CONCRETE MASONRY WALL RETROFIT SYSTEMS FOR BLAST PROTECTION

A Dissertation

by

CAROL FAYE JOHNSON

Submitted to the Office of Graduate and Professional Studies of
Texas A&M University
in partial fulfillment of the requirements for the degree of

DOCTOR OF PHILOSOPHY

Chair of Committee,	Mary Beth D. Hueste
Co-Chair of Committee,	Lynn Beason
Committee Members,	Joseph M. Bracci
	Dara Childs
	Stanley C. Woodson
Head of Department,	Robin Autenrieth

December 2013

Major Subject: Civil Engineering

ABSTRACT

The increased threat against government and public facilities in the United States and abroad has highlighted the need to provide an economic and efficient method to retrofit existing conventional structures. Hollow, unreinforced, concrete masonry unit (CMU) infill walls, commonly used in reinforced concrete or steel framed structures, are particularly vulnerable to blast loads. Facilities that incorporate CMU walls must either be hardened or retrofitted for explosive events. Conventional retrofit techniques that focus on increasing the overall strength of the structure by adding steel or concrete are difficult to implement, time consuming, expensive, and in some cases, increase the debris hazard. The current research presents an alternative retrofit system for CMU walls that involves the application of an elastomeric material applied to the interior surface of the wall to prevent secondary debris in the form of CMU fragments from entering the structure when it is exposed to blast loads.

The experimental program used to evaluate the alternative retrofit systems was divided into three phases. In Phase one, resistance functions for seven different retrofit systems were developed in 24 subscale static experiments. In Phase two, the structural response of the retrofit systems subjected to blast loads was evaluated in 25 subscale experiments. The final phase of the experimental program consisted of 18 full-scale high-explosive (HE) experiments used to validate the structural response observed in the subscale dynamic experiments.

Data generated from the experimental program were used to develop a single-degree-of-freedom (SDOF) model to predict the mid-span deflection of the retrofitted CMU walls subjected to blast loads. The subscale resistance functions from Phase one were scaled and used in the SDOF model. The full-scale experimental results and the predicted results from the model were compared and the retrofit systems were ranked according to the qualitative and quantitative results obtained from the experimental and analytical research.

DEDICATION

This work is dedicated to my Uncle William Frederick Emanuel, Specialist Four, 1st Platoon, Troop F, 17th Calvary Regiment, 196th Infantry Brigade (Light), Americal Division, United States Army Republic of Vietnam, Army of the United States, killed in action on July 02, 1970, by an improvised explosive device in Quang Tin Province, South Vietnam. You will never be forgotten and your legacy will live on in the hearts of all your family members. May we all remember the ultimate sacrifices made by many for the freedoms we have today.

ACKNOWLEDGMENTS

I would like to thank my committee co-chairs, Dr. Beason and Dr. Hueste, and my committee members, Dr. Bracci, Dr. Childs, and Dr. Woodson, for their guidance and support throughout the course of this research.

Thanks also go to my friends, colleagues, and the department faculty and staff for making my time at Texas A&M University a great experience. I would also like to acknowledge Dr. Terry Kohutek a dedicated professor from Texas A&M University, who unfortunately passed away before the document was completed. His support and dedication will always be remembered by all those who worked with him.

I also want to extend my gratitude to the U.S. Army Engineer Research and Development Center (ERDC), which provided the opportunity to pursue a Doctoral Degree at Texas A&M University. The research presented herein was sponsored and conducted by staff of the U.S. Army Engineer Research and Development Center (ERDC), Vicksburg, MS. I would like to thank all of the technicians and engineers from ERDC that assisted in the research program. A full unabridged version of the research presented herein is available for distribution to U.S. Government agencies and their contractors. Requests for the unabridged document shall be referred to U.S. Army Engineer Research and Development Center, ATTN: CEERD-GS-V, 3909 Halls Ferry Road, Vicksburg, MS 39180-6199.

Materials for the experiments were either purchased off the shelf or specifically manufactured for the program by Worthen Industries, Technical Urethanes, Berry

Plastics, Ply Tech, and Sunrez Corporation. The insight provided by the representatives from each company was invaluable.

Finally, thanks to my family and friends for their encouragement, patience, and love.

NOMENCLATURE

A	Area
AFB	Air Force Base
AFRL	Air Force Research Laboratory
α	Decay Coefficient
ANFO	Ammonium Nitrate Fuel Oil
ASTM	American Society for Testing and Materials
AWG	American Wire Gauge
BBTS	Big Black River Test Site
β	Scale Factor
BLS	Blast Load Simulator
CFC	Chloro Fluorocarbons
CMU	Concrete Masonry Unit
CONWEP	Conventional Weapons Effects Program
COTS	Commercial off the Shelf
d	deflection
Δt	Time Increment
δ	Displacement
DL	Driver Length
DP	Driver Pressure
DW	Dynamic Wall
E	Modulus of Elasticity
E_m	Modulus of Elasticity for Masonry
ε	Strain
ERDC	Engineer Research and Development Center
E_v	Modulus of Rigidity
f	Natural Frequency

F(t)	Forcing function
f_m'	Compressive strength of masonry
F_e	Equivalent Force
FOUO	For Official Use Only
FS	Full-Scale
F_T	Total Force
g	Gravity
GFRP	Glass Fiber Reinforced Polymer
h	height
h/t	Slenderness ratio
HE	High Energy Explosive
HTC	Hydrostatic Test Chamber
i_r	Reflected impulse
k	Stiffness
K_L	Load Transformation Factor
K_{LM}	Load Mass Transformation Factor
K_M	Mass Transformation Factor
K_R	Resistance Transformation Factor
L	Span
m	mass
M_e	Equivalent Mass
MEK	Methyl Ethyl Ketone
mils	millionths of inch
MSDS	Material Safety Data Sheets
M_T	Total Mass
NCERD	National Center for Explosion Resistant Design
P	Pressure
P_{abs}	Absolute Pressure
P_{atm}	Atmospheric Pressure

P_{CL}	Centerline Pressure
P_{gauge}	Gauge Pressure
Φ	Strength reduction factor
ϕ	Shape Function
pli	pounds per lineal inch
P_o	Ambient pressure
P_r	Reflected pressure
P_S	Peak incident pressure
PSA	Pressure Sensitive Adhesive
psi	pounds per square inch
PSTC	Pressure Sensitive Tape Council
R	Range
R(t)	Resistance function
SDOF	Single Degree of Freedom
SOP	Standard Operating Procedure
SW	Static Wall
T	Natural Period
t	thickness
t_a	Time of arrival
TDR	Transient Data Recorder
t_{eo}	Equivalent positive time duration
t_o	Positive phase duration
TPU	Thermoplastic Polyurethane
UAHB	University of Alabama at Huntsville
UFC	Unified Facility Code
USACE	United States Army Corps of Engineers
VOC	Volatile Organic Compounds
w	width
w(x)	distributed load

WAC	Wall Analysis Code
$\dot{X}$	Velocity
$\ddot{X}$	Acceleration

TABLE OF CONTENTS

Page

LIST OF FIGURES

Page

LIST OF TABLES

Page

1. INTRODUCTION*

In 1946, the study of blast effects and their mitigations was initiated during World War II by the National Defense Research Committee when the outcome of near-field explosions on structures was examined. Damage criteria for buildings with load bearing walls were developed based on the impulse from the blast wave (Jones, P. 1989). In the Cold War era, aboveground nuclear testing was used to study the responses of one- and two-story masonry buildings to long-duration blast loads. This research led to a failure criterion for masonry walls that was based on the peak pressure from the blast wave (Jones, P. 1989). In 1964, Biggs documented more robust analytical methods that considered the load-time history and structural parameters, such as material strengths and support conditions, in his book *Introduction to Structural Dynamics.*

> Explosions produce a shock wave or high-pressure front that propagates outward from the "point" of detonation. The length of time that it takes for the shock front to propagate to a specific point of interest is defined as the time of arrival, t_a. The shock front depicts an almost instantaneous rise in pressure (Figure 1.1). The peak incident pressure, P_s, is at the end of this initial phase. The

*Part of this chapter is reprinted with permission from "Evolution of Elastomeric Retrofits for Concrete Masonry Unit Walls for Enhanced Blast Resistance at the Engineer Research and Development Center" by Johnson, C.F., B.P. DiPaolo, and S.C.Woodson, 2011. *Journal of Advanced and High Performance Materials*, Winter 2011, 27-30. Copyright 2011 by Matrix Group Publishing Inc. for The National Institute of Building Sciences Advanced Materials Council.

Part of this chapter is reprinted from *Composites: Part B*, Vol. 38, Issues 5-6, by Buchan, P.A. and J.F. Chen, "Blast Resistance of FRP Composites and Polymer Strengthened Concrete and Masonry Structures- A State-of-the-Art Review," 509-522. Copyright 2007 with permission from Elsevier.

Part of this chapter is reprinted with permission from ASCE, "U.S. Embassy Designs Against Terrorism: A Historical Perspective" by Gurvin, Peter E. and Andrew C. Remson III, 2001. *Structures 2001: A Structural Engineering Odyssey, 1-10,* Copyright 2001 by American Society of Civil Engineers. This material may be downloaded for personal use only. Any other use requires prior permission of the American Society of Civil Engineers.

incident pressure is the pressure on a surface parallel to the direction of propagation (Figure 1.2). The propagation velocity decreases with time (and distance), but it is typically greater than the speed of sound in the medium. As the shock front propagates away from the explosion center, the peak incident pressure at the location of the shock front will decrease. When the wave reaches a surface (such as a wall or a structure) that is not parallel to the direction of propagation, a reflected pressure, P_r , will be generated. The reflected pressure will have the same general shape as the incident pressure, but the peak reflected pressure will typically be significantly higher than that of the incident wave. The magnitude of the reflected pressure depends on the magnitude of the incident wave and the angle of the inclined (often vertical) surface. The impulse delivered to the structure is defined as the area under the pressure-time curve, modified to account for "clearing" around the structure.

Clearing around the structure affects the duration of the reflected pressure and depends on the distance to the nearest free surface, which determines the rate of flow around the object (i.e., the flow will try to go around the wall in order to continue behind the obstacle). This secondary flow from the high to the lower pressure regions reduces the reflected pressure to the stagnation pressure, a value that is in equilibrium with the incident wave pressure. If the reflected pressure cannot be relieved by the secondary flow (such as in the case of an infinite plane wave impinging on an infinitely long wall), the incident wave will be reflected at every point on the surface, and the duration of the reflected pressure will be the same as for the incident wave (Johnson, DiPaolo, and Woodson 2011).

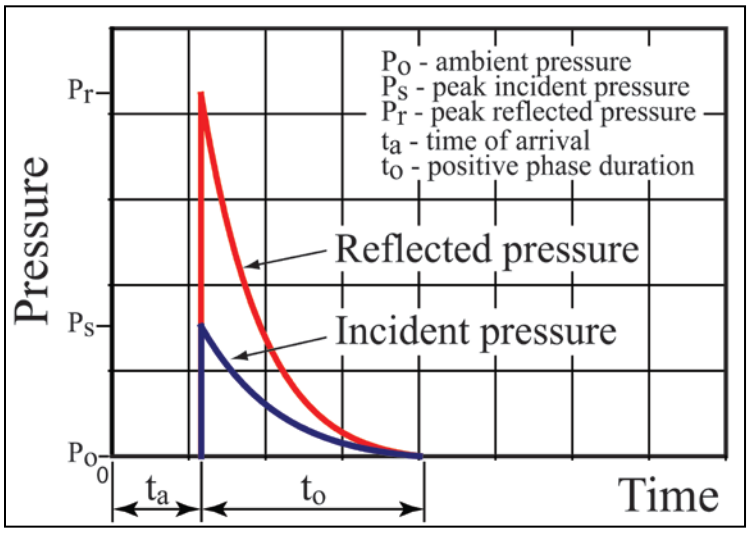

Figure 1.1. Blast loading. (Johnson, DiPaolo, and Woodson 2011)

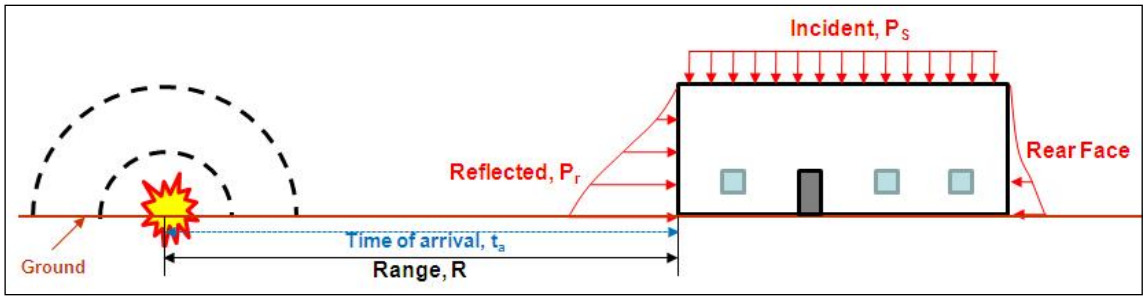

Figure 1.2. Loads on structure from hemispherical surface burst. (Adapted from Woodson 1999; Department of the Army (TM5-855-1) 1986)

The recent increase in domestic and foreign terrorist activity worldwide has demonstrated the vulnerability of existing structures to blast loading. Examples of this vulnerability include government facilities attacked by car bombs at the following locations: West Beirut (1983) resulted in 70 deaths; Kuwait (1983) resulted in 5 deaths; East Beirut (1984) resulted in 11 deaths; Dhahran, Saudi Arabia (1996) resulted in 19 deaths; Nairobi, Kenya (1998) resulted in 218 deaths; and Dares Salaam, Tanzania (1998) resulted in 12 deaths. In the past, military and government facilities on foreign soil were the key targets of terrorists; however, events over the past two decades have shown that high profile public facilities are also viable targets. "The global vulnerability of civilian facilities to terrorist attacks is highlighted in the events in London (2005), Madrid (2004), Istanbul (2003), Bali (2002), and New York (2001)" (Buchan and Chen 2007). The range of building types requiring a blast vulnerability assessment has increased from military barracks, offices, and embassies on foreign soil to include high profile public buildings on domestic soil. Historical monuments, government facilities, courthouses, process industry plants, and other commercial establishments in the United

States might require blast assessment and retrofit systems in the near future. Incidents at the World Trade Center in New York City (1993), in which six people died and more than a thousand people were injured, the Alfred P. Murrah Federal Building in Oklahoma City (1995), in which 168 people were killed and over 800 were injured (Wikipedia 2010), and the devastating second attack on the World Trade Center (2001), where 2,726 people were killed and 1,100 people were injured, demonstrate the viable terrorist threat in the continental U.S.

"The U.S. State Department reported more than 11,000 terrorist attacks globally in 2005 that killed more than 14,600 people." (Buchan and Chen 2007) An assessment of historical terrorism activity data conducted in 2004 by the U.S. Department of State indicated that approximately 85% of recorded incidents involved explosive devices. The U.S. Army Corps of Engineers (USACE), Engineer Research and Development Center (ERDC) in Vicksburg, Mississippi, the Air Force Research Laboratory (AFRL) at Tyndall AFB, Florida, the National Center for Explosion Resistant Design (NCERD) at the University of Missouri-Columbia, the University of Alabama at Huntsville (UAHB), and numerous other universities and government agencies are currently working to develop design criteria for wall systems to resist blast effects.

Ideally, researchers in the field of blast protection would like to completely prevent human injury, loss of life, and structural and property damage, but minimizing these hazards is more realistic. One of the most dangerous aspects of blast response is fragmentation, defined as high-velocity debris originating from pieces of walls, windows, light fixtures, equipment, and furniture.

> For example, the embassy in Nairobi was a robust reinforced concrete structure featuring two-way slab and beam-column frame construction with shear walls on the short sides. The building overall fared well, but considerable non-structural damage to the unreinforced masonry partitions, the elevator and stairway shafts, furniture, drop ceilings, and light fixtures was sustained inside the building. The enormous amount of flying debris is believed to have contributed to the high level of casualties. Forty-four building occupants were killed, and another 21 were seriously injured (Gurvin and Remson 2001).

Rebuilding the structures that currently do not meet blast standards is not feasible. So, the structures must be retrofitted to accommodate cost and time constraints. Reinforced concrete, tilt-up concrete, timber, steel, light metal, reinforced masonry, and unreinforced masonry structures may require different retrofit material systems and application procedures. Therefore, several different methods should be developed and evaluated for each construction type. Conventional retrofit techniques that focus on increasing the overall strength of the structure to mitigate the debris hazard by adding steel or concrete are difficult to implement, time consuming, expensive, and could increase the debris hazard. Retrofit techniques that focus on the ductility of the structural element instead of the mass may be more beneficial. The retrofit techniques must attempt to accommodate a variety of existing conditions while also incorporating aesthetic considerations and operational requirements (Alkhrdaji March 2006; Alkhrdaji October 2006). An easily transportable, effective, expedient, cost-effective, and applicable retrofit method incorporating quality assurance and control must be developed.

Concrete masonry units (CMUs), commonly referred to as concrete blocks or cinder blocks, are one of the most common construction materials used in exterior curtain wall systems of conventional structures throughout the world. The primary advantages of a

CMU wall are its low cost, material availability, and ease of construction. While CMU walls provide adequate strength for conventional design loads, it is widely accepted that CMU infill walls subjected to large lateral loads, such as the transient dynamic loads associated with blast events, almost always fail before the main structural frame of the building is overloaded. When CMU walls are subjected to blast loads, the blocks can break into large fragments ranging in size from full CMU blocks to pebble-size debris. The penetration of the CMU fragments at high velocities into the building's interior can present a severe to lethal hazard for the building's occupants and equipment depending on the severity of the blast (Figure 1.3). Primary debris hazards are defined as fragments that originate from the housing or materials in direct contact with the explosive or munition. The fragments created during the blast event originating from the CMU walls are defined as secondary debris hazards. In Figure 1.3, the wall depictions under (a) represent the respective walls before the airblast impacts the wall surface. The pictures under (b) illustrate the respective wall responses after the airblast has impacted the structure. It is assumed that the magnitude of the range, R, distance from the explosive charge to the structure, is large enough that the airblast impacts the wall as a planar wave. For the airblast wave to be planar in Figure 1.3, the range between the explosive and the CMU walls would need to be increased. ERDC has conducted extensive full-scale and subscale dynamic (explosive) and static (slowly increasing load) tests on unretrofitted CMU walls. The low out-of-plane capacity, due to the low flexural capacity and the brittle mode of failure of CMU walls, make them an excellent candidate for a retrofit system.

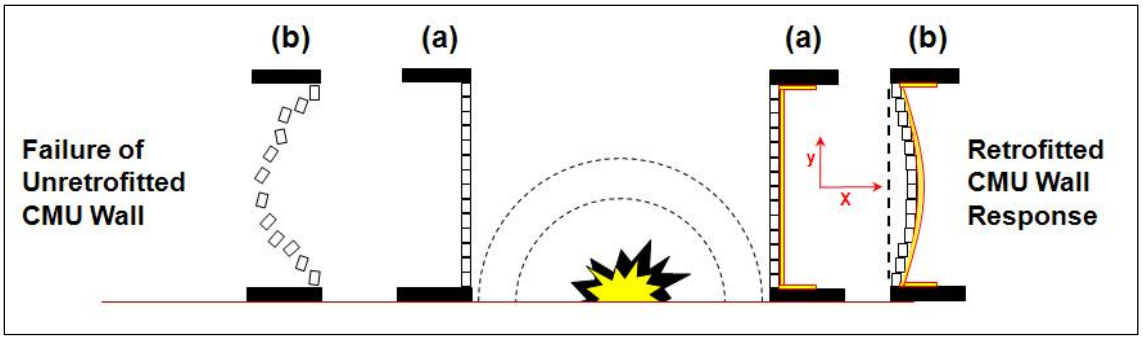

Figure 1.3. Unretrofitted and retrofitted CMU wall response to blast load. (a) Wall before the blast load. (b) Wall response to blast load.

The purpose of the research presented herein was to develop a retrofit system to enhance the blast resistance of hollow, unreinforced CMU infill walls typically used in reinforced concrete or steel framed structures and to explore analysis techniques to make the development of such systems more efficient. As stated earlier, conventional retrofit techniques that focus on increasing the overall strength of the infill walls to mitigate the debris hazard by adding steel or concrete are difficult to implement, time consuming, expensive, and in some cases, increase the debris hazard. A more promising technique involves the application of an elastomeric membrane to the tension side of the CMU wall. This membrane serves to increase the resistance and ductility of the CMU wall assembly. This research began by evaluating the spray-on polyureas commonly used as a spray-on truck bed liner that was identified in 2000 as a retrofit for light-gauge steel buildings (mobile trailers) by the AFRL. Results presented herein show that the spray-on polyurea liners mitigate the debris hazard associated with CMU walls subjected to blast loads; however, installation of such systems require extensive training and expensive equipment. In addition, the spray-on systems also lack the quality assurance and control

for effective use in austere environments. Therefore, additional elastomeric materials and installation techniques were explored to develop an effective, efficient, and economical retrofit system that could be applied to CMU walls with minimal training and equipment requirements.

Once the retrofit materials and installation systems were selected, an experimental program was initiated to identify the performance of the various retrofit systems. The experimental program was divided into two parts based on the loading rate applied to the test specimens. The material characteristics under static and dynamic loading differ, so both loading regimes were evaluated in the research program. First, the static experiments were conducted to identify potential CMU retrofit systems and to determine the physical response of the retrofitted CMU walls loaded at a steady and slow rate. The physical response of the static experiments was quantified by developing resistance functions from the load and deflection data. Once the static experiments were completed, a small number of systems were removed from further consideration because of poor structural performance. The remaining systems were then subjected to subscale dynamic evaluation using high energy explosives (HE) and a Blast Load Simulator (BLS). Based on the subscale results, the original group of systems was further refined, and full-scale dynamic experiments were performed to provide final verification for full-scale prototype systems. The qualitative and quantitative results from the subscale model and full-scale prototype experiments were used to select the most promising retrofit systems.

Subscale static experiments conducted in a laboratory using water as a load are much more economical than either subscale or full-scale dynamic experiments that require a

remote test site, a blaster, and the explosives to create the load. At this stage of development, a full-scale dynamic experiment is ultimately required to validate the performance of any proposed system. This notwithstanding, a considerable amount of effort was expended to develop a method to predict full-scale dynamic behavior from the subscale static experiments in the hope of reducing overall development costs. To accomplish this, results from the subscale static experiments were used to develop full-scale resistance curves. The scaled resistance functions were combined with well accepted techniques first advanced by Biggs to develop a single-degree-of-freedom (SDOF) procedure to predict the full-scale dynamic response. This procedure was demonstrated using all of the full-scale experiments conducted in this program and the results from the full-scale experiments are compared to the predicted results from the SDOF procedure presented herein.

2. PROBLEM DESCRIPTION

Conventional retrofit techniques used to mitigate debris hazards for buildings generally focus on making major modifications to both the primary structural frame and the secondary elements, such as the windows and infill walls. This is commonly referred to as blast hardening and is accomplished by increasing the overall strength of the structure through the addition of mass using concrete or steel. Given enough resources and time, it is possible to greatly enhance the survivability of most existing structures. However, these conventional retrofit techniques are often difficult to implement, time consuming, and expensive, and in some cases, the debris hazard may be inadvertently increased. Depending on the desired level of survivability, fabricating a completely new structure could be more expedient and cost less than hardening an existing structure.

Results from several damage assessments conducted after actual explosive attacks determined that failure of the infill walls is often the primary cause of damage to both the human occupants and the contents of the building. These results led to the conclusion that, in many cases, a significant reduction in secondary debris can be achieved by focusing on retrofitting the wall elements. CMU walls are particularly vulnerable to blast loads. Hollow, unreinforced CMU walls, typically used in steel and reinforced concrete framed structures, tend to disintegrate into a large number of fragments that penetrate into a structure at very high velocities depending on the severity of the blast loads (Figures 2.1a through c). Because of this, retrofit systems

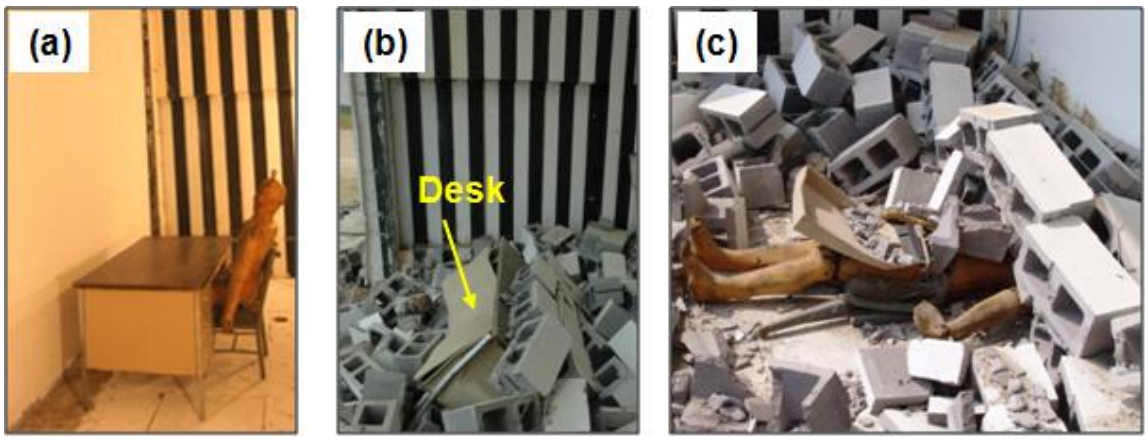

Figure 2.1. Unretrofitted CMU wall. (a) Pretest view of interior. (b) Posttest view of interior. (c) Mannequin after removing the overturned desk and CMU blocks.

for conventional structures have evolved over the years from blast hardening with the addition of mass to the application of lighter, more resilient, and ductile materials. ERDC began the CMU research program using conventional materials such as sheet steel and catcher systems. The catcher systems were not intended to add any additional strength to the wall, but rather served as a net or barrier that would catch the debris and thereby reduce the hazard to occupants in the building.

One of the first catcher systems used was a geotextile or geogrid anchored at the top and bottom floor slabs. These materials are usually stronger in the roll or machine direction and weaker in the cross-roll or cross-machine direction. The retrofit must be applied with the machine-direction (stronger) axis oriented perpendicular to the anchored supports. To anchor the system, the geotextile is wrapped around a steel plate that spans the entire length of the wall and is bolted to the building. Failures in the fabric occur at points of high-stress concentrations, which could occur along the edges of the

anchor plates or CMU fragments. The geofabric system does provide protection from secondary debris hazards, but the application procedure is labor intensive, the fabric could be applied in the wrong direction, extensive anchoring is required, and it is aesthetically unpleasing (Dinan, Coltharp, and Townsend 2002).

Research at ERDC has transitioned from conventional methods to strengthen CMU walls to catcher retrofit systems and the use of elastomeric materials initially evaluated by AFRL on temporary structures. AFRL personnel retrofitted light-gauge steel buildings (mobile trailers) with a spray-on elastomeric liner or coating for blast protection. The primary concern during selection of the polymer was the strength and elongation properties of the material. Secondary factors included effectiveness, expedience, availability, costs, aesthetics, environmental effects, ease of application, and transportation. The elastomeric (polyurea) liner chosen for the test was a two-part spray of polyurea used in commercial applications for spray-on truck bed liners. The materials are shipped in liquid form contained in barrels and can be applied directly to the vertical wall surface with preparation. The polyurea liner bonds quickly to the CMU blocks and forms a continuous bond with the wall surface (Knox, Hammons, Lewis, and Porter 2000). Spray-on elastomeric systems provide a level of protection against the debris hazard; however, the system requires expensive equipment, extensive training, and lacks the quality assurance and quality control needed for effective use in austere environments.

2.1 Objectives

The first objective of the research program was to develop an efficient, engineered, structural retrofit system to effectively mitigate the secondary debris hazard associated with CMU infill walls subjected to blast events. Efficiency in this research was defined by an increase in quality control and assurance, while decreasing the level of training and equipment required for application. Failure of materials in general "refers to any action that leads to an inability on the part of the structural component to function in the manner intended" (Ugural and Fenster 1995). Because of the destructive nature of the dynamic loads investigated, clearly defining the terms success or failure in regards to the research subject is important. In the research program, the CMU wall can lose structural integrity or be compromised, and the retrofit system can still be labeled a success if the retrofit materials prevent secondary debris in the form of CMU wall fragments (secondary debris hazards) from entering the structure. Therefore, the understanding is that the CMU wall can be compromised and will need to be replaced. Failure of the retrofit system is defined first by the presence of a secondary debris hazard and then by the deformation or deflection of the wall into the protected space. Application instructions, failure criteria, design guidelines, and analysis techniques to predict the wall's response under a defined dynamic load were developed for the retrofit systems.

The second objective was to provide an analytical model to predict the wall's response to blast loads. Dynamic analysis of structures can be simplified by applying numerical methods to an idealized system of the true structure of interest. The number of independent coordinates required to define the configuration/position of a system at any

time is referred to as the number of degrees of freedom. The SDOF spring-mass system is the simplest model used to determine the dynamic response of structural components subjected to blast loads (Figures 2.2a and b). A SDOF is defined by a single coordinate or one type of motion. The formulation of the model, the ability to obtain the input parameters simply, and the minimal computational effort required to perform numerous calculations make the SDOF model an advantageous method for dynamic analysis. SDOF models tend to be robust and reliable over a wide range of input parameters, and the capabilities and limitations of the model are usually easy to define or predict.

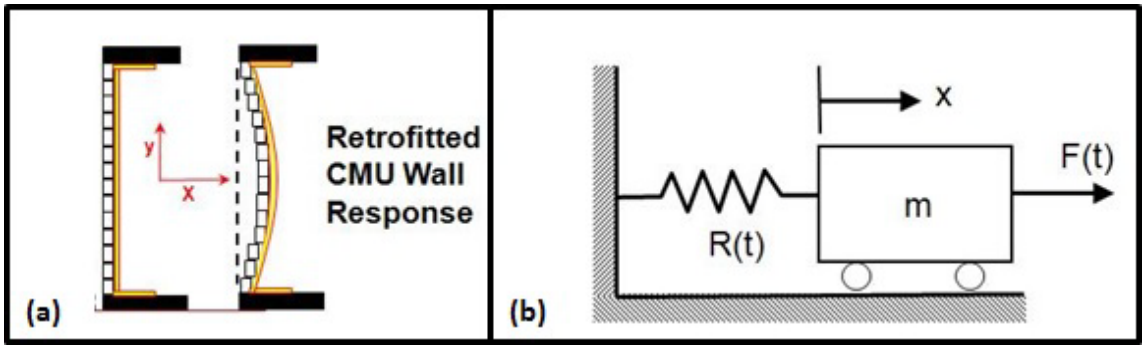

Figure 2.2. Blast response. (a) CMU wall component.
(b) SDOF model used for CMU wall.

The important system parameters used to define an equivalent SDOF model are the spring constant, the weight or mass, and the load function. The properties of the structural component under analysis are used to determine the spring constant or the ratio of force to deflection. If the weight of the structural component is assumed negligible, then the weight or mass of the idealized structure will be the same in the idealized system. If the mass of the structural component is distributed over the

structure, then a mass factor must be applied to obtain the equivalent mass for the idealized system. The load function is typically the same for the two systems, but the magnitude can differ. A properly defined spring-mass system will respond such that the deflection or behavior of the mass in the idealized system will be the same as a significant point on the real structure, which is usually defined by the midpoint deflection of the structural component. In the research program, the unretrofitted and retrofitted CMU walls were the structural component of interest. The wall spans vertically between the bottom and top support with no support from the side walls, which produces a one-way response; so the mid-height deflection of the wall was chosen as the significant point of interest.

2.2 Research Plan

The plan used to achieve the two research objectives is illustrated in Figure 2.3. The retrofit material systems and installation techniques for evaluation as retrofit systems for unreinforced CMU infill walls were selected first. The systems were evaluated in an experimental program divided into two parts. Part 1 consisted of a series of subscale static experiments to characterize the material properties and application techniques. Part 2 consisted of a set of subscale and full-scale dynamic experiments used to evaluate the retrofitted CMU walls' response to blast loads. Once the experimental program was completed, the dynamic analysis of the CMU walls began. An SDOF model developed in Excel was used to predict the mid-span deflection of the retrofitted CMU walls under blast load. The resistance functions created from the static experiments conducted in Part 1 of the experimental program were used in the dynamic analysis. The resistance

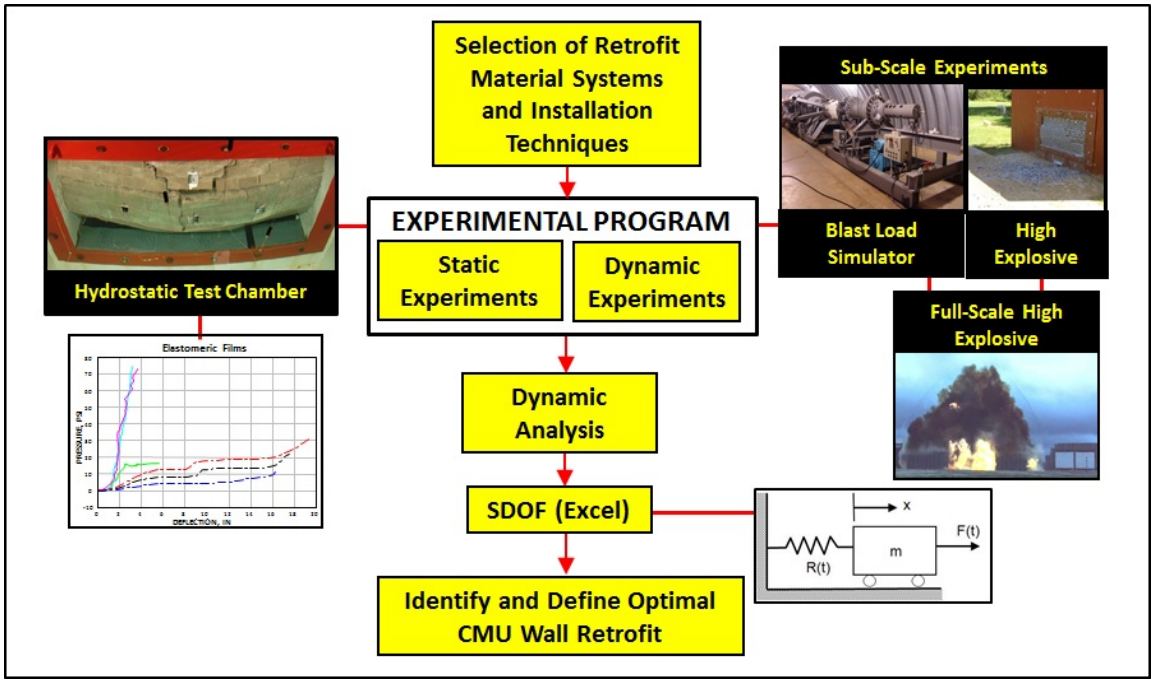

Figure 2.3. Research plan.

functions developed from the subscale static experiments were used in the subscale analysis and the values were increased for the full-scale analysis. The qualitative and quantitative data obtained in the research plan were used to select the optimal retrofit system for blast protection. At the request of the sponsor, the data generated from the static, dynamic, and SDOF analysis were normalized in the document. To further protect the data, the method used to normalize the information has not been included.

3. PRIOR EXPERIMENTAL WORK *

In the late 1990s to 2000, most retrofit procedures concentrated on hardening walls for blast protection. When the research began in 2001, the majority of the research to mitigate secondary debris hazards focused on hardening structures, and only a small number of publications that discussed less evasive measures to control or minimize the debris hazards were researched. Research conducted at ERDC regarding the unretrofitted and retrofitted CMU wall response to explosive loads was discussed first. Over the last decade as the program progressed, research at universities, private consulting firms, and military research labs also increased considerably. Providing detailed information on all of the work that has been conducted at universities and test facilities since the research program began in 2001 would be difficult; therefore, only a short summary of previus work conducted at ERDC was provided. The information provided in Section 3.1 was adapted from the original raw experimental data package, an unpublished report authored by Woodson, Bullock, and Baylot in 2001 who are employees of the Geotechnical and Structures Laboratory at ERDC, and an article in the Journal of Structural Engineering published by ASCE in 2005 with Baylot, Bullock, Slawson, and

*Part of this chapter is reprinted with permission from ASCE "Blast Response of Lightly Attached Concrete Masonry Unit Walls" by Baylot, James T., Billy Bullock, Thomas R. Slawson, and Stanley C. Woodson, 2005. *Journal of Structural Engineering*, Vol. 131, no. 8, 1186-1193. Copyright 2005 by American Society of Civil Engineers. This material may be downloaded for personal use only. Any other use requires prior permission of the American Society of Civil Engineers.

Part of this chapter is reprinted with permission from *CMU Wall Debris and Structural Response Experiments* by Woodson, Stanley C., Billy W. Bullock, and James T. Baylot, November 2001. This work performed by the U.S. Army Engineer Research and Development Center in Vicksburg, MS has not been published to date.

Woodson as authors. The experimental results in Section 3.2 were provided by ERDC, but the information has not been documented in a report to date. An additional list of publications related to blast analysis and CMU wall retrofits obtained during the program is provided in Appendix A.

3.1 Woodson/Bullock Experiments

In 2000, ERDC conducted nine static and forty-three dynamic subscale experiments on reinforced and unreinforced retrofitted and unretrofitted CMU walls. Nineteen of the dynamic experiments were conducted to obtain debris velocities, sixteen were used to define structural damage levels, and eight were retrofitted wall experiments. To model a non-load-bearing exterior wall constructed between two exterior columns, air gaps were left between both sides of the wall and the reaction structure and between the top course of blocks and the top of the reaction structure. A slip dowel created using a 1/8-in. steel dowel was wrapped in foil and grouted into every third cell along the top course of blocks to represent "the clips typically used to connect the top of the wall to the floor slab or edge beam above the wall" (Baylot, Bullock, Slawson, and Woodson 2005). The dowels were wrapped in foil to prevent a bond from forming in the grout. The blocks were placed in a running bond, and the bottom course was placed in a mortar bed to create a simple support.

Four types of CMU wall construction were evaluated. The first group consisted of nine hollow and unreinforced CMU walls. The second group consisted of twenty-two partially grouted lightly reinforced walls. Every third column of cells was filled with grout and reinforced with a nominal 1/8-in.-diameter deformed steel wire in the partially

grouted lightly reinforced CMU walls. The third group of walls consisted of eight fully grouted unreinforced CMU blocks. Every cell in the CMU block wall was filled with grout. The final set of walls evaluated consisted of four fully grouted and lightly reinforced walls. All of the cells were fully grouted, and every third cell corresponding to the cells containing the slip dowels were reinforced with a 1/8-in.-diameter deformed steel wire. Simple and fixed boundary conditions existed depending on the reinforcement used. Walls containing a mortar joint at the bottom support were considered simply supported, while the walls reinforced with the steel wire and a mortar joint were considered fixed. The hollow unreinforced CMU walls evaluated in the referenced experiments are discussed in greater detail (Woodson, Bullock, and Baylot 2001).

Three hollow and unreinforced CMU walls were evaluated in the Hydrostatic Test Chamber (HTC). The corners on the first CMU wall evaluated in the chamber became bound in the top corners, and the high resistance observed in the data is considered to be unrealistic. The diagonal cracking observed in the photos also indicated that the wall was unable to deform freely (Figure 3.1a). The CMU wall in Test 8 failed one course above the midline at approximately 0.0396 (Figure 3.1b). In Test 9, the CMU wall cracked below the top 1/4 span, and the bottom section of the wall fell into the chamber (Figure 3.1c). The resistance functions created from the original pressure and deflection data for each of the experiments were normalized and are provided in Figure 3.2.

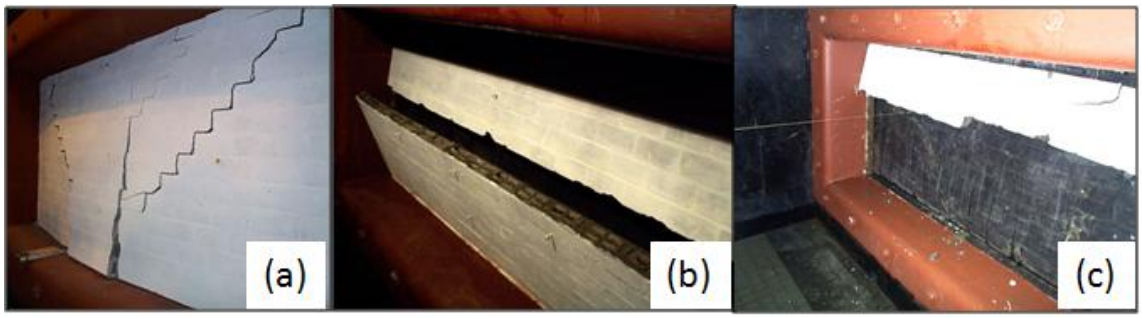

Figure 3.1. Hollow and unreinforced CMU walls. (a) Test 1. (b) Test 8. (c) Test 9. (Woodson, Bullock, and Baylot 2001)

Three retrofit materials were evaluated in the static and dynamic experiments: a glass fiber-reinforced polymer (GFRP), a spray-on polyurea, and a steel sheet. The first material selected was a 0.04-in.-thick unidirectional E-glass fiber-reinforced polymer bonded to the interior surface of the CMU wall using an epoxy (Figure 3.3a). The GFRP overlapped the top and bottom supports and was adhesively attached to the reaction frame in the dynamic experiments. The material properties for the GFRP used in the experiments are provided in Table 3.1. For the second retrofit system, a two part spray-on polyurea commercially used as a truck bed liner was used to coat the interior surface of the CMU wall. The spray-on liner was approximately 1/8-in.- to 3/16-in.-thick with a 2-in. overlap on the top and bottom supports. The properties for the spray-on elastomer used in the Woodson/Bullock experiments can be found in Table 3.2.

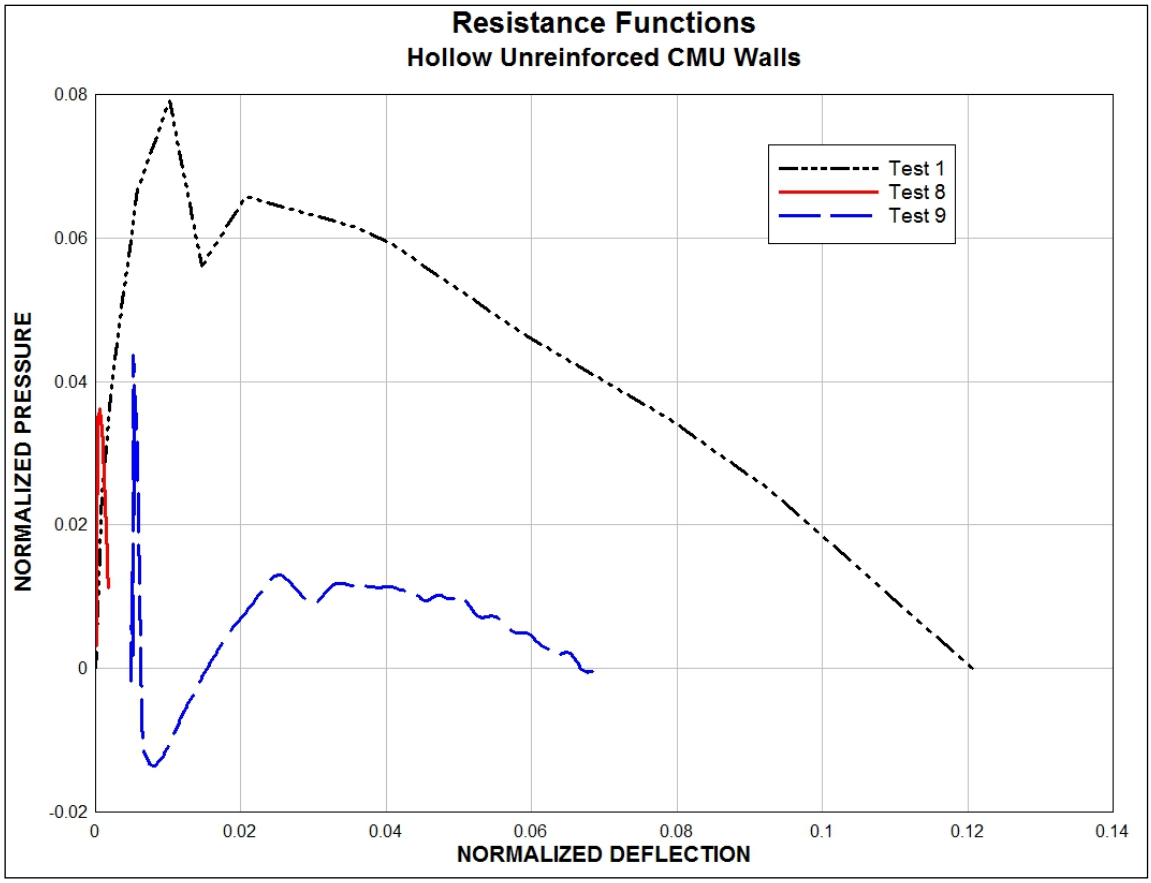

Figure 3.2. Resistance functions for hollow and unreinforced CMU walls.

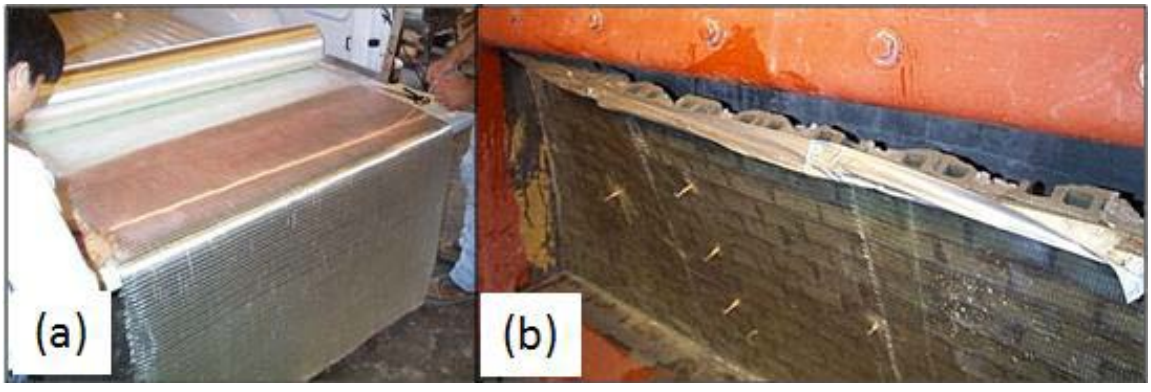

Figure 3.3. GFRP retrofit. (a) Unidirectional GFRP used to retrofit the wall. (b) Retrofit failed when the material peeled off the top support. (Woodson, Bullock, and Baylot 2001)

Table 3.1. GFRP material properties in Woodson/Bullock experiments. (Adapted from Baylot, Bullock, Slawson, and Woodson 2005)

Material Property	GFRP
Modulus of Elasticity	3,790 ksi
Tensile Strength	87 ksi
Elongation at Break	2.24 %
Mass Density	0.000033 lb/in.^{3}

Table 3.2. Polyurea material properties in Woodson/Bullock experiments. (Adapted from Baylot, Bullock, Slawson, and Woodson 2005)

Material Property	Spray-on Polyurea
Modulus of Elasticity	33,940 psi
Secant Modulus	23,930 psi
Yield Strength	1,667 psi
Ultimate Strength	2,000 psi
Elongation at Yield	4.7 %
Elongation at Rupture	89 %

A 20-gauge hot-dipped galvanized A-36 steel sheet was used as the third retrofit system. The steel sheet was only used as a retrofit material in the dynamic experiments. The steel sheet covered the interior surface of the CMU wall, and a 3-in. strip overlapped the top and bottom supports. The sheet was not physically attached to the wall but was anchored to the top and bottom supports with a 1/4-in. by 3-in. steel plate using 1/4-in.-diameter bolts every 6 in. on center.

The hollow unreinforced CMU wall retrofitted with the GFRP (Test 4) failed when the material that overlapped the top support peeled off (Figure 3.3b). The resistance function created from the original pressure and deflection data was normalized and provided in Figure 3.4. The ultimate flexural resistance of the CMU wall occurred at a deflection of 0.0086 and a pressure of 0.426 (Figure 3.4).

The hollow and unreinforced CMU wall retrofitted with the spray-on polyurea (Test 6) failed when the 2-in. overlap peeled off the top support (Figures 3.5a and b). The ultimate flexural resistance of the CMU wall occurred at a deflection of 0.0776 and a pressure of 0.193 (Figure 3.4). The ultimate tensile membrane resistance of the retrofit system occurred at a deflection of 0.405 and pressure of 0.263.

> Data generated from the dynamic experiments were used to define hazard levels based on the horizontal velocity of the debris. Four hazard levels were defined before the experiments began. If the CMU wall did not fail, the hazard to occupants was very low; so a limiting case for wall hazard was the highest load that did not fail the wall. Low hazard was selected as a wall that failed but entered the room at approximately zero horizontal velocity (in-place collapse). The medium and high hazard levels were defined by debris entering the room at an approximate velocity of 0.577 and 1.15, respectively. The hazard levels were defined by the debris velocity and the height of impact of the debris in a 9.8-ft-wide room. For example, debris traveling at a velocity of 1.15 would drop approximately 19.7 in. as it flew across the 9.8-ft-wide room, which would be a high hazard for occupants. If the debris impacted the opposite wall at a low level (less than 19.7 in.) or on the floor, then the debris hazard was considered intermediate (Baylot, Bullock, Slawson, and Woodson 2005).

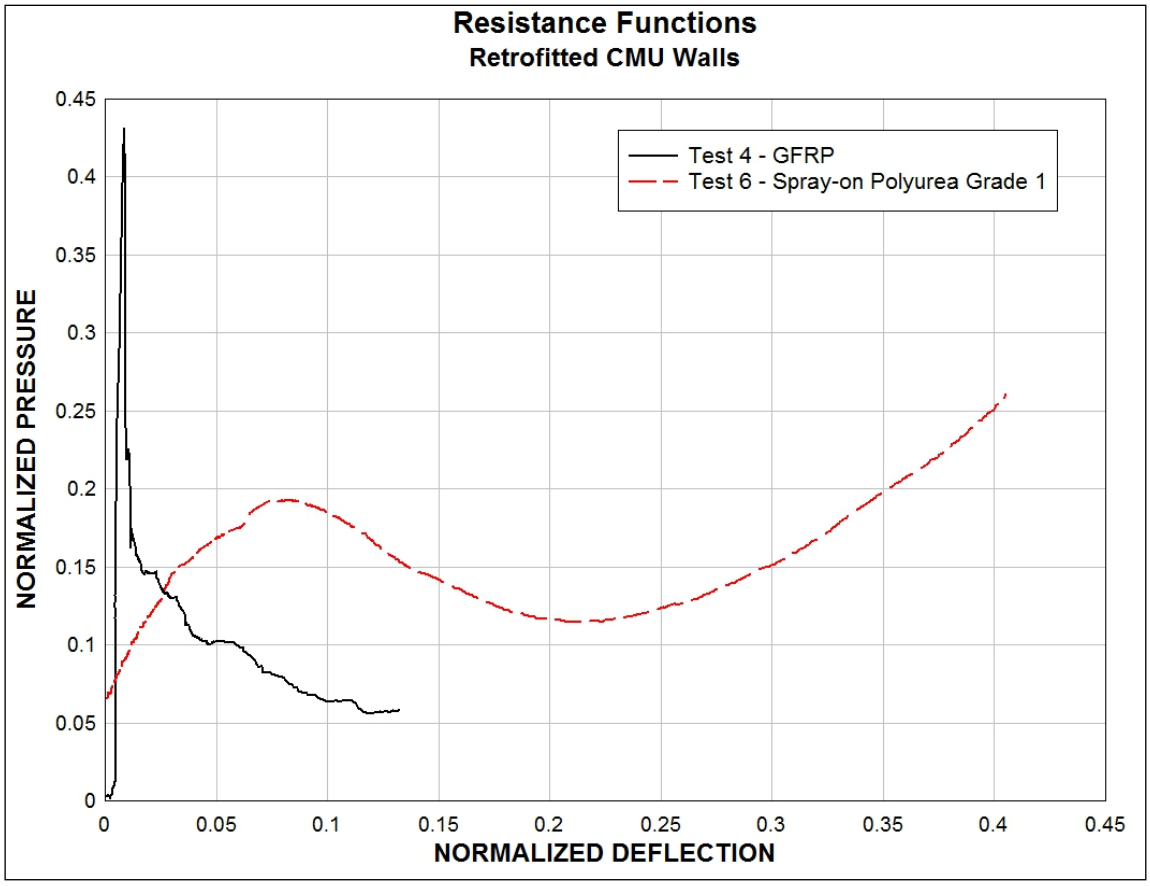

Figure 3.4. Resistance functions for the retrofitted CMU walls.

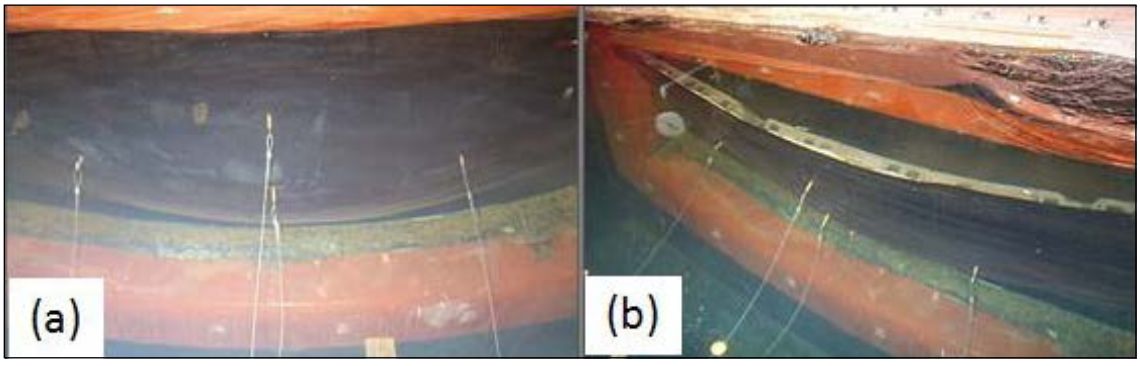

Figure 3.5. Polyurea retrofit. (a) Maximum deformation of polyurea coating occurred at the center of the wall. (b) Retrofit failed when polyurea peeled off the top support.

High, medium, and low levels of structural damage were also defined using the dynamic experiments. High damage was defined by the loss of structural integrity and collapse of the structural element. A wall that needed repair to be returned to proper function was defined as medium damage. Low damage corresponded to a wall that was repaired for aesthetic purposes only (Woodson, Bullock, and Baylot 2001).

Nine dynamic experiments were conducted on the hollow unreinforced CMU walls in the Woodson/Bullock experiments. The first six experiments were conducted on unretrofitted CMU walls to define the reflected pressure and impulse levels required to identify the hazard and damage levels. The walls in Tests 1, 2, 3, and 8 were completely destroyed, and the majority of the debris entered the reaction structure (Figures 3.6 a and b). Observations noted in the Woodson, Bullock and Baylot (2001) report are summarized in the following text. In Test 1, the debris entered the structure at a velocity of 0.269 and was scattered across the floor of the room. Several large pieces of the debris consisted of three to four bricks still intact, but no significant impact marks were identified on the rear wall of the reaction structure. The wall in Test 2 was also

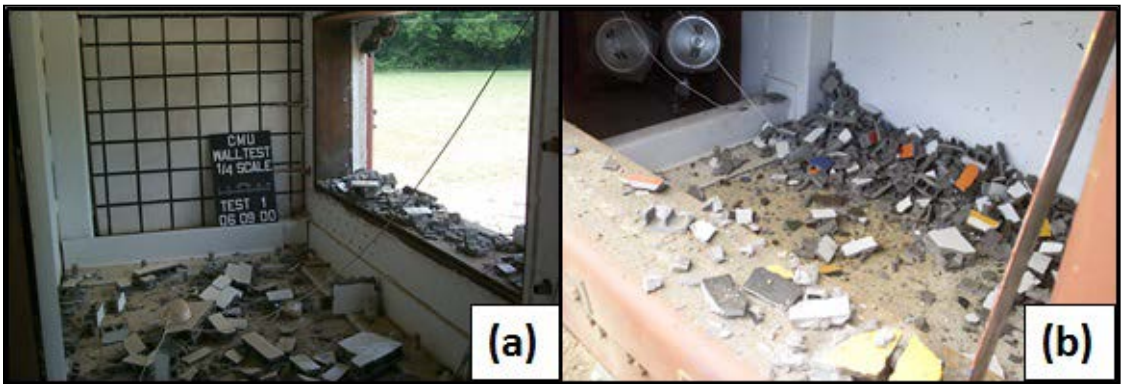

Figure 3.6. Unreinforced, unretrofitted CMU walls. (a) Test 1. (b) Test 2.

destroyed, and the debris entered the structure at a normalized velocity of 1. Marks scattered across the back wall indicated that the debris impacted the wall along the centerline. In Test 3, the CMU debris impacted the rear wall of the structure at a velocity of 0.577. The largest pieces of debris were two to four blocks wide, and the majority of the debris was located inside the reaction structure (Figure 3.7a). A portion of the wall collapsed in Test 8, but the debris fell into the reaction structure. A 1-ft section of the CMU wall wedged into the side walls of the frame, a second section of the wall fell onto the bottom support of the frame, and the third section of the wall fell into the front of the reaction structure at a negligible velocity (Figure 3.7b).

Figure 3.7. Unreinforced, hollow, unretrofitted CMU walls. (a) Test 3. (b) Test 8.

The CMU walls in Tests 4 and 27 were damaged, but neither wall became a debris hazard (Figures 3.8a and b and Figures 3.9a and b, respectively). “Damage to the CMU wall in Test 4 consisted of some spalling along the top of the wall, a crack in the mortar bed that extended the full length of the wall, several hairline cracks were visible in the mortar joints on the exterior and interior face of the CMU wall, and a yield line was

visible across the wall 18 in. above the bottom support." (Woodson, Bullock, and Baylot 2001) There was enough damage to require the wall to be rebuilt. The accelerometers mounted to the wall indicated a 0.112 deflection into the structure at the mid-span and 0.0646 at the quarter point. The wall in Test 27 was also heavily damaged but did not collapse into the structure. The wall had a permanent 0.0862 deflection into the reaction structure at two yield line locations 18 and 24 in. above the bottom support of the frame. The top of the wall permanently deflected 0.0646 into the reaction structure, and a crack was found in the mortar bed that extended the full length of the wall. A few of the blocks along the top support lost a portion of their faceshells, and half of a CMU block in the top corner fell into the reaction structure. The accelerometers indicated a maximum deflection at the mid-span of 0.112 and 0.043 at the quarter point.

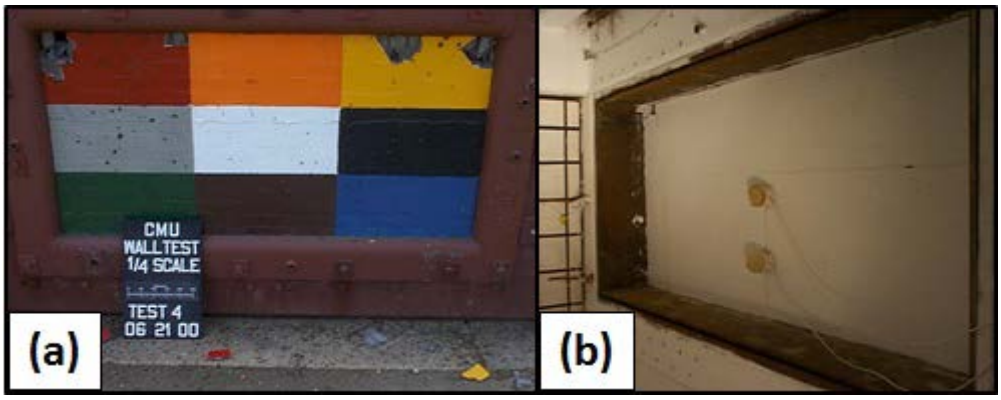

Figure 3.8. Posttest views of unreinforced, unretrofitted CMU wall – Test 4. (a) Exterior. (b) Interior.

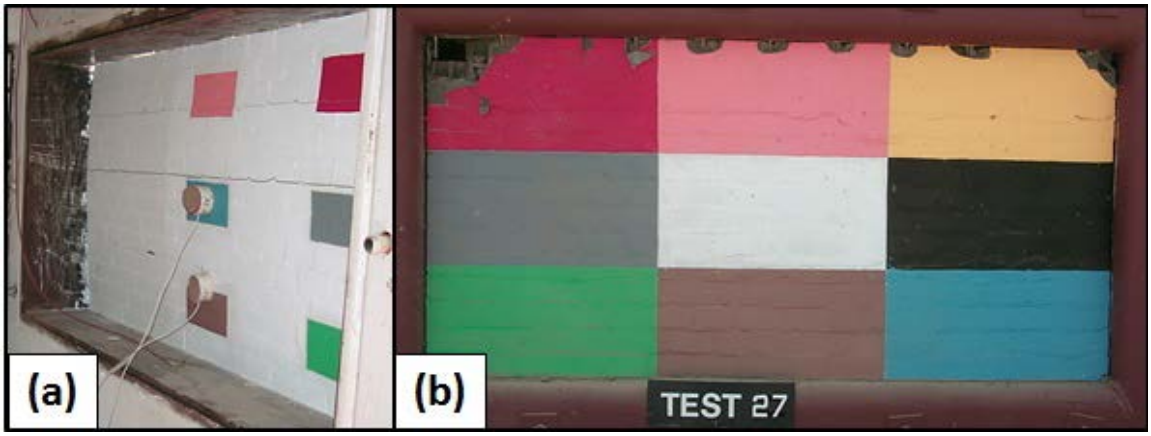

Figure 3.9. Hollow, unreinforced, and unretrofitted CMU wall – Test 27. (a) Interior. (b) Exterior.

The GFRP, spray-on polyurea, and sheet of steel were used to retrofit the three remaining hollow and unreinforced CMU walls. The CMU wall retrofitted with a single layer of GFRP was heavily damaged in the experiment, but none of the debris entered the reaction structure. The fibers in the GFRP layer were aligned in a vertical orientation. The center of the GFRP separated from the steel frame during the wall response and half of the blocks lost their faceshells in the experiment (Figure 3.10a). The bright areas in Figure 3.10b highlight the locations on the wall where the GFRP has pulled away from the frame and no CMU fragments were left attached to the retrofit material in these areas. Two 4-in. tears were also found in the GFRP layer located approximately 10 in. from each edge of the wall (Figure 3.10c).

The hollow CMU wall retrofitted with a coating of the spray-on polyurea Grade 1 remained standing, but the "structural integrity of the wall was lost (Figure 3.11b). The spray-on polyurea separated approximately 2 in. on the lower left (looking at the interior

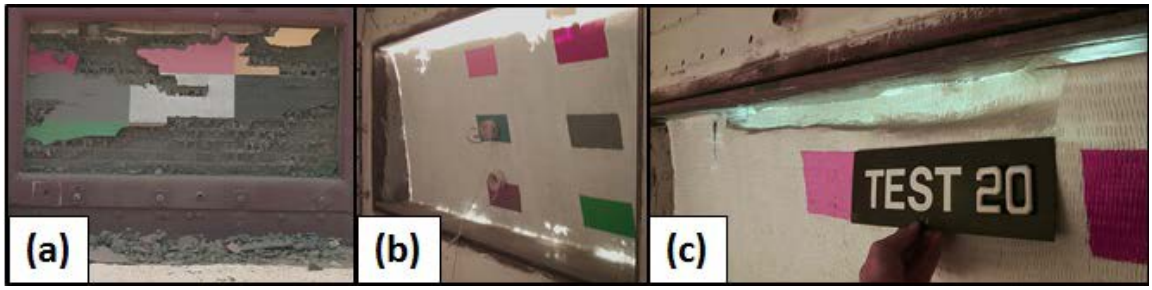

Figure 3.10. Hollow, unreinforced CMU wall with GFRP retrofit. (a) Exterior. (b) Interior. (c) GFRP peeled off top support and material ripped at top support.

face of the wall) and 8in. on the opposite side (Figure 3.11a). The mid-height (center) deflection was consistently 0.259 across the wall and 0.172 to 0.215 along the 1/4-height points." (Woodson, Bullock and Baylot 2001) The faceshells on approximately 28% of the blocks were damaged and landed at the base of the structure.

The wall retrofitted with a 20-gauge sheet of steel failed when the anchor plate, shown in the pretest photo in Figure 3.12a, failed. The bolts securing the plate to the steel reaction frame sheared, and the plate was propelled to the back of the reaction structure (Figure 3.12b). The CMU wall was completely destroyed, and half of the debris from the wall fell into the reaction structure, while the other half fell onto the frame and in an area in front of the reaction structure (Figures 3.13a and b). The steel plate had a permanent deflection of 0.776 into the structure. Large pieces of debris found outside the structure and on the sill of the frame were several blocks wide.

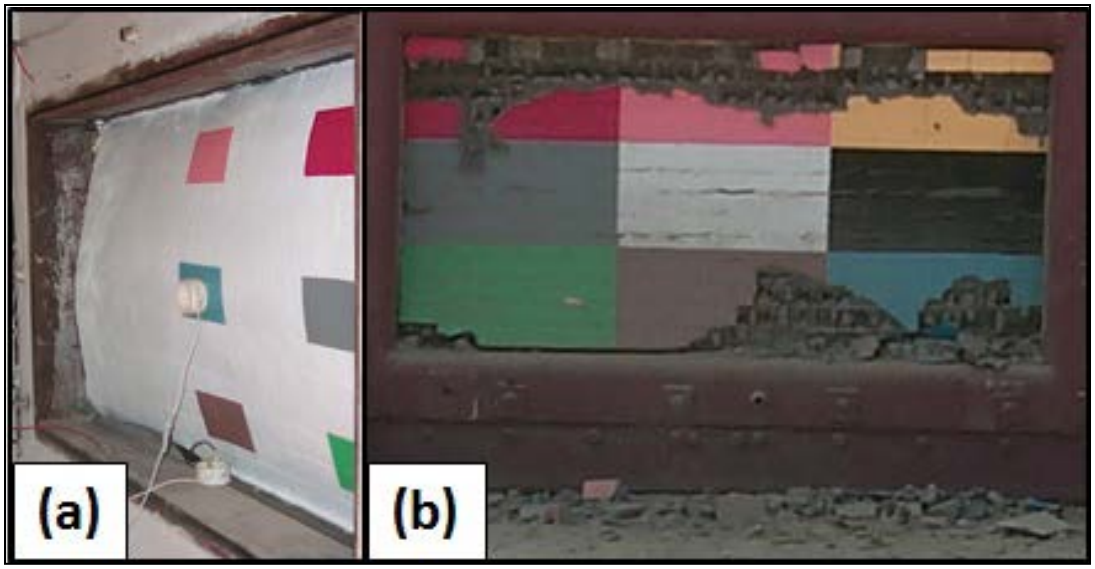

Figure 3.11. Hollow, unreinforced CMU wall with spray-on polyurea retrofit. (a) Interior. (b) Exterior.

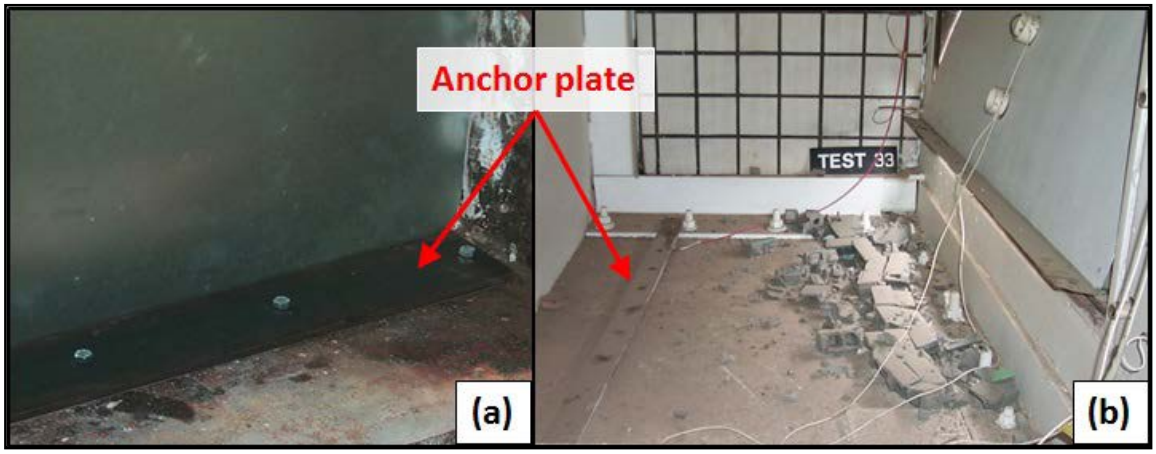

Figure 3.12. CMU wall steel sheet retrofit. (a) Pretest view of anchor plate. (b) Posttest view of anchor plate failure.

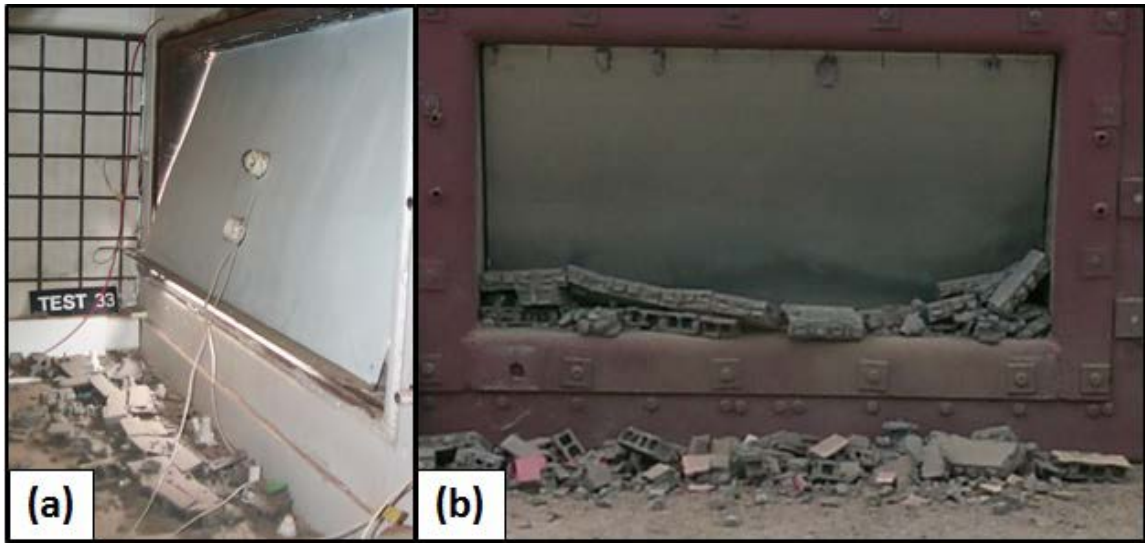

Figure 3.13. Posttest CMU wall with sheet steel retrofit.
(a) Interior. (b) Exterior.

The resistance functions generated from the hydrostatic test chamber experiments were used in the Wall Analysis Code (WAC) to predict the wall responses to the explosive events. The researchers compared the predicted wall response to the results obtained in the dynamic experiments. "The WAC performed well when predicting moderate- and high-hazard debris velocities using the experimentally developed resistance functions, but the program needs a more accurate method to analytically develop resistance functions" (Baylot, Bullock, Slawson, and Woodson 2005).

3.2 Cummins/Bullock Experiment

A multi-bay experiment, conducted at the Big Black River Test Site (BBTS) in 2002, evaluated the response of four hollow unreinforced CMU walls (Figure 3.14a). Wall 1 was a hollow, unreinforced CMU wall with no retrofit applied, Wall 2 was retrofitted with a spray-on elastomer, Wall 3 was retrofitted with an elastomeric film, and Wall 4

was retrofitted with an undisclosed material system under evaluation. The spherical charge of C4 was suspended above ground centered on the middle of the reaction structure using a tripod at a designated standoff.

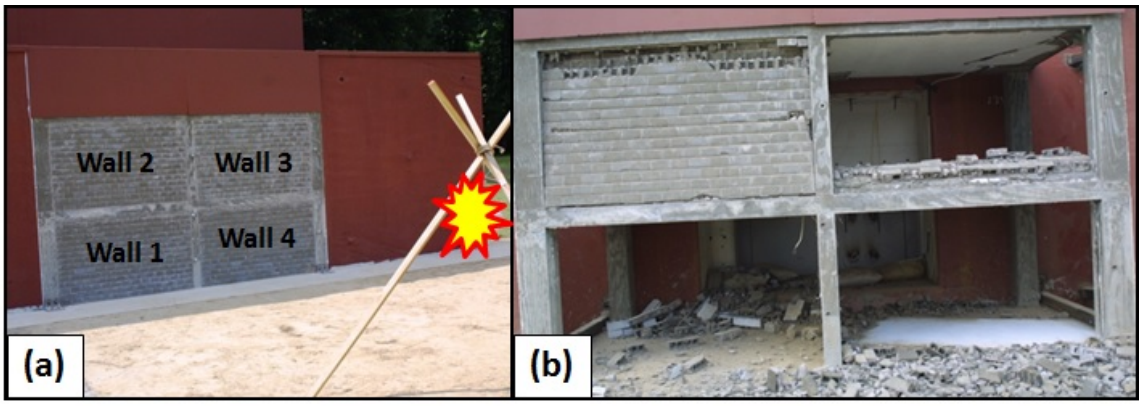

Figure 3.14. **Multi-bay structure at BBTS. (a) Pretest. (b) Posttest.**

Wall 1 was completely destroyed with the majority of the debris impacting the back wall of the reaction structure (Figure 3.15a). The spray-on elastomer applied to Wall 2 performed very well, preventing all of the debris from entering the reaction structure (Figure 3.15b). Posttest exterior and interior photos show that the damage to the wall was concentrated at the top three courses (Figures 3.14b and 3.15b). Lateral deflection did occur at the top support where the overlapped polyurea peeled away from the top support.

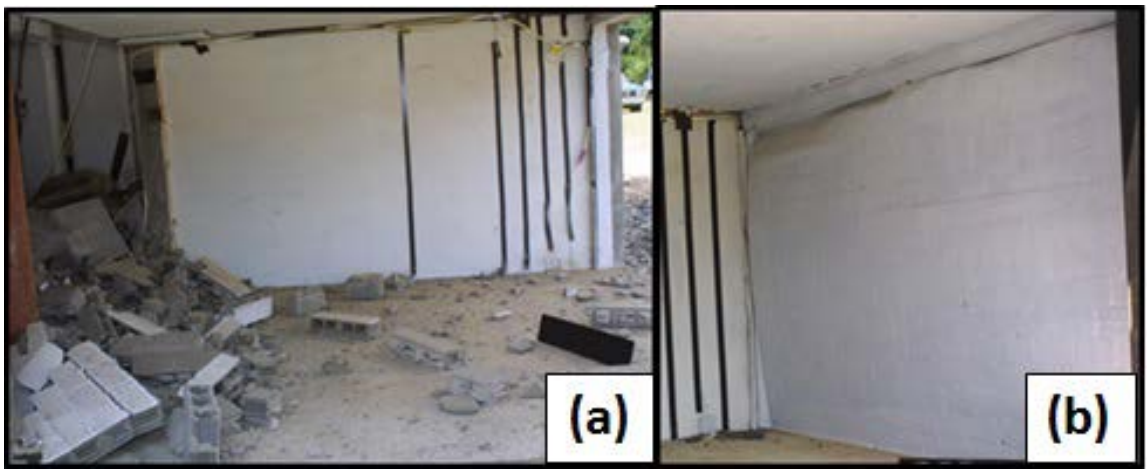

Figure 3.15. Posttest inspection. (a) Interior view of unretrofitted CMU wall. (b) Interior view of Wall 2 retrofitted with a spray-on polyurea Grade 1.

4. CMU WALLS AND RETROFIT MATERIALS*

The research program began by evaluating the effectiveness of the spray-on polyurea material proof tested by the AFRL on mobile temporary metal buildings. As the material systems were evaluated, additional materials in the elastomeric genre, such as polyureas, polyurethanes, thermosets, and thermoplastics, were explored. Additional application techniques, which included trowel-on materials and elastomeric films applied with pressure sensitive adhesives (PSA), were also investigated. Several material characteristics, such as the yield strength and elongation at rupture, were compared to determine the best candidates for potential solutions. Application techniques, equipment requirements, availability, quality control, costs, and transportability were some of the items considered while selecting materials to evaluate. The goal was to select a material or system to mitigate the debris hazard and increase the quality control and assurance while minimizing the equipment and training requirements (Figure 4.1 a to e).

The materials selected for evaluation were items currently available as a commercial off-the-shelf (COTS) product, but the material was used in a different manner or application than the originally intended or designed use. For example, the spray-on polyurea used in the research project is commercially available as a truck bed liner, but was used as a retrofit material to mitigate debris hazards associated with blast loads on unreinforced CMU walls. Some of the materials obtained for assessment were evaluated

* Part of this chapter reprinted with permission from *Reactor®E-30i and E-XP2i: Integrated Proportioning System*, by Graco Inc., 2012, Graco Inc., Minneapolis, MN. Copyright 2012 by Graco Inc. Accessed September 1, 2013. http://www.graco.com/content/dam/graco/aftd/literature/brochures /348500/348500EN-B.pdf.

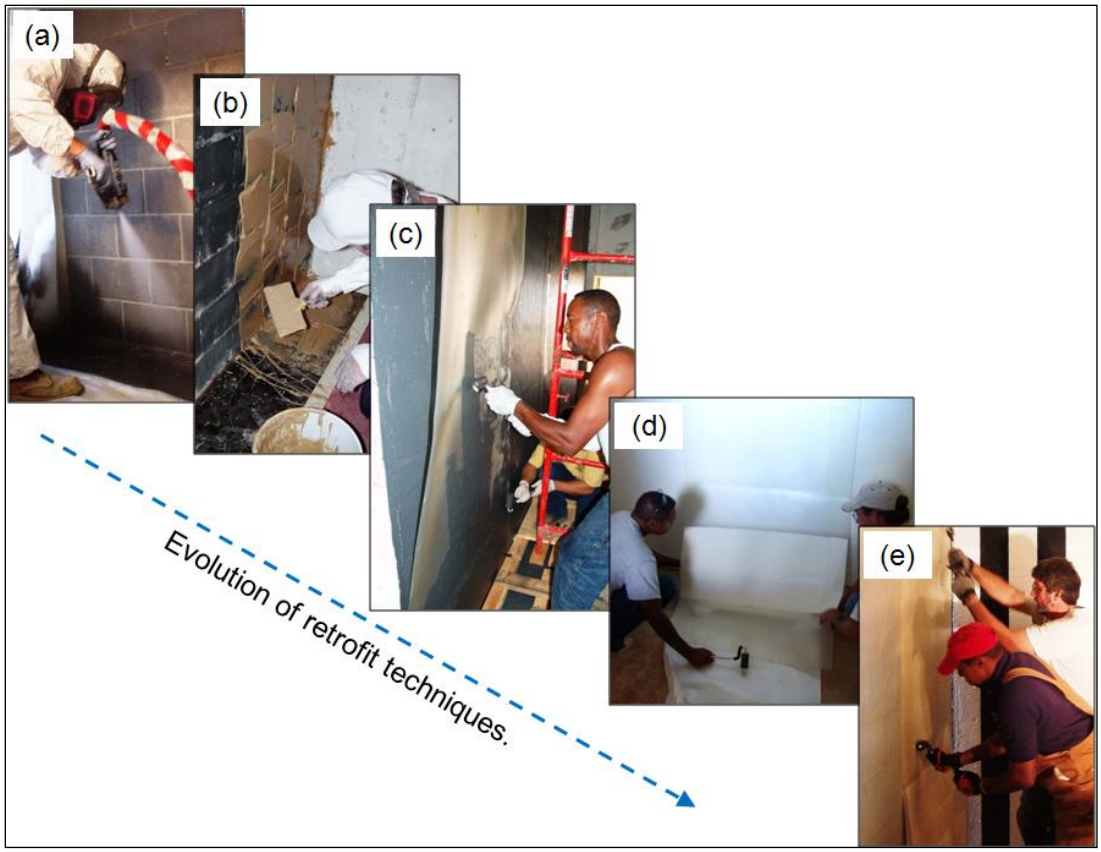

Figure 4.1. Materials and application techniques. (a) Spray-on polyureas. (b) Trowel-on thermoset. (c) Trowel-on thermoset with unreinforced or reinforced elastomeric film. (d) PSA with elastomeric film. (e) PSA with reinforced elastomeric film.

as a singular material, while others were combined with additional COTS materials to form a new composite system for evaluation. To continue with the example discussed earlier, the spray-on polyurea used as a truck bed liner was used in combination with an Aramid fiber-reinforced fabric to create a composite material for debris mitigation. A composite material combines two or more distinct components with significantly different properties to create a new material composed of the best properties of each constituent. Each component had advantages and disadvantages, but the composite

material was developed to promote the best properties of each component. The composite materials used in this research consisted of a matrix and reinforcement.

4.1 Replica Scaling

Subscale models have been used in numerous experiments to determine the response of full-scale prototypes in many applications and fields of study. The book by Baker, Westine, and Dodge, *Similarity Methods in Engineering Dynamics, Theory and Practice of Scale Models*, published in 1973, has been used as a standard in the field of subscale model experimentation. Subscale models of the unretrofitted and retrofitted CMU walls were used in 76% of the static and dynamic experiments conducted in the research. Replica scaling uses a subscale model of exactly the same geometry and materials as a full-scale prototype to replicate the response of the prototype, which is ultimately the system of interest. The response of the subscale models to the static and dynamic loads allowed researchers to efficiently and economically evaluate a larger number of retrofit material systems. The subscale models are capable of predicting the full-scale prototype response because homologous and not identical states of time, location, and force are related. Materials are homologous if they have corresponding but not necessarily equal values of variables.

For geometrically similar scaling to be functional, (1) the subscale models and full-scale prototypes made from an elastic material must have the same values of Young's modulus of Elasticity (E), mass density (ρ), Poison's ratio (ν), yield, ultimate, and compressive stress and (2) the external loads must act at homologous points.

Engineering strain is a good characteristic to relate subscale models and full-scale prototypes, since it is the same for both, independent of the material properties, and is

valid for any type of structural material. The geometric scale factor for a model is:

$$\beta = \frac{\text{sub-scale model}}{\text{full-scale prototype}}$$

where $\beta \leq 1$. Building models consisting of materials that are difficult to obtain or scale can be problematic. For example, blasting sand was used in the mortar mix until it was deemed a hazardous material and removed from the commercial market. Strain rates and gravity forces cannot be scaled according to the elementary principles of geometrically similar scaling (Jones, N. 1989). The model structure may accurately replicate the initial blast response of the prototype, but the posttest response may be significantly different, since the gravitational force, g, for the subscale model according to replica scaling should be g / β. Gravitational forces can affect the distribution of fragments or the collapse of a structural component. The strain rate, 1/s, which should be scaled to $1 / \beta s$, may increase the strength of the model over that of the prototype when subjected to highly impulsive loads. Table 4.1 lists the scale factors for parameters used in the research program.

4.2 CMU Walls

The subscale and full-scale CMU walls used in the research represented simple, hollow, unreinforced, non-participating infill walls structurally isolated from the lateral

force-resisting system commonly used in concrete- and steel-framed structures. In a non-participating infill wall, in-plane loads were not transferred to the wall from the structural frame. To prevent the unintentional transfer of in-plane loads from the

Table 4.1. Scale factors.

Parameter	Full-Scale Prototype	Subscale Model	Parameter	Full-Scale Prototype	Subscale Model
Length	L	$L\beta$	Impulse	I	$I\beta$
Mass	m	$m\beta^3$	Displacement	δ	$\delta\beta$
Area	A	$A\beta^2$	Volume	V	$V\beta^3$
Time	t	$t\beta$	Velocity	v	v
Pressure	P	P	Acceleration	a	a/β
Strain	ε	ε	Stress	σ	σ

bounding frame to the non-participating infill wall, in-plane isolation joints were created by leaving gaps between the top and sides of the masonry. The gaps were required to remain free of any materials (mortar, debris, and other rigid materials) that could transfer load between the infill and bounding frame. However, a resilient material could be placed in the gap, provided that the compressibility of the material was considered when designing the required joint size. In-plane isolation joints were required to be a minimum of 3/8-in.- (9.5-mm-) wide in the plane of the infill. Sections B.1.3 and B.1.4 of the Building Code Requirements and Specifications for Masonry Structures and Commentary (2011) stated that infill walls shall be proportioned so that the nominal

strength multiplied by the strength reduction factor, ϕ is 0.6, equals or exceeds the required strength. The strength reduction factor, ϕ, was applied to the shear, flexure, and axial strength of a masonry infill panel. Mechanical connections were only required between the infill wall and bounding frame, along the perimeter of the infill wall, parallel to the direction of the design span for out-of-plane loads. The mechanical connection had to be attached to the bounding frame and could not transfer in-plane forces. Section B.2.2.4 of the Building Code specified that the maximum spacing allowed along the supported perimeter of the infill was 4 ft (1.22 m).

4.2.1 Concrete Masonry Units

Three different sizes of two-cell U.S. manufactured CMU blocks were used to construct the walls in the static and dynamic experiments (Figures 4.2a and b). The exact dimensions of the blocks used in the experimental program are provided in Table 4.2. The 1/4-scale blocks, nominally 2 in. by 2 in. by 4 in. with an average weight of 0.57 lb, were used as the research program began to construct the subscale static and dynamic CMU walls. The 1/4-scale CMU blocks were replaced with approximately third-scale blocks (0.29 scale factor), nominally 2-1/4 in. by 2-1/4 in. by 4-1/2 in. with an average weight of 1.18 lb, because the manufacturer discontinued the fabrication of 1/4-scale blocks. Standard 8-in. by 8-in. by 16-in. CMU blocks with an average weight of 28 lb were used to construct all of the walls in the full-scale experiments. The three different block sizes used in the research program are identified and compared in Figures 4.2a, b, and c.

The compressive strength of masonry units, $f_m^{'}$, with Type S mortar is available in the 2003 International Building Code in Table 2105.2.2.1.2. The modulus of elasticity, E_m, was based on the compressive strength of masonry from Section 1.8.2.2.1 of the Building Code Requirements and Specification for Masonry Structures (2011)

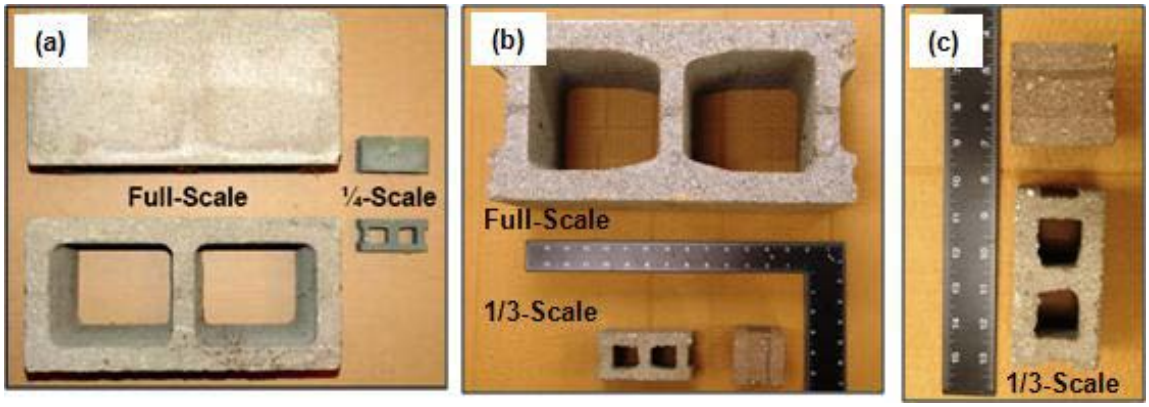

Figure 4.2. CMU blocks for test program. (a) Full-scale and 1/4-scale CMU blocks. (b) Full-scale and 1/3-scale CMU blocks. (c) Close-up of 1/3-scale blocks.

Table 4.2. CMU block dimensions.

Blocks	End Shell, in. (mm)	Face Shell, in. (mm)	Web, in. (mm)	Width, in. (mm)	Height, in. (mm)	Length, in. (mm)	Weight, lb (kg)	Scale Factor
Full-Scale	1.25 (31.75)	1.25 (31.75)	1 (25.4)	7.625 (194)	7.625 (194)	15.62 (397)	28 (12.7)	1
Subscale 1	0.3125 (7.937)	0.375 (9.525)	0.375 (9.525)	1.99 (51)	1.91 (49)	3.86 (98)	0.57 (0.259)	0.25
Subscale 2	0.5 (12.7)	0.5 (12.7)	0.5 (12.7)	2.23 (57)	2.29 (58)	4.54 (115)	1.18 (0.535)	0.29

$$E_m = 900 f'_m \tag{4.1}$$

and the modulus of rigidity for CMU from Section 1.8.2.2.2 was

$$E_v = 0.4 E_m \tag{4.2}$$

4.2.2 Mortar

The Type S mortar, a mixture of portland cement, lime, sand, and water, was used to level, seat, and bond the masonry units together. The minimum average compressive strength of Type S mortar at 28 days was 1,800 psi (12.4 MPa) (Masonry Standards Joint Committee, American Concrete Institute, Structural Engineering Institute, and Masonry Society 2011; Drysdale, Hamid, and Baker 1999; Mamlouk and Zaniewski 1999). Since mortar was used as an adhesive to bond the units together, a complete, strong, and durable bond with the masonry unit was important for quality control. However, the strength of the masonry construction was controlled by the adhesion or bond between the blocks and mortar. The most important property of mortar was not the compressive strength, but the tensile bond strength, which was the force required to separate the units. The tensile bond strength, which ranges from 20 to 80 psi (0.14 to 0.55 MPa), affects the shear and flexural strength of masonry. The workability, tensile strength, compressive strength, resistance to freeze and thaw, and water retention could affect the mortar's performance. As a rule, "thin mortar layers generally produced stronger walls than thick mortar layers" (Mamlouk and Zaniewski 1999).

4.2.3 CMU Wall Construction

All of the CMU walls evaluated in the static and dynamic experiments had the same support conditions required to model a non-participating infill wall. The top and bottom supports were simply supported, and the right and left sides of the walls were free. The free edges on both sides of the wall were created by leaving a 1/4- to 1-in. gap between the sides of the CMU wall and the sides of the respective steel frame or reinforced concrete reaction structure, depending on the construction scale. The gaps prevented the development of arching forces and also prevented the walls from dragging against the frame during the response to loading. At the top support, a gap and a slip dowel connection created a simply supported connection by providing lateral support without adding additional restraint. In the subscale walls, the dowels were fabricated using D1 wire (equivalent to a #4 bar that was used in the full-scale walls) and were located every 6 in. (152 mm) on center (every third cell). Only the cells containing the dowels on the top course were fully grouted. However, before the grout was added to the cells, the dowels were wrapped in aluminum foil to prevent bonding between the dowel and grout, creating the slip dowel connection. The simply supported connection at the bottom of the wall was created by placing the first course of blocks in a mortar bed. The blocks were laid in a running bond in a single wythe.

The subscale CMU walls were constructed in stand-alone steel or concrete frames. All of the subscale static experiments in the HTC were conducted in steel frames (Figure 4.3a), while steel and reinforced concrete frames were used in the subscale dynamic experiments (Figure 4.3b). To expedite the experimental program, multiple

static and dynamic frames were fabricated to house the subscale CMU walls, which allowed the walls to be constructed and retrofitted without extended delays. The frames were transported and bolted into the appropriate testing device for static or dynamic evaluation. The CMU wall was constructed flush with one edge of the 12-in. (305-mm)

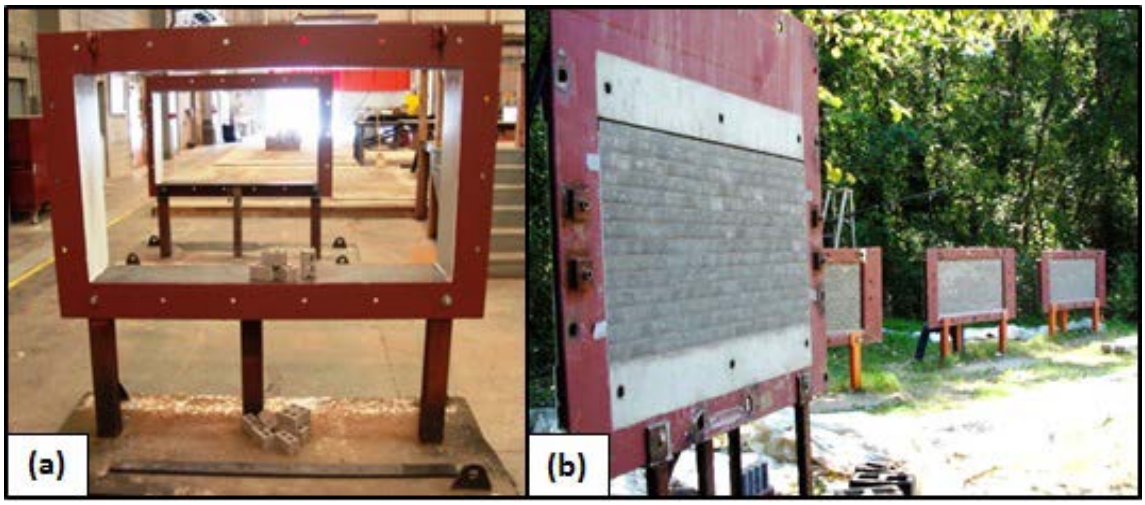

Figure 4.3. Subscale test frames. (a) Steel frames used in the static experiments. (b) Reinforced concrete and steel frames used in HE dynamic experiments.

flange (Figures 4.4a and b), leaving the remaining area on the flange at the top and bottom supports for either an adhesive bond, mechanical bond, or both.

The full-scale CMU walls evaluated at the remote field sites were built by local contractors using common construction procedures and standard 8-in. by 8-in. by 16-in. blocks. To ensure a one-way response, a 1-in. (25.4-mm) gap was left between the sides of the CMU wall and the sides of the concrete reaction structure. The first course of blocks was placed in a 1-in.- (25.4-mm-) thick mortar joint. At the top support a 1-in.

(25.4-mm) gap and slip dowels (PTA Series #420 Anchors) provided lateral support without adding additional restraint. The slip dowels, equivalent to a #4 bar, were used in every third cell (every 16 in. or 406 mm). The PTA Series Anchors (#420) permitted vertical deflection without transferring compressive loads to the CMU wall. A concrete hammer drill, anchor bolts, hammer, and wrench were required to install the slip dowels (Figures 4.5a, b, and c). Horizontal ladder mesh reinforcement (#220) was placed in every other course. Only the CMU cells that contained slip dowels were fully grouted (Figure 4.6a and b).

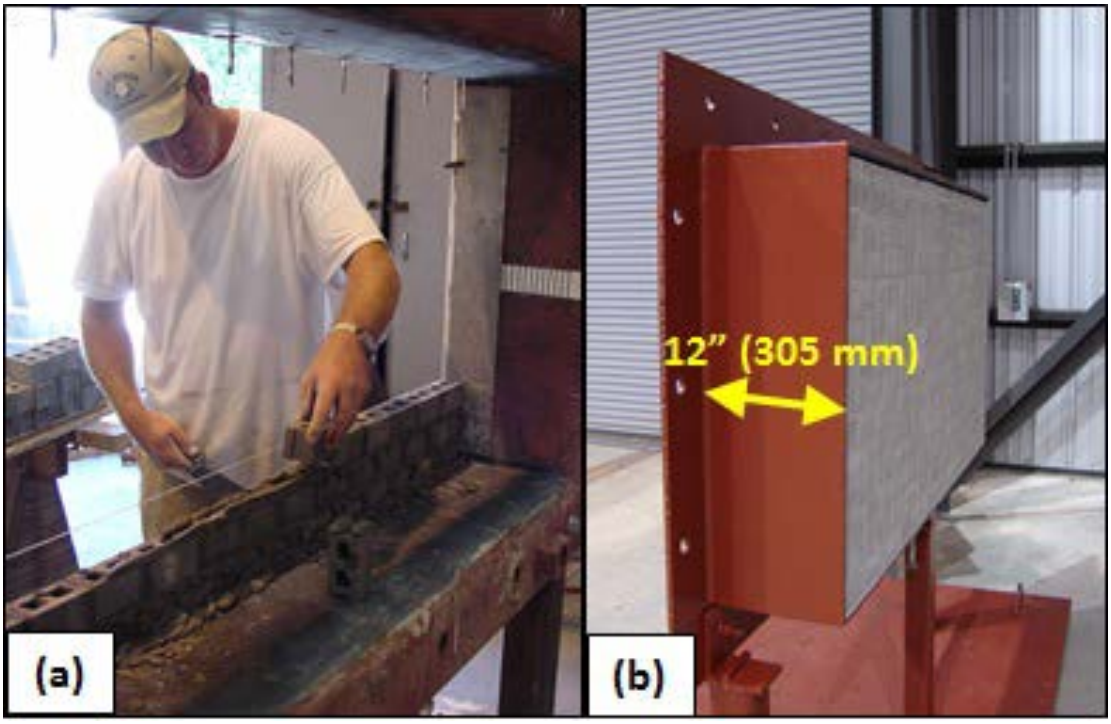

Figure 4.4. **Subscale construction**. **(a) Mason placing CMU blocks. (b) CMU wall flush with edge of frame.**

Figure 4.5. Full-scale construction. (a) Concrete hammer drill. (b) Installing anchor bolts to mount slip dowels. (c) CMU stacked in running bond.

Four CMU wall sizes were used in the full-scale research program, depending upon the availability of the reinforced concrete reaction structures at the remote field site. The reaction structures used to house the CMU walls were constructed based on guidance received from multiple sponsors, who provided funding for the research program over

Figure 4.6. Wall construction. (a) Mason placing top course of blocks with slip dowels. (b) CMU cells with slip dowels fully grouted.

the last ten years. The first set of walls, Bay 1 and Bay 2, nominally 224 in. by 130 in., was 16 courses tall and 14 blocks wide (Figure 4.7a). For a select number of experiments, an extension was placed on the top of Bay 1 or 2 to raise the height to

192 in. (Figure 4.7b). The second set of walls, Bay 3 and Bay 4, nominally 174 in. by 111 in., was 14 courses tall and 11 blocks wide (Figure 4.7c). Bays 3 and 4 were separated, as shown in Figure 4.7d, for select experiments. A fourth reaction structure, 120 in. by 120 in., (Figure 4.7e) was also added to the test site. The substrate at the bottom and top supports on Bays 1, 2, and 5 was all concrete (Figure 4.8a). The bottom supports of Bays 3 and 4 were primarily concrete, but both bays had steel in-bed plates in two small areas of the retrofit anchor zone (Figure 4.8b). The type of substrate in the test frame or reaction structure defined the primers used during the installation of the retrofit materials.

The CMU wall sizes and height-to-thickness ratios for all of the subscale static and dynamic experiments are provided in Table 4.3. The slenderness, or height-to-thickness ratio, of the walls used in the full-scale experiments was 14.5 to 23.2, while the ratio for the subscale experiments was 15.3 to 16.1. One of the key factors when designing the subscale experiments was to maintain a height-to-thickness ratio greater than six to ensure a flexural response in the walls. Ideally the subscale and full-scale walls would all have the same height-to-thickness ratio, but this could not be maintained due to the size limitations of the test devices and reaction structures. If the height to thickness ratios between the different size walls could be maintained, then one can assume a similar response to loading between the subscale models and the full-scale prototypes.

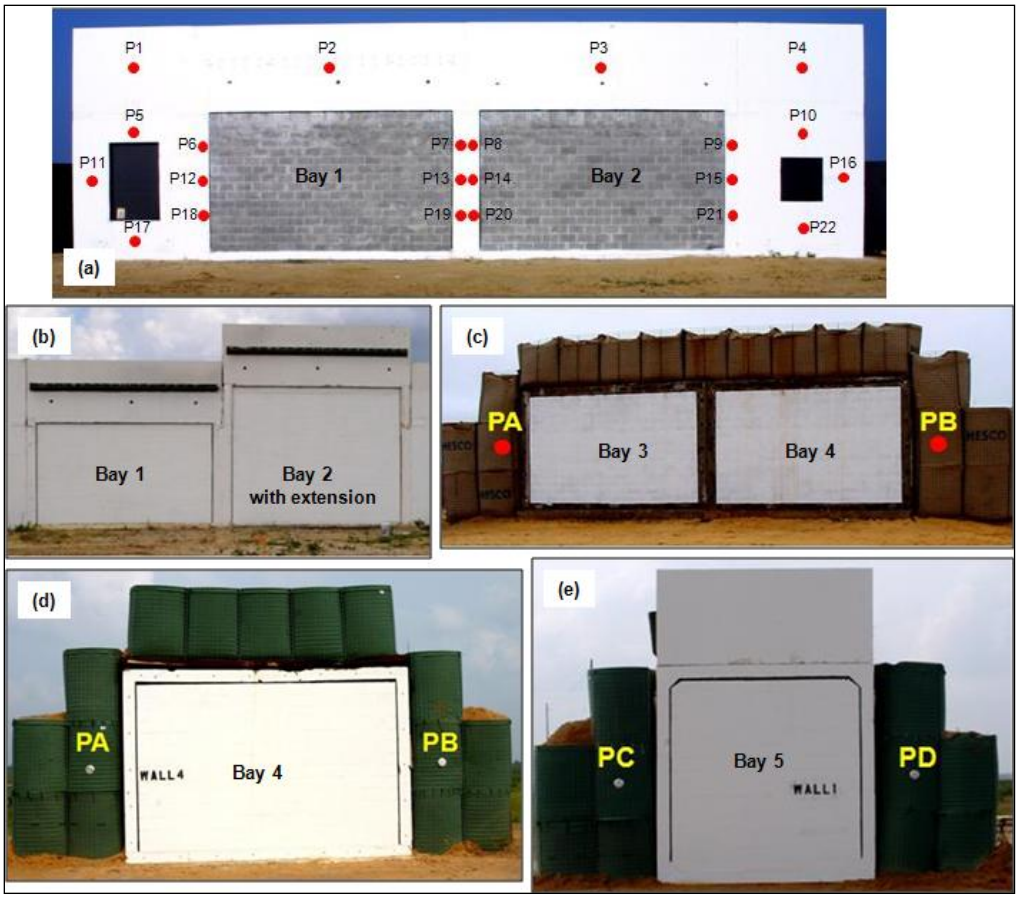

Figure 4.7. Full-scale reaction structures. (a) Bay 1 and Bay 2. (b) Bay 2 with extension. (c) Bay 3 and Bay 4. (d) Bay 3 and 4 were separated for some experiments. (e) Bay 5.

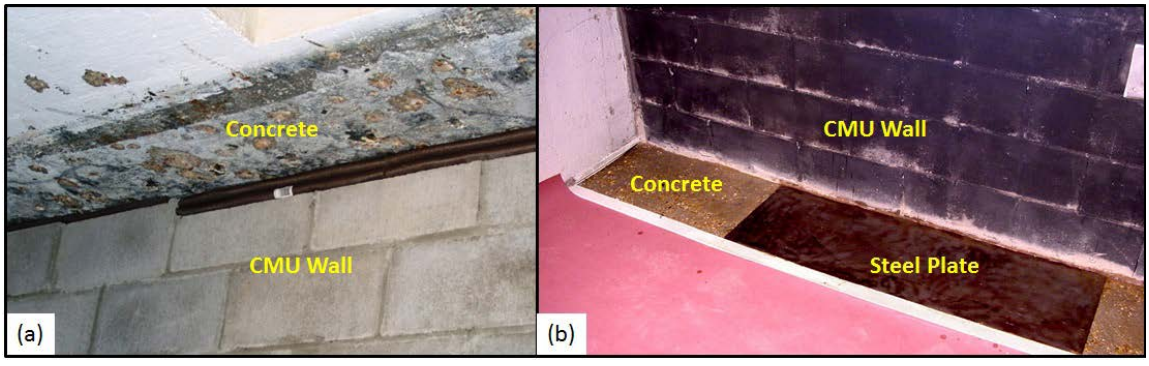

Figure 4.8. Substrate at supports. (a) All concrete substrate at top support. (b) Bays 3 and 4 have a mixed substrate of steel and concrete on the bottom support.

Table 4.3. CMU wall physical properties.

Test Frame Reaction Structure	Block	Wall					
	t in. (mm)	h in. (cm)	h/t	w in. (cm)	No. Courses	Blocks/ Course	Weight lb (kg)
Static Experiments							
Subscale 1	1.99 (51)	31 (78.7)	15.6	61.25 (156)	14	15.5	210 (95)
Subscale 2	2.25 (57.1)	35.55 (90.3)	15.8	61.25 (156)	13	13	340 (154)
Dynamic Experiments							
Subscale 1 (HE)	1.99 (51)	32 (81.3)	16.1	64 (162)	14	15.5	210 (95)
Subscale 2 (BLS)	2.25 (57.1)	34.5 (87.6)	15.3	49.75 (126)	13	13	340 (154)
Bays 1 & 2 (HE)	7.625 (194)	130 (330)	17	224 (569)	16	14	10,100 (4,580)
Bays 1 & 2 Extension (HE)	7.625 (194)	177 (450)	23.2	224 (569)	22	14	13,760 (6,240)
Bays 3 & 4 (HE)	7.625 (194)	111 (282)	14.5	174 (442)	14	11	6,700 (3,040)
Bay 5 (HE)	7.625 (194)	120 (305)	15.7	120 (305)	15	7.5	5,000 (2,268)

4.3 Retrofit Material Systems and Application Techniques

The retrofit systems used in the research program were divided into two basic groups, i.e., unreinforced elastomeric materials and fiber-reinforced elastomeric materials. Most of the individual materials evaluated as retrofit materials were also used in the fiber-reinforced composite materials. For example, the spray-on polyurea was evaluated as an individual retrofit material and at a later date as a composite material containing Aramid fiber reinforcement. Similarly, the trowel-on thermoset was evaluated as an individual material before it was used in conjunction with unreinforced and

reinforced polyurethane and thermoplastic films. The polyurethane and thermoplastic films were also evaluated as individual materials before the fiber reinforcement was added.

The complete retrofit systems consisted of one or more of the following components, i.e., a matrix material, fiber reinforcing fabric, primer, adhesive, and an anchor system at the supports. A brief description of the eight fiber reinforcing fabrics (Figures 4.9 through 4.11), five primers, and seven anchorage systems used in the static and dynamic experiments is provided in Sections 4.3.1, 4.3.2, and 4.3.3, respectively. The procedure used to apply the materials was dictated by the matrix material and adhesive. A description of these components is provided in the appropriate section.

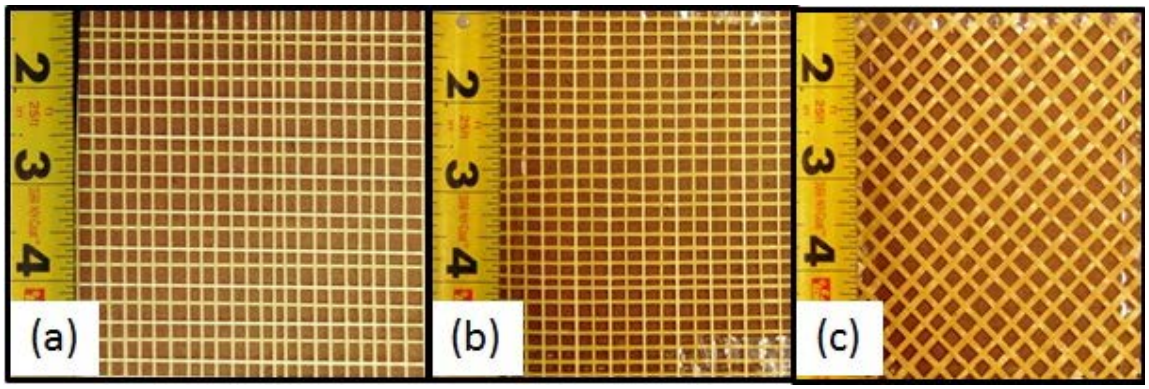

Figure 4.9. Fiber reinforcement. (a) Fabric A. (b) Fabric B. (c) Fabric C.

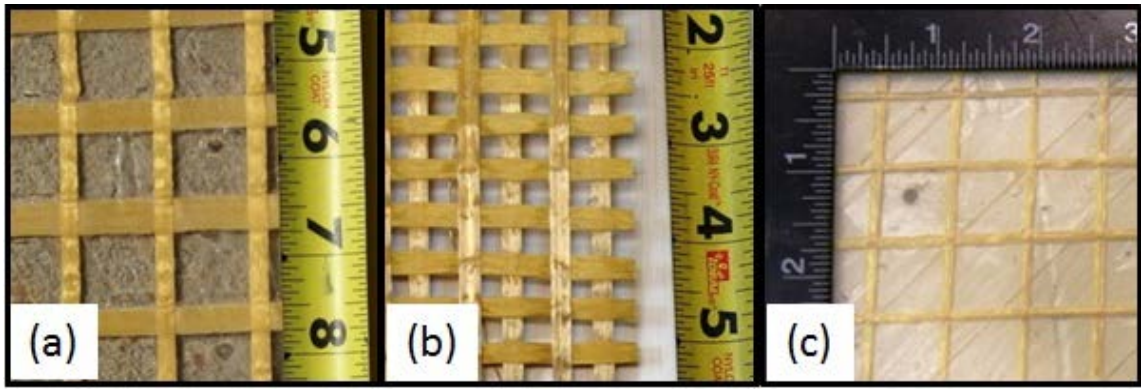

Figure 4.10. Fiber reinforcement. (a) Fabric D. (b) Fabric E. (c) Fabric F.

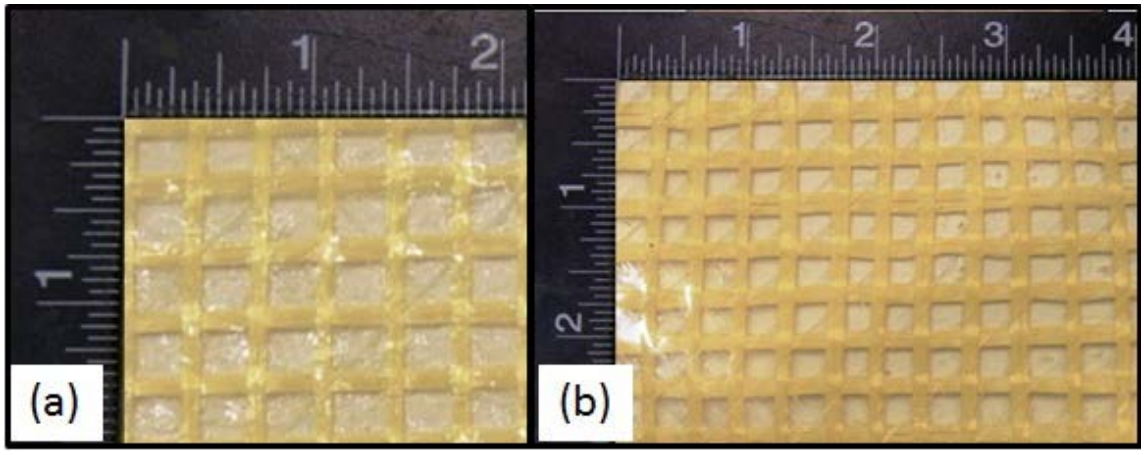

Figure 4.11. Fiber reinforcement. (a) Fabric G. (b) Fabric H.

4.3.1 Aramid Fiber Reinforcement

The organic fiber, Aramid (Kevlar), was selected for use as the reinforcing agent for the composite material. Aramid fibers were developed in the 1960s and were provided commercially by DuPont under the trade name Kevlar in the 1970s. The established use and history of the Aramid fibers as primarily a ballistic resistant material aided in the selection of the open weave Aramid fabrics as the reinforcement for the retrofit systems.

The fabrics constructed of Aramid fiber bundles generally had similar strengths in both the machine and cross-machine directions. The open weave fabric, when used, was encapsulated by the matrix materials.

The fiber strength for each fabric was documented by determining the strength along the direction of the fiber. The fiber orientation was taken into account at a later time. First, a scale was placed perpendicular to the fiber bundles on a sample of the fabric, and then the number of bundles per lineal inch on the scale was counted. For example, if a 1,140 denier Aramid yarn (one yarn per bundle) with a tenacity or tensile strength of 0.0441 lb (20 g) per denier was measured every 0.7 in. (17.8 mm), then the strength of the fabric was documented at 71.7 lb per lineal in. See Table 4.4 for information on each Aramid fabric reinforcement used in the research program.

Table 4.4. Aramid fabric reinforcement properties.

Fabric Label	Fiber Strength, lb/lin in.	Fiber Bundle Thickness	Fiber Area/ sq in.	Fiber Area Ratio Fiber/Void
A	100	0.005	0.394	0.65
B	200	0.006	0.4575	0.84
C	400	0.007	0.5538	1.24
D	800	0.017	0.4384	0.78
E	800	0.017	0.794	3.85
F	200	0.013	0.392	0.61
G	200	0.01	0.4567	1.36
H	600	0.01	0.6356	1.74

4.3.2 Primer

Five different primers were used with selected elastomeric systems to promote the adhesion between the substrate at the top and bottom supports, the adhesive, and the elastomeric films. One of the key requirements considered during the selection of a primer for the evolving retrofit systems was the emission of volatile organic compounds

Two primers were selected for evaluation on metal substrates, i.e., Primer 1 and Primer 2. Primer 1 was advertised as a low viscosity material used to adhere polyurethane and spray elastomers to all types of metals. Primer 1 was a single component applied to the metal substrate using a small paint brush to a thickness of 0.01 to 0.02 in. (0.025 to 0.05 mm). The material has an indefinite pot life and has a long elastomer application window (1 to 16 hr). Primer 2 was also a single component material applied by a paint brush to steel surfaces. Primer 2 could be thinned with methyl ethyl ketone (MEK) to make application easier, but once MEK was added, the material became flammable.

Primer 3 was a water-based epoxy primer applicable for use on concrete, metal, wood, and other rigid substrates. Primer 3 was a two component material blended with a drill mixer at a 1:1 ratio by volume and was applied by paint brush to the concrete substrate. Primer 3 has a pot life of 4 hr and a shelf life of one year.

Primer 4 was a two-component adhesive primer applicable for use on urethane and rubber materials. The two components were mixed 1:1 ratio by volume. Primer 4 was applied to the substrate with a paint brush and has a pot life of 4 hr at 75°F (24°C). Before the elastomeric material was added, the primer was allowed to dry to a tacky film

(20 to 40 min). If the elastomeric material was not applied within 4 hr, then the surface was re-primed. Primer 4 has a shelf life of 3 months and had to be stored in cool (<80°F), dry areas protected from direct sunlight. If the primer was opened and would not be used again for 24 hr, then the container had to be purged with dry nitrogen. If the primer was not applied in open air, then a respirator with chemical cartridges had to be worn.

Primer 5, an aqueous acrylic polymer used as a pressure-sensitive adhesive (PSA) in specialty tape applications, was used as a primer for the reinforced TPU films. Primer 5 aggressively adhered to a variety of surfaces and has high cohesive strength. This was the only primer applied to the complete CMU wall surface and the reaction structure/frame using a regular paint roller. The material was allowed to cure for 24 hr before the elastomeric film was applied. The primer has a shelf life of one year and should be protected from freezing.

4.3.3 Anchorage of Retrofit Systems

The retrofit materials were secured or anchored to the top and bottom supports using a simple adhesive bond or a mechanical and adhesive connection. Initially, a simple adhesive bond was developed through the application of the respective retrofit materials (Figure 4.12). However, as the research program progressed, a mechanical anchorage system was added in addition to the adhesive bond to prevent the retrofit materials from peeling away from the top and bottom supports and to account for poor substrate conditions in the reaction structures. Each connection system was labeled with a system

number to identify the adhesive or mechanical anchorage used in the experimental program.

In the subscale static and dynamic experiments, four anchor systems were evaluated. System 1 evaluated the adhesive strength of the retrofit materials as the only bond between the retrofit system and the steel or reinforced concrete reaction frame (Figure 4.12a). In Systems 2 to 4, an anchor plate secured by bolts was used in addition to the adhesive strength or bond created by the retrofit materials. The anchor plates were bolted to the supports, sandwiching the retrofit material between the anchor plate and the surface of the substrate. In System 2, a 0.25-in.-thick steel plate with rounded edges was secured to the supports using bolts spaced 6 in. on center (Figure 4.12b). The plate in System 2 was sprayed with the polyurea used to retrofit the CMU walls to prevent the

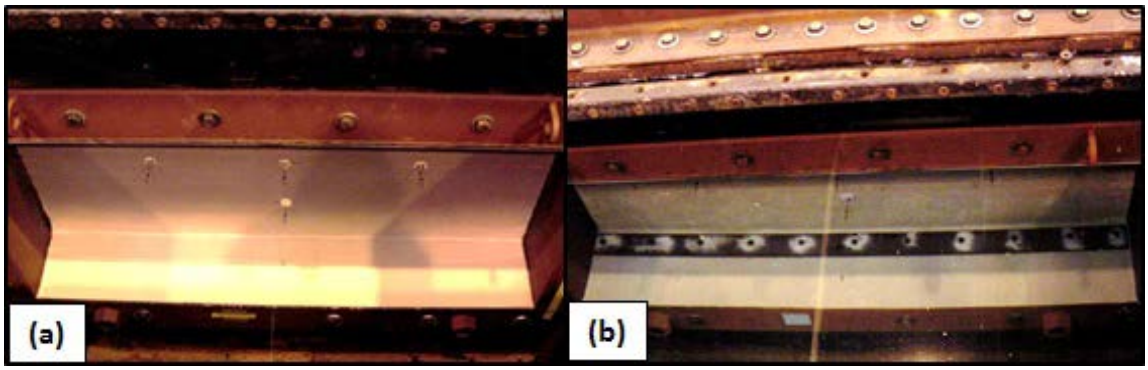

Figure 4.12. Anchorage. (a) System 1 – Relying solely on the adhesive strength of the retrofit material to the steel frame. (b) System 2 – Steel plates bolted to the top and bottom supports to anchor the retrofit material in static experiments.

sharp edges of the plate from shearing the retrofit materials. In System 3, a thin-wall steel stud member (3-in.-wide) was bolted to the bottom and top flanges to anchor the retrofit materials in the BLS experiments (Figure 4.13a). In System 4 (Figure 4.13b), a piece of Superstrut (B-1400-HS) pre-galvanized metal framing channel 1-5/8 in. wide by 13/16 in. tall by 1/16 in. thick with a nominal weight of 1 lb/ft was bolted 1.75-in. from the CMU wall surface to anchor the retrofit materials to the supports.

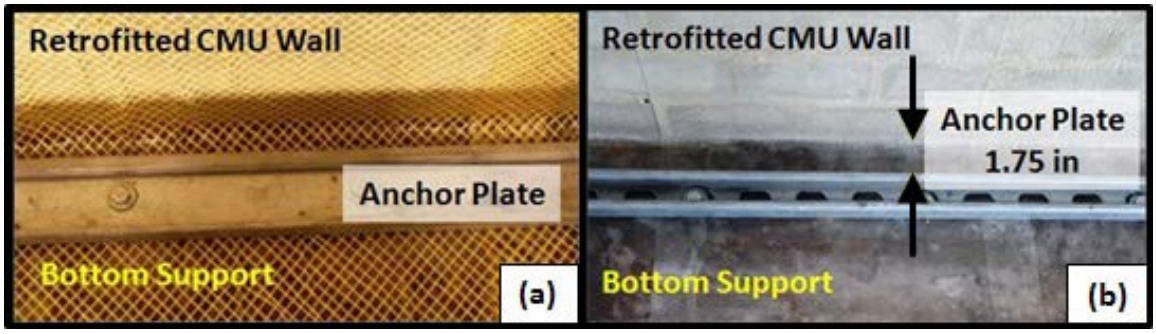

Figure 4.13. Anchorage. (a) System 3 – 3-in.-wide thin wall steel stud used as anchor plate. (b) System 4 – metal framing channel used as anchor plate.

In the full-scale HE experiments, the adhesive bond strength between the substrate and the retrofit materials was evaluated first. The adhesive strength was sufficient in a small number of experiments, but the poor physical condition of the substrate and inclement environmental conditions highlighted the need for an additional mechanical connection in the full-scale experiments. Four different mechanical anchorage systems evolved as the full-scale HE experiments continued. Mechanical anchorage System 5 was very robust and consisted of a steel angle with a structural tube welded along the short leg of the angle, Hilti sleeves, and anchor bolts (Figure 4.14a, b, and c). System 6

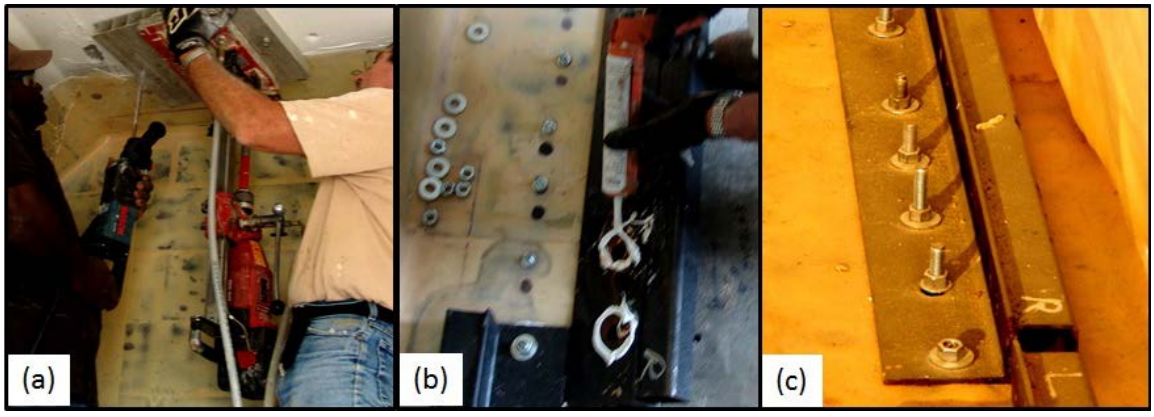

Figure 4.14. Anchor System 5. (a) Hammer and concrete core drill used to drill holes for anchor bolt sleeves. (b) Adhesive applied to bottom of angle. (c) Finished System 5 installed on the bottom support.

used the same fasteners as System 5, but the steel angle and structural tube were replaced by a thin-walled steel stud member (Figure 4.15a). Systems 7 and 8 used thesame thin-walled steel stud member used in System 6, but the robust anchor sleeves and bolts were replaced with smaller Red Head concrete anchors (Figure 4.15b) and a ramset actuator and fastener system, respectively (Figure 4.16a, b, and c). To prevent

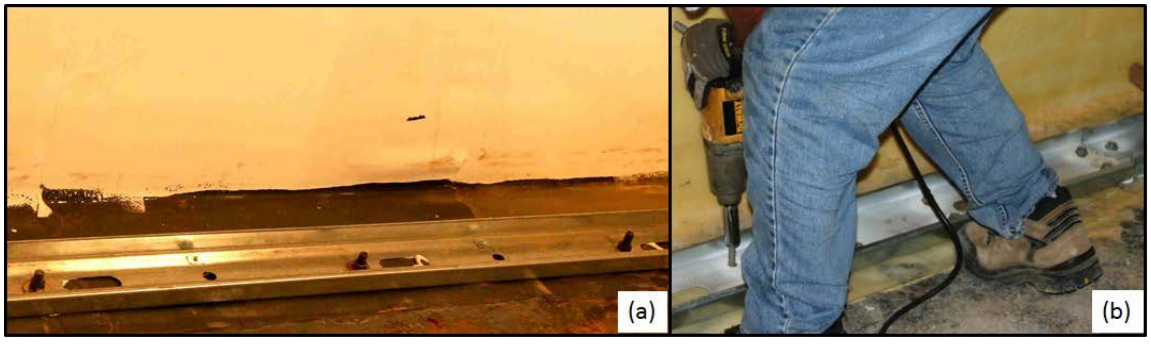

Figure 4.15. Anchorage. (a) System 6 - A thin steel channel secured using anchor bolts and sleeves. (b) System 7 - thin steel channel secured using pilot hole and anchor bolts.

the retrofit materials from sliding between the interface of the mechanical fasteners and the elastomeric materials (Figure 4.16b), extra adhesive was applied to the bottom of all the steel elements used as anchor plates.

Figure 4.16. Anchor System 8. (a) Steel stud member. (b) Adhesive. (c) Ramset and nails required for installation.

The weight of System 5 forced the fabrication of the anchor system to be limited to 8-ft lengths so that the anchor plates could be installed on both the top and bottom supports by a three-person team. The tools and components required to complete the installation of anchor System 5 included an angle, structural tube, welder, hammer drill, concrete core drill, anchor bolts, and hand tools. To prepare for the installation of System 5, a concrete hammer drill was used to drill the bolt holes before the retrofit was installed (Figure 4.14a). The sleeves were installed in the holes, then filled with pipe foam, and taped over to prevent sand, dirt, debris, and the retrofit materials from filling the holes. The installation crew replaced several drill bits during the process because rebar was encountered in the reinforced concrete supports of the reaction structure. A uniform bolt layout could not be achieved due to the rebar; some of the holes had to be

relocated, and some of the bolts could not be installed as deep as others. The need to pre-drill the holes increased installation time and could be hazardous. It is highly recommended that installers use SDS drill bits in the concrete hammer drill, which are specifically used to drill holes in reinforced concrete. If the installers encounter rebar during the process of drilling a hole, there is a risk of injury. If rebar is encountered, it is best to quickly release the drill, so that the force does not transfer to the installer. The torque created by the impact or hammer drill can violently twist an installers arm, causing muscle/ligament damage or bones to break in the hand, wrist, or arm.

The weight of the steel angle and structural tube used in System 5 was drastically reduced in Systems 6, 7, and 8. System 6 used the same anchor bolt system used in System 5, since the sleeves were already available, but replaced the steel angle and tube with a thin-walled steel member. This allowed researchers to determine if the thin-walled steel member was sufficient. To complete installation of System 6, the following items were required, i.e., thin steel channel, concrete core drill, anchor bolts, and hand tools. Systems 7 and 8 further optimized the installation process by replacing the large anchor bolt and sleeve installation with smaller fasteners. Although System 7 used slightly smaller bolts that did not require a drop in sleeve, the method still required a hammer drill to prepare the pilot holes in the concrete substrate and an impact drill to install the bolts. System 8 removed the need to drill holes by replacing the anchor bolts with a ramset actuator and fasteners designed for steel, concrete, or multiple-use substrate fasteners. Installers wore eye and ear protection during installation.

4.4 Spray-on Polyurea

The spray-on retrofit system chosen for evaluation was a two–component, spray-in-place, flexible, 100% solids (0% VOC) thermoplastic polyurethane/polyurea system (TPU). Two grades of the spray-on polyurea were used in the experimental program. Both spray-on products contained no Chloro Fluorocarbons (CFCs) and were environmentally safe. The Grade 1 material was the world's leading spray-on polyurea used on vehicles. Grade 2 was a fast-cure, textured surface, multi-purpose material designed for commercial and industrial applications. The highly flexible material exhibited excellent adhesion to most materials and was typically used as a protective coating for concrete, masonry, wood, metal, and fiberglass surfaces. The material had excellent adhesion to itself, allowing a seamless monolithic-elastomeric membrane to form on the structural element during application.

The first experiment using a spray-on polyurea was conducted in 2000 under the direction of Woodson/Bullock. Since then, ERDC has conducted 21 experiments using variations of the spray-on retrofit system. The spray-on retrofit systems consisted of two groups, i.e., the spray-on polyurea as a singular material and the spray-on polyurea as the matrix with Aramid fibers as the reinforcement. The application procedure varied slightly for each system. The first retrofit system evaluated various thicknesses of the spray-on polyurea. Subscale experiments labeled SW1-SW3 and DW1-DW3 used the spray-on polyurea techniques outlined in Sections 4.4.1.-4.4.5 to apply the retrofit system. The second system consisted of various thicknesses of the spray-on elastomer, a layer of fiber reinforcement, and a second coating of the spray-on elastomer to

encapsulate the reinforcement. The application procedures for the fiber-reinforced, spray-on polyurea system, outlined in Section 4.5, were used in subscale experiments Trial 1, SW4-SW9, and DW4-DW9 and full-scale experiments FS2-FS4.

The spray-on polyurea products were designed for processing through high-pressure, impingement-mix, polyurethane dispensing equipment (Table 4.5). The system

Table 4.5. Requirements for dispensing equipment.

Equipment Requirements	**Value**
Pressure (psi)	1,500 min
Hose Temperature	120 to 140°F
Pre-Heater Temperature	
Component ‘A’	120 to 140°F
Component ‘B’	120 to 140°F

recommended for material application should have satisfied the following requirements, i.e., the Polyol ‘B’ component must be thoroughly power mixed prior to use; the “A’ ISO and ‘B’ Polyol components must be pump fed to a high-pressure spray-in-place plural component dispensing equipment; the material dries in 10 sec and can be walked on or handled within 30 sec of application; and full, unrestricted use of the facility can be restored in 24 hr or less.

In 2001, the Glas-Craft MX II Dispensing System was selected for the research program as it accurately measured, mixed, and dispensed polyurethanes and polyureas without solvents (Figure 4.17). The system was mounted in a standard trailer for

transportation to and from all the test sites used in the program. The cost of the Glas-Craft MX system was $14,950, the Probler dispenser gun was $2,980, and a 35-ft hose was $800. An air compressor capable of maintaining 47 cfm at 100 psi that cost $6,350 was used with the dispensing system. The system was housed in a 12-ft utility trailer that cost $3,500, and the generator required to operate the equipment cost $17,600. The Grade 1 and 2 materials were purchased in drum sets for $2,857 and $3,284, respectively.

The Glas-Craft MX systems are no longer manufactured. The recommended dispensing system in 2012 was the Graco Reactor E-XP2i, which was a self-contained turnkey model consisting of the electric Reactor, a diesel generator, and integrated air compressor as one unit that sold for $75,000. The unit was mounted on a skid that could be loaded by forklift onto a trailer or truck as required (Figure 4.18). The Grade 2 spray-on polyurea used in this research was sold in 925-lb sets of the A and B components. On average, one 925-lb set covered 617 sq ft of surface area at a thickness of 250 mils. The cost of each set ranged from $3,136 to $3,275, depending on the number of sets purchased. As additional sets were purchased, the cost per set decreased. Additional information on the new Graco E-XP2i Integrated Reactor is found at http://www.graco.com/content/dam/graco/aftd/literature/brochures/348500/348500EN-B.pdf.

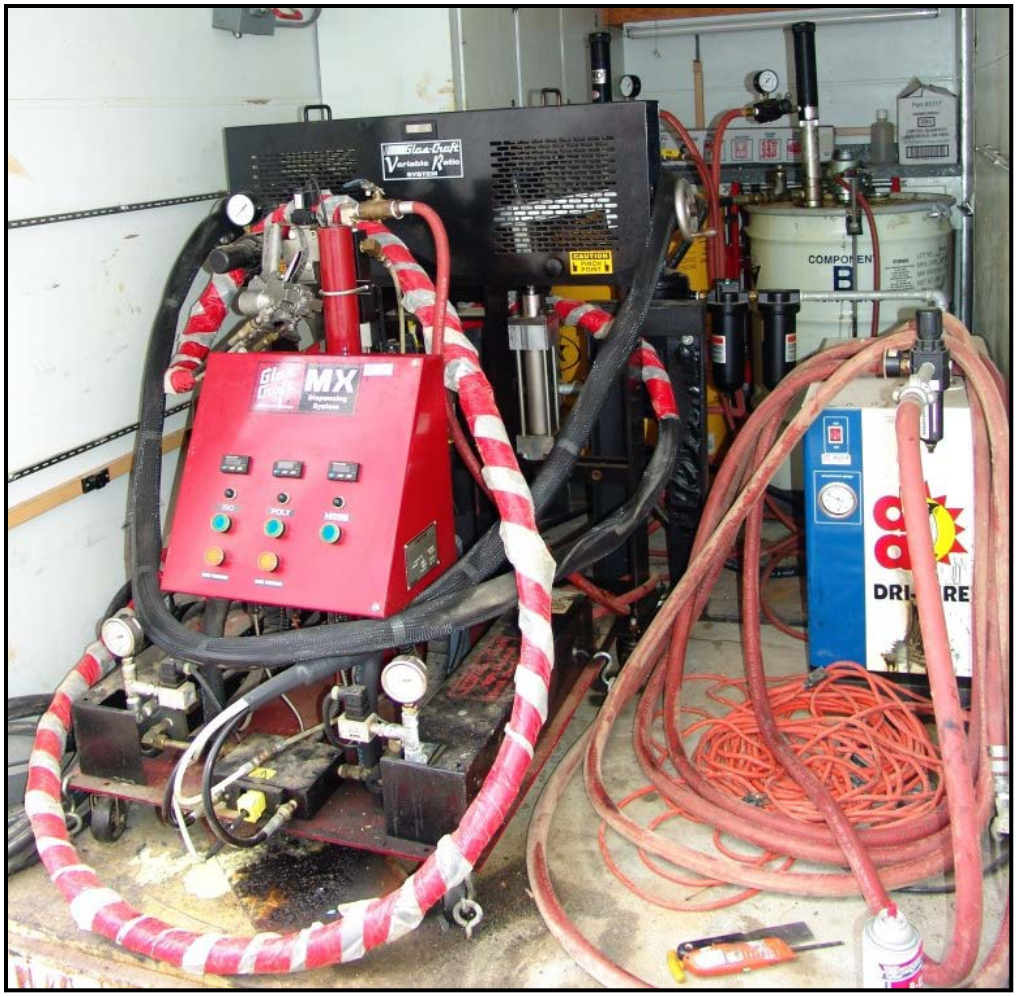

Figure 4.17. Dispensing system used to apply spray-on elastomer.

Figure 4.18. Graco Reactor E-XP2i Unit. (Graco Inc. 2012)

4.4.1 Step 1: Safety Equipment

The two-part spray-on polyurea material required the following safety products during application, i.e., gloves, Tyvek disposable protective coveralls with hood, and respirators with full face shields and fresh air supply pump (Figure 4.19). Safety glasses, gloves, and a respirator were required during application of the primer (Primer 1 or Primer 4) and during the operation of a wire wheel brush or grinder. If a sand blaster was

used during surface preparation, heavy duty protective clothing, leather gloves, and a full-face shield with fresh air supply were worn.

Figure 4.19. Safety equipment required for polyurea application.

4.4.2 Step 2: CMU Wall and Support Preparation

The ideal infill CMU wall for the spray-on retrofit system was a smooth unpainted surface with no tooled or protruding mortar joints. A wall with tooled joints was acceptable, but all protruding mortar must be removed using a masonry chisel, wire brush, masonry brick, or grinder (Figure 4.20a). Gaps in the mortar joints larger than a 1/4-in. were filled with “Concrete and Masonry Silicone Sealant” (Figure 4.20b). A standard cement mortar could have been used to fill the gaps, but would have delayed

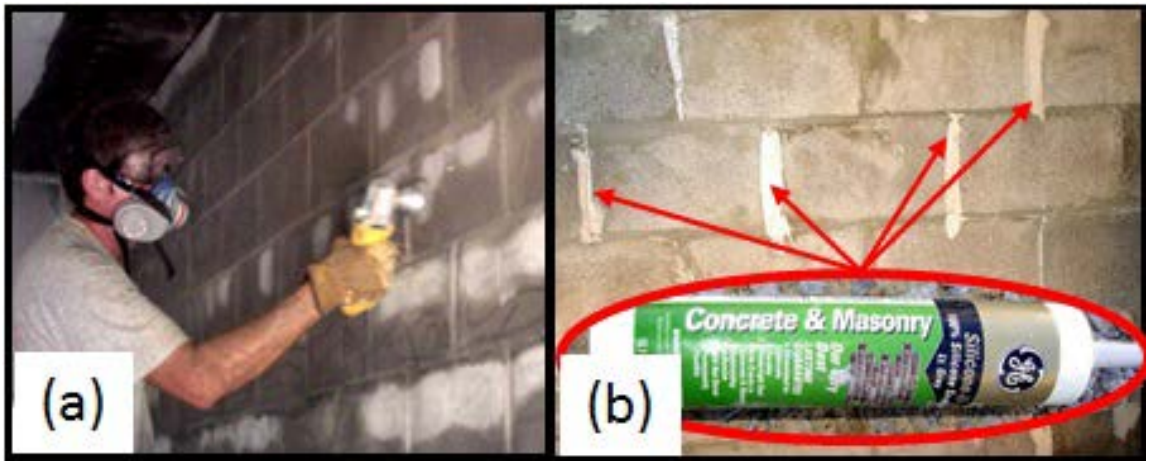

Figure 4.20. CMU wall preparation. (a) Wire brush used to remove excess mortar from face shells and joints. (b) Concrete and masonry silicone used to fill gaps in mortar joints.

the application procedure by 24 hr to allow the moisture in the mortar to cure. Moisture on the wall surface during application of the polyurea prevented or at least weakened the adhesive bond between the CMU wall and the polyurea. The wall surface/substrate was clean, completely cured, firm, and free of dust, oil, wax, or grease. Any foreign matter, such as dust, rust, mildew, or deteriorated coatings, was removed. If the surface to be sprayed had a slick finish from high-gloss paint or fiberglass, the surface was roughened by sanding or a primer was applied. The curing process could be affected if the surface temperature did not fall between 50 and 150°F. If temperatures were extremely low, a portable heater was used to heat the prepared surface or primer. The wall and support surface was required to be dry before the spray-on polyurea was applied, so a heater or portable fans might be used to dry the wall surface. However, heaters were not required while retrofitting the CMU walls in the research program.

Before application of the spray-on polyurea began, the gaps between the sides of the CMU wall and the reaction structure had to be filled with a deformable or temporary material (Figure 4.21). In the full-scale experiments, standard wall insulation foam board

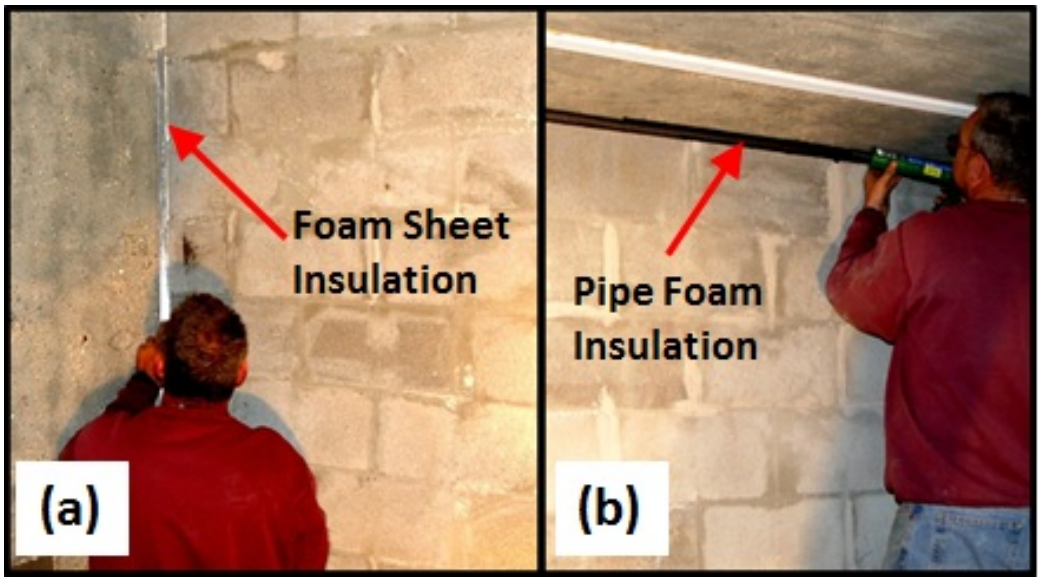

Figure 4.21. Materials used to fill gaps. (a) Wall insulation foam board placed in gap between reaction structure and wall. (b) Pipe foam insulation caulked in place to bridge gap between top support and wall.

was cut to fit and used to bridge the 1-in. gaps between the sides of the concrete reaction structure and the CMU wall (Figure 4.21a). On the subscale experiments, cardboard sheets and silicone were used to bridge the 1/4-in. gaps between the reaction frame and the surfaces of the CMU walls during application of the spray-on polyurea. The 1-in. gap between the ceiling of the concrete reaction structure and the top of the CMU wall was filled with pipe foam (Figure 4.21b). Caulk or silicone was used to secure both the wall insulation board and pipe foam. Wire tape/trim was applied around the perimeter of the

CMU wall to facilitate the easy removal of excess spray-on polyurea around the borders of the test area. The wire tape that was used was a product frequently used by automobile detailers and painters. Plastic sheeting was also secured around the perimeter of the work area to prevent the overspray from adhering to the reaction structure (Figure 4.22a and b).

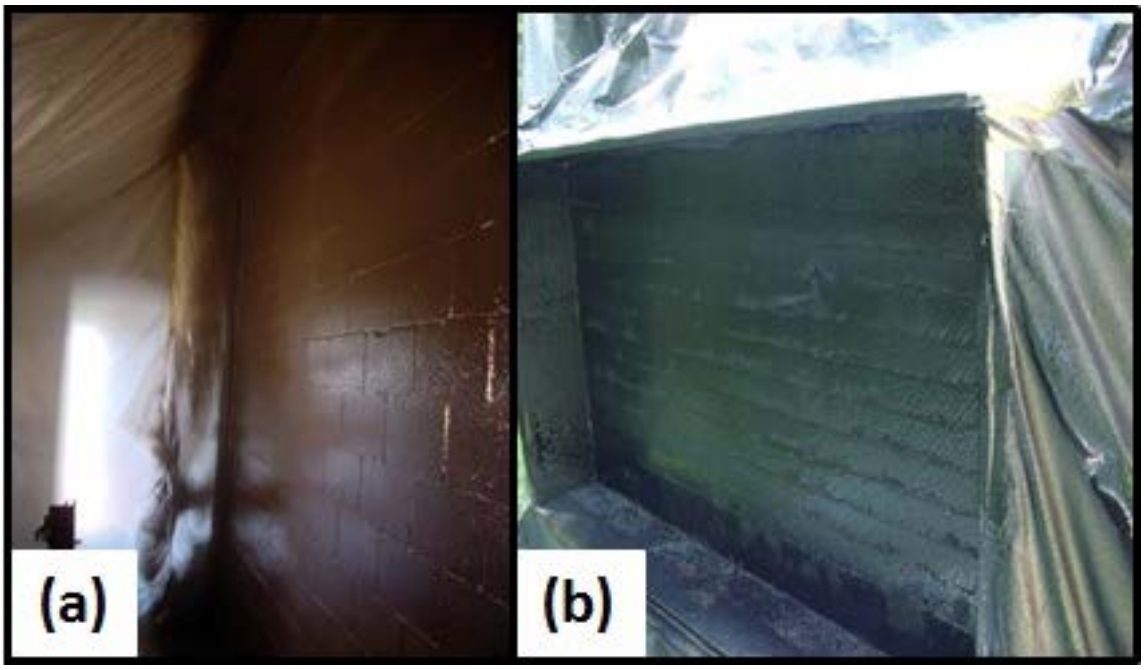

Figure 4.22. Plastic sheeting prevents overspray on areas adjacent to CMU walls. (a) Full-scale. (b) Subscale.

A strip of the structural steel or reinforced concrete elements adjacent to the infill CMU wall served as the area or zone where the retrofit was secured to the supports. These areas were clean, dry, and rough to provide an adequate bonding surface for the retrofit material. The preferred method of support preparation would be sand or grit

blasting; but, if a sand blaster was not available, a wire brush or grinder could be used to prepare the supports (Figure 4.23a and b). The bond between the support surface and the spray-on polyurea had to be as clean, dry, and rough as possible to prevent a peel back failure. A damp surface or layer of dust diminished the bond strength.

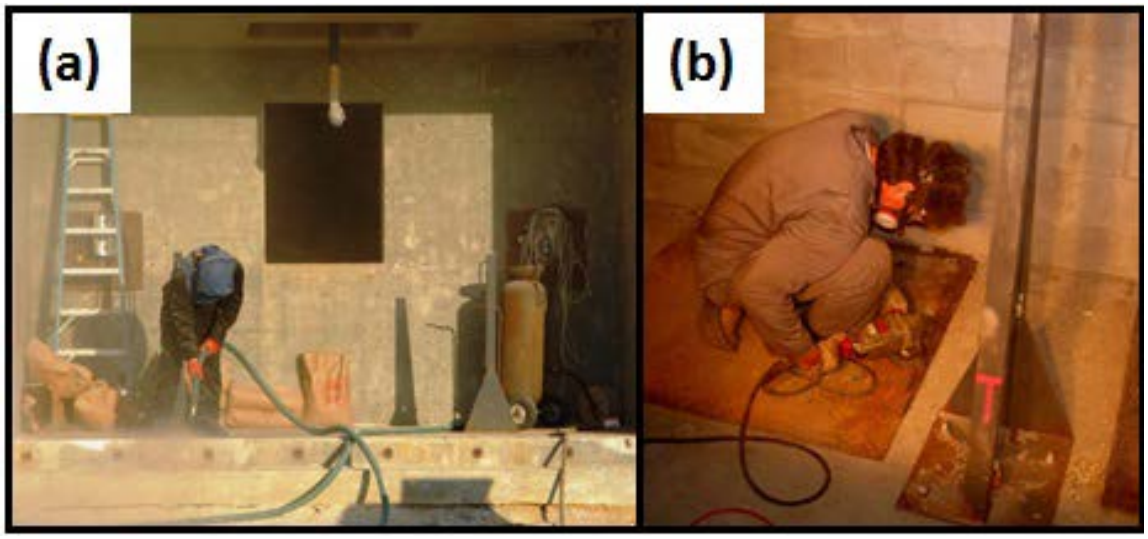

Figure 4.23. Methods to prepare the supports. (a) Sand blaster. (b) Grinder.

4.4.3 Step 3: Priming the Supports

The surfaces selected as supports were primed with either Primer 1, Primer 2, or Primer 4 (Figure 4.24). The primers had a maximum application window of 90 min, so only the amount of primer required for each designated section was prepared for application at one time. A small paint brush was used to apply the primers. Once the primed surface became firm but slightly tacky, which usually occurred after 15 to 40 min at 20°C (68°F), the first coat of spray-on polyurea was applied to the supports. The application window for the spray-on polyurea could be extended by applying an

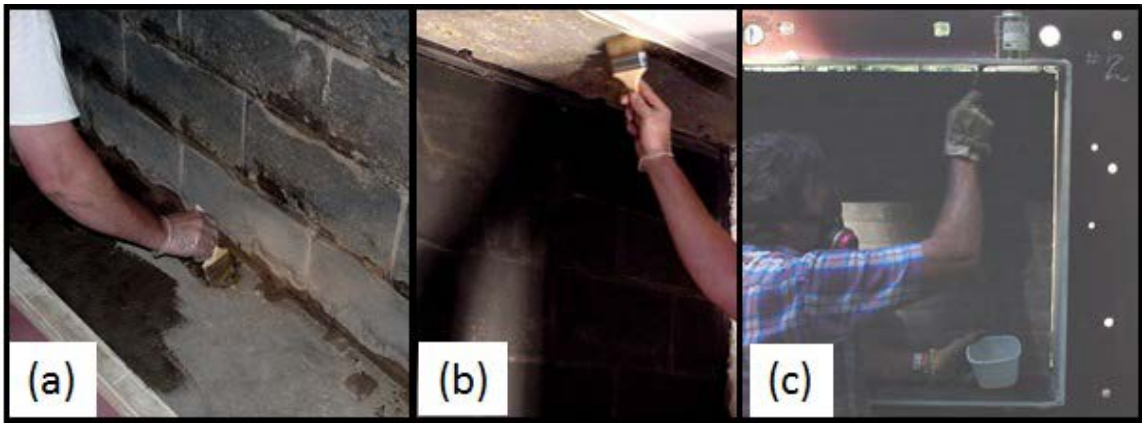

Figure 4.24. Primer application. (a) Primer 1 applied to steel plate on bottom support. (b) Primer 4 applied to concrete top support. (c) Primer 2 applied to subscale steel frame.

additional coat of primer if the polyurea application process was delayed and the surface was no longer tacky. Primer 1 is a single-component primer used on steel surfaces. In areas where concrete and steel surfaces coexisted as shown in Figure 4.24a located in Bays 3 and 4, it was highly recommended that a coat of Primer 1 be applied to the steel surface immediately after preparation and cleaning to prevent the formation of rust. This prevented any need to sand-blast or grind the steel surface a second time if the spray-on polyurea application was delayed for an extended time. If a delay did occur and the substrate was a mixture of steel and concrete, then a coat of Primer 4 could be applied over a layer of Primer 1 preventing the need to mix and apply two different primers prior to application of the spray-on polyurea. For best results, a coat of Primer 1 was applied to any steel substrate after preparation to prevent any form of contamination, and an additional coat of primer was applied an hour or two prior to the application of the spray-on polyurea. Primer 4 is a two-component primer used on concrete supports mixed

at a 1:1 ratio by volume of Part A and Part B (Figure 4.24b). Primer 2 was applied with a paint brush to the steel frame used in the subscale HE experiments (Figure 4.24c).

4.4.4 Step 4: Application of Spray-on Polyurea

Coverage of the spray-on polyurea was approximated based on the number of passes the person applying the material made while covering the wall surface. One pass was defined as the amount of material applied to the wall during a swing of the arm from left to right, right to left, top to bottom, or bottom to top (Figures 4.25a and b). The thickness associated with each pass was therefore controlled by the procedure (distance and speed) of the individual applying the material. Table 4.6 provides an average thickness of the spray-on material based on the employee from ERDC spraying the material. Several samples were sprayed and measured to obtain the average values provided in Table 4.6. The individual tried to maintain smooth and consistent timing throughout the application process to improve consistency. The spray gun was held 1 to 3 ft from the surface to be coated. Applicator experience often yielded a variation in thickness across the wall of ±5%. The individual applying the material practiced the technique before spraying the CMU wall. The ERDC representative sprayed several samples for practice that were later used to gauge the approximate thickness achieved, and the samples were later cut into coupons to be used for the uniaxial tensile experiments. A thin square sheet of steel covered with a layer of wax was used to create the practice squares (Figure 4.25). When the initial coat was applied, it was important to spray the supports and the course of blocks adjacent to the top and bottom supports first while the primer was still tacky (Figure 4.26a). Once the supports were complete, the CMU wall was sprayed

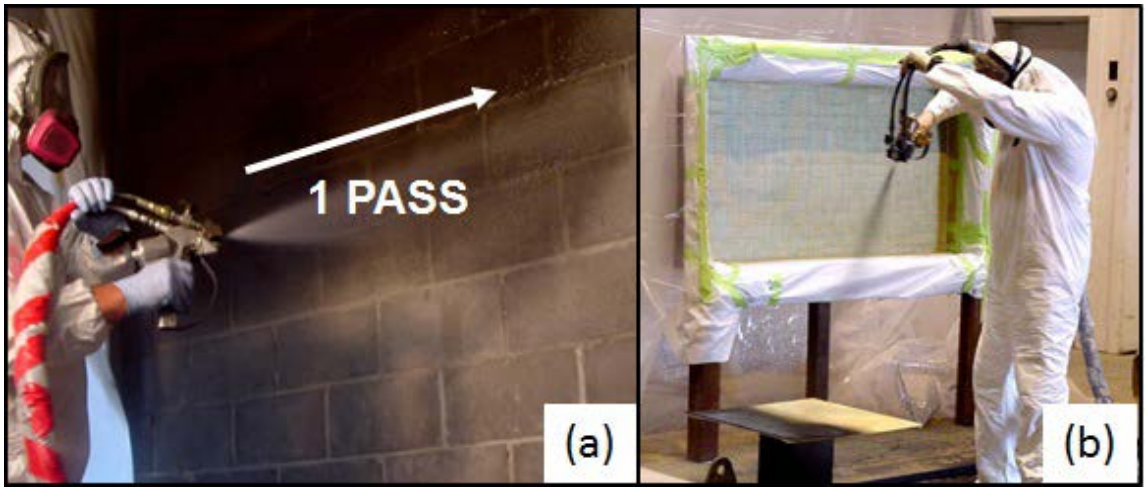

Figure 4.25. Spray technique. (a) Example of one pass by swinging the arm from left to right. (b) Practice sample sprayed to gage the thickness and create coupons for uniaxial tensile experiments.

Table 4.6. Typical spray-on measurements.

Number of Passes	Thickness, in. (mm)
4	0.0625 (1.5775)
8	0.125 (3.175)
16	0.25 (6.35)
32	0.5 (12.7)

(Figures 4.26b and 4.27). If any moisture was on the wall or supports, the polyurea did not adhere well, and bubbles formed in the material layer. If the bubbles were large, they were cut out, and new material was sprayed over the hole until it was the required thickness. The polyurea had very good adhesion to itself; so once the first layer was completed, the remaining application procedure was completed with minimal delays until the final thickness desired was achieved (Figures 4.27a and b). However, if the wall

was left for an extended amount of time and became damp, dirty, or dusty, the adhesion was compromised. A minimal thickness of 0.03 in. was required to complete the curing process.

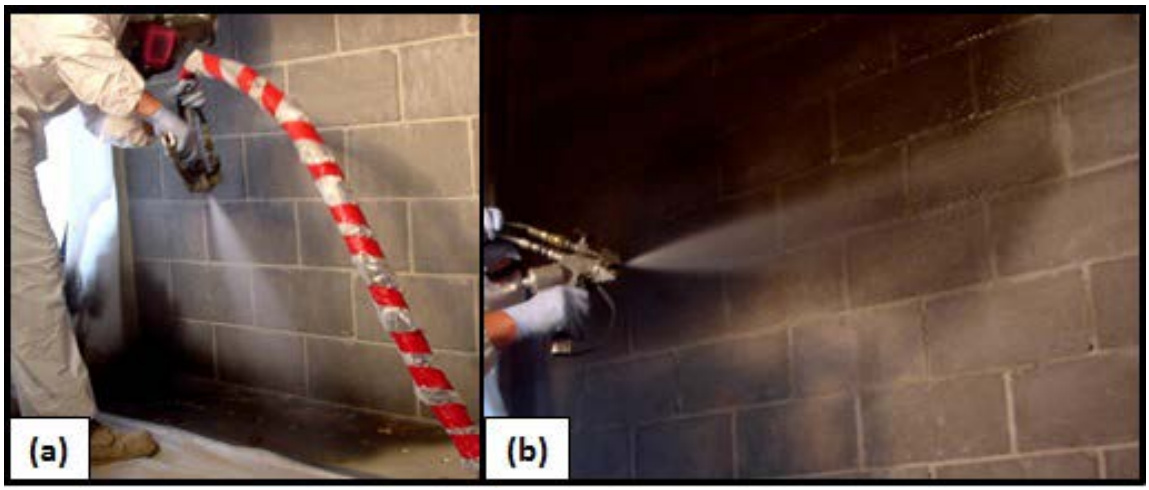

Figure 4.26. Spray-on polyurea. (a) Spray supports first while primer is tacky. (b) Polyurea applied to CMU wall surface.

Figure 4.27. Spray-on polyurea. (a) Spray wall surface in a continuous manner until desired thickness achieved. (b) Application of spray-on polyurea to subscale specimen.

4.4.5 Step 5: Clean-up

The wire tape that was applied around the perimeter of the wall was removed. The wire tape that was pulled away from the wall allowed the overspray or excess to be removed from the side walls of the reaction structure and supports. The plastic sheeting and insulation foam was removed from the gaps along the sides of the CMU walls.

4.5 Fiber-Reinforced Spray-on Polyurea Application

The procedure used to apply the fiber-reinforced spray-on polyurea was similar to that for the unreinforced polyurea, but additional steps were added to incorporate the installation of the fiber reinforcement. The same safety equipment used in the spray-on polyurea application was required for the fiber-reinforced version. No additional safety equipment was required during the application of the Aramid reinforcement; however, it was good practice to wear safety glasses and gloves at all times.

4.5.1 Step 1: CMU Wall and Support Preparation

The same CMU wall and support preparation as discussed in Section 4.4.2 was repeated.

4.5.2 Step 2: Preparation of Fiber Reinforcement

The fiber reinforcing fabric was designed and cut to length before the spray-on process began. The material must cover the entire wall surface and a section of the top and bottom supports. The only fiber reinforcement available for researchers when the reinforced spray-on polyurea experiments began had fiber bundles oriented at 0/90 deg. To facilitate a ±45-deg orientation on the wall, pieces were cut and trimmed to the lengths required to cover the entire surface and applied diagonally onto the wall surface

(Figures 4.28a and b). The sheet layout was designed so that the two longest pieces would be used to cover the wall surface from one corner to the opposite corner, and the sheets would be secured or anchored at both the top and bottom supports. The fibers

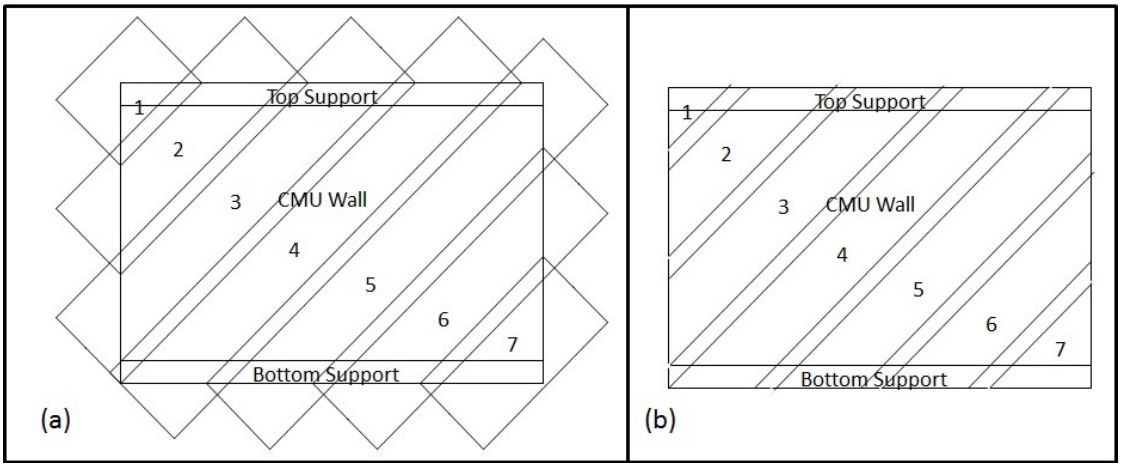

Figure 4.28. Fabric orientation. (a) The fiber reinforcement layout. (b) Fabric coverage after sheets were trimmed to fit wall.

originally oriented at 90 deg on the film were angled 45 deg to the horizontal mortar joints, and the fibers ran the entire length of the sheet from one anchored end to the opposite anchor. The remaining sheets were only anchored at one support. The fabric material was measured and cut to allow a designated width of 12 in. of material to overlap on the top and bottom supports to anchor the fabric. Before the material arrived on site, a PSA was applied to one face of the fabric reinforcement (Figure 4.29a). The fabric reinforcement was then cut to length, and the excess fabric that extended past the right and left side of the CMU wall was trimmed (Figures 4.28b and 4.29b). Each fabric sheet was labeled to ensure proper placement on the wall, and each fabric sheet

overlapped the previous sheet by at least 8 in. in the full-scale walls and 2 in. in the subscale CMU walls.

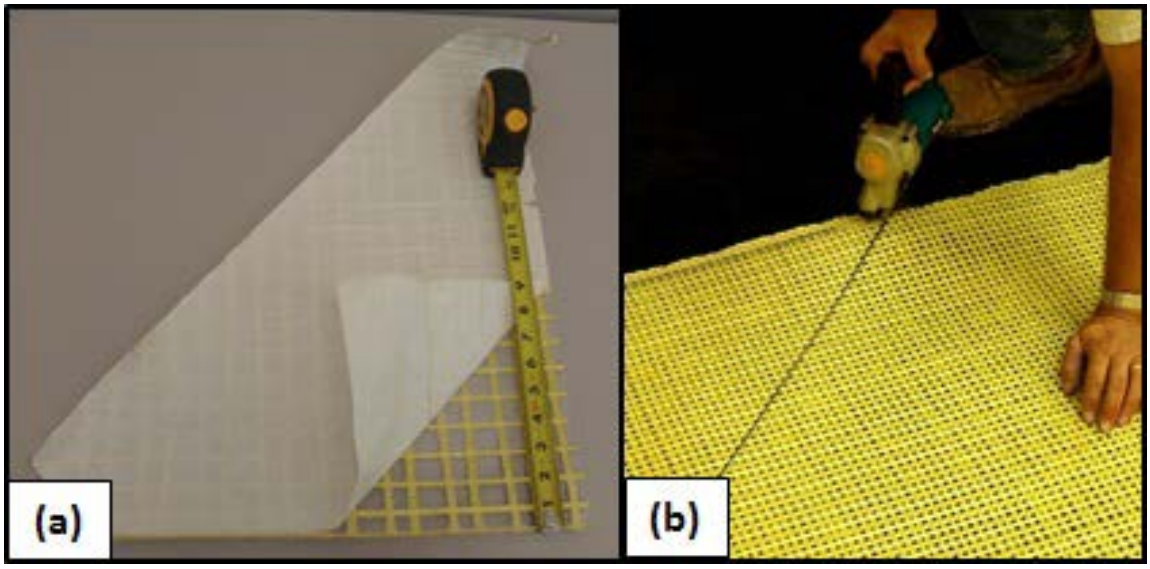

Figure 4.29. Fabric preparation. (a) A PSA was added to one face of the fiber reinforcement. (b) Fabric cut and labeled prior to application of first coat of spray-on polyurea.

4.5.3 Step 3: Priming the Supports

The same procedure used to prime the supports detailed in Section 4.4.3 was repeated.

4.5.4 Step 4: Application of First Layer of Spray-on Polyurea

Step 4 from the spray-on polyurea procedure discussed in Section 4.4.4 was used to apply the first layer of polyurea to the wall. For this system, the first layer of the polyurea was half of the final thickness desired on the wall. The CMU wall surface and supports were the same thicknesses.

4.5.5 Step 5: Application of Reinforcement

Application of the fabric reinforcement began in the top left corner and moved down the wall as shown in Figures 4.28a and b and as the numbers 1 to 7 indicate on Figures 4.28a and b. The reinforcement was also applied to the supports. The area to be adhered to the support was folded and creased prior to placement on the wall, to create as tight a corner as possible (Figures 4.30a and b). The reinforcement was applied by removing the backing paper revealing the PSA. In the full-scale experiments, the reinforcement was too heavy to stick to the wall without additional assistance, so the spray-on polyurea was sprayed at sporadic locations to anchor the reinforcement to the wall Figures 4.31a and b). Each successive sheet overlapped the previous sheet of reinforcement by a minimum length of 8-in. on the full-scale walls to create a continuous mat of reinforcement across the entire surface of the wall and supports (Figures 4.32a and b). After the reinforcement was placed on the wall, the entire surface area was rubbed down to remove all of the excess glue/adhesive that remained on the wall between the fiber bundles. As much of the excess glue as possible was removed to provide a contaminate-free surface for the second layer of spray-on polyurea. If glue remained on the wall surface, a good bond would not be formed between the first layer of spray-on polyurea and the second. The objective was to fully encapsulate the reinforcement between the two coats of spray-on polyurea.

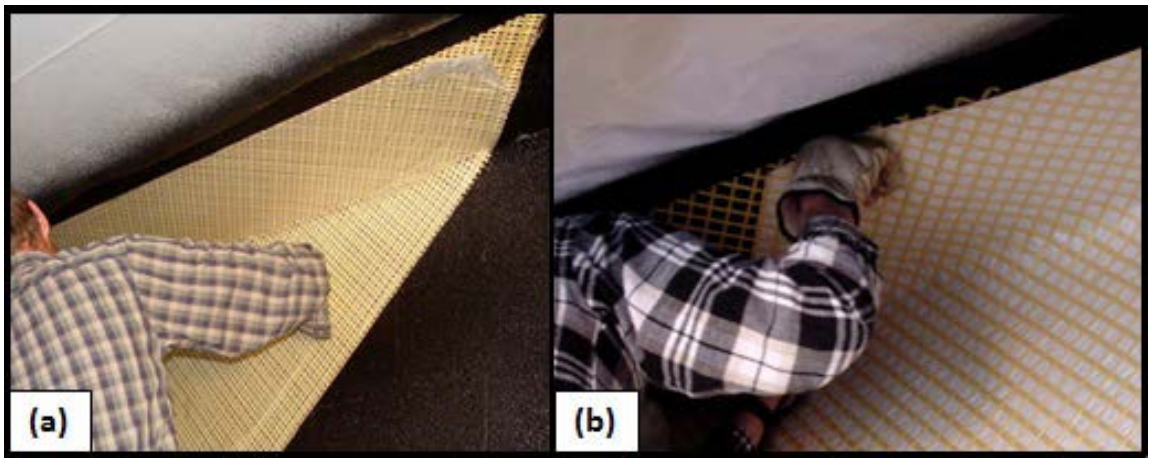

Figure 4.30. Fabric application. (a) Fabric placed on wall beginning at top support. (b) Ensuring placement of sheet before removal of the backing paper that protects the PSA.

The fabric reinforcement used in the subscale experiments was also produced with the fiber bundles running at 0/90 deg. The fabric was specifically cut and placed on the wall to provide fiber reinforcement in the ±45-deg orientation. Each successive sheet of fabric overlapped the previous sheet by approximately 2 in. The fabric was cut to allow at least a 3-in. width of the fabric to overlap the top and bottom supports anchoring the fabric from the wall to the supports (Figure 4.33b). The fabric used in the subscale experiments did not have an adhesive backing. However, the fiber bundles had a coating that would stick to the wall when heated, so a hot iron or hot air gun was used to adhere the fabric to the first layer of polyurea on the wall surface (Figure 4.33a).

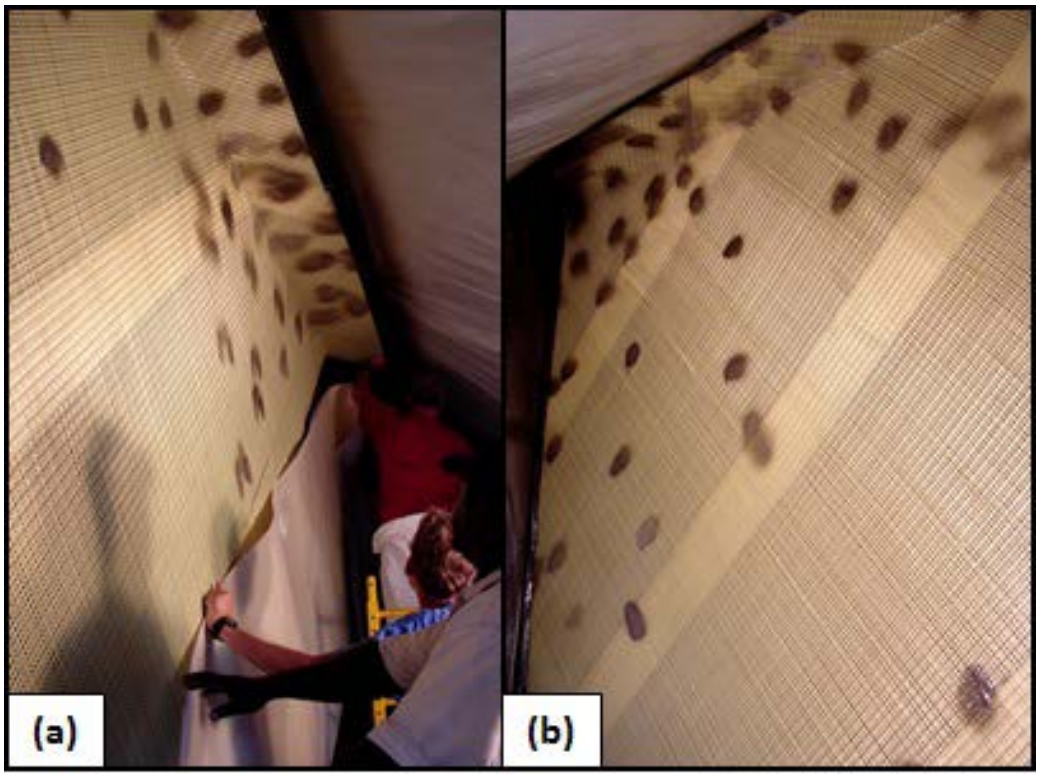

Figure 4.31. Fabric application. (a) Fabric placed diagonally on wall to provide fiber reinforcement in ±45-deg orientation. (b) Spray-on polyurea was used to anchor fabric to wall during application.

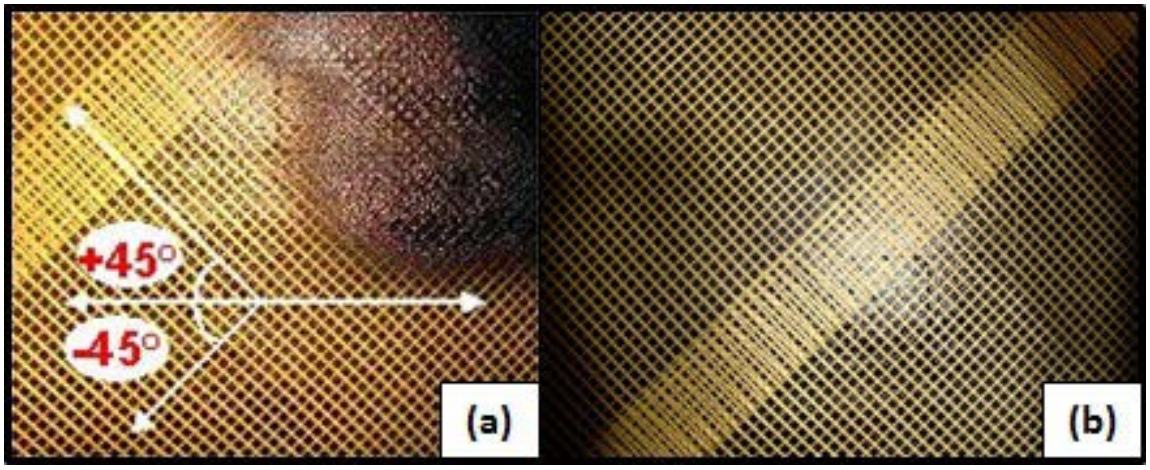

Figure 4.32. Fiber orientation. (a) Aramid fibers in fabric aligned ±45 deg to horizontal mortar joint on CMU wall. (b) Successive pieces of fabric overlapped previous by approximately 8 in.

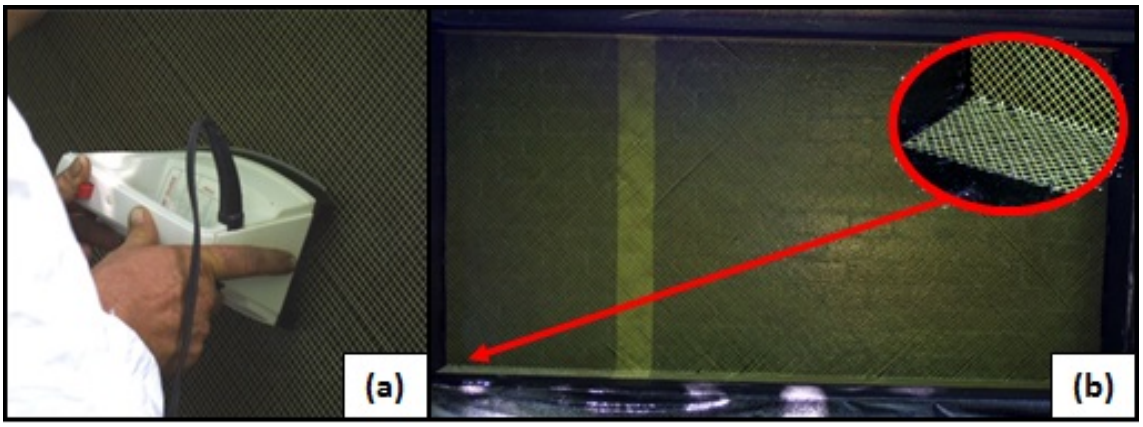

Figure 4.33. Subscale fabric. (a) Hot iron used in subscale experiments to adhere fabric to wall. (b) A 3 in. of fabric overlapped top and bottom supports.

4.5.6 Step 6: Application of Second Layer of Spray-on Polyurea

The second layer of spray-on polyurea was used to encapsulate the reinforcement on the wall (Figures 4.34a and b and Figure 4.35). The spray-on polyurea bonds very well to itself, so the open weave in the fiber reinforcement allowed the new material to bond to the previous layer. The technique used to apply the first coat of spray-on polyurea was repeated for the second layer. Once the desired thickness of the second layer of spray-on polyurea was achieved, the plastic sheeting, wire tape, and trim materials were removed.

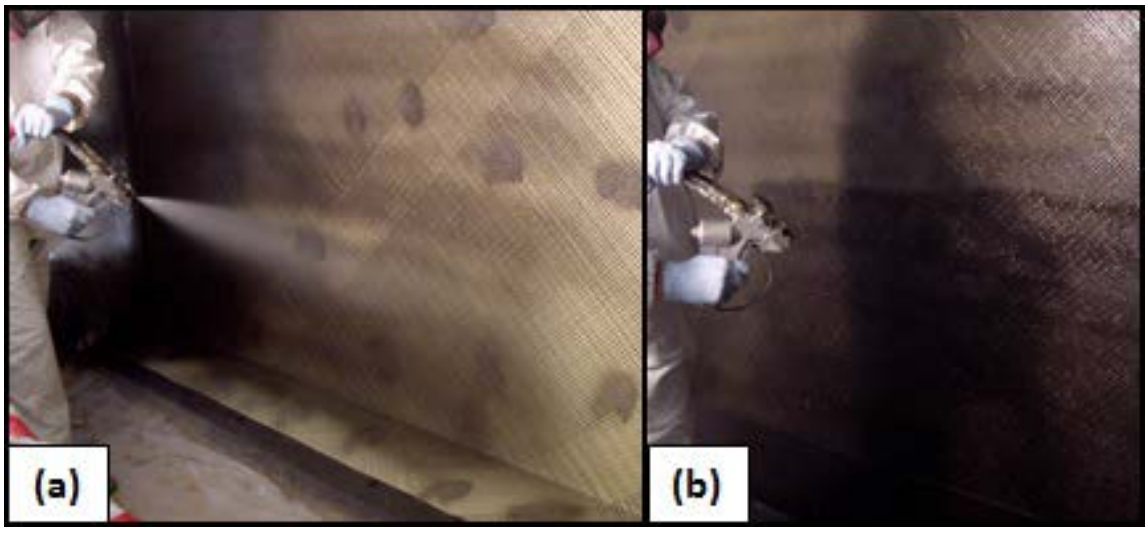

Figure 4.34. Spray-on polyurea. (a) Second coat of polyurea applied to wall. (b) Fabric was encapsulated by polyurea.

4.5.7 Step 7: Anchorage at Supports

Two methods were used to secure the spray-on polyurea with or without reinforcement to the concrete or steel supports. The first method relied solely on the adhesive or bond strength between the steel or concrete substrate and the spray-on polyurea (Figure 4.36a). The quality of the beam/floor slab and the preparation of the substrate were critical when relying solely on the bond strength of the elastomer as the only support system. The second method used the adhesive bond and one of the mechanical anchorage systems discussed in Section 4.3.3. When there was a question as to the strength of the substrate of the reaction structure or one was unable to adequately prepare the supports to insure an adequate adhesive bond, a mechanical anchorage system was used (Figure 4.36b).

Figure 4.35. Application of second coat to subscale specimen.

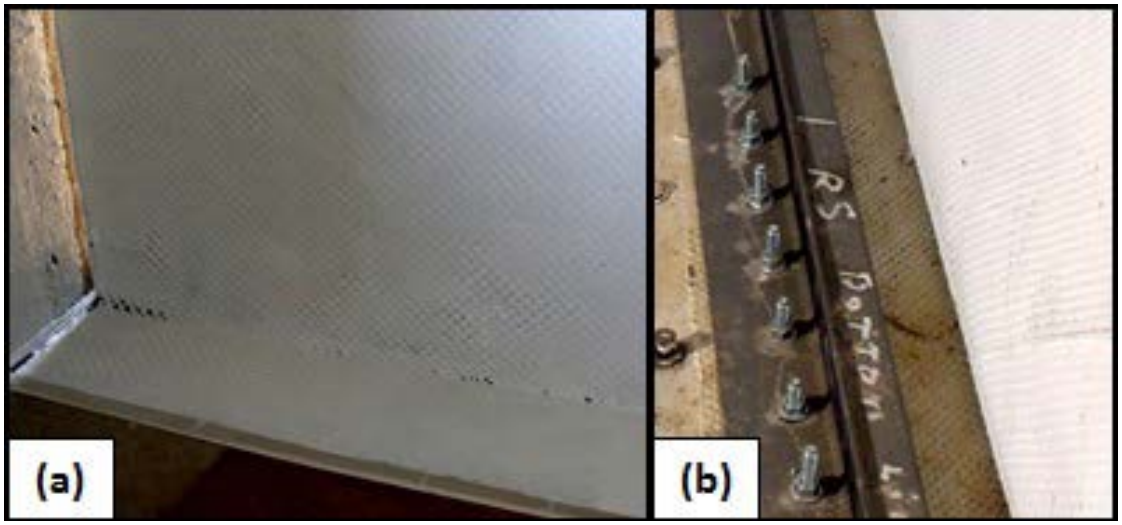

Figure 4.36. Anchor systems. (a) Bottom support relying solely on adhesive strength. (b) Additional anchorage provided by steel plate.

4.6 Trowel-on Thermoset

As a follow-up to the spray-on application technique, a series of experiments using a trowel-on material was evaluated. The material selected for evaluation was a three-component thermoset. Two versions of the trowel-on thermoset material were evaluated. The first version, labeled Grade 1, was evaluated in subscale static and dynamic experiments and in full-scale dynamic experiments. Grade 2, designed to be more economical, was evaluated in one full-scale experiment. The application process for the two trowel-on materials was the same. The equipment required to prepare and apply the retrofit materials were buckets, paddle wheel, drill, notched trowel, flat trowel, and modified plastic putty knife. Subscale experiment SW10, DW10, and DW11 and full-scale experiments FS5, FS6, and FS7 used the trowel-on thermoset procedures to retrofit the walls.

4.6.1 Step 1: Safety Equipment

The application of the trowel-on thermoset retrofit required two safety products, i.e., gloves and safety glasses (Figures 4.37a through c). Safety glasses and gloves were worn at all times. Latex gloves were worn while priming the substrate, mixing materials, and applying the trowel-on material. A respirator was mandatory during the application of the primer (Primer 1 or Primer 4) and during the operation of a sand blaster, wire wheel brush, or grinder. However, a respirator was not required during the application of the trowel-on material. Wearing protective clothing was not mandatory but was highly recommended during the application of the trowel-on material. While applying the

Figure 4.37. Safety equipment. (a) Mandatory: latex gloves, safety glasses, and respirator. (b) Protective clothing disposable paint suit. (c) Latex gloves and sleeves.

material, dropping some of the material on one's arms, head, and clothing was not unusual, so as a protective measure, a hat and a paint suit or sleeves were worn to avoid this nuisance (Figures 4.37b and c).

4.6.2 Step 2: CMU Wall and Support Preparation

The CMU wall and support preparation procedures described in Section 4.4.2 were completed first, with the exception of the plastic sheeting and wire tape, because these items were not required to protect the reaction structure from excessive application. Then the CMU wall surface to be retrofitted was painted with a coat of standard latex matte/flat black paint (Figures 4.38a and b). The paint contrasted with the light colored trowel-on polymer and served as one of two methods used for quality control during the application procedure. If the appearance of black paint was seen through the target thickness of 0.25 in. (635 mm) the trowel-on coating for full-scale walls, then the material was applied too thinly. The subscale CMU wall surfaces were also painted, but

they were painted to replicate the full-scale wall surface and not as a quality control method. The wall and paint had to be dry prior to application of the trowel-on polymer (Figure 4.38b). Paint was not applied to the surface of the supports. The bond between the support surface and the trowel-on thermoset had to be as strong as possible to prevent a peel-back failure, and a layer of paint would have diminished the bond strength at the supports. The wire tape and plastic sheeting used to remove excess material after

Figure 4.38. Quality control. (a) CMU wall surface is painted black; no paint applied to concrete supports. (b) Trowel-on material applied to the clean support and painted CMU wall.

the spray-on application was not needed in the trowel-on material application. Due to the nature of the application process, it was much easier to prevent or quickly remove any material that may have been applied to the reaction structure accidently.

4.6.3 Step 3: Priming the Supports

The priming procedure from Section 4.4.3 was repeated.

4.6.4 Step 4: Coverage of Trowel-on Material

Coverage of the trowel-on thermoset was approximately 1,600 mils thick for 1 ft^2/gal (1 mm thick for 1 m^2/liter). Therefore, the amount of material required to cover 100 ft^2 (9.29 m^2) at a target thickness of 0.25 in. (6.35 mm) was approximately 15.75 gal (59.2 L). Additional material was added to all coverage calculations to account for loss and penetration into the CMU blocks. The amount of loss to factor into the calculation was dependent on material packaging, environmental conditions, pot life of material, mixing, application procedures, and the skill level of personnel. When all the conditions were satisfactory, approximately 10% more material was added to the order. When conditions were not favorable, at least 25% additional material was added to the order.

4.6.5 Step 5: Resin Preparation of Trowel-on Material

The trowel-on thermoset contains three components, i.e., Parts A, B, and C. The quality of each component was evaluated before the mixing process began. All three components were soft and poured easily. Part A was packaged in five gallon buckets and looked like a clear gel. This component could solidify at temperatures below 75°F (24°C), and the solidification could be either complete (solid) or partial (grainy). When solidification occurred to any extent, the containers were exposed to temperatures above 85°F (30°C) until the material returned to a smooth liquid. Submerging the closed material containers in a hot water bath worked very well to reverse the solidification process. When Part A had to be treated for solidification, the material was premixed with a drill using a paddle wheel attachment before the three components were mixed together. When any amount less than a full container was used, the entire container was

stirred before the amount required was removed. Part B was usually stored in plastic bags pre-measured for a specific volume of trowel-on material (Figure 4.39). Part B was beige and had a tendency to separate if stored for long periods of time. When the material separated, red streaks were visible in the material contained in the plastic bag. This was corrected by kneading the plastic bag before opening, which returned the material to its original consistency. Part C was packaged in a small clear plastic bottle and was a clear liquid that could also solidify. Part C was also returned to its original form by heating the bottle in a hot water bath.

4.6.6 Step 6: Mixing Process for Trowel-on Material

The three trowel-on components were packed in containers pre-measured for a particular area of coverage. The mixing process began by adding the entire contents of Part B into the bucket containing Part A (Figure 4.39a). When any amount less than a full container was required, Part A and B were mixed at a 3:1 ratio by weight. The two

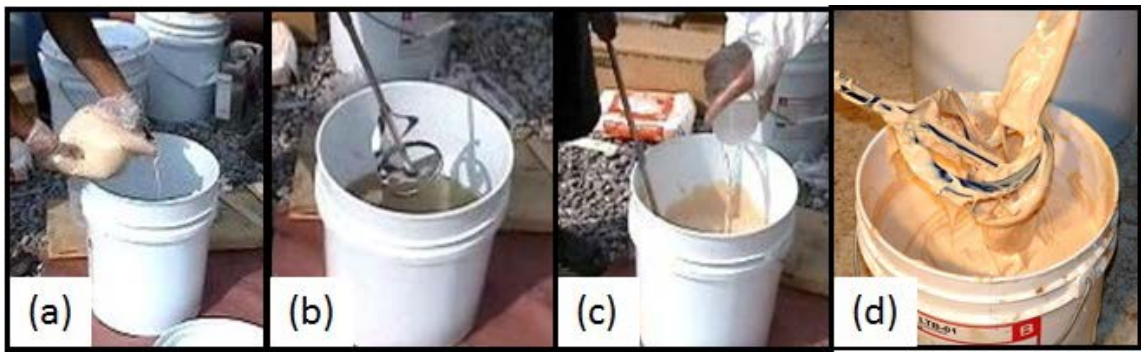

Figure 4.39. Mixing process. (a) Part B is added to Part A. (b) First two components are mixed with a paddle wheel attachment on the drill mixer. (c) Addition of Part C while mixing the material. (d) Material is ready to be applied to the wall.

components were mixed using a paddle wheel attachment on a standard drill (Figure 4.39b). The mixing process was stopped intermittently, and a paint stick was used to scrape the sides, corners, and bottom of the container to ensure that the material was mixed thoroughly. Part C, the "Build Agent" (Figure 4.39c), was added to the bucket last. Once Part C was added and mixed with the other materials, the mix began to thicken. The entire bottle of Part C did not have to be used. The amount of build agent used was dependent on the applicator's ability and environmental conditions. As larger quantities of Part C were added, the material thickened and became harder to apply to the wall. The mixing process was complete when the material became a thick, sticky paste as shown in Figure 4.39d.

4.6.7 Step 7: Pot Life of Trowel-on Material

An exothermic reaction occurred as the materials were added and mixed to form the trowel-on thermoset. The personnel applying the trowel-on material had to move quickly since the material had a twenty minute application window at 75°F (24°C). The curing process began as soon as the materials were mixed, and the workability of the material decreased as the time increased. The pot life increased at cooler temperatures and decreased at higher temperatures. The longer the trowel-on material remained in the warmer confined area of the mixing container, the pot life decreased, reducing the workability time of the material. Therefore, applying the trowel-on material to the wall quickly, which reduced the temperature of the material, was very advantageous, increased the pot life, and maintained the workability of the material.

4.6.8 Step 8: Application of Trowel-on Material

The technique used to apply the trowel-on material was dependent on environmental conditions and the number and skill level of the personnel. Due to the limited pot life of the trowel-on material, it was applied to the wall as quickly as possible. As discussed in the previous step, applying the material to the wall quickly increased the material's working time. Spreading the freshly mixed material was easier. The trowel-on material was applied to the supports and walls in two layers. The first layer served as a guide to control the overall thickness of the complete retrofit. When the first layer had been applied properly to the wall, it contained a consistent groove pattern. The second layer of material was used to fill the grooves, creating one solid coating at the desired thickness. Starting the application process at the top and moving down the wall was best. Several batches of material were needed to complete the application. Figure 4.40 shows a schematic of the wall and illustrates the area of coverage recommended for each batch of material used in the application process. The different colors represent separate batches of material, and the numbers identify the order of application for each additional batch of trowel-on material. The dashed lines identify the areas where multiple batches of material are feathered into each other.

The preferred method of application was the 'notched-trowel' method, which used the following items to apply the material, i.e., a trowel with a notch depth equal to the desired thickness of the retrofit material (Figures 4.41a through c), a flat sheetrock trowel (Figure 4.41a), and a modified plastic putty knife (Figure 4.41c). The trowel-on material was applied in two layers using at least a three-person crew. The first person

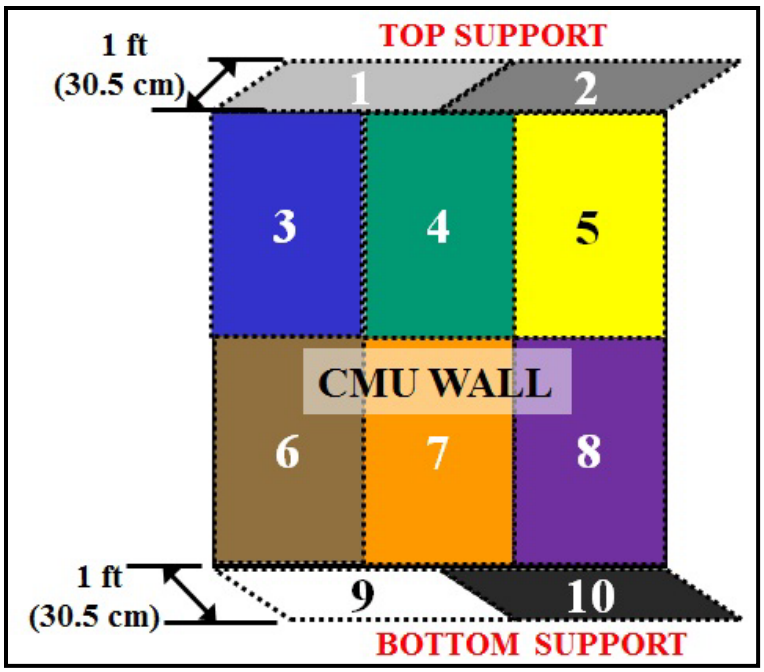

Figure 4.40. Schematic of the wall demonstrating the area of coverage recommended for each batch of material.

was responsible for measuring and mixing the three components to prepare the trowel-on material. The material began to harden after the components were mixed. The first person also scraped and cleaned the tools used in the mixing process between batches so that the application process could continue uninterrupted; at least two sets of trowels were used. While one set of trowels were used to apply a batch of material, the second set was cleaned for use on the next batch. The second person applied the material to the CMU wall in sections using a flat sheetrock or straight trowel (Figure 4.41a) normally used to apply plaster or stucco finishes. To ensure a consistent thickness, a third person followed the second person with the notched trowel (Figure 4.41b) angled perpendicular to the surface of the wall. In the full-scale experiment, the desired thickness was 0.25 in.

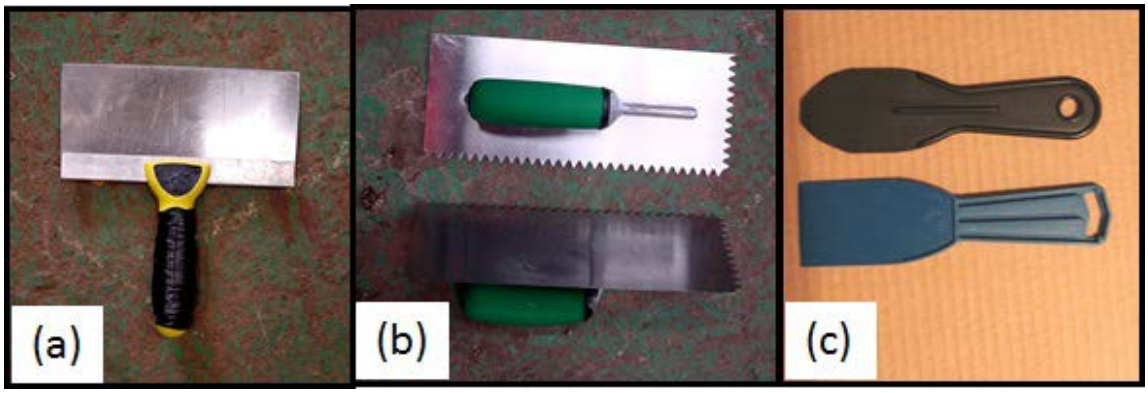

Figure 4.41. Trowels. (a) Flat trowel used to apply material to the wall and to fill in the grooves on the second layer. (b) Notched trowel used to create grooves in the material as a form of quality control. (c) Modified plastic putty knife used to apply the material in the corners.

(6.35 mm), so a notched trowel with a 0.25-in. (6.35-mm) groove was used to form the first layer of material. A small 3-in.- (7.62-cm-) wide plastic putty knife trimmed into an elliptical shape was used to apply a continuous and thick layer of material at the corners (Figure 4.41c). The plastic putty knife was shaped so that it would fit flat against the top support and the CMU wall surface.

The third person began applying the trowel-on material in the top corner using the plastic putty knife (Figure 4.41c). Then, the second person began to apply large quantities of the material to the supports and the CMU wall surface (Figure 4.41a) using the flat trowel. The third person followed the second person and redistributed the material applied with the flat trowel until the material became one consistent grooved layer (Figure 4.41b). The procedure was repeated until the entire wall surface and top and bottom supports were covered with the first layer of material (Figures 4.42a through c).

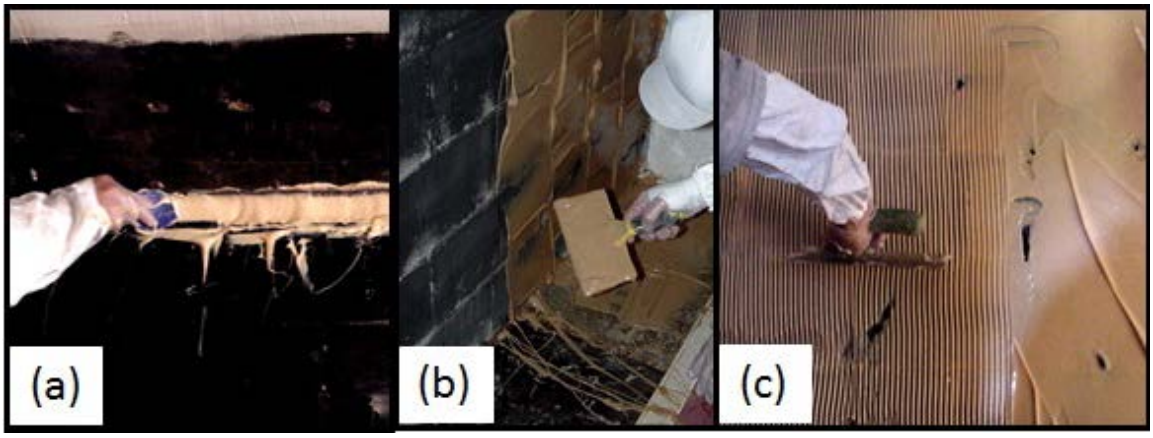

Figure 4.42. Trowel-on application. (a) Modified plastic putty knife used to apply material in corners. (b) First layer of material applied to the wall using a flat trowel. (c) Notched trowel used to create grooves in the material corresponding to the desired thickness of the material.

The trowel-on material has high self-adhesion, so additional preparation between the application of the first and second layer of the trowel-on material was not required (Figures 4.42a through c). However, if more than a day elapsed between the application of the first and second layer, the surface was wiped clean with MEK before the next layer was applied. Once the first layer cured or hardened (material does not deform with pressure), the second layer was applied vertically from the top to the bottom using the flat trowel with medium pressure (Figures 4.43a and b). The material applied during the second layer filled in the grooves left from the notched trowel, creating a continuous layer of trowel-on material at the desired thickness. Air bubbles in the material were avoided. The vertical movement minimized the amount of air bubbles formed in the

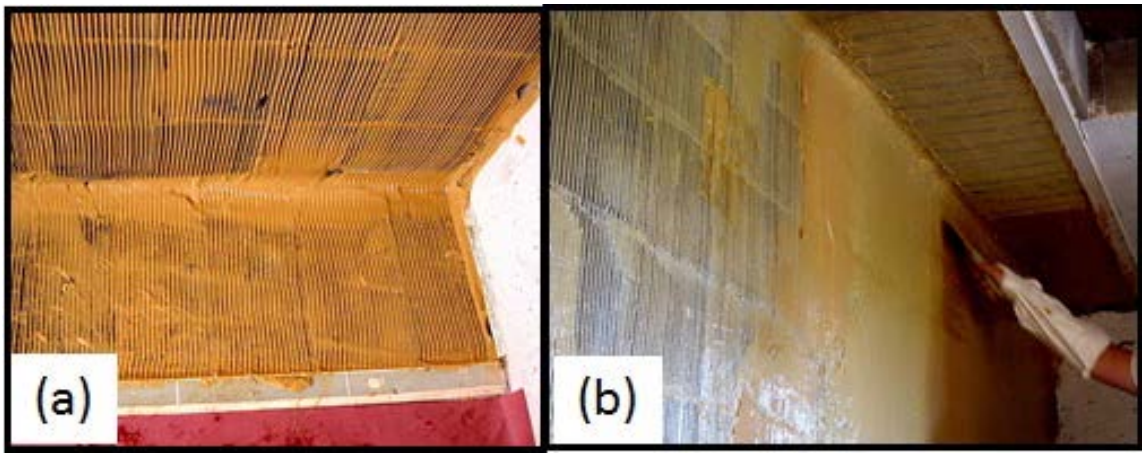

Figure 4.43. Trowel-on application. (a) Grooves from first layer on wall and bottom support. (b) Flat trowel used to fill in the grooves to complete the second layer of the retrofit material.

retrofit while filling in the grooves. The points where the trowels removed from the wall were staggered to prevent a continuous line or pattern from forming on the wall. Exposed voids and other touch-ups were repaired easily at a later time.

After the second layer of material hardened, the retrofitted wall was inspected. If the black paint was visible, then the desired depth was not obtained and additional material was added (Figure 4.44a). If a prolonged period of time had elapsed since the application of the second layer, the area requiring additional material was wiped clean with MEK prior to the application of any additional material. The trowel-on application was complete once the black paint was no longer visible (Figures 4.44b and c).

4.6.9 Step 9: Curing of Trowel-on Material

A minimum of 7 days at 75°F (24°C) was allowed for the trowel-on material to cure. The cure time could be reduced by half for each 18°F (10°C) increase in temperature.

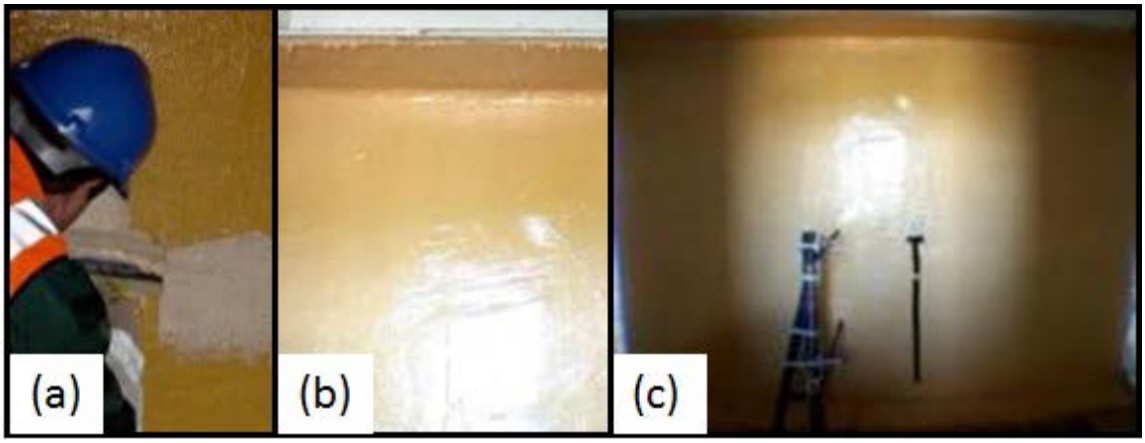

Figure 4.44. Trowel-on application. (a) Extra material added to thin spots. (b) Trowel-on layer on wall and top support. (c) Instrumentation added to retrofitted wall.

4.7 Elastomeric Films w/Trowel-on or Spray-on Adhesives

The first series of elastomeric films evaluated in the research program required an adhesive material to be added for installation to the CMU wall. An adhesive is either a natural or synthetic material in a liquid or semi-liquid state used to bond or fasten items. Adhesives cure by either evaporating a solvent (non-reactive adhesives) or by chemical reactions (reactive adhesives) that occur between two or more constituents. The methods used to bond the films to the wall in the research program included a spray-on material, two trowel-on materials, and three double-sided PSA tapes. Mechanical anchorage using screws or bolts was avoided on the wall surface because holes in the elastomeric film would create stress concentrations that would decrease the physical properties of the film. Using an adhesive distributed the stress evenly over the entire bonded area of the CMU wall surface.

There are many different types and ways to describe or define elastomeric films, but in the research program, the films evaluated in the subscale and full-scale experiments were divided into two categories, i.e., thermoplastic and polyurethane films. The application procedures described from this point on will apply to both film types unless specified differently in the text. The ability to find COTS films in both the third- and full-scale materials became one of the most difficult aspects of the research program as it progressed. The following is a basic description of the materials used and is not a full description of the many materials that could be classified as a polyurethane or thermoplastic elastomeric film. This researcher recommends that the material properties for the respective materials to be used in a particular application be determined before use.

The typical subscale unreinforced polyurethane films used in the research program were 15- to 20 mils thick, produced to length, and packaged on 48-in.-wide rolls, and the target thickness for the full-scale unreinforced films was 60 mils. The first unreinforced elastomeric film (45 mils) was thicker than the desired thickness for a subscale material but it was used in one subscale static experiment, SW17. The second subscale unreinforced film was 14.8 mils thick and it was used in experiments labeled SW21 and BLS4-BLS7. The first full-scale unreinforced thermoplastic film was 60 mils thick and it was used in experiments FS8-FS10. The thickness and strength of the first full-scale unreinforced film was duplicated in the second film.However, the second full-scale unreinforced film used in experiment FS12 was purchased from a second manufacturer due to limited availability of the product.

One of the first subscale reinforced elastomeric films provided by the manufacturer consisted of an open weave Aramid fiber-reinforcement provided by a secondary consultant was encapsulated between two layers of polyurethane film using a lamination process. Then, a PSA purchased from a separate vendor was applied to the reinforced film at the test facility to bond the film to the CMU wall surface. The laminated reinforced material was only used in one subscale static experiment, SW22. A primer was used to strengthen the bond between the film material and the reaction frame at the top and bottom supports in allof the experiments. However, a primer was not used on the CMU wall surface to enhance the bond between the PSA and CMU in the initial experiments.

The final subscale fiber reinforced elastomeric film consisted of an open-weave Aramid fiber-reinforcement that was encapsulated in a 48-in.-wide polyurethane film through an extrusion process. Then, one surface of the film was coated with a hybrid acrylic PSA to bond the film to the CMU wall. The film, with the liner removed, was 30.2 mils thick, and the adhesive and the removable liner were each 7 mils thick creating a film with an overall thickness of 44.2 mils with the protective liner in position. The open-weave Aramid fabric reinforcement with a 200-lb/lineal inch by 200-lb/lineal inch tensile strength had a 1/4-in. web opening. Subscale experiments SW23-SW24, SF1-SF5, and BLS8-BLS11 used this retrofit material.

Four different forms of stress can affect the bond between the film and the CMU, i.e., tensile, shear, cleavage, and peel as illustrated in Figures 4.45a through e (3M 2006; Huntsman 2007; Troughton 2008). The stresses can act singular or in combination on the

bond between the adhesive and substrate. Tensile stresses are created when a force pulls the film away from the CMU equally or uniformly across the entire joint (Figure 4.45b). Shear stresses occur when the forces exerted on the film and the CMU slide over each other, and the stress is parallel to the joint (Figure 4.45c). Cleavage stresses are created when the forces acting on the film and block are concentrated on one edge of the joint, creating a prying or wrenching force on the adhesive (Figure 4.45d). Peel stresses are created when the force is concentrated along a surface or boundary line and the flexible surface of the film pulls or lifts away from the CMU surface (Figure 4.45e). Once the peeling action begins, the stress line remains in front of the advancing separation boundary. Most adhesives perform better when the primary stress is tensile or shear, but a combination of stresses can also affect the bond strength. A combination of cleavage and peel stresses can occur between the substrate and the film through the adhesive and from posttest observations, this combination appeared to affect the bond between the CMU, adhesive, and film during most of the experiments.

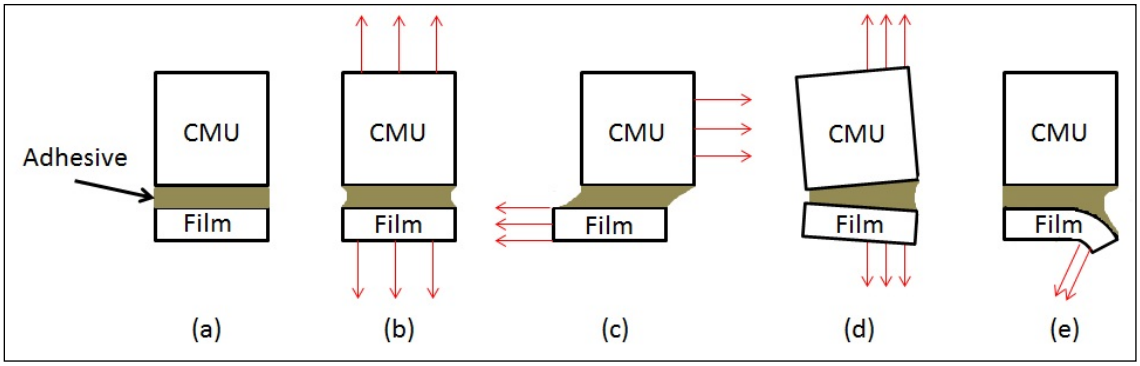

Figure 4.45. Stress modes. (a) Unstressed state. (b) Tensile. (c) Shear. (d) Cleavage. (e) Peel. (Adapted from 3M 2006; Huntsman 2007; Troughton 2008)

4.7.1 Spray-on Synthetic Rubber Based Adhesive and Elastomeric Film

A COTS adhesive was selected for use with one of the thermoplastic films. This material system was used to retrofit walls for one subscale static (SW18) and one dynamic experiment (DW12). In the static experiment, the spray-on synthetic rubber adhesive was only used at the supports. In the dynamic experiment, the spray-on adhesive was used to bond the film to the entire CMU wall surface and the top and bottom supports. The material was marketed as a neoprene high-performance rubber and gasket adhesive used as a general purpose adhesive to bond rubber and gasket materials to metals, enamel, wood, plastics and neoprene, SBR, and butyl rubber. The adhesive and substrate should be at a temperature of at least 65°F (18°C) for best results at time of application. For proper application, this spray-on adhesive had to be applied to the surface of the wall and the elastomeric film's surface.

4.7.1.1 Step 1: Safety Equipment

The spray-on synthetic rubber adhesive required the following safety products during application, i.e., gloves, Tyvek disposable protective coveralls with hood, and respirators with full-face shields. Safety glasses, gloves, and a respirator had to be worn during application of the adhesive and during the operation of a wire wheel brush or grinder during preparation of the supports. When a sand blaster was used during the surface preparation, heavy duty protective clothing, leather gloves, and a full-face shield with a fresh air supply pump had to be worn or used.

4.7.1.2 Step 2: Wall and Support Preparation

All of the same steps described in Section 4.4.2 to prep the wall and supports were also used for this retrofit system since a possibility existed for material overspray during application of the spray-on adhesive.

4.7.1.3 Step 3: Application of Spray-on Adhesive and Elastomeric Film

The manufacturer's instructions require that both the elastomeric film and the CMU wall surface be sprayed for proper application. A uniform coat of the adhesive was applied to the wall surface first (Figures 4.46a and b), and then a layer of the adhesive was applied to one side of the elastomeric film (Figure 4.46b). Once the adhesive was

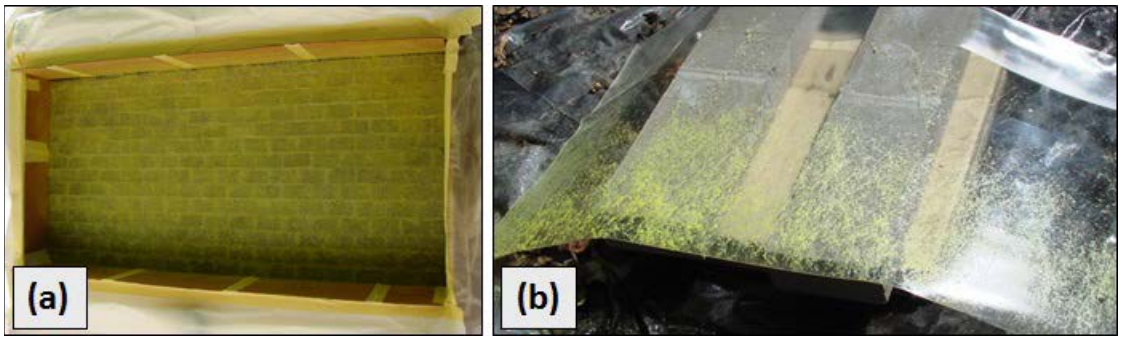

Figure 4.46. Spray-on adhesive. (a) Spray-on adhesive applied to CMU wall surface. (b) Adhesive being sprayed on the film surface before it is applied to the CMU wall surface.

dry, which took less than 5 min, the installers only had an 8- to 12-min window of application based on the adhesive bonding range. Once the film contacted the CMU wall surface, the bond was immediate, and the material could not be repositioned. This made it extremely important to design the sheet application and position before the process

began. The film was applied to the wall from the free edge of the top support, down the surface of the wall, to the free edge of the bottom support. Pressure was applied to the film using a rubber roller to ensure contact between the two surfaces. Any trapped air between the CMU wall surface and the elastomeric film was pushed to the free edges using the rubber roller to improve the bond between the wall and elastomeric film surfaces.

4.7.1.4 Step 4: Apply Mechanical Anchorage

Anchor System 2 was used to secure the retrofit materials to the substrate. While preparing the retrofitted wall for the dynamic experiment, a tear developed in the material at the support, so an additional 1-ft-wide strip of the film was added to the top and bottom supports (Figure 4.47). Then the plates used in System 2 were bolted into place to anchor the film. It is important to note that the elastomeric film systems allowed repairs or extra material to be added easily as was seen in the application process for this wall.

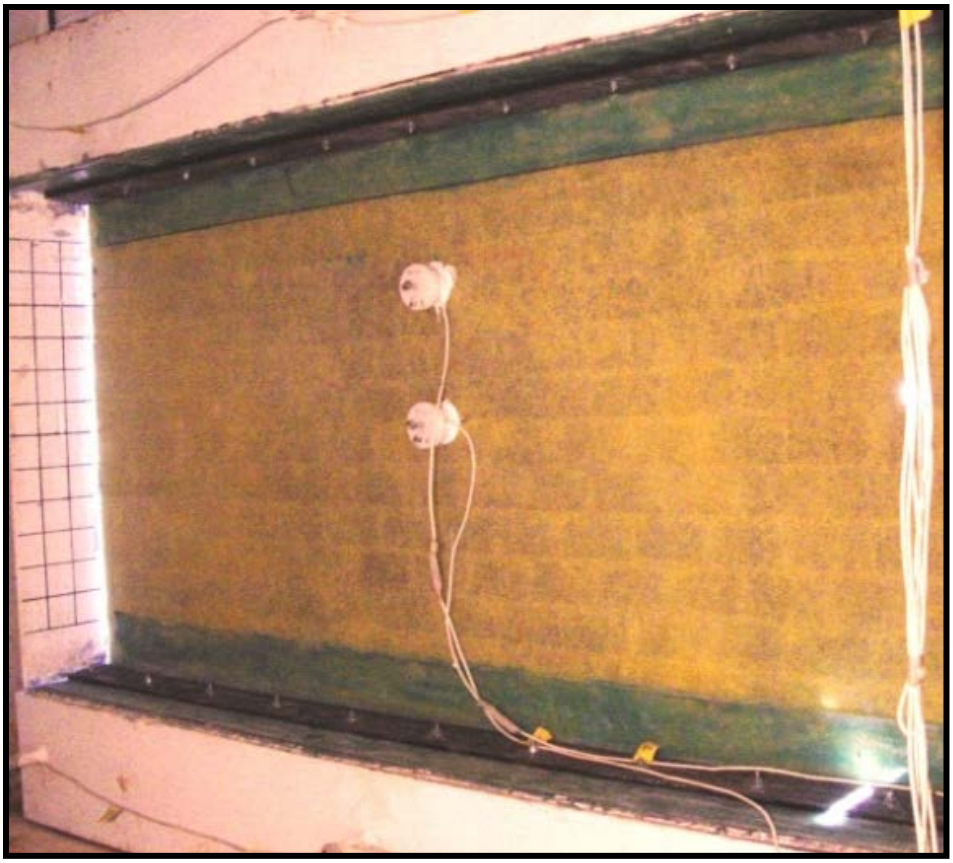

Figure 4.47. Wall retrofitted with spray-on adhesive and elastomeric film with an additional strip of film applied to the supports to repair a defect.

4.7.2 Elastomeric Film with Trowel-on Thermoset Adhesive

New materials were combined with some of the materials and application techniques from previous retrofits to create a new retrofit system. For example, the trowel-on thermoset adhesive used in Section 4.6 was used as the adhesive for the new COTS elastomeric films, and the primers used on the supports in most all of the retrofit systems were also used to prime the elastomeric films in the new retrofit system. Several different unreinforced and reinforced elastomeric films were evaluated using this

application procedure; for clarity, the material properties for each film are provided in their respective experimental results discussion. The reinforcement and the material properties for the films differed, but the procedure used for their application were the same. At least three people participating in the application is recommended. The procedures discussed in this section were used in the subscale experiments SW13 and DW13 and full-scale experiments FS8-FS10.

Wall FS13 was the first experiment conducted on a wall retrofitted with an elastomeric film from the manufacturer that contained Aramid reinforcement in a ±45-deg orientation. In Section 4.5.2, the Aramid reinforcement had to be cut into special shapes to align the fibers in a ±45-deg orientation on the CMU wall surface, and in Section 4.5.5, the procedure to apply a 0/90-deg fiber-reinforced film in a ±45-deg orientation on the CMU wall are described. This was the first film sent from the manufacturer with the film encapsulated in a ±45-deg orientation; thus, the film did not have to be cut into special shapes to create the desired fiber orientation on the wall. The application discussed in the procedure for unreinforced film applied with a trowel-on thermoset adhesive can be used to apply the ±45-deg fiber-reinforced film without the need for additional steps.

The techniques described in earlier sections required each step to be completed individually. In the process used to apply the elastomeric films, most of the steps were repeated for each strip of film. For the CMU wall illustrated in Figure 4.48, three sheets of film were needed to cover the 10-ft by 10-ft wall surface; the steps used to apply each sheet had to be repeated three times. Figure 4.48 shows a schematic of the wall

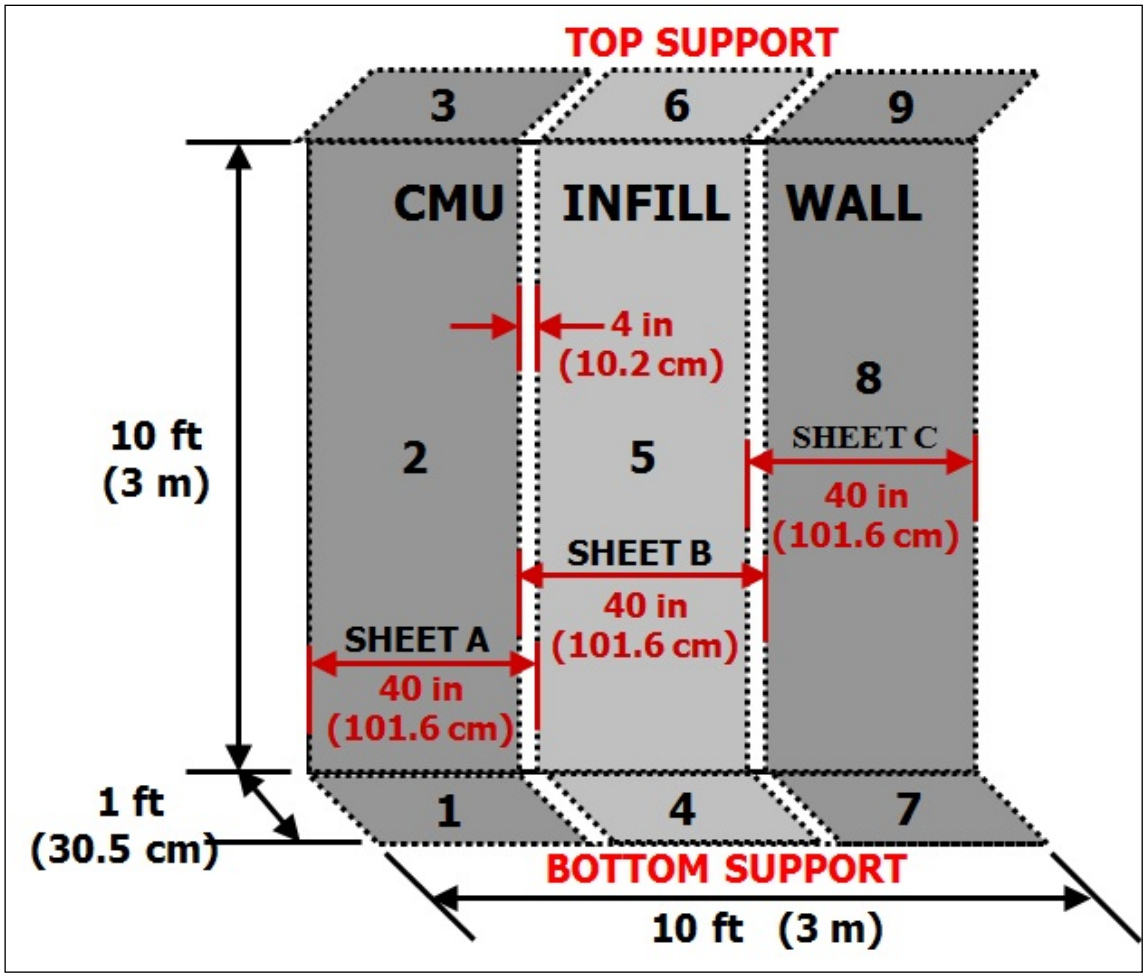

Figure 4.48. Wall schematic illustrating the order of trowel-on and film applications. Notice the 4-in. (10.2-cm) overlap of each film section (white strip). In this illustration, Sheet B overlaps Sheet A, and Sheet C overlaps Sheet B.

demonstrating the area of coverage recommended for each batch of material used in the application process. Beginning application of the trowel-on material at the bottom of the wall and working upward was considered to be the best procedure. The numerical order (1-9) for the trowel-on material's application is labeled on Figure 4.48 as well as the order for each film sheet alphabetically (A-C). The order of operation for the example

illustrated in Figure 4.48 would require the trowel-on material to be applied to Areas 1 through 3, then apply Sheet A, apply trowel-on material to Areas 4 through 6, then apply Sheet B, apply trowel-on material to Areas 7 through 9 and apply Sheet C. This procedure will be discussed in greater detail later in this section.

4.7.2.1 Step 1: Safety Equipment

The trowel-on material used in Section 4.6 was used as the adhesive for the thermoplastic film. The same safety equipment used to apply the trowel-on thermoset was used for the trowel-on and film retrofit system. No additional equipment was required.

4.7.2.2 Step 2: CMU Wall and Support Preparation

The CMU wall and support preparation procedures described in Section 4.4.2 were completed first with the exception of the plastic sheeting and wire tape. The wire tape and plastic sheeting that were used to remove excess material after the spray-on application were not needed in the trowel-on material application. Due to the nature of the application process, the person applying the material could prevent or quickly and easily remove any material that might be applied to the reaction structure accidently.

4.7.2.3 Step 3: Priming the Supports

The procedure used to prime the supports in Step 3 of Section 4.4.3 was repeated for this system.

4.7.2.4 Step 4: Thermoplastic Film Preparation

The unreinforced and reinforced elastomeric films applied to the CMU walls in the research program were produced in rolls of material 40 to 48 in. (101.6 to 121.9 cm) wide (Figures 4.49a and b). The length and number of film sheets required to completely cover the CMU wall were determined and prepped prior to mixing the trowel-on material. The film sheets were applied to the wall vertically beginning on either the right or left edge, with each successive sheet overlapping the previous by at least 4 in. (10.2 cm). Each sheet of material was cut the length required to cover the entire wall height plus an additional 2 ft (61 cm) to cover the material used on the top and bottom supports (areas where the trowel-on polymer and film overlapped the structure's steel or concrete frame). The length of material used at the top and bottom supports should be at least 12 in. (30.5 cm) long. A simple utility knife was used to cut the film material into the required lengths. The application face of each sheet was cleaned with MEK (Figure 4.49b), denatured alcohol, or acetone. In some of the experiments, the elastomeric film was primed with the primer material used on the supports before it was applied to the wall surface.

4.7.2.5 Step 5: Trowel-on Thermoset Preparation

The coverage of the trowel-on material, resin preparation, mixing process, and pot-life discussed in Steps 4 through 7 of Section 4.6 are the same.

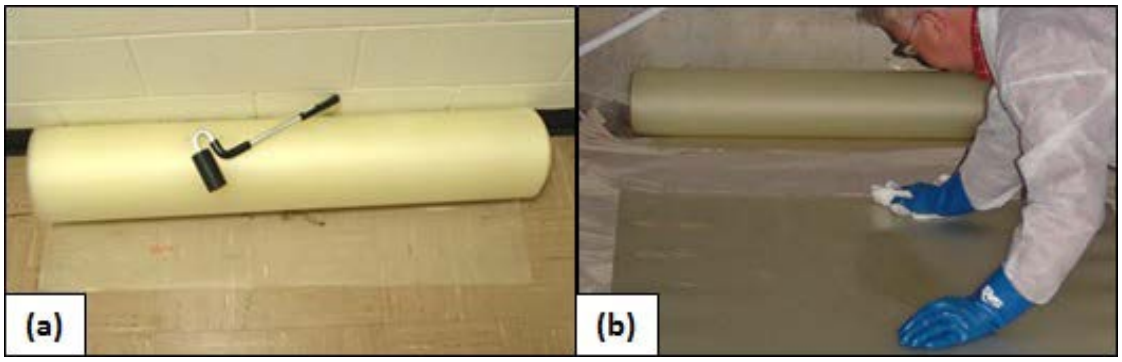

Figure 4.49. Film preparation. (a) Roll of thermoplastic film and a rubber roller used to apply the film to the wall. (b) Thermoplastic film is prepped with MEK prior to application.

4.7.2.6 Step 6: Application of Trowel-on Thermoset

The application process for the trowel-on thermoset was very similar to the process used in Step 8 of Section 4.6.8 with a few modifications. At least three people were needed to complete the trowel-on thermoset and thermoplastic film application. The addition of one to two more people would make the process more efficient and comfortable, but the discussion will be described for the smallest crew required for completion. Three trowels were used to apply the thermoset material (Figure 4.50a), i.e., modified plastic putty knife (A), a flat sheetrock knife (B), and a notched trowel (C). The first person was responsible for measuring and mixing the three components to form the trowel-on material. The material began to harden after the components were mixed, so at least two sets of trowels were used allowing the application process to continue uninterrupted. While one set of trowels was used to apply a batch of material by installers two and three, the second set was cleaned by the first person for use on the next batch. The second person applied the material to the CMU wall in sections equal to

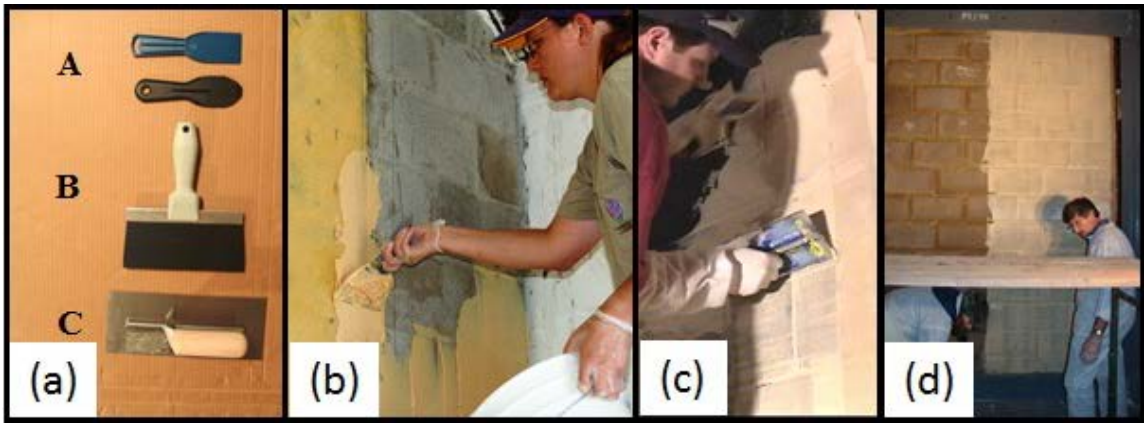

Figure 4.50. Trowel-on material application. (a) Trowels used to apply the thermoset. (b) Flat trowel used to apply material to wall. (c) Notched trowel used to control thickness. (d) One section of trowel-on material is completed and ready for film application.

the width of the thermoplastic film using a flat or straight trowel (Figure 4.50b) normally used in plaster or stucco finishes. The third person immediately followed the second person with a notched trowel (Figure 4.50c) held against the CMU wall's surface at an angle slightly less than perpendicular (90 deg). The notched trowel selected for application should be larger than the desired thickness of the trowel-on polymer. For example, in this experiment, the target thickness was 0.06 in. (1.5 mm), so a notch trowel with a 0.175-in. (4.8-mm) groove was selected. A notched trowel with a 0.1875-in. (4.8-mm) depth applied at an angle to the wall's surface produces a groove of material with a depth of 0.125 in. (3.2 mm). The application of the thermoplastic film redistributed the trowel-on material to a thickness approximately half of the groove depth. Once the trowel-on/film retrofit procedure was completed, the layer of trowel-on material was reduced by half to a depth of 0.06 in. (1.5 mm) with a 0.06-in.- (1.5-mm-) thick film for a total retrofit thickness of 0.12 in. (3.1 mm). The primary purpose of the

notched trowel was to control the consistency or quality of the trowel-on thermoset thickness by removing excess or identifying thin areas of material. Moving the notched trowel from the bottom to the top of the wall prevented material loss by allowing the excess material to accumulate on the trowel instead of dropping to the floor (Figures 4.50b and c). As shown in Figures 4.50d and 4.51a and illustrated in Figure 4.48, only one strip equal to the width of the film was prepared at a time. This prevented the material from hardening before the film could be applied.

The procedure used to apply the trowel-on polymer to the CMU wall (Figures 4.51b and c) was also used at the supports (floor and roof slabs.) The only difference in the procedure was at the corners. A small 3-in. (7.62-cm) plastic putty knife trimmed into an elliptical shape was used to apply a continuous and thick layer of material at the corners (Figure 4.51c). Modifications to the plastic putty knife are shown in Figure 4.50a.

4.7.2.7 Step 7: Film Application

The trowel-on material had a very short pot life, so the trowel-on application process had to move quickly in order to leave adequate time for film application. To prevent the trowel-on material from curing before the application of the film, mixing and applying only enough trowel-on material for each individual sheet was important (Figure 4.50d). The cleaned side of the film was placed against the trowel-on material. The film was applied starting at the bottom support and moved up the wall (Figure 4.51b). Applying the film from the bottom up anchored the film, thereby reducing film movement and redistribution of the trowel-on polymer. Two people were responsible for holding the film away from the CMU wall (Figure 4.52a), while at least one person with a 3-in.-

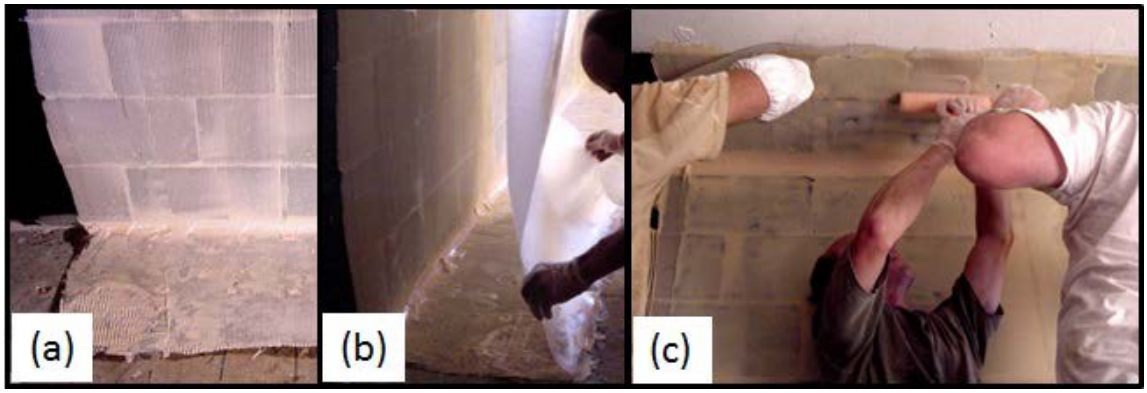

Figure 4.51. Film application. (a) Appearance of grooved trowel-on material before film application. (b) Film application began at the bottom support. (c) Film material applied to top support.

(7.62-cm-) wide rubber roller applied uniform pressure to the film material from the bottom support, up the wall, to the top support in one continuous application (Figures 4.52a through c). Normal CMU wall construction, with tooled joints and uneven placement of CMU blocks, limited the effectiveness of a wider roller. Air bubbles should be prevented from forming under the film. However, if air bubbles formed, the roller was used to move the trapped air toward the sides or leading edge of the film (Figure 4.52b). The amount of air bubbles formed under the film could be minimized if the people holding the film away from the wall could keep it from touching. The person or people applying the pressure dictated the point of contact, speed, and progress of the application to minimize the formation of air bubbles (Figure 4.52c). If pressure was applied at random locations on the wall instead of in a continuous motion, large air voids developed, and an inadequate bond between the trowel-on thermoset and film material developed.

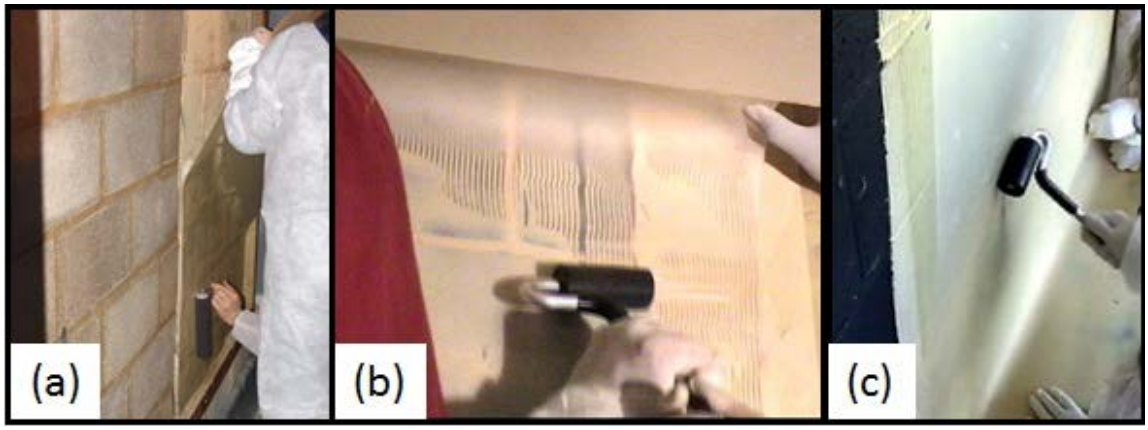

Figure 4.52. Film application. (a) Two people hold the film off the wall while a third applies pressure to the film. (b) Grooves in the trowel-on material became a smooth continuous layer as pressure is applied. (c) Rubber roller works best to apply pressure.

The amount of pressure applied to the wall was controlled by visual inspection of the grooves in the trowel-on material. As pressure was applied to the film using a roller or similar device, the grooved trowel-on material redistributed to form a smooth continuous layer under the film (Figure 4.53a). If groves are visible, more pressure should have been applied or the material began to harden indicating the installer did not apply the material in a timely manner (Figure 4.53b). If the grooves in the trowel-on material were visible, the pressure applied to the film was increased. If the block is visible through the film, too much pressure was applied (Figure 4.53c).

The trowel-on polymer had high self-adhesion and also adhered well to the film. However, the ability of the film to adhere to the trowel-on material was highly time dependent. The film material had to be applied before the trowel-on material began to firm or harden. If the film peeled off the wall after applying pressure, then too much

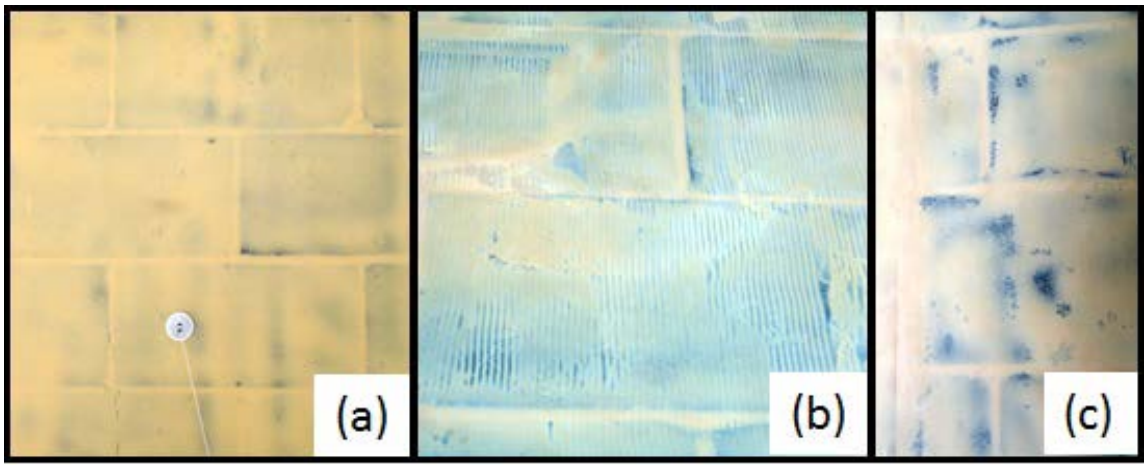

Figure 4.53. Quality control. (a) Smooth continuous layer. (b) Grooves are visible under the film. (c) Block surface is visible under film.

time has expired between the placement of the trowel-on material and the film. Two options can be used to correct the situation. Either new trowel-on material can be added to the existing material at the identified problem areas or the trowel-on material can be removed and replaced with fresh material. The flat trowel used earlier in the application procedure can be used to scrape off the firmed or hardened trowel-on polymer. Freshly mixed trowel-on material can then be placed on the wall to complete the film application.

Multiple sheets of the film were used to cover the entire CMU wall. As Figures 4.54a through c illustrate, each subsequent sheet of thermoplastic film overlapped the previous sheet. The excess trowel-on material not covered by the previous sheet of material had to be removed before the next sheet of film was applied to the wall (Figure 4.54a). This was a quality control measure because the excess material from the previous sheet application would have hardened before the next sheet of film could be applied creating

Figure 4.54. Film application. (a) Excess material to left of film must be cleaned off. (b) MEK was used to clean the strip of film to be overlapped by the next sheet of film. (c) Overlap area is covered with a layer of the trowel-on material.

a weak zone in the retrofit system. The flat trowel used in the application process was also used to scrape off the excess trowel-on material. The overlap area, a 4-in.-(10.2-cm-) wide vertical strip on the edge of the previous sheet of film was cleaned with MEK, denatured alcohol, or acetone and allowed to dry before the next batch of trowel-on material was applied (Figure 4.54b). The trowel-on material was applied to a 4-in. strip of the previous sheet of film to bond each successive sheet into one continuous system (Figure 4.54c). The application procedure was repeated until the CMU wall was completely covered (Figure 4.55).

4.7.2.8 Step 8: Curing

The trowel-on/film retrofit system was allowed a minimum of 7 days at 24°C (75°F) to cure. The cure time can be reduced by half for each 10°C (18°F) increase in temperature.

4.7.2.9 Step 9: Anchorage at Supports

One of the four full-scale mechanical anchorage systems described in Section 4.3.3 was used to secure the retrofit system to the top and bottom supports. System 5 was used on the retrofitted wall shown in Figure 4.55. The anchorage system used for each experiment is discussed in the appropriate experimental results section.

Figure 4.55. Each successive sheet overlaped the previous sheet.

4.7.3 Elastomeric Film and Trowel-on Epoxy Application

The procedure used to apply the trowel-on epoxy system was very similar to the trowel-on thermoset and elastomeric film application with only a few modifications and additional steps added. The trowel-on thermoset used in the previous retrofit system was

replaced with a trowel-on epoxy. The steps to apply the retrofit system were repeated for each successive sheet of film applied as was discussed earlier in Sections 4.7.2.6 and 4.7.2.7. The primary difference between the two systems was the ability and time that it took the trowel-on adhesives to bond to the elastomeric film. The trowel-on thermoset material bonded quickly to the elastomeric film and was able to maintain form on the wall during the application process from the beginning of the application process until the material cured. However, the trowel-on epoxy did not adhere as well to the elastomeric film during the installation process, but bonded well to the CMU wall surface after the curing process. Additional steps and bracing procedures were added to the elastomeric film and epoxy application process to ensure contact between the wall and film materials. Several different unreinforced and reinforced elastomeric films were evaluated using this application procedure; for clarity the elastomeric films are identified in the respective experimental results discussed in Chapters 5 to 7. The reinforcement and material properties for the films may differ, but the procedure used to apply the materials was the same. At least three people participating in the application was recommended. The trowel-on epoxy and unreinforced elastomeric film system were used in subscale experiments SW14 and FS11.

The epoxy chosen for evaluation in the research program is an adhesive used in the construction, industrial, specialty vehicle, transportation, and military industries to bond rubber, metal, wood, plastics, glass, ceramics, and masonry materials. The epoxy is a flexible, two-component gray material consisting of a base and accelerator material that cures at room temperature with high peel and shear strength. It has a 90-min window of

application and reaches handling strength in 10 hr. The full cure time for the epoxy is 7 days at 72°F (22°C). The epoxy has a 24-month shelf life and a gallon kit cost $700/kit.

4.7.3.1 Step 1: Safety Equipment

The safety equipment recommended in Section 4.6.1 is also recommended for this procedure.

4.7.3.2 Steps 2 and 3: CMU Wall Preparation and Priming the Supports

The same procedures discussed in Steps 2 and 3 of Sections 4.6.2 and 4.6.3 were replicated in this procedure to prepare the CMU wall and to prime the supports.

4.7.3.3 Step 4: Film Preparation

The film sheets were cut before the retrofit process began. The height of the wall to be retrofitted was measured, and 2 ft were added to the overall length required to allow 1 ft of material to be used at each support. The elastomeric film used with the epoxy had to be primed to enhance the adhesion between the materials. A full coat of the primer was mixed and applied to the surface of the elastomeric film with a paint brush (Figures 4.56a through c). Multiple sheets of film were required to cover the wall surface, so the 4-in. strip to be covered by each successive sheet was primed (Figure 4.56c). Each successive sheet and overlap area on the previous sheet was primed by the second and third installers, while the first installer began mixing the epoxy. The film surfaces should be primed as needed, but not all at one time. Notice in Figures 4.56b and c that the support and overlap areas were primed in sections before

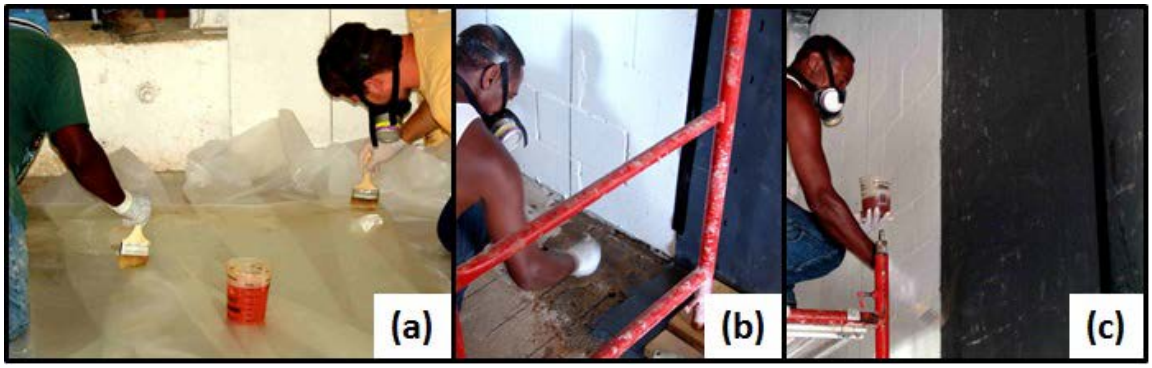

Figure 4.56. Primer application. (a) Prime the film. (b) Prime the support. (c) Prime the 4-in. area on the previous sheet of film that will be overlapped by new sheet.

each successive sheet was applied rather than applying the primer across the entire support region.

4.7.3.4 Step 5: Mixing Process for Trowel-on Epoxy

The base and accelerator components were measured in separate buckets at a 2:3 (Base:Accelerator) mix ratio by volume or 5:7 mix ratio by weight (Figures 4.57a and b). Each smaller bucket was poured into a 5-gal bucket and mixed with a paddle wheel attached to a drill (Figure 4.57c). Once a uniform color was obtained, the material was mixed for an additional 15 sec. Once mixed, the epoxy had a maximum window of application of 90 min. The material's window of application was reduced at higher temperatures and with large quantities of mixture. As in the trowel-on thermoset, the quicker the mixed epoxy was removed from the bucket and applied to the wall, the longer the window of application.

Figure 4.57. Mixing process. (a) Measure component A. (b) Measure component B. (c) Mix component A and B.

4.7.3.5 Step 6: Trowel-on Epoxy Application

The same process used to apply the trowel-on thermoset in Section 4.7.2.6 was repeated to apply the trowel-on epoxy (Figure 4.58 a, b, and c). The procedure illustrated in Figure 4.48 was used to apply the epoxy and elastomeric film.

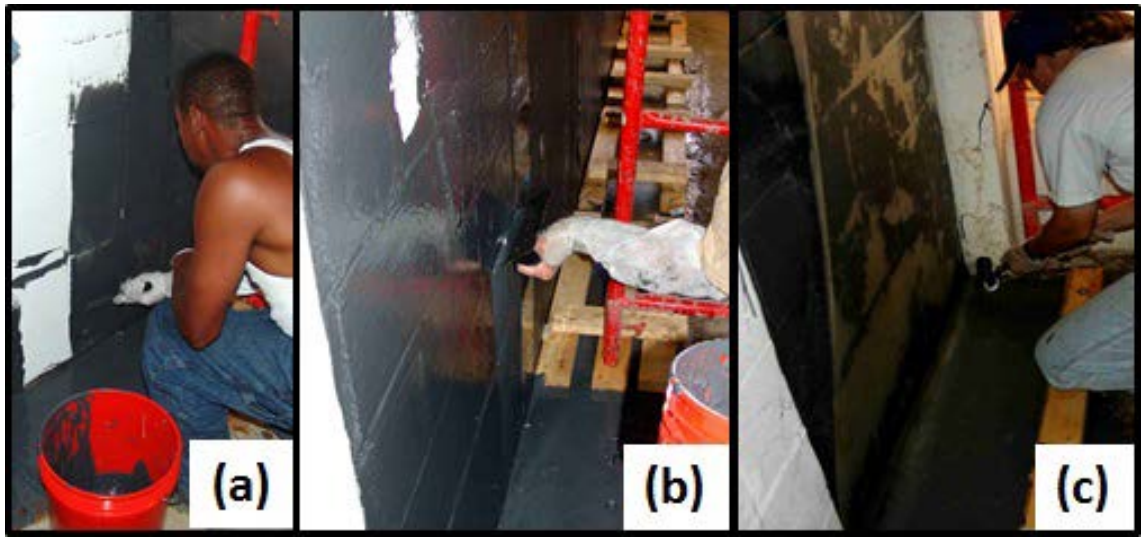

Figure 4.58. Epoxy application. (a) Flat trowel used to apply the epoxy. (b) Notched trowel used to control thickness. (c) Pressure applied using rubber roller to apply film.

4.7.3.6 Step 7: Film Application

The trowel-on material had a very short pot life, so the trowel-on application process had to move quickly in order to leave adequate time for film application. To prevent the trowel-on material from curing before the application of the film, only mixing and applying enough trowel-on material for each individual sheet was important (Figure 4.57). The primed side of the film was placed against the trowel-on material. The film was applied starting at the bottom support and moved up the wall (Figure 4.59c). The trowel-on epoxy takes longer to cure, so temporary braces were used on the top and bottom supports to keep the film in place until the bond was strong enough to maintain contact between the support surface and the film. The braces constructed from

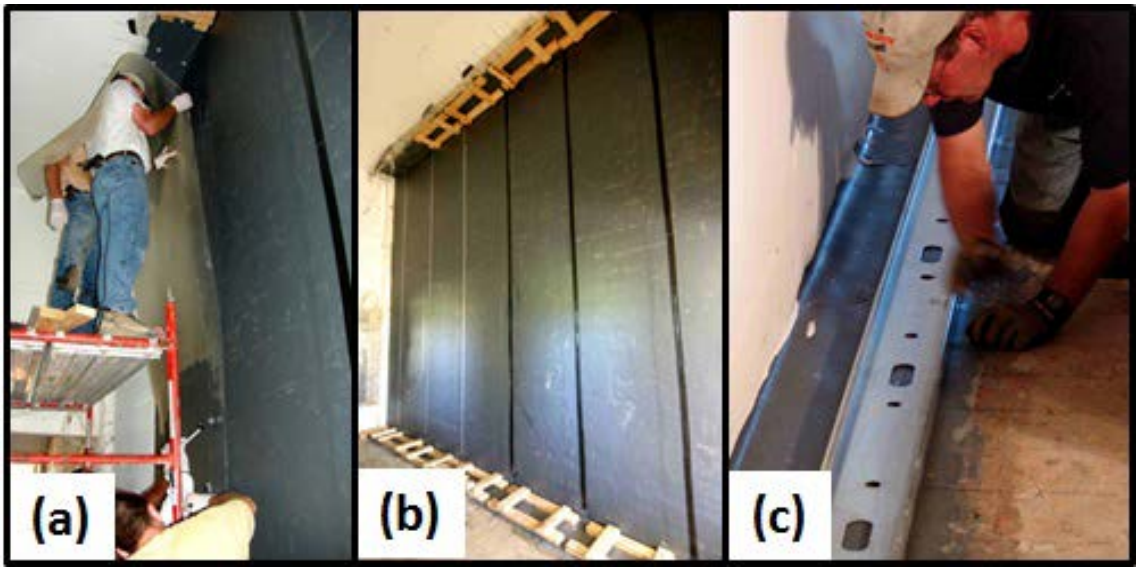

Figure 4.59. Final application steps. (a) Two people hold the film off the epoxy, while others apply pressure during installation. (b) Temporary braces at the supports and duct tape along the film seams were added until the epoxy cured. (c) Installation of a mechanical anchorage system.

dimensional lumber were built before the application process began. Each brace was the same width as the sheets of film, so a brace was installed as each sheet was applied. A ramset nail gun was used to secure the temporary braces to the top and bottom supports. The sides of the film also began to curl away from the wall surface, so duct tape was used to secure the seams. The duct tape and temporary supports were removed once the epoxy cured (Figure 4.59b). Applying the film from the bottom up anchored the film reducing film movement and redistribution of the trowel-on epoxy. Two people were responsible for holding the film away from the CMU wall (Figure 4.59a) while at least one person with a 3-in.- (7.62-cm-) wide rubber roller applied uniform pressure to the film material from the bottom support, up the wall, to the top support in one continuous application (Figure 4.59a). Normal CMU wall construction, with tooled joints and uneven placement of CMU blocks, limited the effectiveness of a wider roller. The formation of air bubbles under the film was avoided. However, if air bubbles were created, the roller was used to move the trapped air toward the sides or leading edge of the film. The amount of air bubbles formed under the film were minimized when the people holding the film away from the wall prevented the film from touching the wall until the person operating the roller initiated the contact. The person or people applying the pressure dictated the point of contact, speed, and progress of the application to minimize the formation of air bubbles. If pressure was applied at random locations on the wall instead of in a continuous motion, large air voids developed, and an inadequate bond between the epoxy and film material developed.

The amount of pressure applied to the wall was controlled by visual inspection of the grooves in the trowel-on material. As pressure was applied to the film using a roller or similar device, the trowel-on material was redistributed to form a smooth continuous layer under the film. If the grooves in the trowel-on material were visible, the pressure applied to the film was increased. If the block became visible through the film, too much pressure was applied.

4.7.3.7 Step 8: Mechanical Anchorage

Once the temporary braces were removed (Figure 4.59b), one of the four full-scale mechanical anchorage Systems 5 through 8 described in Section 4.3.3 was applied to the top and bottom supports (Figure 4.59c). The duct tape was removed after the mechanical anchorage was applied, and the elastomeric film was painted to improve the quality of the high-speed video footage.

4.8 Fiber-Reinforced Elastomeric Film with Trowel-on Epoxy Adhesive

The fiber-reinforced elastomeric film with trowel-on epoxy adhesive was used in subscale experiments SW15-SW16 and DW14 and full-scale experiment FS12. The full-scale reinforced elastomeric film evaluated in the research program was constructed using Fabric E encapsulated in an elastomeric film and required additional application procedures that were later removed from the process as more fiber-reinforced elastomeric films became commercially available. The only Aramid reinforcement available to researchers when the research program began had fiber bundles oriented at 0/90 deg. The fabric, which was provided on a roll, was shipped to a manufacturer to be encapsulated in a resin matrix. To facilitate a ±45-deg orientation on the wall,

researchers cut the pieces at angled lengths and applied them diagonally onto the wall surface (Figure 4.60a). The layout of the sheets was designed first, so that the appropriate lengths and forms of the film could be prepared, as illustrated in Figure 4.28. The material covered the entire wall surface and the top and bottom supports. The sheet layout was designed so that the longest piece would cross the wall surface from one corner to the other and be secured or mechanically anchored at both the top and bottom supports. The remaining sheets were only mechanically anchored at one support. Installers allowed a designated width of material to overlap 12 in. on the top and bottom supports to anchor the fabric, and each successive sheet of film overlapped the previous sheet by at least 8 in. Each fabric sheet was labeled to ensure proper placement on the wall.

4.8.1 Step 1: Wall and Support Preparation

In addition to the procedure outlined in Step 2 of Section 4.6.2 bracing was constructed and added to the structure before the retrofit materials were applied and the CMU wall was not painted. The trowel-on epoxy as seen in the previous retrofit system required time to set before it could maintain contact between the surfaces, and the initial version of the reinforced elastomeric film was heavier than planned, so temporary bracing was required during installation. The temporary bracing built with dimensional lumber was added to the reaction structure before the epoxy was mixed (Figure 4.60b). Enough space was left between the brace and the wall to apply the epoxy and the sheet of film. Plenty of shims of various thicknesses were ready to press the film against the wall.

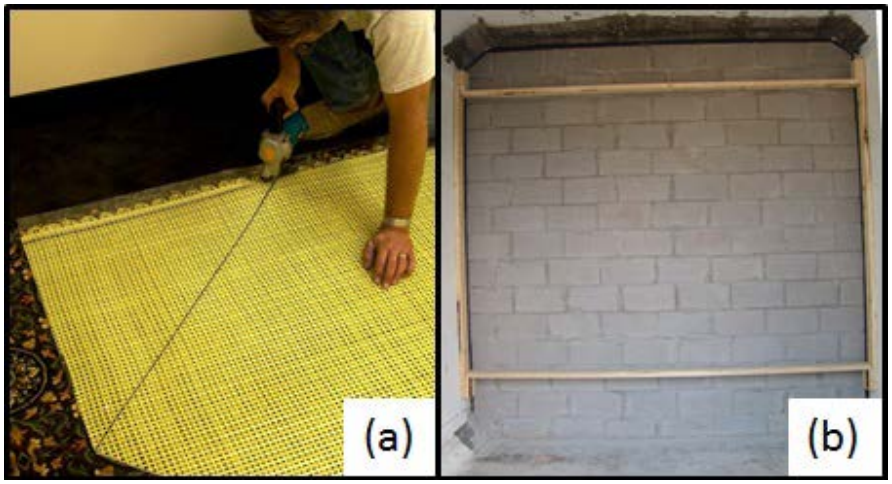

Figure 4.60. Items to prepare for installation. (a) Reinforced elastomeric film. (b) Temporary bracing installed.

4.8.2 Step 2: Mix Trowel-on Epoxy

The same epoxy utilized in Section 4.7.3 was used to apply this version of the fiber-reinforced film. Step 5 in Section 4.7.3.4 was repeated to mix the trowel-on epoxy. Only the quantity required was mixed to apply each sheet of film at one time. If the installers tried to mix enough material to cover the entire wall surface, they ran out of time before the film could be applied.

4.8.3 Step 3: Apply Trowel-on Epoxy

The same procedure and tools discussed in Step 6 of Section 4.7.3.5 were repeated. The only difference between the two procedures was the shape of the area covered. In Section 4.7.3.6, the film was applied in vertical strips, so rectangular sections of the wall were covered with each epoxy mix. For this system, triangular sections that mimic the shape of the fiber-reinforced sheets of film were coated with the epoxy (Figures 4.61a and b).

4.8.4 Step 4: Film Preparation

The same procedures used in Step 2 of Section 4.5.2 were used to prep the reinforced film for application to the wall.

Figure 4.61. Retrofit application. (a) Trowel-on material applied in triangular sections. (b) Applying trowel-on material for film sheet two. (c) Sheet 2 applied to wall. (d) Temporary bracing applying pressure to film until epoxy cured.

4.8.5 Step 5: Fiber-Reinforced Film Application

The epoxy had a very short pot life, so the application process had to move quickly to leave adequate time for film application. To prevent the trowel-on material from curing before the application of the film, only mixing and applying enough epoxy for each individual sheet was important (Figure 4.61b). The primed side of the film was placed against the trowel-on material. The film was applied starting at the bottom corner support and moved up the wall (Figure 4.61c). The trowel-on epoxy took longer to cure, so temporary braces were used to keep the film in place until the bond was strong enough to maintain contact between the support surface and the film (Figure 4.61d). The temporary supports were removed once the epoxy cured (Figure 4.62a). Two people

were responsible for holding the film away from the CMU wall, while at least one person with a 3-in.- (7.62-cm-) wide rubber roller applied uniform pressure to the film material.

The fiber-reinforced film used in this retrofit system required additional material to be applied along the overlap areas of each successive sheet. As illustrated by the arrows in Figure 4.62a, three additional 12-in.-wide strips of the fiber-reinforced film were cut to length and epoxied over the original four sheets of film used to cover the wall surface. This step was added based on the observations on site during the application process. Additional bracing was added to secure the additional strips of elastomeric film.

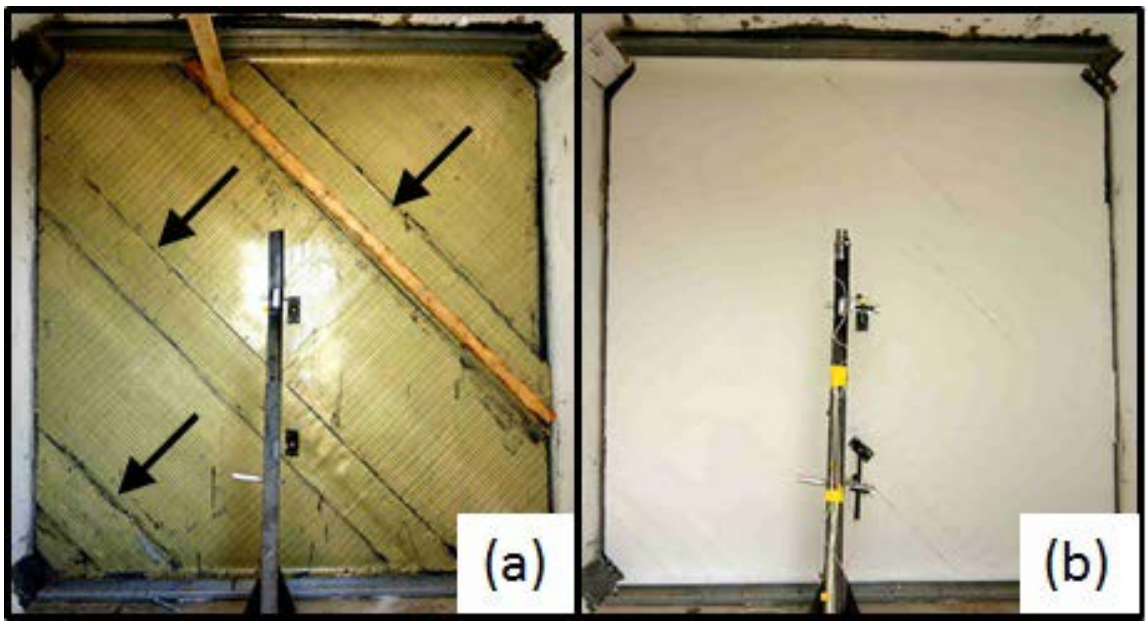

Figure 4.62. Retrofit complete. (a) Extra material added to reinforce seams. (b) Temporary braces removed and instrumentation and mechanical anchors installed.

4.8.6 Step 6: Mechanical Anchorage

Once the temporary braces were removed, one of the four full-scale mechanical anchorage Systems 5 through 8 described in Section 4.3.3 was applied to the top and bottom supports (Figure 4.62b). Only one sheet of film is mechanically anchored at the top and bottom support. Three of the four sheets ended on the side of the CMU wall and were only attached to the CMU wall through the adhesive strength of the epoxy material. The elastomeric film was painted to improve the quality of the high-speed video footage.

4.9 Elastomeric Films with PSAs

The retrofit procedure was simplified by replacing the trowel-on adhesive with a PSA in the final group of retrofit systems evaluated. PSAs were a cost-effective alternative to glues, rivets, mechanical fasteners, and spot welds. Rubber-, acrylic-, and silicone-based adhesives were considered during material selection (Figure 4.63a). Rubber-based adhesives were composed of natural or synthetic elastomers that became tacky by the addition of various resins. These were usually lower-cost adhesives that had good tack and shear properties and offered good adhesion to material with both high- and low-surface energy. Rubber-based adhesives were less suited for use under prolonged UV exposure, solvent contact, or elevated temperature conditions. Acrylic-based adhesives were usually more costly than rubber-based adhesives, but acrylic polymers could be compounded to have a good balance of tack, peel and shear. Acrylics were ideally suited for prolonged UV exposure and elevated temperatures while offering solvent resistance and long-term aging stability. However, they were less effective on materials with low-surface energy. Silicone-based adhesive systems combined the

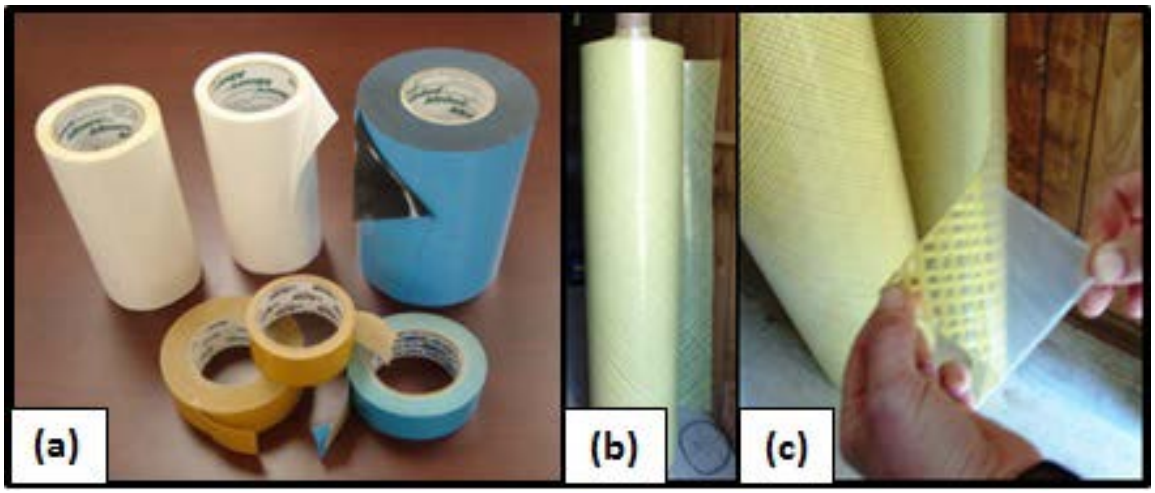

Figure 4.63. PSA. (a) The first group of PSAs considered for evaluation had to be applied to the films in the field. (b) Final retrofit material ±45-deg fiber-reinforced elastomeric film with PSA applied. (c) Protective backing removed to expose PSA.

flexibility of silicone rubber with the temperature resistance of silicone resin. They offered the widest service temperature range along with good resistance to a variety of solvents and to thermal/oxidative degradation. These systems had good adhesion to materials with low-surface energy, but exhibited lower tack and significantly higher cost compared to acrylics. Figures 4.63b and c show a retrofit material with a PSA applied.

Subscale walls SW17 and SW18 were the first walls to be retrofitted with a PSA. The PSA selected for these experiments was a 1-in.-wide, double-sided tape that was used to adhere the elastomeric films to the wall surface. Subscale walls SW19-SW20 and BLS4-BLS7 and full-scale experiments FS14-FS18 were retrofitted with elastomeric films adhered to the wall with a PSA that was purchased on a separate roll and applied to the elastomeric films in the field. Subscale experiments SW21-SW24 and BLS8-BLS11 were retrofitted with elastomeric films with a PSA that was applied to the films during

the manufacturing process, which removed the need to apply the adhesive to the film in the field. Both application processes are described in this section.

4.9.1 Rubber Adhesive

One of the first PSAs selected for evaluation in a full-scale experiment was a multi-purpose double-sided cloth tape advertised for carpet installation on interior floors and stairs of commercial aircraft and industrial mounting in machining processes. The construction of the tape consisted of a cotton cloth with reclaimed rubber adhesive. The tape was 13 mils thick and it delivered to the test site in 48-in.-wide rolls. The material was only used to retrofit one full-scale wall, FS14.

4.9.2 Acrylic Adhesive

PSA1 is a thick high-performance industrial material consisting of a high-tack, double-coated, acrylic-based adhesive on a clear polyester (PET) carrier film with a paper release liner. Each layer of the adhesive is 3.5 mils thick, the carrier film is 1 mil thick, and the release paper is 3.2 mils thick. The total thickness of the PSA is 8 mils, and with the release paper, the total thickness is 11.2 mils. The adhesive is advertised to have excellent bond strength to foams, rubbers, most plastics, metals, and low-surface energy materials. The material is conformable and ideal for rough surfaces where the requirements to fill gaps may be required. Performance advantages include instant bonds, conformability, easy-to-handle and safe, no messy clean-up or chemicals, uniform thickness, and consistent performance under stress and temperature changes. The elastomeric films were adhered to the CMU wall in subscale experiments SW19-SW20 and BLS4-BLS7 and full-scale experiments FS15-FS18 using PSA1.

4.10 Elastomeric Films with PSAs and Trowel-on Adhesive at Supports

4.10.1 Step 1: Safety Equipment

If a sand blaster is used during surface preparation along the supports, heavy-duty protective clothing, leather gloves, and a full-face shield with a fresh air supply must be worn. Safety glasses, gloves, and a respirator should be worn during the operation of a wire-wheel brush or grinder and when applying Primer 1 or Primer 4 to the supports. Safety glasses and gloves are not required for application of the elastomeric films but are recommended to be worn for general safety measures.

4.10.2 Step 2: Prepare Elastomeric Film

The CMU wall surface was measured, and two additional feet were added to the length of each sheet to cover the top and bottom supports. At least a 4-in. overlap to the previous sheet was factored into the design. The film sheets were cut to length using cutting shears or a sharp knife. A flat clean surface to apply the PSA was needed. The elastomeric film was stretched on a flat surface, then the PSA was unrolled onto the film. One person could hold the roll of PSA but using two people was easier as shown in Figure 4.64. The hardest part of this process was to keep the PSA and film straight. The third person applied pressure using a rubber roller to ensure contact between the PSA and film surface. The person applying pressure to the PSA to prevent or remove air bubbles from forming between the two materials was important.

4.10.3 Step 3: CMU Wall and Support Preparation

The ideal infill CMU wall for the film application was a smooth unpainted surface with no tooled or protruding mortar joints. A wall with tooled joints or painted was

Figure 4.64. Acrylic adhesive applied to the elastomeric film in the field.

acceptable, but all protruding mortar joints had to be removed. A masonry brick, wire brush, masonry chisel, or grinder could be used to remove the protruding mortar joints. The CMU wall surface and supports were clean, dry, completely cured, and free of dust, oil, wax, or grease.

4.10.4 Step 4: Film Application

To begin the film application measure, the first foot of material on each end of the sheet was folded down and secured. This material was used at the supports and was not applied to the support area until after the supports were primed and the trowel-on thermoset or epoxy had been applied. The film was folded over onto itself and secured with a piece of duct tape. The film was applied from the top of the wall to the bottom of the wall moving from one edge of the wall to the opposite edge (Figures 4.65a and b). Once all the sheets were applied, the material was secured at the top and bottom supports, respectively. It took at least two people to apply the film to the CMU wall

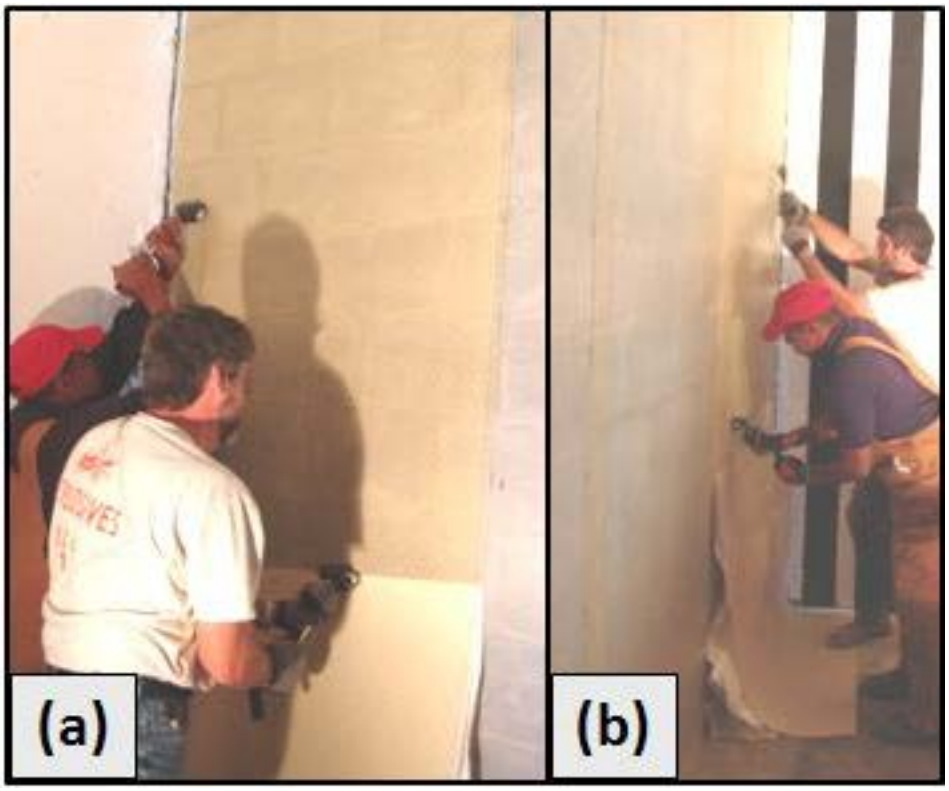

Figure 4.65. Film application. (a) Pressure applied to first sheet of film. (b) Each additional sheet overlaps the previous until the CMU wall surface is covered.

surface. The crew tore off one to two feet of the backing paper and pressed the film against the CMU wall surface. Additional pressure was applied using a rubber roller to ensure good contact between the film and wall surface. The rubber rollers were also used to push any air trapped between the film and wall surface to a free edge of the film. If too much of the backing paper was removed, the film touched the surface before the installers were prepared and made it very difficult to reposition the film once it touched the surface. If the film was repositioned, then part of the PSA might be lost resulting in a weak spot when the film was reapplied. Once the first sheet was applied to the wall

(Figure 4.65a), it was recommended that the installers measure and mark the overlap area on the previous sheet. This aided the installers to maintain a straight line as the second sheet was installed overlapping the first. This process continued until each sheet was applied. Each successive sheet overlapped the previous sheet by at least 6 in. (Figure 4.65b). This procedure was repeated until all of the film sheets were applied to the CMU wall surface.

4.10.5 Step 5: Priming the Supports and Elastomeric Film

The procedures discussed in Step 3 of Section 4.4.3 could be used to apply the primer to the top and bottom supports. It was recommended that a respirator be worn during the mixing and application of primers Primer 1 or Primer 4 (Figure 4.66a). A coat of the primer was also applied to the top and bottom sections of the film to enhance the adhesion between the film and the trowel-on material (Figure 4.66b). Only the 12-in.

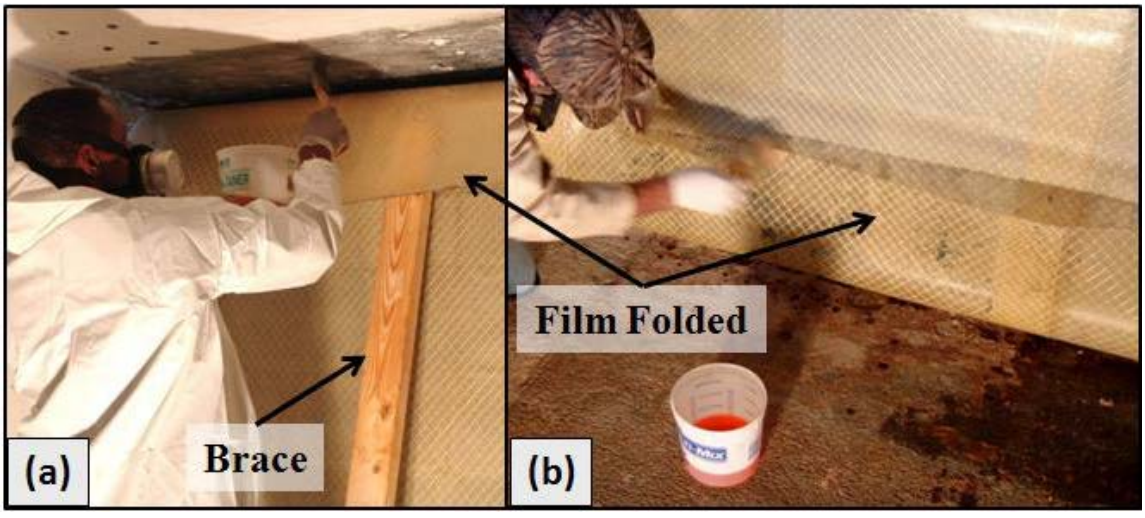

Figure 4.66. Primer application. (a) Applied to top support. (b) Applied to film surface and the bottom support.

area that will be applied to the support was covered, not the film area that touched the CMU wall. Temporary bracing was required while the supports were being primed and the trowel-on material was applied. A piece of dimensional lumber, as shown in Figure 4.66a, could be used to prevent the weight of the elastomeric film from peeling the material away from the wall surface.

4.10.6 Step 6: Apply Trowel-on Adhesive to Supports

The tools required to apply the trowel-on adhesive at the supports included a drill mixer, paddle wheel attachment, mixing cups, flat and notched trowels, modified putty knife, shears, knife, and a rubber roller. If a trowel-on thermoset was applied as the adhesive at the supports, the coverage of the material, resin preparation, mixing process, and pot-life discussed in Steps 4 to 7 from Sections 4.6.4 to 4.6.7 were used. If a trowel-on epoxy was applied to the supports, the mixing procedure discussed in Step 5 from Section 4.7.3.4 was followed. The application procedure in Step 6 of Section 4.7.2.6 was used to apply the trowel-on materials. The trowel-on material was applied to the top support first (Figure 4.67a) then to the bottom support (Figure 4.67b). If the material was applied to the bottom support first, the installers might damage the film or squeeze the trowel-on material by placing a scaffold wheel or ladder leg on the material. Once the trowel-on material was applied, the duct tape securing the elastomeric film was removed (Figure 4.67b), and pressure was applied using a rubber roller to secure the film to the supports (Figure 4.68a). Enough pressure was applied to create a smooth surface and to remove any trapped air beneath the film. When rolling the top and bottom supports, the installer started from the film edge and moved toward the corner (Figures 4.68b and c).

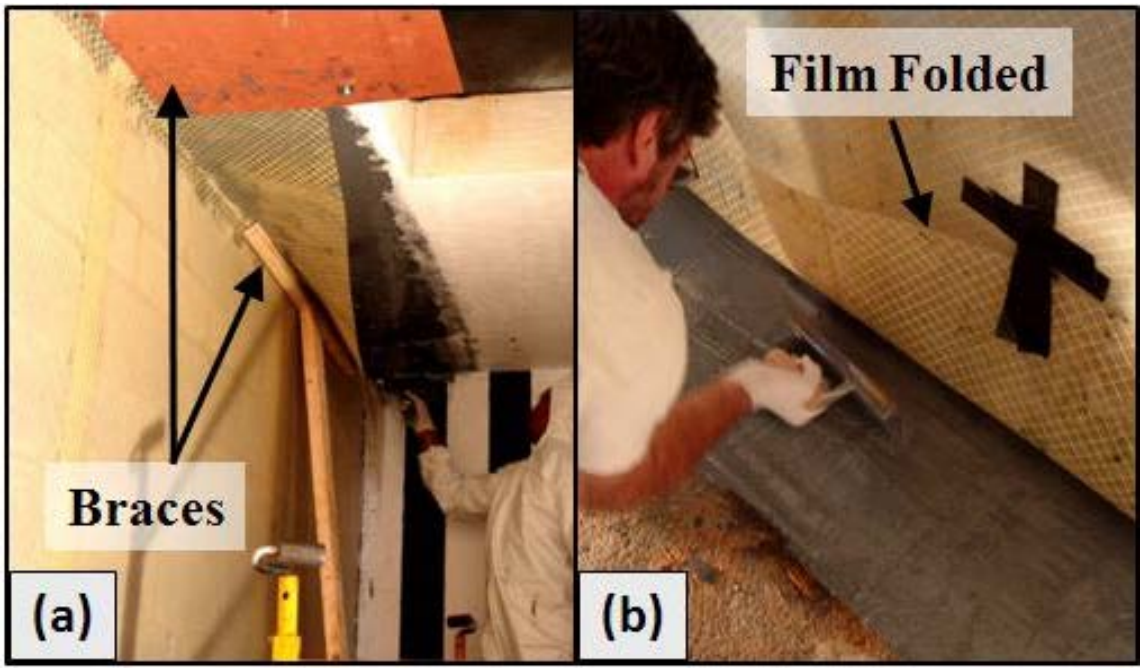

Figure 4.67. Trowel-on application at supports. (a) Epoxy applied to top support while braces secure the film to the support. (b) Notched trowel used to apply epoxy at desired thickness while film secured by duct tape.

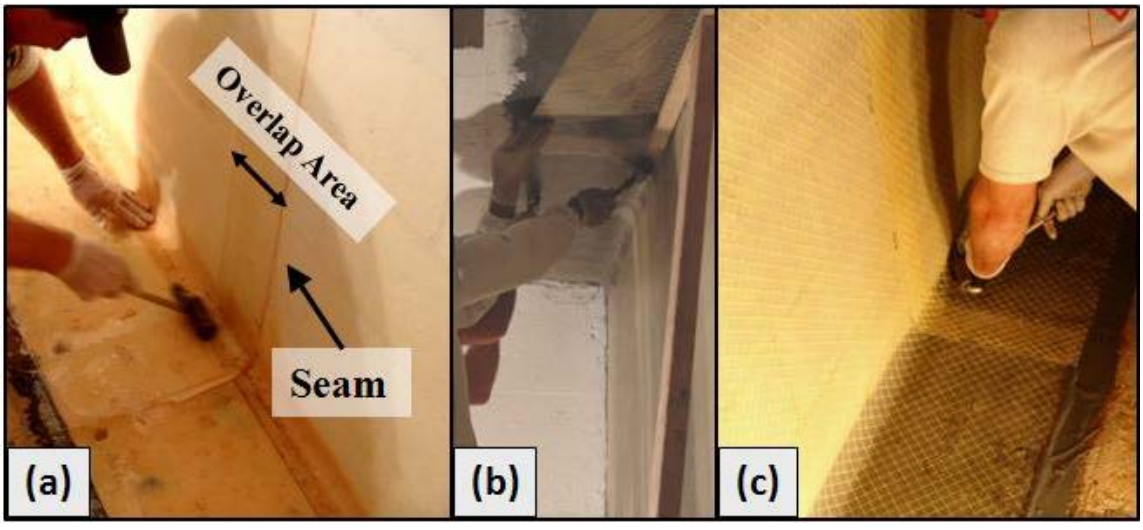

Figure 4.68. Film application. (a) Rubber roller used to apply pressure to the support. (b) Pressure applied to secure the film to the top support. (c) Film applied to bottom support.

This pushed the excess material into the corner where it could be used to fill voids. If the installer moved from the corner of the wall and support interface to the end of the film, the material would be squeezed out of the film area, which could result in a coat of trowel-on material that was too thin. If the trowel-on material was squeezed from under the film, it could not be replaced, because it would be too difficult to pull the film sheet away from the support without disturbing other areas. Temporary bracing was required until the final mechanical anchorage system was completed (Figure 4.67a.).

4.10.7 Step 7: Mechanical Anchorage at Supports

Depending on the wall scale, one of the anchorage systems described in Section 4.3.3 was used to secure the retrofit material. For full-scale walls, System 7 or 8 would be the least evasive to complete the retrofit system. As shown in Figure 4.69a, the mechanical anchorage system could be applied over the temporary bracing. The mechanical anchorage was applied to the top support first (Figure 4.69b) and then to the bottom support (Figure 4.69c).

4.11 Fiber-Reinforced Elastomeric Film with PSA

The trowel-on adhesive was removed from the system as the development of the PSA evolved. The final retrofit system that was evaluated did not require the use of a trowel-on adhesive along the top and bottom supports. The retrofit system consisted of three materials, i.e., a primer applied directly to the CMU wall and reaction structure supports, an elastomeric film, and two thin-wall steel channels. The tools required to install the final retrofit system consisted of a paint roller, shears/knife, laminate roller, a ramset nail gun, and charges and fasteners for the nail gun. If a ramset nail gun was not

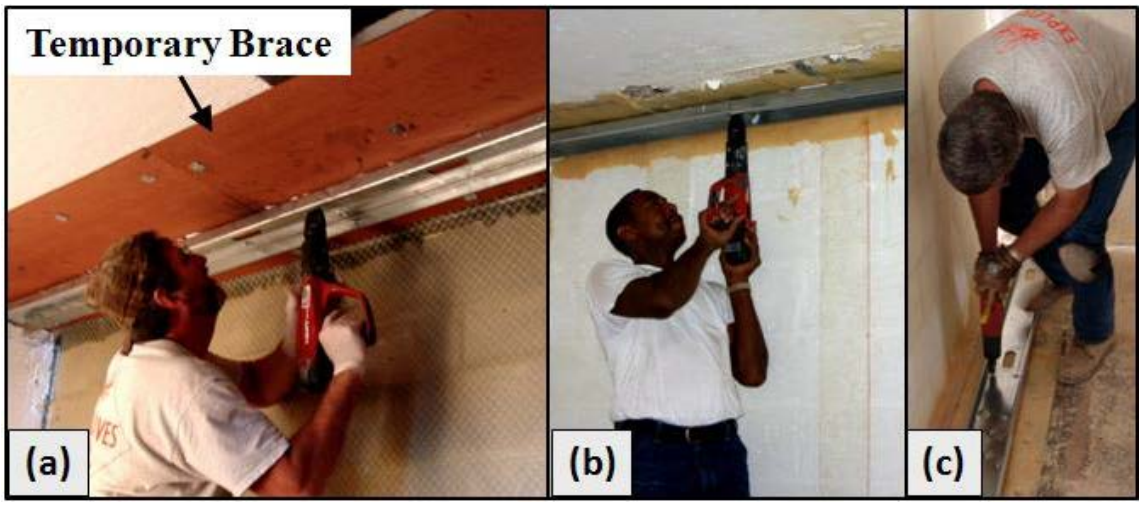

Figure 4.69. Anchor plate. (a) Mechanical anchorage placed over temporary bracing. (b) Ramset and nails used to secure thin steel stud channel to top support. (c) Bottom support secured completing anchor System 8.

available, a drill, bit, wrench, and small anchor bolts could be used to anchor the steel stud channel to the reaction structure.

4.11.1 Step 1: Safety Equipment

No safety equipment was required, but it was recommended that personnel always wear safety glasses and gloves.

4.11.2 Step 2: Film Preparation

The elastomeric film was packaged in rolls approximately 48 in. wide. The film was cut using shears or a knife into full width sheets with lengths equal to the height of the wall plus 24 in. for the top and bottom supports. At least an 8-in. overlap to the previous sheet was factored into the design.

4.11.3 Step 3: CMU Wall and Support Preparation

Step 2 was repeated in Section 4.7.2.2 for the CMU wall and support preparation. At a minimum, the support surface should be cleaned. The steel frame used to evaluate the subscale retrofits in the HTC was wiped with denatured alcohol before moving to Step 3 (Figure 4.70a).

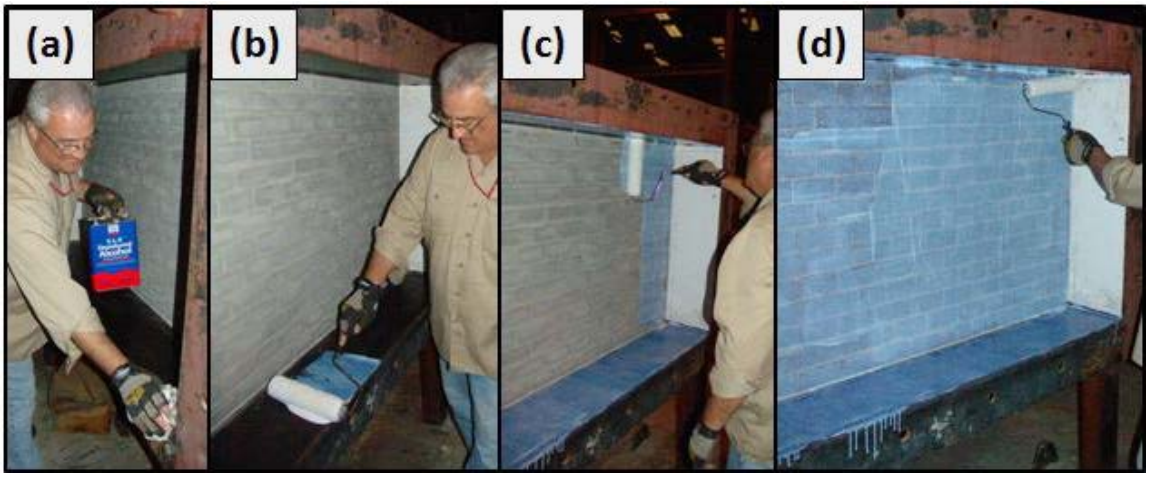

Figure 4.70. Primer application. (a) Cleaning the support surface with denatured alcohol. (b) Primer applied to supports. (c) Primer applied to CMU wall surface. (d) Primer applied to top support.

4.11.4 Step 4: Priming the CMU Wall Surface

The final retrofit system evaluated used a roll-on primer, Primer 5, applied directly to the CMU wall surface and the supports (Figures 4.70b and c). The primer was applied to the wall surface using a standard paint roller. The primer was allowed to cure for a minimum of 15 min until the surface became tacky to the touch. The primer could be applied up to 24 hr before the application of the film, but the wall surface was checked

before moving to Step 4. If the primer surface was no longer tacky, a new layer of primer was applied (Figure 4.70d).

4.11.5 Step 5: Film Application

The film sheets were applied from one side of the wall to the other overlapping each sheet by 8 in. The film was applied to the top support first then down the surface of the CMU wall to the bottom support (Figures 4.71a and b). Getting the film to fit tightly into the corner was difficult, so installers found it easier to fold the material at the point where the top support and CMU wall intersected, mark it with a straight line, and apply the material along the marked line into the corner first, and then apply pressure to apply it to the top support. About a foot or two of the backing paper was removed as the film was applied to the CMU wall surface (Figure 4.71c). If too much was removed, the film may have touched the surface before the installers were prepared, and to reposition the film once it had touched the surface was very difficult. If the film was repositioned, a chance existed that part of the PSA would be lost resulting in a weak spot when the film was repositioned. Once the first sheet was applied to the wall (Figure 4.72a), the installers measuring and marking the overlap area on the previous sheet was recommended. This aided the installers to maintain a straight line as the second sheet was installed overlapping the first (Figures 4.72b and c). This procedure was repeated until the entire CMU wall surface had been covered.

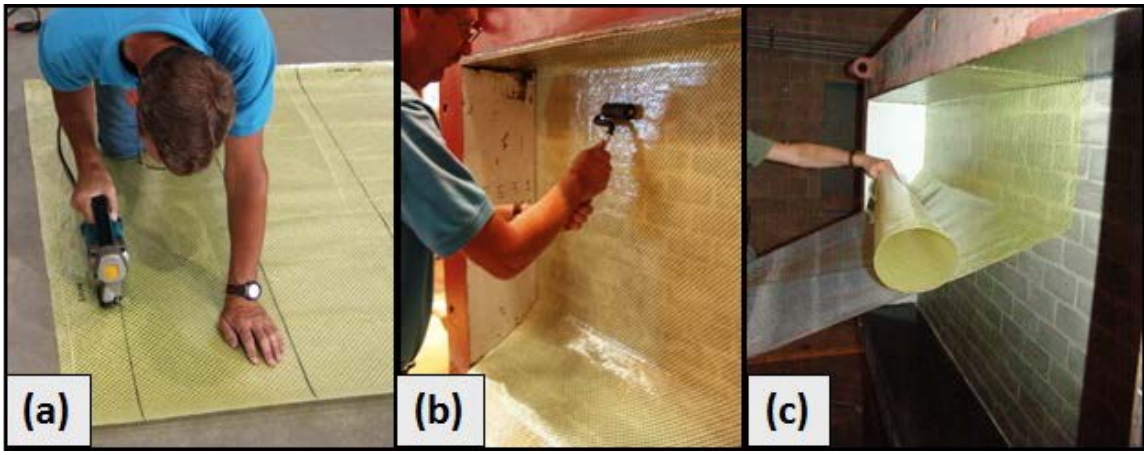

Figure 4.71. Reinforced film. (a) Film cut to size using mechanical shears. (b) Rubber roller used to apply pressure to film. (c) Backing paper removed as film application continued.

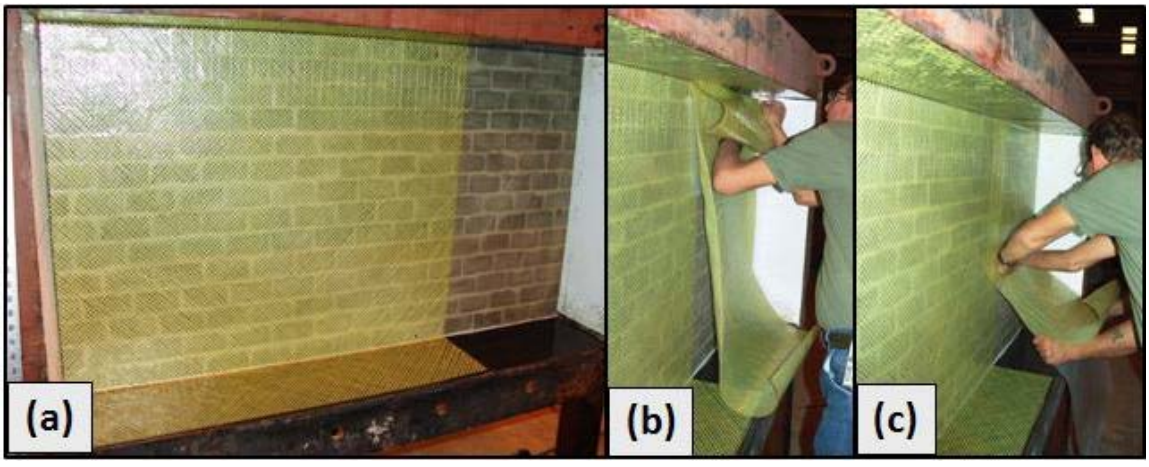

Figure 4.72. Film application. (a) First sheet has been applied. (b) Fold material at corner support to get tight fit. (c) Final sheet of film applied to wall surface.

4.11.6 Step 6: Mechanical Anchorage at Supports

Depending on the wall scale, one of the anchorage systems described in Section 4.3.3 was used to secure the retrofit material. For full-scale walls, System 7 or 8 was the least evasive to complete the retrofit system.

4.12 Test Matrix for Retrofit Material Systems

The experimental program consisted of static and dynamic experiments used to evaluate the global response of the retrofitted CMU walls. The subscale static experiments were conducted first, followed by subscale and full-scale dynamic experiments. HE field experiments and the BLS, a compressed gas driven shock tube, were used to evaluate the subscale retrofitted walls in the dynamic experiments. Candidate materials that performed well in the subscale experiments were selected for evaluation in a full-scale HE event. Full-scale HE experiments were used to validate the subscale experiments and provided a final evaluation of the retrofit materials/systems. Dynamic experiments are vital to the characterization of the retrofit materials, since most of the materials evaluated in the program are highly dependent on the loading rate.

The test matrix identifying the application techniques and material genres evaluated in the static and dynamic experiments are listed in Table 4.7, as well as the number of experiments conducted to evaluate the response of each wall retrofit. The results from each of the experimental procedures shown in Table 4.7 are discussed in Chapters 5 to 7.

Table 4.7. Wall retrofit test matrix.

	Static	Dynamic			
	Subscale	Subscale			Full-Scale
		HE BBTS		BLS	HE
Retrofit Method	HTC	Concrete	Steel	Steel	Concrete
Baseline Wall with no Retrofit	2	0	2	2	2
Spray-on Polyurea	2	1	2	0	0
Spray-on Polyurea with Fiber Reinforcement	7	1	6	0	3
Trowel-on Thermoset	3	2	0	0	3
Trowel-on Thermoset with Elastomeric Film	3	1	1	1	4
Trowel-on Thermoset with Fiber-Reinforced Elastomeric Film	1	0	0	1	1
Elastomeric Film w/PSA	3	0	0	2	3
Fiber-reinforced Elastomeric Film w/PSA	3	0	0	2	2

5. SUBSCALE STATIC EXPERIMENTS*

The global response of the subscale, hollow, unreinforced CMU walls retrofitted with the materials and application techniques discussed in Chapter 4 was evaluated using the HTC, which was designed and constructed to test conventionally constructed walls in the upright/vertical position (Figure 5.1). The HTC determined the physical response of 27 subscale unretrofitted and retrofitted CMU walls loaded at a steady and slow rate. The material's strain rate can be used to quantify or define the load as static or dynamic. Strain rates on the order of 10^{-4} sec^{-1} are regarded as "static" loading conditions (Ugural and Fenster 1995). The HTC was used to obtain quantitative data in the form of resistance functions from the static experiments for use in the dynamic analysis in Chapter 8. The resistance functions developed through the use of most static wall test apparatus, such as vacuum chambers or air bags, do not provide data beyond the first crack of the CMU wall due to the brittle and dynamic nature of the CMU wall failure. "The HTC used an incompressible fluid (water) to create the pressure load, which allowed the user to capture the complete loading cycle, including the first crack of the CMU wall, failure of the CMU wall, and post-crack behavior including the tensile membrane response of the retrofit systems" (Johnson, Davis, Coltharp, Durst, and Smith 2010).

*Part of this chapter is reprinted with permission from *X-Flex™ Retrofit: Results from Subscale Static and Dynamic Experiments*, by Johnson, Carol F., James L. Davis, David L. Coltharp, Bartley P. Durst, and Lonnie L. Smith, 2010, U.S. Army Engineer Research and Development Center, Vicksburg, MS. Due to "Limited Distribution" statement, the material was adapted for public release.

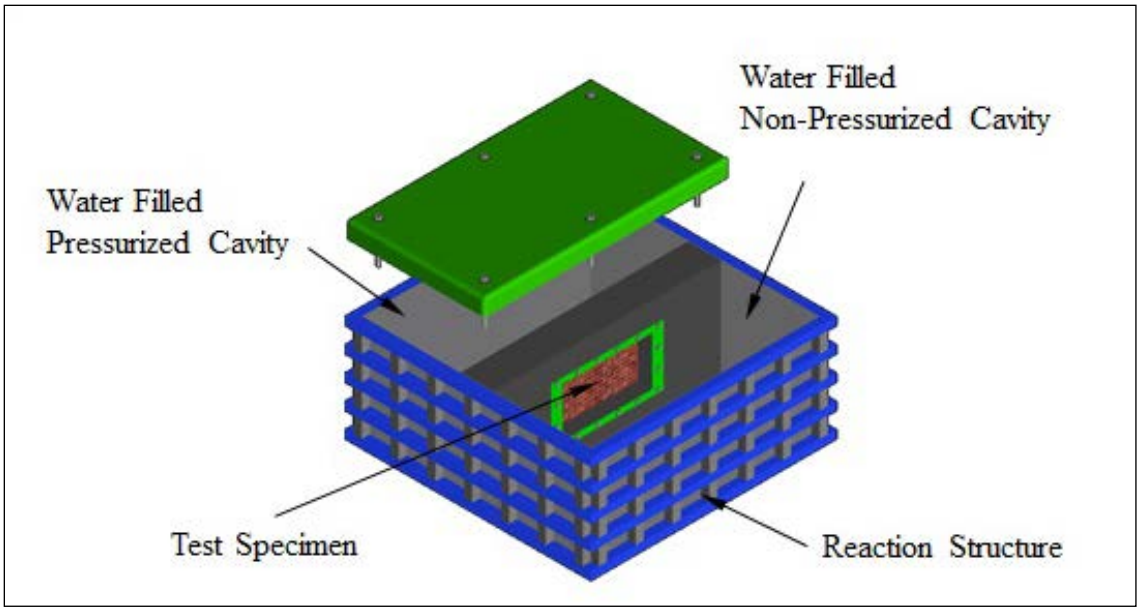

Figure 5.1. Static test chamber for subscale CMU wall experiments. (Adapted from Johnson, Davis, Coltharp, Durst, and Smith 2010)

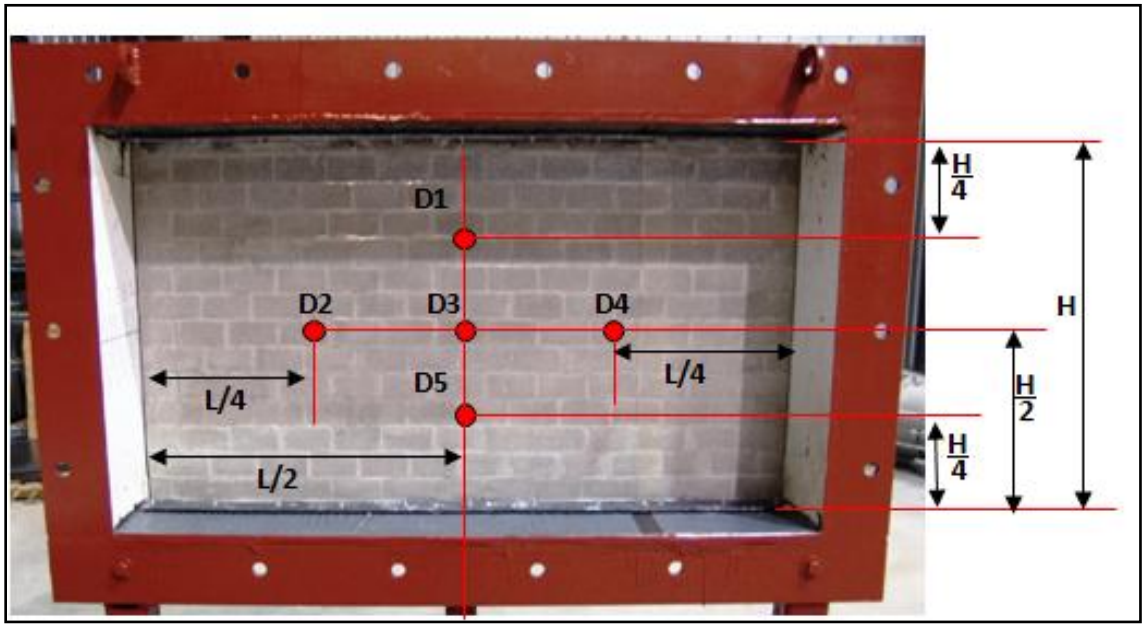

Figure 5.2. Deflection gauge locations for static experiments. (Johnson, Davis, Coltharp, Durst, and Smith 2010)

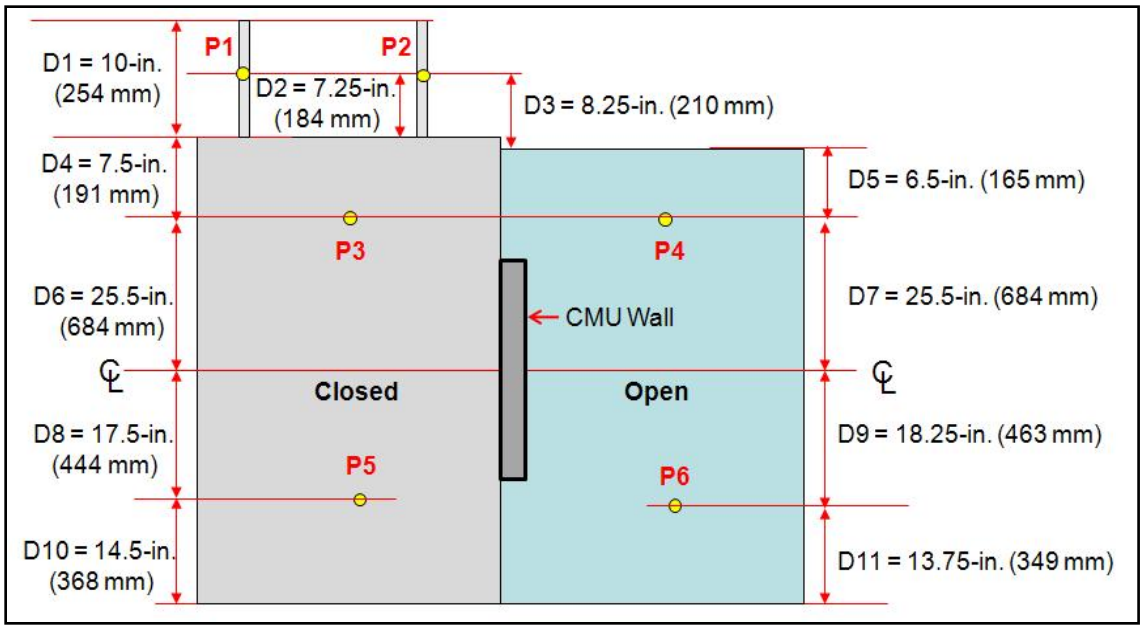

Figure 5.3. HTC: pressure gauge locations.

The instrumentation plan for the static experiments, as shown in Figures 5.2 and 5.3, consisted of five deflection gauges (D1-D5), three to six pressure gauges (P1-P6), still photography, and a normal-speed video camera above and below the water line. UniMeasure Model PA-20 and PA-30 precision potentiometers (deflection gauges) were used to monitor the response/lateral deflection of the wall during the loading process. Three deflection gauges (D2, D3, and D4) were located along the mid-height of the wall, and two deflection gauges (D1 and D5) were placed along the vertical centerline to verify one-way action. The deflection gauges were initially housed outside the exterior wall of the open chamber, and the wire potentiometers were fed through a hole in a rubber pad used to cover the holes in the HTC. This allowed the wire gauges to be set up directly in line with the wall deflection points. However, the excessive deformation of

the walls created a binding condition in the wall, so the deflection gauges were relocated on a bar sitting across the open chamber. The wire from the potentiometers was fed through eyehooks and attached to the wall at the necessary deflection points. The Kulite Models XTM-190SG and XTL-140 pressure gauges were peizo-resistive transducers used to monitor the water pressure in the two chambers. Four pressure gauges (P1-P2, P3, and P5) were used to monitor the water pressure in the closed chamber, and two pressure gauges (P4 and P6) were used to monitor the hydrostatic pressure in the open chamber. Initial experiments conducted in the test chamber only used two pressure gauges, P1 and P2, located in the relief pipes on the pressure chamber lid; gauges P3 and P4 were added at a later date to capture additional pressure data, and finally gauges P5 and P6 were added before the end of the test series to allow the pressure on the specimen to be monitored while the two water chambers were filled.

> Appropriate corrections to the raw data were made to account for the differential head from the pressurized cavity to the non-pressurized cavity of the chamber. The raw data from the multiple pressure gauges were used to determine the magnitude of the pressure exerted on the center of the test specimen. All of the data were transmitted over 22 American wire gauge (AWG) 4 conductor shielded mil spec cable and were recorded on 12-bit bipolar Pacific Instruments, Model 9830, Transient Data Recorders (TDRs). Technicians amplified and conditioned the signal using ERDC built instrumentation. The TDRs' sample rates were set for 16,384 msec per point for the pressure and deflection measurements, yielding a maximum recording time of 31 minutes (Johnson, Davis, Coltharp, Durst, and Smith 2010).

Fluid pressure is defined as the measure of the force per-unit-area exerted by a fluid that acts perpendicular to all surfaces of contact, since no shearing stresses are present. Pressure measurements can be divided into three different categories: absolute pressure, gauge pressure, and differential pressure. Absolute pressure, P_{abs}, is the total pressure,

which is the difference between the pressure at a given point in a fluid and the absolute zero pressure or perfect vacuum. Gauge pressure, P_{gauge}, is the difference between the absolute pressure and the local atmospheric pressure. Atmospheric pressure, P_{atm}, is the pressure caused by the weight of the earth's atmosphere. The standard atmospheric pressure at sea level is 14.7 psi or 101 kPa absolute. Differential pressure is simply the measurement of one unknown pressure relative to another unknown pressure.

Since the two separate containers shared a common surface, namely, the test specimen, the differential pressure was calculated. The fluid pressure exerted on the test specimen was measured in both containers. The differential pressure at the centerline of the specimen was calculated and used to develop resistance functions for each of the retrofit systems. Each compartment had at least one pressure gauge to monitor any changes in the fluid pressure. The fluid used in the tanks (water) had a specific weight, γ, of 62.4 pcf (9.81 kN/m^3). Once the open container was filled, it was in a static state. The pressure is zero at the upper surface and will vary linearly with depth, *h*, until it is equal to γh at the bottom. Therefore, the absolute pressure in a static fluid at any given depth, *h*, can be calculated using the equation:

$$P_{abs} = P_{atm} + \gamma h \tag{5.1}$$

The differential pressure acting on the wall was calculated using the gauge pressure measured in the closed container minus the absolute pressure measured in the open chamber. The differential pressure was plotted with the measured deflection to develop resistance functions for each retrofit system. The following Equations 5.2 to 5.9 were

used to calculate the pressure at the centerline of the wall, P_{CL} , using the listed pressure gauges. In Equations 5.2 and 5.5 measurements from P1 or P2 are used as P.

$$P_{CL} = P + 0.2979\,psi \tag{5.2}$$

$$P_{CL} = P3 - 0.2347\,psi \tag{5.3}$$

$$P_{CL} = P3 - P4 \tag{5.4}$$

$$P_{CL} = P - P4 + 0.5326\,psi \tag{5.5}$$

The quantitative data obtained from the static experiments were used to develop a global relationship (resistance function) between the load and displacement of the structural element. The resistance function for each retrofitted wall provides a definition of the resistance (internal force attempting to restore the component to its original position) of the wall as a function of displacement. The relationship (load vs. deflection) represents the internal potential strain energy of the element.

Several key areas on the resistance function (Figure 5.4) were used to characterize, evaluate, and compare the various retrofit material systems used to retrofit the CMU walls. The first area of interest was the initial slope (Region 1) of the load - deflection curve up to the point of ultimate flexural resistance or failure of the CMU wall, as shown in Figure 5.4. The second point of interest was the wall response at ultimate flexural resistance, which represents the brittle failure of the CMU wall. This point (labeled Point 2 in Figure 5.4) was easily recognized by finding the location of the first peak. The third area of interest was the tensile membrane response of the retrofit system being evaluated on the CMU wall identified as Region 3 in Figure 5.4. These data are captured once the CMU wall has failed, the pressure has equalized, and the retrofit system began to carry

the load until complete failure of the retrofit system occurred. The final area of interest, Point 4, was the ultimate tensile membrane resistance defined by the maximum pressure and deflection captured by the gauges during the experiment (Johnson, Davis, Coltharp, Durst, and Smith 2010).

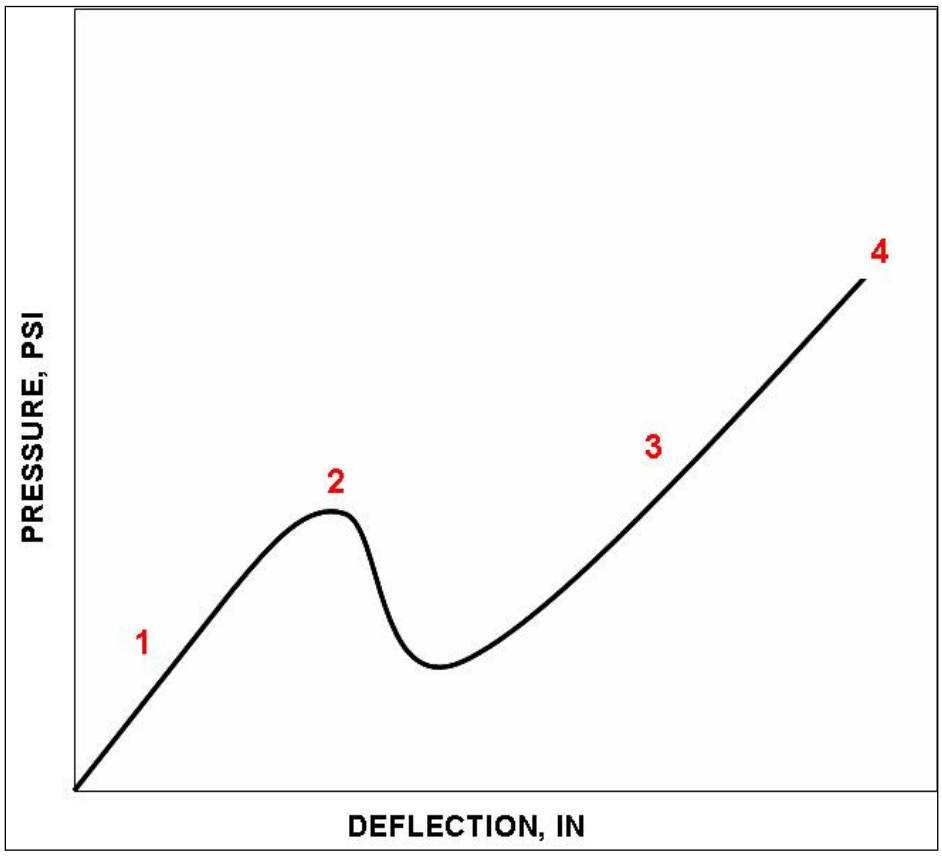

Figure 5.4. Sample resistance function displaying areas of interest. (Johnson, Davis, Coltharp, Durst, and Smith 2010)

In addition to the quantitative description of the response provided in the form of the resistance function, a qualitative description of the physical response of each retrofitted wall was provided. The seven failure modes observed during the execution of the CMU walls and retrofit systems were documented. The different failure modes observed during the execution of the experiments included a tear in the retrofit materials at the

mid-span, shear in the retrofit materials at top, bottom, or both supports, peel-back of the retrofit material at top, bottom, or both supports, failure by deformation of the film at the seams, or failure of the HTC by membrane failure. The HTC test matrix and failure modes for each experiment are provided in Table 5.1. The standard operating procedure developed during execution of the experimental program is provided in Appendix C.

5.1 Trial 1

The first subscale experiment conducted in the HTC was performed to establish testing protocols. The wall retrofit consisted of a spray-on aerosol adhesive, Fabric C applied with the fibers oriented at 0/90 deg, and four passes of the Grade 1 spray-on polyurea. The over-the-counter aerosol spray-on adhesive was sprayed on the wall first; then Fabric C was applied to the wall surface with a 2-in. overlap on the top and bottom supports. A layer of spray-on polyurea was applied over the reinforcement to cover the wall. The spray-on polyurea was also allowed to overlap the top and bottom supports by 2 in. creating an adhesive bond. Anchorage at the top and bottom support relied solely on the adhesive strength of the spray-on polyurea.

The wall failed very early in the loading process. When the wall reached a deflection of 2 in., the retrofit layer peeled away from the top support moving from right to left (Figures 5.5a and b). Based upon the results from this trial experiment, several procedures were changed. First, the aerosol spray adhesive was no longer used to adhere the reinforcement to the wall and to prevent a peel back failure; the area of overlap on the top and bottom supports was increased from 2 to 12 in. Additional information regarding the mechanical anchorage systems used was provided in Section 4.3.3.

Table 5.1. Test matrix for HTC.

Wall	Matrix	Fiber Reinforcement	Failure Mode
Trial 1	Spray-on Polyurea Grade 1	Fabric C at 0/90 deg	5
Base1	None	None	1
Base2	None	None	1
SW1	Spray-on Polyurea Grade 1	None	1
SW2	Spray-on Polyurea Grade 1	None	2
SW3	Spray-on Polyurea Grade 2	None	1
SW4	Spray-on Polyurea Grade 2	Fabric A at 0/90 deg	2
SW5	Spray-on Polyurea Grade 1	Fabric C at ±45 deg	5
SW6	Spray-on Polyurea Grade 1	Fabric A at ±45 deg	3
SW7	Spray-on Polyurea Grade 2	Fabric A at ±45 deg	3
SW8	Spray-on Polyurea Grade 2	Fabric B at ±45 deg	5
SW9	Spray-on Polyurea Grade 2	Fabric B at ±45 deg	2
SW10	Trowel-on Thermoset Grade 1	None	2
SW11	Trowel-on Epoxy	None	1
SW12	Trowel-on Epoxy	None	1
SW13	Trowel-on Thermoset & Thermoplastic Film	None	2
SW14	Trowel-on Epoxy & Elastomeric Film	None	2
SW15	Trowel-on Epoxy & Elastomeric Film	Fabric B at ±45 deg	6
SW16	Trowel-on Epoxy & Elastomeric Film	Fabric B at ±45 deg	1
SW17	Polyurethane Film	None	6
SW18	Spray-on Adhesive and Thermoplastic Film	None	2
SW19	PSA & Elastomeric Film	None	6
SW20	PSA & Elastomeric Film	None	2
SW21	PSA & Polyurethane Film	None	2
SW22	PSA & Polyurethane Film	Fabric G at ±45 deg	7
SW23	PSA & Polyurethane Film	Fabric G at ±45 deg	7
SW24	PSA & Polyurethane Film	Fabric G at ±45 deg	7

Failure Mode: (1) Tear at mid-span; (2) Shear at top support; (3) Shear at bottom support; (4) Shear at both supports; (5) peel-back failure at supports; (6) Membrane failure, (7) Failure by deformation at the film seams.

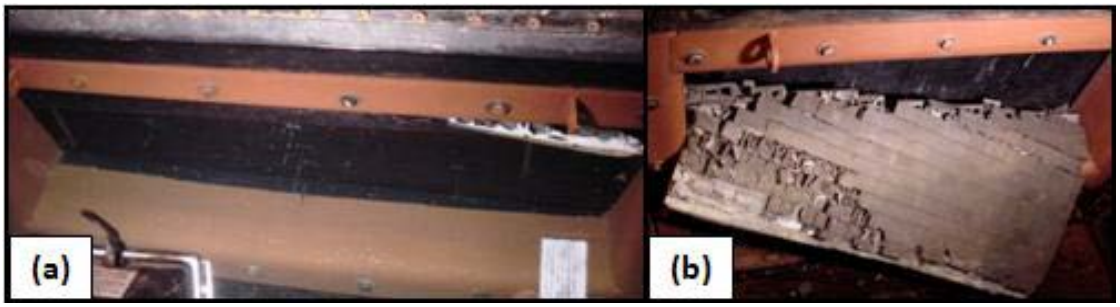

Figure 5.5. Trial 1. (a) Failure began at top support. (b) Complete failure of the retrofit material at the top support.

5.2 Baseline/Unretrofitted CMU Wall (BASE1-BASE2)

5.2.1 BASE 1

The first baseline or hollow, unreinforced, and unretrofitted CMU wall tested in the HTC was so weak that the wall failed before the relief valves could be closed and the data acquisition system started. The water in the two chambers reached the top of the open chamber before the wall failed; so, the hydrostatic pressure applied to cause failure of the wall was created within the 11-in. height difference between the top of the open chamber and the top of the relief valves. The maximum hydrostatic pressure at the point the relief valves are closed is equal to 0.4 psi, which implies that the Base 1 wall failed at a pressure between 0 and 0.4 psi. When the wall failed, it broke into four sections. The bottom course constructed in a mortar bed remained in the test frame (Figure 5.6) and the top section of the wall, where the blocks were grouted in around the dowels, lodged in the top of the steel reaction frame. One section of blocks fell onto the bottom flange of the steel frame and the remaining section of blocks fell onto the floor of the open test chamber.

Figure 5.6. Posttest view of wall debris in chamber.

5.2.2 BASE 2

The execution of the first baseline CMU wall experiment, Base 1, identified a faulty test setup in the HTC apparatus. Changes to the test apparatus and operating procedure were incorporated into the test plan before the second baseline CMU wall test, Base 2, was executed. First, additional pressure gauges, P3-P6, were placed in the walls of the open and pressurized chamber; so, the hydrostatic pressure could be monitored as the water filled the two chambers eliminating the potential loss of data due to early failure of the wall. The data acquisition system in Base 1 was never started, because the standard operating procedure at that time was to start the data acquisition system when the relief valves were closed. To prevent this failure from occurring in the remaining experiments (Step 23 in the Standard Operating Procedure in Appendix C), the data acquisition system was started when the water reached the bottom of the test specimen which is nominally the height of pressure gauges P5 and P6.

The baseline CMU wall once again failed very early during the experiment; however, due to the changes in the test procedure data was collected. Once the wall cracked the blocks begin to deflect and rotate at the mortar joints and the wall continued to resist pressure up to a maximum pressure of 0.035 and a deflection of 0.0276 (Figure 5.7).

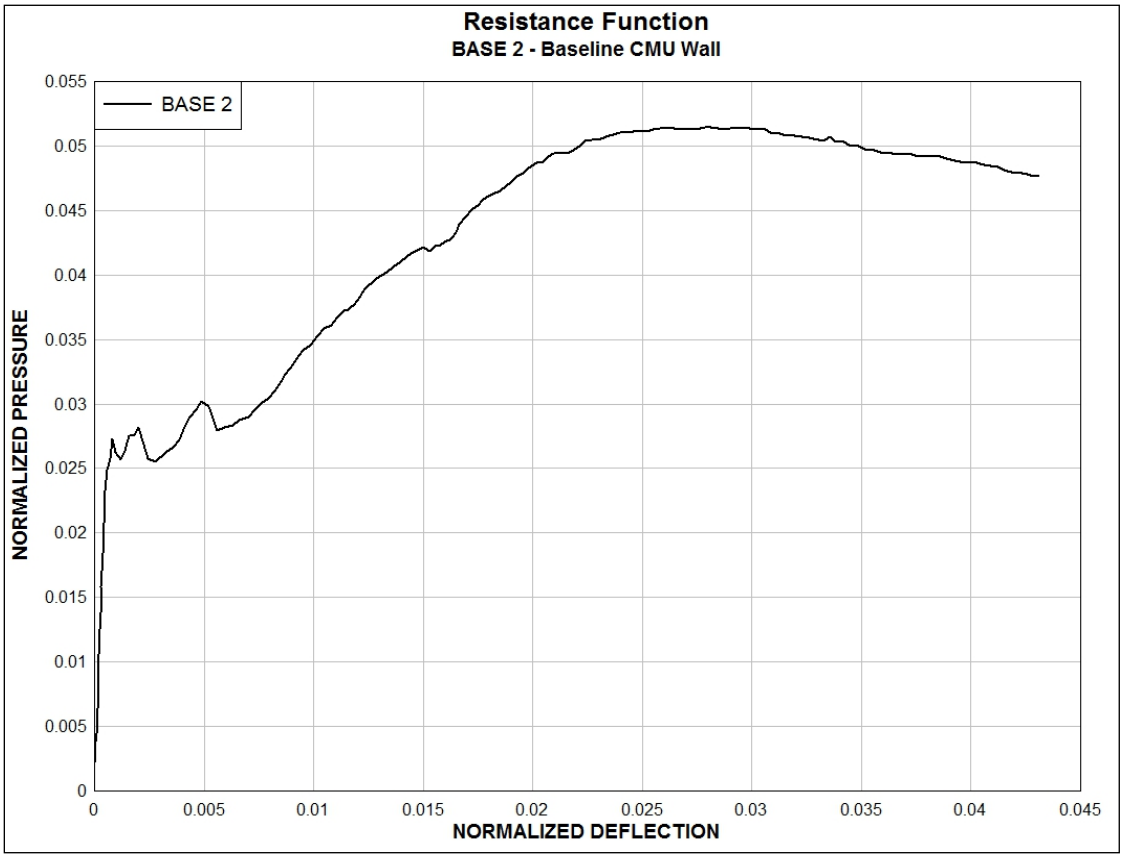

Figure 5.7. Resistance function for baseline CMU wall, Base 2.

5.3 Spray-on Polyurea (SW1-SW3)

5.3.1 Wall SW1

Wall SW1 was retrofitted with four passes of the Grade 1 spray-on polyurea material (Figure 5.8a). The procedure used to retrofit wall SW1 was detailed in Section 4.4. The spray-on polyurea was also applied to the full 12-in. width of the top and bottom supports to adhesively bond the coat of polyurea to the steel reaction frame. A leak in the HTC was identified during the first attempt to load the specimen. The experiment was halted, the water was drained out of both chambers, the steel frame was resealed, and the experiment was continued the following day. When the first attempt to test the wall failed, a deflection of 0.009 was recorded, so the wall was slightly damaged during the first attempt. During the second experiment, CMU debris appeared to lodge between the steel frame and the membrane causing the wall to bind on one side at approximately 0.172 of deflection. The loading continued and the debris appeared to clear itself. As

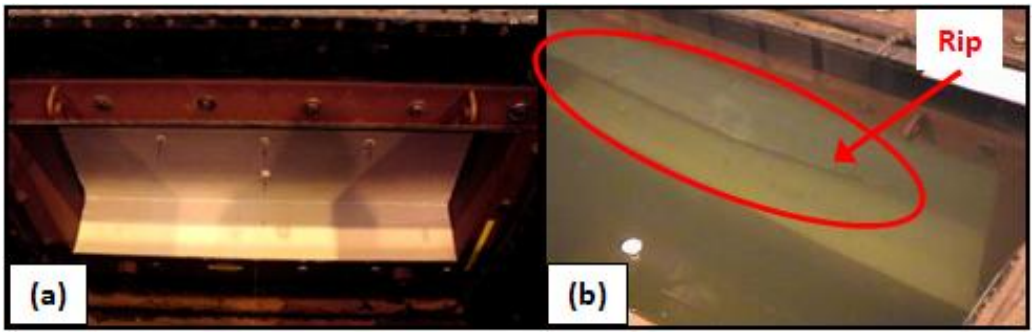

Figure 5.8. SW1. (a) Pretest photo of Wall SW1. (b) Rip in the polyurea coat propagated from left to right across the wall along the centerline mortar joint.

seen in Figure 5.8b, failure of the retrofit occurred when a tear beginning at the centerline mortar joint propagated across the wall from left to right. The ultimate flexural resistance of the CMU wall was noted at a deflection of 0.0603 and a pressure of 0.0731 (Figure 5.9). The wall continued to deform as the tear propagated across the wall to a final deflection of 0.676 and a pressure of 0.244.

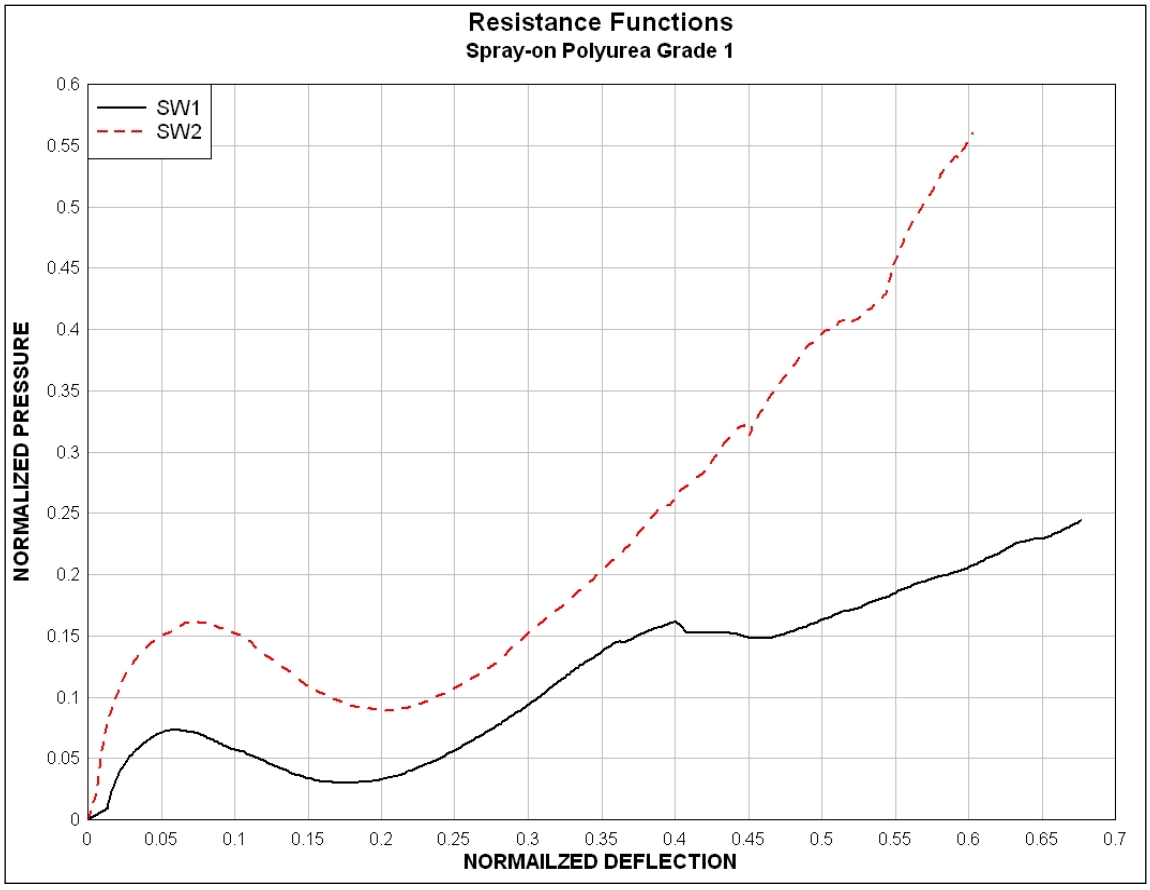

Figure 5.9. Resistance functions for Wall SW1 and SW2.

5.3.2 Wall SW2

The retrofit material and procedure for SW1 was duplicated on wall SW2 (Figure 5.10). While the wall was being prepared for the experiment, a section of the spray-on polyurea was torn. The area surrounding the tear was removed and new spray-on polyurea was applied to repair the area. The patched area was thicker than the initial layer; which caused the wall to bind on the left side during the loading process.

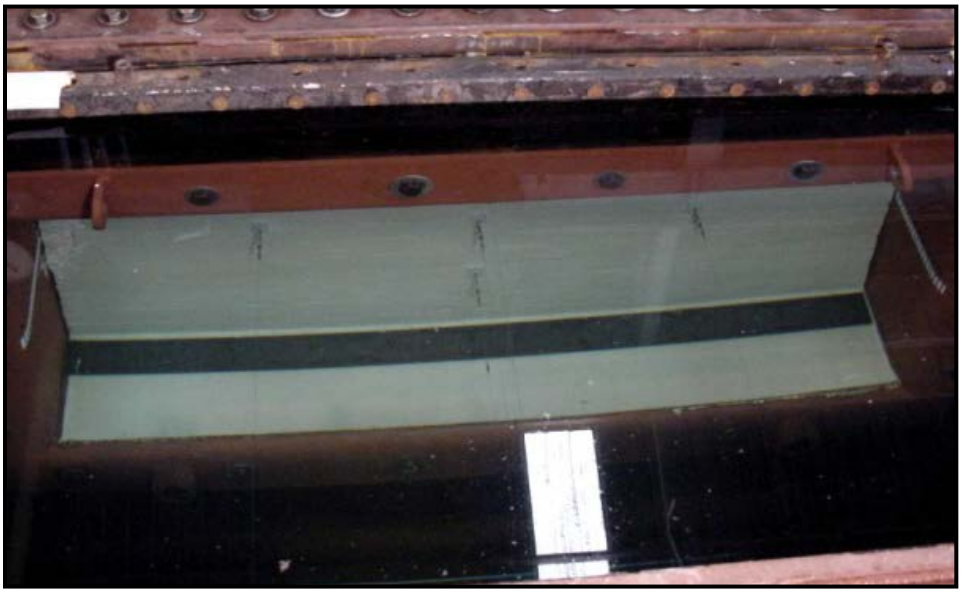

Figure 5.10. Pretest photo of Wall SW2.

The ultimate flexural resistance of the CMU wall was noted at a deflection of 0.0721 and a pressure of 0.163 (Figure 5.9). The adhesive anchoring all three of the deflection gauges along the mid-height of the wall failed at different times during execution of the experiment, so the three curves were averaged to obtain a composite resistance function to represent the material. Each curve on Figure 5.11 represents one of the three

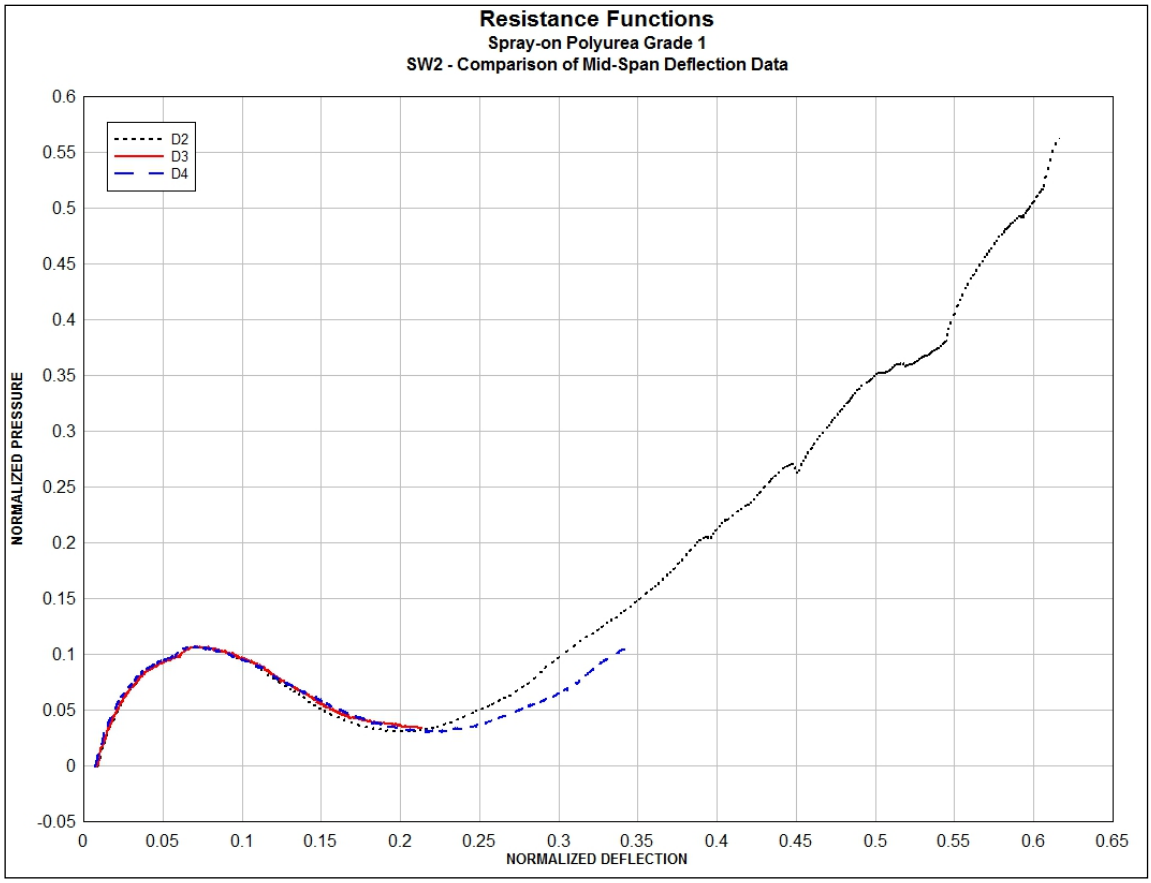

Figure 5.11. Resistance function for Wall SW2.

deflection gauges along the horizontal center line (D2, D3, and D4). Deflection gauge D3 failed first at a wall deflection of 0.2 at a pressure of 0.0366. Deflection gauge D4 failed next at a pressure of 0.106 and a deflection of 0.393. Gauge D2 failed last at a pressure of 0.56 and a deflection of 0.602. During the experiment it appeared that CMU debris lodged between the frame, membrane, and retrofit causing the left side of the specimen to bind affecting the deflection measurements of gauge D2. This incident could account for the difference in slope between curves D2 and D4 beginning at a deflection of 0.215. The wall deformed substantially before it began to tear from right to

left across the top of the wall (Figures 5.12a and b). The anchored elastomeric material was still intact under the plate, so the coat of polyurea sheared across the steel anchor plate while the material deflected laterally.

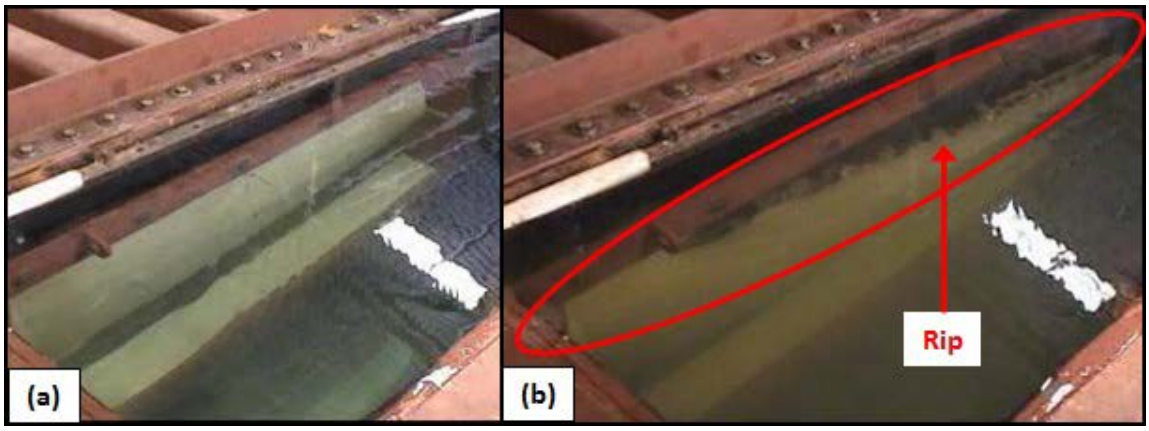

Figure 5.12. SW2. (a) Wall deflection during loading. (b) Complete failure of retrofit resulting from polyurea tear along top support.

5.3.3 Wall SW3

Wall SW3 was retrofitted with four passes of the Grade 2 spray-on polyurea (Figure 5.13a). The polyurea was applied to the CMU wall surface and the top and bottom supports. Anchor plates were also used to secure the retrofit to the steel frame. One can document the deformation in the wall by observing the location of the pressure gauge mounts as the wall was loaded in Figures 5.13b, 5.14a and b, and 5.15a and b. The adhesive used to secure deflection gauge D3 failed during the experiment, so gauge D5 was used to create the resistance function. The ultimate flexural resistance of the CMU wall was noted at a deflection of 0.0746 and a pressure of 0.165. A tear in the retrofit began slightly left of the geometric center of the wall at a lateral deflection of

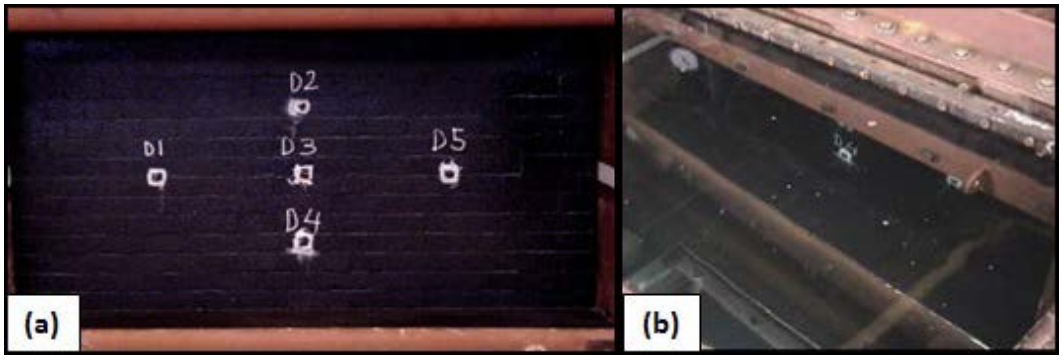

Figure 5.13. SW3. (a) Pretest photo of Wall SW3. (b) Two deflection gauges visible early in the experiment.

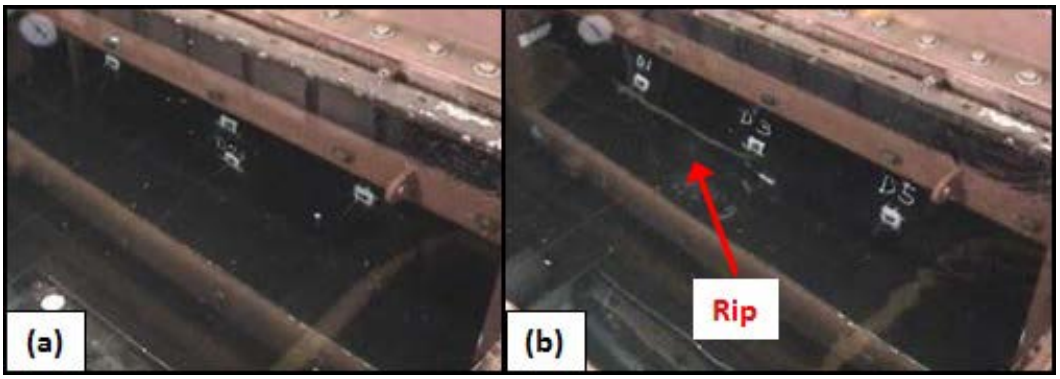

Figure 5.14. SW3. (a) All three mid-height deflection gauges were revealed as deformation continued. (b) Tear in the polyurea propagated from left to right along the mid-height mortar joint.

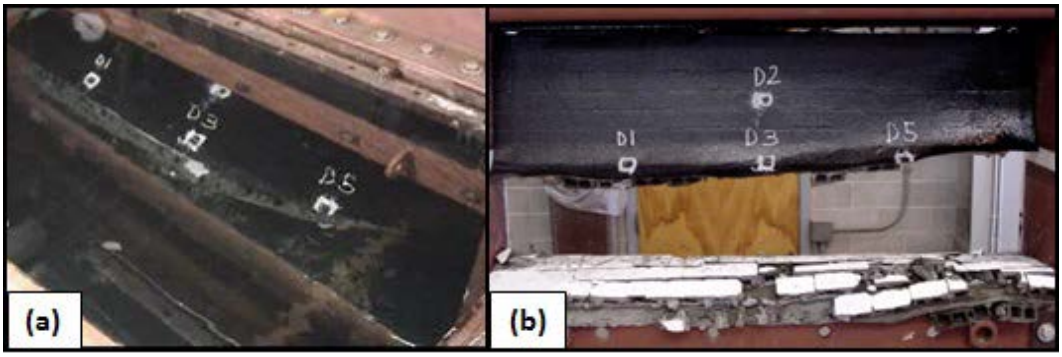

Figure 5.15. SW3. (a) As the retrofit material tore, the wall continued to deform rapidly. (b) Failure occurred at the mid-height and at the top support.

approximately 0.319 and a pressure of 0.198. As the loading process continued, the tear continued to propagate across the wall from left to right. At approximately 0.43 of deflection, the tear was half-way across the wall (Figure 5.14b). Posttest inspection of the wall (Figure 5.15b) also identified an area along the top right corner of the wall where the elastomer sheared along the top plate. Unfortunately, this area of the wall was not visible during loading, so it is not known when this tear developed. The specimen continued to deform until complete failure of the retrofit occurred at a deflection of 0.895 and a pressure of 0.452 (Figure 5.16). The data for the spray-on polyurea experiments were listed in Table 5.2.

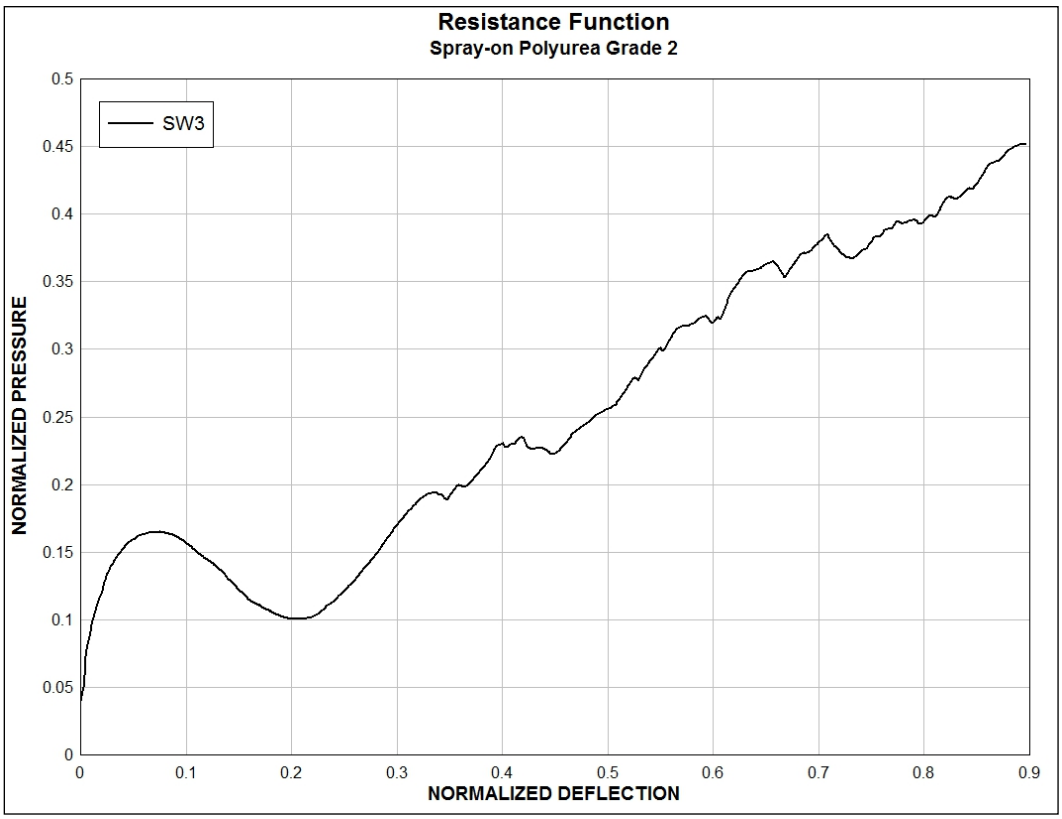

Figure 5.16. Resistance function for SW3.

Table 5.2. Normalized pressure (P) and deflection (d) data for spray-on polyurea.

Wall	Retrofit	CMU Wall Failure		Retrofit Failure	
		P	d	P	d
SW1	Spray-on Polyurea Grade 1	0.0731	0.0603	0.244	0.676
SW2	Spray-on Polyurea Grade 1	0.162	0.0721	0.56	0.602
SW3	Spray-on Polyurea Grade 2	0.165	0.0746	0.452	0.895

5.4 Fiber-Reinforced Spray-on Polyurea Retrofit (SW4-SW9)

5.4.1 Wall SW4

The retrofit system on Wall SW4 consisted of two passes of Grade 2 spray-on polyurea, followed by Fabric A (100 lb/in.) arranged so that the fibers were oriented at 0 and 90 deg to the horizontal mortar joint on the wall. Then two additional passes of Grade 2 polyurea were added to encapsulate the fabric on the wall. The procedure used to apply the retrofit system for SW4 was detailed in Section 4.5. Mechanical anchorage was provided to the top and bottom supports to prevent peel-back failure. Data collection ended when the spray-on polyurea and fiber reinforcement sheared along the steel plate along the top support (Figures 5.17a and b) at a pressure of 0.476 and a deflection of 0.346. Figure 5.17a indicated that there was substantial CMU debris generated from the top half of the wall, since there are no CMU attached to the elastomeric film in the posttest photo. The ultimate flexural resistance of the CMU wall was noted at a deflection of 0.0324 and a pressure of 0.25 (Figure 5.18). The data for all of the spray-on fiber reinforced polyurea experiments were listed in Table 5.3.

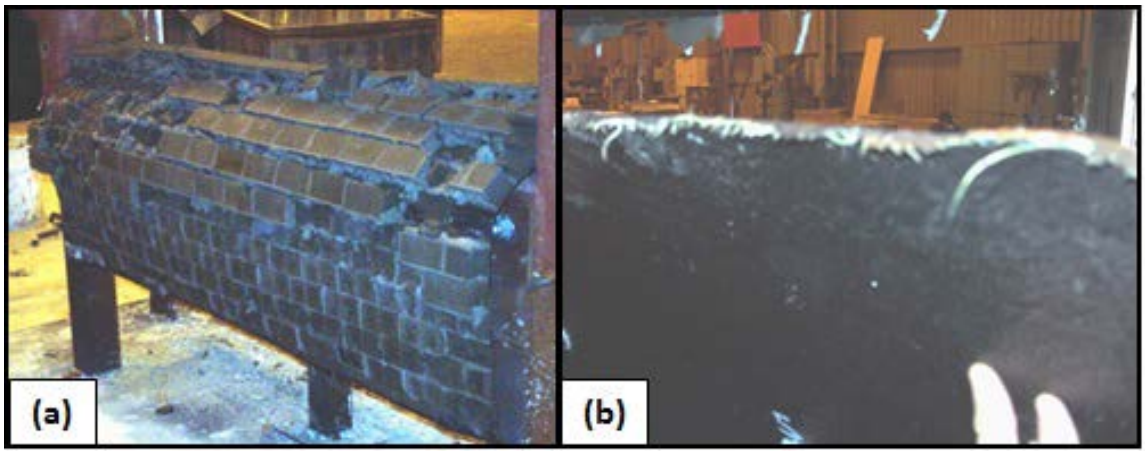

Figure 5.17. SW4. (a) Failure of Wall SW4. (b) Retrofit failed when it tore along the top support.

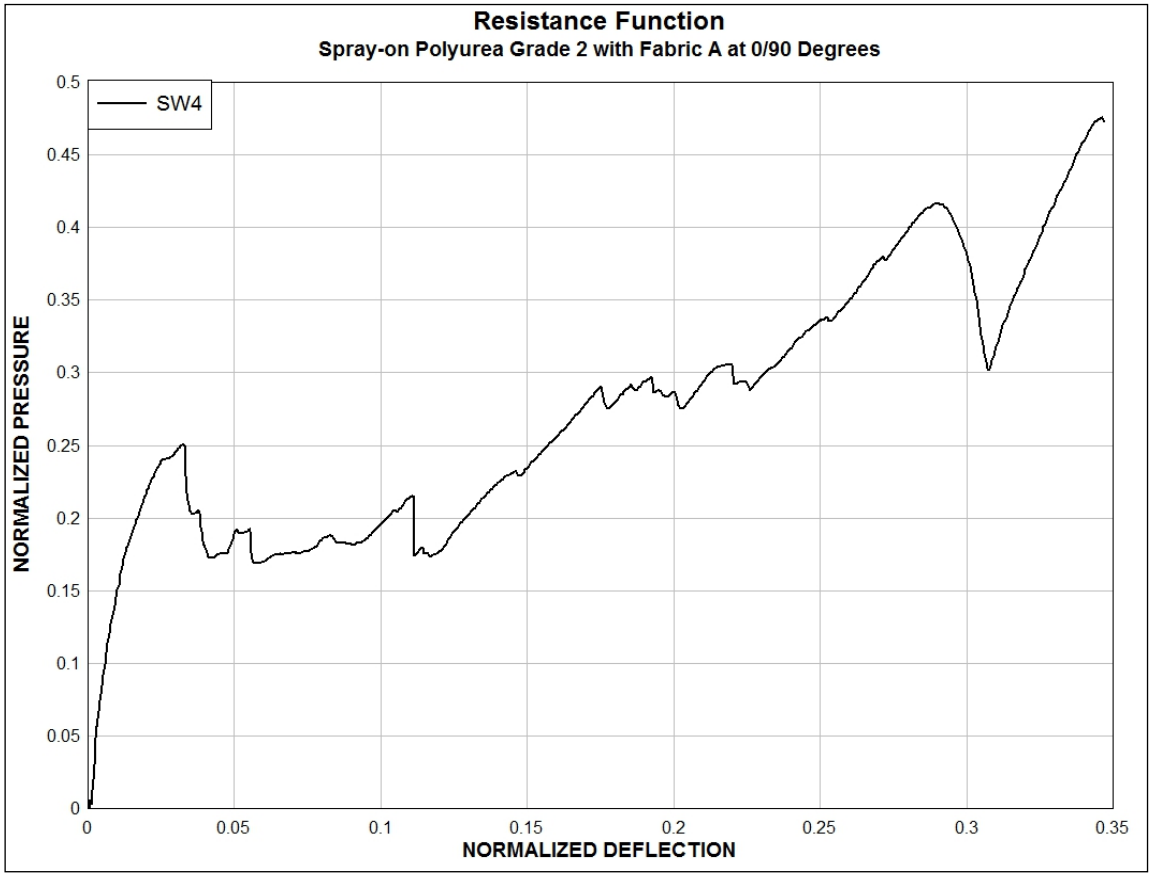

Figure 5.18. Resistance function for Wall SW4.

Table 5.3. Normalized pressure (P) and deflection (d) data for spray-on reinforced polyurea.

Wall	Retrofit	CMU Wall Failure		Retrofit Failure	
		P	d	P	d
SW4	Spray-on Polyurea Grade 2 with Fabric A at 0/90 deg	0.25	0.0324	0.476	0.346
SW5	Spray-on Polyurea Grade 1 with Fabric C at ±45 deg	0.261	0.0238	1.07	0.46
SW6	Spray-on Polyurea Grade 1 with Fabric A at ±45 deg	0.25	0.0891	0.363	0.456
SW7	Spray-on Polyurea Grade 2 with Fabric A at ±45 deg	0.299	0.0537	0.543	0.4
SW8	Spray-on Polyurea Grade 2 with Fabric B at ±45 deg	0.25	0.0347	0.146	0.349
SW9	Spray-on Polyurea Grade 2 with Fabric B at ±45 deg	0.333	0.0312	0.908	0.408

5.4.2 Wall SW5

Wall SW5 was retrofitted with a reinforced spray-on polyurea material detailed in Section 4.5. First, two passes of the Grade 1 spray-on polyurea was applied to the wall, followed by a layer of Fabric C applied with the fibers oriented ±45 deg to the wall. Then two additional passes of the spray-on polyurea were applied over the fabric to encapsulate the reinforcement between the two layers of the spray-on polyurea The spray-on polyurea and Fabric C were applied to the entire 12-in. top and bottom flanges of the steel test frame (Figure 5.19a). In addition to the adhesive bond, mechanical anchorage was also provided by bolting steel plates to the top and bottom flanges

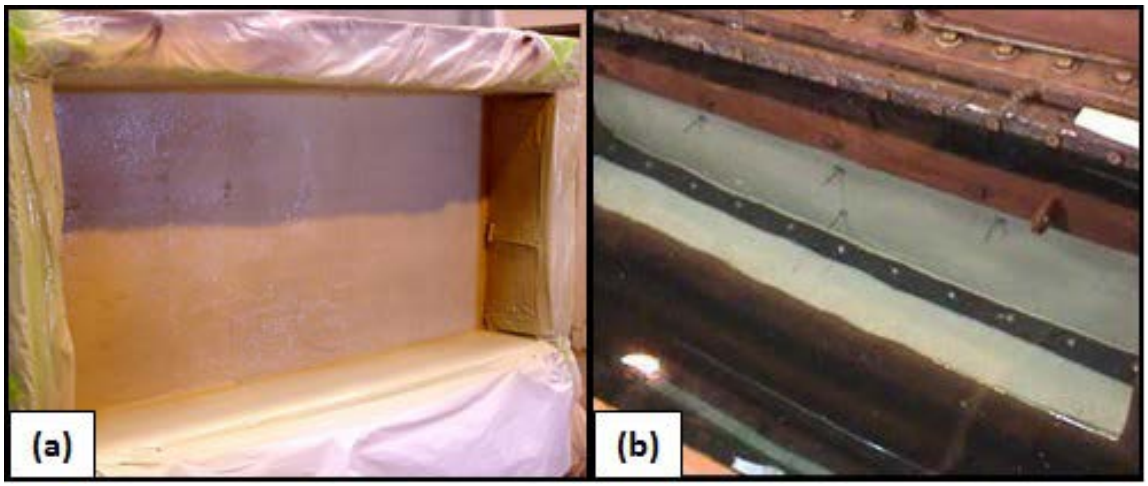

**Figure 5.19. SW5. (a) Wall SW5 during retrofit application.
(b) Deformation of wall during the experiment.**

clamping the reinforced elastomeric material between the steel frame and steel anchor plate.

The ultimate flexural resistance of the CMU wall was marked at a deflection of 0.0238 and a pressure of 0.261. Figure 5.19b illustrates the initial flexural response of the retrofitted wall. The specimen continued to be loaded past this point, and at a deflection of 0.46 and a pressure of 1.07, the bolts holding the anchor plate to the frame failed. Some of the bolts sheared while others yielded once the plate began to deflect into the chamber (Figure 5.20a). This point can be identified on the resistance function by locating the point at which the pressure dropped by 0.79. The elastomeric coating showed no visible tears. Once the mechanical anchorage failed, the adhesive bond between the elastomer and the frame began to fail by peeling back off the supports (Figure 5.20b). Complete failure of the retrofit system occurred when the material peeled off the bottom support (Figure 5.21).

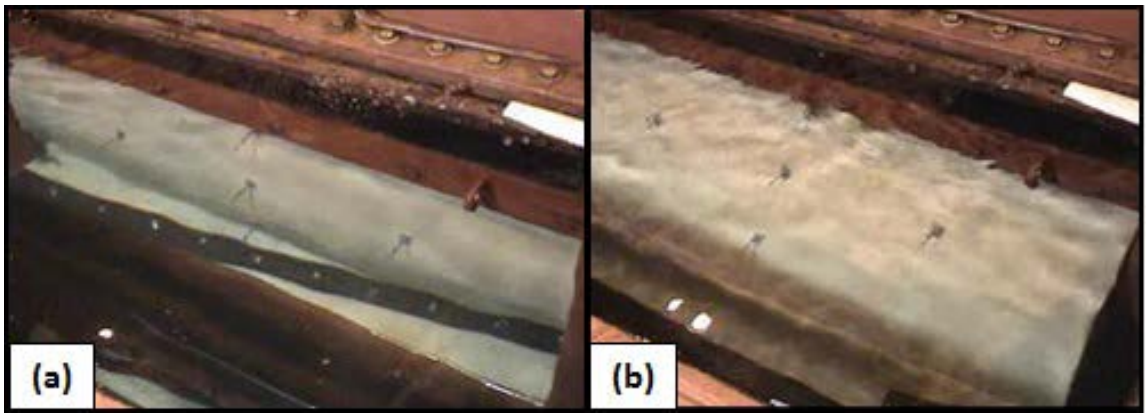

Figure 5.20. SW5. (a) Failure of mechanical anchorage on Wall SW5. (b) Adhesive bond failed after the mechanical anchorage failed.

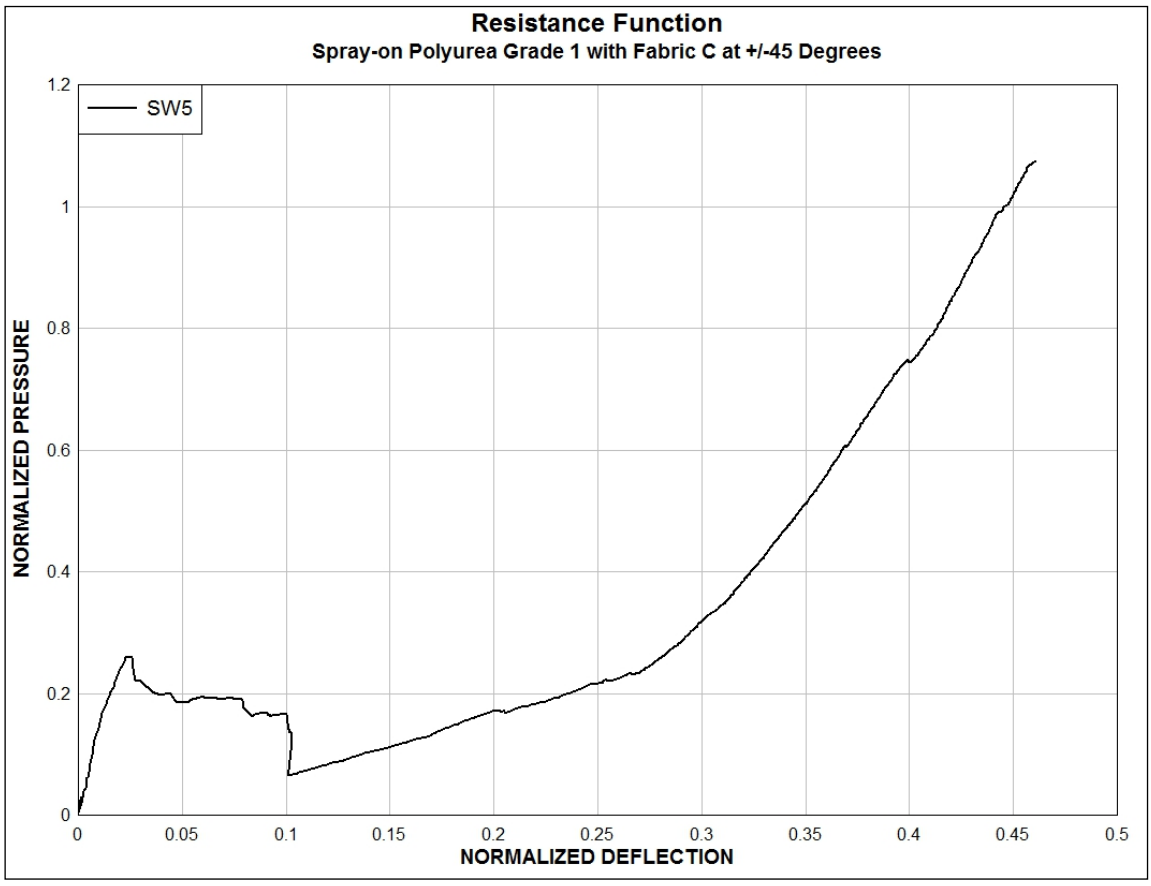

Figure 5.21. Resistance function for Wall SW5.

5.4.3 Wall SW6

Wall SW6 was also retrofitted with a reinforced spray-on polyurea detailed in Section 4.5. First, two passes of the Grade 1 spray-on polyurea were applied to the wall surface, followed by a layer of Fabric A applied with the fibers oriented ±45 deg to the wall. Then two additional passes of the spray-on polyurea were applied over the fabric to encapsulate the reinforcement between the two coatings of the spray-on polyurea. The spray-on polyurea was applied to the entire 12-in. top and bottom flanges of the steel test frame to provide an adhesive bond. Some areas of the fabric were not flat against the wall, which prevented the fabric from being completely encapsulated by the spray-on polyurea (Figure 5.22a). The bolts anchoring the plate to the frame were replaced with high strength bolts due to the failure of the mechanical anchorage in experiment SW5.

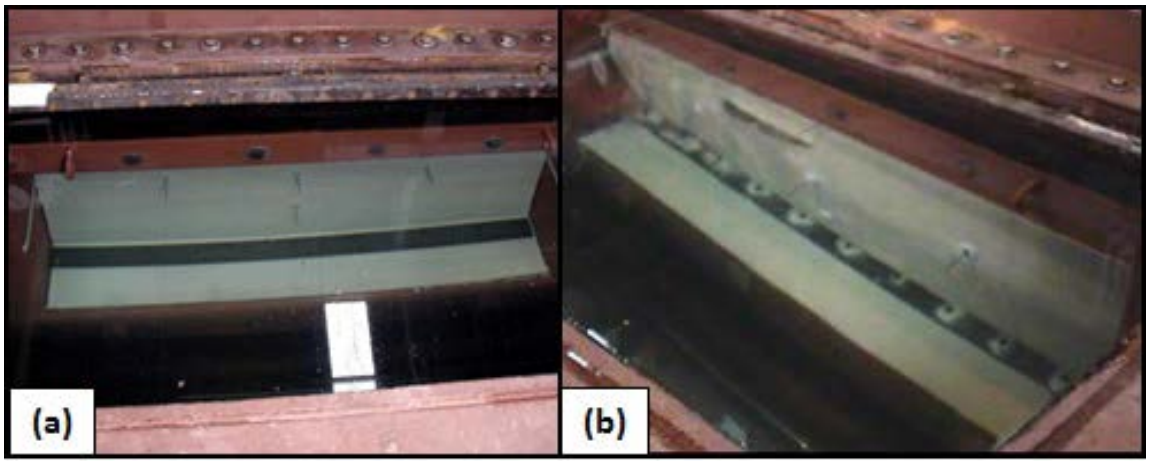

Figure 5.22. SW6. (a) Pretest photo of Wall SW6. (b) Retrofit continued to deform after the rip developed.

The ultimate flexural resistance of the CMU wall was identified at a deflection of 0.0891 and a pressure of 0.25. A tear developed in the retrofit material along a mortar joint located four courses from the top (Figure 5.22b). The ultimate tensile membrane resistance occurred at a deflection of 0.456 and a pressure of 0.363. As the wall continued to deform, the spray-on material began to tear along the bottom support beginning at the center and propagating uniformly in both the left and right directions. The experiment was complete when the retrofit material sheared across the anchor plate at the bottom support (Figure 5.23). A final deflection of 0.738 and a pressure of 0.254 were documented but not included in the resistance function (Figure 5.24).

Figure 5.23. Ultimate failure of the retrofit occurred when the materials tore along the bottom anchor plate.

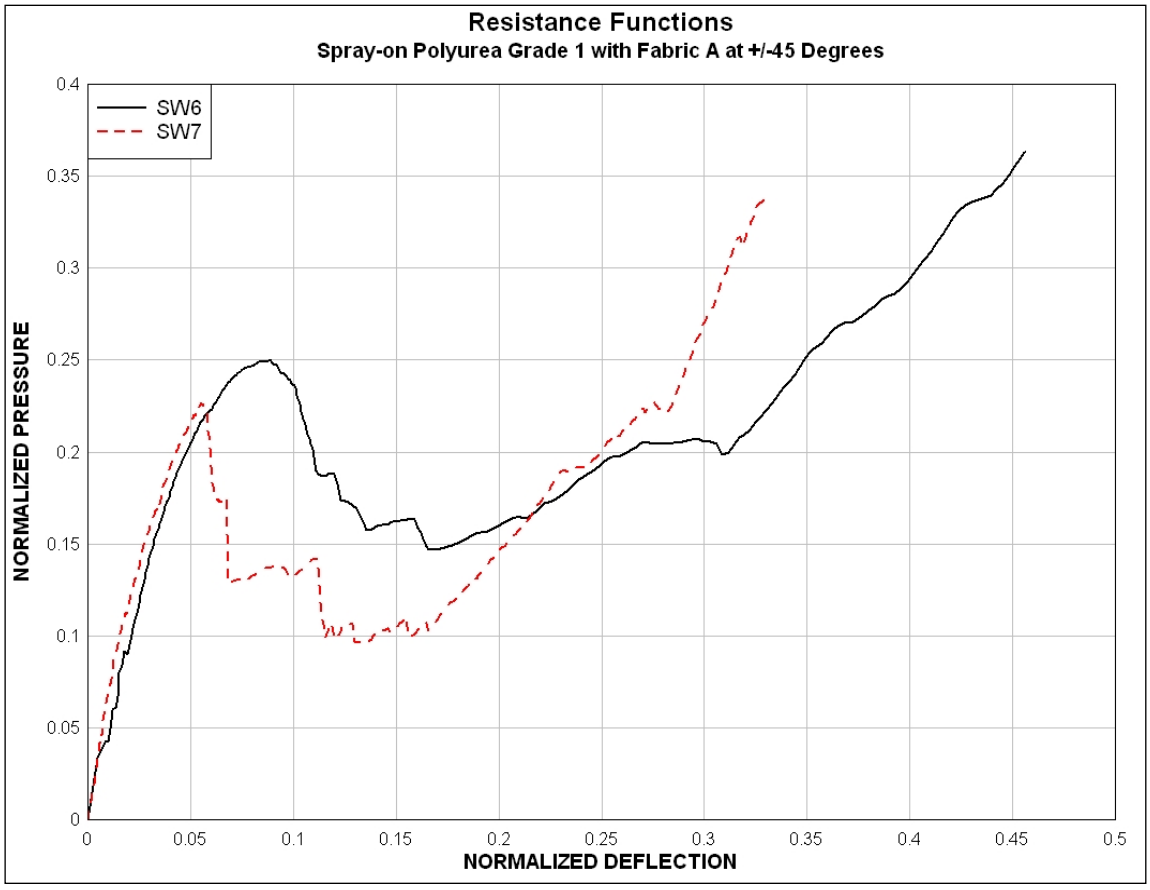

Figure 5.24. Resistance functions for Wall SW6 and SW7.

5.4.4 Wall SW7

Wall SW7 was retrofitted with two passes of Grade 2 spray-on polyurea, a layer of Fabric A with the fibers oriented ±45 deg to the wall, and two additional passes of the spray-on polyurea were applied to encapsulate the fabric (Figure 5.25a). Anchor plates were used to secure the retrofit materials on the top and bottom supports. Wall SW7 was loaded twice because a leak developed in the HTC during the loading process at a pressure of 0.2. The resistance function for the complete loading cycle (loading and unloading) of the center line deflection gauge in Experiment 1 is shown in Figure 5.26.

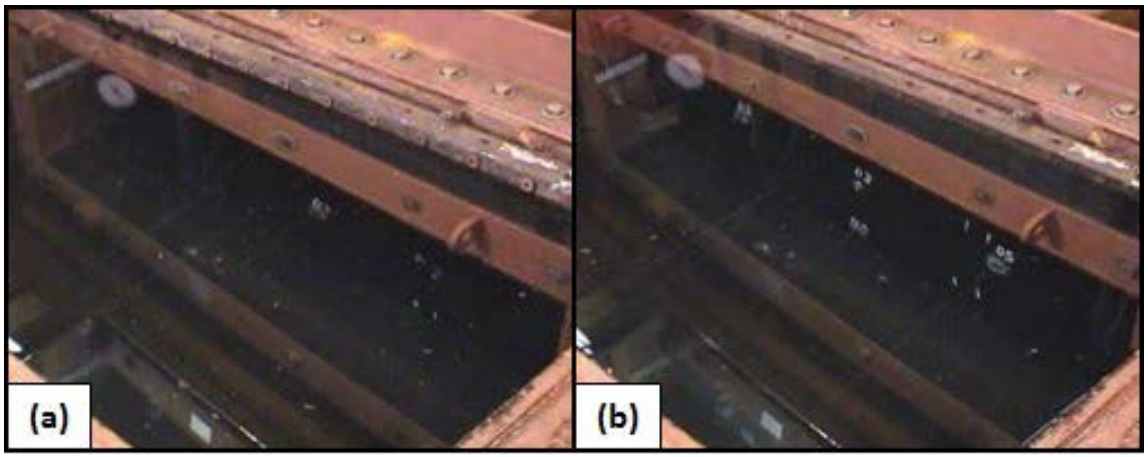

Figure 5.25. SW7. (a) Pretest photo of Wall SW7. (b) As the wall deformed all three centerline gauges became visible.

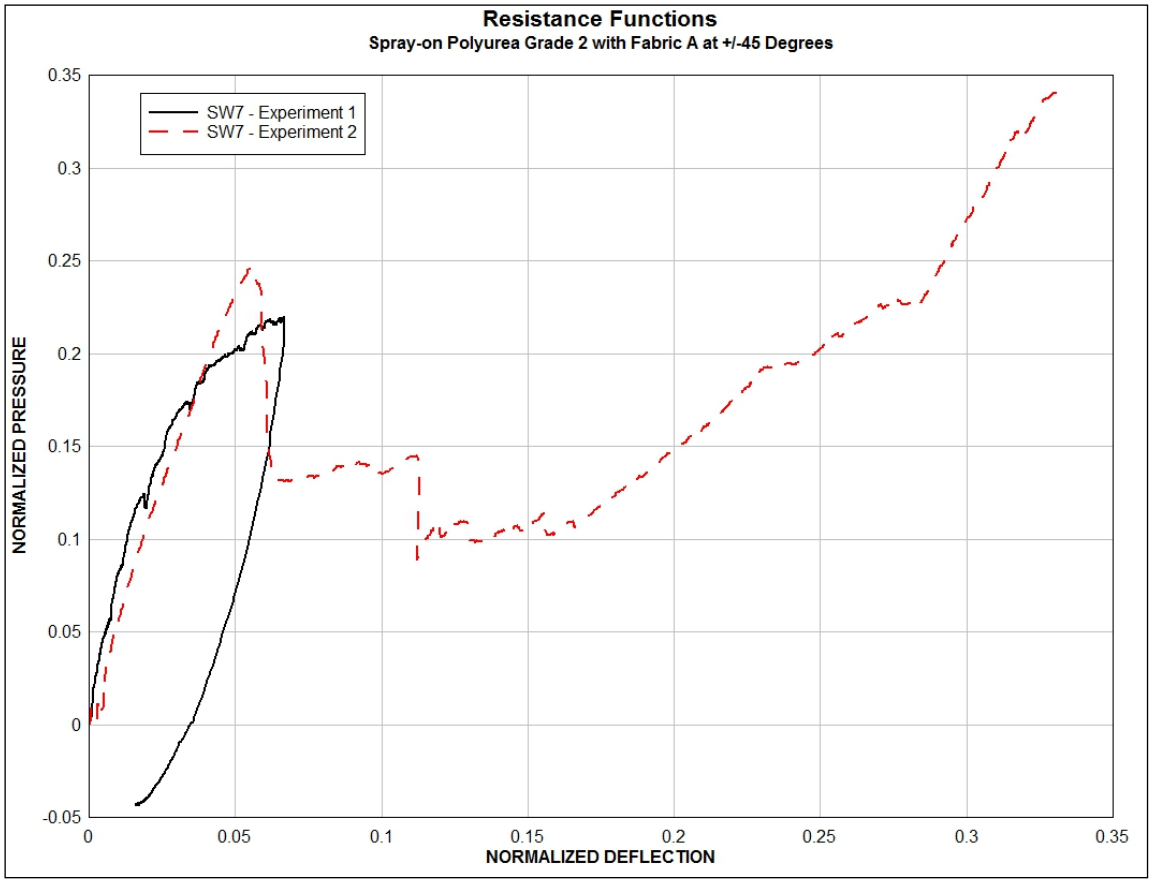

Figure 5.26. Resistance functions for Wall SW7 Experiments 1 and 2.

The wall exhibited some permanent deformation after unloading. The maximum pressure achieved during Experiment 1 was 0.218 at a maximum deflection of 0.067. The wall was removed and the chamber was resealed to continue the evaluation. The second experiment on SW7 was executed to failure of the retrofit. However, during the execution of Experiment 2 the adhesive securing deflection gauge D3 failed at a pressure of 0.341 and a deflection of 0.332 (Figure 5.26). Initially the point of maximum deflection occurred along the mid-line (Figure 5.25b). The retrofit tore at the center of the bottom support (Figure 5.27a) and propagated uniformly to the edges of the wall (Figure 5.27b). The retrofit system failed at a deflection of 0.4 and a pressure of 0.543. The insert in Figure 5.28 provides a view of the sheared section of the elastomer including the fiber reinforcement ends. Once the wall was removed from the chamber, it was clearly visible (Figure 5.29) that the CMU along the bottom half of the wall were heavily damaged. The ultimate flexural resistance of the CMU wall was noted at a

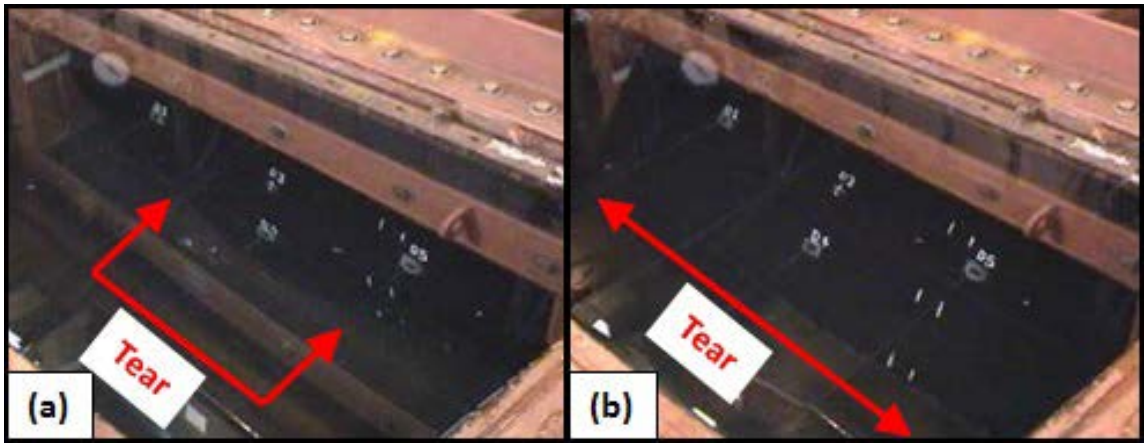

Figure 5.27. SW7. (a) Retrofit began to tear at the center of the bottom support. (b) Tear propagated entire length of wall.

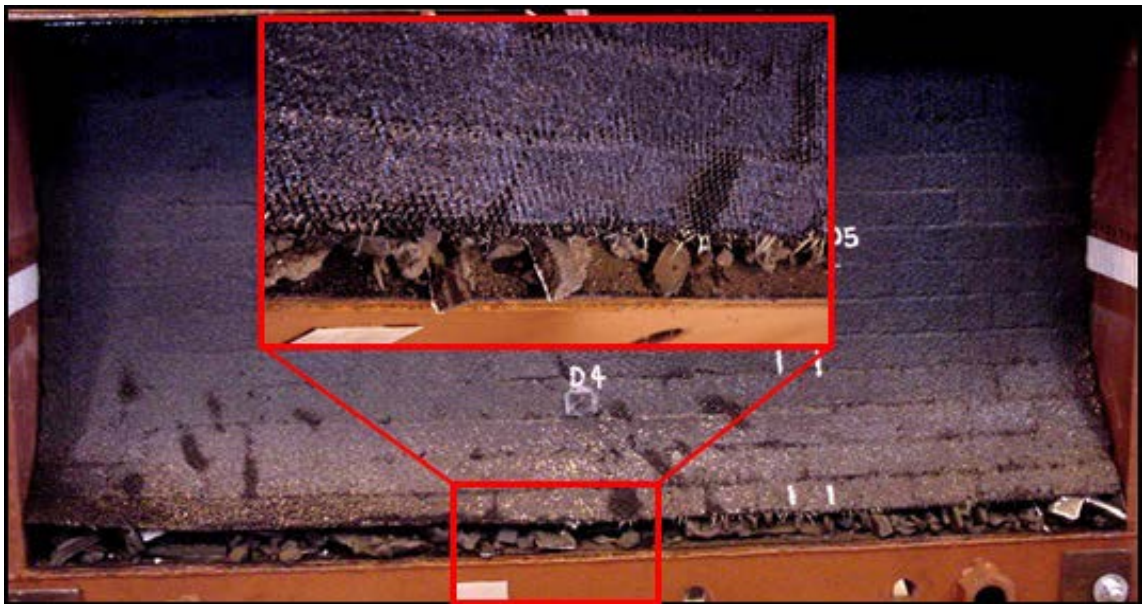

Figure 5.28. Failure at bottom support of elastomer and fabric reinforcement.

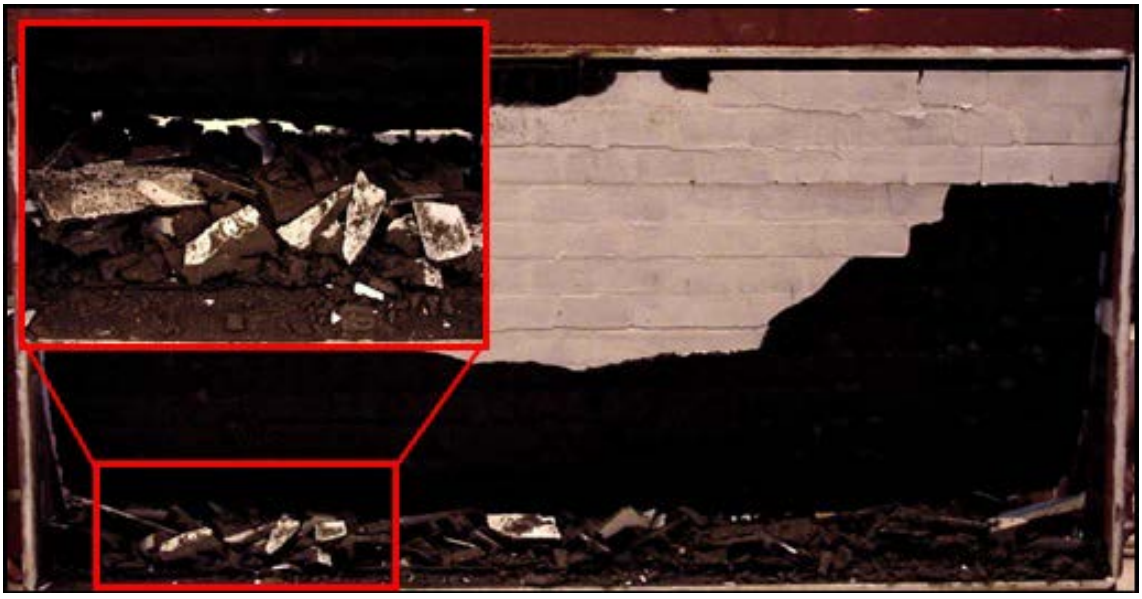

Figure 5.29. Accumulation of CMU debris on bottom flange of frame.

deflection of 0.0537 and a pressure of 0.299. The resistance functions for Experiment 1 and 2 shown in Figure 5.30 were used to develop a composite resistance function for SW7.

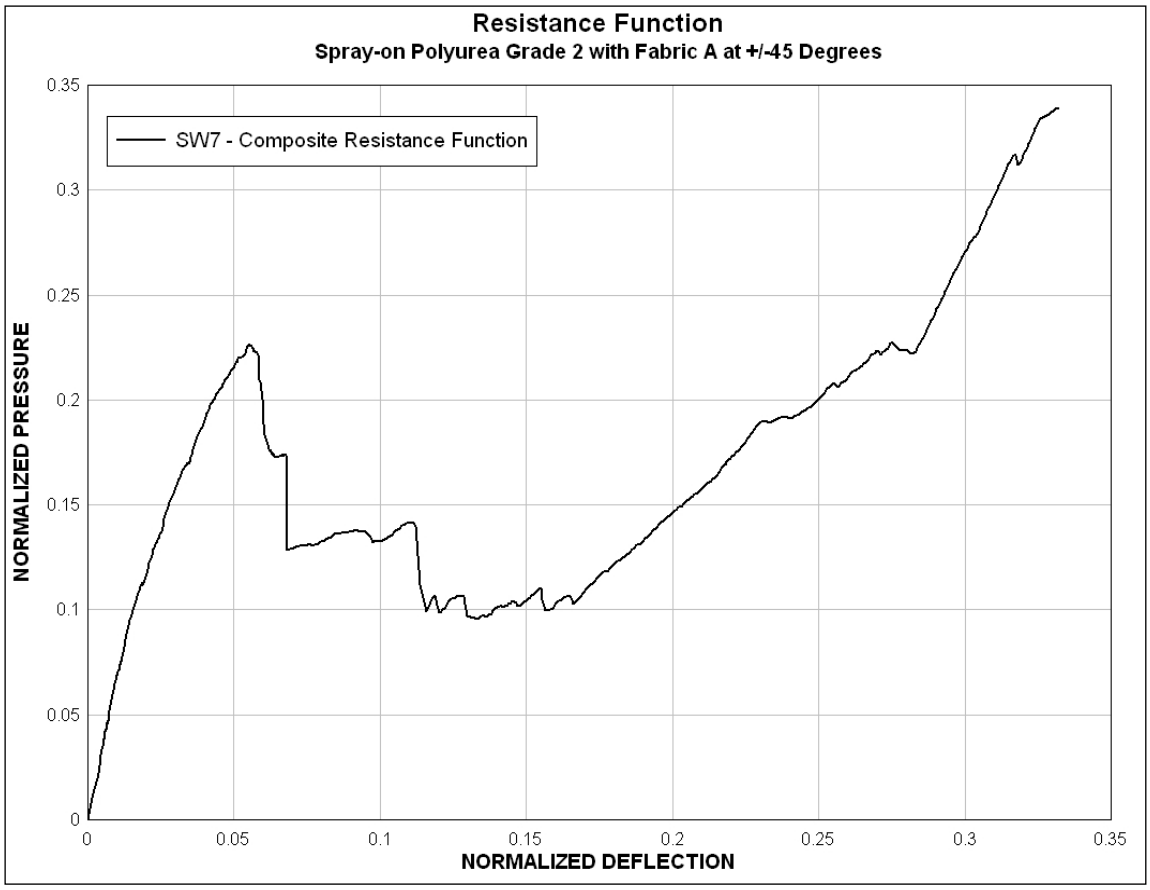

Figure 5.30. Creation of composite resistance function for Wall SW7.

5.4.5 Wall SW8

The retrofit system on SW8 consisted of two passes of Grade 2 spray-on polyurea, followed by Fabric B (200 lb/in.) arranged so the fibers were oriented at ±45 deg on the wall, and covered with two additional passes of Grade 2 polyurea to encapsulate the

fabric. Additional spray-on polyurea was added to the top and bottom supports in lieu of mechanical anchorage. Relying on the adhesive bond as the sole support condition continued to be a problem as the retrofit failed when the polyurea layer peeled back as the loading increased on the wall. The material began peeling off of the left side and propagated across the bottom support. The retrofit system peeled off of the supports before any rips developed in the material (Figures 5.31a and b). The ultimate flexural resistance of the CMU wall was noted at a deflection of 0.0347 and a pressure of 0.25 (Figure 5.32). Complete failure of the retrofit occurred at a deflection of 0.349 and a pressure of 0.1446.

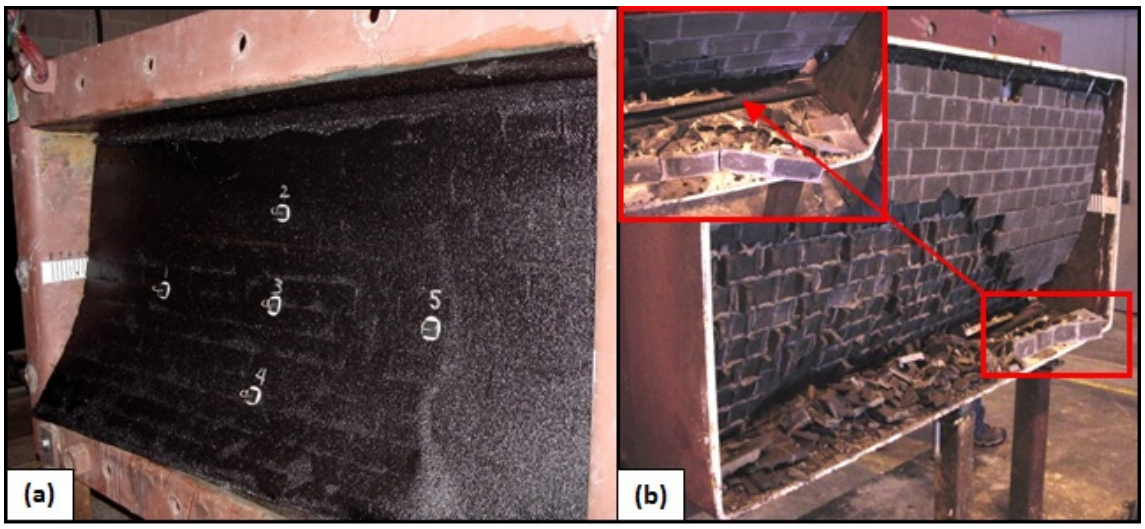

Figure 5.31. SW8. (a) Posttest photo of Wall SW8. (b) Failure occurred when the elastomeric material peeled off the bottom support.

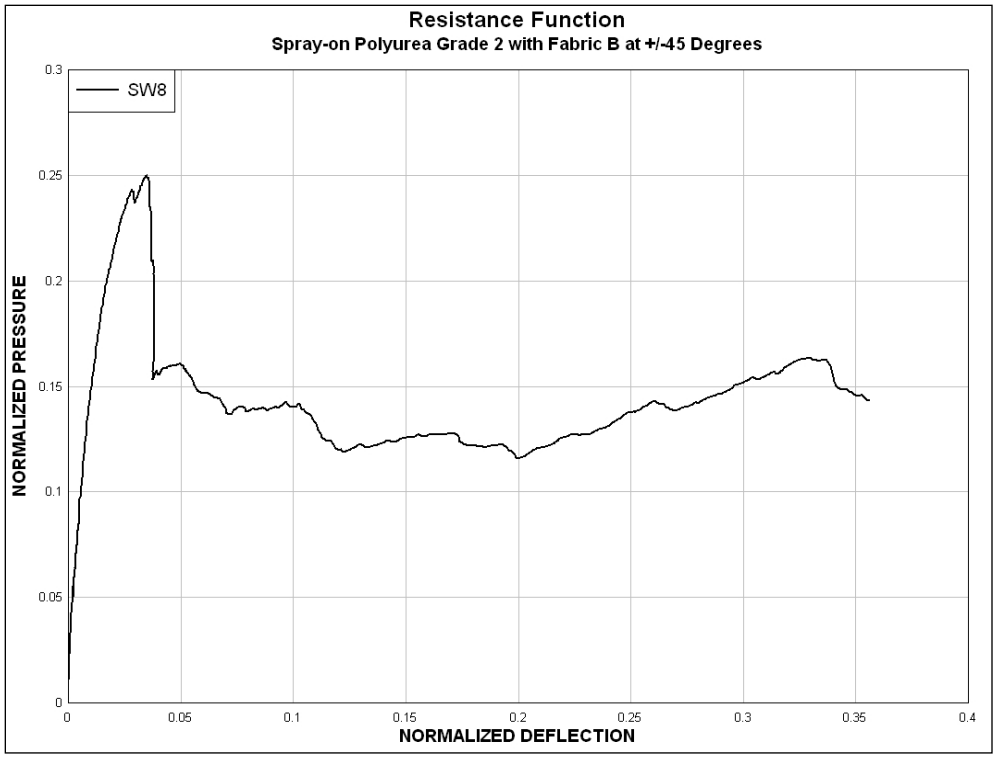

Figure 5.32. Resistance function for Wall SW8.

5.4.6 Wall SW9

The retrofit material and procedure for Wall SW9 duplicated Wall SW8 except for the addition of mechanical anchors to the top and bottom supports to prevent the peel-back failure that occurred in SW8. Posttest inspection of the wall showed that almost all of the CMU blocks were heavily damaged, leaving only remnants of the mortar attached to the elastomer (Figure 5.33a). A peel-back failure was prevented; however, failure of the retrofit occurred at the top support when the spray-on coating and fabric tore along the anchor plate (Figure 5.33b). The ultimate flexural resistance of the CMU wall was noted at a deflection of 0.0312 and a pressure of 0.333 (Figure 5.34). Complete failure of the retrofit occurred at a deflection of 0.408 and a pressure of 0.908.

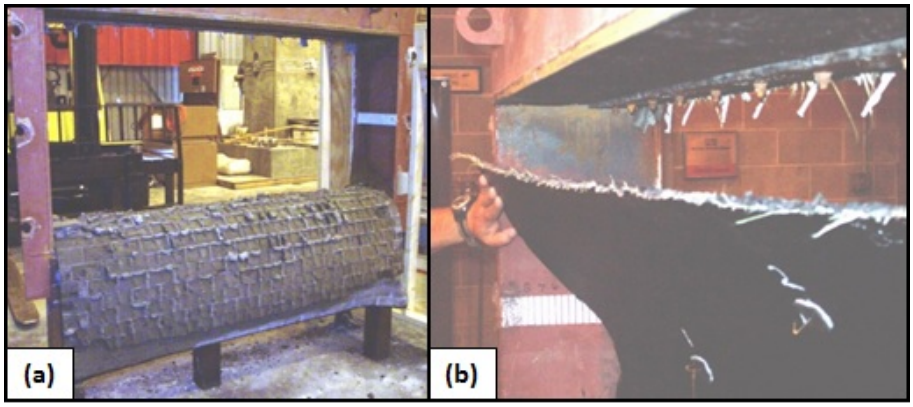

Figure 5.33. SW9. (a) Posttest photo of Wall SW9. (b) Retrofit system failed along the top support.

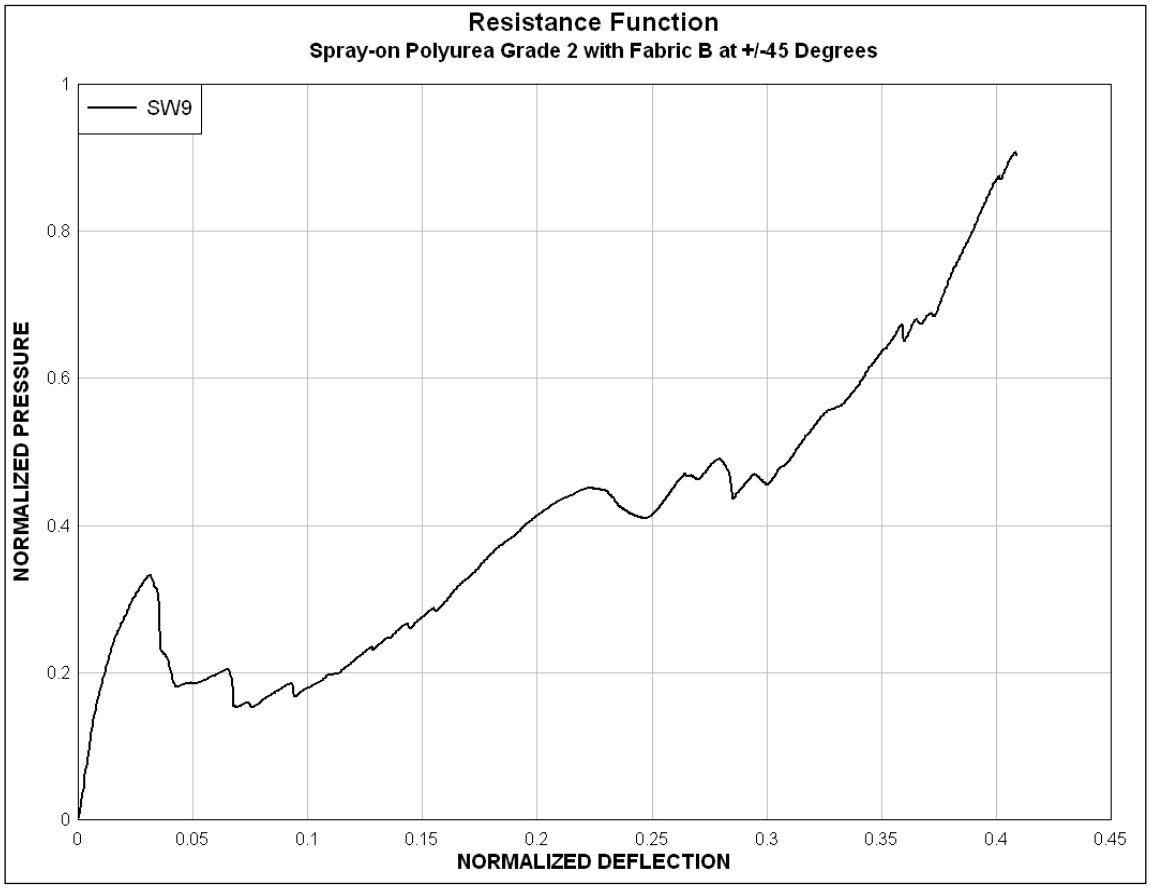

Figure 5.34. Resistance function for Wall SW9.

5.5 Trowel-on Retrofits (SW10-SW12)

5.5.1 Wall SW10

Wall SW10 was retrofitted with a trowel-on thermoset material using the procedure detailed in Section 4.6. First, a layer of thermoset was applied to the wall and to the top and bottom supports using a notched trowel. A second layer of material was applied to the same area using a flat trowel to fill in the grooves until the desired retrofit thickness was achieved on the CMU wall and steel supports (Figure 5.35). No mechanical anchorage was used to secure the retrofit material. The retrofitted wall failed when the trowel-on material sheared along the top support. The ultimate flexural resistance occurred at a pressure of 0.0889 and a deflection of 0.0568. (Figure 5.36). The membrane continued to deform until final failure occurred at a pressure of 0.536 and a deflection of 0.744.

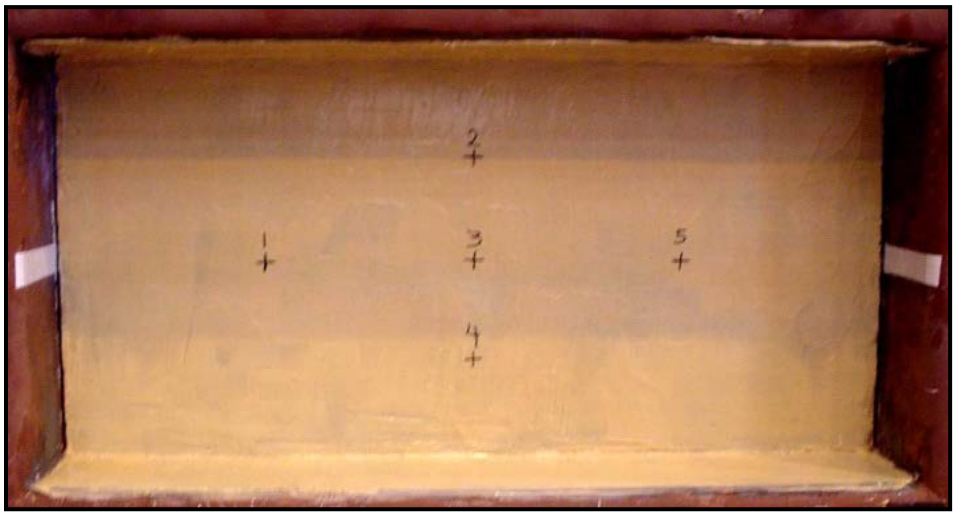

Figure 5.35. SW10 retrofitted with trowel-on thermoset.

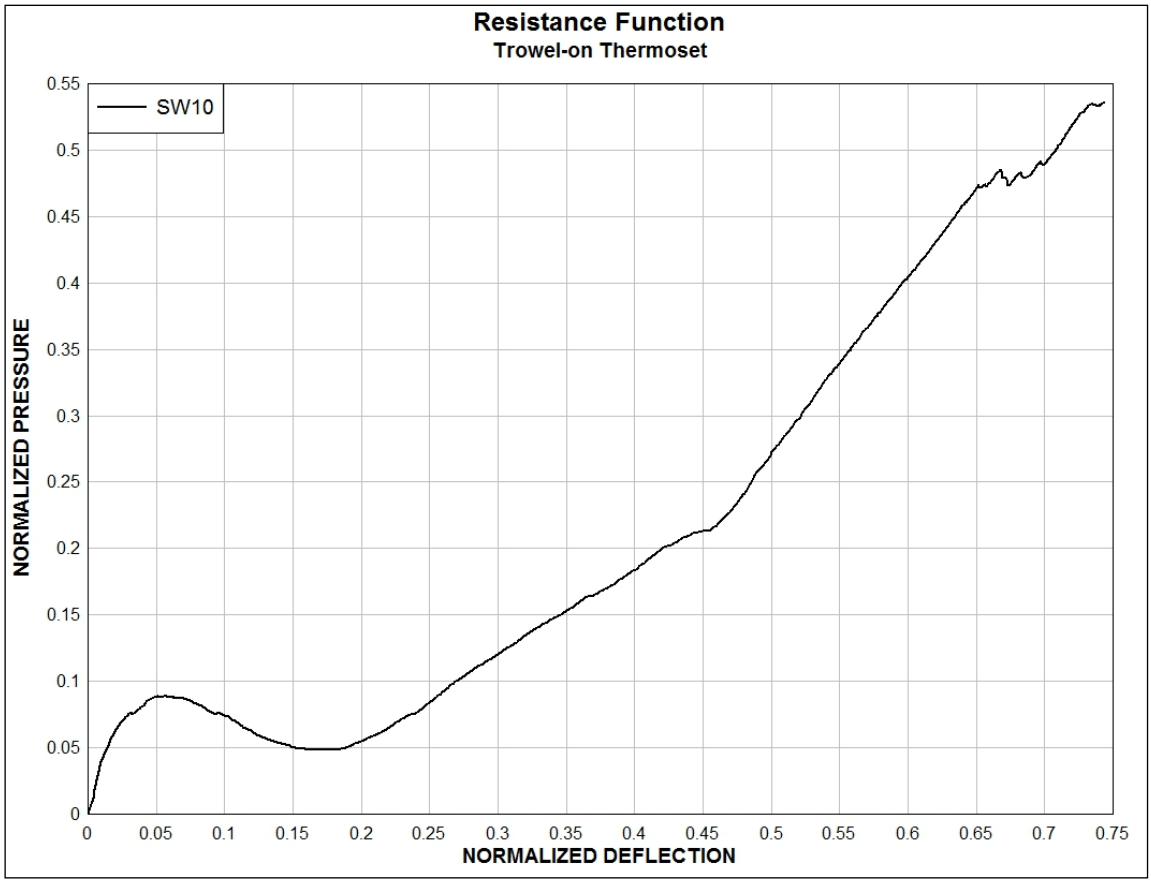

Figure 5.36. Resistance function for SW10.

5.5.2 Wall SW11

Wall SW11 was retrofitted with a trowel-on epoxy (Figure 5.37a). Unlike the first 10 experiments, SW11 was evaluated to determine the contribution of the trowel-on epoxy to the resistance of the CMU wall and not as a singular retrofit system. The trowel-on epoxy was not selected as a retrofit material, but as an adhesive to be used with additional materials. A layer of epoxy was applied to the wall and the top and bottom supports using a flat trowel until the desired thickness representative of an adhesive layer on the CMU wall and steel supports was achieved. Several runs

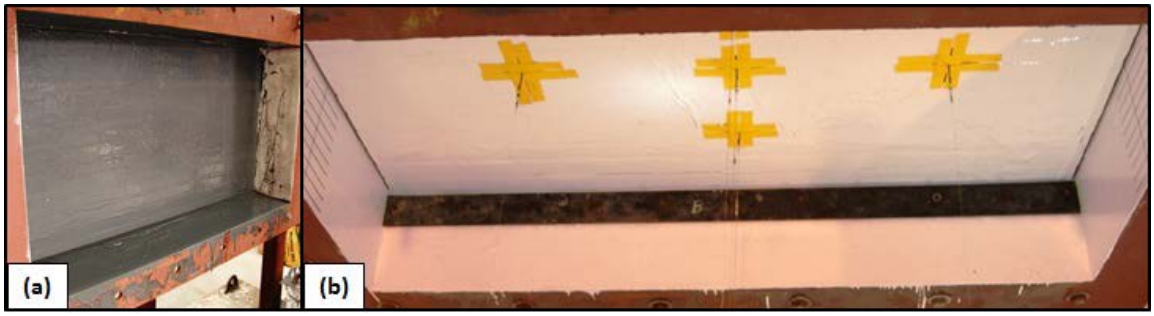

Figure 5.37. SW11. (a) Wall retrofitted with trowel-on epoxy. (b) Epoxy painted white so cracks could be seen during deformation.

developed in the epoxy material in the center of the wall, suggesting that the layer was not uniform and was less than the desired thickness in random areas on the wall. In addition to the adhesive bond between the epoxy and the steel flanges, mechanical anchorage was added by bolting steel plates to the top and bottom flanges clamping the epoxy layer between the steel frame and anchor plate (Figure 5.37b). The epoxy was painted white, so any cracks that developed in the epoxy during the execution of the experiment could be documented.

As the HTC was filling a defect in the epoxy along the top of the first course of blocks in the center of the wall became evident (Figure 5.38a). As the center of the wall approached a 1-in. deflection, the defect along the top of the first course of blocks became even more pronounced and a tear began to develop at the mortar joint (Figure 5.38b). As the center of the wall approached a 2-in. deflection, a tear developed from the left edge of the wall along the seventh course of blocks to the first deflection hook on the left side of the wall (Figure 5.39a). As the center of the wall approached a 3-in. deflection, the existing cracks at the center of the wall began to grow wider as the

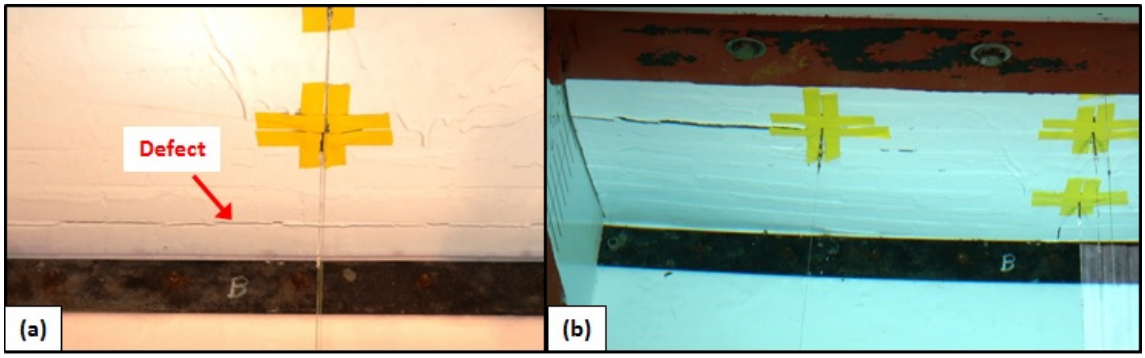

Figure 5.38. SW11 (a) Location of defect in retrofit. (b) Tear in epoxy layer began on the left side of the wall.

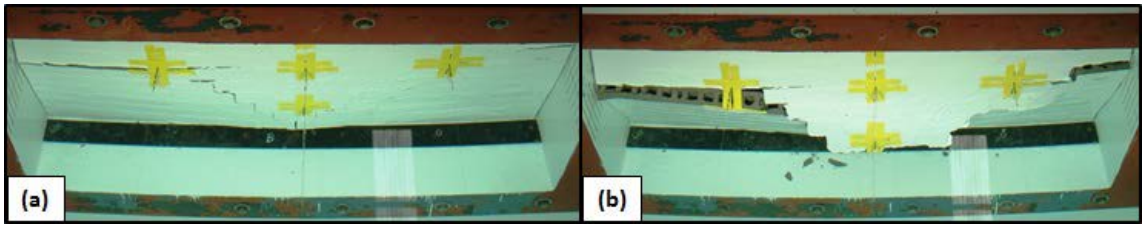

Figure 5.39. SW11. (a) The tear in the epoxy traveled diagonally from the first gauge on the left to the bottom gauge at the center of the wall. (b) Complete failure occurred when crack propagated the full width of the wall.

CMU rotated along the mortar joint and diagonal cracks began to develop from the tear along the left side to the tear along the bottom course of blocks. As the wall passed the 3-in. deflection mark, the diagonal cracks grew wider and a second diagonal crack became very visible as the crack propagated to the right edge of the wall. From the video it was observed that the maximum deflection occurred at the bottom of the wall until the diagonal crack along the third course of blocks became more dominant. Mortar and block debris began to fall out of the cracks once the wall deflection passed the 4-in. deflection mark. When the wall completely failed, the blocks remained attached to the

liner (Figure 5.39b). The ultimate flexural resistance of the CMU wall occurred at a pressure of 0.0834 and a deflection of 0.128 and the ultimate failure of the retrofit occurred at a pressure of 0.0751 and a deflection of 0.453 (Figure 5.40).

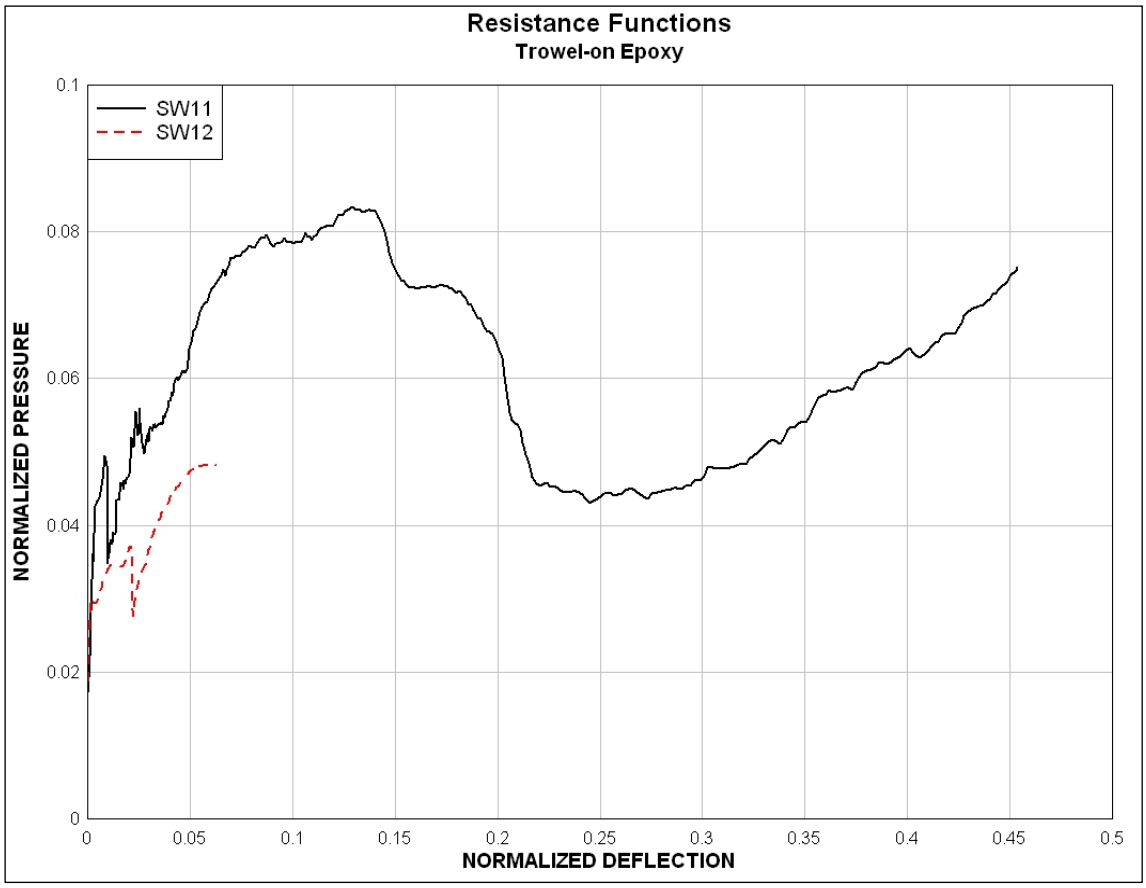

Figure 5.40. Resistance functions for SW11 and SW12.

5.5.3 Wall SW12

The retrofit procedure used for SW11 was repeated on SW12. The procedure differed only in an attempt to prevent the material from running down the face of the CMU wall. After the epoxy was applied to the CMU wall, a layer of aluminum foil was

placed across the wall surface. The foil was later removed from the wall, but some of the foil could not be removed from the top and bottom supports. The foil prevented the material from running, but it left a very uneven layer of epoxy on the wall surface as seen in Figures 5.41a and b. In addition to the adhesive bond between the epoxy and the steel flanges, mechanical anchorage was added by bolting steel plates to the top and bottom flanges.

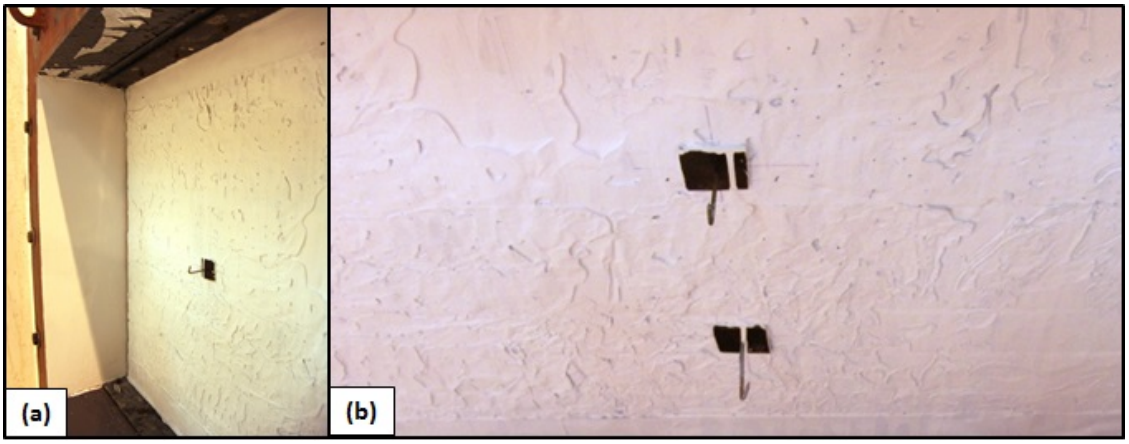

Figure 5.41. SW12. (a) CMU wall retrofitted with trowel-on epoxy. (b) Uneven epoxy surface.

The retrofitted wall failed after a crack developed uniformly across the full length of the wall at the mid-span (Figure 5.42a). The crack developed at a pressure of 0.0267 and deflection of 0.00241. The pressure in the HTC continued to increase until failure occurred at a maximum pressure of 0.0484 at a deflection of 0.0602 (Figure 5.40). The wall broke into two sections (Figure 5.42b). The top half of the wall hung from the top support and the bottom half of the wall settled on the bottom support. The CMUs were

still attached to the epoxy indicating a good adhesive bond between the epoxy and the block surface. The data for the trowel-on material experiments were listed in Table 5.4.

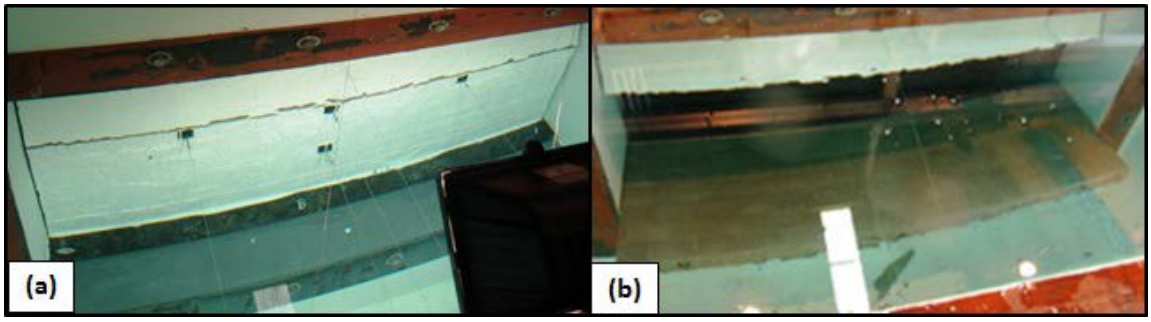

Figure 5.42. SW12. (a) Failure occurred along the mid-span. (b) Wall broke into two sections.

Table 5.4. Normalized pressure (P) and deflection (d) data for trowel-on materials.

Wall	Retrofit	CMU Wall Failure		Retrofit Failure	
		P	d	P	d
SW10	Trowel-on Thermoset	0.0889	0.0568	0.536	0.744
SW11	Trowel-on Epoxy	0.0834	0.128	0.0751	0.453
SW12	Trowel-on Epoxy	0.0484	0.0602	NA	NA

5.6 Unreinforced Film and Trowel-on Adhesive Retrofits (SW13-SW14)

5.6.1 Wall SW13

Wall SW13 was retrofitted with the trowel-on thermoset material used in SW10 and an unreinforced layer of elastomeric film (Figure 5.43a). First, a layer of thermoset was applied to the wall and the top and bottom supports using a grooved trowel. A single

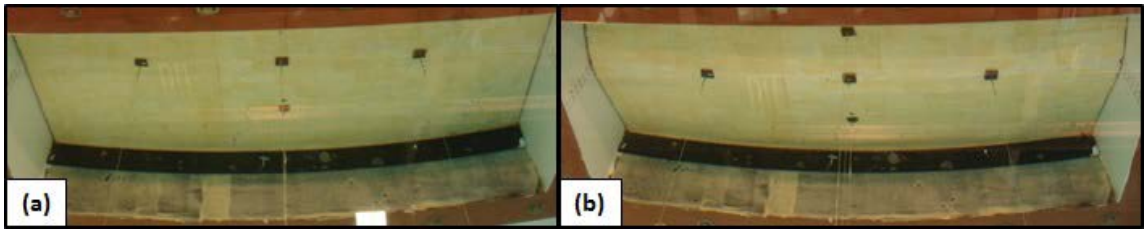

**Figure 5.43. SW13. (a) Pretest view of retrofitted wall.
(b) Mid-span wall deflection at 3 in.**

layer of the elastomeric film was applied to the wall surface and pressure was applied using a rubber roller to secure the adhesive bond between the trowel-on thermoset and the elastomeric film. The procedure used to apply the retrofit materials was discussed in detail in Section 4.7.2. In addition to the adhesive bond, mechanical anchorage was added by bolting steel plates to the top and bottom flanges clamping the retrofit material to the test frame.

The retrofitted wall exhibited a toughness not observed on any of the previous experiments. The wall deformation began along the mid-span of the wall (Figure 5.43b) and continued to be the area of maximum deformation until the elastomeric film sheared along the anchor plate at the top support (Figure 5.44b). The deformation in the retrofit was consistent across the mid-span of the wall until the deformation exceeded the 8-in. mark (Figures 5.45a and b). This appeared to be a limitation of the membrane separating the two chambers of water. Because the membrane is bolted on all four sides, it could not continue to deform uniformly with the wall, which is why the deflection of the film continued to increase at the center of the wall as illustrated in Figures 5.44a and b,

Figures 5.45a and b. and Figure 5.46a. The trowel-on thermoset used as the adhesive for the film began to fail along the mortar joints, which represent the high strain locations,

Figure 5.44. SW13. (a) Deformation extends past the reaction structure frame. (b) Failure of the film occurred when the material sheared at the top support.

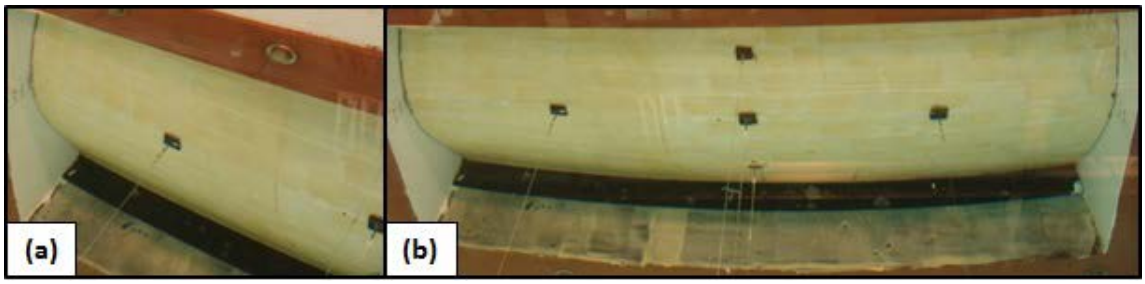

Figure 5.45. SW13. (a) Mid-span deflection at 8 in. (b) Uniform deflection across the wall.

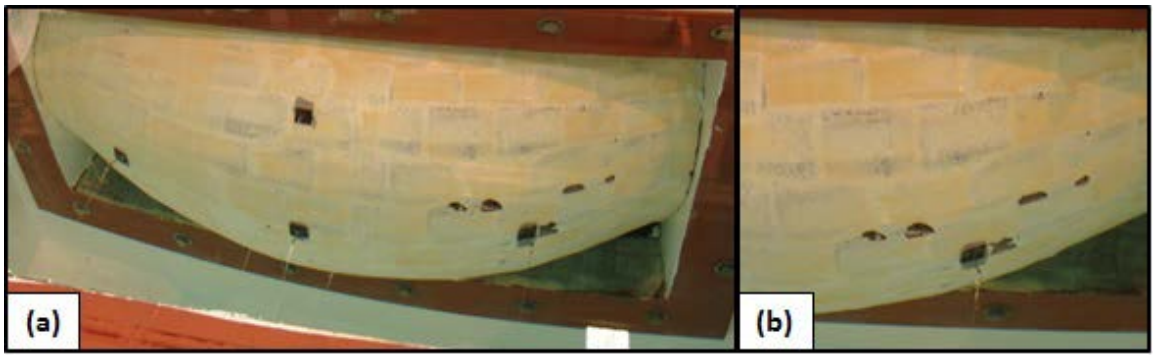

Figure 5.46. SW13. (a) Extreme deformation of the retrofitted CMU wall. (b) Thermoset used as an adhesive begins to tear under the film.

as the pressure and deformation continued to increase (Figure 5.46b.). The CMU wall cracked at a pressure of 0.0723 and a deflection of 0.0728 (Figure 5.47). The collection of deflection data stopped at 0.991, but from the still pictures it appeared that the film deformed past this value. The maximum pressure the retrofitted wall sustained was 0.634.

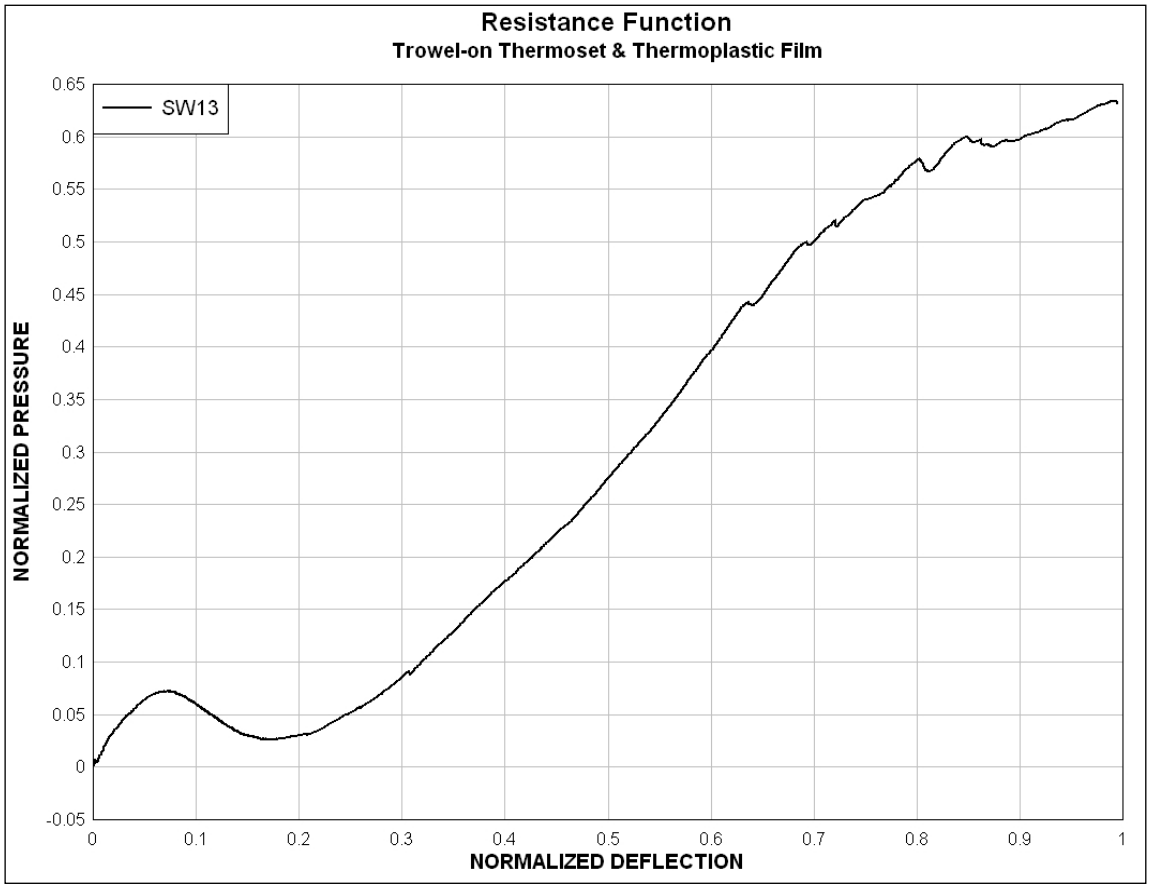

Figure 5.47. Resistance function for SW13.

5.6.2 Wall SW14

Wall SW14 was retrofitted with the trowel-on epoxy used in SW11 and SW12 and an unreinforced layer of elastomeric film. First, a layer of epoxy was applied to the wall and the top and bottom supports using a grooved trowel. A single layer of the elastomeric film was applied to the wall surface and pressure was applied via a rubber roller to secure the adhesive bond between the trowel-on epoxy and the elastomeric film. The procedure used to apply the retrofit materials was discussed in detail in Section 4.7.3. In addition to the adhesive bond between the epoxy and the steel flanges, mechanical anchors were added to the top and bottom flanges by bolting steel plates to the test frame. The epoxy color made it difficult to observe deformation in the wall, so the elastomeric film was painted to aid the documentation process.

The retrofitted wall underwent a large deformation before failure of the film occurred at the top support. Cracks in the paint layer formed as the retrofitted wall deflected (Figure 5.48a). The cracks in the paint indicated high strain regions and the number of cracks in the paint increased as the pressure and deflection continued to increase (Figure 5.48b). The mortar joint and the increase in deflection between the CMU courses increased as shown in Figures 5.49a and b. The film resisted load until it sheared along the steel anchor at the top support (Figures 5.50a and b). The ductility of the film allowed the CMU blocks and film to deform without crushing the CMU blocks as demonstrated in Figures 5.51a and b.

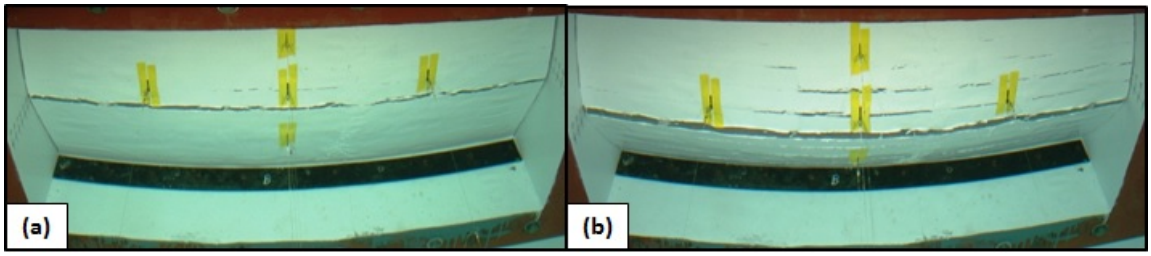

Figure 5.48. SW14. (a) Deflection at 0.259 (b) Cracks in paint indicate high strain regions. Deflection at 0.517.

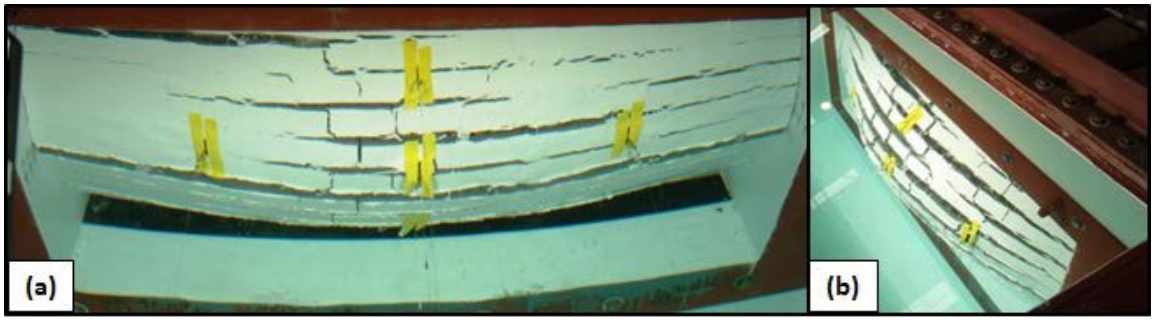

Figure 5.49. SW14. (a) High strain regions outlined by cracks in the paint along the mortar joints. (b) Point before the membrane failed.

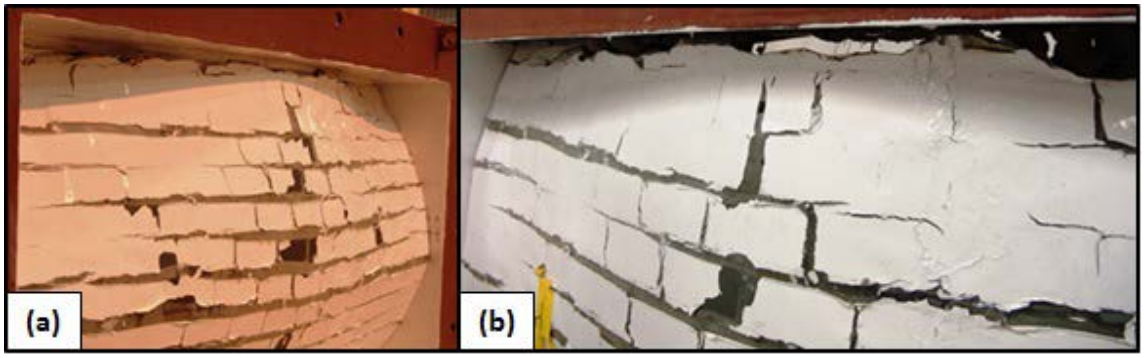

Figure 5.50. SW14. (a) Plastic deformation in film and tear along the top support. (b) Film tore along the center of the film at the top support.

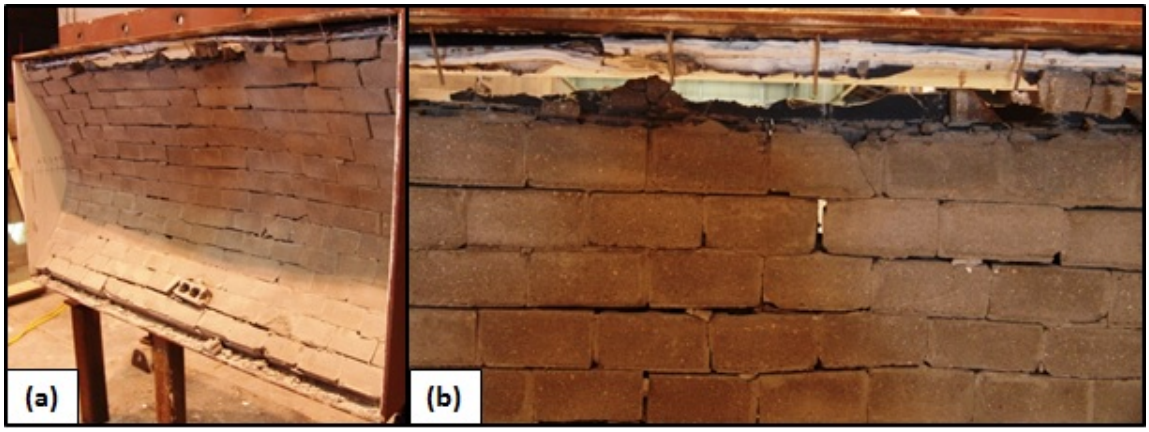

Figure 5.51. SW14. (a) The mortar joints on the CMU wall were compromised, but the face shells were undamaged. (b) Tear in the film and mortar joints failed.

The CMU wall failed at a pressure of 0.0978 and a deflection of 0.105. It appears that the elastomeric film began to tear along the top support at approximately 0.421 and 0.776 of deflection. This could not be seen on the video or in the still pictures, but the resistance function plateaus at this point and slightly decreases before the deflection and pressure increase at a different rate (Figure 5.52). The maximum pressure and deflection recorded by the data system was 0.743 at a deflection of 1.29. The data for the unreinforced films with trowel-on adhesives are listed in Table 5.5.

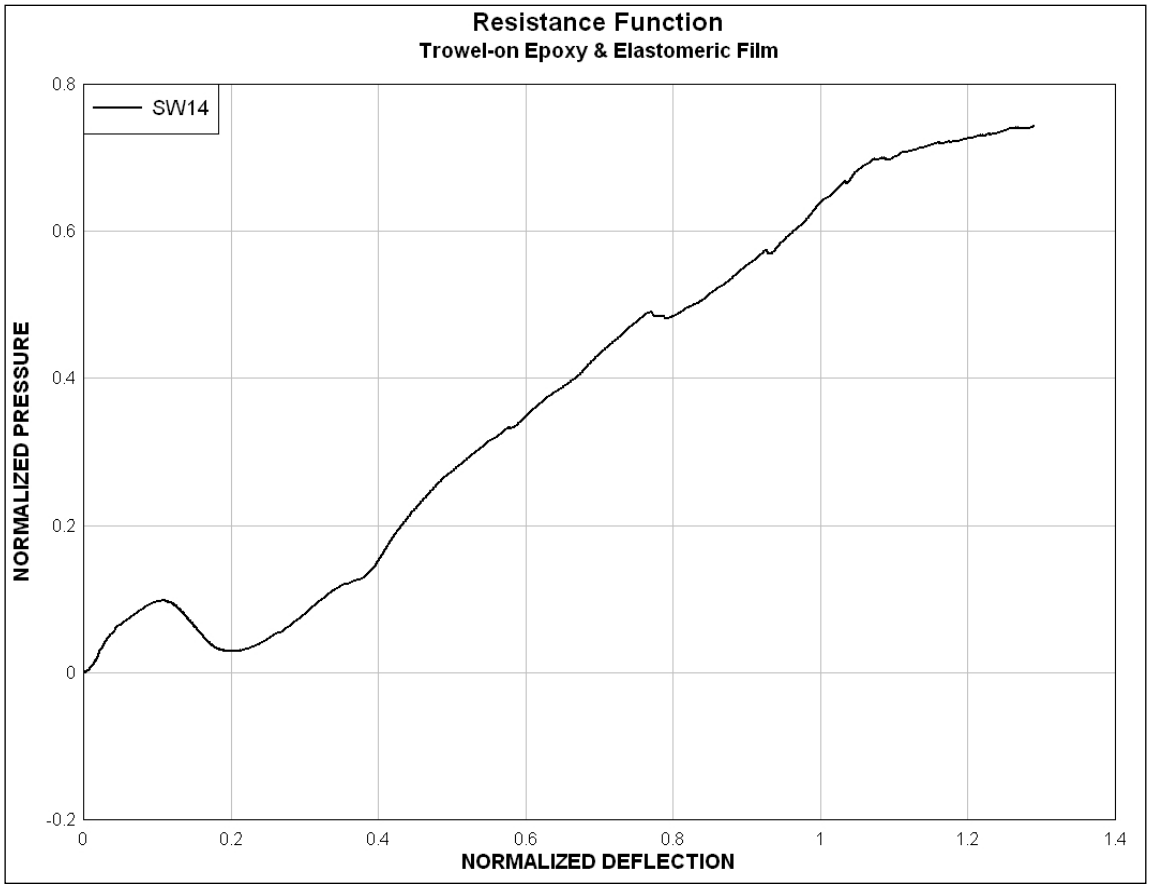

Figure 5.52. Resistance function for SW14.

Table 5.5. Normalized pressure (P) and deflection (d) data for unreinforced films with trowel-on adhesives.

Wall	Retrofit	CMU Wall Failure		Retrofit Failure	
		P	d	P	d
SW13	Trowel-on Thermoset and Thermoplastic Film	0.0723	0.0728	0.634	0.991
SW14	Trowel-on Epoxy and Elastomeric Film	0.0978	0.105	0.743	1.29

5.7 Reinforced Film and Trowel-on Adhesive Retrofit (SW15-SW16)

5.7.1 Wall SW15

Wall SW15 was retrofitted with the trowel-on epoxy used in SW11, SW12, and SW14 and a reinforced layer of elastomeric film. First, a layer of epoxy was applied to the wall and the top and bottom supports using a grooved trowel. A single layer of the fiber-reinforced elastomeric film was applied to the wall surface and pressure was applied via a rubber roller to secure the adhesive bond between the trowel-on epoxy and the elastomeric film. The fiber-reinforced elastomeric film was produced with fibers oriented at 0/90 deg and cut such that the fibers would align at ±45 deg on the wall. The film sheets cut at the specified angle created a diagonal seam across the center of the wall. The seam was secured using an additional layer of trowel-on epoxy (Figure 5.53a). The procedure used to apply the retrofit materials was discussed in detail in Section 4.8. In addition to the adhesive bond between the epoxy and the steel flanges, mechanical anchors were added to the top and bottom supports by bolting steel plates to the top and bottom flanges. Both sheets of film were anchored to the top and bottom supports.

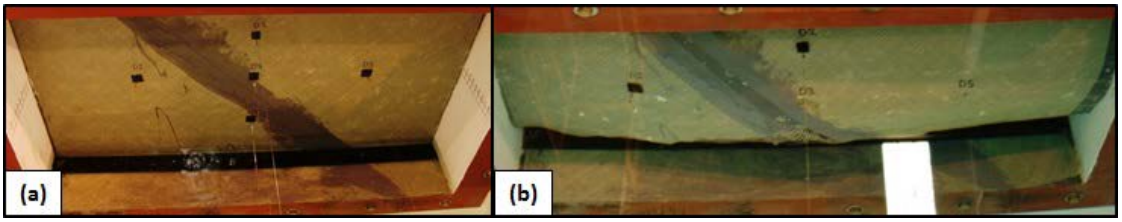

Figure 5.53. SW15. (a) Pretest view. (b) As the retrofitted wall deformed under load, the film began to pull away from the right edge of the wall.

The retrofit system was not tested to failure because the membrane burst during the execution of the HTC experiment. The deformation in the retrofitted wall was uniform until the CMU began to lodge against the side of the frame (Figure 5.54a). As the retrofitted wall deflected, the film began to pull away from the right edge of the wall surface (Figure 5.53b). As the loading on the specimen continued, the seam across the center of the wall began to open (Figure 5.54b) and the adhesion between the film and epoxy was lost (Figure 5.54c). Posttest inspection of the specimen indicated that the fibers deformed at the high strain points along the wall (Figures 5.55a and b). It was also evident during the inspection that the mortar bed at the bottom of the wall did not adhere to the steel frame. The mortar bed remained intact and adhered to the bottom course of CMU blocks as the wall rotated as shown in Figure 5.56b. The CMU blocks lodging between the film and the frame created an alternate crack pattern in the wall than what was observed in previous experiments (Figure 5.56a). The CMU wall failed at 0.34 and a deflection of 0.0684. The maximum pressure and deflection recorded by the data system was a pressure of 0.468 at a deflection of 0.627 (Figure 5.57). The data for the fiber reinforced films with trowel-on adhesive experiments were listed in Table 5.6.

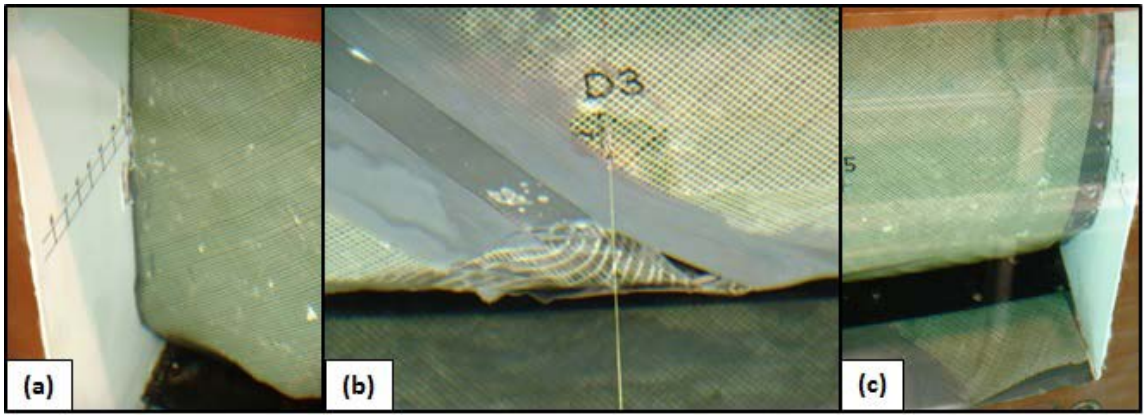

Figure 5.54. SW15. (a) Right edge of retrofitted wall lodged against the steel frame. (b) Seam at the overlap opened during the experiment. (c) Adhesion was lost between the film and epoxy.

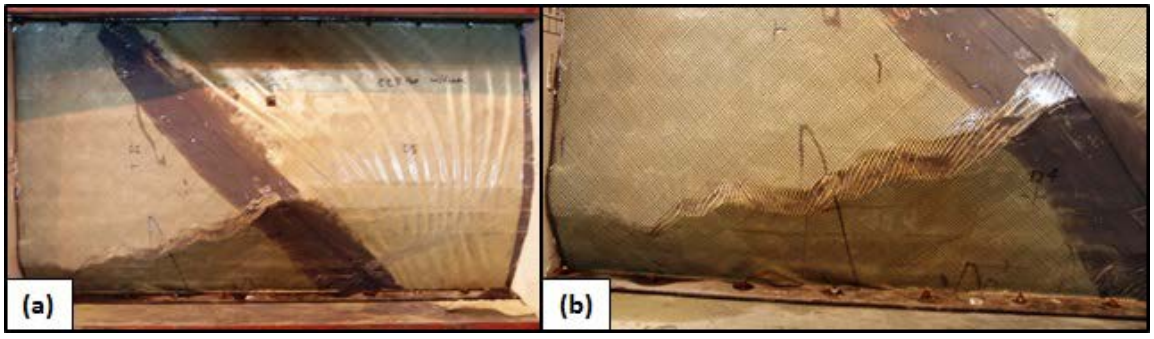

Figure 5.55. SW15. (a) Posttest view. (b) Stressed fibers in the film.

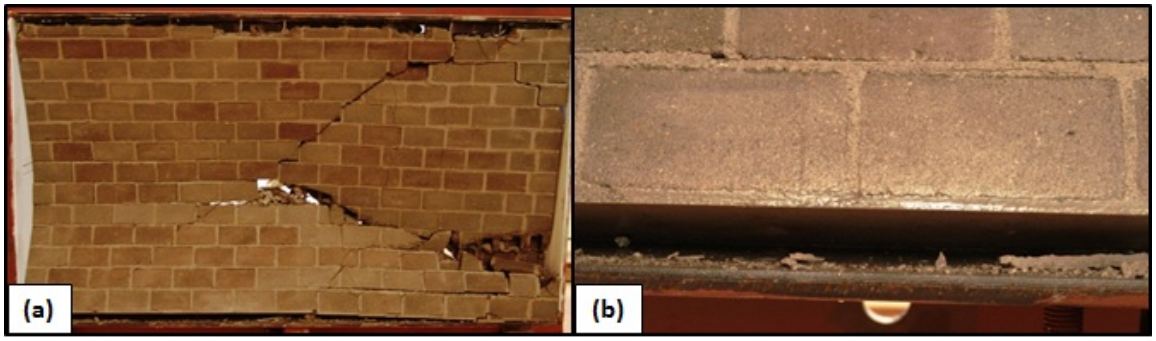

Figure 5.56. SW15. (a) The CMU blocks lodging against the side of the steel frame forced an alternate failure pattern. (b) Mortar joint at the bottom course of blocks did not bond to the steel frame.

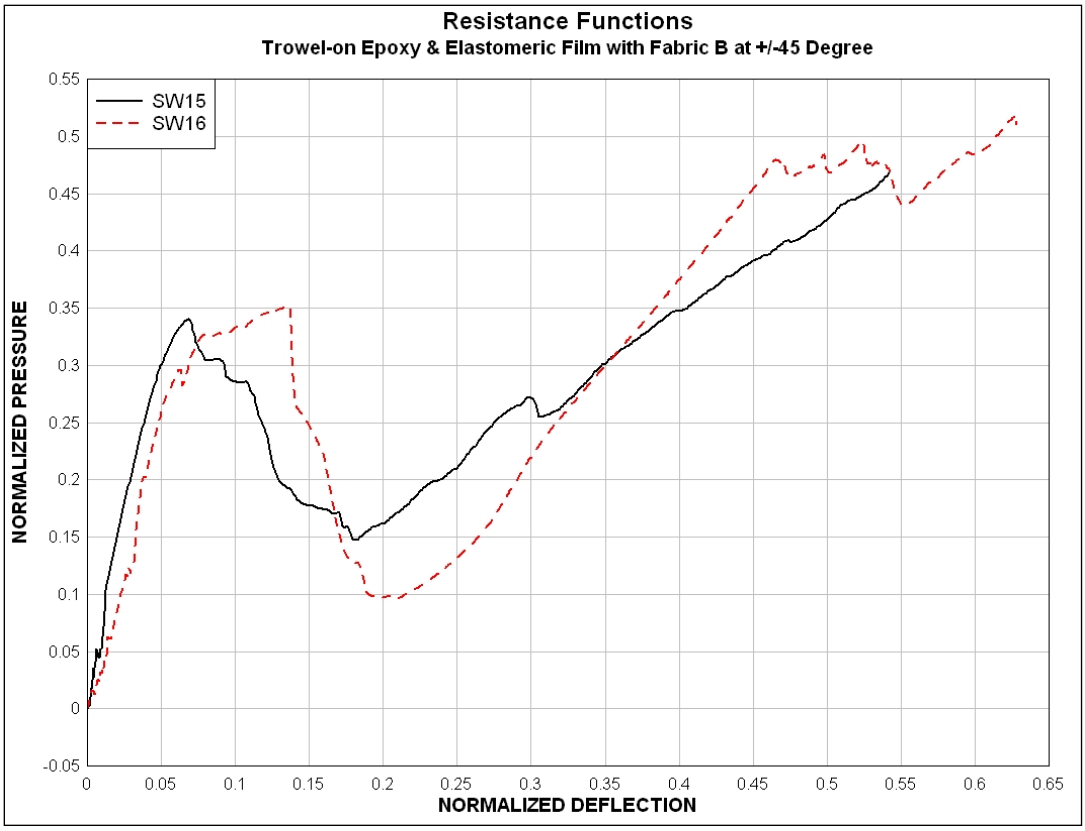

Figure 5.57. Resistance functions for SW15 and SW16.

Table 5.6. Normalized pressure (P) and deflection (d) data for fiber reinforced films with trowel-on adhesives.

Wall	Retrofit	CMU Wall Failure		Retrofit Failure	
		P	d	P	d
SW15	Trowel-on Epoxy and Elastomeric Film with Fabric B at ±45 deg	0.34	0.0684	0.468	0.542
SW16	Trowel-on Epoxy and Elastomeric Film with Fabric B at ±45 deg	0.351	0.135	0.518	0.627

5.7.2 Wall SW16

Wall SW16 was retrofitted using the same technique and materials used for SW15 (Figure 5.58a). The maximum deformation was consistent along the mid-span of the retrofitted wall and a crack developed along the mortar joint at the mid-height of the wall (Figure 5.58b). The crack grew as the retrofitted wall deformed under an increasing load. The fibers began to reorient from the ±45-deg orientation to a 90-deg orientation as the deformation increased (Figures 5.59a and b). Notice that both fibers began to span the crack vertically (Figure 5.60a and b). If the fibers in the film were oriented in a 0/90-deg orientation then only half of the fibers (90-deg fibers) would have been engaged. The horizontal, 0-deg, fibers would not have carried any load. By using the ±45-deg orientation the retrofit system can absorb more energy as both sets of fibers reorient along the high strain location at mid-span. Ultimate failure of the reinforced elastomeric film occurred when the film tore from left to right across the length of the wall (Figures 5.61a and b). The ultimate flexural failure of the wall occurred at a pressure of 0.351 and a deflection of 0.135 and the ultimate failure of the retrofit system occurred at a pressure of 0.518 and a deflection of 0.627 (Figure 5.57).

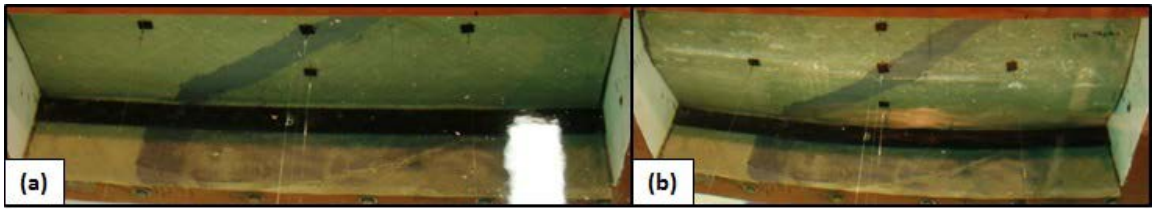

Figure 5.58. SW16. (a) Pretest view. (b) Change in appearance at the mid-span indicates a high strain location.

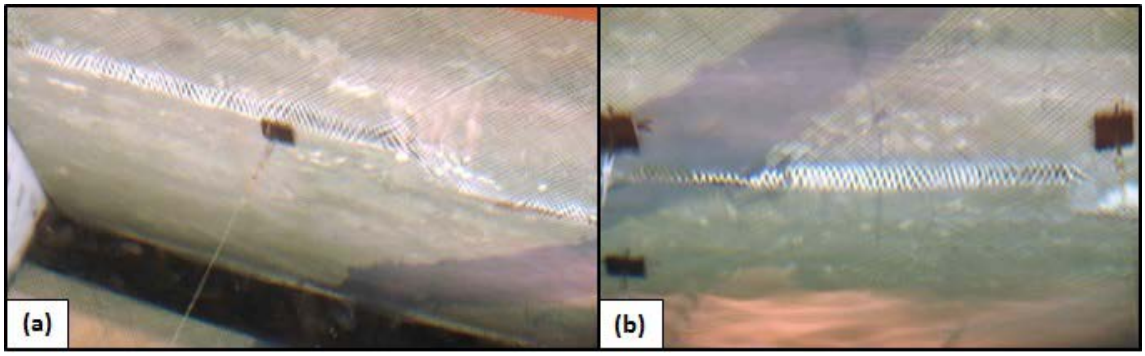

Figure 5.59. SW16. (a) Fibers along the mid-span mortar joint began to reorient. (b) Epoxy along seam cracked and fibers reorient.

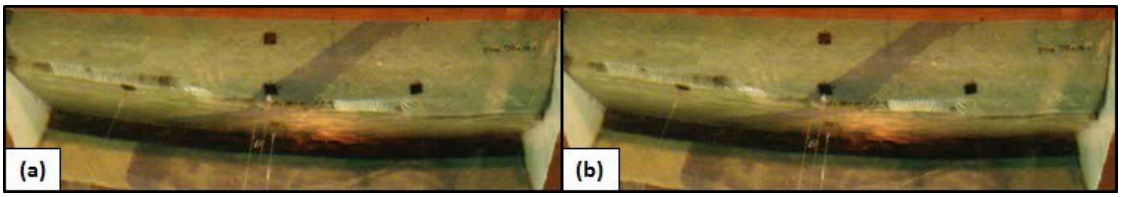

Figure 5.60. SW16. (a) The fibers continued to reorient from ±45 deg to 90 deg across crack. (b) Fibers began to fail as the deformation continued.

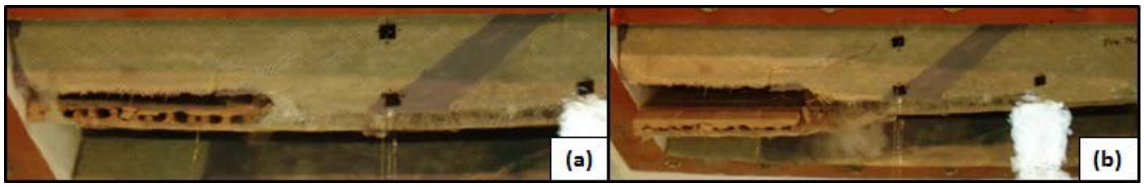

Figure 5.61. SW16. (a) Film and fibers continued to fail as the pressure increased. (b) Rip continued across the length of the retrofit.

5.8 Unreinforced Film with PSA (SW17-SW21)

5.8.1 Wall SW17

Wall SW17 was retrofitted with an unreinforced elastomeric film adhered to the wall and supports using a double sided tape (Figure 5.62a). A spray-on adhesive was used to

Figure 5.62. SW17. (a) Pretest view. (b) Posttest view of the retrofit system.

secure the film to the top and bottom supports. Anchor System 2 was added to mechanically secure the elastomeric film to the test frame. The membrane failed before the film could be tested to failure. The maximum deformation occurred at the mid-span and as the film deformed it was snagged by the bolts securing the anchor plates. The holes created in the film by the bolts did not cause the film to tear or rip indicating that it was a tough material. However, the film and CMU blocks deformed more than 1.38 at the center, which almost exceeded the acceptable deflection. The film plastically deformed under load and the blocks lost adhesion along the center of the film as illustrated in Figures 5.62b and 5.63. The CMU wall failed at a pressure of 0.0723 and a deflection of 0.0501 (Figure 5.63). The documentation of the retrofit's deformation ended when the membrane failed at a pressure of 0.84 and a deflection of 1.4 (Figure 5.64). The data for the unreinforced film with PSA experiments were listed in Table 5.7.

Figure 5.63. Damaged CMU blocks and area where the blocks lost adhesion.

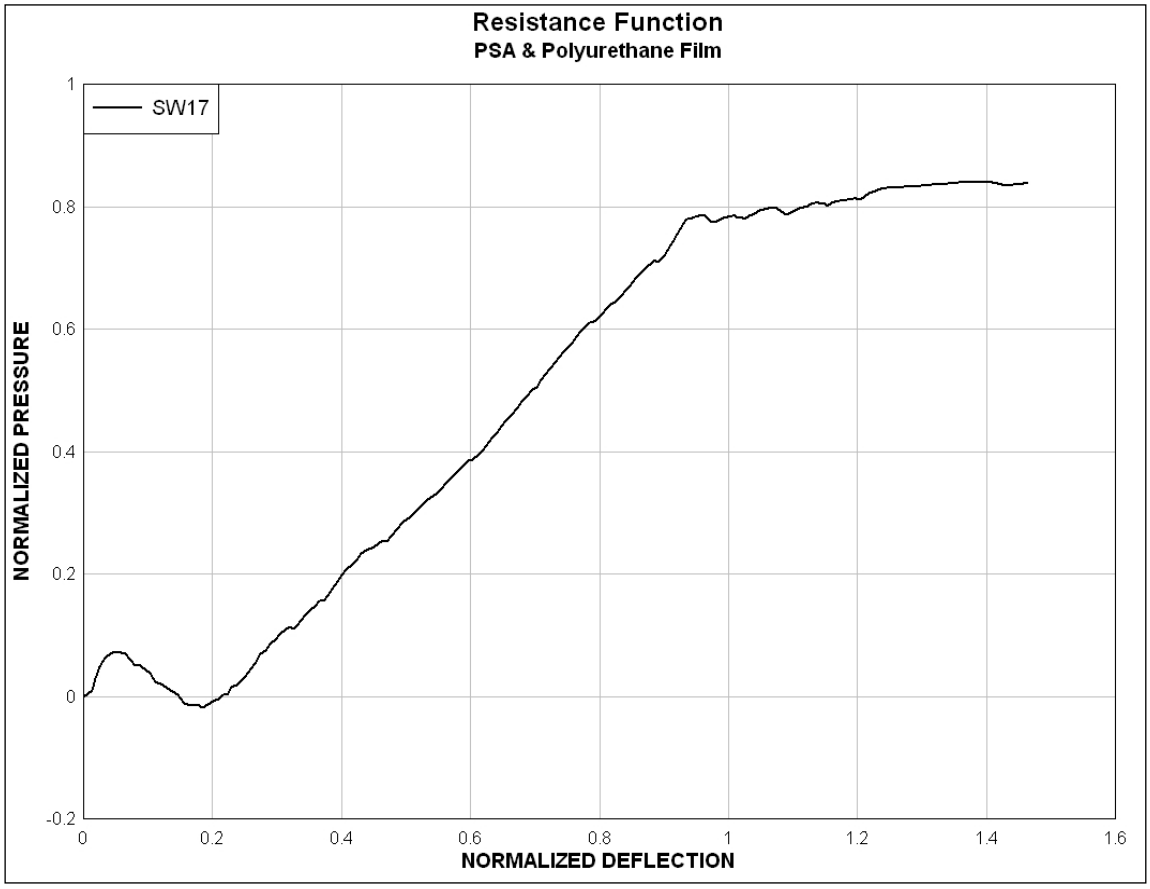

Figure 5.64. Resistance function for SW17.

Table 5.7. Normalized pressure (P) and deflection (d) data for unreinforced films with PSA.

Wall	Retrofit	CMU Wall Failure		Retrofit Failure	
		P	d	P	d
SW17	Polyurethane Film	0.0723	0.0501	0.84	1.41
SW18	Spray-on Adhesive Thermoplastic Film	0.104	0.05	0.733	0.839
SW19	PSA and Elastomeric Film	0.0297	0.0723	0.525	0.926
SW20	PSA and Elastomeric Film	0.062	0.0969	0.367	1.15
SW21	PSA and Polyurethane Film	0.116	0.0696	0.998	0.997

5.8.2 Wall SW18

Wall SW18 was retrofitted with an unreinforced elastomeric film adhered to the wall using a double sided tape. A spray-on synthetic rubber adhesive and anchor System 2 was used to secure the elastomeric film to the top and bottom supports (Figure 5.65a). The transparent film and adhesive allowed the deformation and damage in the CMU wall to be viewed under loading. The maximum deformation of the retrofitted wall was not consistent across the mid-span (Figure 5.65b). The wall deformed in large sections that consisted of two to three courses of CMU (Figure 5.66a). As the deformation continued vertical cracks in the wall sections began to develop around the center of the wall (Figure 5.66b). The width of the cracks continued to increase until the film tore along the anchor plate on the top support (Figures 5.67a and b). The CMU wall failed at a pressure of 0.104 and a deflection of 0.05 (Figure 5.68). The film failed at a pressure of 0.733 and a deflection of 0.839.

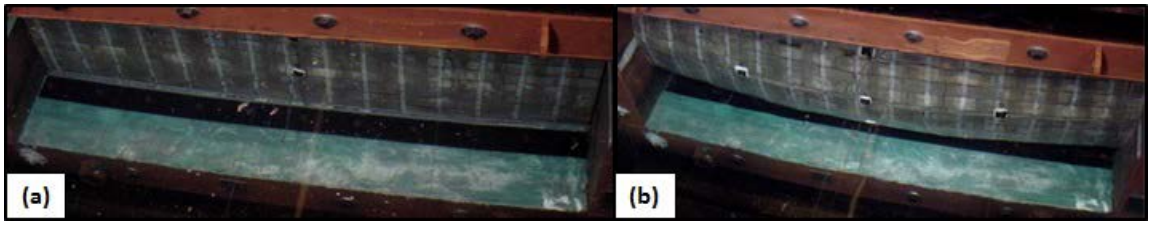

Figure 5.65. SW18. (a) Pretest view. (b) CMU blocks and retrofit did not deform consistently at mid-span.

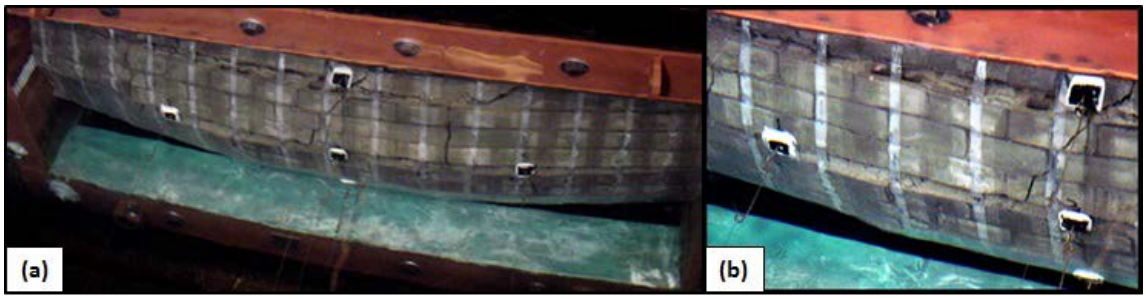

Figure 5.66. SW18. (a) Cracks in wall are visible as the wall deforms. (b) Cracks in the mortar joint continue to enlarge as the wall deforms.

Figure 5.67. SW18. (a) Retrofit failure occurred when the film tore along the top support. (b) Tear in the elastomeric film.

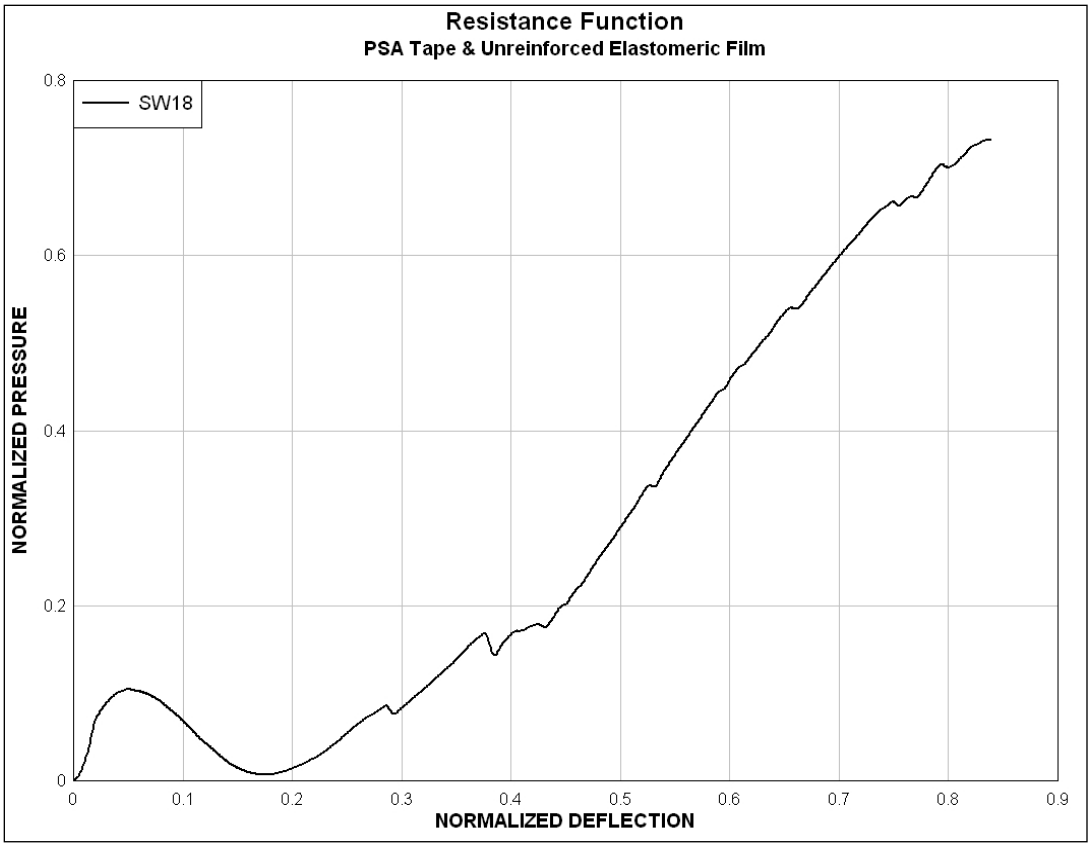

Figure 5.68. Resistance function for SW18.

5.8.3 Wall SW19

Wall SW19 was retrofitted with an unreinforced elastomeric film applied to the CMU wall using a sheet of PSA on the wall surface and a trowel-on epoxy on the top and bottom supports (Figure 5.69a). Mechanical anchorage System 2 was applied to the top and bottom supports. The retrofit system consisted of an unreinforced elastomeric film, Primer 1 for the supports, a PSA for the wall, and a trowel-on epoxy for the supports. The procedure used to retrofit SW19 was detailed in Section 4.10. The anchor plates were applied using nuts and bolts once the epoxy dried, and the wall was allowed to sit for at least 24 hr before it was evaluated in the HTC.

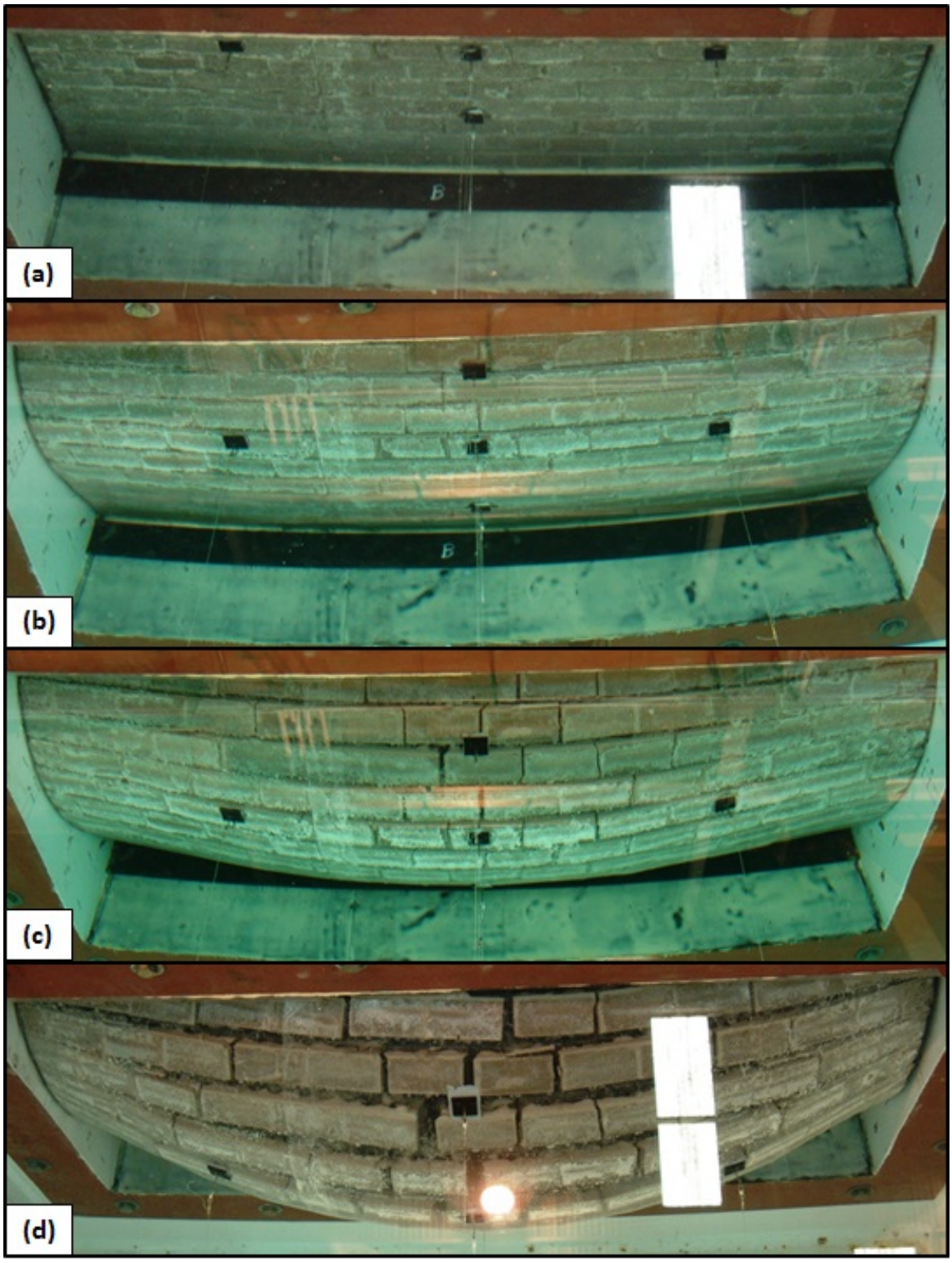

Figure 5.69. SW19. (a) Pretest view. (b) Deflection at 0.388. (c) Deflection at 0.603. (d) Deformation exceeded the test frame.

Specimen SW19 could not be evaluated to failure because the membrane failed during test execution. The film plastically deformed, but no tears were visible in the film during the posttest inspection of the specimen. During the initial response of the retrofitted wall, the maximum deformation of the wall was consistent along the mid-span (Figure 5.69b); however, as the loading and deformation increased the center of the wall began to have larger deformations than the sides or centerline (Figure 5.69c). The horizontal and vertical mortar joints were compromised across the entire surface of the wall and the CMU blocks were held between the elastomeric film and the membrane (Figures 5.69d and 5.70b). The retrofit deformed past the plane of the steel frame before the membrane failed (Figure 5.70a). The CMU wall failed at a pressure of 0.0297 and a deflection of 0.0723 (Figure 5.71). The membrane failed at a pressure of 0.525 and a deflection of 0.926.

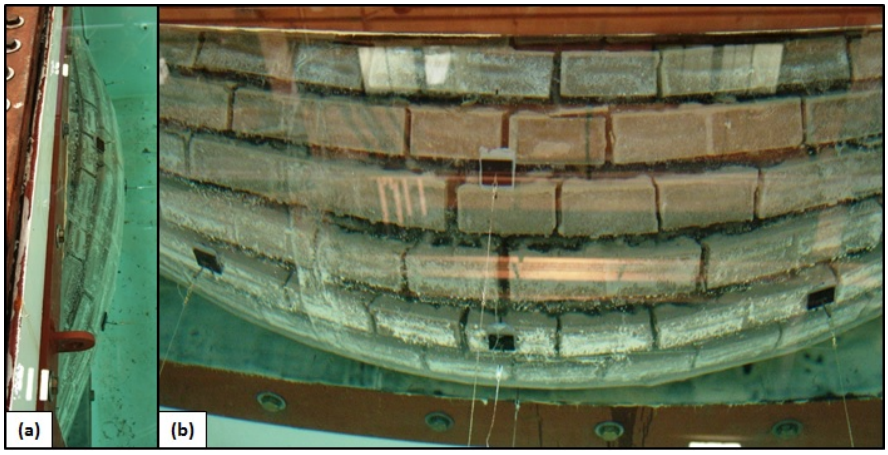

Figure 5.70. SW19. (a) Deformation exceeded beyond plane of steel frame. (b) Failure of horizontal and vertical mortar joints at large deformation.

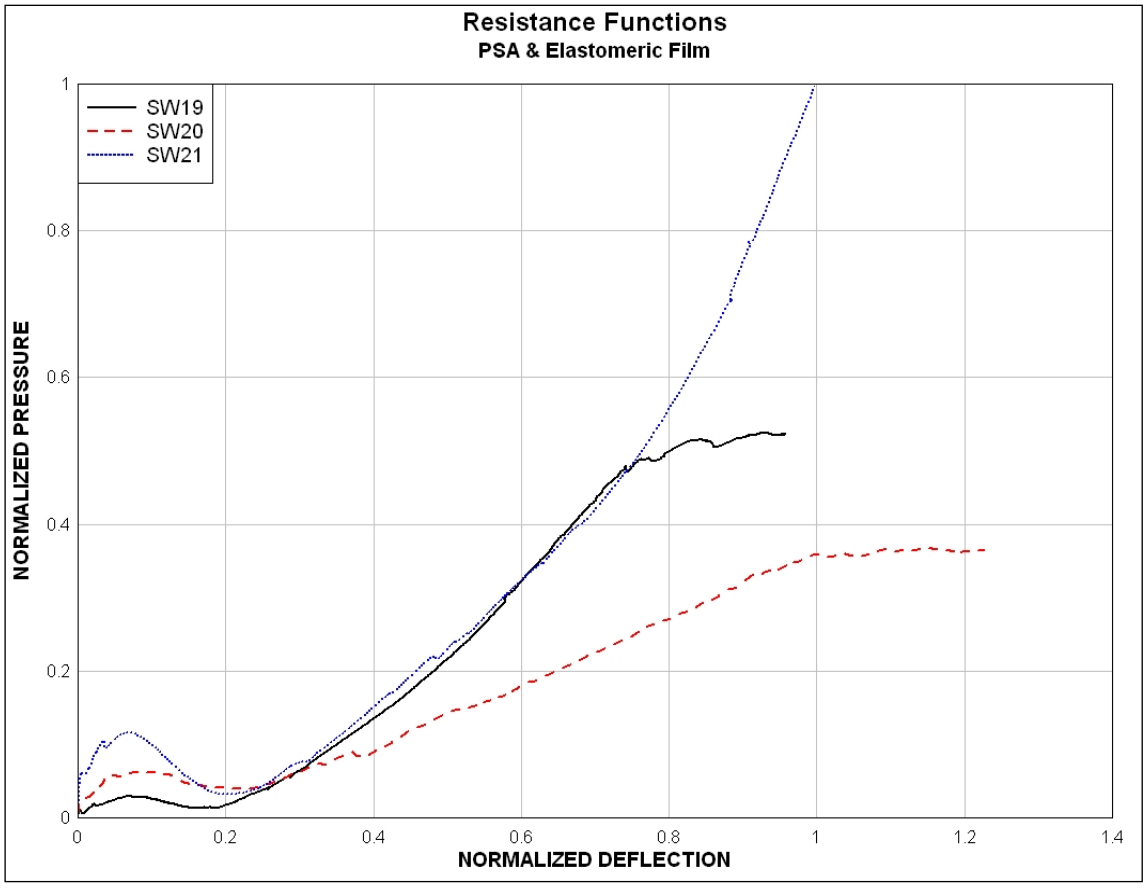

Figure 5.71. Resistance functions for SW19, SW20, and SW21.

5.8.4 Wall SW20

The application procedure used to retrofit SW19 was duplicated on wall SW20 (Figure 5.72a). The CMU wall failed at a pressure of 0.062 and a deflection of 0.0969. The retrofit system applied to SW20 was very ductile, allowing an overall deformation of 1.15 at a peak pressure of 0.367 before it sheared along the top support. The unreinforced and transparent film used to retrofit SW20 allowed witnesses to watch as the cracks formed during the loading process (Figure 5.732b).

Witnesses watched as air bubbles trapped between the CMU wall surface and film traveled through the cracks formed in the CMU wall. As SW20 deformed, multiple cracks developed horizontally and vertically along the entire CMU wall surface. The ductility of the material is evident in Figures 5.73a and b as the wall extends past the steel frame surface. As the pressure continued to increase, the cracks in the wall continued to widen, and the PSA began to tear as the film stretched under the increasing deformation (Figure 5.74). As the PSA continued to tear, sections of the wall and film no longer carried any adhesion between the two surfaces. Deflection gauge, D1, was unable to maintain adhesion to the film during the deformation process and disengaged before complete failure occurred (Figures 5.73c and 5.74). Complete failure of the retrofit system occurred when the film tore along the top support. The resistance function developed from the pressure and deflection data for SW20 is plotted on Figure 5.71 (Johnson, Davis, Coltharp, Durst, and Smith 2010).

Figure 5.72. SW20. (a) Pretest view. (b) Deflection reaches 0.474. (Adapted from Johnson, Davis, Coltharp, Durst, and Smith 2010)

Figure 5.73. SW20. (a) Deformation passed the frame. (b) Vertical and horizontal cracks on wall continued to expand. (c) Gauge D1 disengaged from film surface. (Adapted from Johnson, Davis, Coltharp, Durst, and Smith 2010)

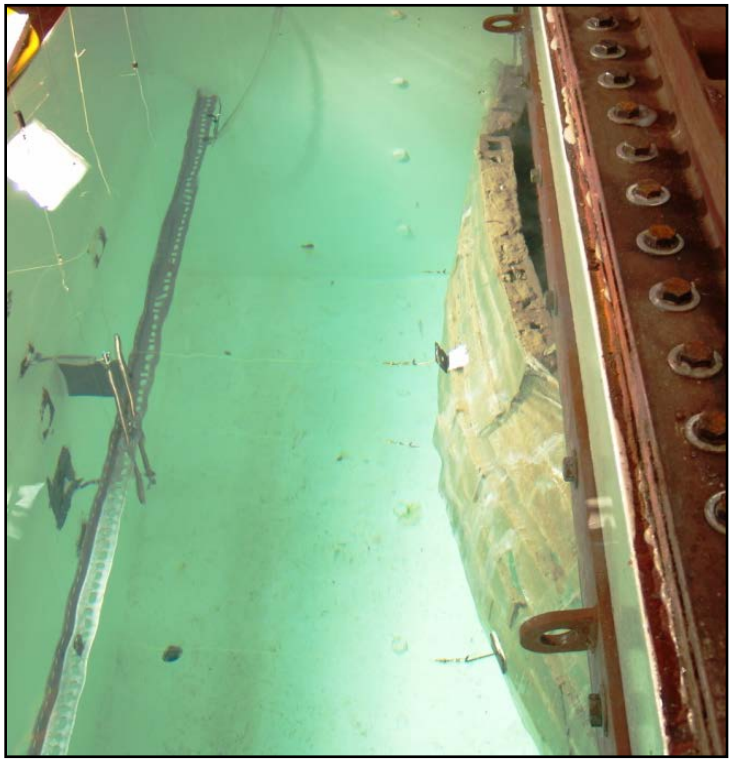

Figure 5.74. SW20– Final failure occurred as the film tore across the top support. (Johnson, Davis, Coltharp, Durst, and Smith 2010)

5.8.5 Wall SW21

The retrofit materials/system and installation process for SW20 was repeated on SW21. A pretest view of the retrofitted CMU wall and the anchoring system are shown in Figures 5.75a and b, respectively.

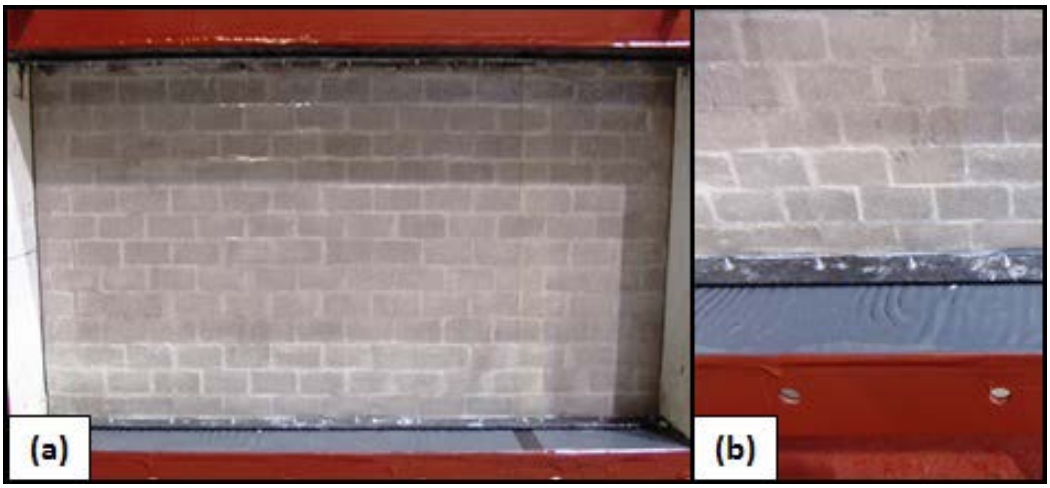

Figure 5.75. SW21. (a) Unreinforced elastomeric film retrofit. (b) Epoxy and mechanical anchorage at bottom support.

The SW21 retrofit system was very ductile, allowing an overall deformation of 0.997 at a peak pressure of 0.998 (Figure 5.71). The CMU wall failed at a pressure of 0.116 and a deflection of 0.0696. As SW21 was loaded, the first crack developed horizontally along the fourth mortar joint from the top, one course below deflection gauge D1. A second horizontal crack developed two courses below the middle gauge and like the first crack, extended the entire width of the wall. The second crack occurred as the wall reached approximately 0.0645 deflection (Figure 5.76a). A third horizontal crack formed two courses below the second crack.

The wall appeared to break into three sections or layers. The three layers were divided as follows: a bottom layer consisting of five courses of block, a second layer containing the five center courses, and then a final layer containing all the remaining courses up to the dowels. Maximum deformation was centered between the D3 and D5 gauges. As the pressure continued to increase, the cracks continued to widen and vertical cracks began to form through the center of the

wall. Inspection of the video indicated that the edges of the CMU wall wedged into the steel frame at approximately 0.431. (Figure 5.76b). Vertical cracks formed at the center of the wall when it wedged against the steel frame and distorted the data (Figure 5.77b). As the pressure increased, the cracks in the wall continued to widen, and the PSA began to tear beneath the film. The film was undamaged, but sections of the PSA were stretched beyond capacity leaving the film and CMU wall unengaged at spots (Figure 5.77a). Complete failure of the retrofit system occurred when the film tore at the center of the top support. Posttest inspection of the blocks indicated that most of the cells were almost completely filled with grout, which would increase the mass of the wall. In this case, the wall should be classified as a partially grouted wall, rather than a hollow wall. The increased mass of the wall strengthened it at least up to the point of ultimate flexural resistance (Johnson, Davis, Coltharp, Durst, and Smith 2010).

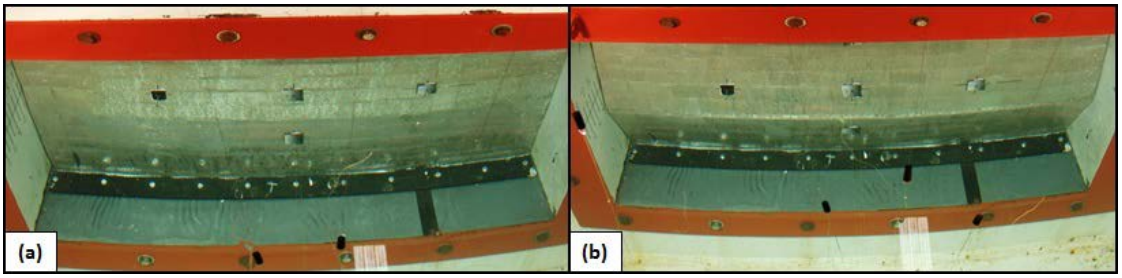

Figure 5.76. SW21. (a) Wall cracks. (b) Crack continues to deform at mid-span. (Johnson, Davis, Coltharp, Durst, and Smith 2010)

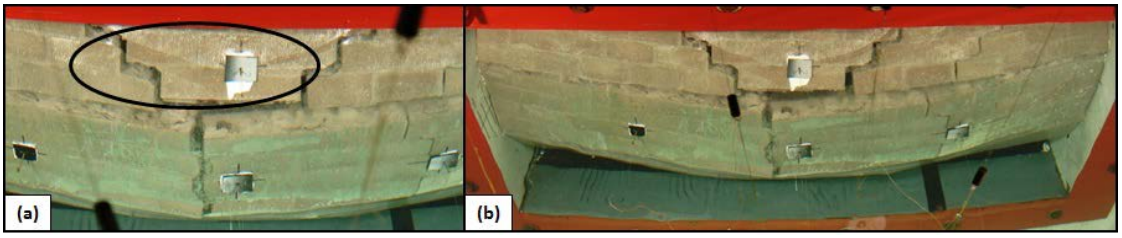

Figure 5.77. SW21. (a) Area where PSA has separated, but film is still intact. (b) Final image at failure. (Johnson, Davis, Coltharp, Durst, and Smith 2010)

5.9 Reinforced Film with PSA (SW22-SW24)

5.9.1 Wall SW22

The retrofit system for SW22 consisted of Primer 5 for the supports and CMU wall surface, a ±45-deg fiber reinforced film (Fabric G) and anchor System 2 (Figure 5.78a). The reinforced film was constructed by laminating an open weave fiber reinforcement between two sheets of elastomeric film. The reinforced film arrived at the ERDC with a PSA that was applied in the factory prior to shipment. The procedure used to retrofit the CMU wall was detailed in Section 4.11.

The response of the laminated composite material on Wall SW22 differed greatly from the previous experiments. The composite film did not rupture, but the construction of the material failed. As the retrofitted wall was loaded, the composite material delaminated and became three individual layers of material.

> The first crack developed horizontally along the centerline of the wall under gauges D2, D3, and D4 (Figure 5.78b) and additional cracks developed along the horizontal mortar joints as the pressure increased. The transparency of the film allowed witnesses to observe the movement of air bubbles originally trapped in the CMU cells through the horizontal and vertical cracks as the retrofitted wall deformed under load (Figure 5.79b) (Johnson, Davis, Coltharp, Durst, and Smith 2010).

The elastomeric film also began to deform as the blocks on both sides began to appear as the tensile load in the film increased (Figures 5.79a and c). As shown in Figure 5.80a, the reinforced film sheets are overlapped (2 in.) during the application to create a

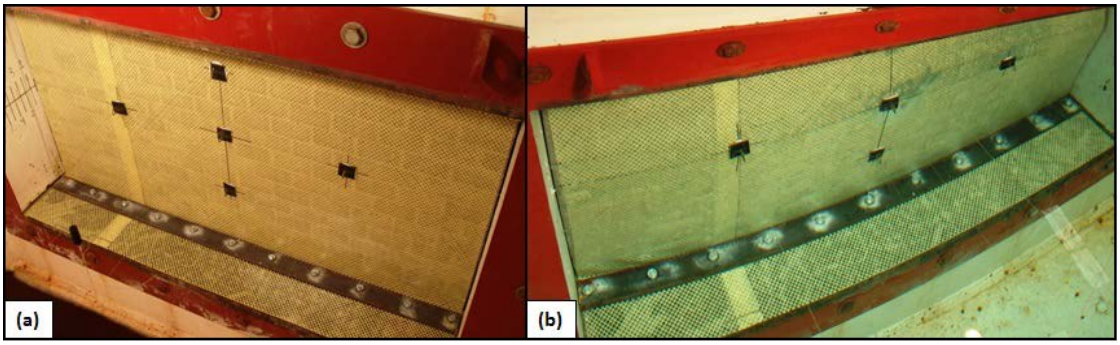

Figure 5.78. SW22. (a) Pretest view. (b) CMU wall cracked along horizontal mortar joint at mid-height. (Johnson, Davis, Coltharp, Durst, and Smith 2010)

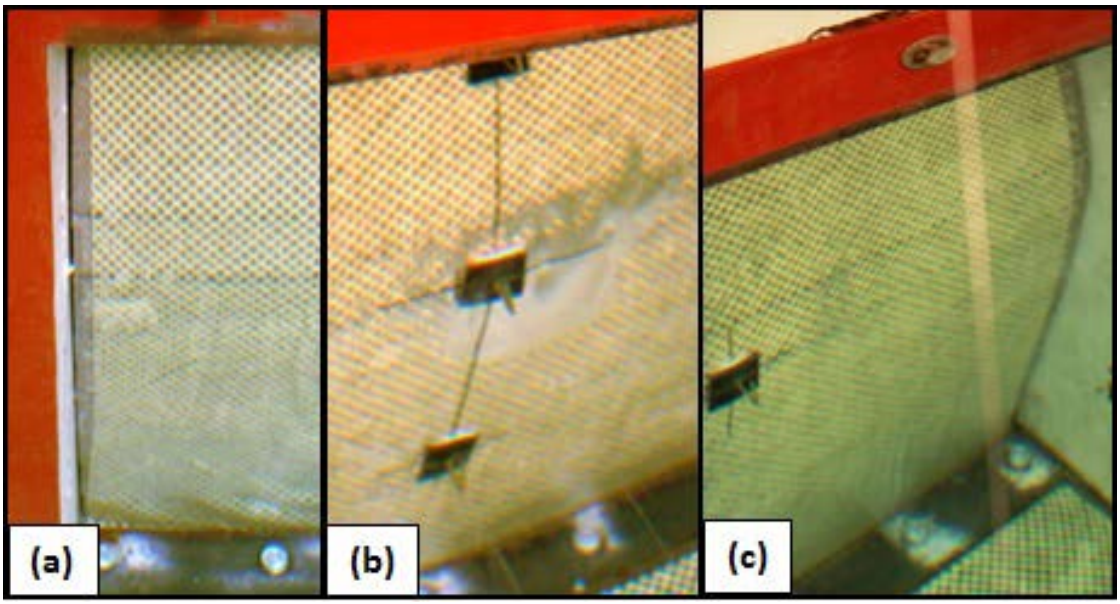

Figure 5.79. SW22. (a) Film deformed exposing the blocks on the left. (b) Air pocket formed between the CMU wall and film. (c) Film deformed exposing the blocks on the right side of the wall. (Adapted from Johnson, Davis, Coltharp, Durst, and Smith 2010)

continuous layer on the wall. As the wall deformed it appeared that the overlapped area opened exposing the CMU; however, the film remained in place but delaminated during the loading process. The delamination allowed the fibers along the edges of the sheets to

slip and recede between the two sheets of film (Figure 5.80a, b, and c). “All of the fibers receded along the seam leaving the area unreinforced during the loading process,

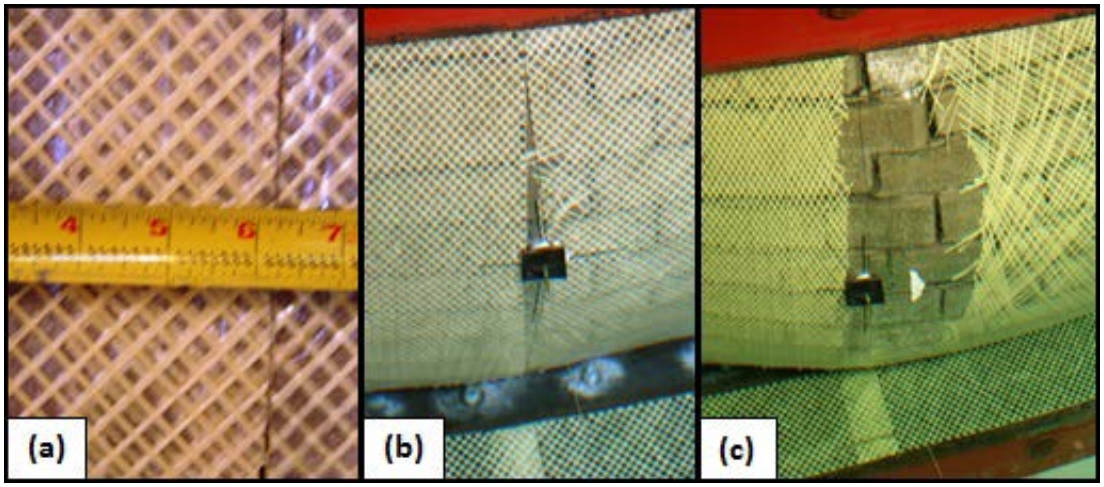

Figure 5.80. SW22. (a) The 2-in. overlap of the film before the experiment began. (b) Fibers began to slide between the two sheets of laminated film. (c) Fibers continued to slide between the two sheets, but the film maintained the seam. (Johnson, Davis, Coltharp, Durst, and Smith 2010)

which created a weak spot on the wall. The maximum wall deformation transitioned from the mid-height line to the seam/overlap area once the fibers shifted (Figure 5.81).” (Johnson, Davis, Coltharp, Durst, and Smith 2010) The PSA was not strong enough to maintain the adhesive bond along the supports and the film in the bottom right corner and the top left corner was pulled under the anchor plate (Figures 5.81, 5.82, and 5.83b). The CMU wall failed at a pressure of 0.0765 and a deflection of 0.137. The experiment was halted at a deflection of 0.831 at a peak pressure of 1.08 (Figure 5.84).

Figure 5.81. SW22 – maximum wall deformation transitioned from mid-height to the seam/overlap area. (Johnson, Davis, Coltharp, Durst, and Smith 2010)

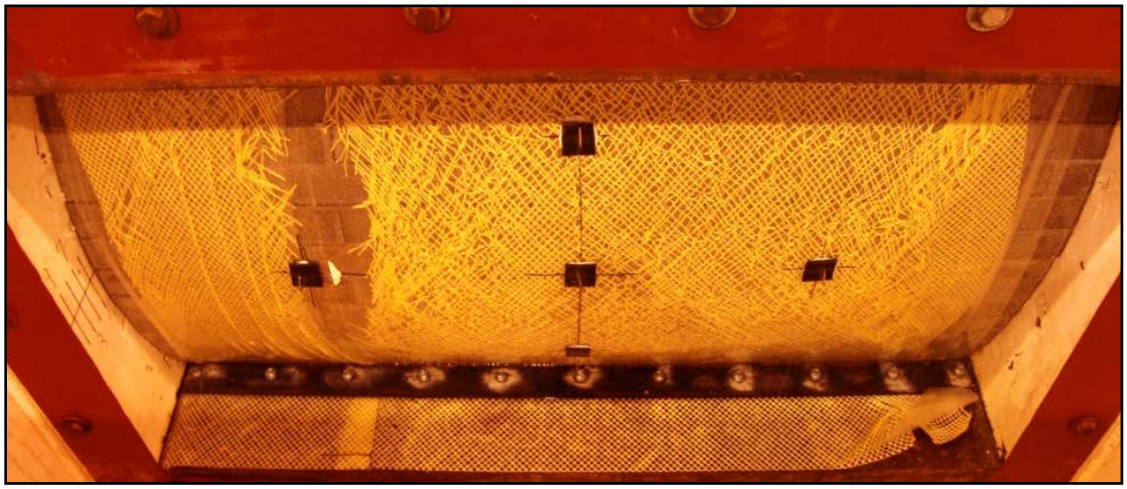

Figure 5.82. SW22 – Once pressure was relieved the fiber reinforcement was permanently deformed. (Johnson, Davis, Coltharp, Durst, and Smith 2010)

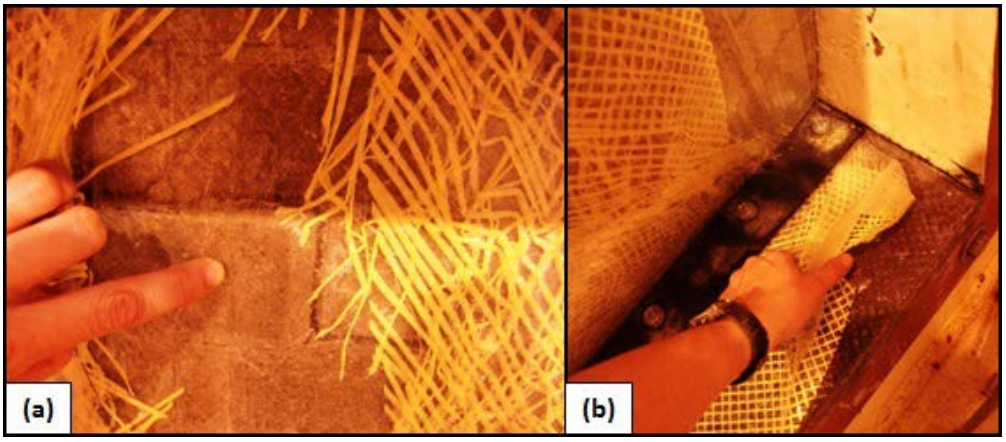

Figure 5.83. SW22. (a) Bottom layer of film and PSA remained attached to wall. (b) Film on bottom support delaminated and deformed under loading. (Johnson, Davis, Coltharp, Durst, and Smith 2010)

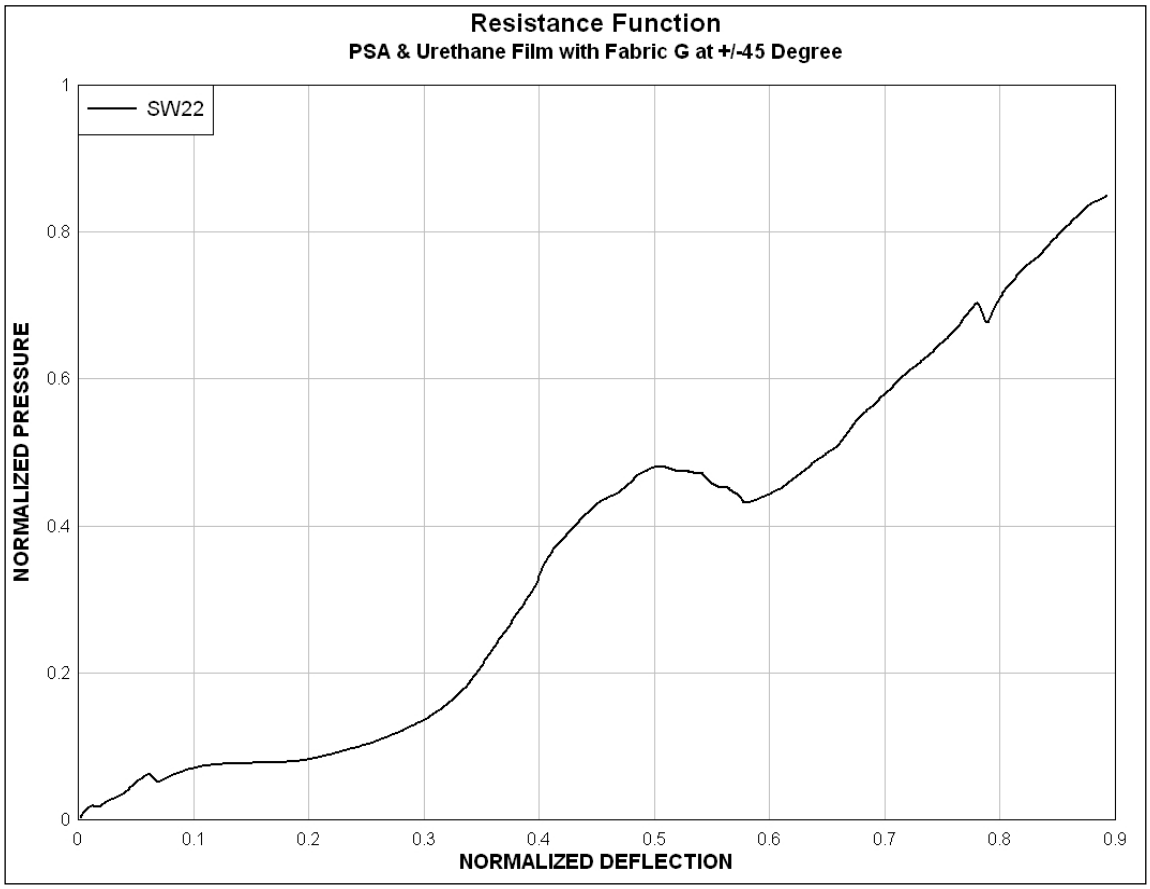

Figure 5.84. Resistance function for SW22.

Posttest inspection of the wall and retrofit indicated that the delamination of the composite film was complete. In Figures 5.85a, b, and c, one can see that there was no adhesion between the two layers of elastomeric film and the reinforcing fabric. When the water was released from the pressurized chamber, the load on the elastomeric film was removed and the fibers relaxed no longer holding their initial form or orientation (Figure 5.82). Figure 5.83a identifies the point where the seam between the two sheets existed. The bottom layer is still there, but the fibers have receded. Complete delamination was also evident at the bottom corner of the right support (Figure 5.83b). This confirms that the load was strong enough to pull the film under the anchor plate, so adhesion at both the supports is important (Johnson, Davis, Coltharp, Durst, and Smith 2010).

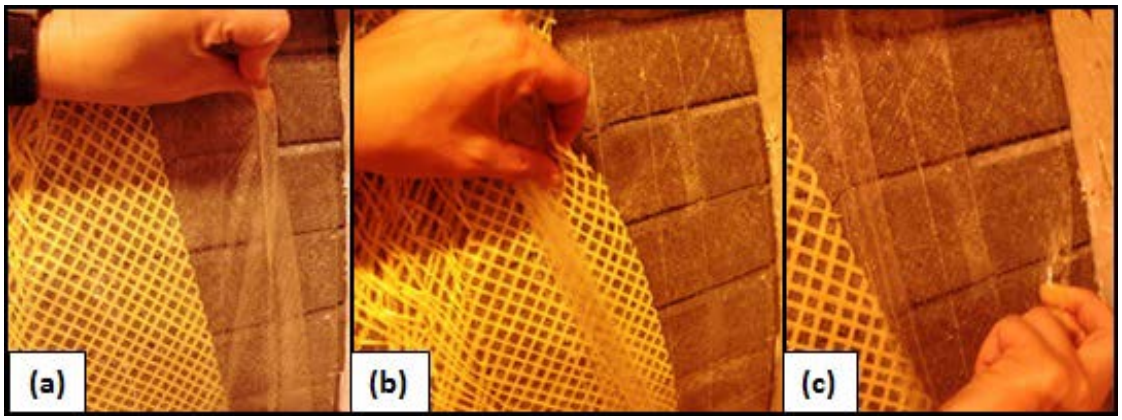

Figure 5.85. SW22. (a) Top layer of film. (b) Fiber reinforcement maintained orientation in lower strain regions, but deformed in high strain regions. (c) Bottom layer of film. (Johnson, Davis, Coltharp, Durst, and Smith 2010)

5.9.2 Wall SW23

The retrofit applied to SW23 also consisted of an elastomeric film that encapsulated an open-weave aramid fiber reinforcement (Figure 5.86a). The construction process between the two fiber reinforced films differed for SW22 and SW23. The film used on SW22 was laminated and the film used on SW23 was constructed by encapsulating the open weave fiber reinforcement with an elastomeric material through an extrusion

process. A PSA was applied to the film in the factory before it was shipped to the ERDC. The application process used on SW22 was repeated for SW23 and the details of the process are described in detail in Section 4.11. The evaluation of the retrofit system applied to SW23 ended earlier than expected when the overlapped area failed.

As the load on SW23 increased, the wall deformed along the mid-height of the wall (Figure 5.86b). However, as the wall deformation continued, the film began to stretch and deform along all of the edges of the film (Figures 5.87a and b). The seam became the weak spot and the deformation transitioned from the center of the wall to the seam/overlap region. As the elastomeric film continued to stretch, the film edges began to distort. In the previous experiment, SW22, the fibers shifted between the two sheets of film and the film maintained its integrity across the seam. However, in this experiment the bond between the film and fibers was strong, which prevented the fibers from distorting. This caused the entire film to recede from the seam (Figure 5.88). The extrusion process used to encapsulate the fibers in the film created a much stronger bond than the delamination process used in SW22. The experiment ended when the opening at the seam exposed an entire CMU. When the water was released from the pressurized chamber, the film exhibited permanent deformation as indicated by the wrinkles shown in Figure 5.88 (Johnson, Davis, Coltharp, Durst, and Smith 2010).

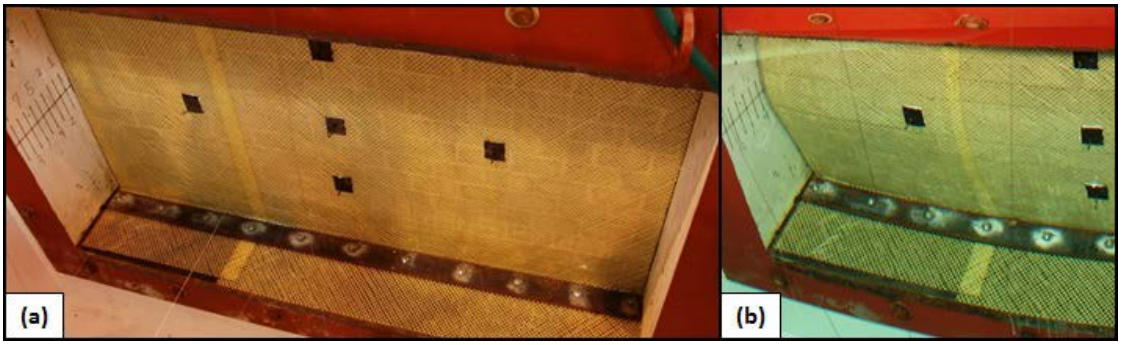

Figure 5.86. SW23. (a) Pretest view. (b) Deflection at 3 in.

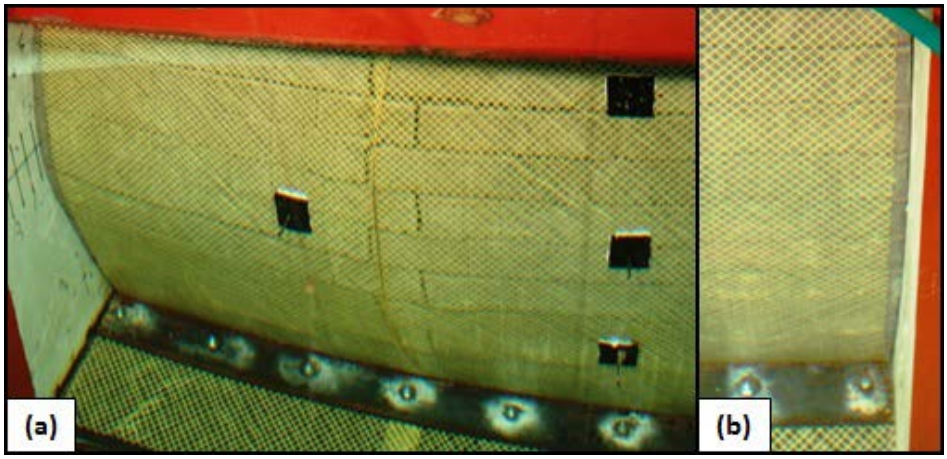

Figure 5.87. SW23. (a) The 2-in. overlap/seam is close to separating. (b) Blocks exposed on right edge. (Johnson, Davis, Coltharp, Durst, and Smith 2010)

The CMU wall failed at a pressure of 0.0972 and a deflection of 0.146. The experiment ended due to failure at the seam at a pressure of 0.443 and a deflection of 0.526 as seen on the resistance function in Figure 5.89.

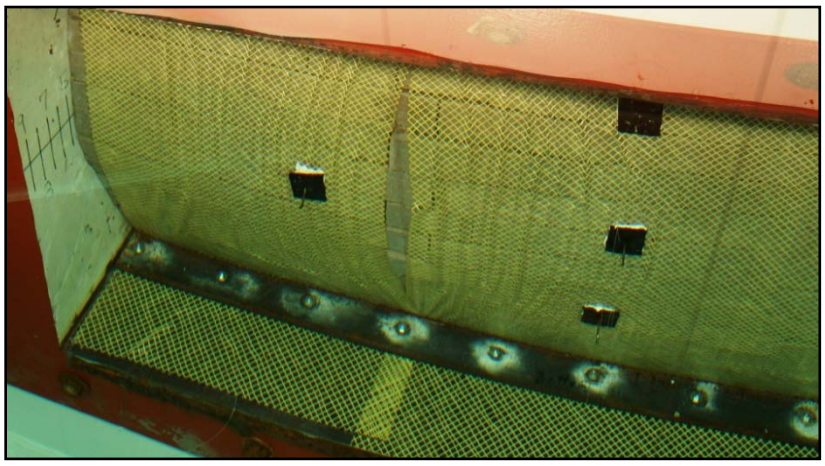

Figure 5.88. SW23 – state of elastomeric film when the pressure on the wall was removed. (Johnson, Davis, Coltharp, Durst, and Smith 2010)

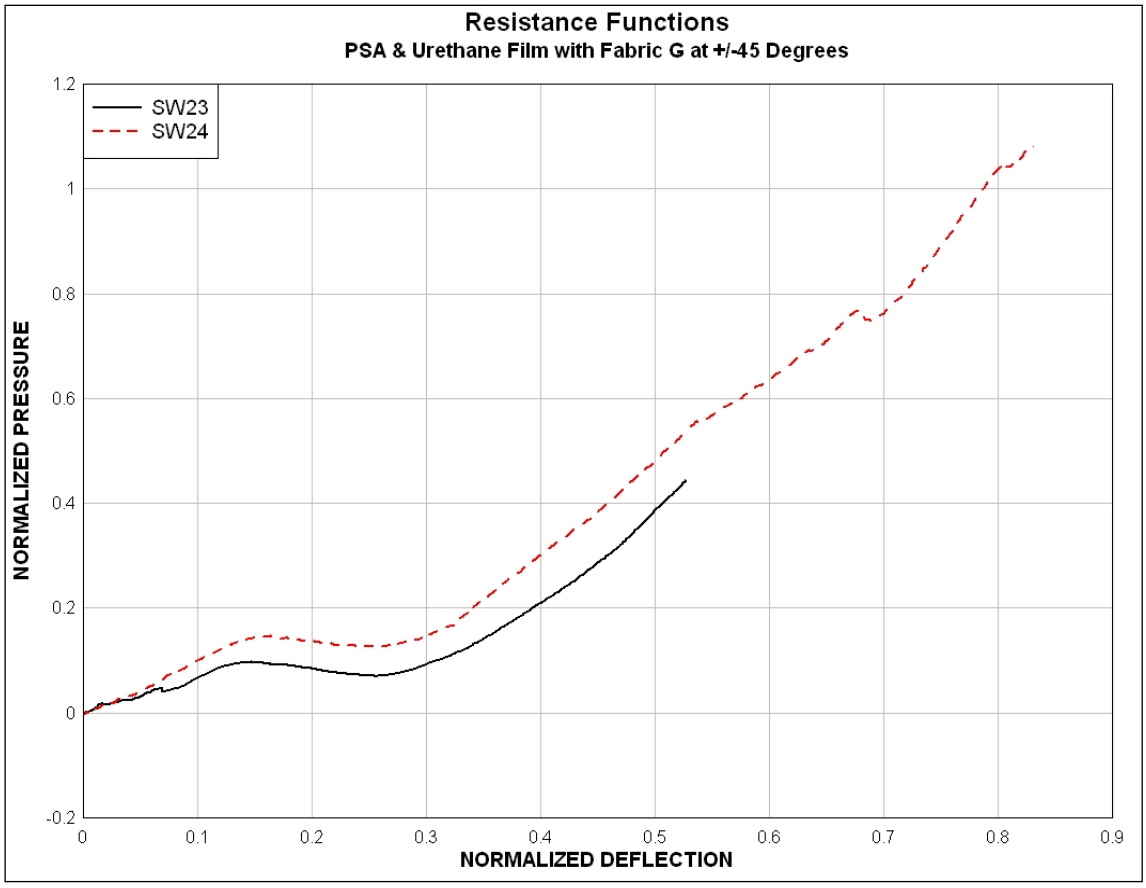

Figure 5.89. Resistance functions for SW23 and SW24.

5.9.3 Wall SW24

The retrofit system and application process used on SW23 was duplicated on wall SW24. The width of the overlapped area on SW24 was increased to delay or prevent the same failure observed in SW23. An extra strip of film had to be added to the right edge of SW24 (Figure 5.90a), because the material was not applied squarely on the wall leaving a strip of blocks exposed. The procedure outlined in Section 4.11 was used to retrofit the CMU wall in SW24.

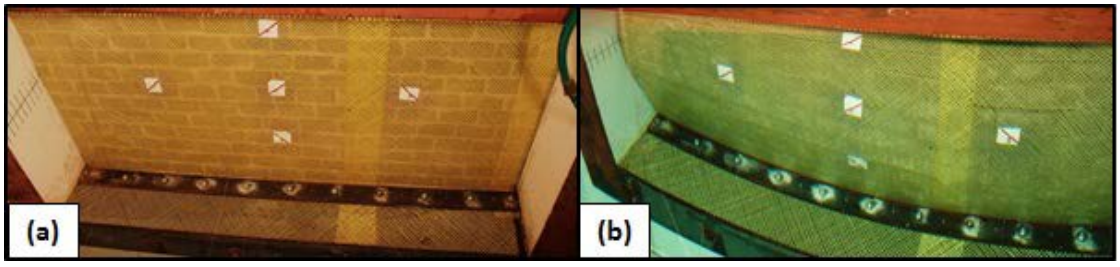

Figure 5.90. SW24. (a) Pretest view. (b) Wall response during evaluation.

The retrofit systems used in SW23 and SW24 had very similar responses. At the beginning of the experiment, the maximum deformation occurred along the centerline (Figure 5.90b). The wall appeared to lodge against both sides of the frame at a deflection of 0.517 as shown in Figures 5.91b and c. The elastomeric film began to pull away from the edges of the CMU wall and the seam began to deform as the pressure continued to increase. Also illustrated in Figures 5.91a, b, and c, the maximum deformation began to occur at the seam representing the weakest point as the load continued to increase. The failure of the seam forced the experiment to be halted and the film was not loaded to failure. However, the retrofit material was loaded past the elastic limit based on the response of the reinforced elastomeric film and the plastic deformation exhibited in the film as the pressure was reduced (Figure 5.91d). The data for the fiber reinforced films with PSA experiments were listed in Table 5.8.

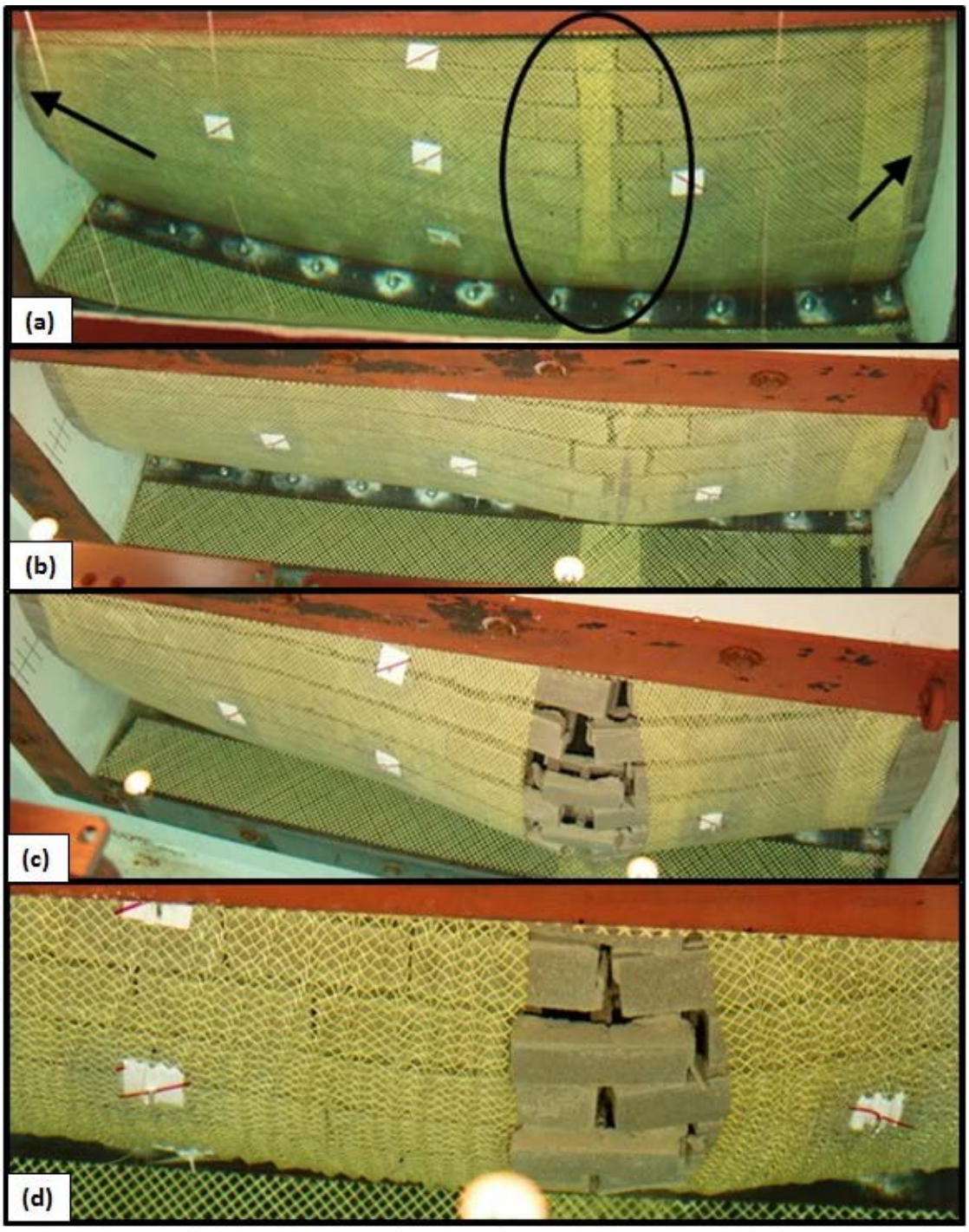

Figure 5.91. SW24. (a) Areas where the reinforced elastomeric film deformed are identified. (b) Film continued to pull away at the edges. (c) Seam opened exposing the CMU. (d) Film and fibers began to relax as pressure was decreased.

Table 5.8. Normalized pressure (P) and deflection (d) data for fiber reinforced films with PSA.

Wall	Retrofit	CMU Wall Failure		Retrofit Failure	
		P	d	P	d
SW22	PSA and Polyurethane Film with Fabric G at ±45 deg	0.0765	0.137	0.85	0.892
SW23	PSA and Polyurethane Film with Fabric G at ±45 deg	0.0972	0.146	0.443	0.526
SW24	PSA and Polyurethane Film with Fabric G at ±45 deg	0.147	0.159	1.08	0.831

5.10 Comparison and Analysis of Subscale Static Experiments

The subscale static experiments were used to evaluate the application procedures, observe the response of the materials under a steady and increasing load, identify failure modes for the materials, and develop a quantitative means to compare the retrofit systems using resistance functions. The resistance functions developed from the experimental data were used to compare the contribution of the different systems to the enhanced strength and ductility of the CMU walls, to determine the total energy absorbed, and as input relating the wall displacement to the load applied for the SDOF analysis discussed in Chapter 8. The data from a hollow, unretrofitted, CMU wall experiment was added as a baseline to demonstrate the capacity of the CMU wall alone and the increase in ductility and strength gained by the retrofit systems. The unretrofitted, CMU wall labeled Base 2 on the resistance functions failed at a pressure of 0.0346 and a deflection of 0.0276. Some of the retrofit systems were removed from further consideration before the subscale dynamic experiments were conducted.

The first two retrofit systems investigated were the unreinforced Grade 1 and Grade 2 spray-on polyurea materials. The Grade 1 and 2 materials were developed and obtained from the same manufacturer. The specimens retrofitted with the Grade 1 material (SW1 and SW2) demonstrated a significant difference in structural response from the baseline/unretrofitted CMU wall (Figure 5.92). However, the response of SW1 and SW2 differed significantly, even though the samples were retrofitted with the same material and procedures. The difference in the ultimate flexural resistance of the CMU walls occurred because SW1 had to be loaded twice due to a leak in the HTC. The specimen was inspected after the initial experiment, and no defects were visible. However, it is clear from the results of SW1 and SW2 that the wall was compromised during the first attempt to evaluate the wall. SW2 had a 122% increase in the pressure values at ultimate flexural resistance over specimen SW1 and a 368% increase over the baseline sample, Base 2. The deflection measurements for SW1 and SW2 were almost identical at the point of ultimate flexural resistance (SW1 at 0.06 and SW2 at 0.07). Both SW1 and SW2 demonstrated a significant increase in displacement over Base 2 of 0.0276. The pressure and deflection values related to the ultimate tensile membrane resistance for sample SW2 were compromised due to instrumentation problems encountered during the experiment. The deflection gauges used to monitor the wall's deflection disengaged at a deflection of 0.341 and a pressure of 0.133. The average resistance function for the Grade 1 material was developed from the experimental results recorded in SW1 and SW2.

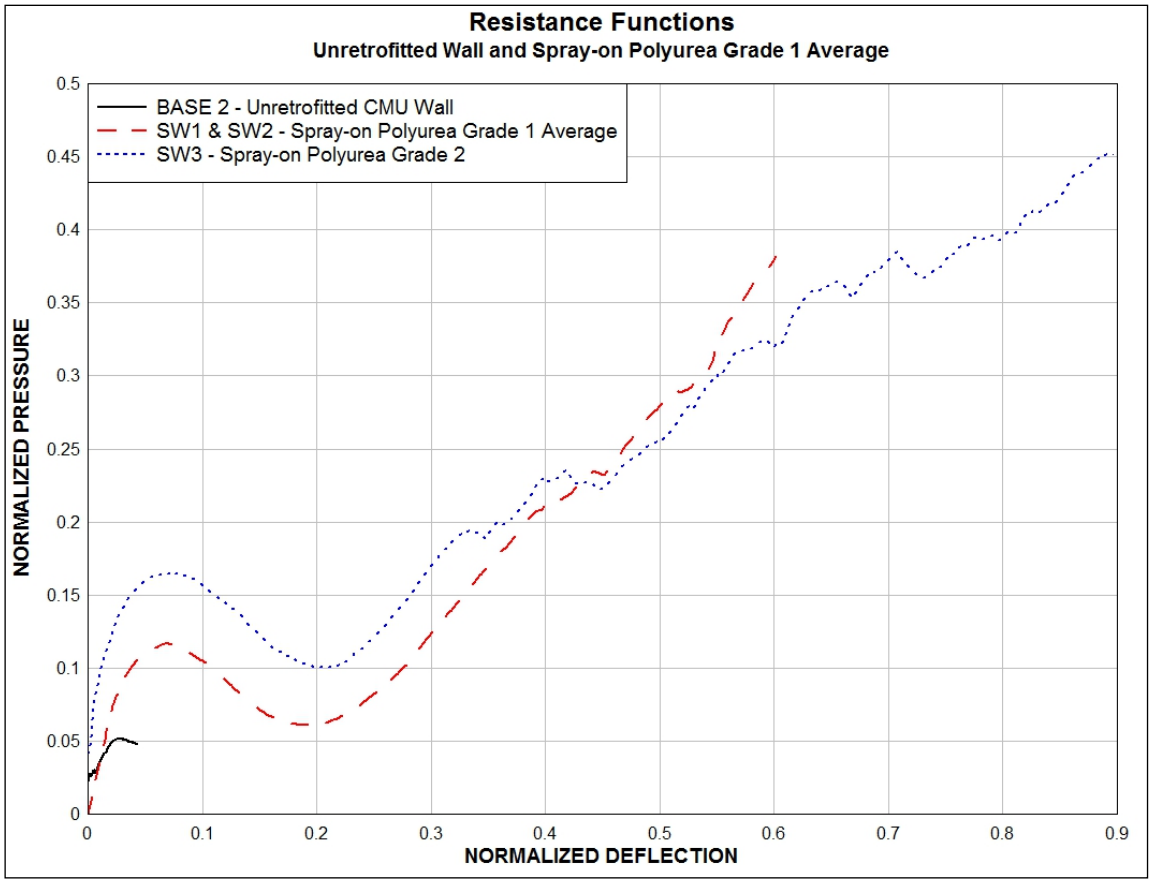

Figure 5.92. Resistance functions for spray-on polyurea Grade 1 and 2 and an unretrofitted CMU wall.

The response of the specimen retrofitted with the Grade 2 material (SW3) improved over the specimens retrofitted with the Grade 1 material (Figure 5.92). SW3 had a 1.8% increase in the pressure value at ultimate flexural resistance over specimen SW2 and a 377% increase over Base 2. The deflection measurements were only slightly different at the point of ultimate flexural resistance for SW2 and SW3 (SW3 at 0.0746 and SW2 at 0.0721). The pressure and deflection values related to the ultimate tensile membrane resistance for sample SW3 could not be compared to the Grade 1 samples due to the

problems encountered during the evaluation of SW1 and SW2. However, the data do demonstrate an increase in pressure and deflection for specimen SW3 when compared to the values obtained from the Grade 1 and baseline experiment.

The next series of retrofit experiments evaluated the spray-on polyurea with encapsulated reinforcement at 0/90 (SW7)- and ±45 (SW4)- degree fiber orientations. Figure 5.93 compares the response of the specimens retrofitted with the Grade 2 spray-on polyurea reinforced with Fabric A (SW7 and SW4). The fabric in SW7 was applied to the wall with the fibers oriented at ±45 deg to the horizontal mortar joints, and SW4 used the same fabric with the fibers oriented at 0/90 deg to the horizontal mortar joints. The specimen, SW7, using the fabric in the 0/90-deg orientation, was stiffer allowing a deflection of 0.0537 at ultimate flexural resistance compared to the 0.0324 allowed by specimen SW4. The pressure at ultimate flexural resistance for the two walls only differed by 0.088. Specimen SW7 encountered similar problems to samples SW1 and SW2 during evaluation. During the first experiment on SW7, a leak in the chamber developed, requiring the experiment to be stopped and repeated the following day. During the second experiment, SW7 exhibited extreme deformation, which caused the deflection gauge, D3, to peel off. This information was documented in Section 5.4.4. Specimens SW7 and SW4, respectively, had a 764% and 622% increase in the pressure values at ultimate flexural resistance over Base 2. The orientation of the fabric also affected the ultimate tensile membrane resistance. The ultimate tensile membrane resistance for SW4 was identified at a pressure of 0.476 and a deflection of 0.346. The ultimate tensile membrane resistance for specimen SW7 was marked at a pressure of

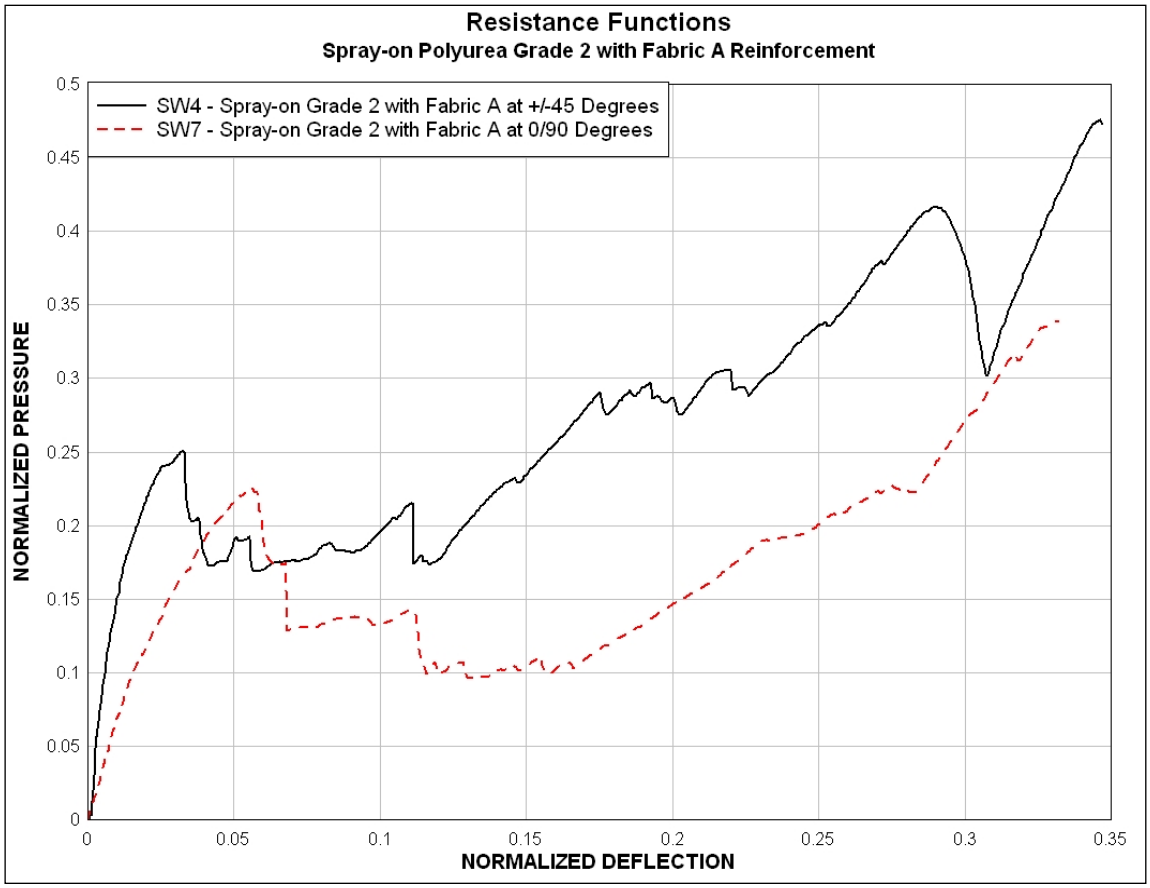

Figure 5.93. Resistance functions for SW4 and SW7.

0.543 and a displacement of 0.4. The Grade 2 spray-on polyurea reinforced with Fabric A in a 0/90-deg orientation (SW7) was slightly stronger than the ±45-deg reinforced wall in the static experiments, so it was selected as a candidate for evaluation in the subscale dynamic program.

All of the responses from the CMU walls retrofitted with ±45-deg fiber reinforced spray-on polyurea were compared in Figure 5.94. The CMU walls retrofitted with the Grade 1 material and ±45-deg fiber reinforcement (SW5 and SW6) were compared first. Two different fabrics (A and C) were evaluated with the Grade 1 material. The stronger

fabric, C, did demonstrate a significant difference in stiffness over Fabric A. Specimen SW6 was retrofitted with the 100-lb/in. fabric A and increased the pressure values at ultimate flexural resistance by 54% over the unreinforced Grade 1 spray-on polyurea specimen SW2 and a 622% increase over Base 2. The deflection measurements differed at the point of ultimate flexural resistance by 0.017 (SW6 at 0.0891 and SW2 at 0.0721). SW5, using the 400-lb/in. fabric, had a 61% increase in the pressure values at ultimate flexural resistance over specimen SW2 and a 654% increase over Base 2. The

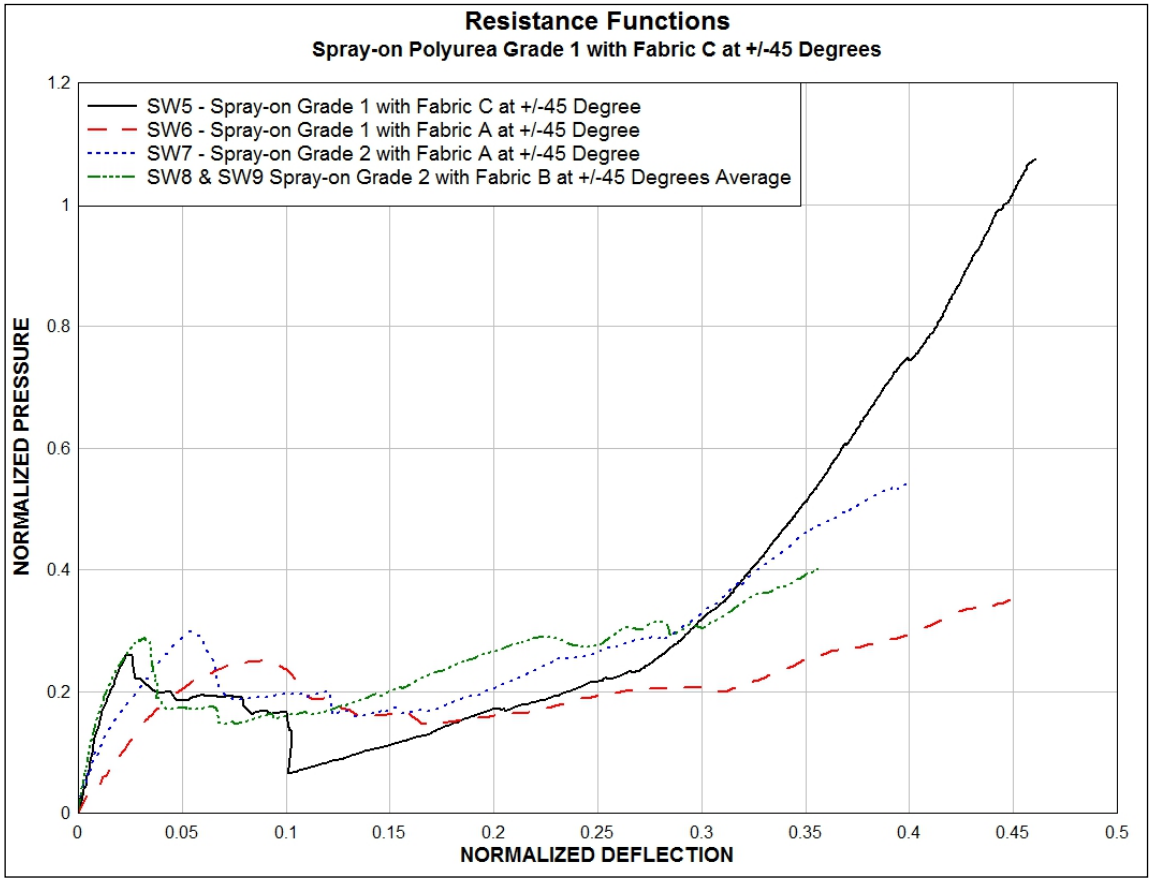

Figure 5.94. Resistance functions SW5, SW6, SW7, and average of SW8 and SW9.

deflection measurements were quite different. SW5 was quite stiffer than the other specimens and was limited to a deflection of only 0.0238 at CMU wall failure. The difference between the tensile strength in the Fabric C (400 lb/in.) and A (100 lb/in.) was a multiple of four and the difference between the deflections at ultimate flexural resistance was increased by a factor of 3.7 (SW5 at 0.0238 and SW6 at 0.0891), but the magnitude of the pressure did not change by the same factor. Specimen SW5 had a 4.21% increase in pressure over SW6 at ultimate flexural resistance.

The increased strength of the fabric in SW5 was significant when the second stage of the resistance function, the tensile membrane resistance, was evaluated. The ultimate tensile membrane resistance was designated as the point at which the retrofit no longer provided any additional strength or ductility to the wall. Additional data might be provided past the point identified on some resistance functions, but this information relates to progression of the initial failure in the retrofit material. For example, the formation of a tear could be marked as the ultimate tensile membrane resistance, but in this example, it took an additional 250 data points for the tear to propagate across the entire wall. The ultimate tensile membrane resistance for SW5 was identified at a pressure of 1.07 and a deflection of 0.46. Specimen SW5 had a 195% increase in pressure over SW6 with only a slight difference in displacement at the ultimate tensile membrane resistance. The point of ultimate tensile membrane resistance for specimen SW6 was marked at a pressure of 0.363 and a displacement of 0.456. The magnitude of the pressure and deflection at ultimate tensile membrane resistance reversed at the ultimate tensile membrane resistance. The peak pressure of SW5 increased by a factor of

3 over SW6, and the peak deflection was the same for both walls. One reason for the difference in response from ultimate flexure to ultimate tensile membrane could be attributed to the failure mechanism. SW5 failed when the bolts holding the anchor plate sheared and the retrofit peeled back off of the supports, which increased the magnitude of the deflection; SW6 sheared at the bottom support. Again data for SW5 and SW6 could not be compared to the unreinforced Grade 1 specimens, SW1 and SW2, due to the instrumentation problems encountered during the experiments. However, the data and retrofitted wall responses clearly demonstrated an increase in capacity of the reinforced spray-on retrofits compared to the unreinforced and baseline specimens.

The responses of the CMU walls retrofitted with the same reinforcing Fabric A, but different grades of the spray-on material (SW6 and SW7) were also compared. The wall responses differed because the spray-on material used to encapsulate the fibers was different. SW7 had a 19.6% increase in pressure over SW6 at ultimate flexural resistance (SW6 at 0.25 and SW7 at 0.299), but the difference was reflected in the displacement. The data indicated that the Grade 2 material was slightly stiffer, thereby reducing the deflection in the wall response which was expected based on the results observed in the unreinforced Grade 1 and 2 spray-on polyurea experiments in Figure 5.92. SW6 (Grade 1) reached ultimate flexural resistance at a deflection of 0.0891, while SW7 (Grade 2) was noted at 0.0537. The difference in stiffness was noted again when the ultimate tensile membrane resistance was evaluated. SW7 (Grade 2) reached this point at a deflection of 0.4, while SW6 deformed to 0.456. The pressure at ultimate tensile membrane resistance for both specimens differed by 0.18.

The effect of increasing the tensile capacity of the fiber reinforcement from Fabric A (100 lb per linear inch) to Fabric B (200 lb per linear inch) was observed when the results from SW7 were compared to the SW8 and SW9 static experiments. All three walls used the Grade 2 polyurea to encapsulate the fiber reinforcement. The resistance functions for walls SW8 and SW9 were averaged and plotted in Figure 5.94. The increase in tensile capacity from the fiber reinforcement decreased the deflection of the CMU wall from 0.0537 (SW7) to 0.0315 (avg. SW8 and SW9) while maintaining the pressure at approximately 0.3 when the CMU wall failed. The ultimate tensile membrane resistance observed in SW8 and SW9 was very similar to the results from SW7, but the ultimate deflection achieved was decreased by 0.044. This indicated that the deformation into the structure was decreased by increasing the tensile capacity of the fiber reinforcement. All of the resistance functions created from the fiber reinforced retrofits in Figure 5.94 compared to the unreinforced spray-on retrofits in Figure 5.92 demonstrated that there was a clear difference between the walls' responses when a reinforcing fabric was encapsulated by the spray-on material.

The resistance functions for the unreinforced Grade 2 spray-on polyurea (SW3) was compared to the Grade 1 trowel-on thermoset (SW10) in Figure 5.95. There was a 46% increase in the maximum pressure and a 24% increase in deflection at the peak ultimate flexural resistance. However, at the ultimate tensile membrane resistance the trowel-on material had a 19% increase in pressure with a 17% decrease in deflection. The objective was to find a material that could provide similar or improved pressure and deflection values using a material or application procedure that was either more economical or

could be applied to the wall easier with better or equal quality control. The unreinforced spray-on polyurea materials were removed from further consideration based on the results obtained from the unreinforced spray-on polyurea, the reinforced polyureas, and

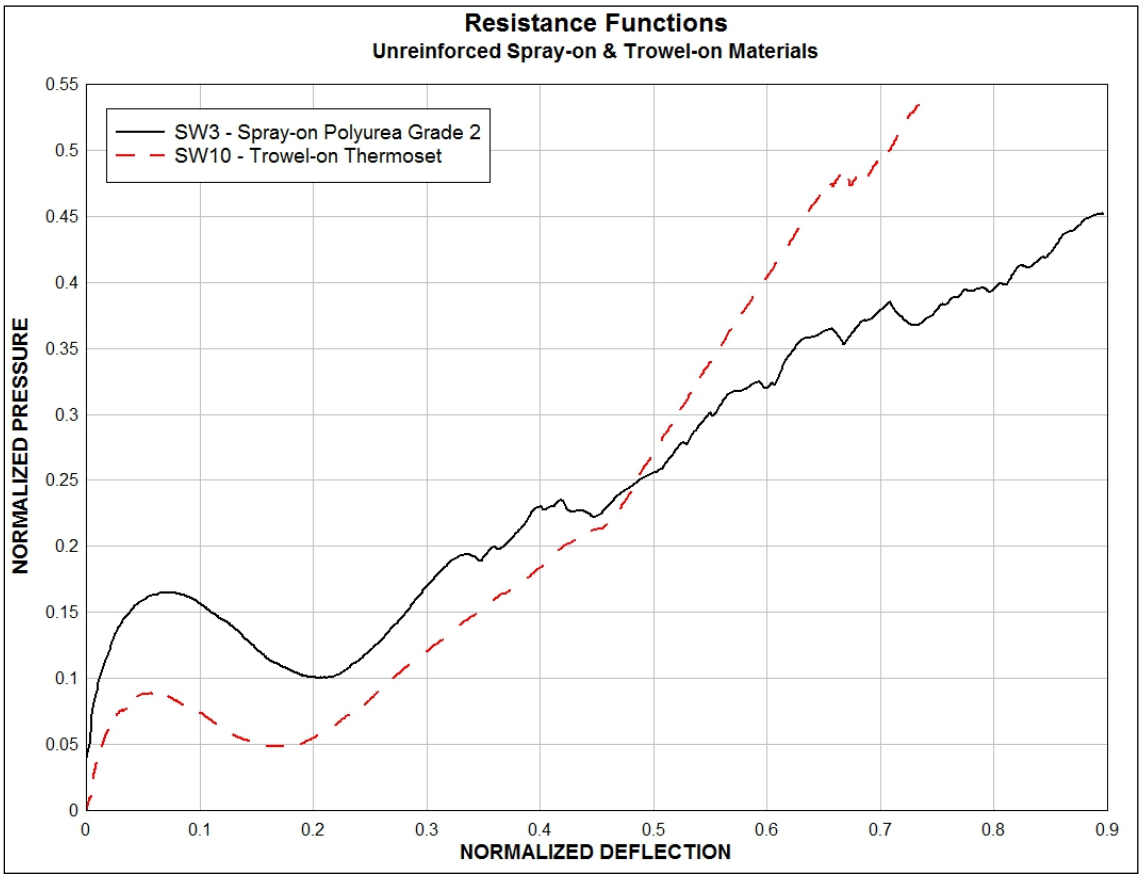

Figure 5.95. Comparison of unreinforced spray-on and trowel-on retrofit materials.

the unreinforced trowel-on thermoset. The trowel-on thermoset was chosen for evaluation in the subscale dynamic experiments over the unreinforced spray-on material because it was able to resist a larger pressure with a reduced deflection using a more economical material and application procedure.

The unreinforced trowel-on thermoset (SW10) and the unreinforced thermoplastic film applied to the CMU wall using a trowel-on thermoset (SW13) were compared in Figure 5.96 to see if the unreinforced film that offered better quality control and a simpler application procedure would have a similar response to the unreinforced trowel-on thermoset. The pressure and deflection at the point of ultimate flexural resistance between the two resistance functions only differed by a magnitude less than 0.02 and 0.02. The trowel-on thermoset failed at a pressure of 0.536 and a deflection of 0.744 in.

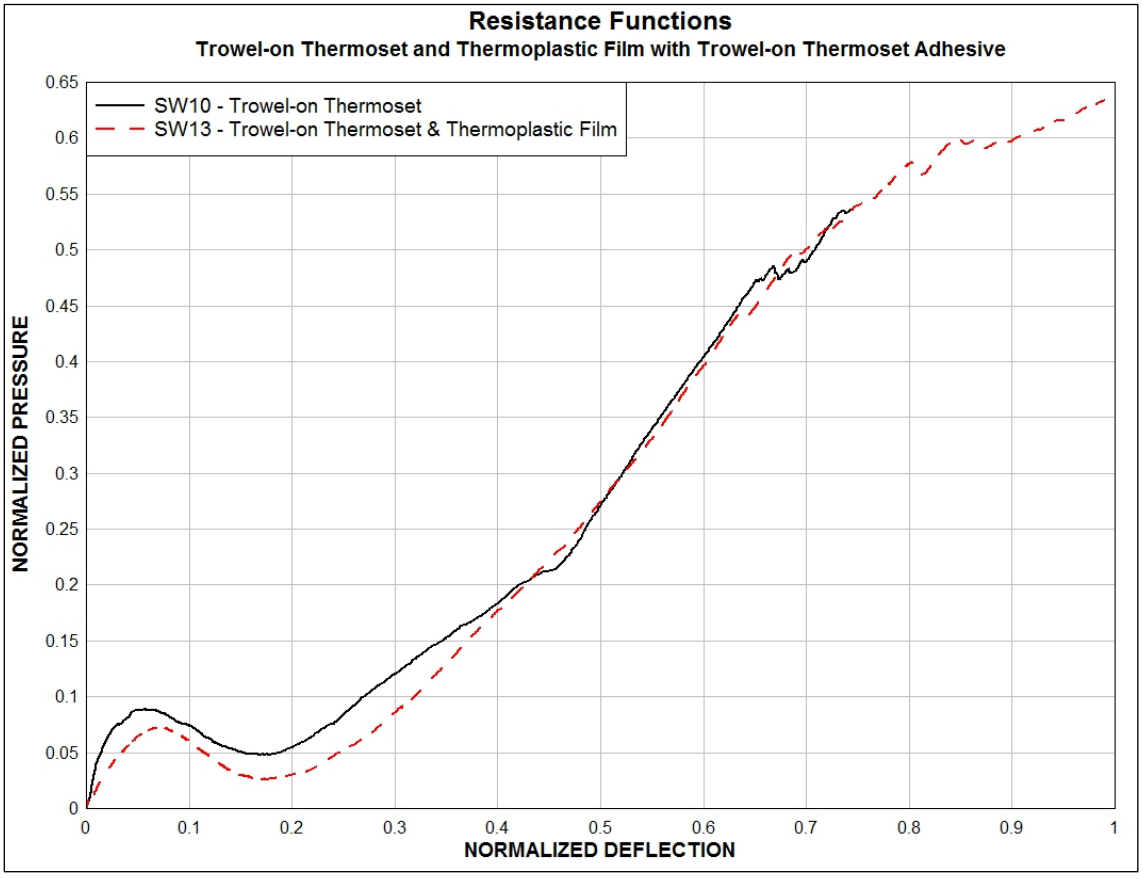

Figure 5.96. Comparison of trowel-on and thermoplastic film with trowel-on thermoset adhesive.

while the thermoplastic film was able to withstand a larger pressure of 0.634 and a deflection of 0.991. Since the resistance functions were so similar, both retrofit systems were selected for further evaluation in the subscale dynamic experiments.

Two versions of an unreinforced elastomeric film and trowel-on adhesive were compared in Figure 5.97. The thermoplastic film applied with a thermoset (SW13) and the elastomeric film applied with an epoxy (SW14) were evaluated and the resistance functions had similar characteristics. The initial slope of both resistance functions were

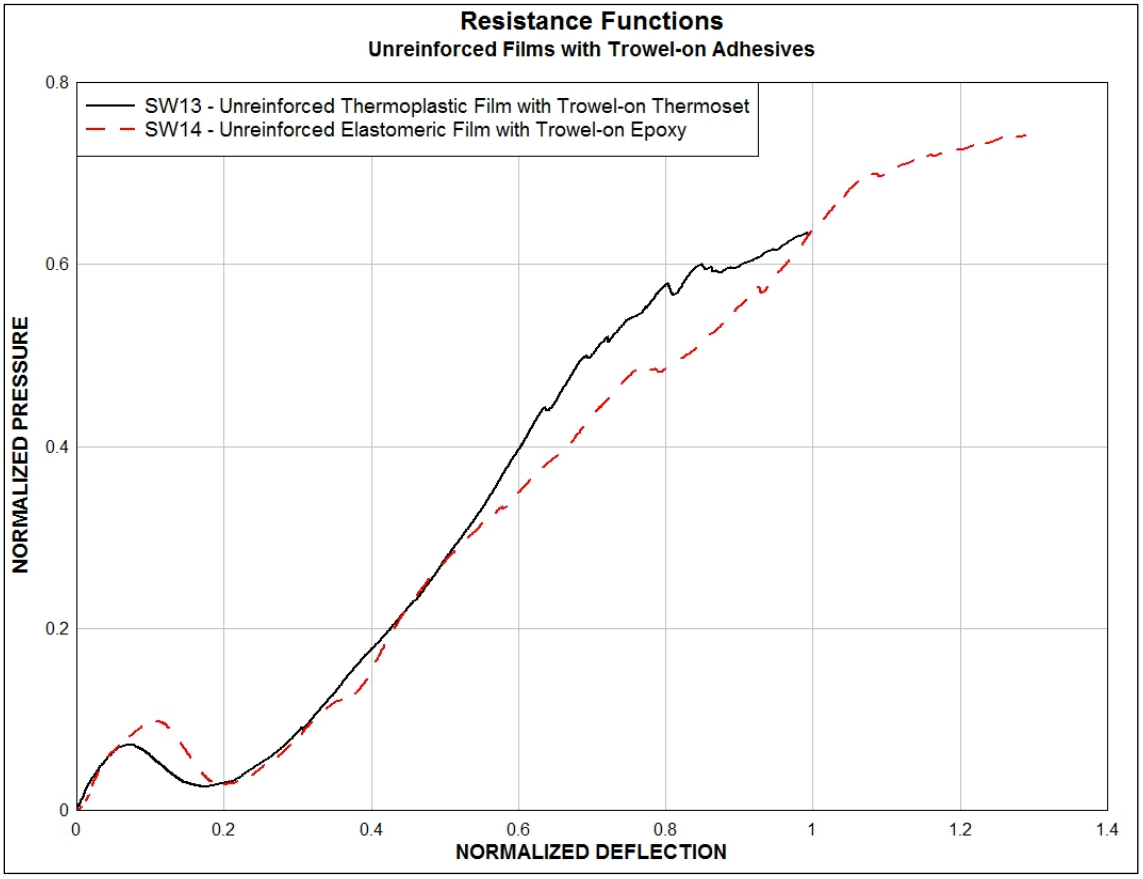

Figure 5.97. Comparison of unreinforced films with trowel-on adhesives.

the same. SW13 reached the point of ultimate flexural resistance at a pressure of 0.0723 and a deflection of 0.0728 and SW14 was able to sustain a pressure up to 0.0978 at an increased deflection of 0.105. SW14 was also able to sustain a pressure at the tensile membrane resistance of 0.743, while SW13 failed at a pressure of 0.634. SW14 was also more ductile allowing the film to deflect 1.29 before the retrofit completely failed and SW13 failed at 0.991. The thermoplastic film with a thermoset adhesive was already selected for further evaluation and the elastomeric film with trowel-on epoxy was also selected for further evaluation.

The next series of resistance functions were compared in Figure 5.98 to determine the contribution of each additional component to the overall resistance functions for CMU walls retrofitted with a trowel-on epoxy (SW11), an unreinforced elastomeric film with a trowel-on epoxy (SW14), and the average resistance function created from two walls (SW15 and SW16) retrofitted with a ±45-deg fiber reinforced (Fabric B) elastomeric film with a trowel-on epoxy were compared on Figure 5.98. The trowel-on epoxy (SW11) that would be used to attach the unreinforced and reinforced films to the CMU wall was evaluated first at the thickness required to attach the films and not as a singular material. Unlike the trowel-on thermoset, the trowel-on epoxy was never considered as a singular retrofit material. The epoxy then was applied to the second wall with an unreinforced elastomeric film added for SW14. This allowed researchers to determine the contribution of the elastomeric film. Then the same epoxy thickness was used to adhesively attach an elastomeric film with ±45-deg fiber reinforcement (Fabric B) to a third wall to determine the contribution of the off-axis fibers.

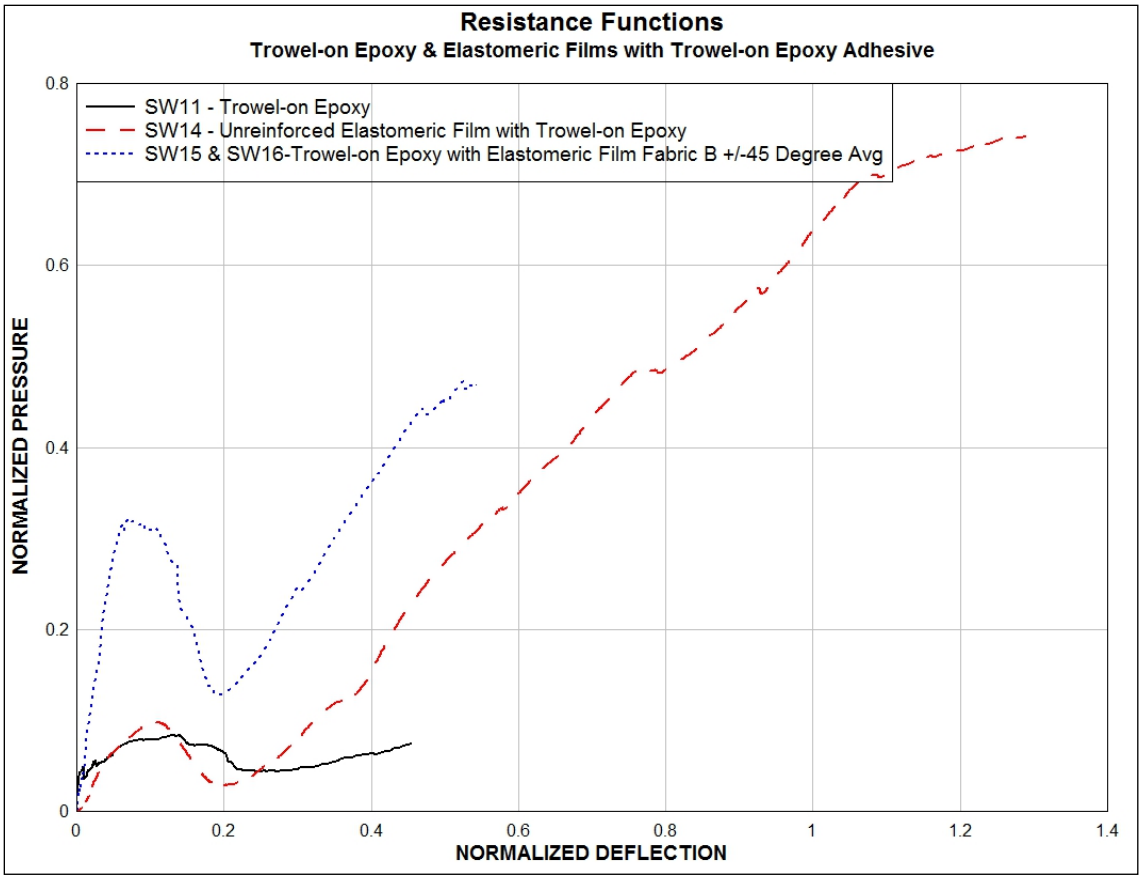

Figure 5.98. Comparison of trowel-on epoxy and elastomeric films with trowel-on epoxy adhesives.

SW11 and SW14 were similar at the point of ultimate flexural resistance. By adding the film to the wall the ultimate flexural resistance went from a pressure of 0.0834 at a deflection of 0.128 for SW11 to a pressure of 0.0978 at a deflection of 0.105. The film added some additional stiffness to the wall over the plain epoxy wall, but the primary difference between the two occurred in the tensile membrane resistance. The epoxy alone did not add significant resistance past the point of ultimate flexural resistance and failed at a deflection of 0.453 at a reduced pressure of 0.0751. The film/epoxy system (SW14) demonstrated that the film does add considerable resistance and ductility to the

retrofit system past the point of ultimate flexural resistance. The film/epoxy system failed at a pressure of 0.743 and a deflection of 1.29 and provided an 889% increase in pressure and a 185% increase in deflection over SW11. The contribution of the off-axis fibers was determined by comparing the average resistance function created from SW15 and SW16 to the data from SW14. First, the pressure at the ultimate flexural resistance increased to 0.323 at a deflection of 0.0707, which are a 230% increase in pressure and a 33% decrease in deflection from SW14. However, the fiber reinforced retrofit did fail at a lower pressure and deflection than the unreinforced film. The fiber reinforced film failed at a pressure of 0.472 and a deflection of 0.524, which was 0.271 lower than the unreinforced film with 59% less deflection.

The average resistance function created from the unreinforced elastomeric films adhesively applied to the walls using a trowel-on material (SW13 and SW14) was compared to the average resistance function developed from unreinforced elastomeric films applied to the wall using a PSA (SW19, SW20, and SW21) in Figure 5.99. The pressure and deflection at the point of ultimate flexural resistance was 0.0798 at a deflection of 0.0884 for the unreinforced elastomeric films with trowel-on adhesive, and 0.0689 at a deflection of 0.0723 for the unreinforced films with a PSA. The two retrofits failed within 0.0109 (16%) and 0.0161. (22%) from each other, which indicated that the ultimate failure of both retrofit systems was slightly effected by the method used to attach the films. The trowel-on adhesive added some additional stiffness to the films when one evaluates the slope of the lines past the point of ultimate flexural resistance to the point of retrofit failure. Both retrofit systems were selected for further evaluation. All

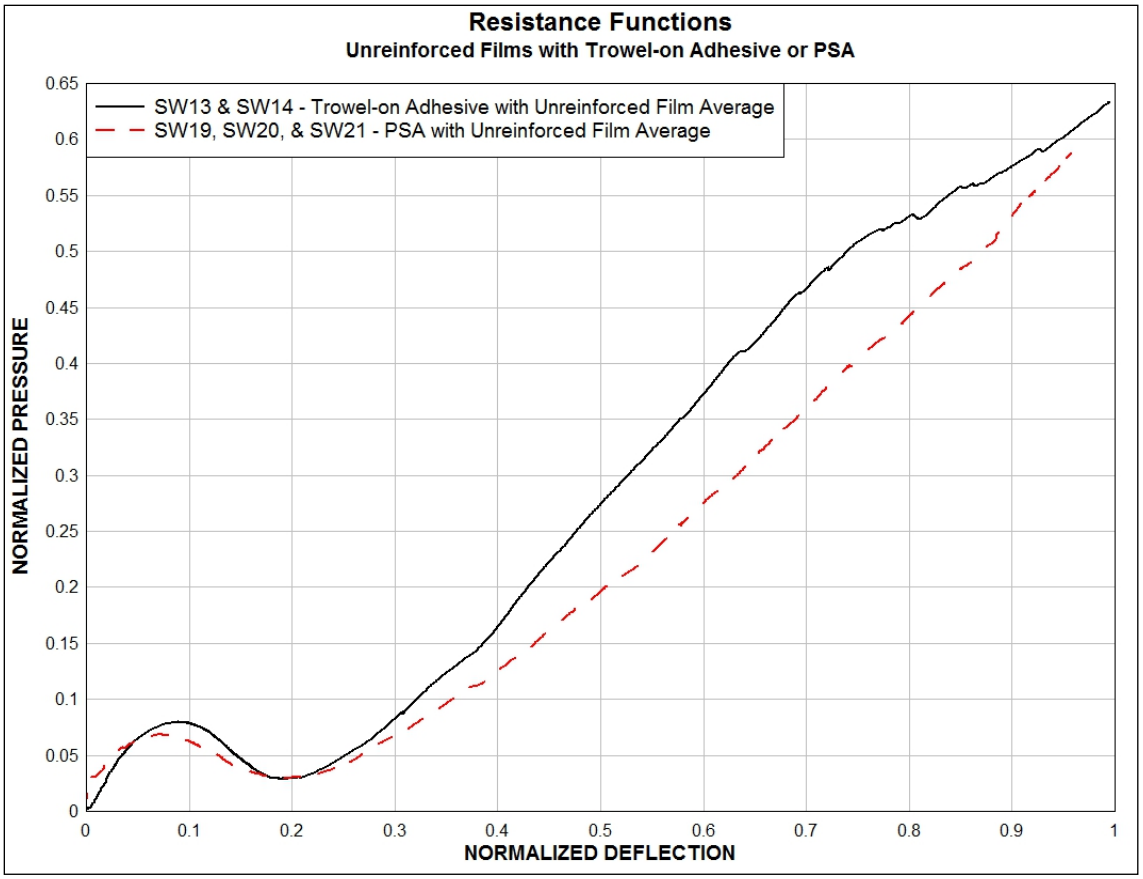

Figure 5.99. Comparison of unreinforced elastomeric films with trowel-on adhesive versus PSA.

of the retrofit systems in this group with the exception of SW19 failed when the retrofit material sheared along the top anchor plate. The evaluation of SW19 ceased due to a membrane failure in the HTC.

The walls retrofitted with unreinforced and reinforced elastomeric films adhered to the wall with a PSA were compared in Figure 5.100. The reinforced films were stiffer than the unreinforced films past the point of ultimate flexural resistance, but the ultimate deflection at the point the experiment was stopped or when the retrofit materials failed as

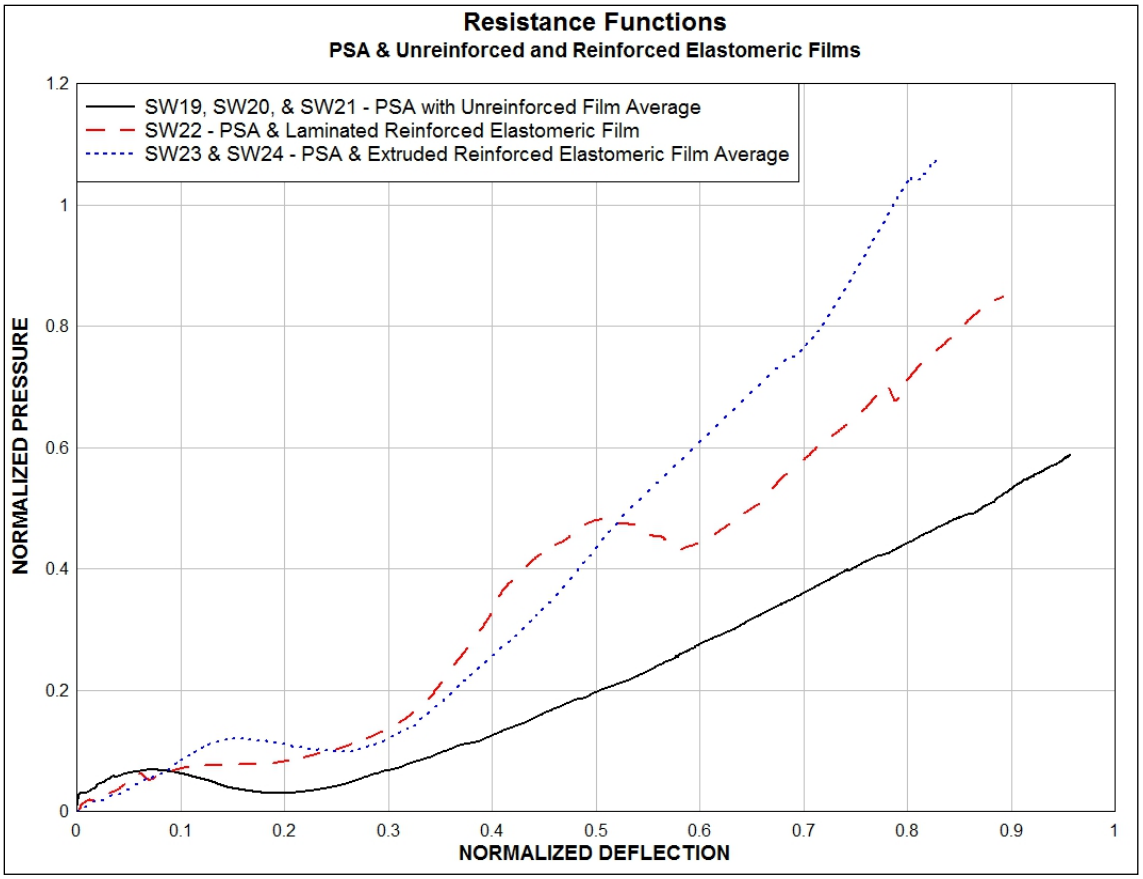

Figure 5.100. Comparison of unreinforced and fiber reinforced elastomeric films with PSA.

in SW19, SW20, and SW21 were relatively similar. The average resistance function from walls SW23 and SW24 are compared to SW22 to see how the laminated or extruded construction of the composite film affected the response of the retrofit. The resistance function for SW22 shows that the ultimate flexural failure occurred at a pressure of 0.0765 and a deflection of 0.137. The film responded quickly and the pressure quickly rebounded and continued to load the reinforced film. As discussed in Section 5.9.1, the sheets of film delaminated during the test allowing the fibers to distort. This was an interesting phenomenon and one that highlights the effects of film

construction. The bond between the encapsulated fibers and the polyurethane film was much stronger for the extruded material in SW23 and SW24. The ultimate effect could not be monitored due to the nature of the walls' failure. The fiber/film strength overwhelmed the PSA at the seam allowing the area to recede and expose the CMUs. This weakened the material at the seam/overlap joint and the point of maximum deformation shifted from the center of the wall at gauge D3 to the seam at gauge D2. Section 5.9.2 includes several figures that show the progression of the failure at the seam.

The laminated reinforced film and the extruded reinforced films demonstrated an 11% and 76% increase, respectively, in pressure over the unreinforced elastomeric films at ultimate flexural resistance. The extruded reinforced films showed a 76% and 58% increase in pressure at ultimate flexural resistance over the unreinforced and laminated reinforced films, respectively. An increase in the pressure was also seen at the ultimate membrane failure for the laminated and extruded reinforced films. The laminated film had a 44% increase in pressure and the extruded film had an 84% increase in pressure over the unreinforced films. The displacement at the point documented as the ultimate tensile membrane failure decreased as the film strength increased. The unreinforced film had the largest average deflection at 0.957 followed by the laminated film at 0.892 and the extruded film at 0.831. The laminated film was removed from further evaluation, but the unreinforced and extruded fiber reinforced film systems were used in the subscale dynamic experiments.

The next group of walls compared ±45-deg fiber reinforced films applied to the walls with various construction methods to encapsulate the fibers and adhesives to apply the materials to the walls in Figure 5.101. The spray-on fiber reinforced system (SW8 and SW9) and the reinforced films with trowel-on epoxy (SW15 and SW16) both used the same Fabric B for reinforcement. The spray-on encapsulated fiber retrofit systems were stiffer than the fiber reinforced elastomeric films using trowel-on adhesives and the fiber reinforced films applied to walls with a PSA. However, the reinforced film systems were

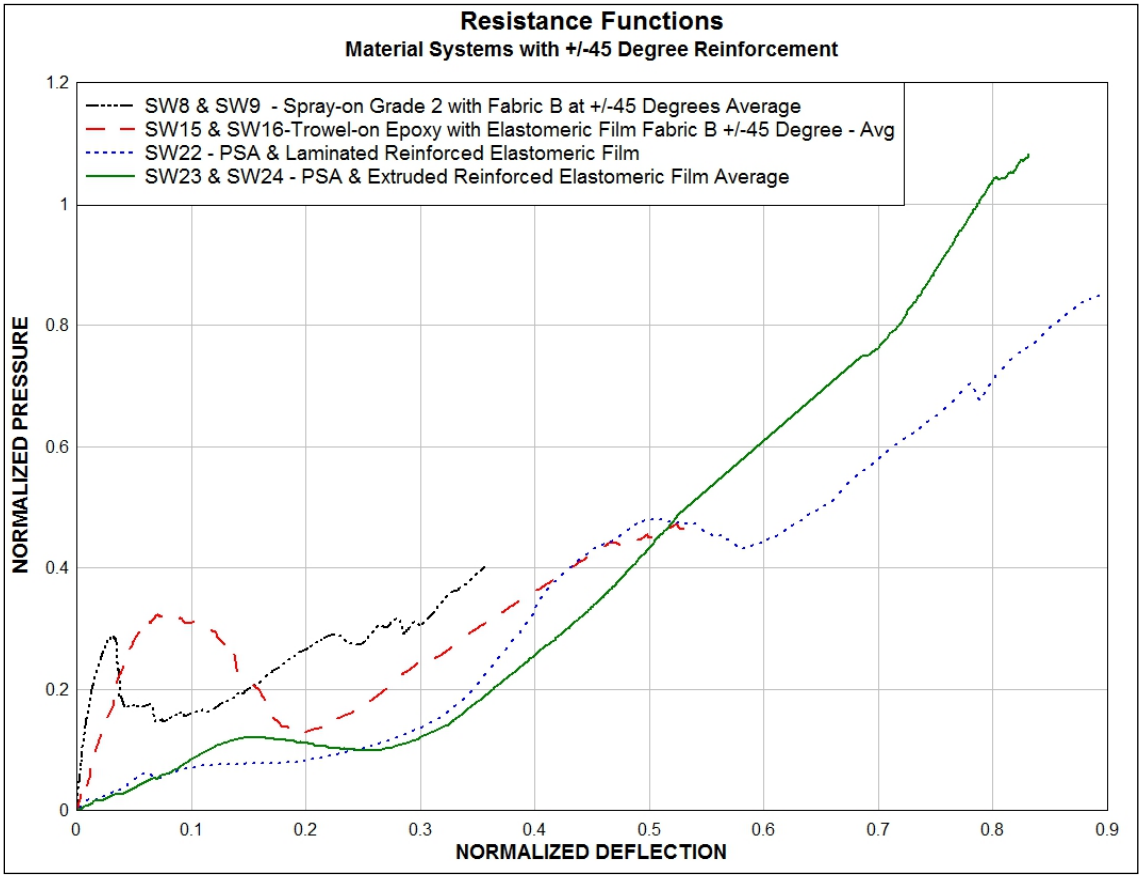

Figure 5.101. Comparison of material systems with ±45-deg reinforcement.

more ductile allowing the retrofit system to deform to a larger degree before the materials failed or the experiment was stopped. The laminated reinforced film had the largest deflection at failure of 0.892, followed by the extruded reinforced films that had an average deflection of 0.831. The reinforced films applied with the trowel-on material only allowed a deflection of 0.524, and the reinforced spray-on material limited the deflection the most at 0.356. At this point in the program, it was hard to determine if a strong bond between the retrofit system and CMU wall was the most beneficial or not. Therefore, a version of each retrofit was used in the subscale dynamic experiments to determine which method of adhesion applied to the CMU walls would have the best global response to a dynamic load.

The results from all of the HTC experiments are graphically depicted in Figures 5.102 to 5.105. The pressures when the CMU wall and retrofit system failed are shown on Figure 5.102. The deflections when the CMU wall and retrofit system failed are illustrated on Figure 5.103. In Figure 5.104, the deflection and pressure at the point when the retrofit system failed are plotted on the x and y axis, respectively. Due to time, material availability, and funding constraints, all of the retrofit systems evaluated in the HTC could not be evaluated in the subscale dynamic experiments. Ten of the retrofit systems were selected for further evaluation in the subscale dynamic experiments. In Figure 5.105, only the retrofit systems selected for further evaluation were plotted.

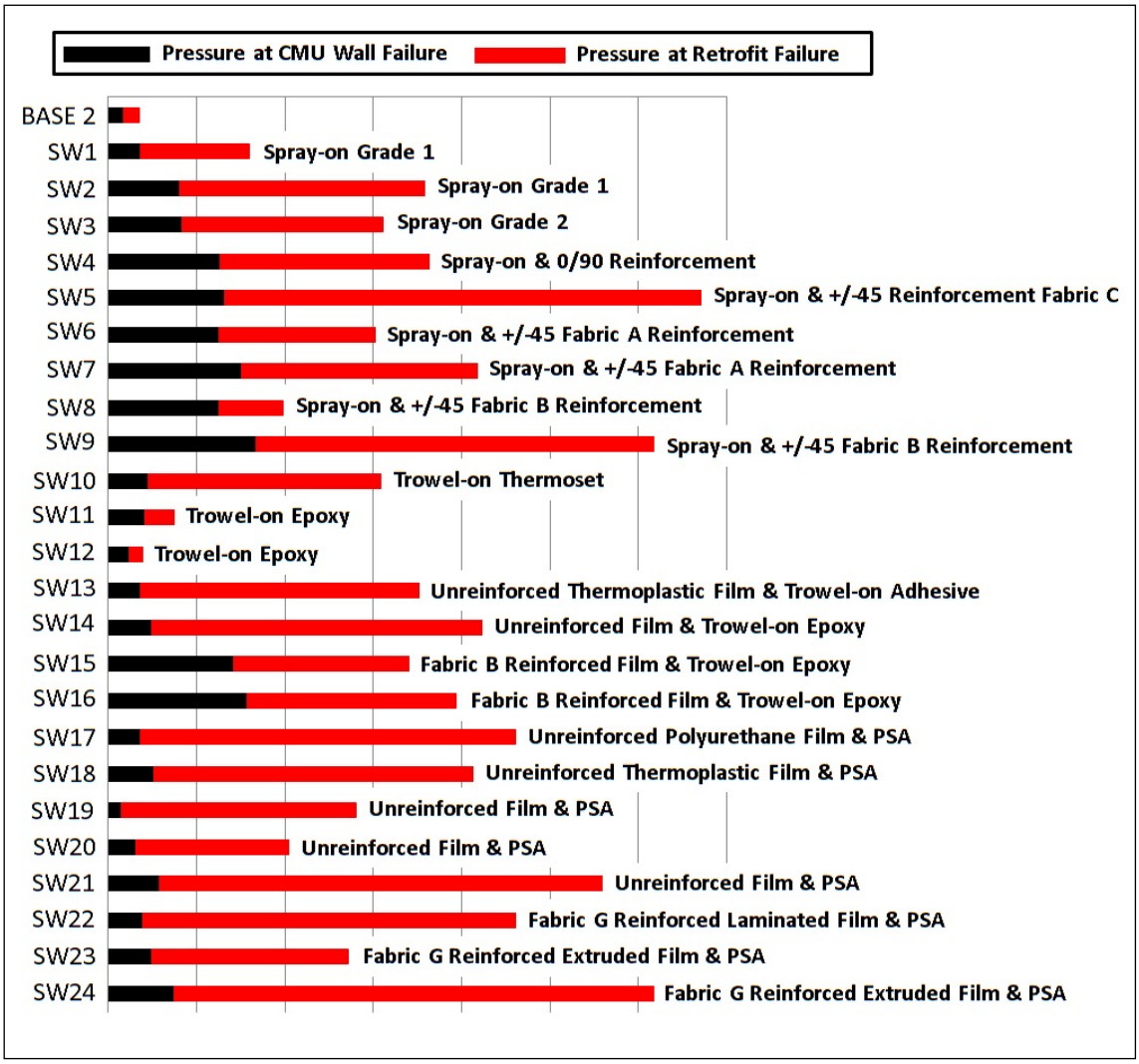

Figure 5.102. Pressure for all of the HTC experiments.

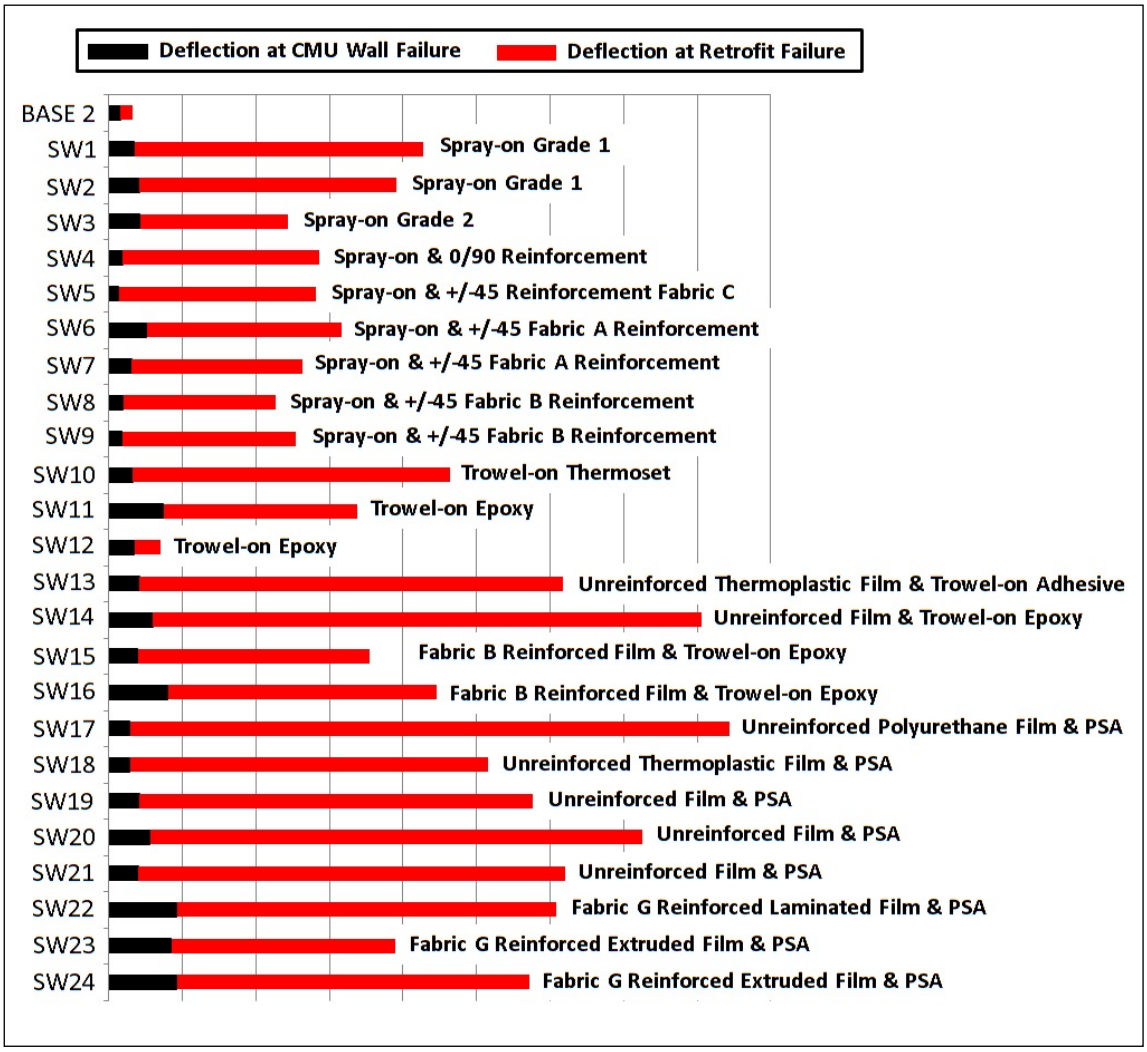

Figure 5.103. Deflection for all of the HTC experiments.

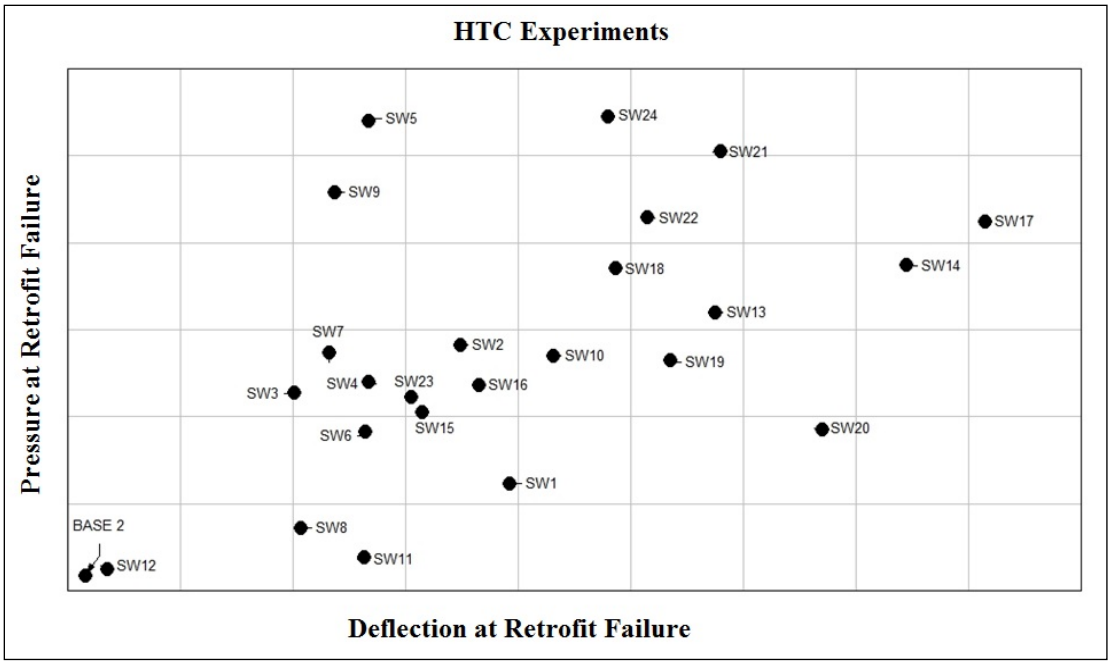

Figure 5.104. Ultimate tensile membrane resistance for all of the static experiments.

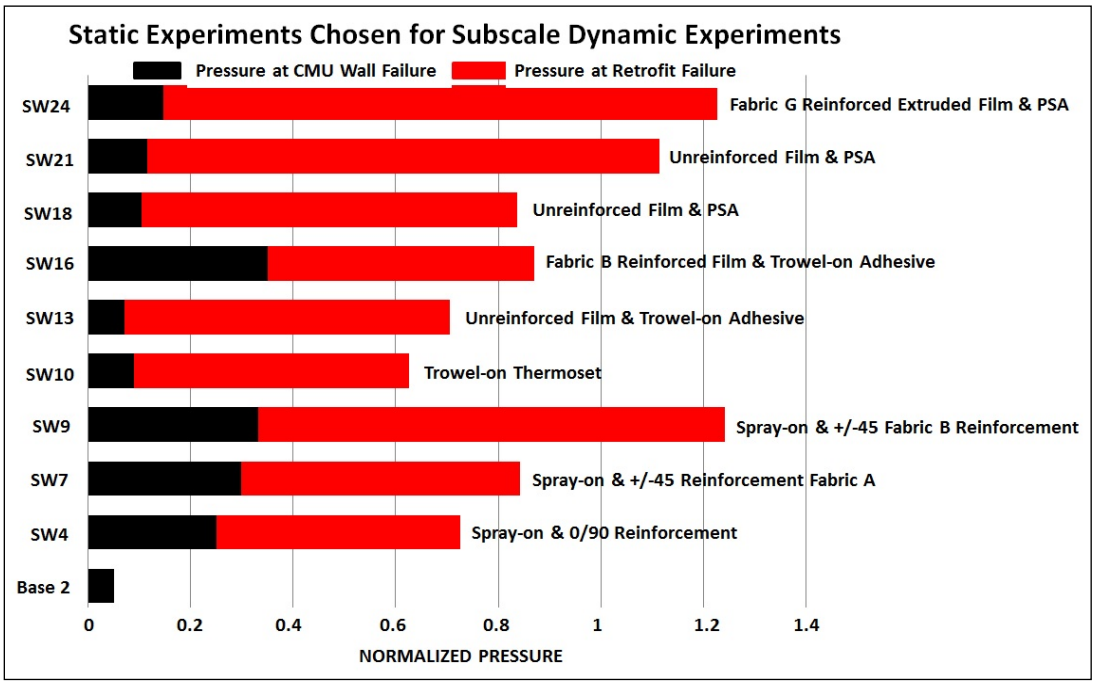

Figure 5.105. Retrofit systems selected for evaluation in the subscale dynamic experiments.

6. SUBSCALE DYNAMIC EXPERIMENTS*

The global response of the CMU walls retrofitted with the elastomeric systems was evaluated in subscale dynamic experiments to investigate the effectiveness of the retrofit systems under a load rate appropriate for blast events. The subscale dynamic experiments were conducted using HE and BLS experiments (Figure 6.1). The initial evaluation of the retrofit material systems began with subscale HE experiments conducted at the BBTS in Vicksburg, MS. Additional subscale dynamic experiments were conducted in the BLS at ERDC once the facility became operational. At the start of the research program, the BLS was in the design phase, and the construction of the facility and device had not begun.

The software program CONWEP 2.1.0.8 (Hyde 1993) was used to predict the blast loads in the dynamic analysis and to develop the experimental layout for the subscale and full-scale blast events. The program was developed in the late 1980s as a computerized version of the Army Technical Manual 5-855-1 "Design and Analysis of Hardened Structures to Conventional Weapon Effects." CONWEP computes the effect

---

*Part of this chapter is reprinted with permission from *Blast Load Simulator/Shock Tube Testing Facilities in the United States*, by Johnson, Carol F. and Lebron Simmons, 2008. Report was prepared for U.S. Army Engineer Research and Development Center, in Vicksburg, MS and has not been published to date.

Part of this chapter is reprinted with permission from *X-Flex™ Retrofit: Results from Subscale Static and Dynamic Experiments*, by Johnson, Carol F., James L. Davis, David L. Coltharp, Bartley P. Durst, and Lonnie L. Smith, 2010, U.S. Army Engineer Research and Development Center, Vicksburg, MS. Due to "Limited Distribution" statement, the material was adapted for public release.

Part of this chapter is reprinted with permission from "Development of a Blast Load Simulator," by Slawson, Thomas R., Carol F. Johnson, and Reed L. Mosher, 2001. *Proceedings of the 72nd Shock and Vibration Symposium*, 2001 by Shock and Vibration Information Analysis Center, Falls Church, VA (Limited Distribution).

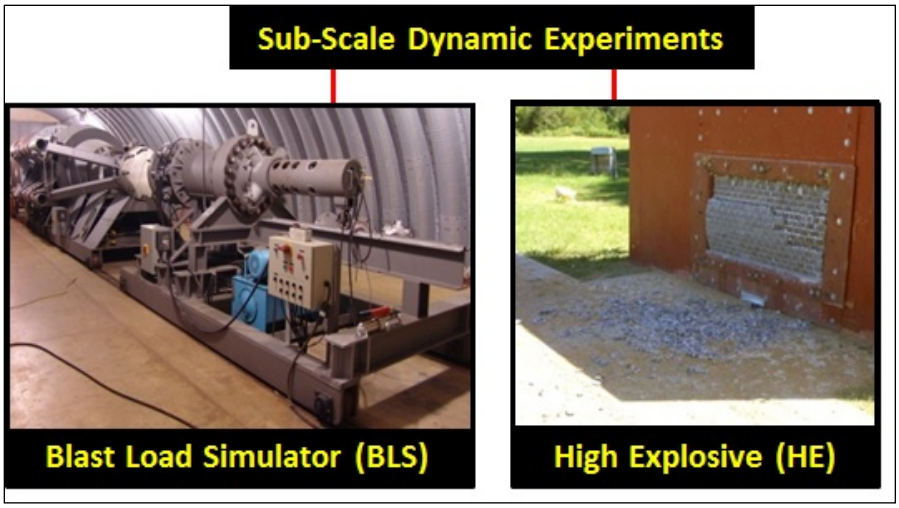

Figure 6.1. Dynamic experiments.

of conventional weapons on user defined structures. The program uses the equations in ARBRL-TR-02555, commonly referred to as the Kingery-Bulmash equations, to determine the airblast parameters, i.e., the peak incident and reflected pressures and impulses, positive phase duration, and time of arrival (Kingery and Bulmash 1984). The modified Friedlander equation in CONWEP, assumes an exponential decay of pressure with time of the form

$$P_r(t) = P_s(1-\frac{t-t_a}{t_o})e^{-\alpha\left(\frac{t-t_a}{t_d}\right)} \qquad (6.1)$$

where:

$P_r(t)$ = pressure at time t

P_s = peak incident pressure

t_o = positive phase duration

t_a = arrival time

α = decay coefficient.

The corresponding reflected impulse, i_r, is the value obtained by integrating the reflected pressure curve over the duration of the positive phase to calculate the area beneath the pressure-time curve.

$$i_r = \int P_r(t)dt \tag{6.2}$$

Typical input and output screens for the program are provided in Figures 6.2 and 6.3.

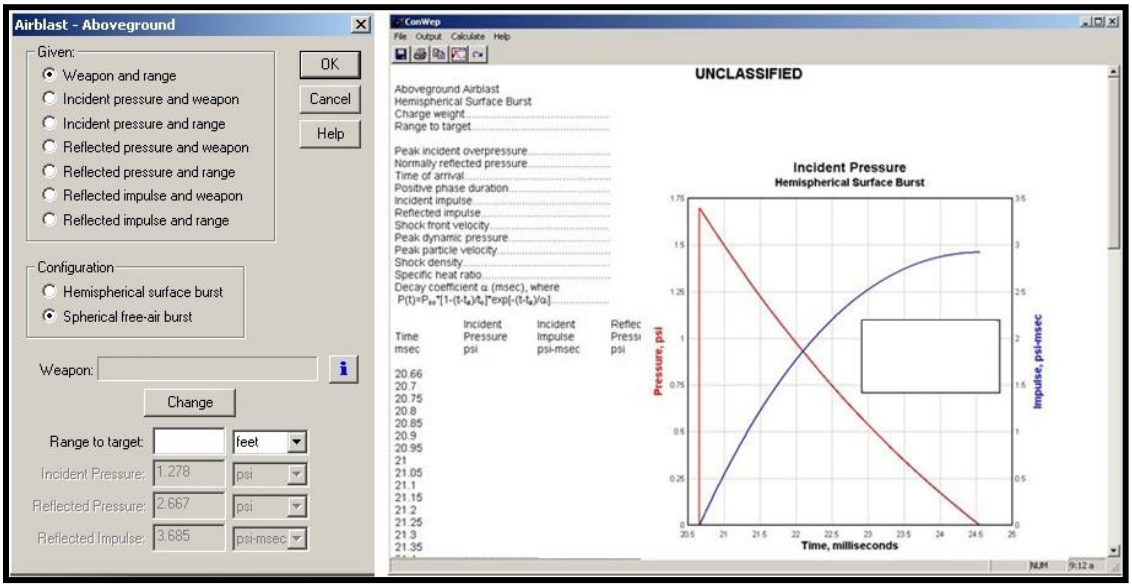

Figure 6.2. CONWEP screens for airblast.

6.1 Subscale HE Experiments

In the subscale HE experiments, the explosive, Composition C-4, was placed at ground level at designated standoffs, R, from the front face of the CMU wall and

reaction structures (Figures 6.4a and b). The standoff distances were based on the predicted reflected pressure and impulse values obtained from the software program CONWEP 2.1.0.8. The response of each retrofitted wall was captured by high-speed video cameras and appropriate instrumentation.

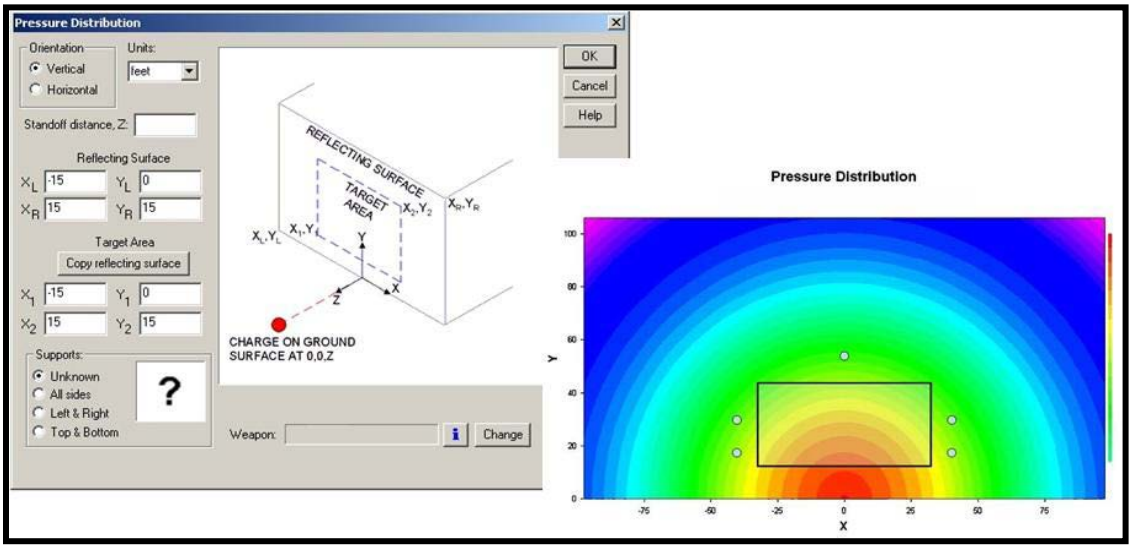

Figure 6.3. CONWEP screens for slab loading from airblast.

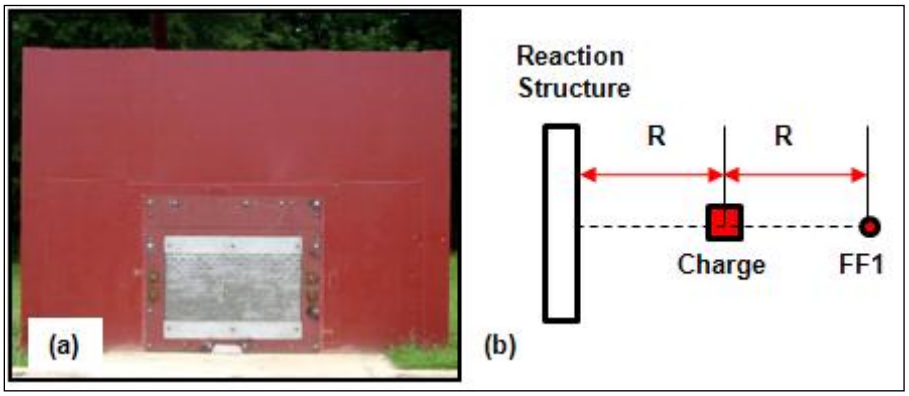

Figure 6.4. HE dynamic experiments. (a) Subscale CMU wall in reaction structure at BBTS. (b) Test site layout at the BBTS (plan view).

The experimental and instrumentation plans for the subscale HE experiments shown in Figure 6.4b and Figures 6.5a and b consisted of seven blast pressure gauges (P1-P6 and FF1) to document the pressure wave created by the blast event and six gauges to measure the retrofitted walls' responses. Two accelerometers (A1, A2), two lasers (L1, L2), two wire deflection gauges (D1, D2), posttest debris distribution, still photos, and two high-speed video cameras were used to document the walls' response to the blast loads (Figures 6.5c and d). The pressure gauges and accelerometers are both

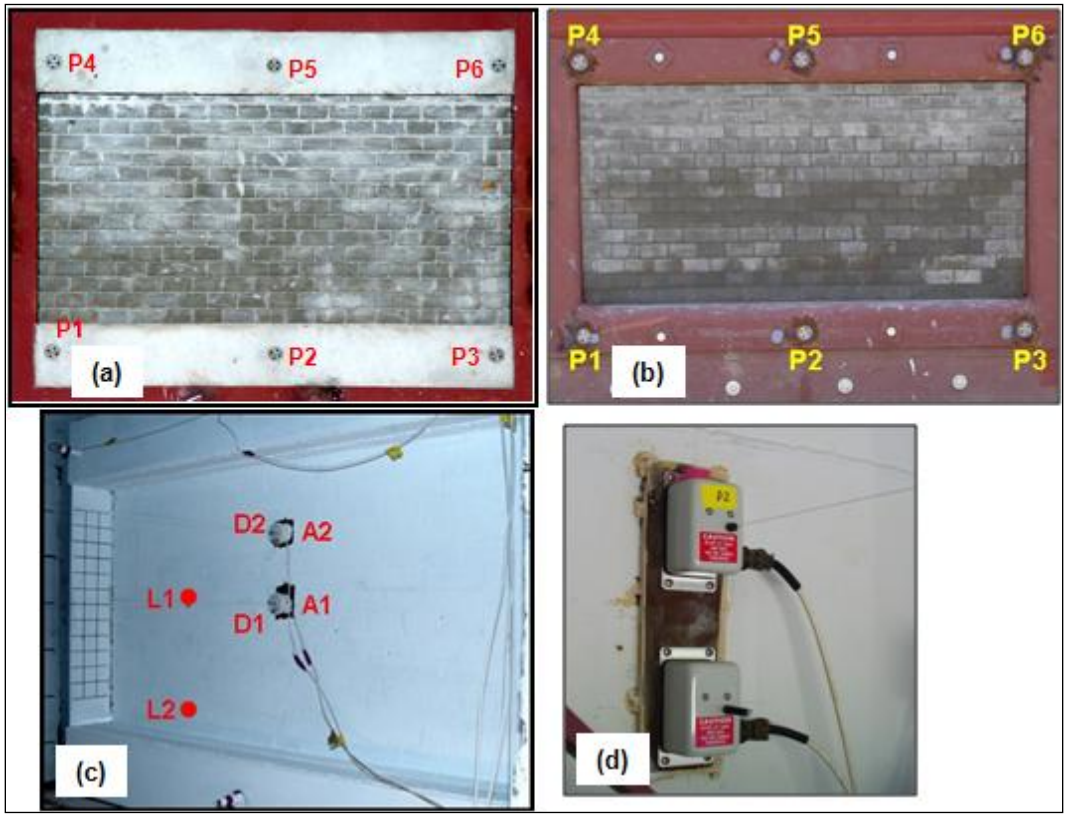

Figure 6.5. Instrumentation used in dynamic experiments. (a) Pressure gauge layout for subscale CMU wall in concrete frame. (b) Pressure gauge layout for CMU wall in steel frame. (c) Accelerometer, laser, and wire deflection gauge layout on CMU wall. (d) Precision potentiometer and wire deflection gauges.

piezo-resistive transducers. The data was transmitted over 22 AWG 4 conductor shielded mil spec cable and recorded on a 12-bit bipolar Pacific Instruments, Model 9830, TDR after the signal was amplified and conditioned using ERDC built instrumentation. The cables tuned to approximately 10 kHz transmitted the data from the test site to an instrument trailer located approximately 800 ft (244 m) away. The TDR's sample rate was set for one microsecond per point for the pressure and acceleration measurements, yielding a record time of –0. 01638 to 0.2294 sec. The sample rate for the deflection measurements was set for two microseconds per point, yielding a record time of -0.015 to 0.229 sec. The negative time increment refers to the pre-trigger, which is the length of measurements saved before the actual signal to record was activated. The pre-trigger prevents the loss of data due to experimental timing miscues.

Kulite Model XT-190SG pressure gauges with a B-Screen filter were used to measure the free-field and reflected pressure on the specimen for each blast event. The six pressure gauges, P1 through P6, were located around the perimeter of the wall to document the reflected pressure and impulse (Figures 6.5a and b). The seventh pressure gauge, FF1, was placed 180 deg from the CMU wall directly in line with the explosive. The range between the explosive and the front face of the wall was also used as the standoff between the explosive and the pressure gauge, FF1. The data from FF1 was used to document the free-field pressure and to determine if the explosive charge achieved full detonation to create the pressure and impulse levels predicted by CONWEP.

Three different methods were used to measure the wall's lateral deflection: accelerometers, lasers, and deflection gauges. The measurements from the three methods were compared to determine the accuracy of each. The acceleration, velocity, and deflection of the wall during the response to the blast load were measured using an Endevco Model 7270A accelerometer. The two accelerometers, A1 and A2, were placed at the mid- and quarter-points. The deflection measurements, D1 and D2, were obtained using Celesco and UniMeasure precision potentiometer and wire deflection gauges. Acuity Research AccuRange 4000 laser range finders, L1 and L2, documented the deflection at mid-height and the movement of the wall at the support.

The dynamic response of the retrofitted CMU walls was obtained in 25 subscale and 18 full-scale dynamic experiments. The dynamic evaluation of the materials/systems began by conducting 14 subscale HE experiments at the BBTS. Two primary limitations at the BBTS affected the test matrix and schedule. First, the test site borders the Big Black River in Vicksburg, Mississippi, and is prone to flooding for extended lengths of time, which damages instrumentation lines and increases labor and material costs for post flood clean-up. Second, the maximum explosive weight allowed at the test site was restricted, and the limit was reduced further through the winter season, which added additional constraints to the test matrix and schedule. The completion of the BLS facility at ERDC alleviated the two primary constraints at the BBTS. The dynamic load was increased, and weather conditions were no longer a constraint. The BLS Facility was used to conduct 11 additional subscale dynamic experiments. Once the subscale evaluations were completed, retrofit materials/systems were selected for validation and

evaluation in 18 full-scale experiments at an AFB in Florida. The dynamic load levels used in the subscale and full-scale dynamic experiments are listed in Table 6.1.

The 14 HE experiments conducted at the BBTS were used to evaluate five different retrofit systems that were installed in steel or reinforced concrete frames. The subscale dynamic experiments evaluated the responses of the CMU wall retrofits,

Table 6.1. Dynamic load level based on normalized peak reflected impulse.

Level	Impulse	Level	Impulse
1	0.3-0.4	5	0.7-0.8
2	0.4-0.5	6	0.8-0.9
3	0.5-0.6	7	0.9-1.1
4	0.6-0.7		

including the effects of the support conditions. The two frames allowed the adhesive strength of the retrofit systems to be evaluated for potential use in conventional steel or reinforced concrete framed structures. The ability to evaluate both substrates allowed researchers to assess the effect of the support conditions on the wall's response to blast loads. An adhesive bond was used in all of the experiments and an additional mechanical anchorage, provided by bolting a steel plate to the frames, was used in select experiments to prevent the retrofit materials from peeling off the supports. Each wall evaluated in the research program is described in the following sections of this chapter

along with a brief description of each retrofit and the results of each dynamic experiment. The complete test matrix for the experiments conducted at the BBTS is provided in Table 6.2.

Table 6.2. Test matrix for subscale HE experiments.

Wall Label	Frame	Matrix	Reinforcement	Dynamic Load Level
DW1	Steel	Spray-on Polyurea Grade 2	None	3
DW2	Concrete	Spray-on Polyurea Grade 2	None	2
DW3	Steel	Spray-on Polyurea Grade 2	None	2
DW4	Steel	Spray-on Polyurea Grade 2	Fabric A at 0/90 deg	3
DW5	Concrete	Spray-on Polyurea Grade 2	Fabric A at ±45 deg	3
DW6	Steel	Spray-on Polyurea Grade 2	Fabric A at ±45 deg	3
DW7	Steel	Spray-on Polyurea Grade 2	Fabric B at ±45 deg	3
DW8	Steel	Spray-on Polyurea Grade 2	Fabric B at ±45 deg	4
DW9	Steel	Spray-on Polyurea Grade 2	Fabric B at ±45 deg	4
DW10	Steel	Trowel-on Thermoset Grade 1	None	3
DW11	Steel	Trowel-on Thermoset Grade 1	None	3
DW12	Concrete	Elastomeric Film & Spray-on Adhesive	None	3
DW13	Concrete	Elastomeric Film & Trowel-on Thermoset	None	4
DW14	Steel	Elastomeric Film & Trowel-on Epoxy	Fabric B at ±45 deg	4

6.1.1 Spray-on Polyurea Retrofit (DW1-DW3)

6.1.1.1 DW1

Wall DW1 was constructed in a steel frame (Figure 6.6a) and retrofitted with four passes of spray-on polyurea material Grade 2. The spray-on polyurea was allowed to overlap the top and bottom supports, anchoring the polyurea layer to the steel frame with an adhesive bond. No mechanical anchorage (steel plate) was used in this experiment (Figure 6.6b). The wall was exposed to dynamic load level 3, defined on Table 6.1. The accelerometer located at the center of the interior face on the CMU wall immediately disengaged from the wall and the quarter-point accelerometer disengaged at approximately 0.104– to 0.139-in. deflection of the wall. The second and third courses of

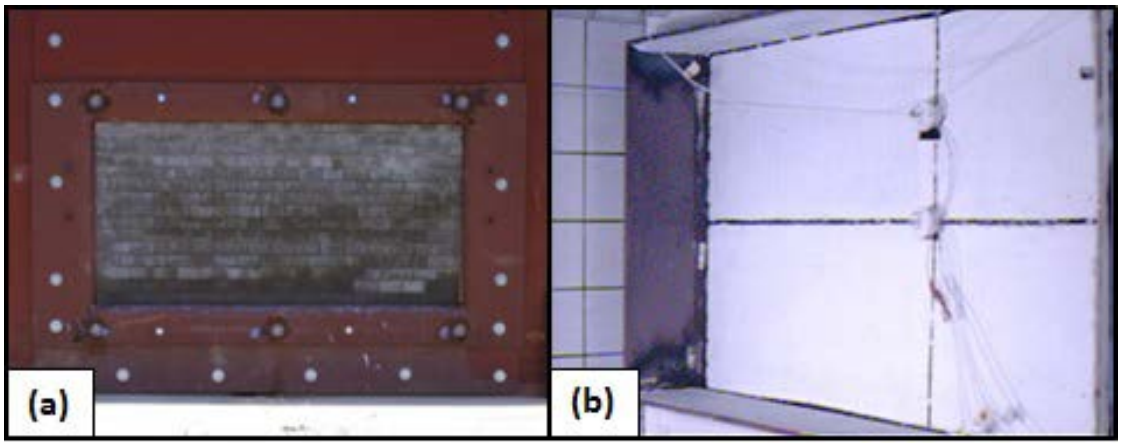

Figure 6.6. DW1. (a) Pretest exterior view. (b) Pretest interior view.

block from the top were damaged. Wall failure occurred at mid-height when the polyurea failed. Figure 6.7 contains several frames (a to d) from the high-speed video camera that chronologically display the wall response. Most of the blocks remained

attached to the polyurea layer (Figure 6.8b). Face shells from the second and third courses from the top littered the area outside the structure, but only a handful of debris was found inside the structure (Figure 6.8a). Based on the data gathered from the six pressure gauges mounted on the reaction structure, pressure gauge P2 appeared to be faulty and was replaced before the next experiment. Samples of the retrofit material were cut from the debris and measured to determine the quality of the application procedure. The average thickness of the retrofit material was 0.13 in., and the thinnest and thickest sample measurements were 0.069 in. and 0.232 in., respectively.

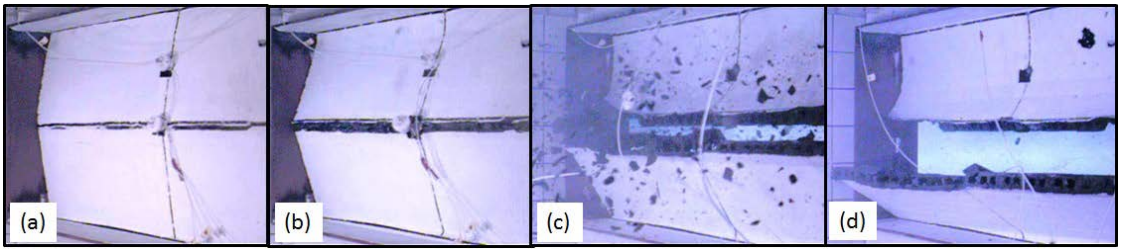

Figure 6.7. DW1: Frames from high-speed camera. (a) Wall cracks at midheight. (b) Wall hesitates slightly before complete failure. (c) CMU debris enters reaction structure. (d) Final wall position.

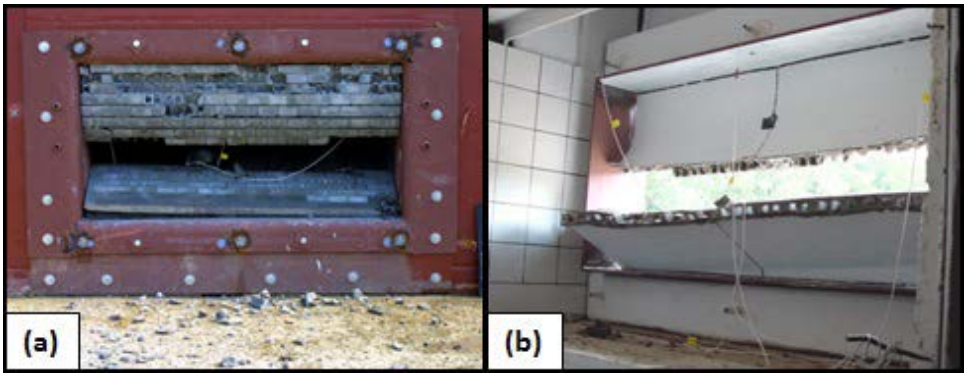

Figure 6.8. DW1. (a) Exterior view. (b) Interior view.

6.1.1.2 DW2

The retrofit material and application procedure for DW2 duplicated DW1. DW2 was constructed in the concrete frame to evaluate the adhesive bond of the spray-on elastomer. DW2 was evaluated at dynamic load 2. The polyurea liner ripped at the top and bottom support and landed outside the reaction structure (Figure 6.9a). Very little debris was found inside the structure. Most of the CMU blocks remained attached to the polyurea when it folded upon itself on the ground (Figure 6.9b). Posttest inspection of the liner and CMU wall outside the structure displayed no visible damage (Figure 6.10a).

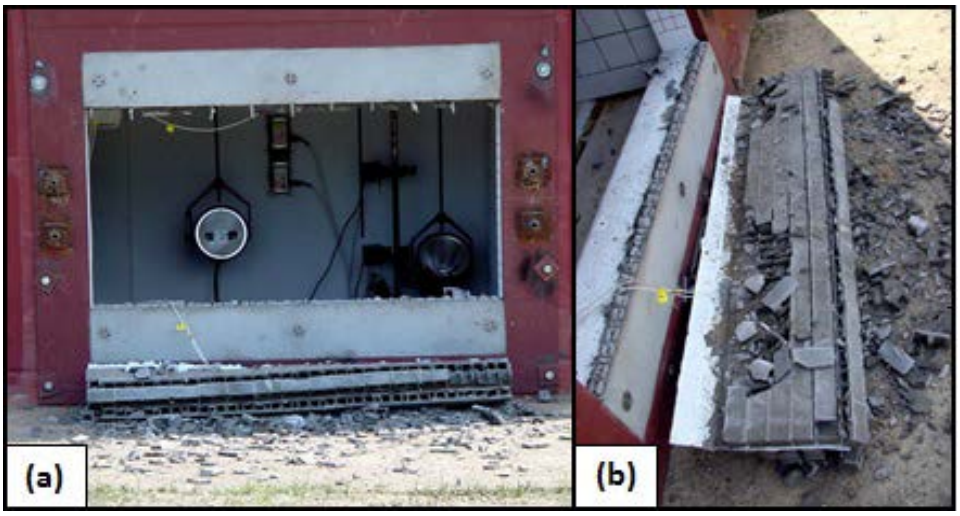

Figure 6.9. DW2. (a) Posttest exterior view. (b) Elastomeric material with blocks attached settled outside of the structure.

The average thickness of the retrofit samples that covered the CMU wall surface was 0.11 in., and the thinnest and thickest samples measured were 0.081 in. and 0.15 in., respectively. Inspection of the supports indicated that the polyurea coat was extremely thin at both the top and bottom supports (Figure 6.10b), causing the elastomer to tear and

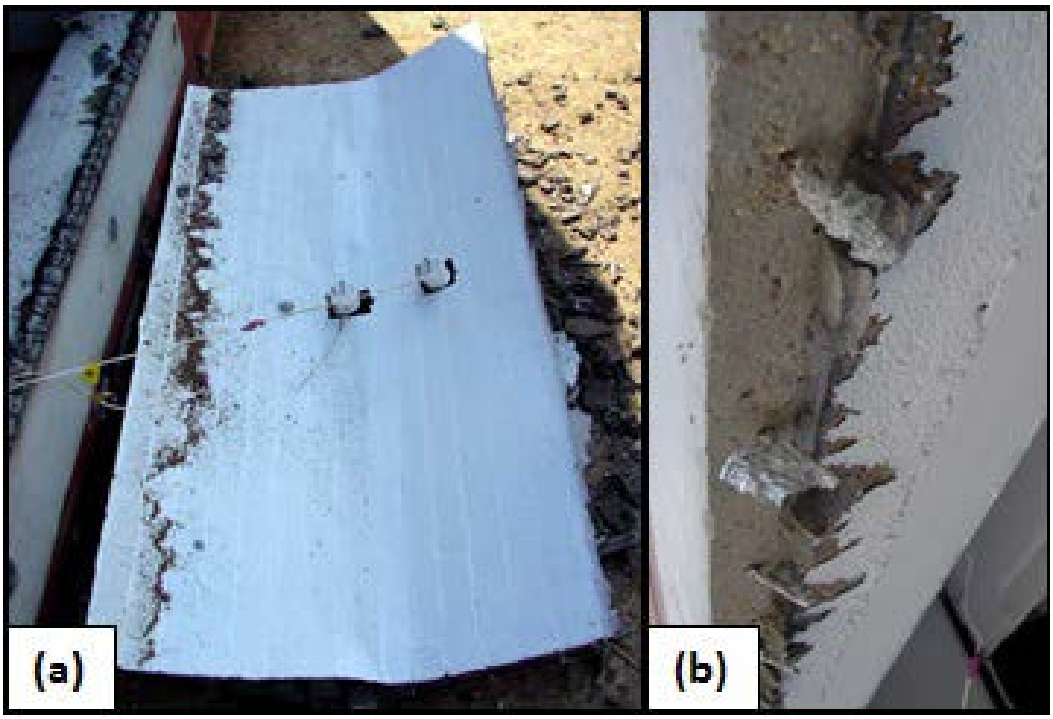

Figure 6.10. DW2. (a) No visible damage to the liner applied to the CMU blocks. (b) Failure due to extremely thin layer of spray-on polyurea at the supports (top support shown).

failure of the system. Data from the accelerometers, lasers, and deflection gauges indicated that the wall deformed into the structure approximately 0.139 to 0.243 in. before it rebounded. The high-speed camera failed to trigger, so video could not be inspected to determine the failure sequence. One could conclude that the polyurea layer tore along the top and bottom supports during the rebound phase of the wall response, since no debris was found inside the reaction structure, and the entire wall and retrofit layer were found folded along the centerline lying outside the structure.

6.1.1.3 DW3

The retrofit materials and application procedure for Wall DW3 was similar to DW1 and DW2, but DW3 was the first dynamic experiment that used a primer to promote the adhesion of the retrofit material to the reaction structure. DW3 was evaluated in the steel frame that was used for DW1. Before the retrofit was applied to the wall, the supports were cleaned with a wire wheel brush, and a steel primer (Primer 1) was applied to the top and bottom supports of the steel frame. Once the supports were prepped, DW3 was retrofitted with four passes of spray-on polyurea Grade 2. The spray-on polyurea was allowed to overlap the top and bottom supports, creating an adhesive bond. No mechanical anchorage (steel plate) was used in this experiment. Since DW2 failed due to the thinness of the polyurea material at the support, the dynamic load for DW3 was maintained at level 2. Wall deformation did occur, but the elastomeric system survived with no visible defects in the polyurea layer. The high-speed camera footage clearly shows that the retrofit layer has not peeled off the top or bottom supports when the wall reaches the maximum deflection into the structure, but the polyurea has significantly peeled off the supports when the wall reaches the maximum deflection during the rebound phase (Figures 6.11a, b, and c). Only a few CMU blocks lost face shells, and none of the debris was found inside the reaction structure (Figures 6.12a and 6.13a). The displacement gauge, D1, and the laser, L1, both measured a maximum deflection into the reaction structure of 0.174 in. at mid-span. Approximately half of the polyurea material overlapping the top and bottom supports peeled back as the wall rebounded during the later phases of the loading cycle (Figures 6.12b and 6.13b). The average thickness of the

retrofit samples was 0.17 in., and the thinnest and thickest samples measured were 0.12 in. and 0.28 in., respectively.

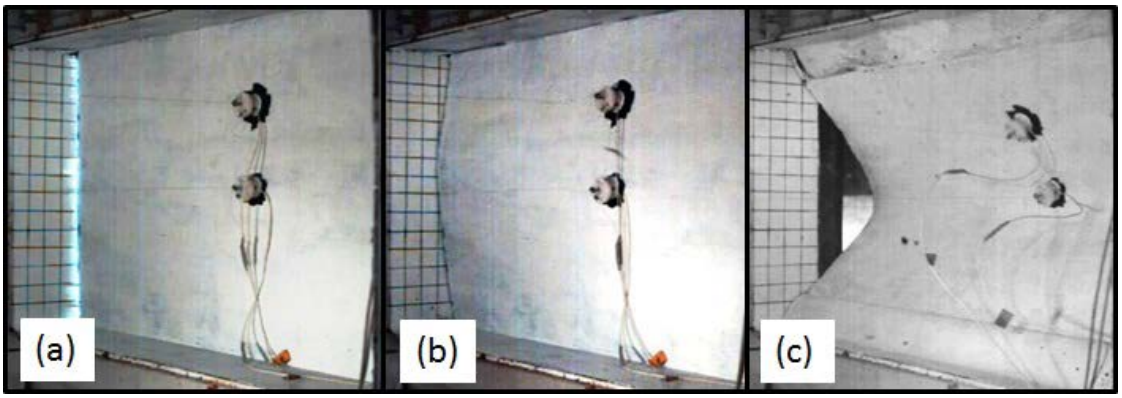

Figure 6.11. DW3. Frames from high-speed camera. (a) Flash from blast. (b) Maximum deflection into the structure. (c) Maximum deflection during the wall rebound.

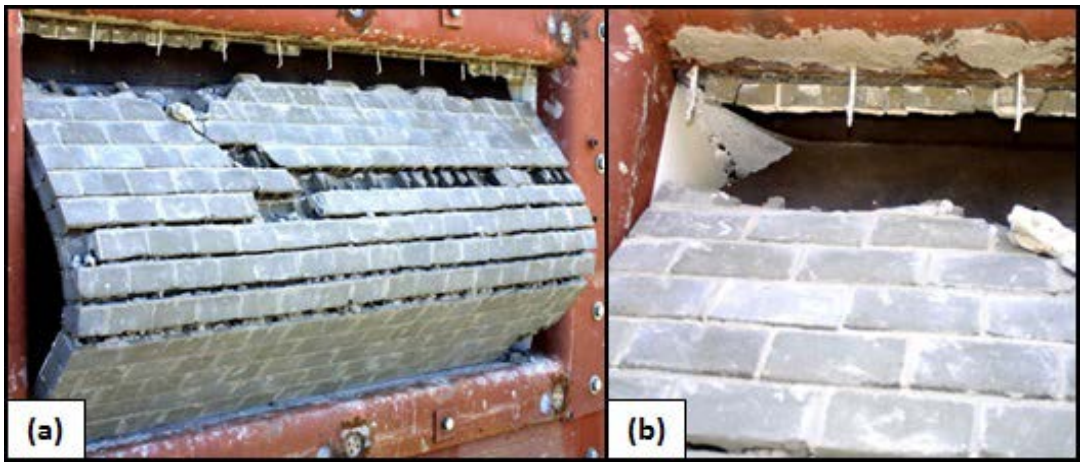

Figure 6.12. DW3. (a) Exterior view. (b) Peel back at top support.

Figure 6.13. DW3. (a) Interior view. (b) Peel back at top and bottom supports.

6.1.2 Fiber-Reinforced Spray-on Polyurea Retrofits (DW4-DW9)

6.1.2.1 DW4

Wall DW4 was retrofitted with a reinforced spray-on polyurea Grade 2. First, two passes of the spray-on polyurea were applied to the wall followed by a layer of Fabric A applied with the fibers oriented at 0/90 deg to the horizontal mortar joints of the wall. The fabric was encapsulated when two additional passes of the spray-on polyurea were applied over the fabric. DW4 was evaluated at dynamic load level 3. The retrofit sheared at the top support and folded over on itself (Figures 6.14a and b). The bottom support remained attached to the frame. High-speed video indicated that the wall deflected minimally before failure of the fiber reinforcement occurred at the top support (Figures 6.15a to d). While evaluating the high-speed camera footage, the wall appeared to transfer the load directly to the top support where the polyurea material and fibers failed along the top course of blocks. The wall failed during the initial deformation into

**Figure 6.14. DW4. (a) Exterior view.
(b) Exterior profile.**

the structure. Posttest inspection of the top support indicated that none of the material peeled off the support as seen during the response of the previous wall evaluated DW3. Inspection of the polyurea and fabric reinforcement at the failure line indicated that intermittent sections of the reinforcement fabric were pulled out of the polyurea layer (Figure 6.16a), but that the material failed the full width of the wall at the top support. A minimal amount of debris was found inside the reaction structure while most of the CMU was still adhered to the polyurea layer (Figure 6.16b). A small amount of debris accumulated in front of the reaction structure (Figure 6.14b). The average thickness of the retrofit samples was 0.12 in., and the thinnest and thickest samples measured were 0.086 in. and 0.18 in., respectively.

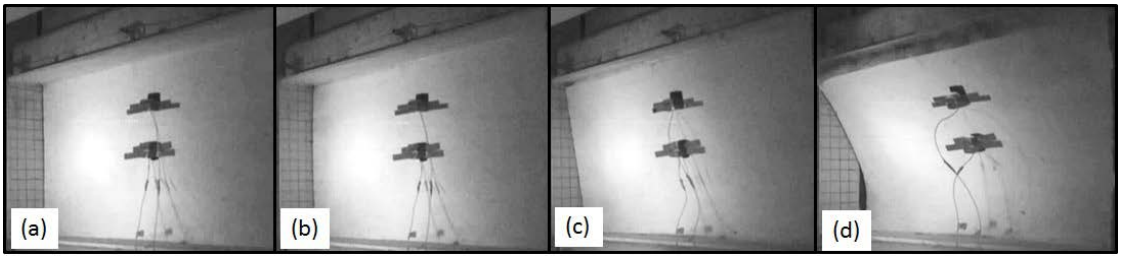

Figure 6.15. DW4: Frames from high-speed video. (a) Pretest interior camera view. (b) Initial wall response. (c) Maximum deflection point transfers to top support. (d) Retrofit completely torn along top support.

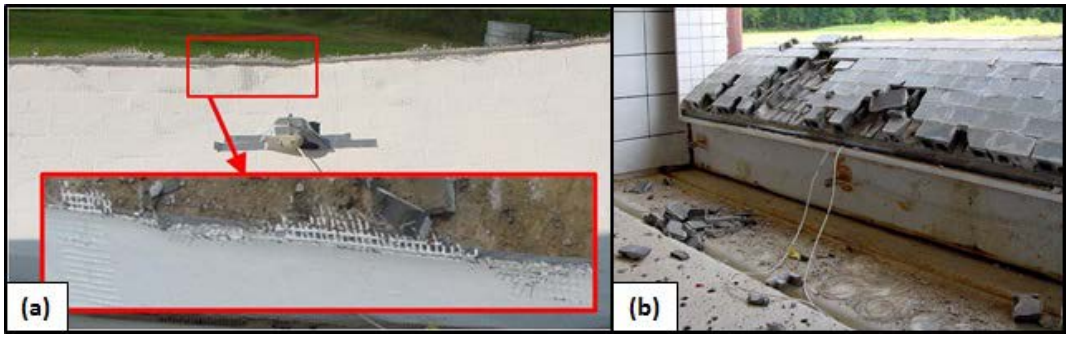

Figure 6.16. DW4. (a) Most of the fibers failed directly at corner, but some fibers pulled out of the polyurea. (b) Interior view.

6.1.2.2 DW5

Wall DW5 was constructed in the reinforced concrete frame to evaluate the bond strength of the retrofit materials to a concrete substrate. The wall was retrofitted with a reinforced spray-on polyurea Grade 2. First, two passes of the spray-on polyurea were applied to the wall, followed by a layer of Fabric A applied with the fibers oriented ±45 deg to the wall. The fabric was encapsulated when two additional passes of the spray-on polyurea were applied over the fabric. DW5 was evaluated at dynamic load level 3. The reinforced polyurea coating was not breached, and most of the blocks

remained attached to the polyurea layer (Figures 6.17a and b). The center four courses of block were heavily damaged across the entire wall span, but again none of the debris was found in the reaction structure (Figure 6.18a). Approximately 30% of the CMU blocks were damaged during the experiment. The center of the retrofitted wall deflected 0.167 in. into the structure. The polyurea did peel back on the top and bottom supports, but the overlap was large enough to prevent failure. In Figure 6.18b one can see that some of the concrete pulled off the support when the spray-on material peeled back, indicating that the bond strength between the elastomer and concrete was very good. High-speed video footage showed that the peel back of the elastomeric material at the bottom and

Figure 6.17. DW5. (a) Exterior view.
(b) Permanent deflection.

top supports occurred during the wall's rebound (Figures 6.19a to d). Maximum displacement occurred during the peak of the rebound cycle. The average thickness of the retrofit samples was 0.13 in., and the thinnest and thickest samples measured were 0.12 in. and 0.35 in., respectively.

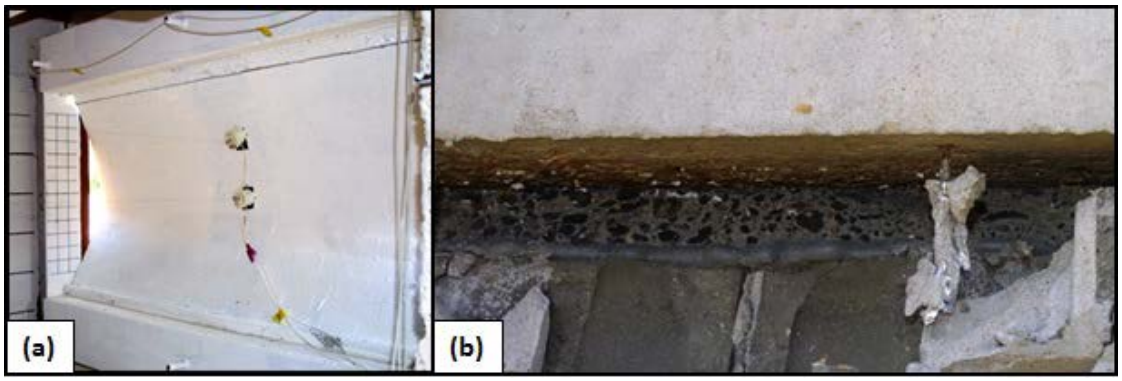

Figure 6.18. DW5. (a) Interior view. (b) Layer of concrete pulled off the support when the polyurea layer peeled back.

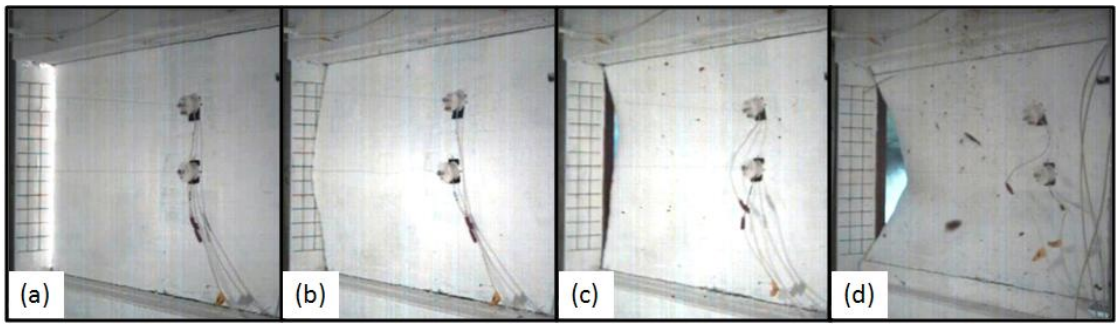

Figure 6.19. DW5: Frames from high-speed video. (a) Flash from explosive detonation. (b) Maximum deformation into structure. (c) Wall displacement on rebound prior to retrofit peel at supports. (d) Maximum displacement during rebound phase.

6.1.2.3 DW6

The retrofit material and procedure for Wall DW6 duplicated DW5. The wall was constructed in the steel frame and the dynamic load was maintained at level 3. The retrofit performed well, allowing none of the CMU wall debris to enter the reaction structure (Figure 6.20a). The reinforced polyurea material was not breached, and almost all of the blocks remained adhered to the polyurea (Figure 6.20b). High-speed video and instrumentation indicate that the maximum deflection of the wall into the reaction structure was 0.18 to 0.194 in. (Figures 6.21a and b). The spray-on polyurea ripped along the top support, but the fiber reinforcement, which was pulled out of the polyurea layer, remained attached and prevented failure at the top support (Figure 6.22a). A rip in the elastomer and fabric developed mid-height on the left edge of the wall and propagated 10 in. to the right (Figure 6.22b). The average thickness of the retrofit samples was 0.11 in., and the thinnest and thickest samples measured were 0.083 in. and 0.15 in., respectively.

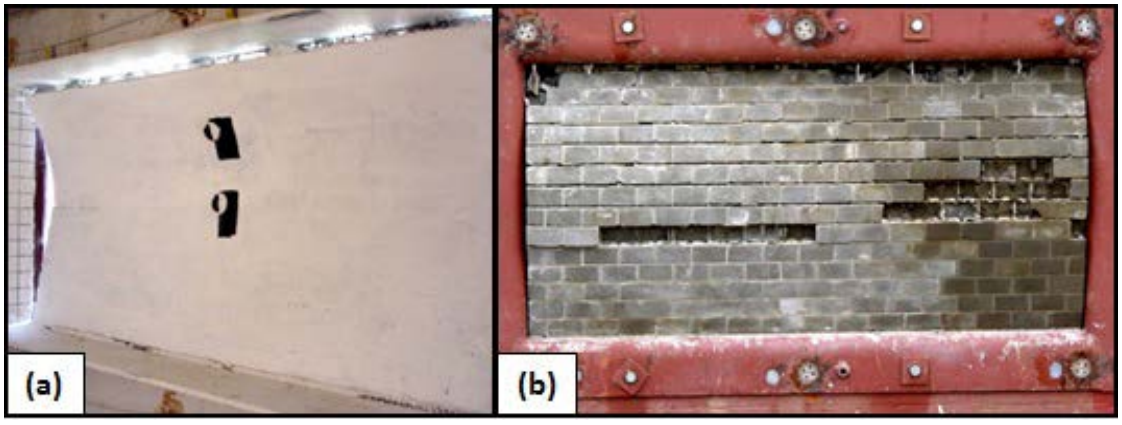

Figure 6.20. DW6. (a) Interior view. (b) Exterior view.

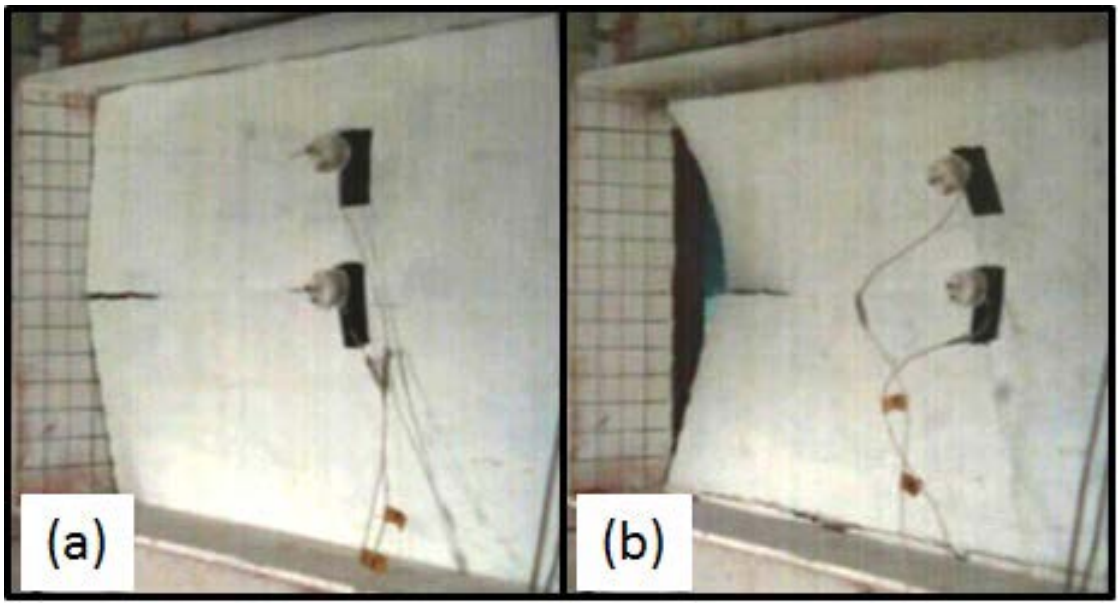

Figure 6.21. DW6: Frames from high-speed camera. (a) Deflection into the structure. (b) Maximum deflection during wall rebound.

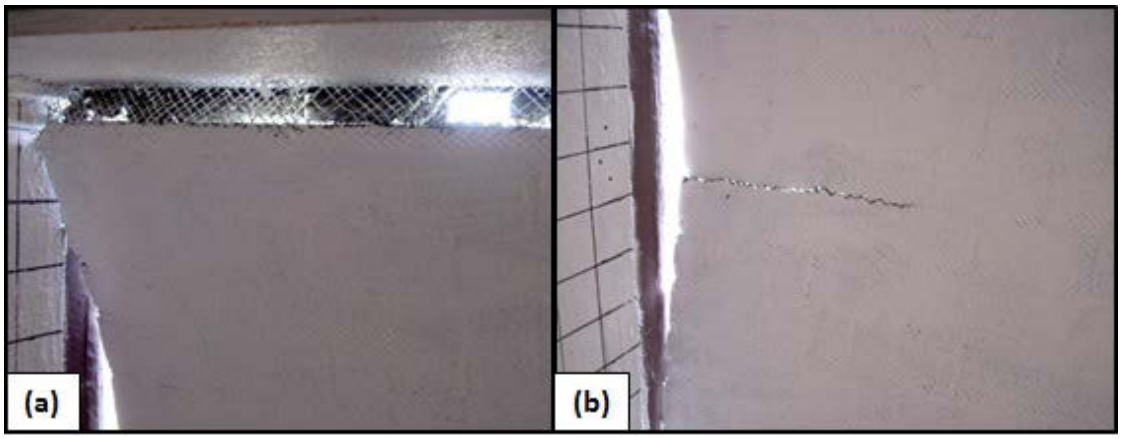

Figure 6.22. DW6. (a) Elastomer ripped but fabric reinforcement remained intact. (b) A 10-in. rip in liner and fabric at mid-height.

6.1.2.4 DW7

Wall DW7 was retrofitted with a reinforced spray-on polyurea Grade 2 and was evaluated at dynamic load level 3. First, two passes of spray-on polyurea were applied to the wall followed by a layer of Fabric B applied with the fibers oriented at ±45 deg to the wall. The fabric was encapsulated when two additional passes of the spray-on polyurea were applied over the fabric. Additional spray-on polyurea was added to the top and bottom supports. The retrofit responded well, allowing none of the CMU wall debris to enter the reaction structure (Figure 6.23a). More than 66% of the CMU blocks were destroyed (Figure 6.23b) and settled outside the reaction structure. High-speed video indicated that the maximum deflection into the reaction structure of 0.312 to 0.347 in. occurred at the bottom quarter-point (Figures 6.24a to d). The center of the wall was measured using three different devices: an accelerometer, a wire displacement gauge and a laser. The accelerometer measured a displacement of 0.208 The wire

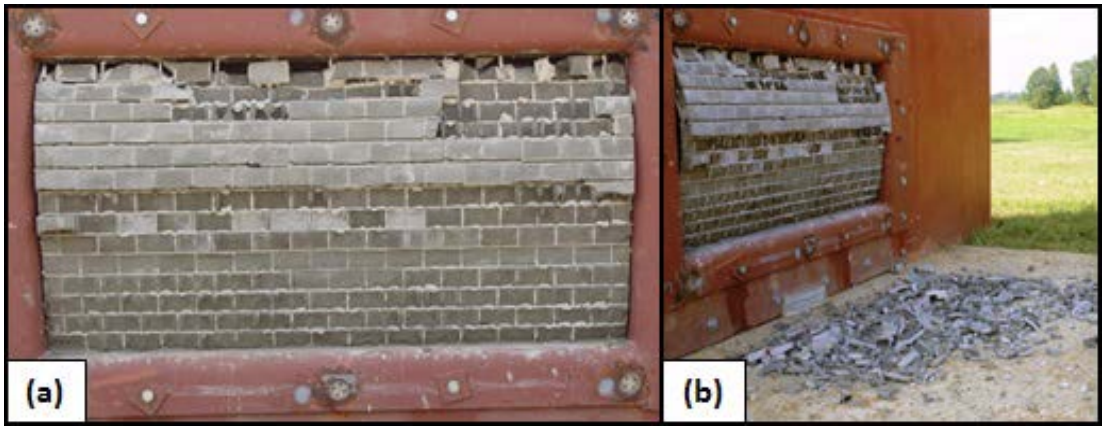

Figure 6.23. DW7. (a) Exterior view. (b) CMU wall debris outside reaction structure.

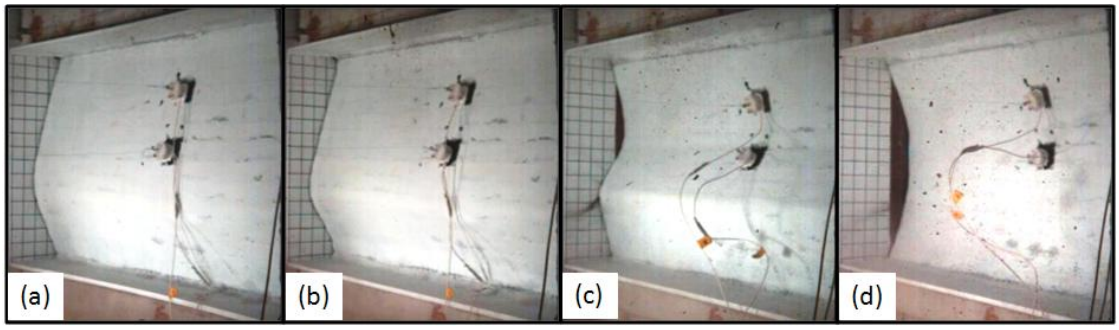

Figure 6.24. DW7: Frames from high-speed video. (a) Wall deflection into structure as retrofit began to peel off top support. (b) Maximum deformation into structure. (c) Wall response during rebound. (d) Maximum deformation during rebound.

displacement gauge measured 0.222 and the laser recorded a deflection 0.25. The reinforced spray-on polyurea appeared to be undamaged during the posttest inspection. No tears were visible in the material (Figure 6.25a); however, the elastomeric system did peel back on both supports as Figure 6.25b demonstrates. This was the first retrofitted wall to peel off the supports during the initial deformation into the structure. The average

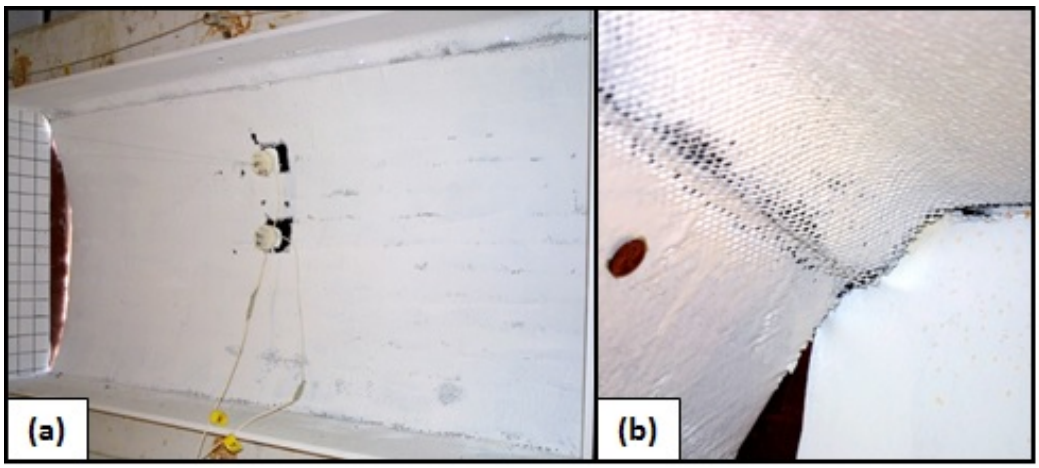

Figure 6.25. DW7. (a) Posttest interior view. (b) Material peeled back at top support.

thickness of the retrofit samples across the wall was 0.19 in., and the thinnest and thickest samples measured were 0.13 in. and 0.33 in., respectively.

6.1.2.5 DW8

Wall DW8 was retrofitted with the reinforced spray-on polyurea system used in DW7 with the addition of a steel primer (Primer 1) to enhance the adhesion on the supports. The dynamic load was increased to level 4, since DW7 survived at level 3. The retrofit successfully prevented the CMU wall debris from entering the reaction structure (Figure 6.26a). More than 59% of the CMU blocks were destroyed with the majority of the damage concentrated at the bottom of the wall (Figures 6.26b and c). The retrofit system held at the supports with minimal peel back or deformation at either support (Figures 6.27a to c). Inspection of the high-speed video showed that the maximum deflection (0.278) of the wall into the reaction structure occurred at the top course of blocks and the maximum deflection into the reaction structure at mid-height was 0.174 (Figure 6.27b). The accelerometer, wire deflection gauges, and the laser all measured a

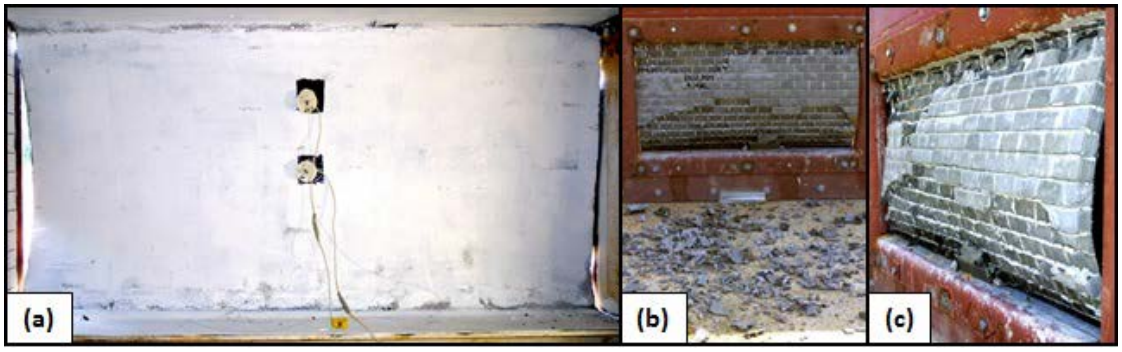

Figure 6.26. DW8. (a) Posttest interior view. (b) Exterior view. (c) Profile view.

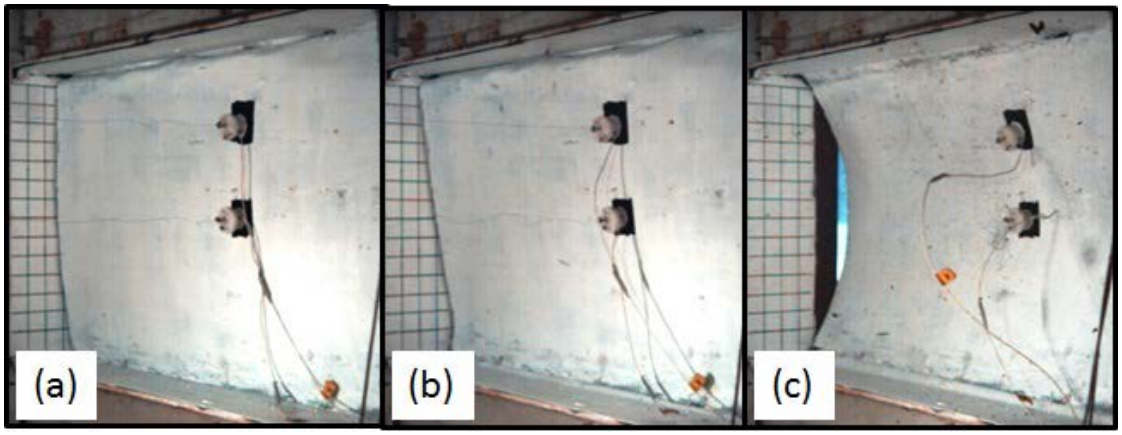

Figure 6.27. DW8: Frames from high-speed camera. (a) Maximum deflection of wall at centerline. (b) Maximum wall deflection at top support. (c) Maximum wall deflection during rebound.

center line deflection of 0.16 to 0.167. The average thickness of the retrofit samples across the wall was 0.19 in., and the thinnest and thickest samples measured were 0.13 in. and 0.25 in., respectively.

6.1.2.6 DW9

The retrofit material and application techniques used on DW8 were duplicated on DW9. The retrofit performed well at dynamic load level 4, allowing none of the CMU wall debris to enter the reaction structure (Figure 6.28a). More than 46% of the CMU blocks were damaged with the majority of the damage concentrated at the top of the wall (Figure 6.28b). The retrofit system held at the supports with little peel back deformation at either support (Figures 6.29a, b, and c). Instrumentation indicated that a maximum deflection of 0.222 occurred at mid-height. The average thickness of the retrofit samples across the wall was 0.19 in., and the thinnest and thickest samples measured were 0.13 in. and 0.35 in., respectively.

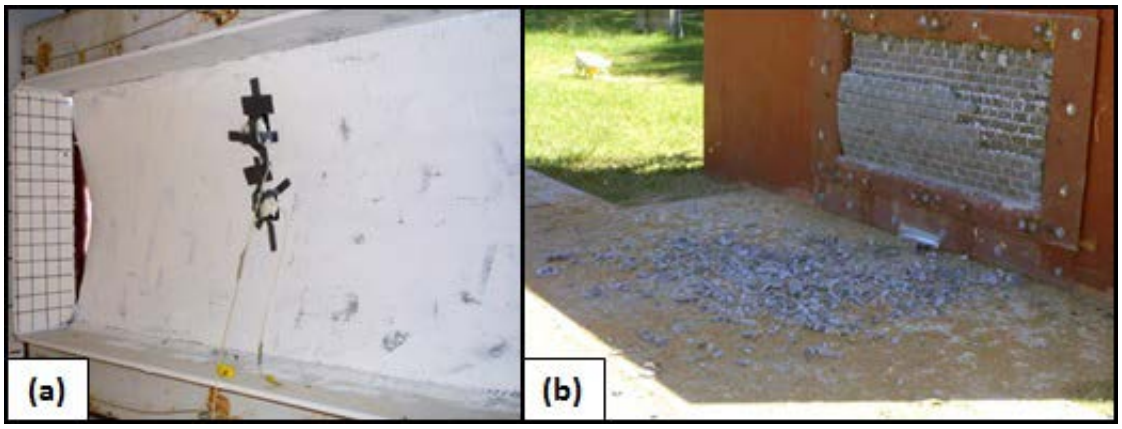

Figure 6.28. DW9. (a) Posttest interior view. (b) Exterior view.

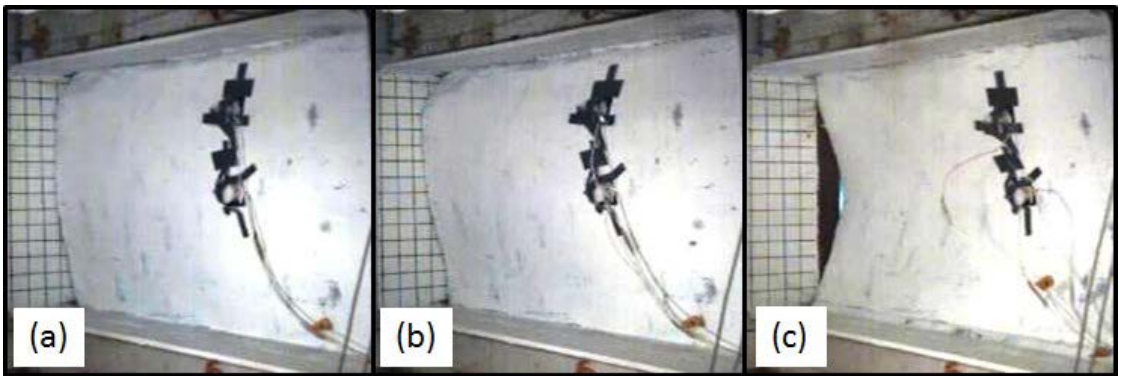

Figure 6.29. DW9: Frames from high-speed camera. (a) Maximum deflection at the center line. (b) Maximum wall deflection occurred near the top of the wall. (c) Maximum wall deflection during rebound.

6.1.3 Trowel-on Retrofit (DW10-DW11)

6.1.3.1 DW10

Wall DW10 was retrofitted with a trowel-on thermoset. The application procedure is provided in Section 4.6. The trowel-on thermoset overlapped the top and bottom supports, creating an adhesive bond with the steel frame housing the test wall. No mechanical anchorage (steel plate) was used in this experiment. The wall was exposed to

dynamic load level 3, which was higher than the load that the unreinforced spray-on polyurea retrofitted wall, DW3, survived. Wall failure occurred at mid-height when the thermoset failed (Figures 6.30b and c); no additional rips or damage was found. None of the retrofit material peeled back from the supports. Evaluation of the high-speed video of the wall response indicated there was a slight delay in the ultimate failure (Figures 6.30a, b, and c). The wall deflected, hesitated for a couple of milliseconds, and then the wall fell into the structure. Most of the blocks remained attached to the retrofit layer (Figures 6.31a and b). Only a few small pieces of block were found inside the structure.

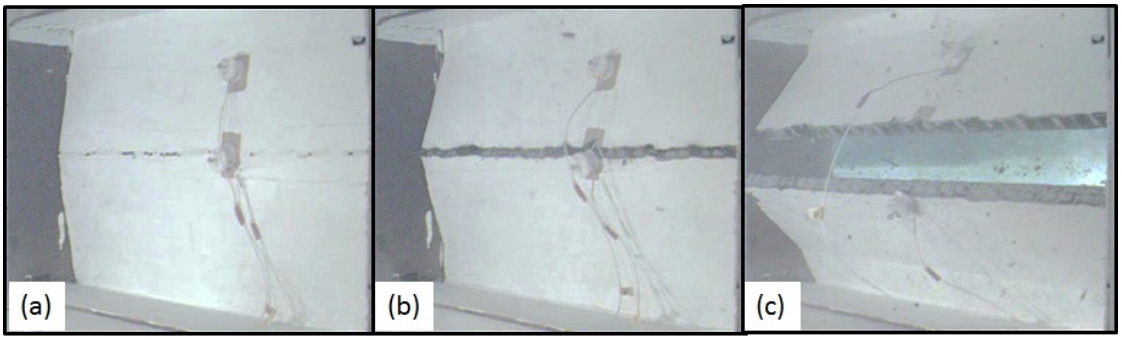

Figure 6.30. DW10: Frames from high-speed video. (a) Crack begins at centerline. (b) Wall responds as three hinge mechanism. (c) Wall completely fails at centerline.

Samples of the retrofit material were cut from the debris and measured to determine the quality of the application procedure. The average thickness of the retrofit material was 0.088 in., and the thinnest and thickest sample measurements were 0.046 in. and 0.25 in., respectively.

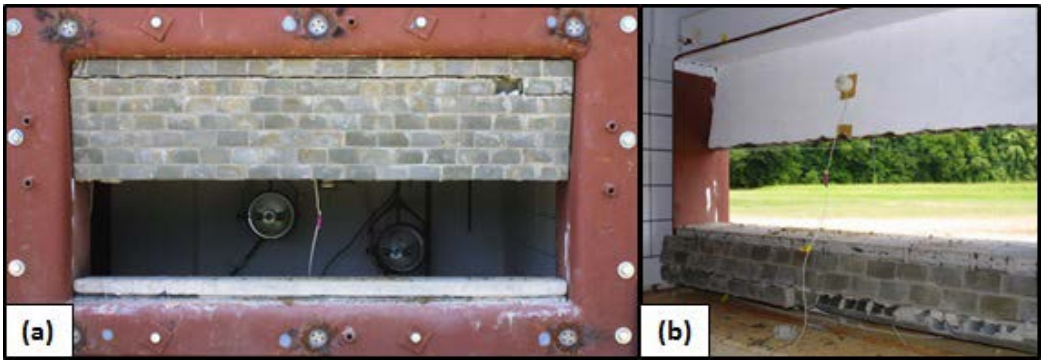

Figure 6.31. DW10. (a) Exterior view. (b) Interior view.

6.1.3.2 DW11

The retrofit material and application procedure for DW11 duplicated DW10. Wall DW11 was maintained at dynamic load 3, since DW10 failed at level 3. The wall response and failure location duplicated DW10. Wall failure occurred when the thermoset failed at mid-height (Figures 6.32a and b), no additional damage to the thermoset material was found. None of the retrofit material peeled back from the supports. All of the blocks remained attached to the thermoset material. Only a few small pieces of debris were found inside the structure.

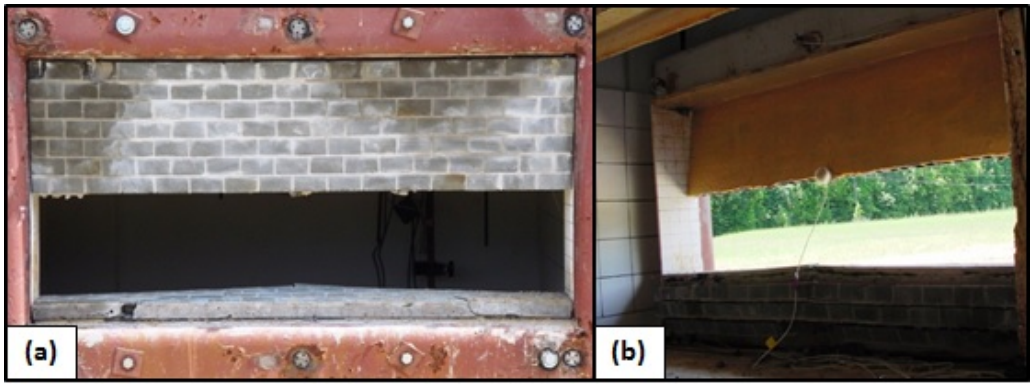

Figure 6.32. DW11. (a) Exterior view. (b) Interior view.

6.1.4 Unreinforced Film and Trowel-on or Spray-on Adhesive Retrofits (DW12-DW13)

6.1.4.1 DW12

Wall DW12 was retrofitted using a spray-on adhesive to adhere an unreinforced film to the interior surface of the CMU wall. An off-the-shelf spray-on adhesive was used to attach the thermoplastic film to the CMU wall. The adhesive was a yellow-solvent type synthetic rubber-based adhesive. It is a general purpose adhesive that can be used for bonding most rubber and gasket materials to most metal, baked enamel, wood, plastics and neoprene, SBR and butyl rubber. During the installation process, the unreinforced material tore at the bottom support, so additional strips of the unreinforced material were added at the top and bottom supports to prevent the material from ripping at the supports. The additional material extended across the full length of the top and bottom flanges and 6 in. onto the wall (Figure 6.33a). In addition to the adhesive bond created

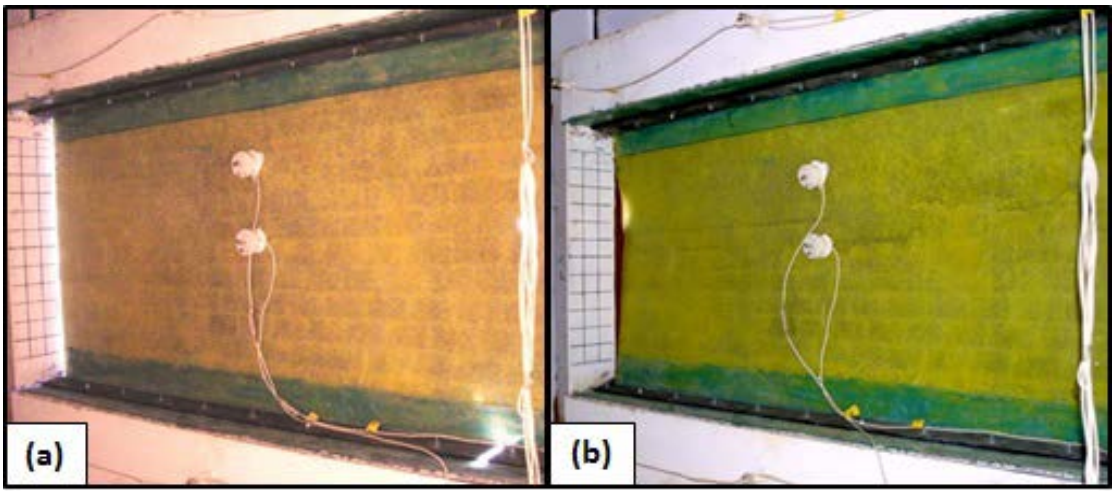

Figure 6.33. DW12. (a) Pretest interior view.
(b) Posttest interior view.

from the spray-on material, a mechanical anchorage in the form of an anchor plate was added to the system. The anchor plate was bolted onto the frame sandwiching the elastomeric film between the steel plate and frame.

DW12 was exposed to dynamic load level 3, which was higher than the load that the unreinforced spray-on polyurea retrofitted wall, DW3, survived. Wall deformation did occur, but the elastomeric system survived with no visible defects in the film (Figure 6.33b). High-speed video indicated that the maximum deflection (0.208) into the reaction structure occurred one course above the mid-height of the CMU wall (Figures 6.34a and b). None of the CMU blocks lost face shells (Figures 6.35a and b).

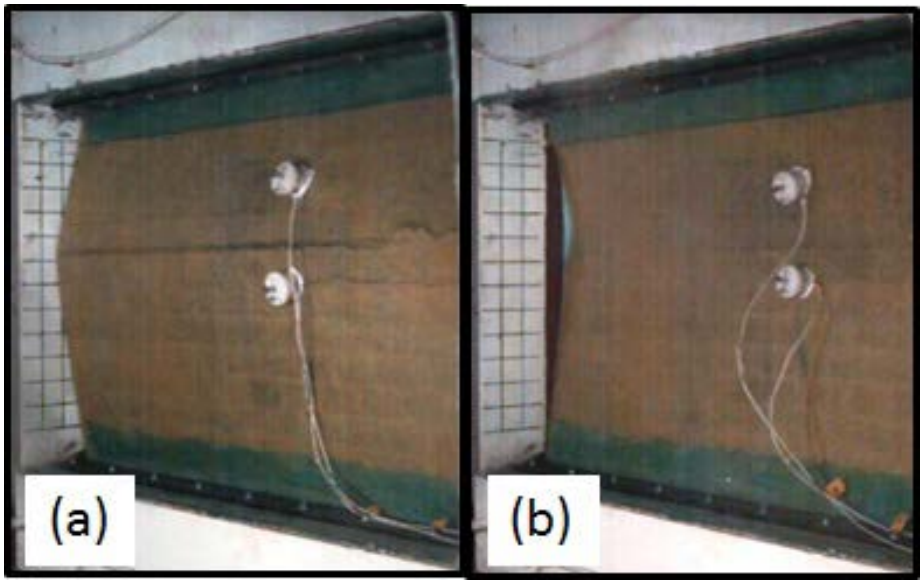

Figure 6.34. DW12: Frames from high-speed camera. (a) Maximum deflection into the structure. (b) Maximum wall deflection during rebound.

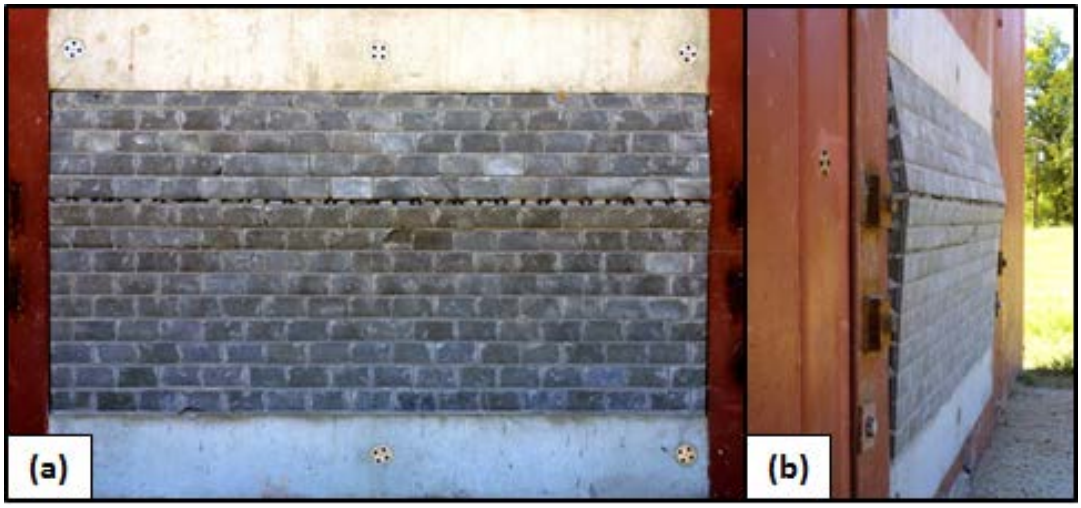

Figure 6.35. DW12. (a) Posttest exterior view. (b) Posttest exterior profile view.

6.1.4.2 DW13

Wall DW13 was retrofitted using the trowel-on thermoset used in DW10 and DW11 as an adhesive to install an unreinforced film to the interior surface of the CMU wall (Figure 6.36a). In addition to the adhesive bond created from the trowel-on material, an anchor plate was added to secure the retrofit system.

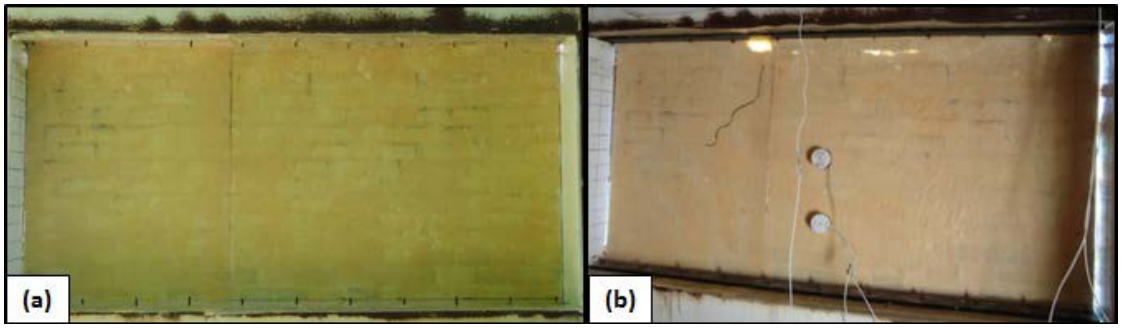

Figure 6.36. DW13. (a) Pretest interior view before anchor plates were installed. (b) Posttest interior view.

DW13 was exposed to dynamic load level 4, which was higher than the load the unreinforced spray-on polyurea retrofitted wall, DW3, survived. Wall deformation did occur, but the elastomeric system survived with no visible defects in the film (Figure 6.36b). Due to a problem with the trigger system used to activate the high-speed cameras and data acquisition system no deformation data was acquired. More than 31% of the CMU blocks were damaged with the majority of the damage concentrated at the top left of the wall (Figures 6.37a and b), and no debris was found inside the reaction structure.

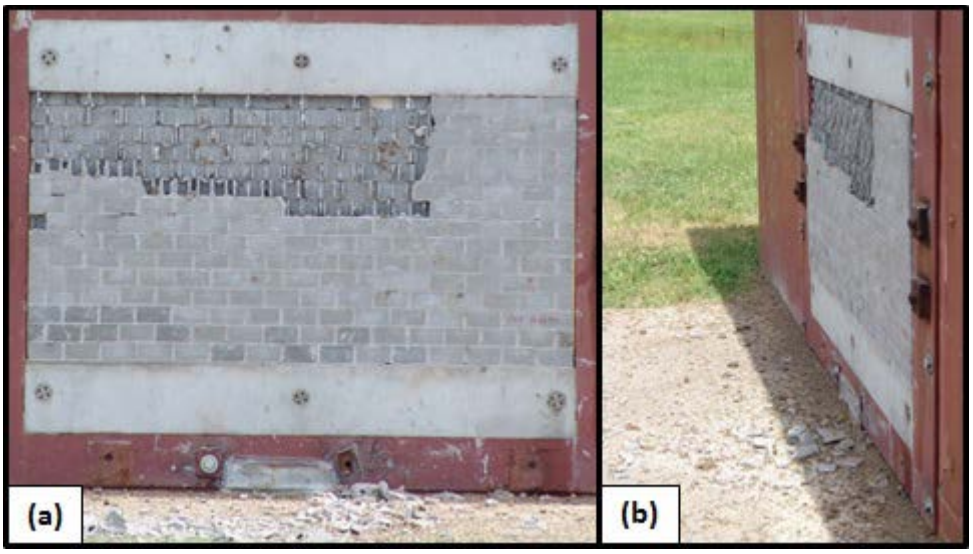

**Figure 6.37. DW13. (a) Posttest exterior view.
(b) Posttest profile view.**

6.1.5 Fiber-Reinforced Film and Trowel-on Adhesive Retrofit (DW14)

Wall DW14 was retrofitted using a two part trowel-on epoxy to adhere a fiber-reinforced film to the interior surface of the CMU wall. When this experiment was conducted, a fiber-reinforced film with fibers oriented at a 45-deg angle to the horizontal line across the film could not be manufactured. The fabric with fibers oriented at 0 and 90 deg was purchased from a supplier and sent to a manufacturer to create the fiber encapsulated film. The film was laid out and cut (Figure 6.38a), so that when the film was applied to the wall, the fibers would be oriented at + 45 and -45 deg to the horizontal support. Two pieces of film were needed to cover the wall surface, and one piece of material overlapped the previous sheet by 2 in. Extra epoxy was added at the seam to prevent the material from peeling back at the seam (Figure 6.38b). In addition to

the adhesive bond created by the trowel-on material, a mechanical anchorage in the form of an anchor plate was added to the top and bottom supports.

DW14 was exposed to dynamic load level 4, which was greater than or equal to the load that the 45-deg fiber-reinforced spray-on polyurea retrofitted walls, DW5, DW6, DW7, and DW8 survived. Wall deformation did occur, but the elastomeric system

Figure 6.38. DW14. (a) Cutting film to orient fibers 45 deg to the horizontal mortar joints of the wall. (b) Two sheets of film used to cover CMU wall with epoxy seam along the center.

survived with no visible defects in the elastomeric film. Due to a problem with the trigger system used to activate the high-speed cameras and data acquisition system, no deformation data was acquired. More than 40% of the CMU blocks lost face shells (Figures 6.39a and b), and none of the debris was found inside the reaction structure. DW14 was the final subscale HE experiment conducted at the BBTS.

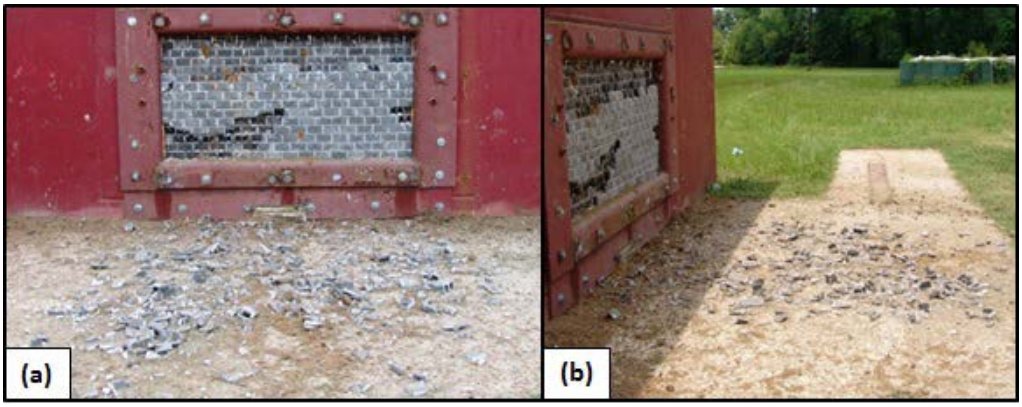

Figure 6.39. DW14. (a) Posttest exterior view. (b) Debris from wall.

6.2 Subscale BLS Experiments

Once the BLS at ERDC became operational, the subscale dynamic events conducted at the BBTS were moved to the BLS facility. The BLS was designed to be a highly tunable compressed-gas-driven shock tube capable of simulating the positive phase of the waveform for explosive yields equivalent to a maximum charge value of 20,000 lb (9,072 kg) of TNT (Figure 6.40). The BLS was developed to evaluate windows, walls, structural retrofit systems, and related targets to airblast loads. The device was designed to simulate blast waveforms "from very low pressures, 1 to 2 psi (7 to 14 kPa), related to failures of conventional annealed glass and hollow CMU walls, to much higher pressures, maximum of 80 psi (552 kPa), related to very large truck bombs" (Slawson, Johnson, and Mosher 2001; Johnson and Simmons 2008). The target vessel in the BLS can accommodate a target 71 in. tall by 53 in. wide (180 cm by 135 cm), so a reaction frame was built to house a 34-in.-wide by 49-in.-tall third-scale CMU wall.

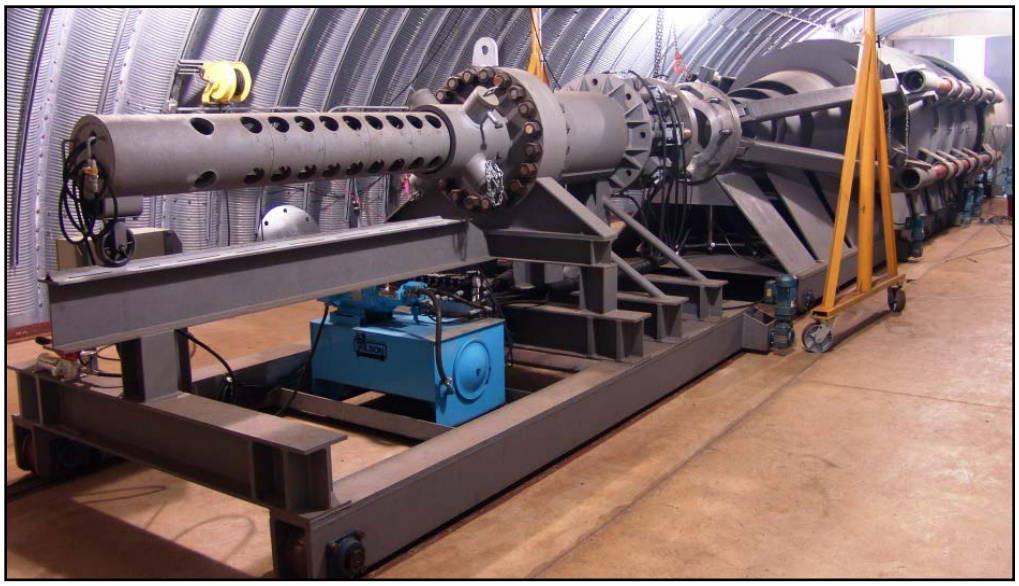

Figure 6.40. BLS at ERDC. (Johnson and Simmons 2008)

The BLS device consists of a driver system, a transition cone, expansion rings, cascade, and a target vessel all housed in an underground enclosure to attenuate the acoustics and contain the blast pressures. The driver system consists of a cylindrical pressure vessel, a push-pop device, and a mechanical striker/diaphragm system (Figure 6.41a). The driver contains the high-pressure source, created by pumping air or an air/helium mixture into the pressure vessel. The gases are confined in the vessel by a predetermined number of steel or aluminum diaphragms. When the diaphragms rupture, compressed gases are released into the transition cone (Figure 6.41b). As the shock propagates downstream through the transition cone to the expansion rings and the cascade (Figure 6.41c), the pressure wave is shaped into the desired waveform. The transition cone consists of three consecutively larger rings attached to a sled that allows the shock pulse to flow freely downstream while expanding at each transition. The vents also allow the pressure that is reflected off the target vessel to vent the BLS device into the underground enclosure reducing, delaying, or removing the rebounding load completely.

The shock pulse travels through the transition cone into the expansion rings and the cascade to the face of the target vessel. The expansion rings consist of two individual steel pieces with the same diameter that are aligned to create venting strategies that will be used to alter the shock pulse to create the negative phase of the blast wave. The magnitude of the pressure created in the negative phase is directly related to the number and magnitude of the gaps that can be used between the transition cone, each expansion ring, and the cascade. The final piece of the transition system is the cascade. The cascade consists of two steel rings, one

slightly larger than the other, that telescope in and out. This will allow the user to make additional changes to the waveforms by adjusting the overall length of the device.

The target vessel is an enclosed steel tube with a framed opening in the face to mount targets and provide a personnel access door in the rear. All of the debris generated from the test article is contained in the target vessel. This allows the users to clean the vessel, remove any of the remaining target from the frame, and reload a new target quickly and easily (Figure 6.41d) (Johnson and Simmons 2008).

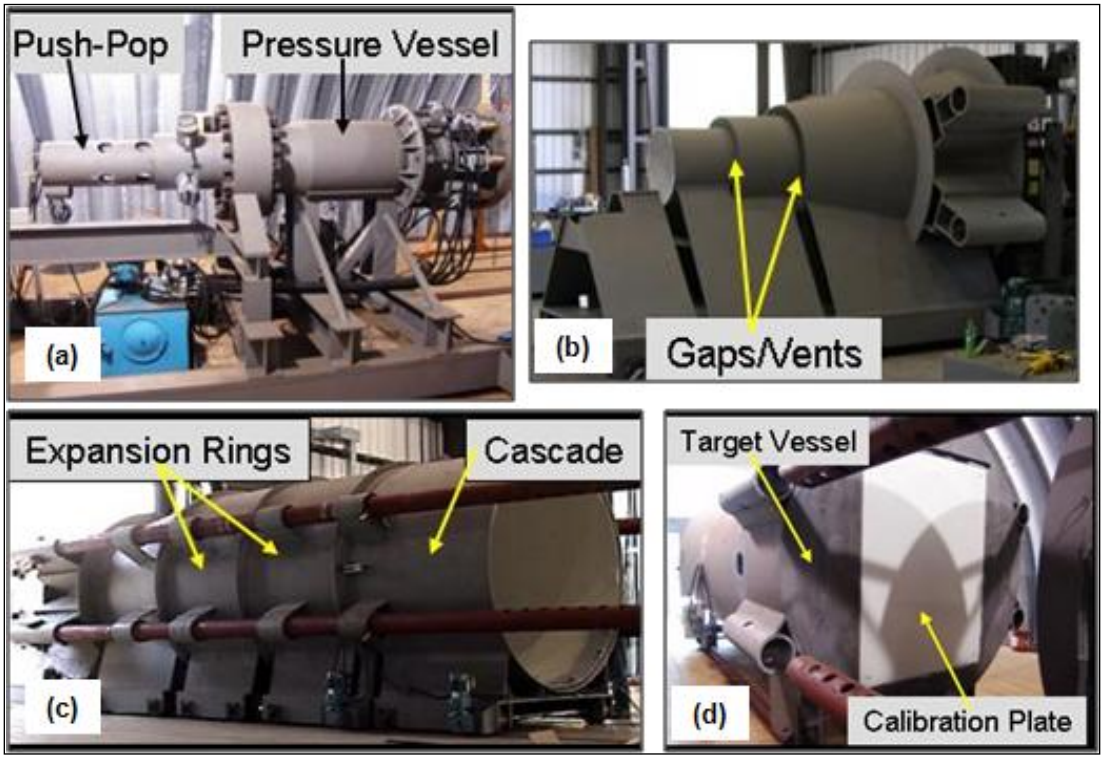

Figure 6.41. BLS. (a) Driver system. (b) Transition cone. (c) Expansion rings and cascade. (d) Target vessel.

Initial proof tests conducted in the BLS facility demonstrated the ability to replicate HE blasts loads over a broad range of interest. However, before the retrofitted walls were evaluated in the BLS, a series of calibration shots were performed to determine the relationship between the components of the device and the changes in the waveform.

The goal for this project was to determine the BLS setup required to mimic the HE experiments to be conducted at the BBTS and at an AFB in Florida. The parameters that must be determined for each dynamic load included the driver pressure (DP), air/helium ratio (Air/HE), driver length (DL), diaphragm quantities, ring orientations, cascade length, gap locations, and gap sizes.

Some of the global relationships between the components and the waveform that had been provided to researchers by the designers will be outlined next; however, the quantitative relationships are still unknown. Several different characteristics of the waveform can be modified by varying the different components of the BLS.

> The four most important waveform characteristics at the target are the peak reflected pressure, peak impulse, shape of the waveform (specifically rise and decay time), and the magnitude of the pressure generated in the negative phase. The peak pressure at the target is controlled by the magnitude of the pressure in the driver, the capacity of the selected diaphragms used to confine the compressed gases, the air-to-helium ratio, the length of the cylindrical driver, the number and locations of the gaps in the expansion rings, and the length of the cascade. The impulse at the target is primarily controlled by the volume of the driver, which can be modified linearly in 6-in. (152-mm) increments using the push-pop. The push-pop is a pipe that plunges in and out of the pressure vessel to define the length and resulting volume of the driver. The magnitude of the pressure, air/helium ratio of the gases in the driver, and the location and number of gaps in the transition and expansion section also affect the impulse at the target. The negative phase created in the waveform is dictated by the number and location of the gaps in the transition and expansion rings (Johnson and Simmons 2008).

The shape of the waveform is affected primarily by the air-to-helium ratio. A higher percentage of helium increases the peak pressure and results in a faster decay of the pressure wave.

A statistical analysis program was used to develop the first round of experiments to define the operational capabilities of the BLS based on the BLS variables: driver volume

length, driver pressure, air-to-helium ratio, gap magnitude, gap location, and cascade length. The driver length can only be modified in 6-in. increments from 6 in. (152 mm) to 5.5 ft (168 cm). The pressure vessel is limited to 1,500 psi (10.3 MPa), and 40 psi (276 kPa) was set as the lowest level. Each gap is limited to a maximum of 12 in. (305 mm), and the cascade length can be modified from 0 to 18 in. (0 to 457 mm). In addition to the individual variable constraints, one global constraint had to be taken into account; the overall length of the device cannot exceed 153 in. (389 cm). Once the experiments were completed, the maximum and minimum reflected pressure, positive phase duration, and peak reflected impulse were documented.

Once the operational requirements were defined for the BLS, the setup required to mimic the HE experiments conducted at the BBTS were developed. Once the setup was determined, the subscale dynamic events to evaluate the remaining wall retrofits were conducted in the BLS. The instrumentation plan for the BLS experiments is shown in Figure 6.42a and b. Data recovery consisted of 12 Kulite Model HKS-11-375SG pressure gauges (P1-P10, PD, and PE) located around the perimeter of the wall to document the reflected pressure and impulse on the specimen (Figure 6.42a). The lateral deflection of the walls was documented using two accelerometers or one laser (Figure 6.42b). The two Endevco Model 7270A accelerometers, A1 and A2, were placed at the mid- and quarter-points to document the wall deflection. Additional deflection measurements were obtained using an Acuity Research AccuRange 4000 laser range finder. The laser, L1, was placed at mid-height to document the wall's deflection. In addition to the instrumentation, pretest and posttest still photos, and two high-speed

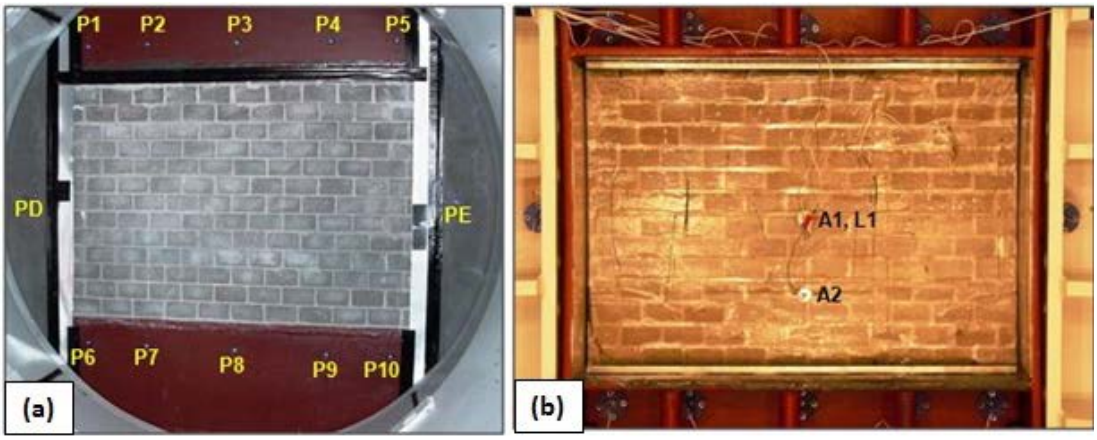

Figure 6.42. Dynamic BLS experiments. (a) Pressure gauge layout. (b) Accelerometer and laser gauge layout on interior face of CMU wall.

video cameras were used to document the wall's response. Pressure gauges were used to measure the reflected pressure on the specimen. The pressure gauges and accelerometers were both piezo-resistive transducers. The data were transmitted over 22 AWG 6 conductor shielded mil spec cable and recorded on a 14-bit bipolar Hi-Techniques Model HT-600 Data Acquisition System. The cables transmitted the data from the target vessel to the control room located approximately 100 ft (30 m) away. The acquisition system's sample rate was set for 0.5 microseconds per point for the pressure, deflection, and acceleration measurements. A recording time of 250 milliseconds was selected based on past experiments. High-speed cameras positioned safely outside of the target vessel were used to capture high-resolution videos from the camera portals on each side and on the rear of the target vessel.

Eleven additional dynamic experiments were performed in the BLS Facility. Three baseline unretrofitted CMU wall experiments were conducted in the BLS to validate the airblast produced by the BLS and to evaluate the test procedure. Once the test setup and blast loads were confirmed, eight retrofitted wall experiments were conducted. The complete test matrix for the BLS experiments is provided in Table 6.3.

6.2.1 Unretrofitted CMU Walls (BLS1-BLS3)

6.2.1.1 BLS1

The first experiment conducted in the BLS was an unretrofitted (baseline) CMU wall, BLS1, conducted at dynamic load level 3 (Figure 6.43a). The construction details for the CMU walls used in the HE experiments were duplicated on the BLS experiments. The difference from the field construction was the addition of a pre-mixed all-purpose drywall joint compound used to fill in the gaps on the right, left, and top sides of the wall (Figure 6.43b). The joint compound sealed the gaps and prevented the blast load from flowing through the gaps and loading the interior surface of the CMU wall. BLS1 failed as expected (Figure 6.44a), but high-speed video indicated that the wall experienced some arching effects during the loading. The diagonal cracks that formed during the wall's response to the blast load indicated that load was transferred between the CMU wall and the steel frame (Figure 6.44b). The gap between the CMU wall and the steel frame may have been large enough to prevent the CMU wall from binding on the edges of the steel frame.

Table 6.3. Test matrix for subscale BLS experiments.

Wall Label	Support	Matrix	Reinforcement	Dynamic Load Level
BLS1	NA	None	None	3
BLS2	NA	None	None	3
BLS3	NA	None	None	3
BLS4	Primer, Epoxy, Anchor Plate	PSA on Polyurethane Film	None	3
BLS5	Primer, Epoxy, Anchor Plate	PSA on Polyurethane Film	None	5
BLS6	Primer, Epoxy, Anchor Plate	PSA on Polyurethane Film	None	6
BLS7	Primer, Epoxy, Anchor Plate	PSA on Polyurethane Film	None	6
BLS8	Anchor Plate	PSA on Polyurethane Film	Fabric ±45 deg	6
BLS9	Anchor Plate	PSA on Polyurethane Film	Fabric ±45 deg	7
BLS10	Primer, Anchor Plate	PSA on Polyurethane Film	Fabric ±45 deg	5
BLS11	Primer, Anchor Plate	PSA on Polyurethane Film	Fabric ±45 deg	3

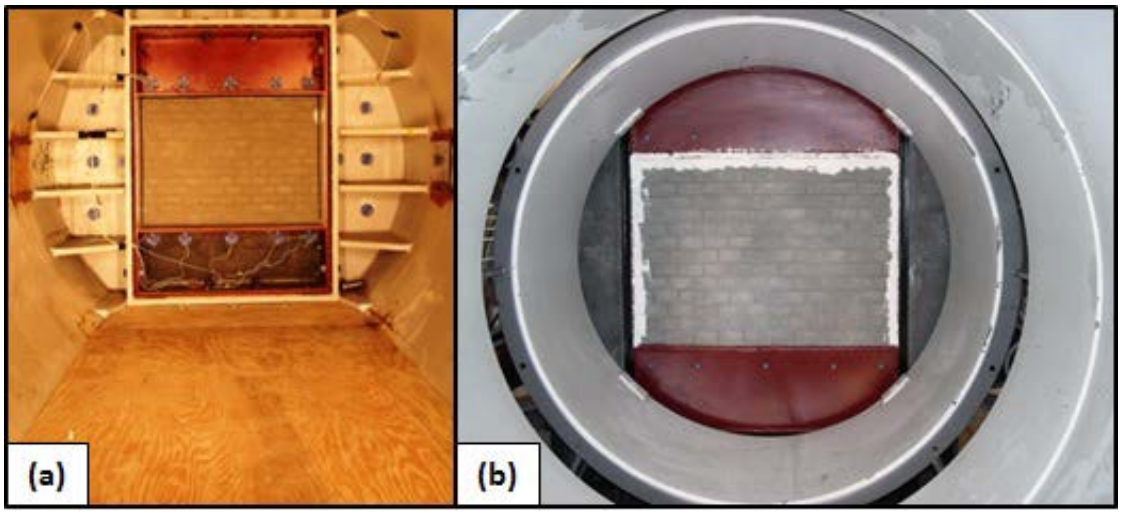

Figure 6.43. BLS1. (a) Pretest interior view of target vessel. (b) Gaps between the CMU wall and steel frame filled with drywall joint compound.

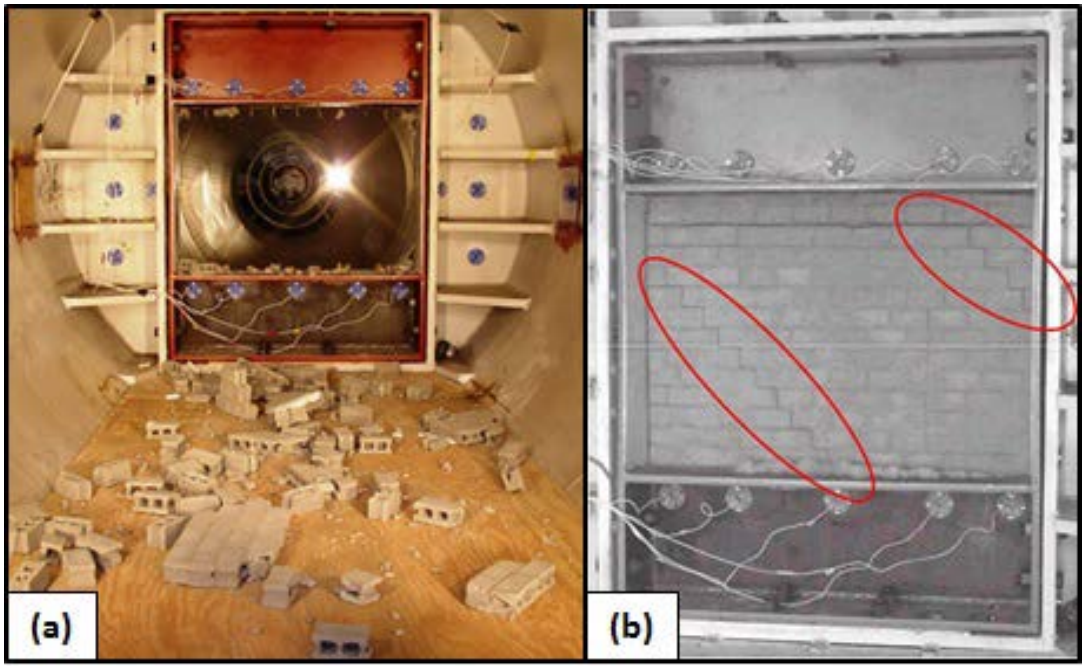

Figure 6.44. BLS1. (a) Posttest view of the debris in the target vessel. (b) Frame from high-speed video illustrating the formation of diagonal cracks.

6.2.1.2 BLS2

The construction of BLS2 mimicked the setup used for BLS1. BLS2 was subjected to dynamic load level 3. Once again, the wall failed and the CMU created a secondary debris hazard (Figures 6.45a and b). However, the diagonal cracks that developed during the response indicated that the wall's response was affected by arching, or the wall experienced some resistance from the side walls of the steel frame. The primary difference between the responses of BLS1 and BLS2 was the direction of the diagonal cracks. Some of the wall debris, illustrated in the bottom right corner of Figures 6.46a and b, was affected by the steel frame. The wall appeared to drag against the edge of the frame, causing it to change orientation. To prevent arching effects in future experiments, the wall construction, frame, and test setup were investigated.

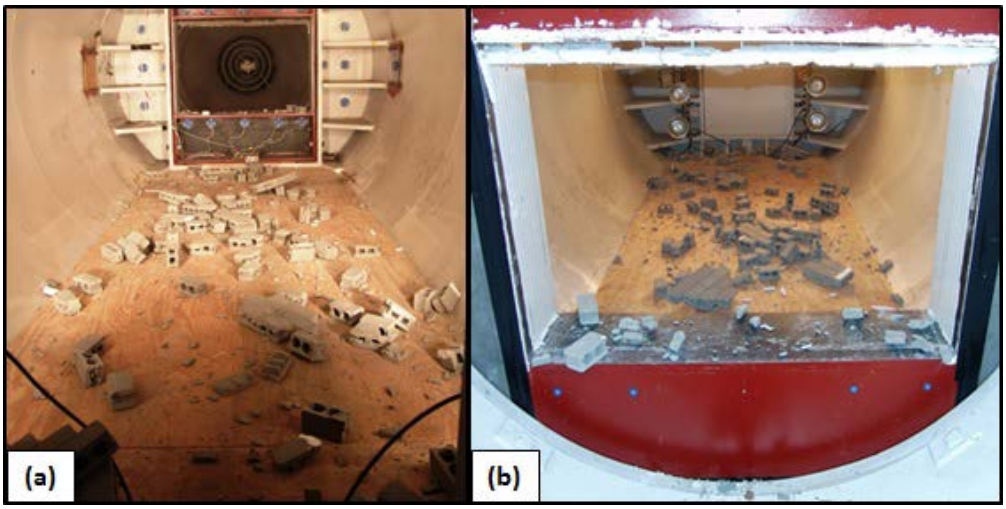

Figure 6.45. BLS2. (a) Interior view of debris in target vessel. (b) Posttest view from blast face of target vessel.

After further investigation, an alteration was made to the test setup and to the steel frames used in the BLS experiments. First, the use of the drywall joint compound to fill the gaps was discontinued. Second, it appeared from photographs and high-speed video that the steel walls of the reaction structure that framed the test specimens were not straight (Figure 6.47a). After a discussion with the welding crew that fabricated the frame, it was discovered that, during the fabrication of the test frame, stiffeners were placed on the edge of the blast face where the wall would be built in order to hold the steel components square while welding, but no stiffeners were placed along the interior

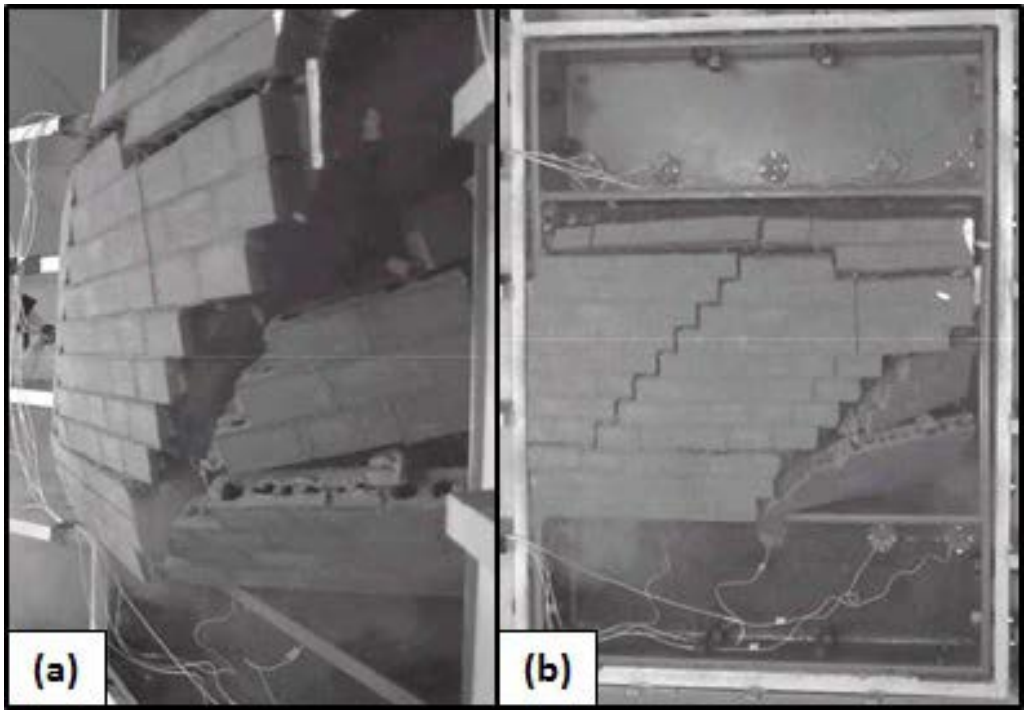

Figure 6.46. BLS2. (a) Frame from high-speed video illustrating debris hazard. (b) Frame from high-speed video with diagonal cracks visible.

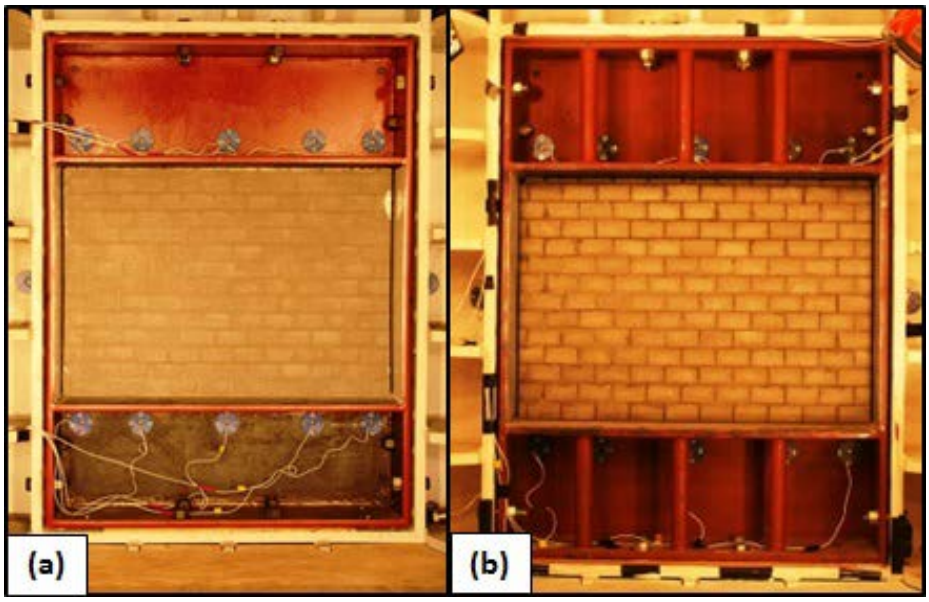

Figure 6.47. Target frames. (a) Original CMU wall frame for BLS experiments. (b) Modified CMU wall frame for BLS experiments.

edge of the frame. It appears that the side walls framing the wall response area deformed due to the lack of stiffeners during the fabrication process. The frames were returned to the welding shop and heat treated to straighten the deformed side flanges, and additional bracing was added to the top and bottom support flanges to prevent further deformation (Figure 6.47b).

6.2.1.3 BLS3

A third baseline CMU wall, BLS3, was tested to determine if the modifications to the steel reaction frame were successful. The dynamic load level of 3 in BLS1 was also used for BLS3. Instead of using the drywall joint compound, thin aluminum strips of flashing and duct tape were used to cover the gaps between the target vessel, the steel reaction frame, and the CMU wall edges (Figure 6.48a). The gaps between the CMU

wall and the steel frame were cleaned thoroughly to prevent the wall from dragging against the frame (Figure 6.48b). If the modifications were successful, the wall would fail during execution of the experiment, but no diagonal cracks would form during failure of the CMU wall.

The high-speed video indicated that the wall failed as desired (Figures 6.49a, b, and c and Figures 6.50a, b, and c). Horizontal cracks formed at the center of the wall, and no diagonal cracks were observed. Posttest photographs indicated that the aluminum flashing prevented the initial airblast from entering the target vessel, and the tape was still in place after the experiment (Figure 6.51a). The debris generated from the CMU wall was scattered across the target vessel (Figure 6.51b).

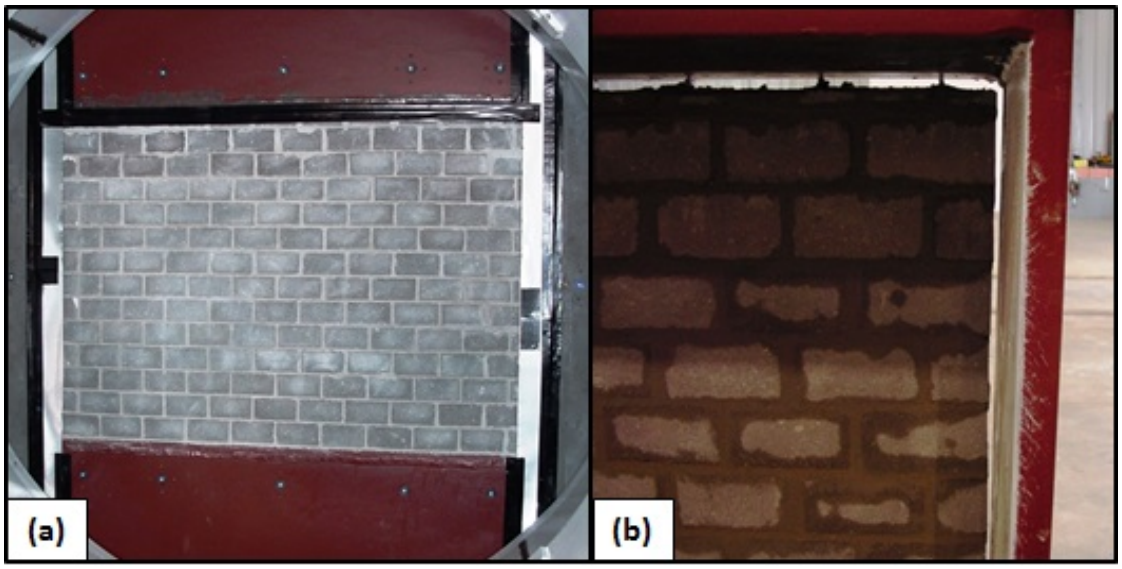

Figure 6.48. BLS3. (a) Aluminum flashing taped over gaps. (b) Gap sizes were increased to prevent the wall from dragging across sides of frame.

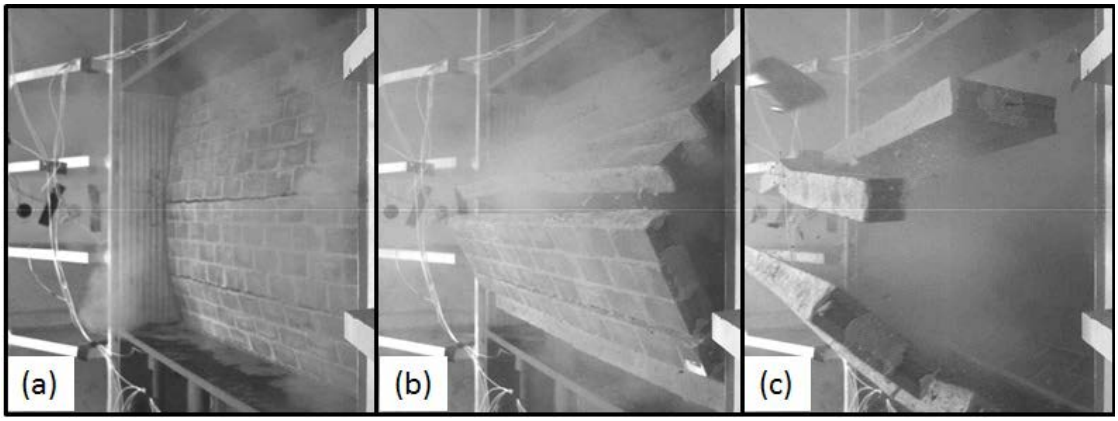

Figure 6.49. BLS3: Frames from high-speed video. (a) Horizontal cracks develop in wall. (b) No diagonal cracks formed. (c) Wall debris did not drag across the frame.

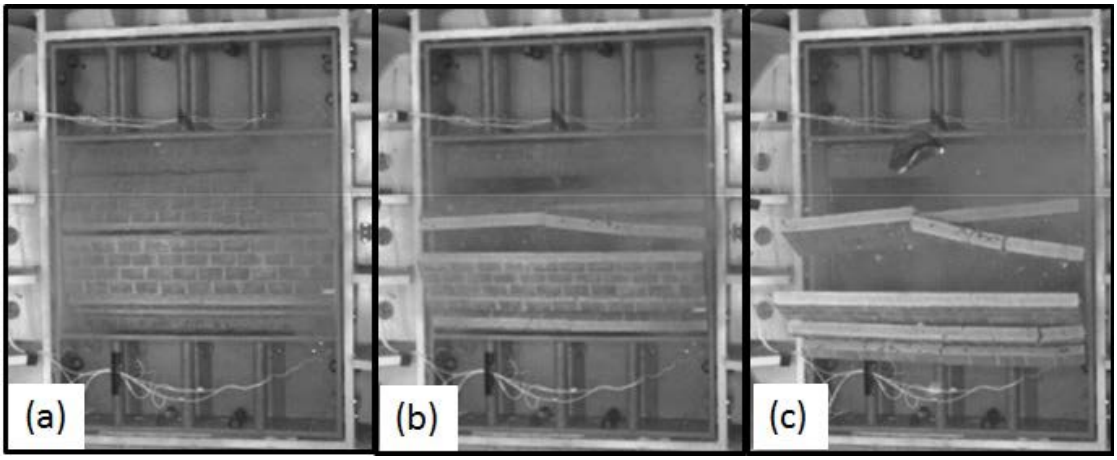

Figure 6.50. BLS3: Frames from high-speed video. (a) No diagonal cracks formed in the wall. (b) No arching effects are evident in the wall's response. (c) Debris hazard created from CMU.

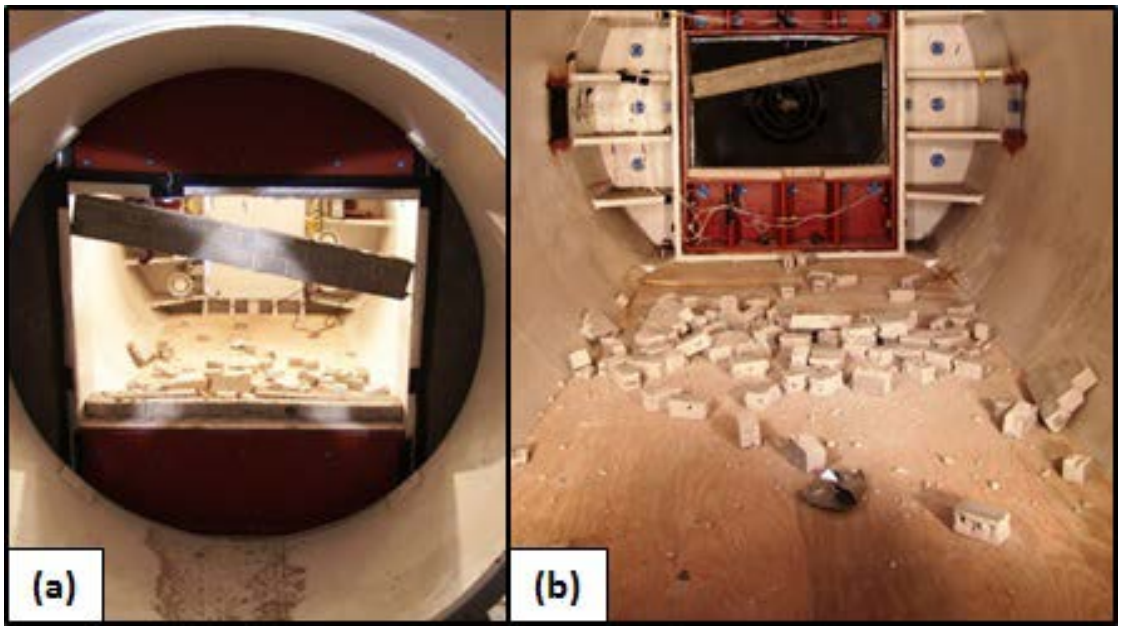

Figure 6.51. BLS3. (a) Aluminum flashing remained taped to the target vessel. (b) Posttest interior view of target vessel and debris generated from the CMU wall.

6.2.2 Unreinforced Film with PSA (BLS4-BLS7)

6.2.2.1 BLS4

The retrofit system used on wall BLS4 consisted of a primer (Primer 1), a PSA, a trowel-on epoxy, and an unreinforced elastomeric film (Figures 6.52a and b). BLS4 was subjected to a blast load that generated an average reflected impulse equal to dynamic load level 3. As discussed earlier, both the unreinforced spray-on polyurea and the trowel-on thermoset failed at dynamic load levels equal to or less than the level used on BLS4. In addition to the adhesive bond, an anchor plate was bolted to the steel frame to secure the retrofit system.

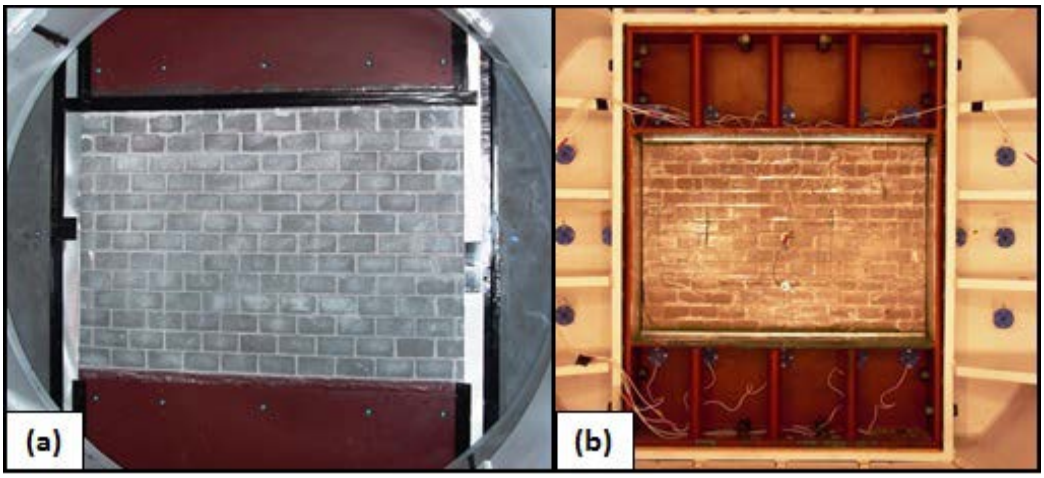

Figure 6.52. BLS4. (a) Pretest exterior face of wall.
(b) Pretest interior face of retrofitted wall.

The retrofit system used in BLS4 successfully prevented the CMU wall from becoming a secondary debris hazard (Figure 6.53b). The CMU wall did lose its integrity, and all of the mortar joints were compromised (Figure 6.53a). The wall would have to be

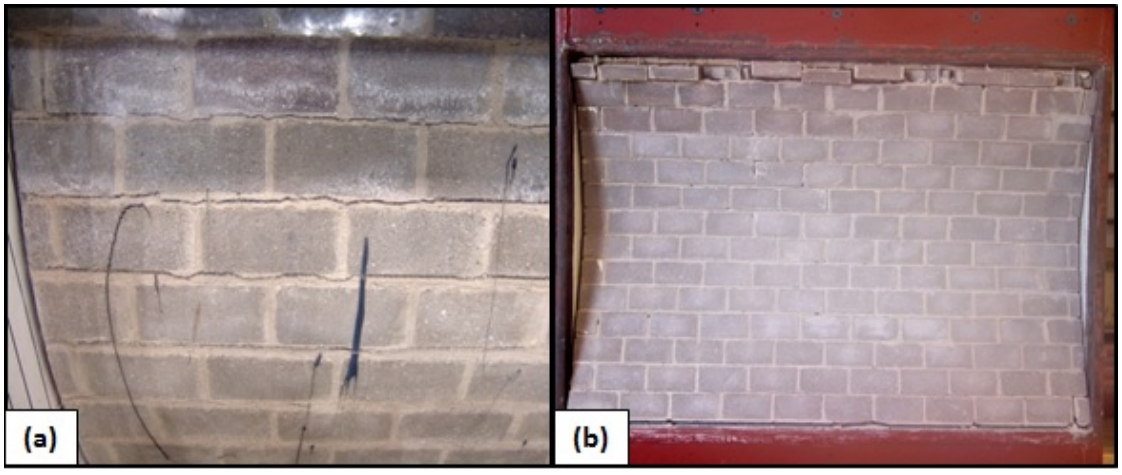

Figure 6.53. BLS4. (a) Mortar joint cracks. (b) Posttest view of exterior face.

replaced in an actual event; however, the blocks were undamaged demonstrating the high ductility of the film (Figures 6.53b and 6.54a). The elastomeric film sustained some damage at the top and bottom supports. Small tears along the edges of the top and bottom supports were found during the posttest inspection. The force of the wall crushed the flanges on the steel anchor plates used on the top and bottom supports (Figure 6.54b). Inspection of the high-speed video indicated that the retrofitted wall deflected 0.312 to 0.347. The wall exhibited a permanent lateral deflection of 0.139, and the PSA was strong enough to prevent the blocks above the center of the wall from falling out of the reaction structure after the experiment (Figures 6.55a and b).

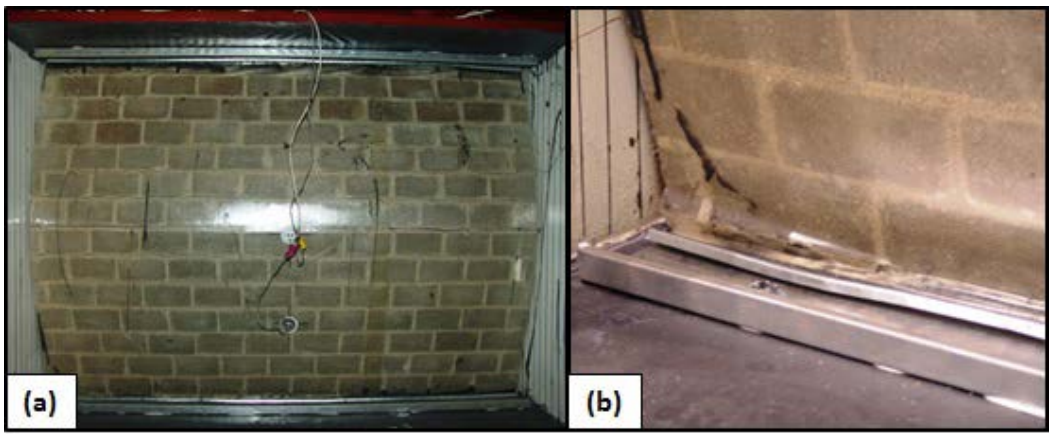

Figure 6.54. BLS4. (a) Posttest view of interior face. (b) Wall response bent the anchor plates.

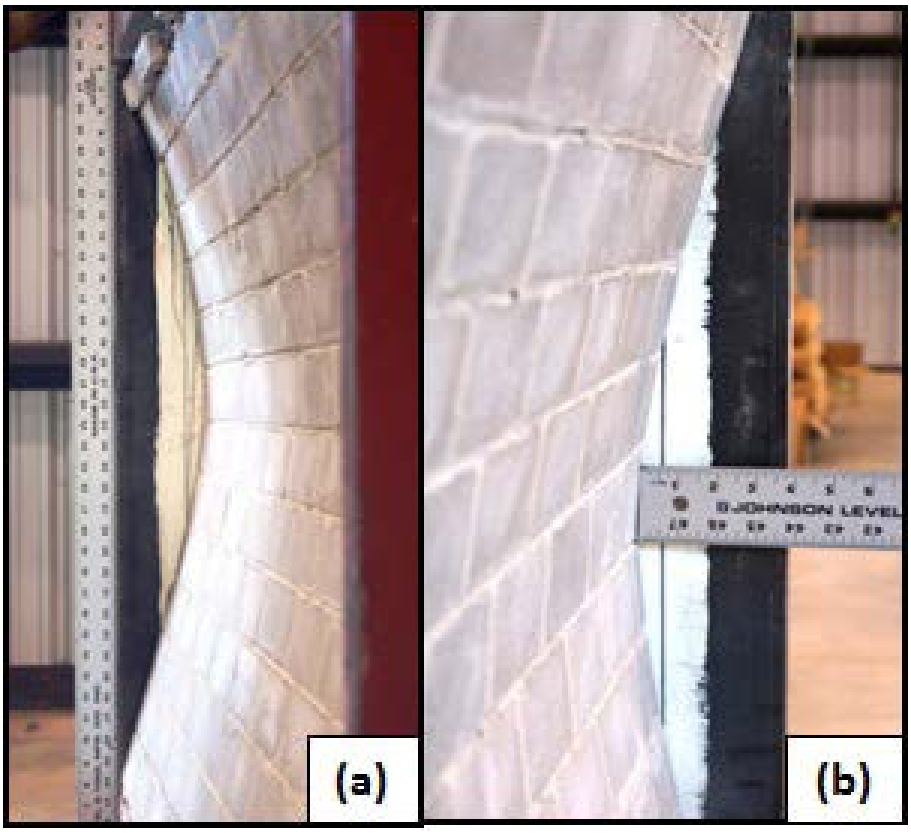

Figure 6.55. BLS4. (a) Final position of wall. (b) A 2-in. permanent deflection in the retrofitted wall.

6.2.2.2 BLS5

Wall BLS5 had the same application procedure and materials used in BLS4. The only difference between the construction, retrofit materials, and procedures used on BLS4 and BLS5 was a layer of paint that was applied to the interior face of the specimen. The intense lighting required to capture the high-speed video created a harsh reflection on the clear elastomeric film in BLS4, which made it difficult to observe the wall damage during the blast event; hence, a layer of white paint was applied to the wall's surface to improve the quality of the high-speed video. Since BLS4 performed

well at level 3, the reflected impulse load was raised to level 5 for BLS5. Figure 6.56a is a still frame of the interior retrofitted surface of the wall before impact of the airblast.

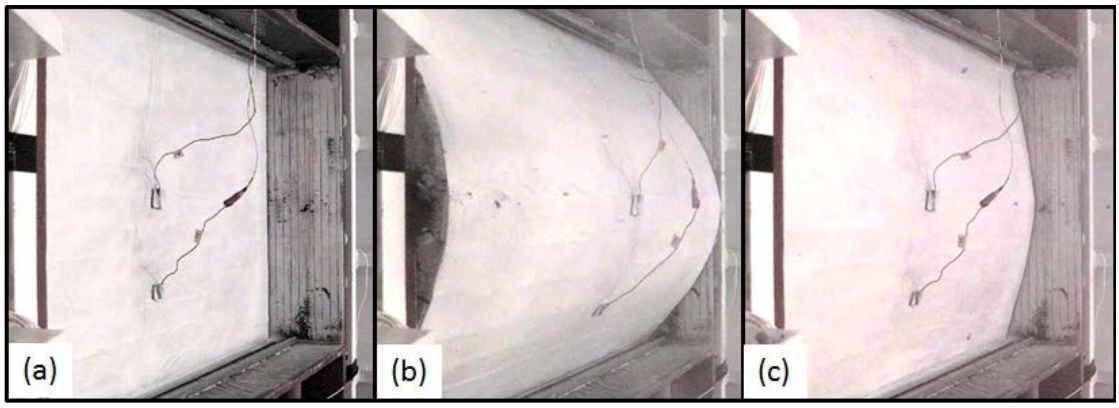

Figure 6.56. BLS5: Frames from high-speed video. (a) Pretest view before airblast arrives. (b) Point of maximum deflection. (c) Final wall position.

The response of BLS5 (Figure 6.57a) to the increased dynamic load was similar to that of BLS4; however, the elastomeric film was damaged during BLS5. A small tear was found in the upper right corner of the film (Figure 6.57b). Review of the high-speed video indicated that the retrofitted wall deflected 0.799 to 0.833 (Figures 6.56a, b, and c), and a handful of CMU debris entered the reaction structure from the edges of the retrofit during the rebound response that occurred after the maximum deflection. The top half of the block wall disengaged from the elastomeric film and fell out of the test frame into the BLS device after the initial wall response. The CMU debris was initially in the steel ring (Figure 6.58a), but fell to the concrete floor when the BLS device was opened for posttest documentation (Figure 6.58b). The blocks on the bottom half of the wall were still securely attached to the film and were forcibly removed (Figure 6.59a). The

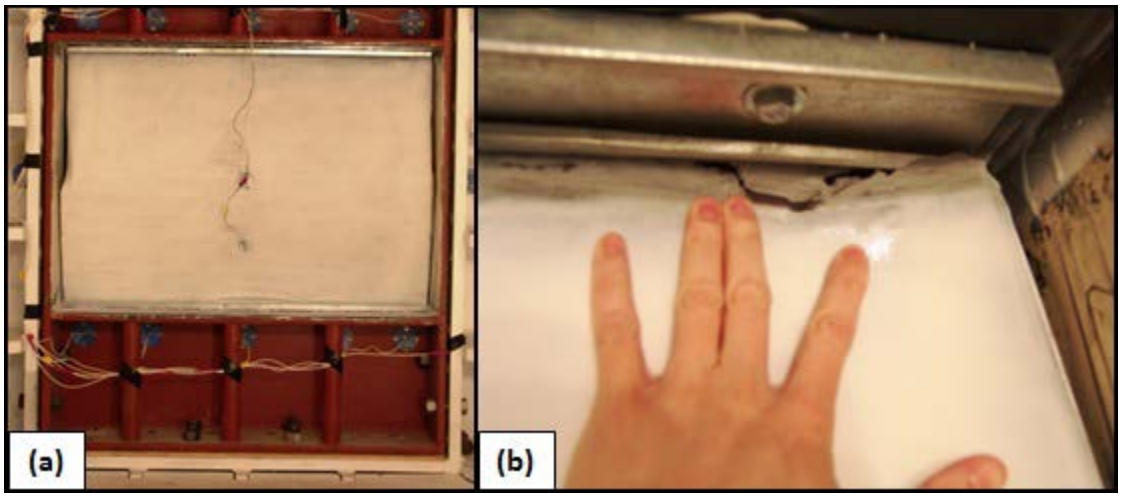

Figure 6.57. BLS5. (a) Posttest view of retrofitted/interior face of wall. (b) Tear along top corner of film.

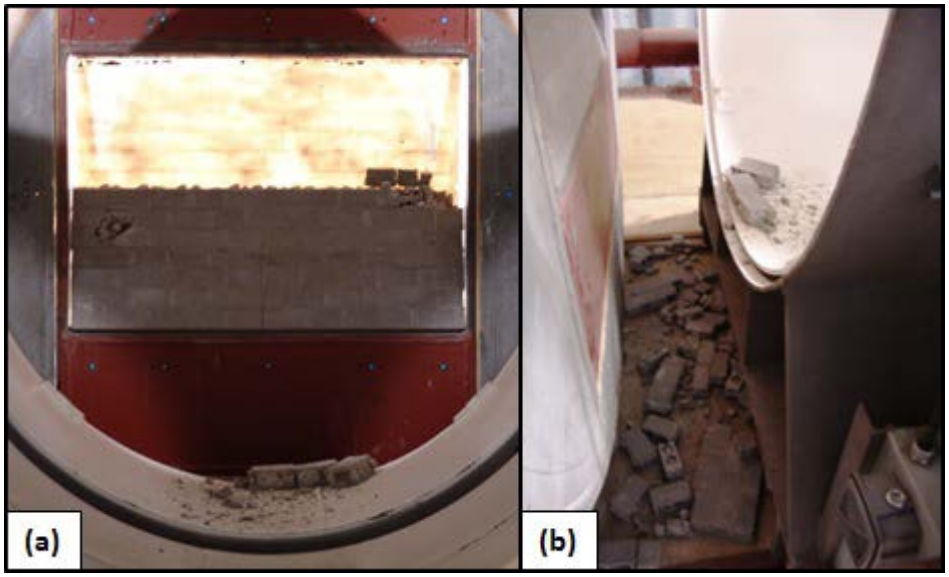

Figure 6.58. BLS5. (a) Exterior view. (b) Debris found outside the reaction structure.

force of the wall also damaged the flanges of the steel stud anchor plates used on the top and bottom supports (Figure 6.59b).

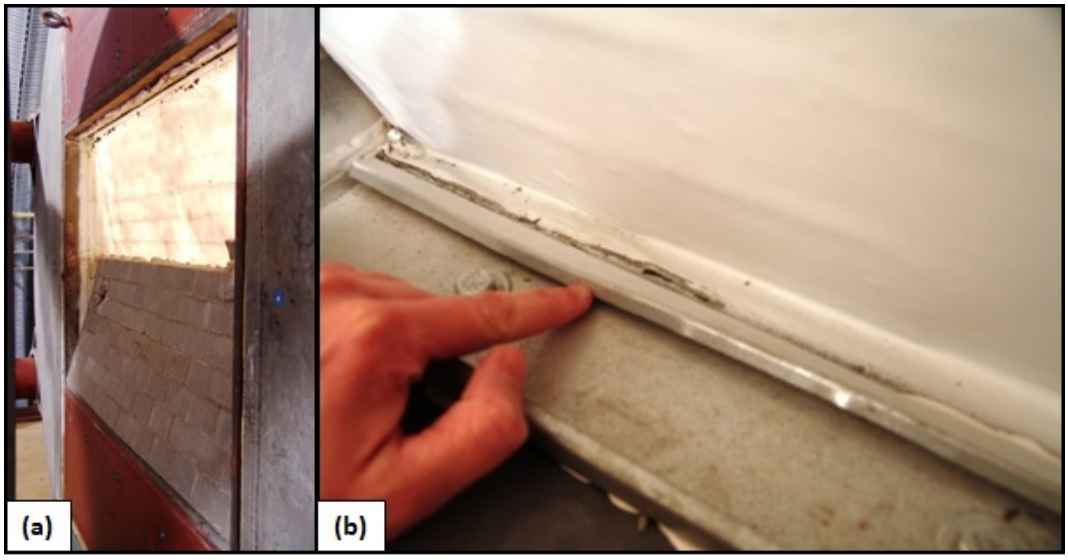

Figure 6.59. BLS5. (a) Posttest exterior face of wall after the CMU blocks on the top half of the wall fell to the floor due to gravitational forces. (b) Force of wall response bent the flanges on the steel studs.

6.2.2.3 BLS6

The retrofit materials used on BLS6 were the same as those on BLS4 and BLS5, but the installation procedure used on BLS6 was slightly different. To cover the entire surface of full-size CMU walls, multiple sheets of the elastomeric film are required. The film can be produced in various widths, but it is recommended for ease of application to limit the production width to 4 ft. To create a continuous layer with no weak areas, multiple sheets overlap the previous sheet by 2 to 6 in. For example, a 12-ft-wide wall would need three sheets 48 in. wide and one additional sheet 18 in. wide to cover the entire wall surface (this includes a 6-in. overlap technique). The elastomeric film for the subscale experiments was produced in 40- to 48-in. widths; thus, one full-sheet and a piece of a second sheet were used to cover the interior face of the subscale CMU wall. In

the subscale experiments to date, only one seam was evaluated during the blast event. As discussed earlier, a full-size CMU wall would require multiple sheets with more than one seam to cover the entire wall surface. To replicate the full-scale experiments, the elastomeric film used in BLS6 was cut into smaller widths so that multiple sheets would be used and more than one seam would be created (Figure 6.60a). The elastomeric film was not painted white before the experiment, but 2-in. by 2-in. black blocks were painted on the film at random points across the wall (Figure 6.60b). The black blocks allowed the elongation and strain rate of the film under dynamic load to be evaluated using the high-speed video. The anchor plate used to secure the retrofit systems to the reaction frame in the BLS experiments was bolted 1.75 in. from the interior face of the CMU wall (Figure 6.60b).

The elastomeric film system applied to BLS6 did not allow any CMU debris to enter the structure, but the elastomeric film was damaged during this experiment executed at dynamic load level 6. Laser L1 recorded a maximum mid-span deflection of 1 into the reaction structure and a final position of 0.549 (Figures 6.61a and b). The large deflection experienced by the wall forced the retrofit system to peel back until the anchor plates engaged, but the wall continued to deform pulling the film over the anchor plates until the film stopped the wall's momentum. The CMU wall was sitting between the top and bottom anchors after the experiment, which were 1.75 in. behind the face of the CMU wall pretest. The anchor plates that were not visible from the blast face before the experiment were clearly visible during the posttest inspection (Figure 6.62a). In Figure 6.62b, only one edge of the anchor plate was still visible from inside the target

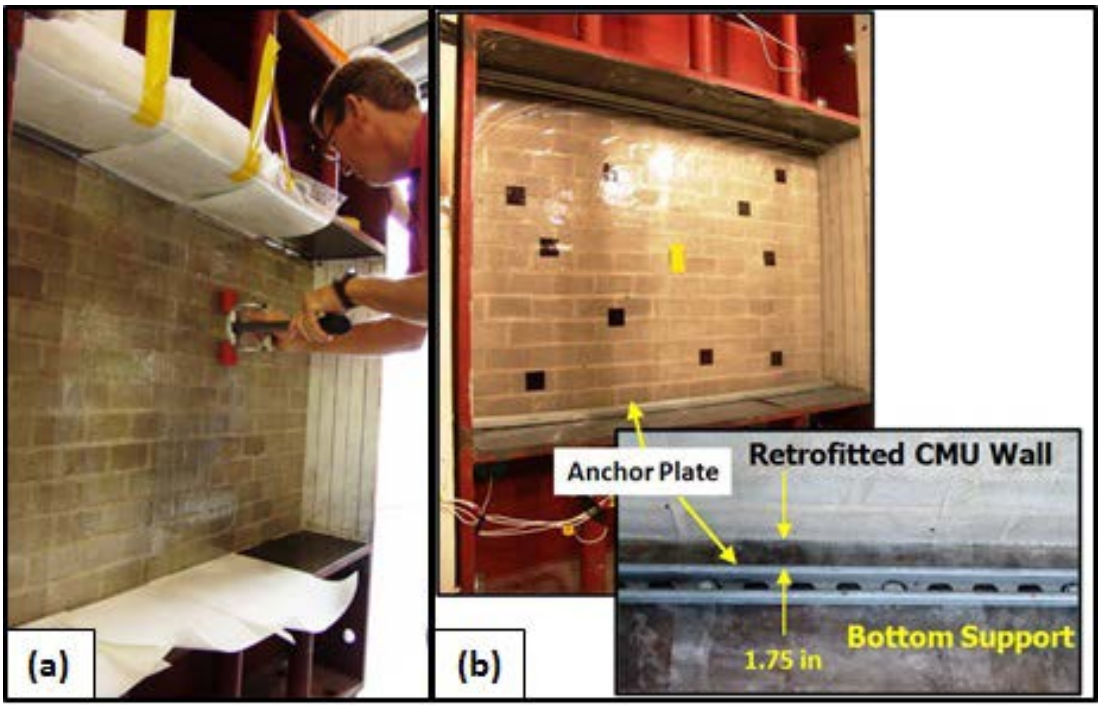

Figure 6.60. BLS6. (a) Multiple sheets and seams evaluated in BLS6. (b) Black squares painted on elastomeric film and location of anchor plate relative to wall surface.

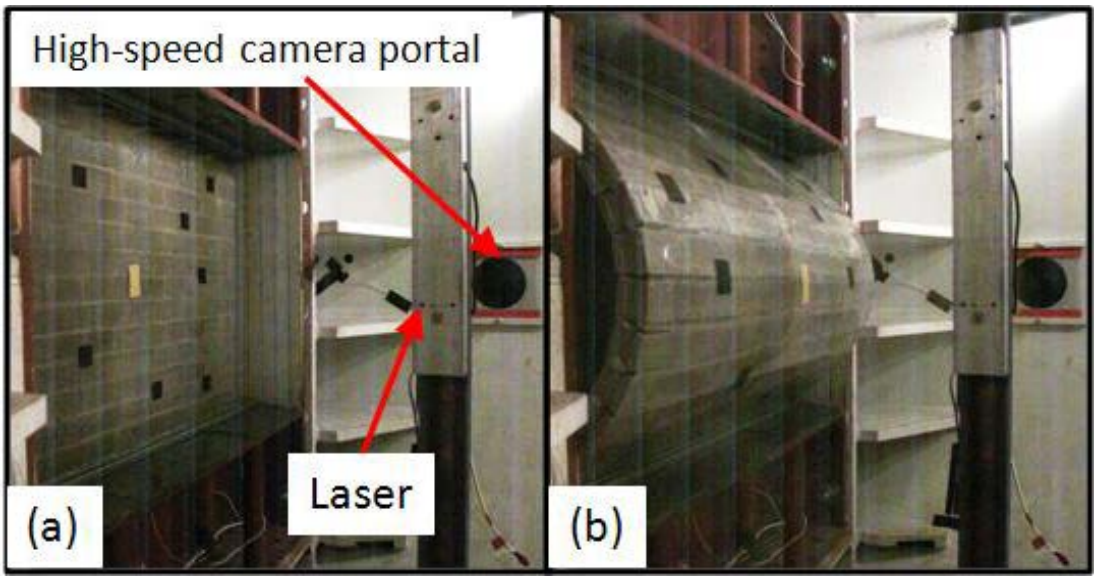

Figure 6.61. BLS6: Frames from high-speed video. (a) Pretest camera view. (b) Maximum deflection.

vessel after the experiment. The film was torn in three places, but was still anchored by the plate. Three small tears were found along the top and bottom supports during the posttest inspection (Figure 6.63a). Seven blocks, or 5% of the CMU wall, lost face shells during the experiment (Figure 6.63b). The blocks above the centerline of the wall began to fall off the film as the weight of the blocks overcame the adhesive strength of the PSA (Figure 6.64a). During the posttest inspection, all of the blocks were removed from the film, and the film was inspected for damage (Figure 6.64b). The edges of the film exhibited some plastic deformation as the material was stretched, but the seams remained secure (Figure 6.64b).

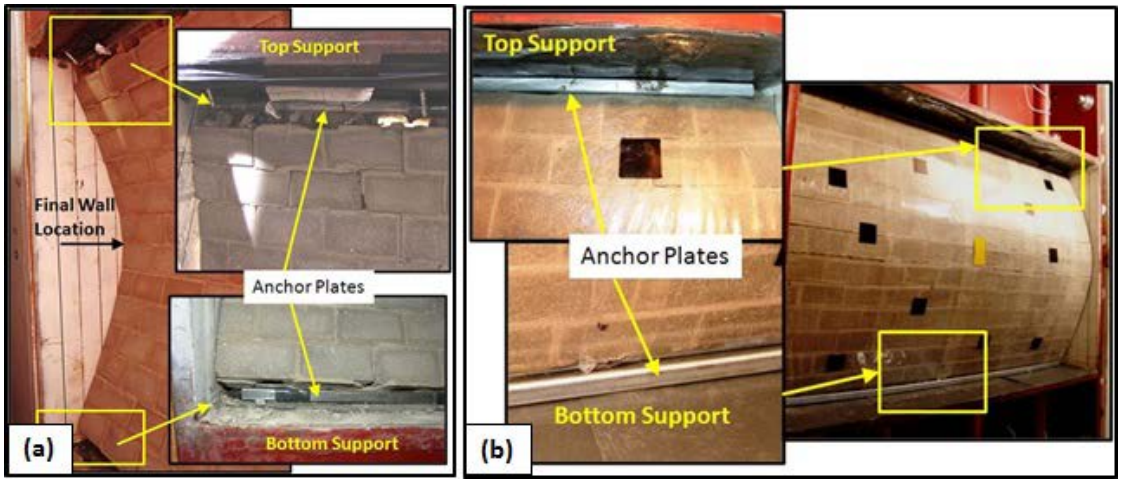

Figure 6.62. BLS6. (a) Final position of CMU wall with anchor plates visible. (b) Interior view of anchor plates.

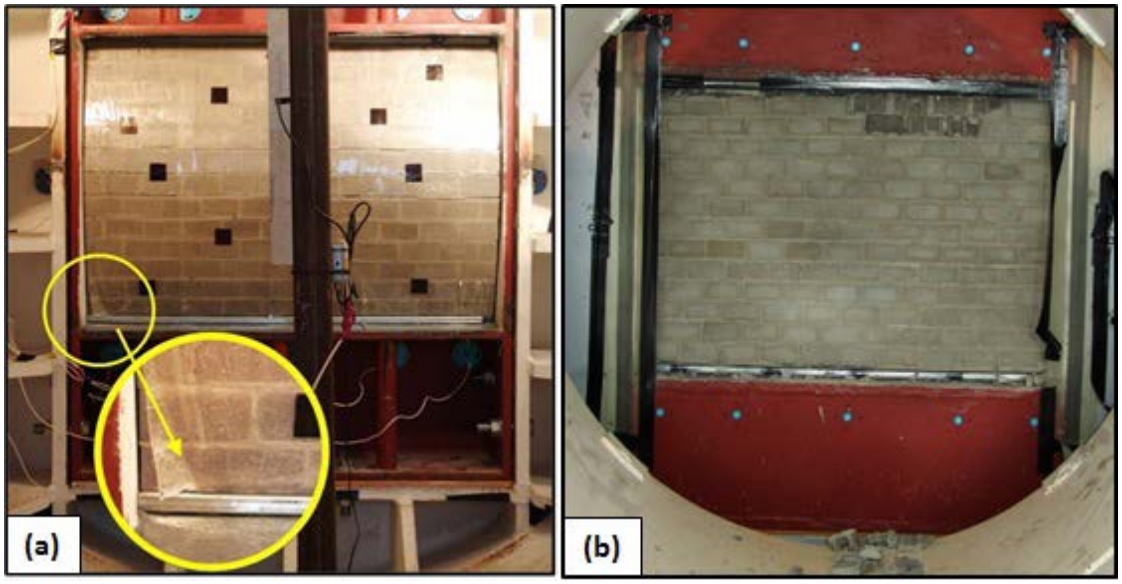

Figure 6.63. BLS6. (a) Posttest interior view of retrofit, small tear in film found in left corner. (b) Posttest exterior view of damaged wall.

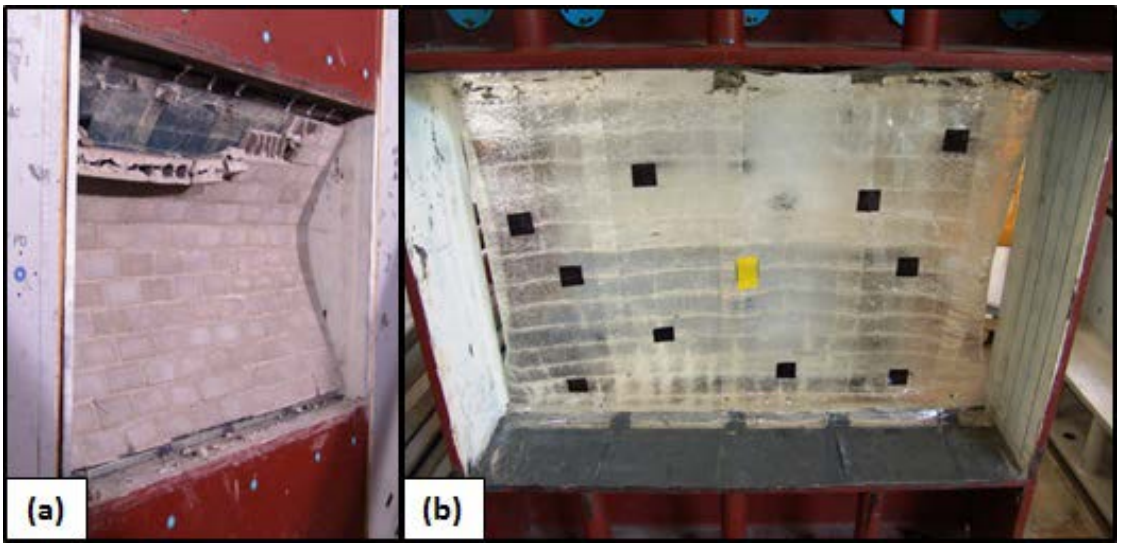

Figure 6.64. BLS6. (a) Gravitational forces pulled the blocks off the elastomeric film. (b) Posttest inspection of film after removal of blocks.

6.2.2.4 BLS7

The retrofit procedure used on wall BLS7 replicated BLS6 except for one detail at the support. In past experiments, a trowel-on thermoset or epoxy was used to create the adhesive bond at the supports. For BLS7, the PSA used to secure the film to the CMU blocks was also used to secure the film to the frame. Anchor plates were used on the top and bottom supports to provide a mechanical anchorage. BLS7 was evaluated at the same dynamic load level of 6 that was used for BLS6.

The retrofit system on BLS7 failed when 90% of the elastomeric film sheared along the edge of the anchor plate on the bottom support, and 22% of the film failed along the edge of the anchor plate on the top support (Figures 6.65a through e, 6.66 and 6.67). Although the elastomeric film tore, most of the blocks remained adhesively engaged to the film. Thirty percent of the blocks were missing from the film (Figure 6.68a), 21% were found in the BLS device, and 9% of the debris was found in the target vessel.

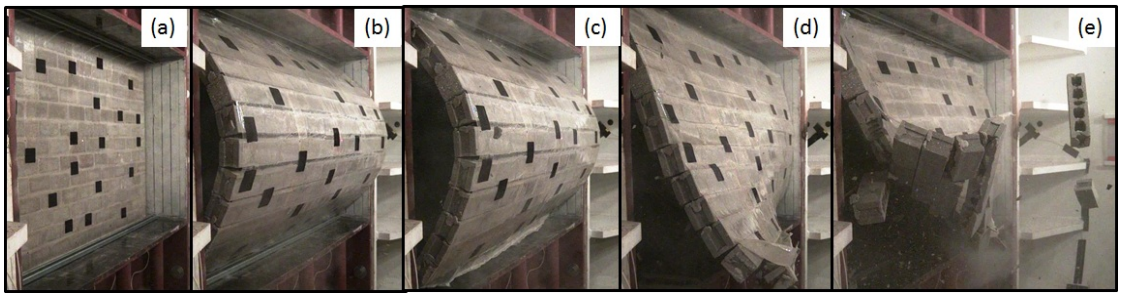

Figure 6.65. BLS7: Frames from high-speed video. (a) Pretest camera view. (b) Maximum deflection before film shears. (c) Shear failure of film along bottom support. (d) Film continues to deform. (e) CMU debris hazard.

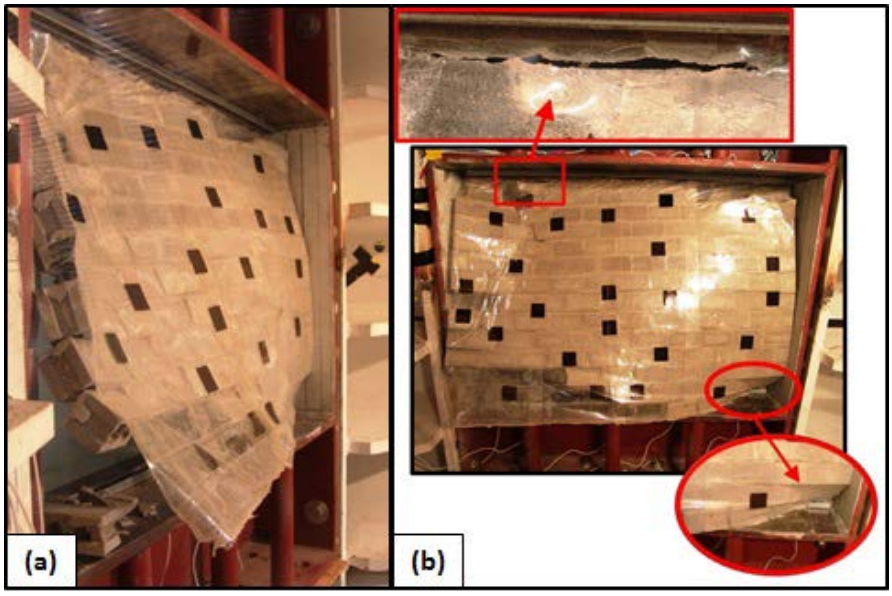

Figure 6.66. BLS7. (a) Final position.
(b) Tear in elastomeric film.

Almost 8% of the debris in the target vessel was found within 4 ft of the interior wall surface (Figure 6.68b). Two blocks were found 10 ft and 12 ft away from the original wall location.

The difference between the responses of BLS6 and BLS7 could be attributed to the lack of an epoxy or thermoset adhesive applied to the supports. The energy that would have been absorbed by the process of peeling back the film from the trowel-on material was applied directly to the film/anchor plate interface.

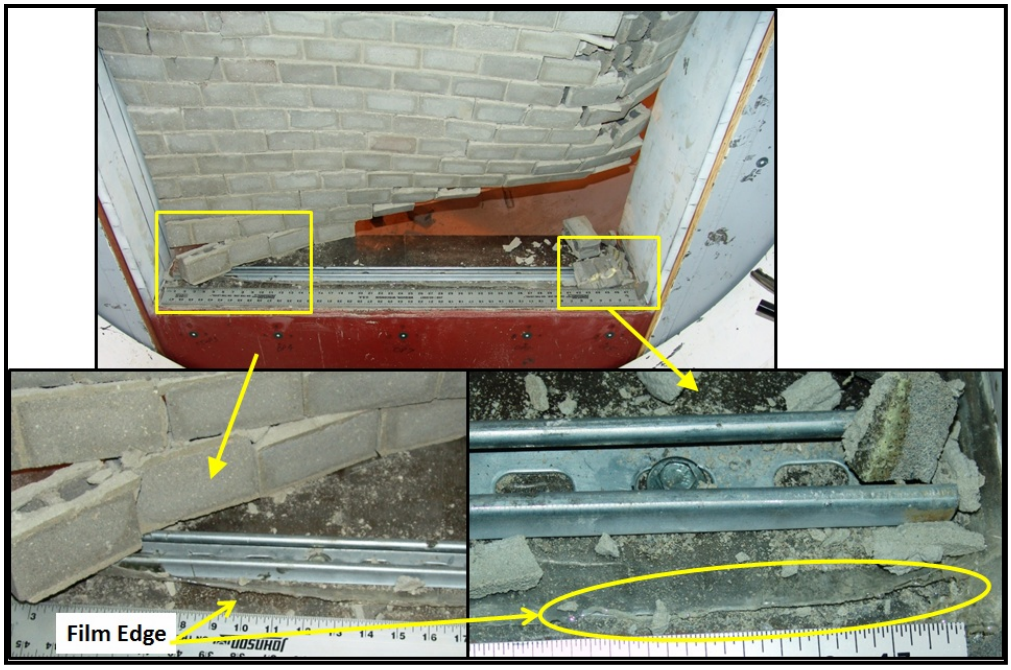

Figure 6.67. Film sheared along the edge of the anchor plate.

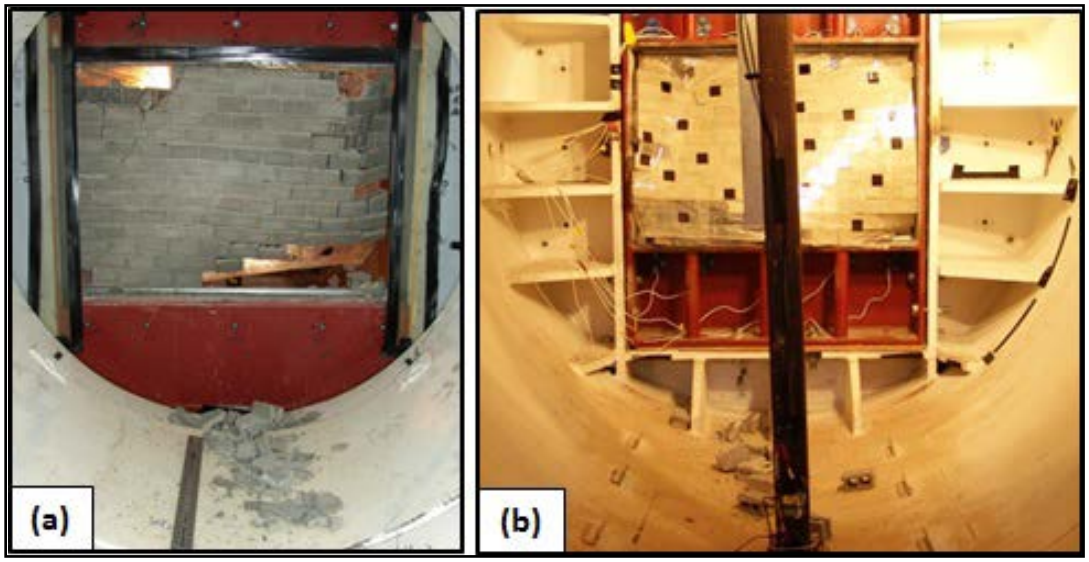

Figure 6.68. BLS7. (a) Damage to CMU wall. (b) Debris found in target vessel.

6.2.3 Fiber-Reinforced Film with PSA (BLS8-BLS11)

6.2.3.1 BLS8

The retrofit system for BLS8 consisted of an open-weave fiber-reinforced Fabric G encapsulated in an elastomeric film (Figure 6.69a). The PSA on the elastomeric film used in this experiment was applied to the film by the manufacturer before it was shipped to the ERDC. The application process used on BLS7 was repeated for BLS8. Figure 6.69b shows the 1-in. setback of the thin steel channel with a deformed leg used as an anchor plate from the interior face of the CMU wall. The anchor plate used in BLS8 was damaged in a previous experiment. BLS8 was subjected to dynamic load level 6, which was the dynamic load at which BLS7 failed and BLS6 was successful.

BLS8 prevented any CMU debris from entering the target vessel, and the magnitude of the deflection into the target vessel was smaller than the deflection measured in BLS6. Inspection of the high-speed video indicated that the maximum deformation occurred at the top of the retrofitted wall and was estimated to be 0.625 to 0.66 (Figures 6.70a, b, and c). The steel channel used to anchor the retrofit system was engaged during the wall's response and was bent almost in half (Figure 6.71). The deformation of the channel ended at the anchor bolts, which were bolted through the center of the channel web. In some locations, the channel and film were pulled around the anchor bolts as seen in Figure 6.72. Fourteen percent of the blocks from the top three courses of blocks were damaged, but the CMU debris was propelled outside the target vessel. The diagonal nature of the cracks formed in the mortar joints from the third course up and the unusual wall deformation during the wall's response could indicate that the wall was pinched,

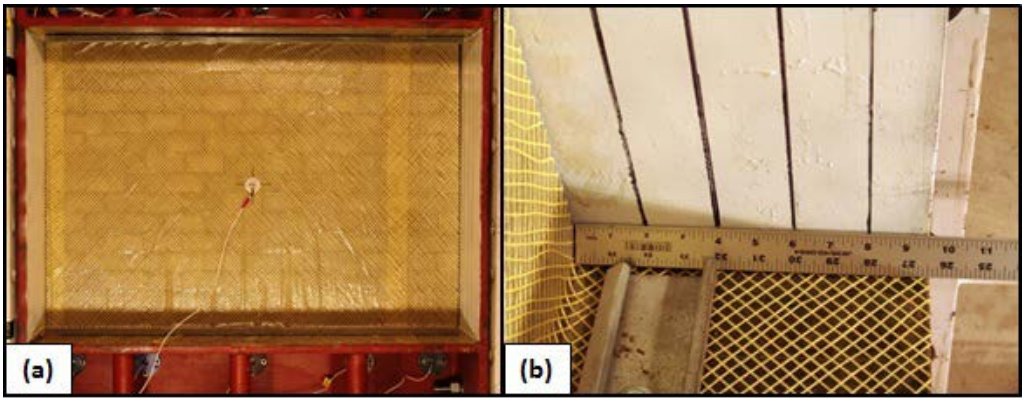

Figure 6.69. BLS8. (a) Pretest interior face of retrofitted wall. (b) Anchor plate deformed in a previous experiment bolted to test frame 1 in. behind wall.

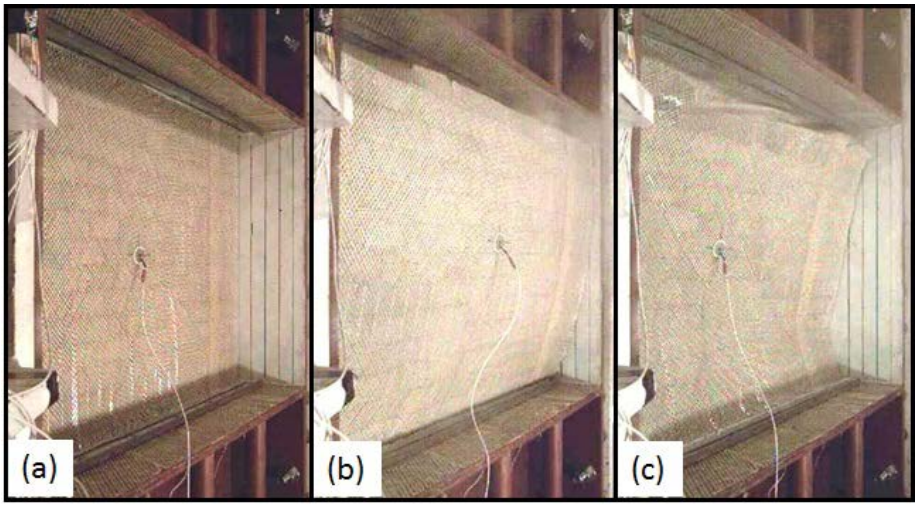

Figure 6.70. BLS8: Frames from high-speed video. (a) Camera view before airblast arrives. (b) Maximum deflection at top support. (c) Final wall position.

jammed, or dragged across the sides of the steel frame during the blast event (Figure 6.72). The bottom course of blocks placed in the mortar bed rotated and deflected at least 0.139 units into the reaction structure. The blocks remaining on the film after the experiment were still securely attached to the film, and some force was required to remove them during the posttest inspection.

Figure 6.71. Interior view of retrofitted wall BLS8 and the damaged anchor plates.

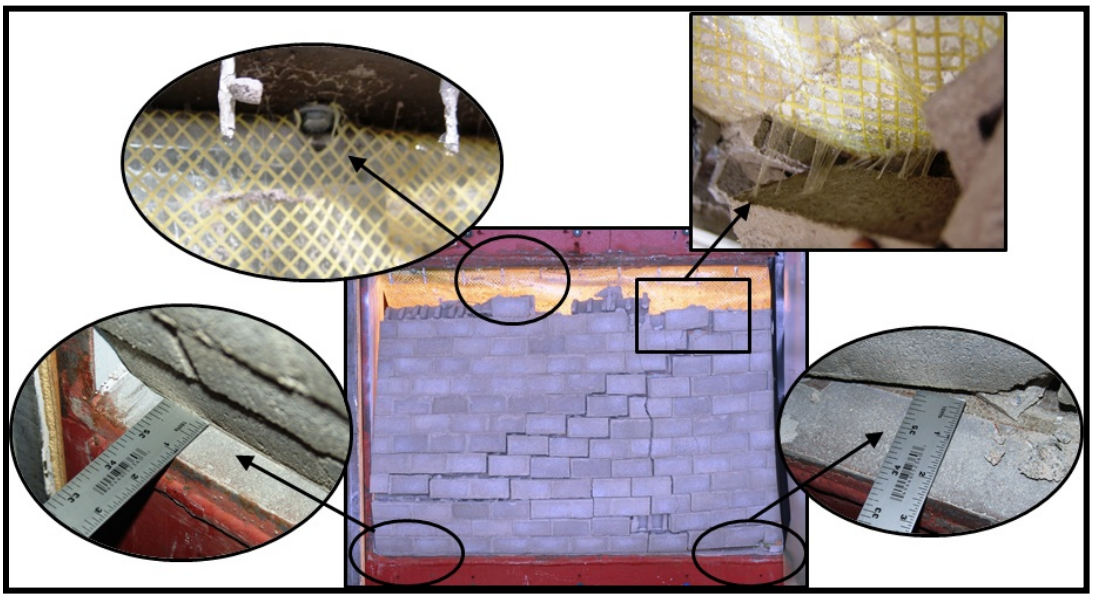

Figure 6.72. BLS8: Exterior view of bottom support, film adhesive, and bolts used on anchor system.

6.2.3.2 BLS9

The materials and application procedure used in BLS8 was duplicated in BLS9. Since BLS8 survived at dynamic load level 6, the load for BLS9 was increased to level 7. It appeared that wall BLS8 experienced some arching effects, so the wall and

retrofit system was inspected closely before the test on BLS9 was conducted. The gaps were cleaned to free any debris that may have been trapped, and the retrofit material was trimmed along the sides of the wall to ensure that the film did not drag along the side walls of the reaction frame.

The retrofit system used on BLS9 catastrophically failed along the mid-height of the wall allowing CMU debris to be thrown 16 ft into the reaction structure. There appeared to be no interaction with the steel frame to cause any localized effects. From the images provided by the two high-speed cameras, the reinforced system's response and development of the tears along the horizontal mortar joint can be observed (Figures 6.73a to d and Figures 6.74a to d). As the wall deflected, cracks developed between the mortar joints and CMU. The cracks continued to increase under load, and the reinforced elastomeric film was engaged. As the cracks continued, the film elongated, and the fibers reoriented from a 45-deg orientation to a 90-deg orientation as shown in the series of Figures 6.75, 6.76, and 6.77. The wall continued to deflect into the structure, and the mortar crack continued to increase until the fibers failed breaking the wall into two pieces. Each wall section impacted the respective supports. It appeared that the film failed first, and then the fibers were pulled out of the film until ultimate failure occurred. This response was evident on the still frames in Figures 6.73, 6.74, 6.75, 6.76, and 6.77 captured from both high-speed cameras.

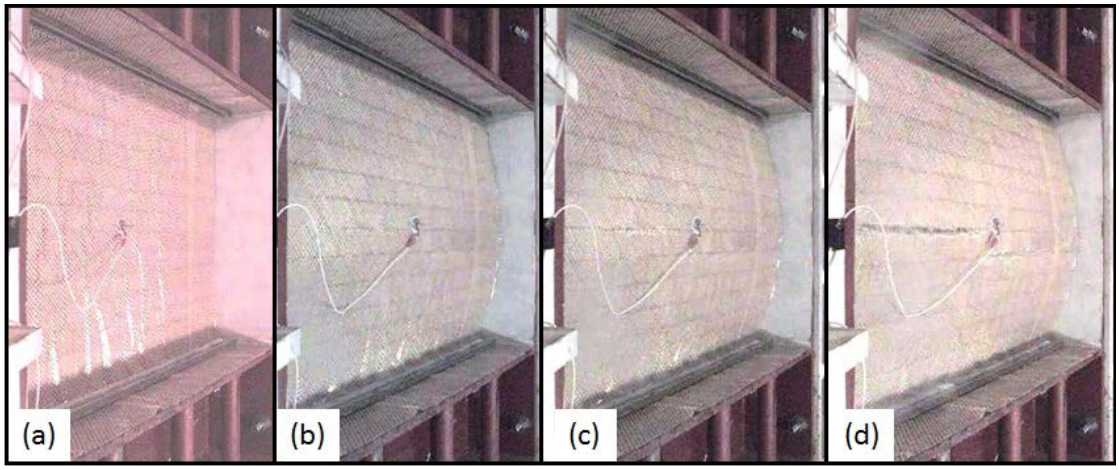

Figure 6.73. BLS9: Frames from high-speed video. (a) Camera view before airblast arrives. (b) Wall begins to deform. (c) Crack forms at centerline. (d) Crack at centerline continued to increase (Adapted from Johnson, Davis, Coltharp, Durst, and Smith 2010).

While most of the blocks remained attached to the film, debris originating around the tear entered the target vessel. The PSA was unable to maintain the adhesive bond between the film and steel frame during the blast load, and this area of the film peeled back to the anchor plates on both the top and bottom supports (Figure 6.78). Without the anchor plates, the size and percentage of debris found inside the target vessel would have been much higher (Johnson, Davis, Coltharp, Durst, and Smith 2010).

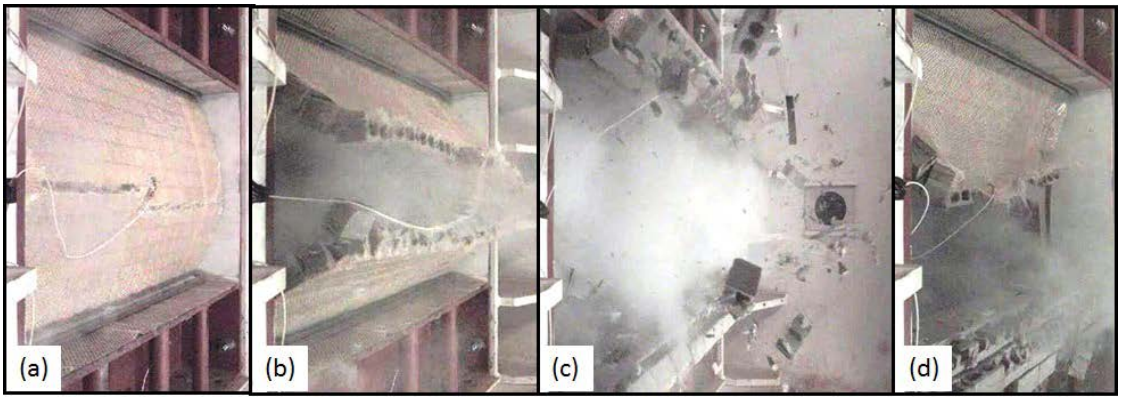

Figure 6.74. BLS9: Frames from high-speed video. (a) Film tore along crack. (b) Complete failure of reinforced film. (c) CMU debris generated from failure edge. (d) CMU above and below failure line remained attached to the film. (Adapted from Johnson, Davis, Coltharp, Durst, and Smith 2010)

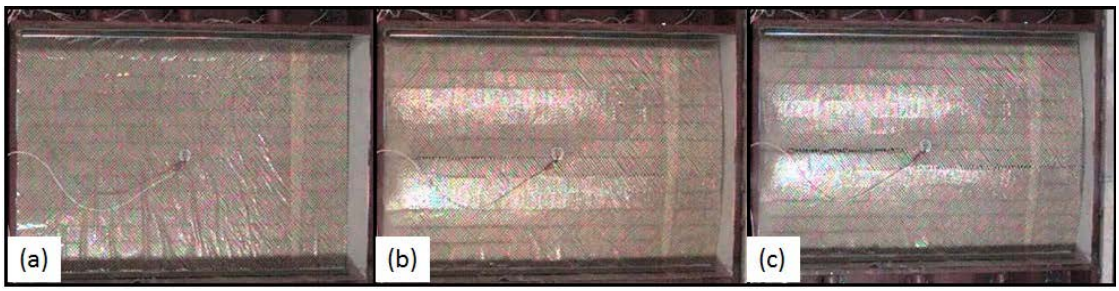

Figure 6.75. BLS9: Frames from high-speed video. (a) Pretest camera view. (b) Cracks in mortar visible. (c) Film begins to tear and fibers realign. (Adapted from Johnson, Davis, Coltharp, Durst, and Smith 2010)

The anchor plates were not visible from the blast face before the experiment, but both anchor plates can be seen in the posttest pictures in Figure 6.78. The fibers that were pulled out of bundles from each half of the wall can be seen in Figure 6.79.

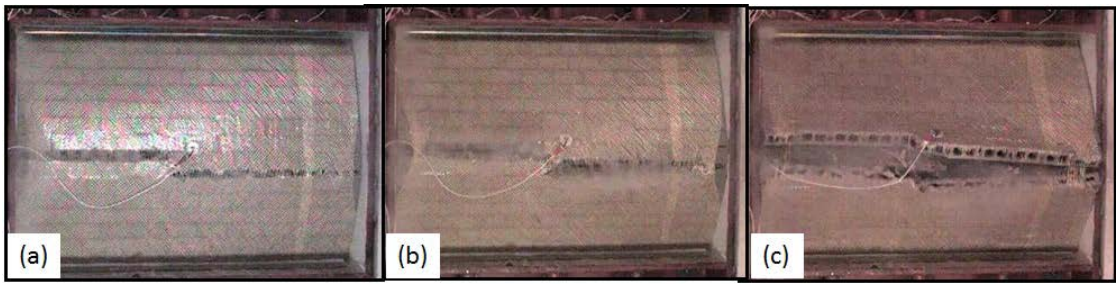

Figure 6.76. BLS9: Frames from high-speed video. (a) Fibers realign to 90-deg. (b) Fibers begin to fail. (c) All fibers along centerline have failed and wall deflects into target vessel. (Adapted from Johnson, Davis, Coltharp, Durst, and Smith 2010)

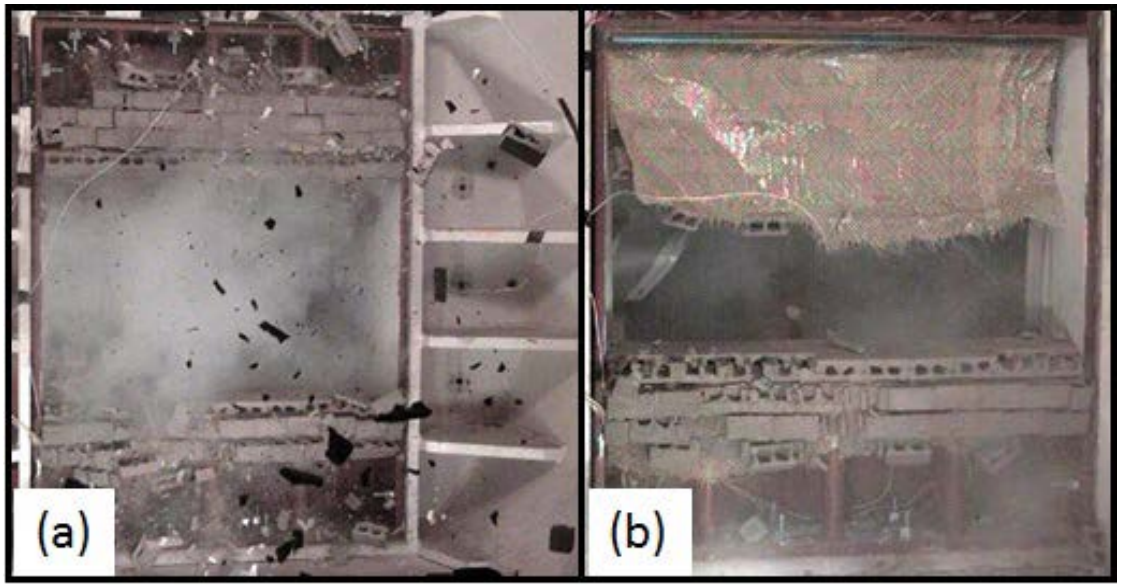

Figure 6.77. BLS9: Frames from high-speed video. (a) CMU debris and wall/retrofit impact reaction frame. (b) Final wall position. (Adapted from Johnson, Davis, Coltharp, Durst, and Smith 2010)

Figure 6.78. BLS9: Exterior view of anchor plates on the supports and damaged wall/retrofit materials. (Adapted from Johnson, Davis, Coltharp, Durst, and Smith 2010)

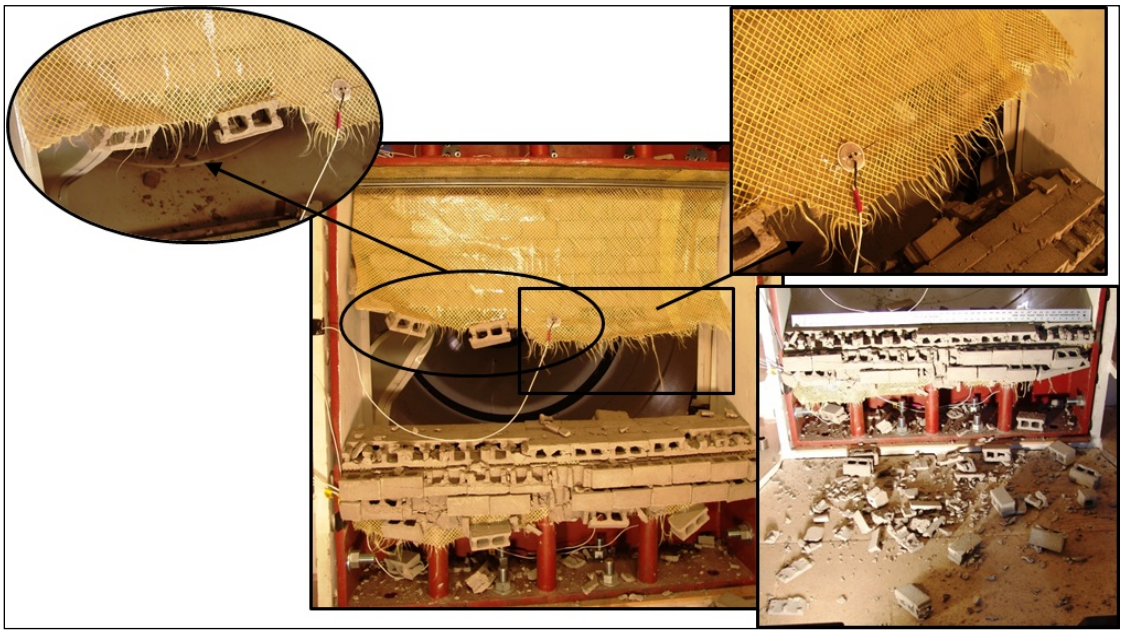

Figure 6.79. BLS9: Interior view of debris and elastomeric film with fiber strands visible. (Adapted from Johnson, Davis, Coltharp, Durst, and Smith 2010)

6.2.3.3 BLS10

Wall BLS10 repeated the application procedure and materials used in BLS8 and BLS9; however, the two materials did differ. Both materials contained the same resin and reinforcement material, but something differed in the manufacturing process. The installers accidently peeled off the elastomeric film sandwiching the fabric reinforcement from one side of the material exposing the reinforcement while trying to peel the backing paper off of the PSA. Additional material from the order was inspected, and the delamination was found to be common. The defective material was evaluated to determine if the delamination would affect the global response of the wall under dynamic loading. During the application process, each successive sheet applied to the wall overlapped the previous sheet by 3 to 3-3/4 in. The dynamic load for BLS10 was reduced to level 5 since BLS9 failed catastrophically.

The reinforced elastomeric film used to retrofit BLS10 was successful, but did sustain damage as shown in the series of Figures 6.80, 6.81, and 6.82. The film and fibers tore at two locations along the mid-height of the wall (Figure 6.82). BLS9 and BLS10 had similar responses, but BLS10 did not reach failure. The two high-speed cameras recorded the wall response under load. As the wall deflected, cracks developed between the mortar joints and the CMU along the centerline. The cracks expanded as the deflection continued to increase, and the reinforced elastomeric film was engaged. As the deflection increased, the film elongated, and the fibers reoriented from a 45-deg orientation to a 90-deg orientation. As the deflection increased, the seams on the elastomeric film began to deform reducing the overlap area. The wall continued to

deflect into the structure, and the mortar crack continued to increase until the fibers failed along the centerline at two wall locations. Blocks were exposed at the first seam on the left when the wall reached maximum deflection.

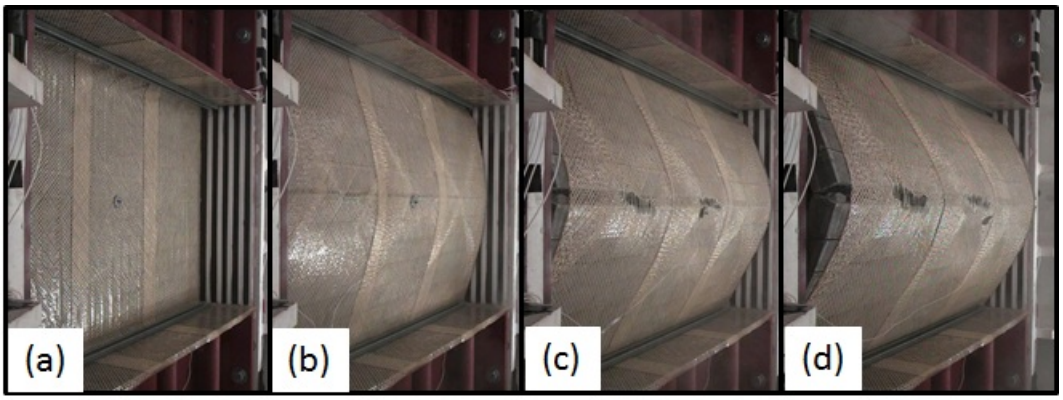

Figure 6.80. BLS10: Frames from high-speed video. (a) Pretest camera view. (b) Crack at centerline. (c) Film tears and fibers reorient. (d) Point of maximum deflection.

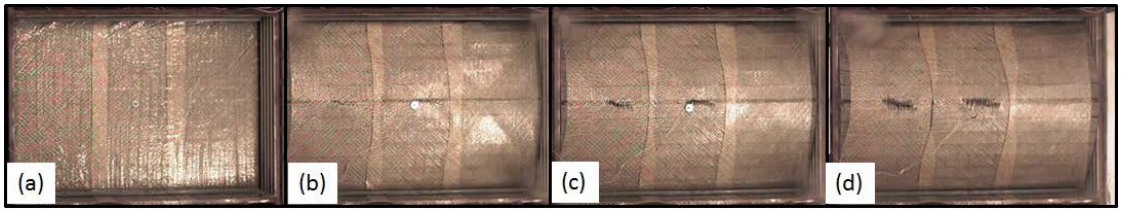

Figure 6.81. BLS10: Frames from high-speed video. (a) Pretest camera view. (b) Crack at centerline. (c) Film tears, fibers reorient, and seam opening. (d) Holes in film and seams open at maximum point of deflection.

The high-speed camera located on the left side of the target vessel captured images of the wall's response that appeared to punctuate the high stress and strain areas in the elastomeric film. The lighting and camera angle appeared to highlight these areas in the

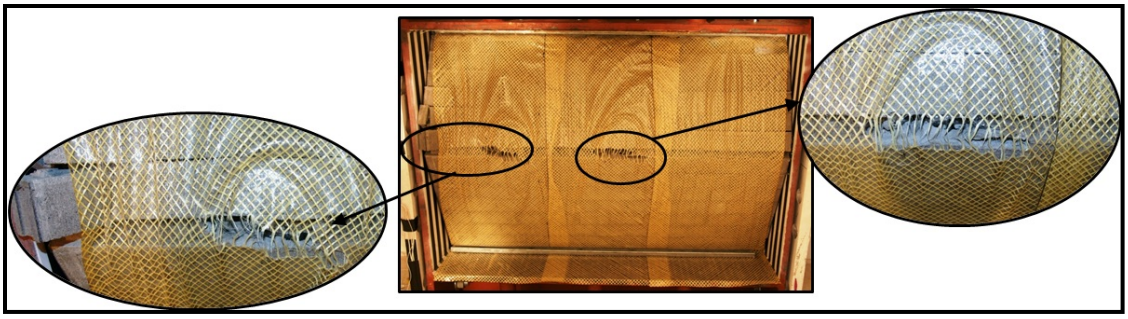

Figure 6.82. BLS10: Posttest interior view of damaged reinforced film.

mid-section of the wall where the fibers were engaged during the wall's deformation. One still frame from the video was chosen as an illustration (Figure 6.83). Dashed lines were added to the frame on the left to highlight the areas of interest on the frame to the right.

Eleven percent of the blocks were damaged during the blast event. The damage was concentrated across the top of the wall (Figure 6.84a). As the wall began to rebound from the point of maximum deflection, the blocks along the right edge at the centerline were trapped between the steel frame and the film damaging the blocks. The anchor plates on the top and bottom supports prevented the wall from deflecting any further into the target vessel (Figure 6.84b). The accelerometer at the center of the wall indicated a deflection of 0.833 into the reaction structure.

Figure 6.83. The two photos illustrate the pattern created in the elastomeric film at high stress and strain areas.

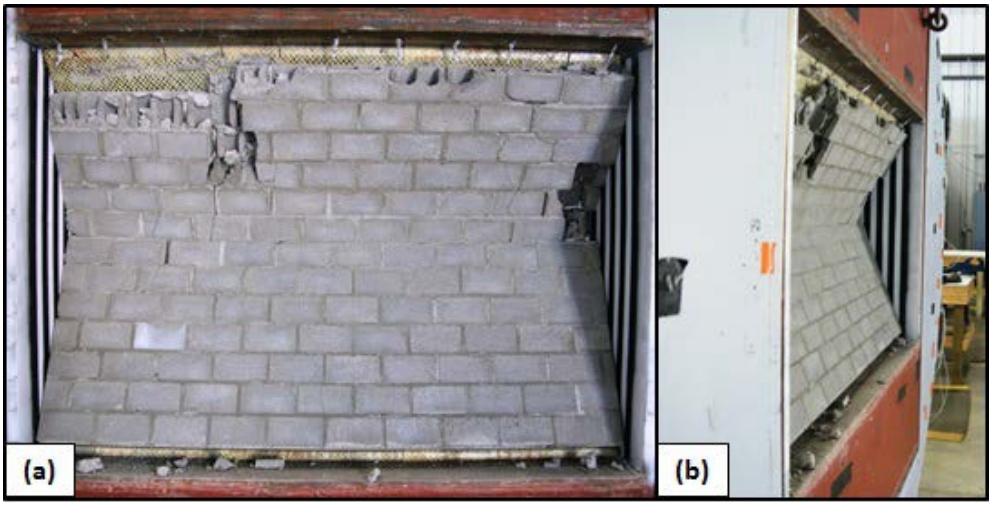

Figure 6.84. BLS10. (a) Posttest exterior view. (b) Final position of deformed wall.

6.2.3.4 BLS11

The reinforced elastomeric film used on BLS11 was obtained from the same roll of material used to retrofit BLS8 and BLS9. The dynamic load for BLS11 was reduced to level 3 to obtain the wall's response for a mid-level load. The response of the elastomeric film to the dynamic load was captured in high-speed video (Figure 6.85a). Even at the reduced dynamic load, the PSA could not prevent the elastomeric film from disengaging at the bottom support. The film did fold up against the anchor plate when the wall deformed into the structure (Figure 6.86). None of the CMU face shells sustained damage during the event, but the mortar joints were damaged (Figure 6.87). No tears or plastic deformation was observed on the elastomeric film during the posttest inspection (Figure 6.86). The accelerometer at the center of the wall indicated a maximum deflection of 0.326 (Figure 6.85b). The retrofitted wall's final position was 0.104 units from the original location (Figure 6.87).

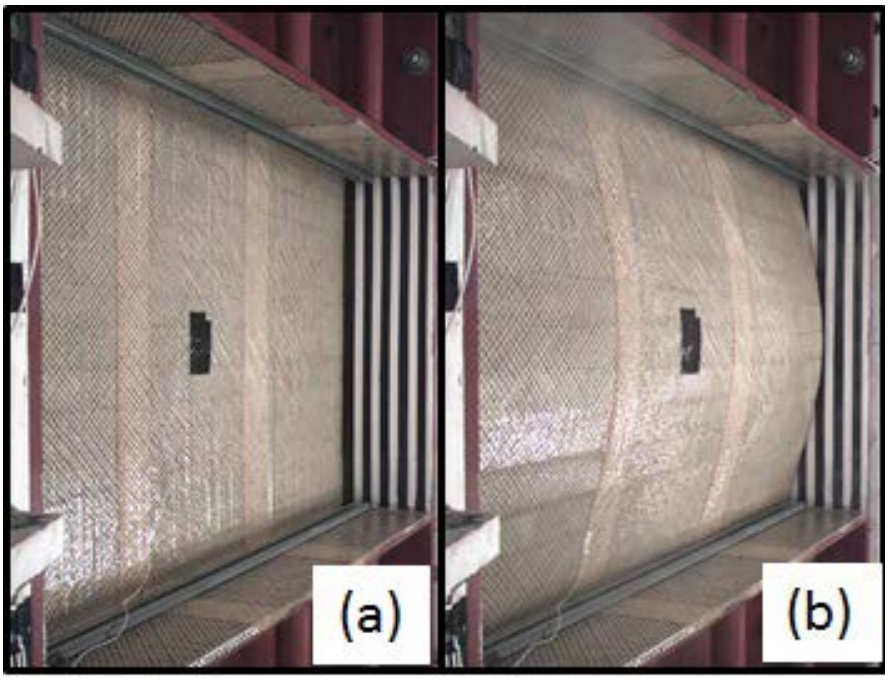

Figure 6.85. BLS11: Frames from high-speed video. (a) Pretest camera view. (b) Maximum wall deflection.

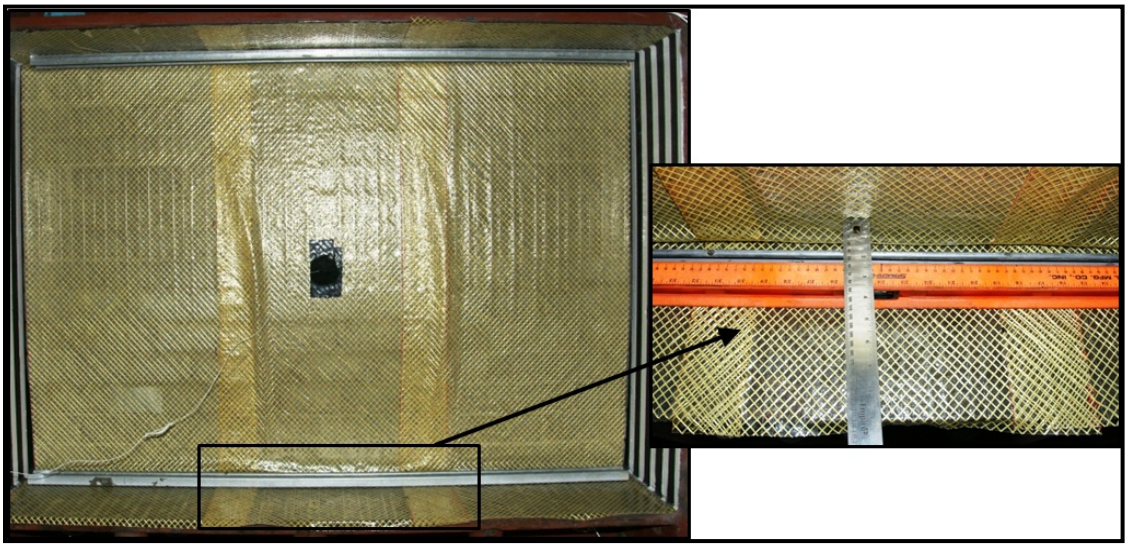

Figure 6.86. Posttest interior view of BLS11. The entire wall permanently deflected into the structure.

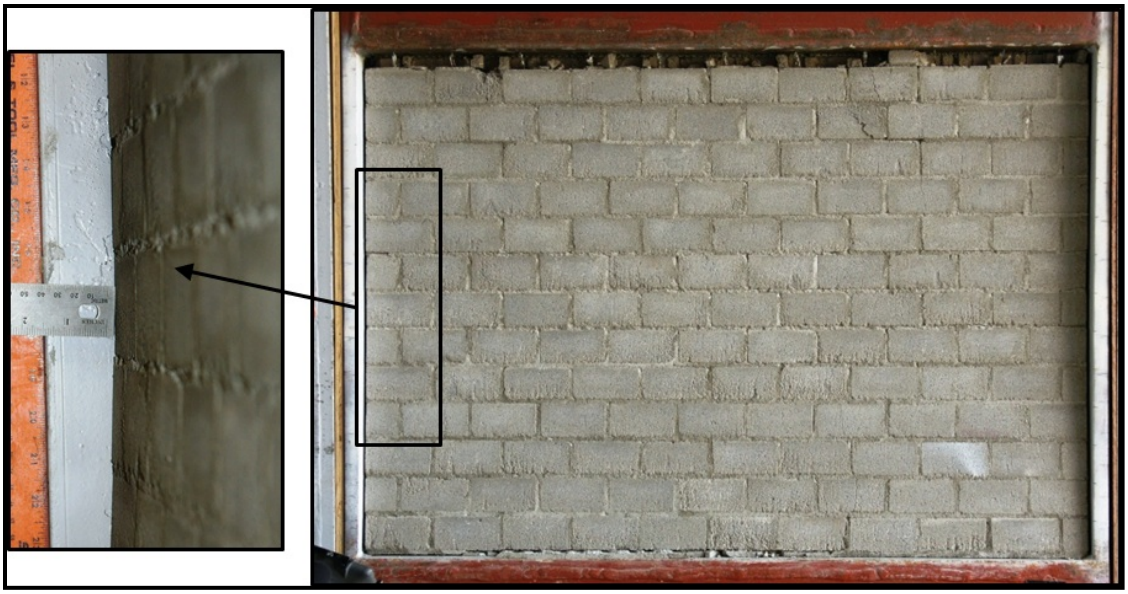

Figure 6.87. Posttest exterior view of BLS11. Permenant deflection of the wall into the structure.

6.3 Comparison and Analysis of Subscale Dynamic Experiments

Fifteen of the 22 subscale experiments successfully demonstrated the effectiveness of the retrofit systems to mitigate debris hazards associated with blast loads. The dynamic load level for each unretrofitted and retrofitted wall evaluated is graphically depicted on Figure 6.88. The first three walls (BLS1, BLS2, and BLS3) evaluated in the BLS were conducted to demonstrate the debris hazard associated with the blast load associated with dynamic load level 3. The responses of BLS4, BLS5, BLS6, BLS8, BLS10, and BLS11 clearly demonstrated that the unreinforced and reinforced films using a PSA can provide a high level of protection for personnel located in rooms retrofitted with these types of systems. Examination of the interior of the target vessel following the experiments, along with the high-speed camera coverage, showed that no

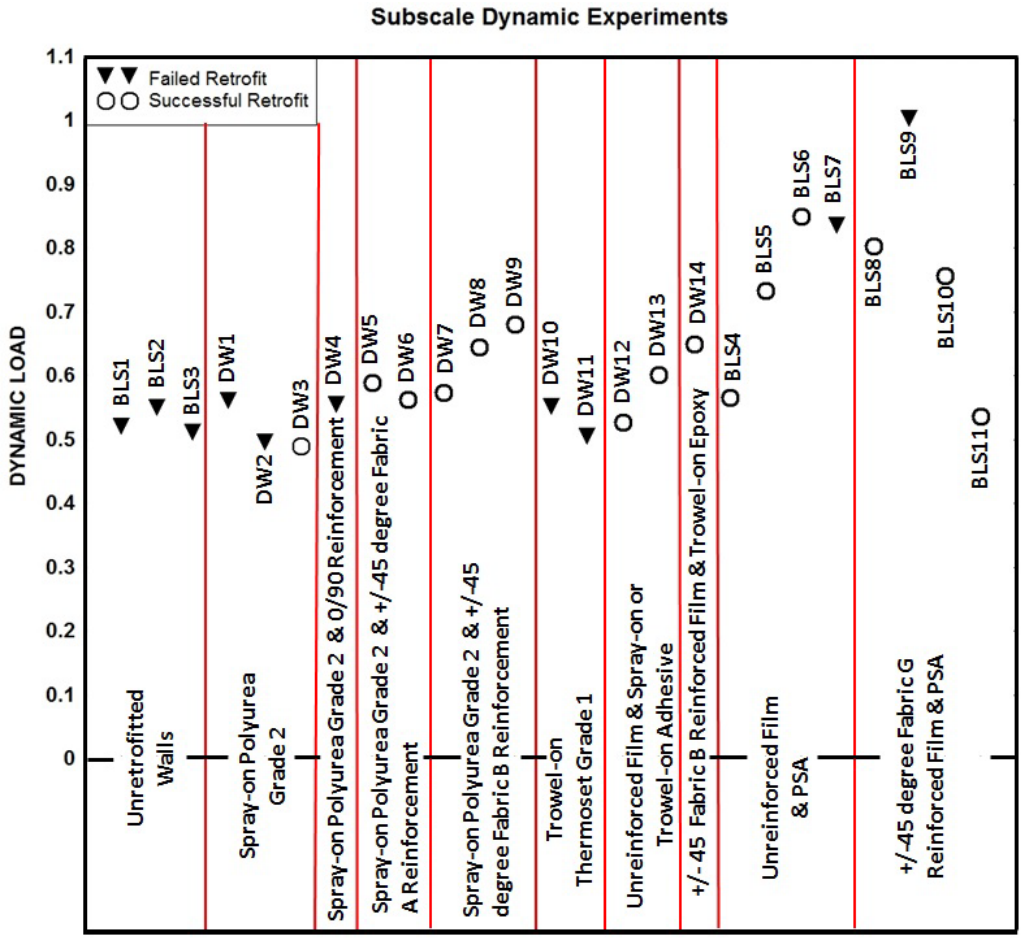

Figure 6.88. Subscale dynamic experiments normalized results.

significant debris was generated. The unreinforced and ±45-deg reinforced films (Fabric G) applied to the wall with PSAs survived the highest dynamic load of all the retrofits evaluated in the subscale experiments. All of the data documented from the subscale experiments is provided in Table 6.4.

The first system evaluated was the unreinforced spray-on polyurea Grade 2 (DW1, DW2, and DW3). DW1 was evaluated at dynamic load level 3 in a steel frame and the

Table 6.4. Data from subscale dynamic experiments.

Test Label	Dynamic Load Level	Material Thickness, in.			Normalized Deflection	CMU Damage, %	Failure Mode
		Min	Max	Avg.			
DW1	3	0.069	0.232	0.13	Fail	Fail	1
DW2	2	0.081	0.15	0.11	Fail	Fail	4
DW3	2	0.12	0.28	0.17	0.174	7	PASS
DW4	3	0.086	0.18	0.12	Fail	Fail	2
DW5	3	0.12	0.35	0.13	0.167	30	PASS
DW6	3	0.083	0.15	0.11	0.194	7	PASS
DW7	3	0.13	0.33	0.19	0.347	66	PASS
DW8	4	0.13	0.25	0.19	0.278	59	PASS
DW9	4	0.13	0.35	0.19	0.222	46	PASS
DW10	3	0.046	0.25	0.088	Fail	Fail	1
DW11	3	0.0876	0.0876	0.0876	Fail	Fail	1
DW12	3	0.0655	0.0655	0.0655	0.208	0	PASS
DW13	4	0.0655	0.0655	0.0655	BAD	31	PASS
DW14	4	0.0255	0.0255	0.0255	BAD	40	PASS
BLS1	3	None	None	None	Fail	Fail	1
BLS2	3	None	None	None	Fail	Fail	1
BLS3	3	None	None	None	Fail	Fail	1
BLS4	3	0.019	0.02	0.0195	0.347		PASS
BLS5	5	0.019	0.02	0.0195	0.833	50	PASS
BLS6	6	0.015	0.0195	0.0173	1	5	PASS
BLS7	6	0.015	0.0195	0.0173	Fail	30	3
BLS8	6	0.03	0.03	0.03	0.66	14	PASS
BLS9	7	0.03	0.03	0.03	Fail	Fail	1
BLS10	5	0.03	0.03	0.03	0.833	11	PASS
BLS11	3	0.03	0.03	0.03	0.326	0	PASS

Failure Mode: (1) Tear at mid-span; (2) Shear at top support; (3) Shear at bottom support; (4) Shear at both supports.

elastomeric liner ripped across the center line of the wall. Since DW1 failed at level 3, the dynamic load was reduced to level 2 for DW2. The entire wall ripped at the top and bottom support and settled at the base of the reaction structure. It appeared that the polyurea coat on DW2 was too thin at the supports. A third specimen, DW3, was used to repeat the experiment at dynamic load level 2 in a steel frame using a thicker application at the top and bottom supports. The spray-on polyurea applied to DW3 successfully demonstrated the ability of the material to mitigate the debris hazard, but it also demonstrated the importance of quality control, specifically the material thickness at the supports. The unreinforced Grade 2 spray-on polyurea retrofit system was not selected for further evaluation in the full-scale experiments.

The Grade 2 spray-on polyurea reinforced with Fabric A in 0/90-deg orientation applied to wall DW4 failed to mitigate the debris hazard for dynamic load level 3. DW4 failed when the system sheared at the top support. It appeared that the fibers oriented in the 0/90-deg orientation limited the wall deflection, forcing the system to be overloaded at the supports and ultimately to fail. Since the wall failed at dynamic load level 3, the decision was made not to repeat the retrofit experiment or re-evaluate it at a reduced load. The retrofit system was also not selected for further evaluation in the full-scale dynamic experiments.

The Grade 2 spray-on polyurea reinforced with Fabric A in the ±45 deg orientation applied to walls DW5 and DW6 both effectively demonstrated the ability of the system to mitigate the debris hazard for dynamic load level 3. DW5 was evaluated in a frame using concrete beams at the supports, while DW6 was evaluated in a steel frame.

Instrumentation results from both walls registered a maximum deflection of 0.174. DW5 peeled back at both the top and bottom supports, but no visible damage to the elastomeric liner or reinforcement was found during the posttest inspection. Since some of the energy from the blast was absorbed during the peel back response of the wall, little damage was observed across the interior surface of Wall DW5. DW6 did not appear to peel back at the top support in the high-speed video; instead the fiber reinforcement was pulled out of the spray-on material. Because the reinforcement and spray-on material did not act as one entity at the supports, it appeared to stiffen the specimen and forced a 10-in. rip to develop along the center line on the right side of the wall. Both walls effectively demonstrated the ability of the retrofit system to mitigate the debris hazard, but they also demonstrated the importance of encapsulating the reinforcement at the support/wall interface.

The three walls (DW7, DW8 and DW9) retrofitted with the Grade 2 spray-on polyurea reinforced with Fabric B in a ±45-deg orientation effectively mitigated the debris hazard associated with dynamic load levels 3 and 4. All three walls were evaluated in a steel frame and the last two, DW8 and DW9, used a primer at the top and bottom supports. The dynamic load was increased as each wall was evaluated. The use of the primer along the top and bottom supports did appear to affect the adhesive strength between the spray-on material and steel supports. Comparatively for the three walls in the group, DW7, which did not use the primer, had the most peel back along the supports; while DW8 and DW9 exhibited only a slight peel back response. Out of the

nine walls retrofitted with the spray-on polyurea material, this retrofit system was selected for validation in full-scale dynamic experiments.

The two walls (DW10 and DW11) retrofitted with the trowel-on thermoset Grade 1 both failed at dynamic load level 3. Both walls failed when the retrofit tore along the centerline. No additional damage was found in the thermoset layer during the posttest inspection. After watching the footage from the high-speed video, it appeared that DW11 was very close to surviving the experiment. The retrofitted wall appeared to hesitate on the high-speed video for a millisecond or two at the maximum deformation point before the two sections of the CMU wall failed at the centerline. The retrofit system should have been evaluated at level 2, so a direct comparison could be made with the Grade 2 spray-on polyurea, but material and time constraints prevented any further subscale evaluations using the trowel-on thermoset material.

The two walls (DW12 and DW13) retrofitted with the unreinforced elastomeric films successfully mitigated the debris hazard subjected to dynamic load levels 3 and 4, respectively. DW12 used a spray-on adhesive to adhere the film to the CMU wall and DW13 used the trowel-on thermoset to apply the film to the wall. DW12 responded very well at dynamic load level 3, but problems were encountered during the application process. The film was torn at the bottom support, and an additional strip of film had to be added to strengthen the weakened area. To maintain symmetry on the wall, an additional strip was added to the top support. The double layer of material strengthened the retrofit at the supports, but questions were raised as to the validity of the experiment. DW13 responded well at level 4 and the application process was more efficient. The

majority of the CMU blocks on the top half of the wall lost faceshells, but the wall returned to the original position in line with the reaction structure after responding to the blast load. A variation of the retrofit systems used in DW12 and DW13 was selected for full-scale validation.

Wall DW14 was retrofitted with a ±45-deg fiber reinforced (Fabric B) elastomeric film applied to the wall using a trowel-on epoxy and successfully mitigated the debris hazard associated for dynamic load level 4. The retrofit performed well and was selected for further evaluation in the full-scale experiments.

Three of the four walls (BLS4, BLS5, BLS6, and BLS7) retrofitted with the unreinforced elastomeric film applied to the wall using a PSA successfully mitigated the debris hazard subjected to dynamic load levels 3, 5, and 6. The three walls that survived the airblast were very ductile deforming 0.312 to 1into the reaction structure. BLS6 and BLS7 were both evaluated at level 6 with mixed results. The same retrofit materials and application procedure was used for BLS6 that survived and BLS7 that failed at the bottom support when the film tore along the bottom anchor plate. The unreinforced elastomeric film applied with a PSA was selected for evaluation in the full-scale experiments.

Three of the four subscale dynamic experiments (BLS8, BLS9, BLS10, and BLS11) retrofitted with an elastomeric film reinforced with Fabric G in a ±45-deg orientation successfully demonstrated the effectiveness of the retrofit systems to mitigate the debris hazards for dynamic load levels 6, 7, 5, and 3, respectively. It is important to note that the reinforced films evaluated in the dynamic events used the extruded material and not

the laminated version. The failure of BLS9 does show that the strength of the system can be overcome, and debris along the failure line could become a hazard. The failure of BLS9 also highlighted the response of the fibers used as reinforcement in the film. It was interesting to note that individual fibers were pulled out of the bundles on both sides of the tear. One might expect an entire bundle to have sheared or failed at the boundary, but all of the edges along the tear on both halves had loose fibers. This indicated that the fibers were literally pulled out of the fiber bundles and film during deformation. The retrofit system used in BLS8, BLS9, BLS10, and BLS11 was also selected for further evaluation.

7. FULL-SCALE HE EXPERIMENTS

The results obtained in the subscale dynamic events were validated by conducting full-scale HE field experiments at an Air Force Base (AFB) in Florida. The full-scale HE dynamic experiments conducted in the research program are listed in Table 7.1. Four wall sizes were used in the full-scale experimental series depending on the availability of the reinforced concrete reaction structures at the AFB (Figure 7.1). The reaction structures used to house the CMU walls were built based on guidance received from sponsors funding the research program over the last ten years. All of the walls used in the full-scale experiments represented a hollow unreinforced CMU wall typically used in reinforced concrete or steel-framed structures. The first set of walls (Bay 1 and Bay 2), nominally 224 in. by 130 in. (569 cm by 330 cm), were 16 courses tall and 14 blocks wide (Figure 7.1a). An extension was placed on the top of Bay 1 or 2 on select experiments to raise the height to 192 in. (488 cm) (Figure 7.1b) and 24 courses tall. The second set of walls (Bay 3 and Bay 4), nominally 174 in. by 111 in. (442 cm by 282 cm), were 14 courses tall and 11 blocks wide (Figure 7.1c). Bays 3 and 4 were separated for select experiments as shown in Figure 7.1d for testing purposes. A fourth reaction structure, 120 in. by 120 in (305 cm by 305 cm) and 15 courses tall and 7.5 blocks wide (Figure 7.1e), was also used. The areas in the reaction structure used to anchor the retrofit systems on Bays 3 and 4 were primarily reinforced concrete, but there were two steel in-bed plates on the bottom support. The supports on Bays 1, 2, and 5 were all concrete.

Table 7.1. Test matrix for full-scale HE experiments.

Wall Label	Reaction Structure	Matrix	Reinforcement	Dynamic Load Level
FS1	Bay 2 and Extension	None	None	4
FS2	Bay 3	Spray-on Polyurea Grade 2	Fabric D at ±45 deg	3
FS3	Bay 4	Spray-on Polyurea Grade 2	Fabric E at ±45 deg	3
FS4	Bay 2	Spray-on Polyurea Grade 2	Fabric E at ±45 deg	2
FS5	Bay 3	Trowel-on Thermoset Grade 1	None	3
FS6	Bay 4	Trowel-on Thermoset Grade 2	None	2
FS7	Bay 3	Trowel-on Thermoset Grade 1	None	2
FS8	Bay 1	Trowel-on Thermoset Grade 1 & Thermoplastic Film	None	2
FS9	Bay 5	Trowel-on Thermoset Grade 1 & Thermoplastic Film	None	1
FS10	Bay 3	Trowel-on Thermoset Grade 1 & Thermoplastic Film	None	3
FS11	Bay 1 and Extension	Trowel-on Epoxy & Polyurethane Film	None	3
FS12	Bay 5	Trowel-on Epoxy & Elastomeric Film	Fabric D at ±45 deg	1
FS13	Bay 5	Trowel-on Thermoset & Elastomeric Film	Fabric F at ±45 deg	4
FS14	Bay 2 and Extension	PSA & Elastomeric Film	None	3
FS15	Bay 3	PSA & Thermoplastic Film	None	2
FS16	Bay 1	PSA & Elastomeric Film	None	4
FS17	Bay 3	PSA & Reinforced Elastomeric Film	Fabric F at ±45 deg	3
FS18	Bay 4	PSA & Reinforced Elastomeric Film	Fabric F at ±45 deg	4

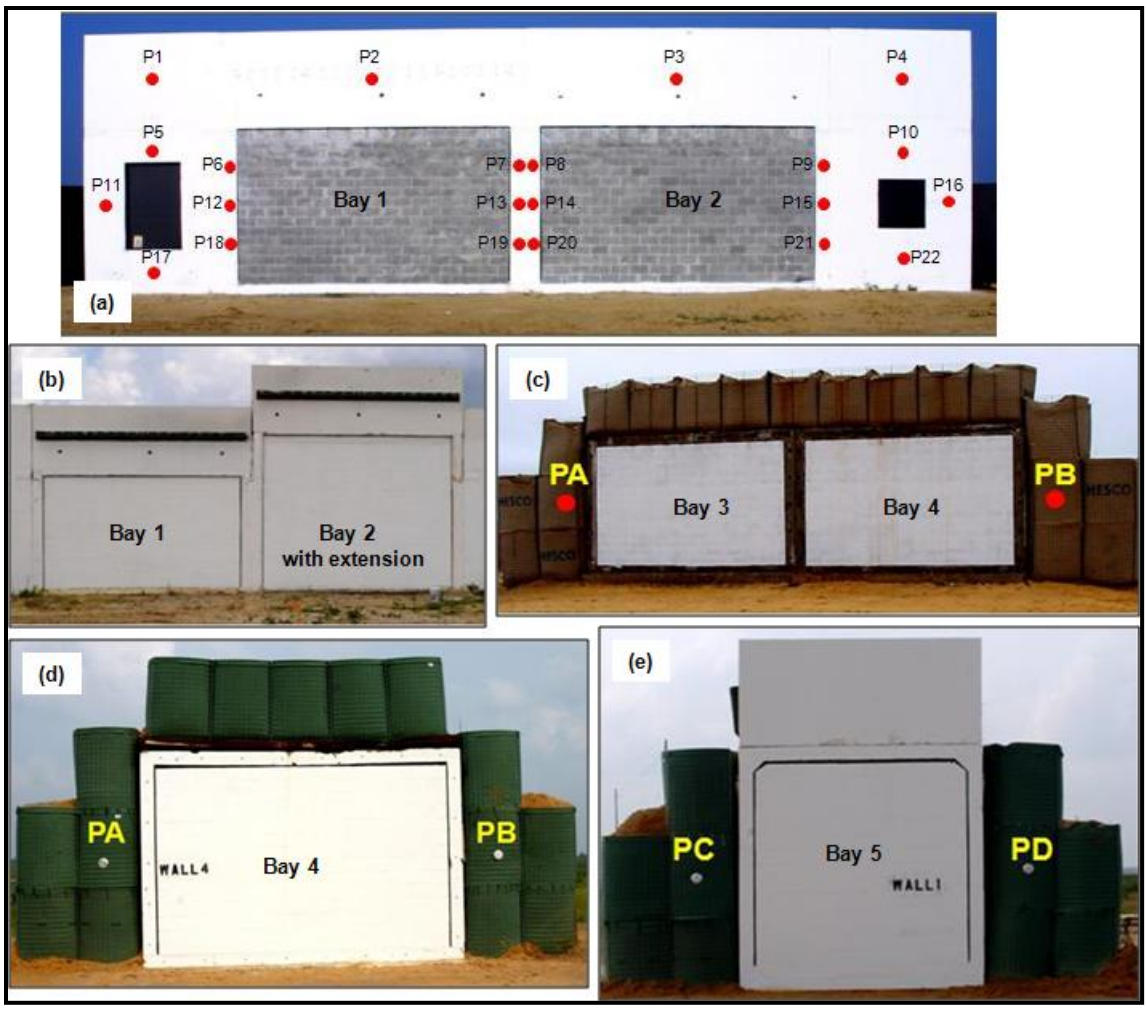

Figure 7.1. Full-scale CMU walls with gauge locations. (a) Bay 1 and Bay 2. (b) Bay 2 with extension. (c) Bay 3 and Bay 4. (d) Bay 3 and Bay 4 were separated for some experiments. (e) Bay 5.

The instrumentation plan for the full-scale experiments consisted of pressure gauges, lasers, accelerometers, deflection rods, still photography, and high-speed cameras. Data recovery consisted of 22 blast pressure gauges located on the reaction structure containing Bays 1 and 2 (P1-P22), two accelerometers used as deflection gauges (D1, D2) on each wall, and two high-speed digital video cameras. The 22 pressure gauges

documented the reflected pressure and impulse on the reaction structure (Figure 7.1a). Pressure gauges (PA, PB, PC, and PD) installed around Bays 3, 4, and 5 were placed in the earthen bins used to create clearing walls around the reaction structure (Figures 7.1c, d, and e). One pressure gauge was placed in the earthen bins at mid-height of the CMU wall on each side. Unless otherwise specified in the individual wall descriptions the two accelerometers, D1 and D2, were placed at the mid- and quarter-point wall heights to document the wall's deflection.

The reflected pressure was measured by Kulite Model XT-190SG pressure gauges with B-Screen filters to measure the reflected pressure on or around the reaction structures. Endevco Model 7270A accelerometers were used to measure acceleration, velocity, and deflection of the retrofitted wall as it responded to the blast load (Figure 7.2b). As shown in Figure 7.3c and d, two different mounts were used to attach the accelerometers to the wall. The pressure gauges and accelerometers were piezo-resistive transducers. The deflection measurements were monitored using an ERDC-built Model LS deflection gauge that consists of pinion-and-spur-gear driven potentiometer gauges (Figures 7.2a and b). When available an Accu-Range 4000 laser was used to measure the deflection at the center of the wall (Figures 7.3a and b). The data were transmitted over 22 AWG 4 conductor shielded mil spec cable and were recorded on 12-bit bipolar Pacific Instruments, Model 9830, TDR after the signal was amplified and conditioned using in-house instrumentation. The cable run from the test site to the instrumentation trailer located behind a berm was approximately 2,500 ft (762 m) away with an average loop resistance of 103 ohms. The cables were tuned to approximately

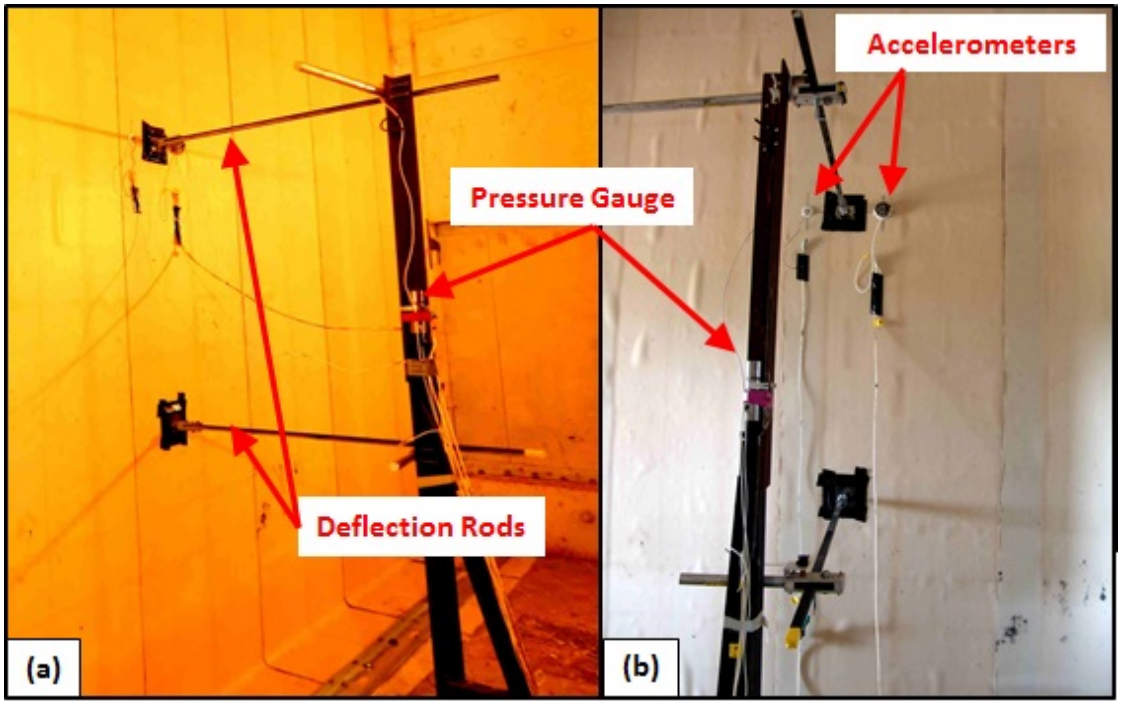

Figure 7.2. Instrumentation. (a) ERDC built Model LS deflection gauge that consists of pinion-and-spur-gear driven potentiometer gauges. (b) Endevco Model 7270A accelerometers were used to measure acceleration.

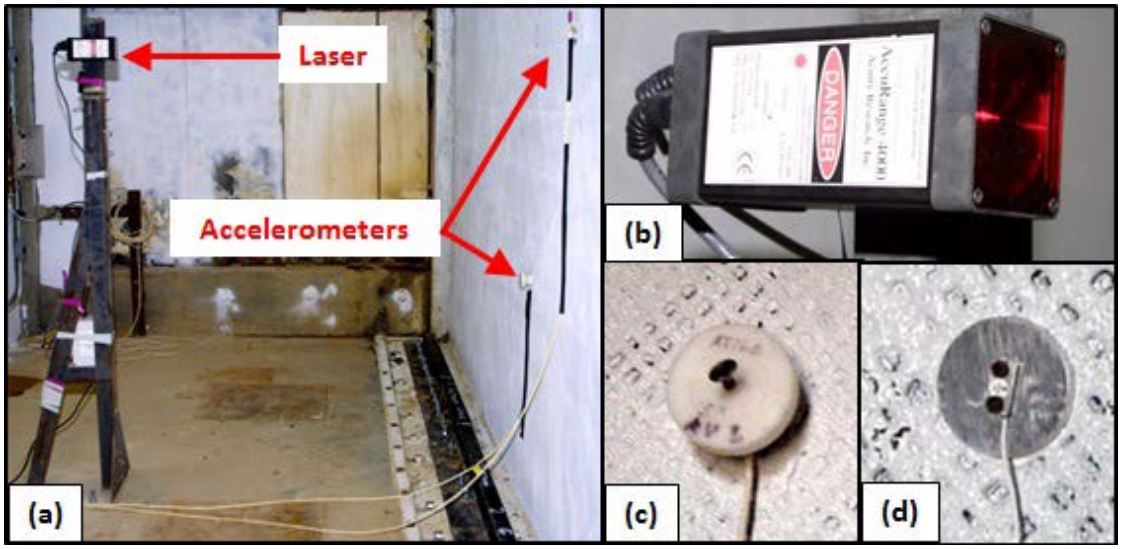

Figure 7.3. Instrumentation. (a) Laser and accelerometers. (b) AccuRange-4000 Laser. (c) Accelerometer mount 1. (d) Accelerometer mount 2.

10 kHz. The sample rate for the TDRs was set for two microseconds per point for the pressure and acceleration measurements, yielding a record time of –0.01638 to 0.2294 sec. The sample rate for the deflection measurements was set for 16 microseconds per point, yielding a record time of -0.122 to 1.835 sec. The different settings were required because the pressure wave moves much faster than the specimens can react to it.

7.1 Unretrofitted CMU Wall (FS1)

The first full-scale experiment evaluated at the AFB was an unretrofitted (baseline) CMU wall. The baseline wall was used to validate the secondary debris hazard associated with a blast load that was previously observed in the subscale HE and BLS experiments. The wall was constructed in the largest reaction structure available, Bay 2 with the extension (Figure 7.4a). A thin metal desk and a mannequin sitting in a steel chair were placed behind the test wall (Figure 7.4b).

Figure 7.4. FS1. (a) Pretest view of exterior. (b) Interior view.

As expected, the CMU wall was completely destroyed at dynamic load level 4. A few pieces of debris were found outside the reaction structure, but 99% of the debris was inside the structure. The wall's response would have been deadly for occupants (Figure 7.4). The mannequin was completely covered with full CMU blocks (Figures 7.5a and b), and the steel chair was flattened under the weight of the debris. Frames from the high-speed video are displayed in Figures 7.6a through d. The CMU wall started to crack at the top of the desk. In Figures 7.6c and d, the wall has translated into the reaction structure; and the test site outside the reaction structure became visible in Figure 7.6d. The debris was removed, and the mannequin was retrieved as shown in Figure 7.7a through d.

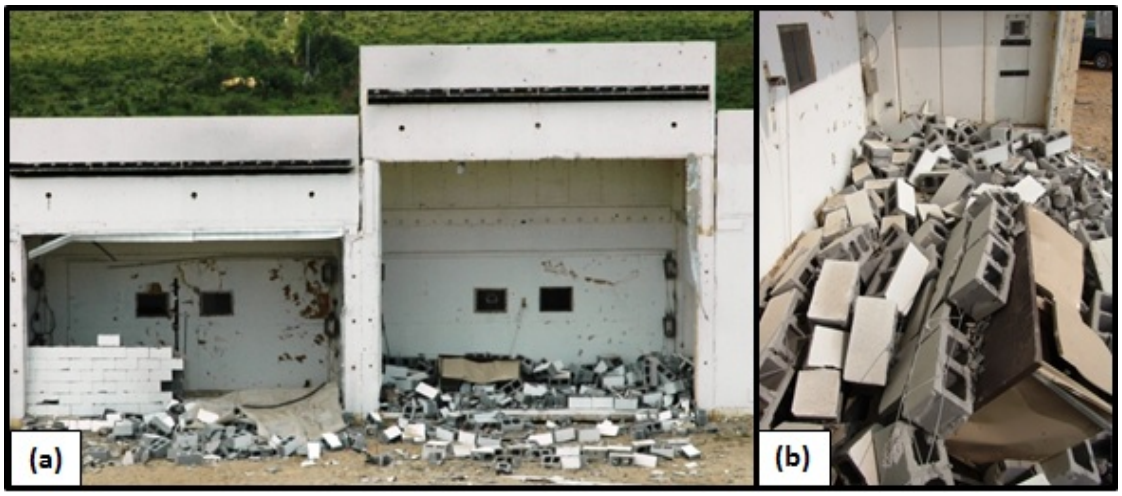

Figure 7.5. FS1. (a) Posttest exterior view. (b) Interior view.

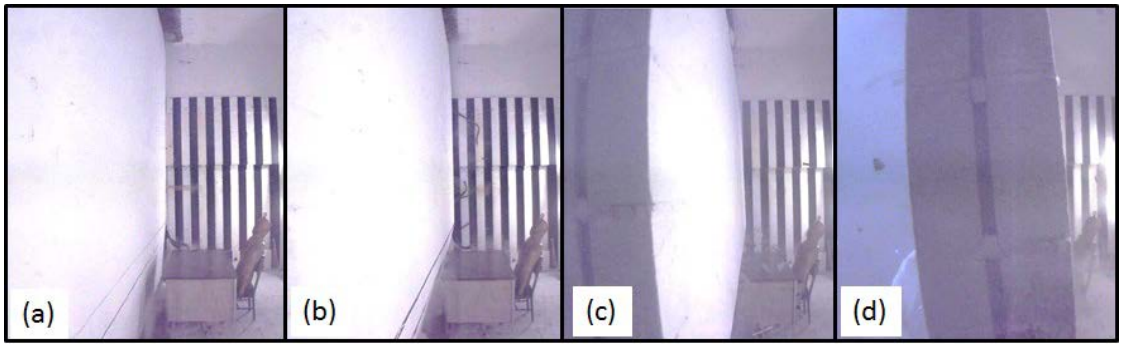

Figure 7.6. FS1: Frames from high-speed video. (a) First crack develops at desk height. (b) Wall deflection before the desk is impacted. (c) CMU wall has deflected completely into structure. (d) CMU wall has impacted test mannequin and camera views exterior of structure.

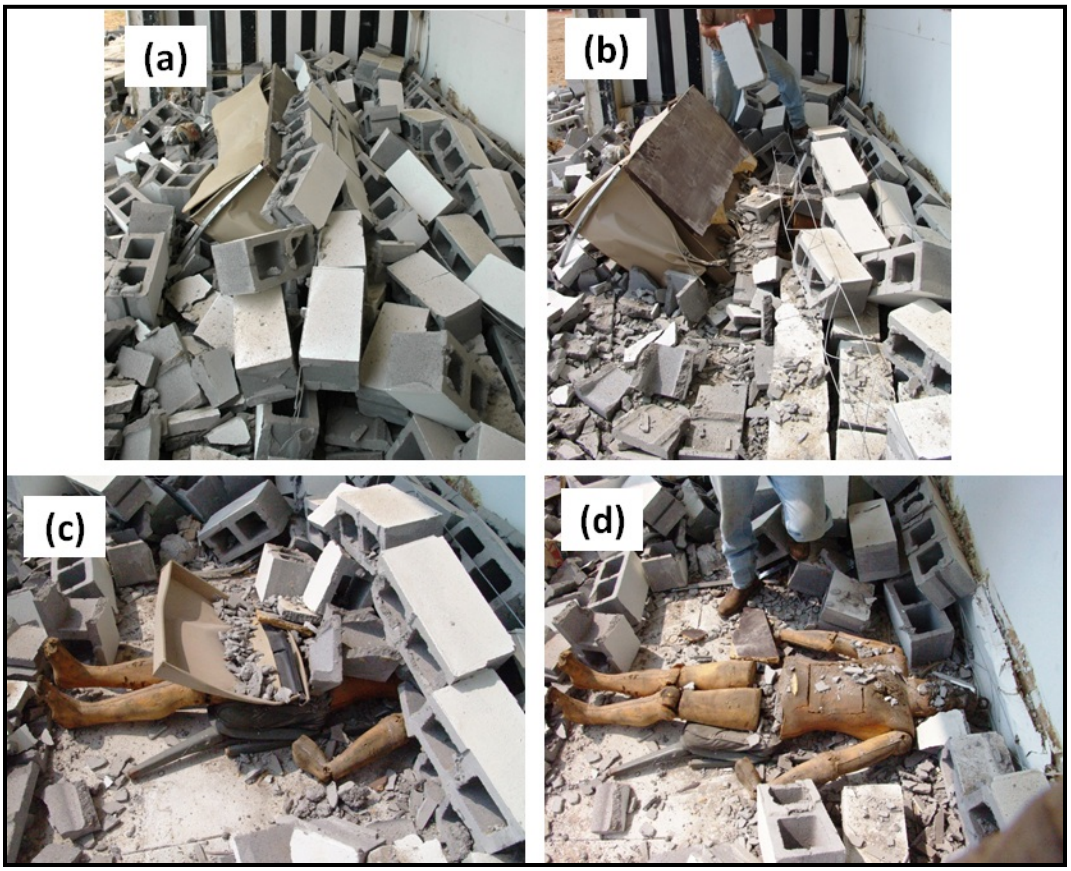

Figure 7.7. Debris removed to uncover mannequin. (a) Orginal debris pile. (b) Blocks removed from area around desk. (c) Desk removed. (d) Mannequin found wih flattened steel chair.

7.2 Fiber-Reinforced Spray-on Polyurea Retrofits (FS2-FS4)

Three full-scale dynamic experiments on CMU walls retrofitted with fiber-reinforced spray-on polyurea retrofits were conducted at a remote test site in Florida. Two separate events were used to evaluate three fiber-reinforced spray-on retrofitted CMU walls. The 45-deg fiber-reinforced polyurea was the most impressive spray-on retrofit system evaluated in the subscale dynamic experiments, so it was selected for validation in the full-scale field events. The first full-scale field event evaluated walls FS2 and FS3 (Figure 7.8). Walls FS2 and FS3 were constructed in Bays 3 and 4, respectively. Both walls were 174 in. wide by 111 in. tall. These experiments were conducted at dynamic load level 3. The second field event evaluated wall FS4 at the reduced dynamic load level of 2. Wall FS4 was constructed in Bay 2 and was 224 in. wide by 130 in tall. Construction details for all three walls are in Section 4.2.3.

Figure 7.8. Pretest photograph of walls FS2 and FS3.

7.2.1 FS2

Wall FS2 was retrofitted with a reinforced spray-on elastomer. First, eight passes of Grade 2 spray-on polyurea were applied to the wall followed by a layer of Fabric D applied with the fibers oriented ±45 deg relative to the horizontal mortar joints of the CMU wall. The reinforcement was applied to the wall by technicians using a PSA that was applied to one side of the reinforcement during production. The fabric was encapsulated by eight additional passes of the spray-on polyurea. The spray-on polyurea and fabric overlapped the top and bottom supports that created an adhesive bond. The wall was prepared according to the application procedures discussed in Section 4.5. However, the top and bottom supports where damp when the spray-on elastomer was applied. Due to the extremely wet conditions at the field site and the tight test schedule, the supports could not be completely dried before the retrofit was applied.

Wall failure did not occur during the initial response. High-speed video indicated that the peel-back failure at the top support occurred after the initial loading and during the rebound of the wall (Figures 7.9a through c and Figures 7.10a through e). The adhesive bond was inadequate to maintain the retrofit integrity at the top support. The lack of adhesion could be attributed to the condition of the supports during the application of the retrofit. A 3-ft portion of the retrofit located at the bottom left corner support also peeled back. Although the retrofit system failed at the supports (Figure 7.10), no CMU wall debris was discovered inside the reaction structure. Posttest inspection of the material indicated that the liner had no visible damage and peeled off

the reaction structure as one entity (Figures 7.11 and 7.12a and b). None of the CMU blocks remained adhered to the layer of polyurea.

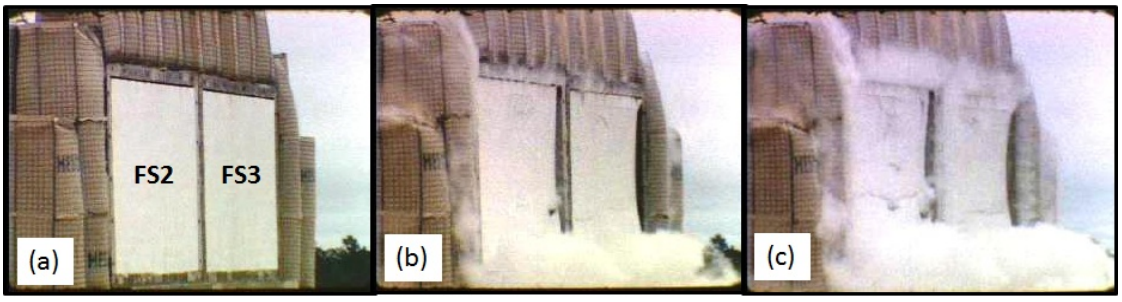

Figure 7.9. FS2 and FS3: High-speed video from exterior camera. (a) Pretest camera view. (b) Blast pressure impacts walls. (c) CMU blocks begin to disengage from retrofit.

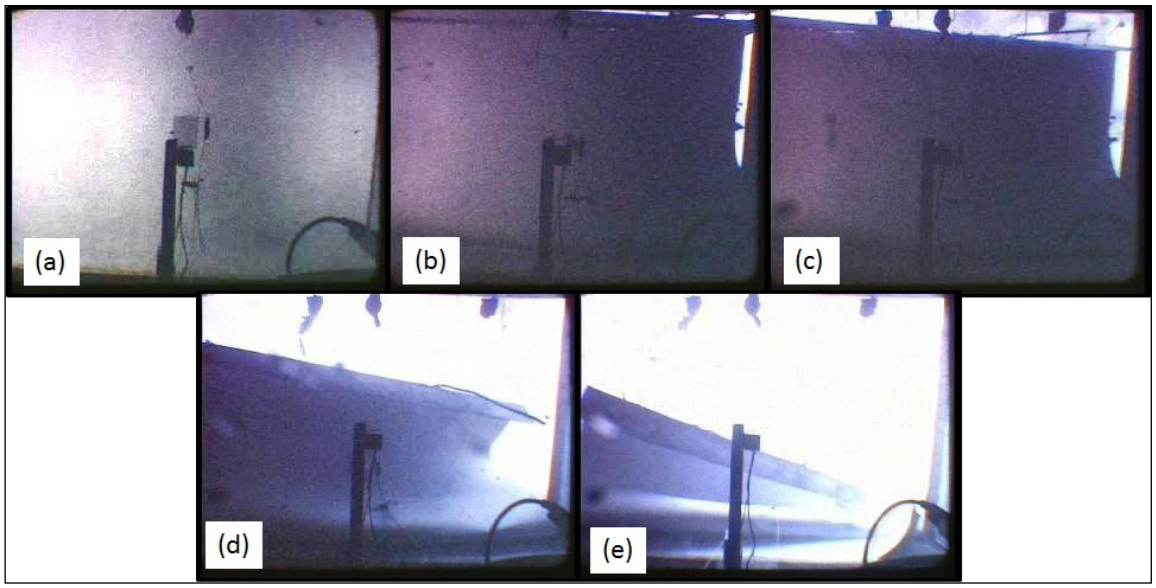

Figure 7.10. FS2: Frames from high-speed video. (a) Wall deflected into structure. (b) Retrofit begins to peel off top support during rebound. (c) Retrofit disengages from right to left. (d) Retrofit completely disengaged. (e) Weight of retrofit falling down pulls the retrofit off the bottom support in the right corner.

Figure 7.11. Posttest photograph of walls FS2 and FS3.

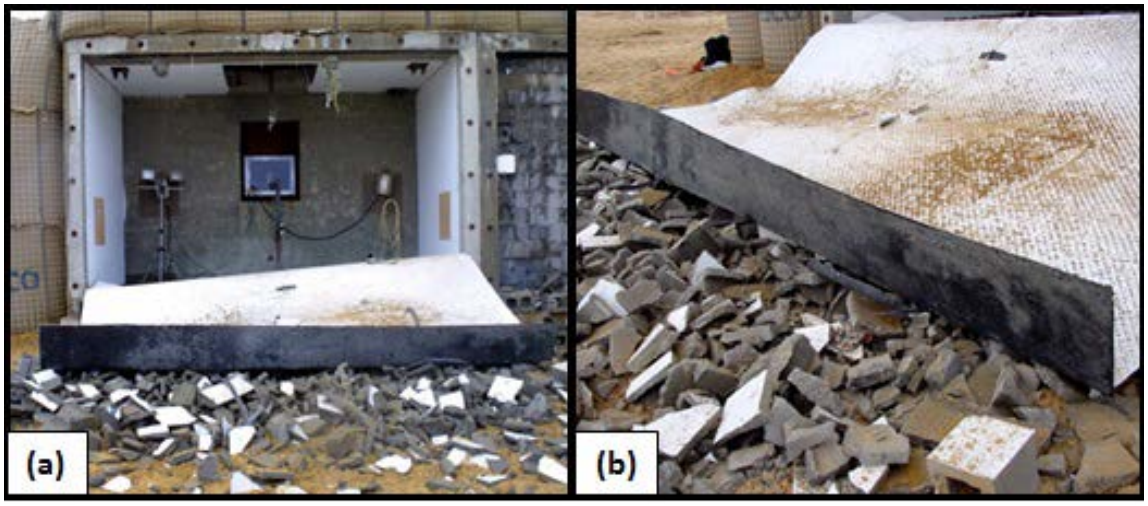

Figure 7.12. FS2. (a) CMU debris and retrofit coating was outside the reaction structure. (b) Retrofit failed due to loss of adhesion at the top support.

7.2.2 FS3

The retrofit procedure for wall FS2 was repeated on wall FS3. The only difference between the two walls was that fiber reinforcement Fabric E was used on FS3. The clear area between the fiber bundles was slightly larger on Fabric D, but the tensile strength per fiber bundle was the same. First, eight passes of Grade 2 spray-on polyurea were applied to the wall followed by a layer of Fabric E applied with the fibers oriented ±45 deg to the horizontal mortar joints of the CMU wall. The reinforcement was applied to the wall by technicians using a PSA that was applied to one side of the reinforcement during production. The fabric was encapsulated when eight additional passes of the spray-on polyurea were applied over the fabric. The spray-on polyurea and fabric overlapped the top and bottom supports, creating an adhesive bond. The retrofit system was applied to wall FS3 before the heavy rain began on site.

The retrofit performed well, allowing none of the CMU wall debris to enter the reaction structure (Figure 7.13a). The reinforced elastomeric material was not breached, and almost all of the CMU blocks lost their front face shells. Only six and a half blocks remained whole and attached to the polyurea material (Figure 7.13b). The polyurea did not appear to pull back at the top or bottom supports. The accelerometer mounted at the center of the retrofitted CMU wall produced a maximum deflection of 0.397.

7.2.3 FS4

Wall FS4 was constructed in Bay 2 and it was also retrofitted with a reinforced spray-on elastomer (Figure 7.14). First, eight passes of Grade 2 spray-on polyurea were applied to the wall, followed by a layer of Fabric E applied with the fibers oriented

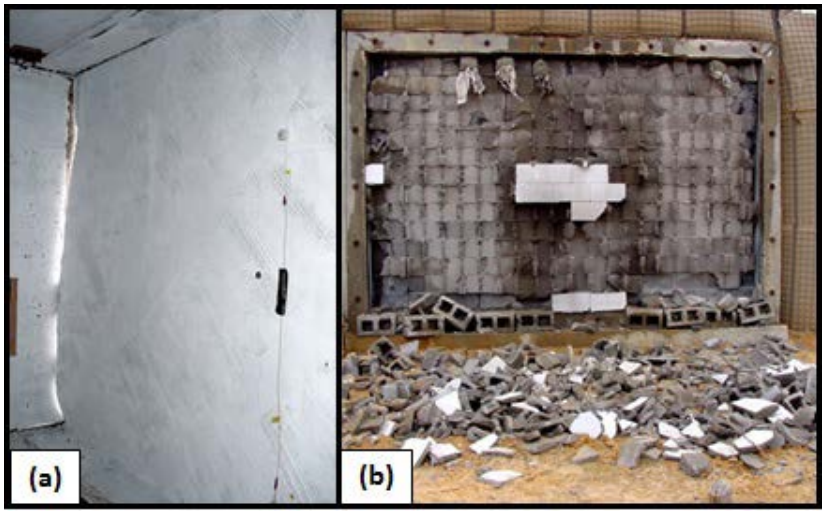

Figure 7.13. FS3. (a) Posttest interior view. (b) CMU debris found outside the reaction structure.

Figure 7.14. Pretest exterior view of retrofitted CMU walls FS4 and FS8.

±45 deg to the horizontal mortar joints of the CMU wall. The reinforcement was applied to the wall by technicians using a PSA that was applied to one side of the reinforcement during production. The fabric was encapsulated when eight additional passes of the spray-on polyurea were applied over the fabric. The spray-on polyurea and fabric overlapped the top and bottom supports creating an adhesive bond. Anchor plates were

added to the top and bottom supports prior to testing in the full-scale experiment to prevent a peel-back failure of the retrofit system (Figure 7.15a). The plates were not applied directly at the wall/support interface but instead were moved 4 in. away, allowing the material to peel back a defined distance before the mechanical connections would engage (Figure 7.15b). Anchor bolts were used to secure the plates to the concrete supports. Wall FS4 was exposed to a reduced dynamic load of 2.

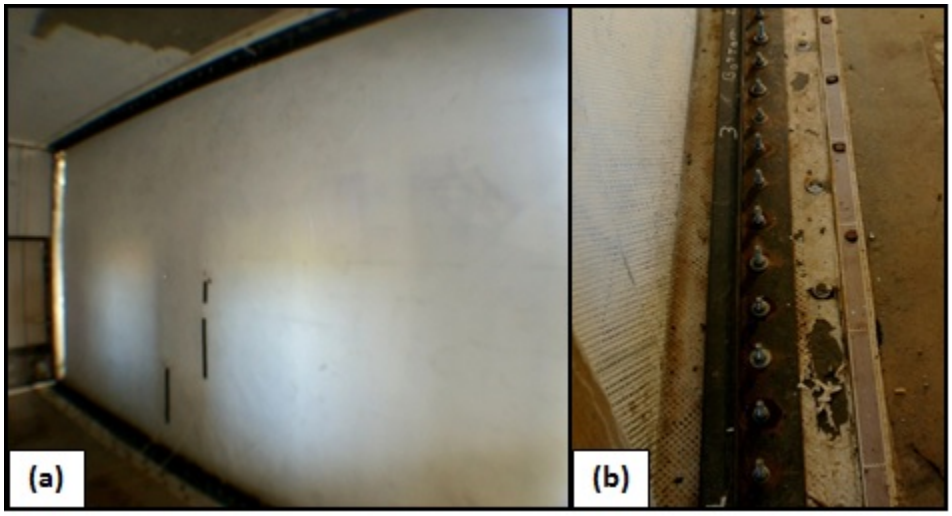

Figure 7.15. FS4. (a) Pretest interior view.
(b) Anchor plates on top and bottom supports.

The retrofit performed well, allowing none of the CMU wall debris to enter the reaction structure (Figure 7.16a). The reinforced elastomeric material was not breached, and almost all of the CMU blocks lost their front face shells. Only 21 blocks remained whole and attached to the polyurea (Figure 7.16b). The reinforced spray-on polyurea system did exhibit evidence of peel back. However, the mechanical connections

prevented additional peel back and failure of the retrofit system. No visible damage was found on the liner during the posttest inspection, and no tears were found. The accelerometer at mid-height indicated a maximum deflection of 0.52. However, high-speed video indicated that the maximum deflection occurred at a height approximately 3.5 ft. from the floor. Unfortunately, the magnitude of the maximum deflection at this point could not be determined from the high-speed video.

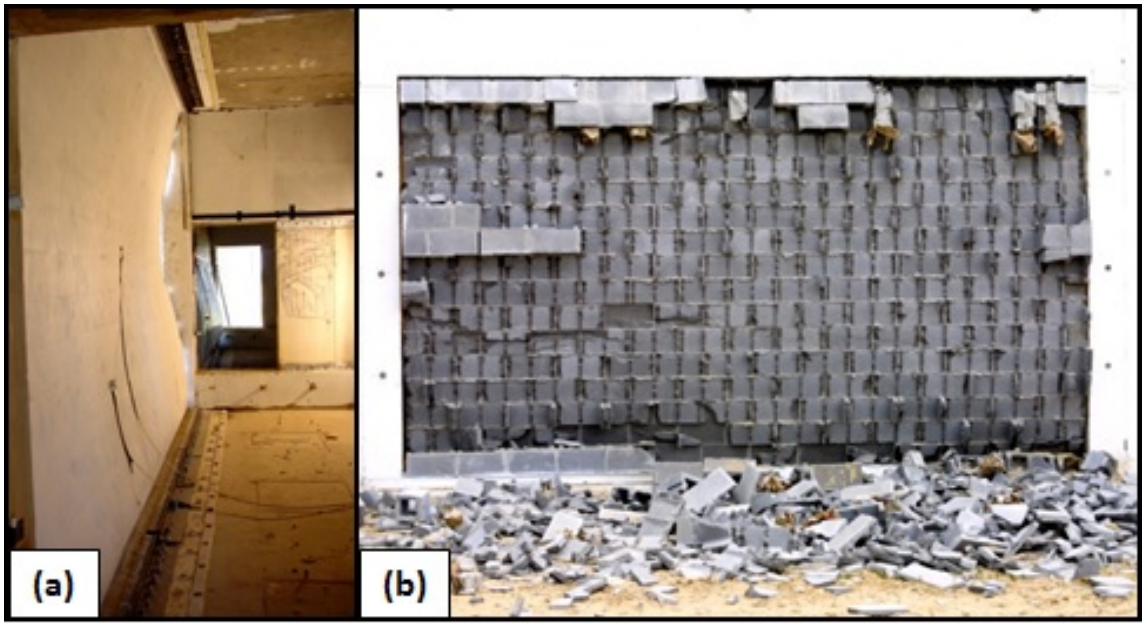

Figure 7.16. FS4. (a) Posttest interior view.
(b) Posttest exterior view.

7.3 Trowel-on Thermoset Retrofit (FS5-FS7)

7.3.1 FS5

Wall FS5 was built in Bay 3 and retrofitted with a trowel-on thermoset. The application procedure used to apply the materials was discussed in Section 4.6. The CMU wall construction and instrumentation plan for FS5 differed from the plan used in all of the other full-scale experiments. The CMU wall built in Bay 3 did not leave a gap on either side or at the top of the wall so that arching forces could be developed during the wall's response. The dashed black lines in Figure 7.17a are slightly outside of the perimeter of the CMU wall and mark the seam between the concrete reaction structure and the wall. The pressure gauges were placed in fully grouted CMU blocks on each side of the test specimen instead of in the concrete reaction structure or HESCO containers (extra large sand bags) surrounding the CMU wall. Then the steel plates used to secure the deflection rods were bolted to the CMU blocks on the test wall. The steel plates were then covered with the trowel-on thermoset as the retrofit was applied to the test specimen (Figure 7.17b). All of the instrumentation was placed along a horizontal line mid-height of the wall.

The retrofit system for FS5 performed well at dynamic load level 3 and allowed no debris to enter the reaction structure (Figure 7.17a). The pressure gauge mounts, which consisted of steel pipe with the gauge mount secured on the end, were fully grouted in two CMU blocks and are visible in the posttest photograph in Figure 7.17b. The

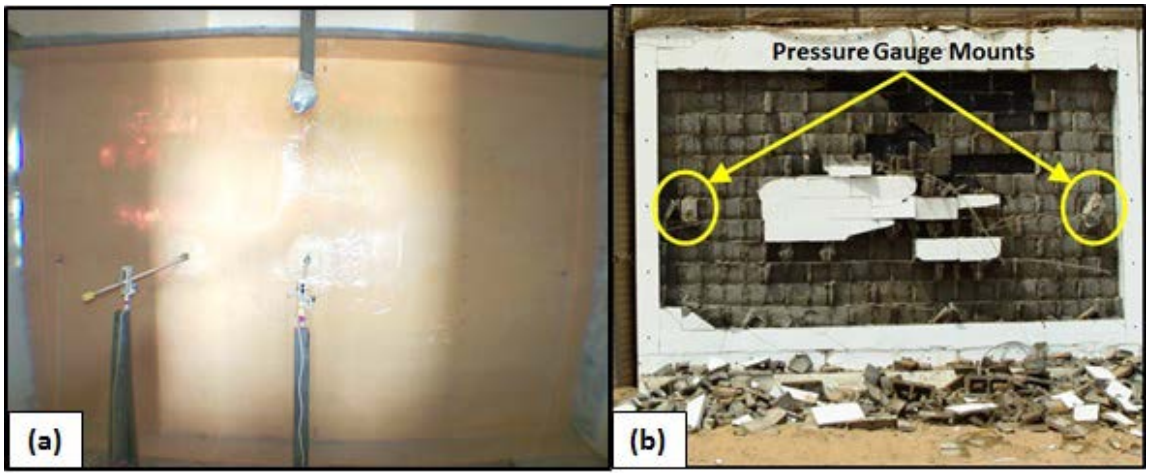

Figure 7.17. FS5. (a) Posttest interior view. (b) Posttest exterior view.

mechanical deflection rod placed at the quarter point along the mid-height line of the wall recorded a max deflection of 0.37. The deflection rod placed at the center point along the mid-height wall line recorded a maximum deflection of 0.42.

7.3.2 FS6 and FS7

Walls FS6 and FS7 were constructed in Bays 4 and 5, respectively (Figure 7.18a). Both walls were constructed with gaps between the sides of the CMU wall and the reaction structure and a 1-in. gap at the top support. Wall FS7 was retrofitted with the Grade 1 trowel-on thermoset material used in FS5 (Figure 7.19a). FS6 was retrofitted with a more economical version Grade 2 of the trowel-on thermoset (Figure 7.18b). The alternate version had a very loud (likened to cooked cabbage) odor that should be considered when designing for use. The very hot and humid conditions at the field site may have intensified the odor associated with the material. The procedure used to apply the materials was discussed in Section 4.6.

FS6 and FS7 both failed at dynamic load level 2 when the trowel-on thermoset layer peeled off the top supports (Figure 7.19b). The high-speed cameras setup to capture the walls' response failed to trigger, so the wall response must be determined from instrumentation and posttest inspection of the debris. Posttest inspection of the interior of the reaction structure suggested that the material peeled off the supports during the

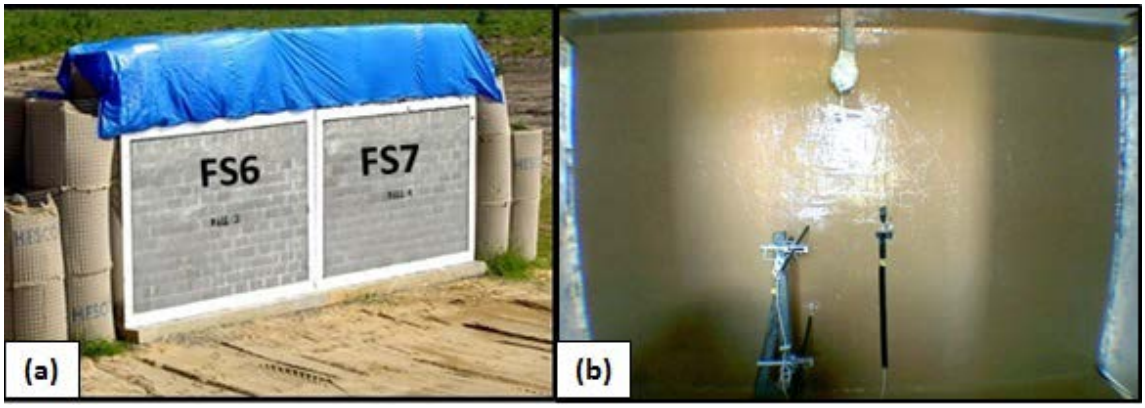

Figure 7.18. FS6 and FS7. (a) Pretest exterior view. (b) Pretest interior view of FS6.

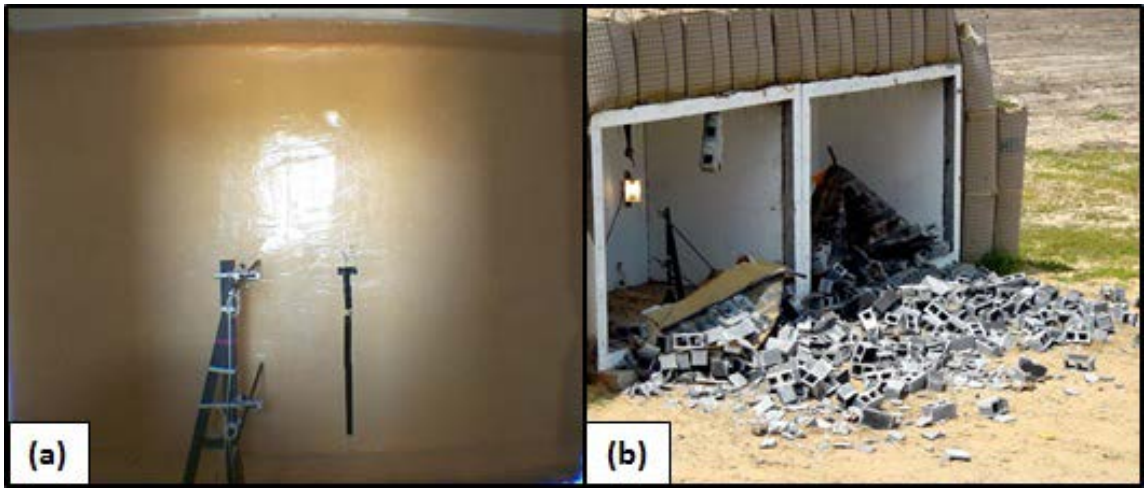

Figure 7.19. FS6 and FS7. (a) Pretest interior view of FS7.
(b) Posttest exterior view of FS6 and FS7.

rebound phase of the response for FS6, since the retrofit layer was found outside the threshold of the reaction structure (Figure 7.20a). Data from the center mechanical deflection gauge indicated that the wall initially deformed 0.493 into the reaction structure and then rebounded to over 0.639. Deflection measurements at the quarter point also indicated that the wall deformed 0.674 into the structure, and then rebounded

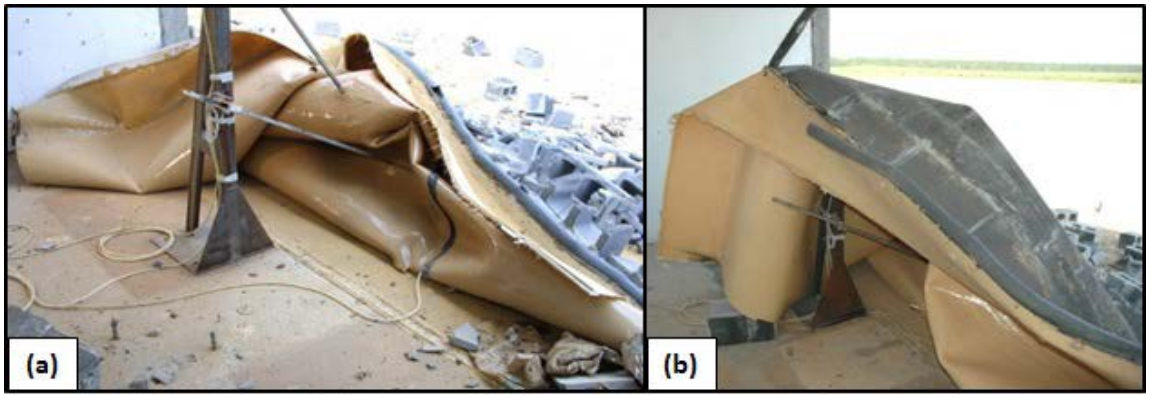

Figure 7.20. FS6 and FS7. (a) Posttest view of failed retrofit of FS6. (b) Posttest view of failed retrofit of FS7.

to over 0.776. The thermoset layer from FS6 was removed from the debris, and samples were obtained from the material for quality inspection.

Details from the inspection of FS7 did not clearly indicate when the retrofit peeled off the support. A minimal amount of debris was found inside the structure, and most of the CMU blocks were no longer attached to the liner, which typically indicates that the retrofit failed during the rebound. However, the liner was found inside the reaction structure, which would be hazardous to occupants (Figure 7.20b). The quarter-point

and center mechanical deflection gauges both exceeded the maximum deformation measurements, which would also indicate that the wall failed during the initial wall response. Voids in the thermoset layer were also discovered in both materials during the posttest inspection (Figure 7.21b). The appearance of linear strips that peeled away from the liner in Figure 7.21a may indicate that the trowel-on material did not bond to itself during the application process creating weak points in the material. The linear strips were equivalent to the size of the notches on the trowel. Although these defects were identified, it appeared that the defects did not initiate failure. The liner peeled off the concrete support cleanly leaving no thermoset remnants on the concrete surface or concrete on the thermoset material.

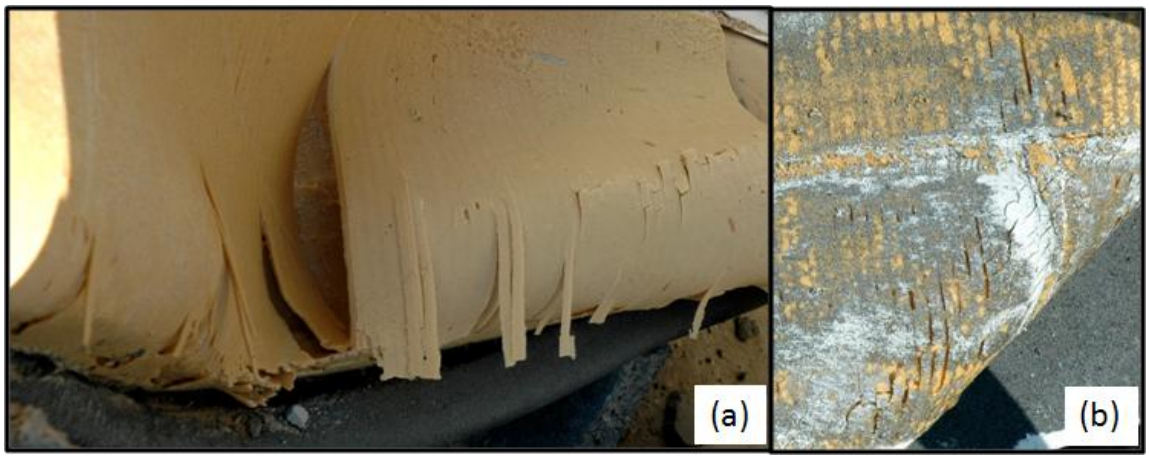

Figure 7.21. Defects in trowel-on layer on Walls FS6 and FS7. (a) Material did not adhere to itself very well. (b) Voids found in the trowel-on material.

7.4 Unreinforced Film and Trowel-on Polymer Adhesive (FS8-FS11)

7.4.1 FS8

Wall FS8 was built in Bay 1 and retrofitted with a trowel-on thermoset coupled with a thermoplastic film (Figures 7.22a and b). The retrofit was anchored to the floor and ceiling with mechanical anchor plate System 2. The application procedure for the trowel-on thermoset and thermoplastic retrofit system was discussed in Section 4.7.2.

The response of the CMU wall to dynamic load level 2 documented the success of the retrofit system (Figures 7.23a and b). The retrofit contained all of the wall debris allowing no debris to enter the reaction structure. Damage to the exterior face of the CMU wall was limited to loss of the CMU block face shells at the bottom corners of the wall and cracking along the mortar joints. The wall had a peak deflection at mid-span of approximately 0.365 to 0.457. Forty-six of the blocks or 21% of all the blocks completely disengaged from the retrofit material along the top right section of the wall

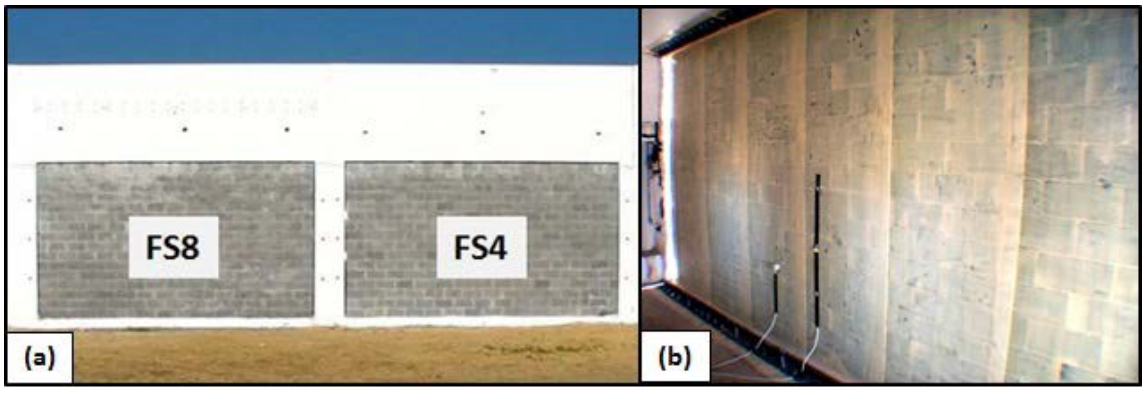

Figure 7.22. FS4 and FS8. (a) Pretest exterior view. (b) Pretest interior view of Wall FS8.

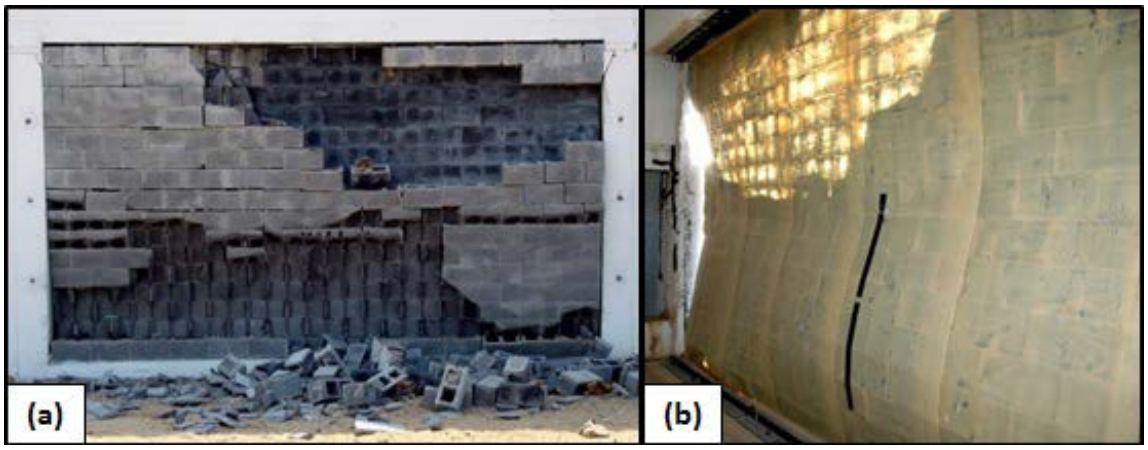

Figure 7.23. FS8. (a) Posttest exterior view. (b) Sunlight left a glow on the retrofit where the blocks were completely lost.

(Figure 7.23a). Sixty-one blocks or 27% of the blocks from the mid-height down lost the front face shells of the CMU blocks, while the back face shell remained adhered to the retrofit material (Figures 7.24a and b). About 48 of the CMU blocks became debris due to the response to the blast event. Looking from the interior of the reaction structure in Figure 7.23b, the sunlight highlights the area where all of the CMU blocks were lost. No tears were found on the thermoplastic film during the posttest inspection.

A heavy duty anchor system was used in this experiment to prevent a peel back failure at the support. The anchor plates were constructed in 8-ft lengths to make the plates light enough for three people to install the system. A structural tube was welded to the short leg of the angle to prevent the retrofit from tearing along the angle edge (Figure 7.25a). The anchor plates performed well, the bolts remained engaged at the

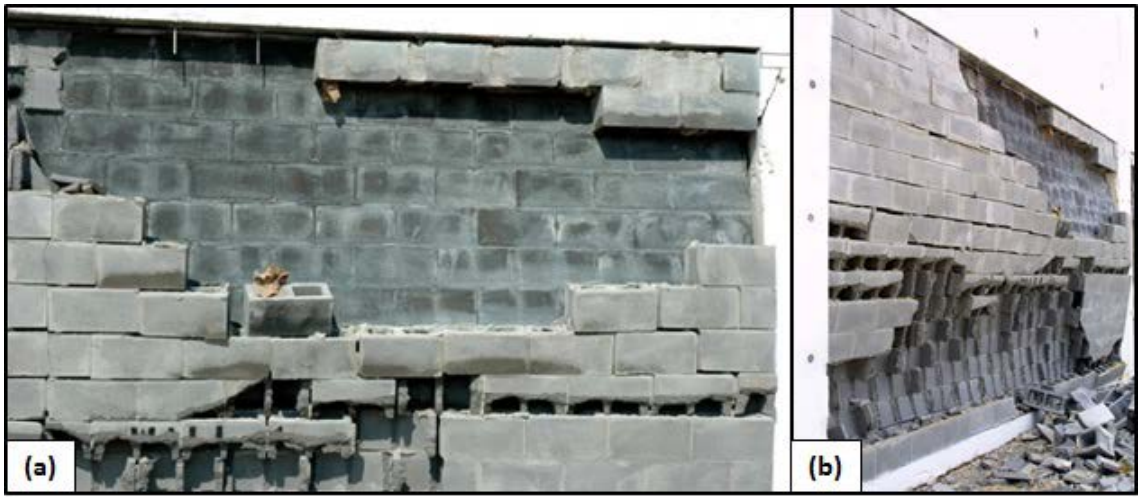

Figure 7.24. FS8. (a) No block remnants remained attached to the top right corner of the retrofit. (b) Face shells remained adhered to the trowel-on material and film from mid-height down across the bottom of the wall.

support, and the retrofit material did not tear along the anchor plate edge. Posttest observations and photographs of the supports showed that the material did not peel back to the anchor plates along the top or bottom supports (Figures 7.25a and b).

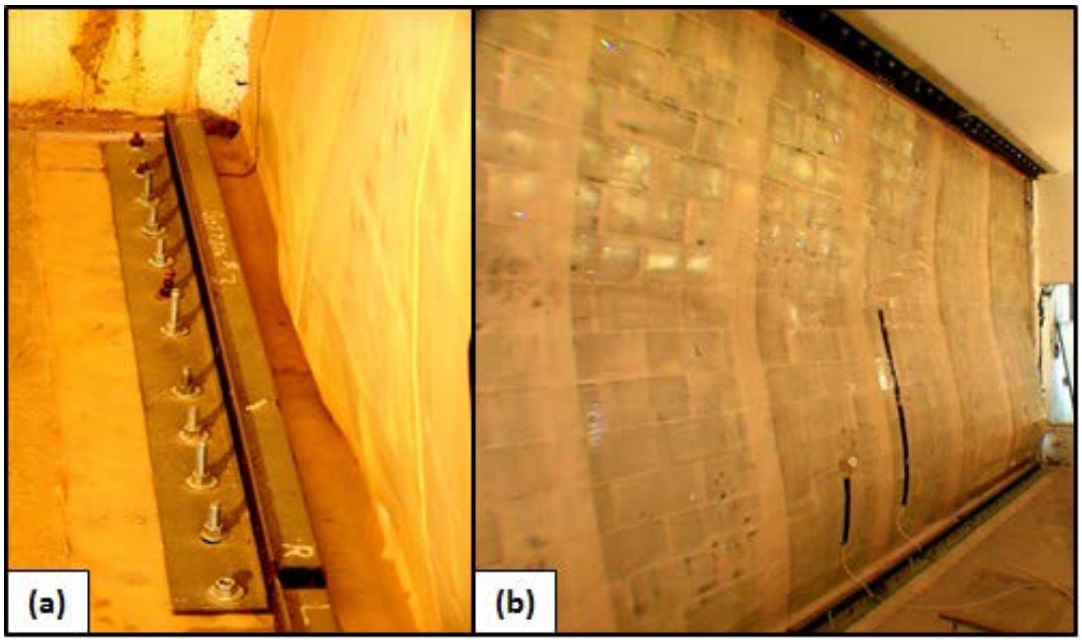

Figure 7.25. FS8. (a) Posttest view of retrofit supports. (b) Posttest view of top and bottom retrofit anchors.

7.4.2 FS9

Wall FS9 was built in Bay 5, and the trowel-on thermoset and thermoplastic film materials, application procedure, and retrofit anchor system used in FS8 were duplicated (Figures 7.26a and b). FS9 was subjected to a reduced dynamic load of 1 and the retrofit system performed well during the blast event. None of the debris entered the reaction structure, and 94% of the CMU blocks remained in the wall plane (Figure 7.27a). Only seven blocks or 6.2% of the face shells were damaged during the blast (Figure 7.27b). However, there were numerous visible cracks in the CMU wall. No visible damage of the film was discovered. The film peeled off at the top right corner of the wall, but the anchor system prevented the material from peeling off the support. Posttest inspection of the CMU wall indicated that the wall experienced arching effects during the initial

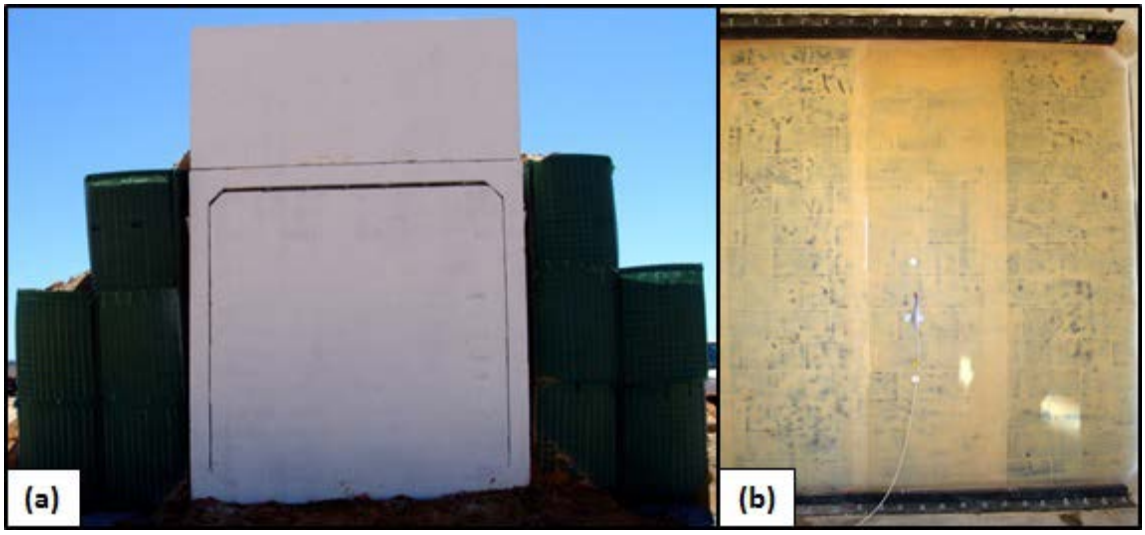

Figure 7.26. FS9. (a) Pretest exterior view. (b) Pretest interior view.

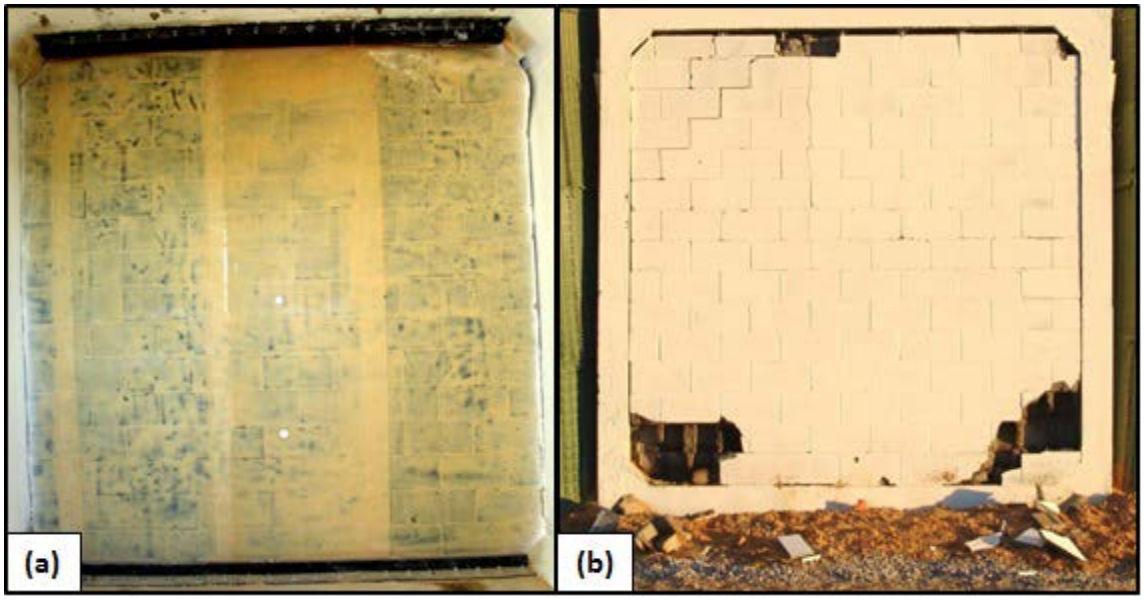

Figure 7.27. FS9. (a) Posttest interior view. (b) Posttest exterior view.

response to the blast load. The block damage and diagonal crack pattern from the bottom corners were a clear indication that some of the load was transferred to the reaction structure (Figure 7.28a). There was also a vertical crack extending from the broken block

on the top course that extended down the wall to the diagonal crack. The air blast produced from the explosive event or the wall dragging along the side of the reaction structure forced the film to disengage from the CMU wall at the top right corner as seen in Figure 7.28b.

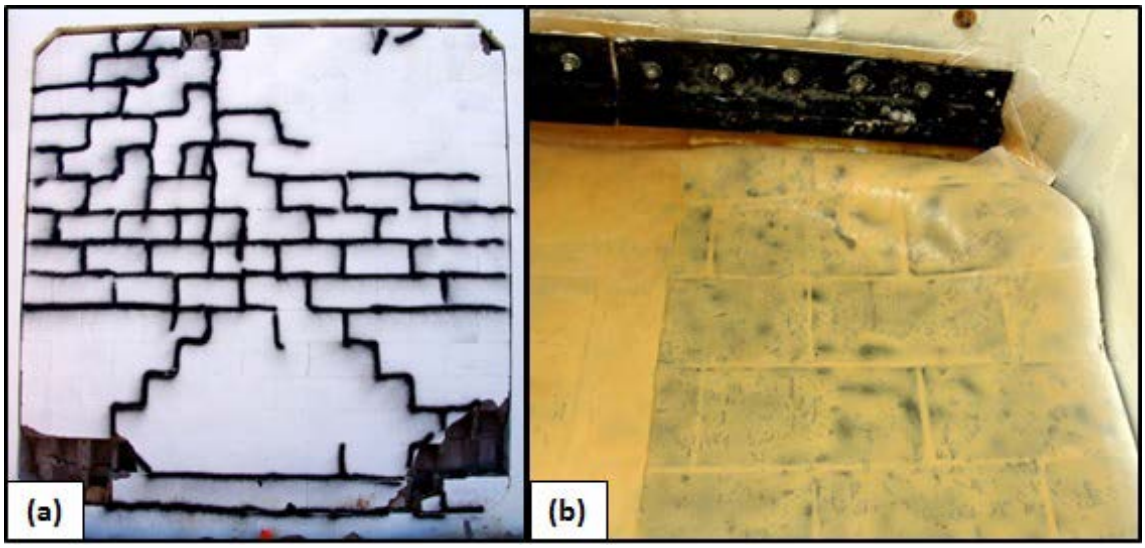

Figure 7.28. FS9. (a) Crack pattern in CMU wall outlined with black paint. (b) Retrofit material disengaged from CMU in top right interior corner.

7.4.3 FS10

Wall FS10 was built in Bay 3, and the trowel-on thermoset and thermoplastic film materials and application procedure used in FS8 and FS9 were duplicated (Figures 7.29a and b). The mechanical connection used to secure the retrofit materials was changed from System 2 to System 3. A thin-wall steel stud member was used instead of the robust steel anchor plate, and the Hilti anchor bolts were replaced with Red Head concrete bolts (Figure 7.30a). A single continuous steel stud member was not installed;

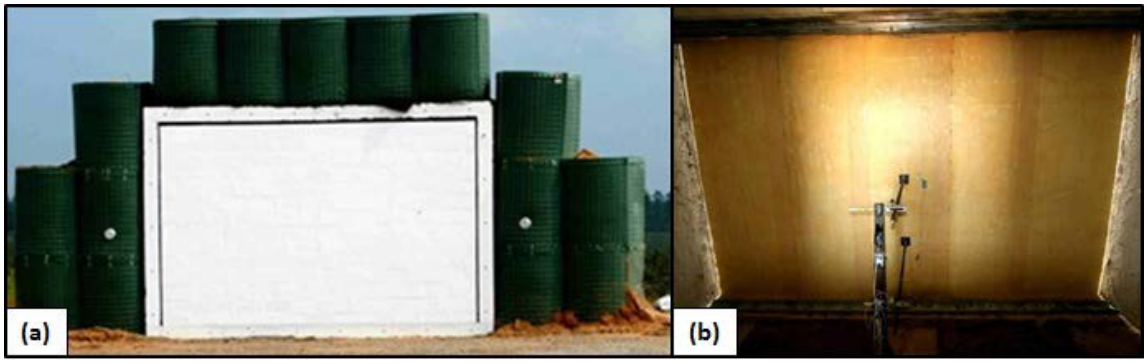

Figure 7.29. FS10. (a) Pretest exterior view of Bay 3. (b) Pretest interior view.

instead, three pieces were used to cover the full length of the wall. Two small sections were used on the right and left sides of the support, and a longer piece was used to cover the center of the wall to prevent a seam or joint at the center of the wall support (Figure 7.30b). The wall was subjected to dynamic load level 3, which was larger than the dynamic loads used on FS8 or FS9.

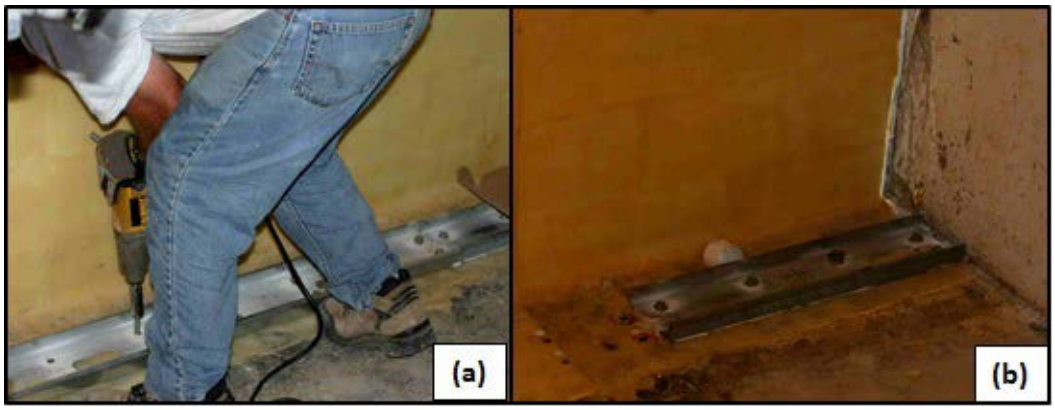

Figure 7.30. Anchor installation. (a) Concrete bolts installed with impact wrench. (b) One of three pieces of the steel studs used to anchor bottom support.

The response of the CMU wall to load level 3 documented the success of the retrofit system. The retrofit prevented debris originating from the CMU wall from entering the structure (Figure 7.31a). Figure 7.32a through d illustrate the stages of wall response under the blast load. The blast wave forced the thermoplastic film to disengage from the trowel-on thermoset at the top support (Figures 7.32b and c). The area continued to expand as the wall was loaded. The small circles located at the mortar joints in Figure 7.32d are areas where the trowel-on thermoset was stretched past its limit; however, the film was undamaged.

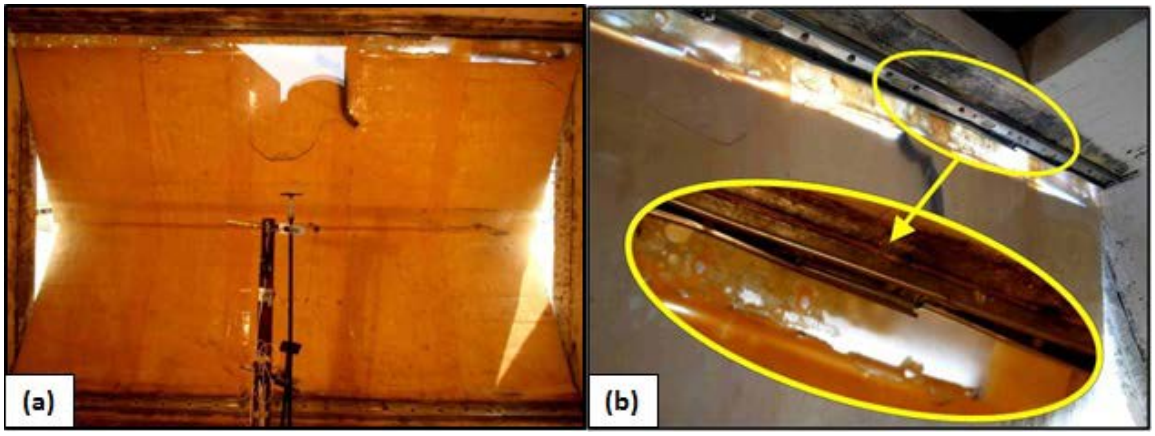

Figure 7.31. FS10. (a) Posttest interior view. (b) Top anchor was deformed during wall response.

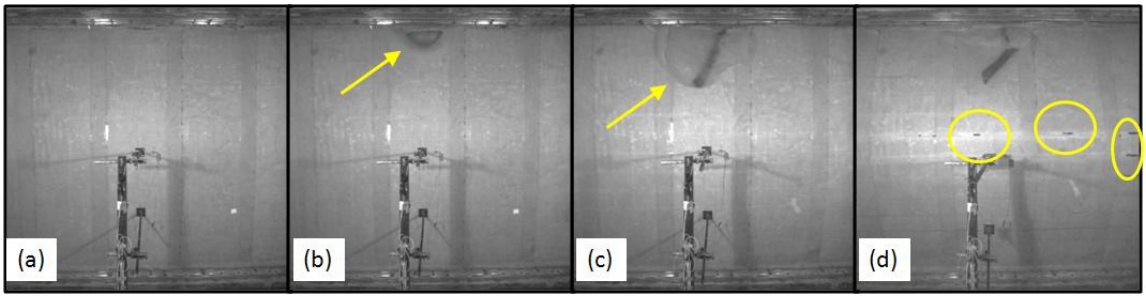

Figure 7.32. FS10: Frames from high-speed video. (a) Wall prior to blast load. (b) Blast wave begins to force the film to disengage at the center of the top support. (c) Area continued to grow while the wall responded. (d) Thermoset was stretched thin along the mortar joints, but the film was still undamaged.

Eight of the blocks or 5% of the total blocks were damaged (Figure 7.33a). The wall had a peak deflection at mid-span of approximately 1 unit into the reaction structure and a permanent deflection of approximately 0.411 out of the structure (Figure 7.33b). The top and bottom anchors used to secure the retrofit were engaged during the wall's response, and the top anchor plate was deformed (Figure 7.31b). The side wall of the steel channel adjacent to the CMU wall on the bottom support was also deformed as shown in Figure 7.34a. Hours after the blast event, the weight of the blocks on the retrofit along the bottom half of the wall disengaged and fell to the ground (Figure 7.34b).

**Figure 7.33. FS10. (a) Posttest exterior view.
(b) View of permanent deformation.**

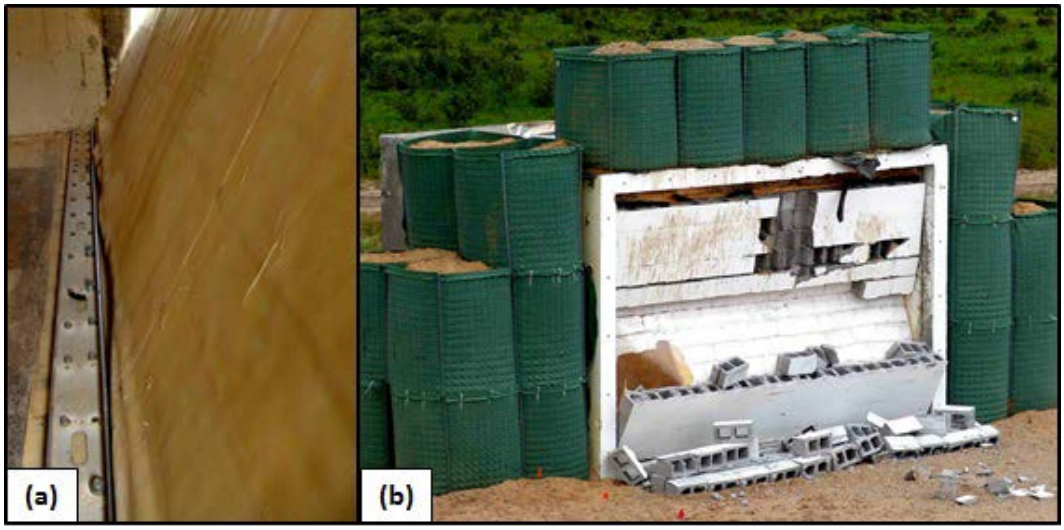

Figure 7.34. FS10. (a) Bottom support was engaged during wall response. (b) Hours after the blast event, the bottom section of the wall disengaged from the retrofit material.

7.4.4 FS11

Wall FS11 was built in Bay 1 with an extension to increase the wall height to 177 in., and the trowel-on epoxy and polyurethane film application process was similar to the procedure used in FS8-FS10 (Figures 7.35a and b). The epoxy/polyurethane combination did not bond as well as the thermoset/thermoplastic combination, so additional bracing was used at the top and bottom supports until the epoxy cured. The complete application procedure used to install the retrofit system was discussed in Section 4.7.3. Once the epoxy cured, the temporary braces were removed, and mechanical anchor System 2 was installed to secure the retrofit system. The polyurethane film was painted white to improve the quality of the video, since high-speed cameras require a significant amount of light to record at the speeds and resolution required for dynamic experiments. However, the white paint also provided an added benefit that was not planned. The white paint highlighted the high stress and strain areas on the wall. These high stress and strain areas located at the mortar joints in the central portion of the wall were identified when the paint deformed beyond its limit. As shown in Figures 7.36a, b, and c and Figures 7.37a and b, the paint failure along the mortar joints was very clear.

The retrofit system on FS11 was subjected to the same dynamic load level (3) that FS10 survived. Five of the seven polyurethane sheets did peel down two to three blocks along the top of the CMU wall (Figures 7.37a and b and Figure 7.38a). The peel back of the film along the top support of the CMU wall could be contributed to the 1-in. gap at the top of the wall. Pipe foam was placed in the gap, but it did not completely fill the

**Figure 7.35. FS11. (a) Pretest exterior view.
(b) Pretest interior view.**

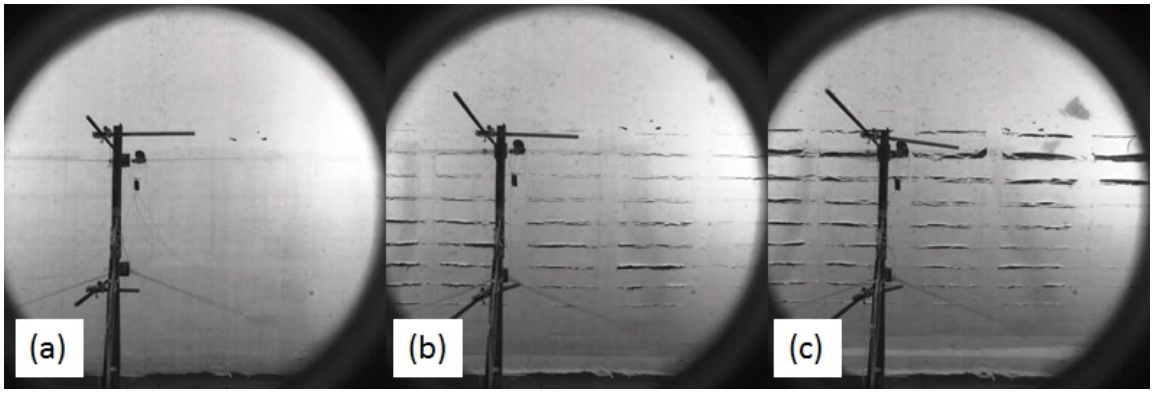

Figure 7.36. FS11: Frames from high-speed video. (a) CMU wall painted white for high-speed video. (b) White paint is stretched beyond its limit and tears at the mortar joints. (c) Paint continues to tear as the wall continues to deform.

void. The blast pressure may have jetted through the voids and applied a direct load to the adhesive between the film, epoxy, and CMU. No tears were found in the polyurethane film during the posttest inspection. The polyurethane film did not peel back at the bottom support (Figure 7.38b). The external high-speed video frames in Figure 7.39a, b and c show that the wall deflected at least 0.365 into the reaction

structure. No debris was found inside the structure, and only four blocks lost their face shells (Figure 7.40a). Although the wall was compromised, it remained in the reaction structure. It appears that the wall was close to falling out of the reaction structure during the rebound phase because the wall was leaning out of the structure at the top course by ¾ of a block width (Figure 7.40b).

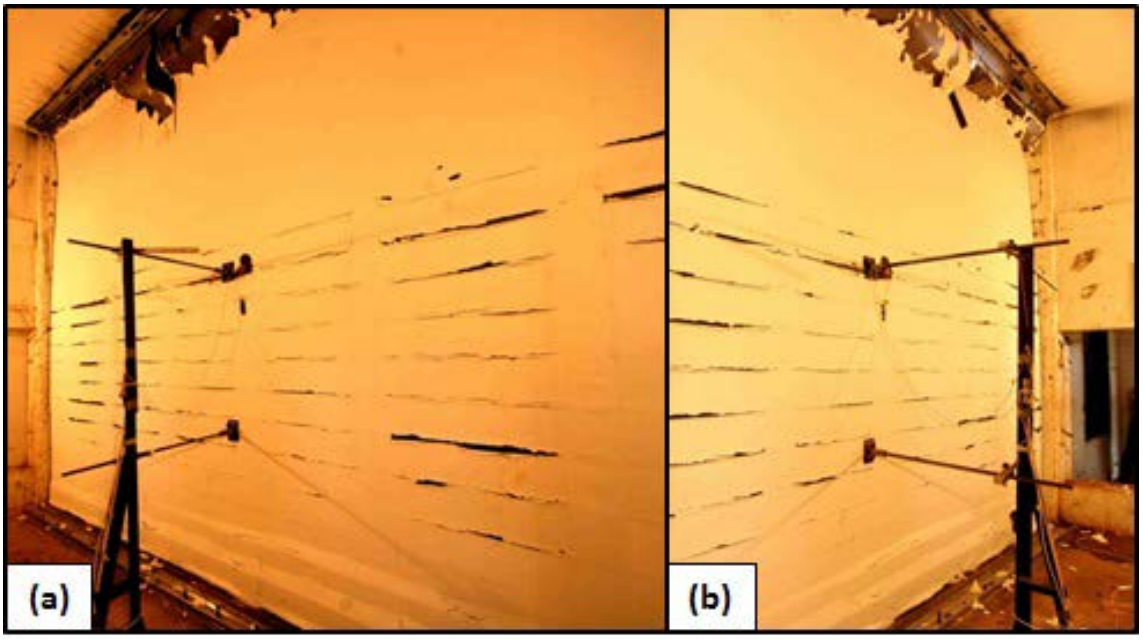

Figure 7.37. FS11. (a) High stress and strain rate locations are evident by the tears in the paint layer. (b) Film peeled off the wall along the top two courses.

Figure 7.38. FS11. (a) Five of the seven sheets of film peeled off the top of the CMU wall. (b) Film at the bottom support did not appear to peel back.

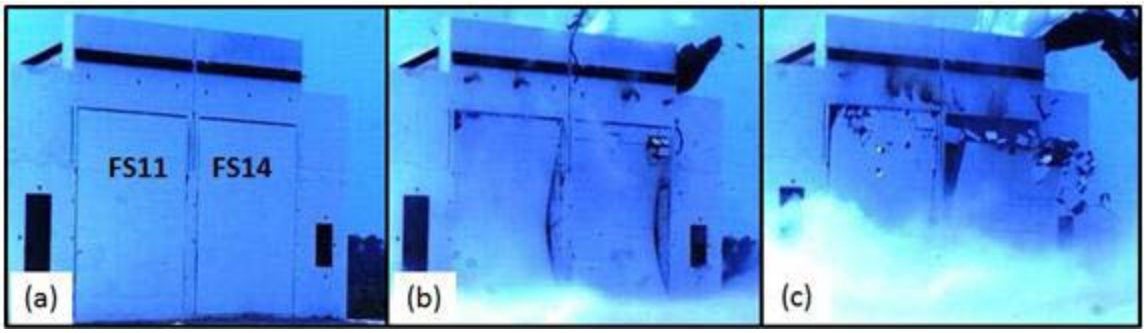

Figure 7.39. Frames from high-speed video. (a) Pretest view of walls. (b) Maximum deflection of walls. (c) Blocks remained attached to liner in FS11 and blocks peel off retrofit on FS14.

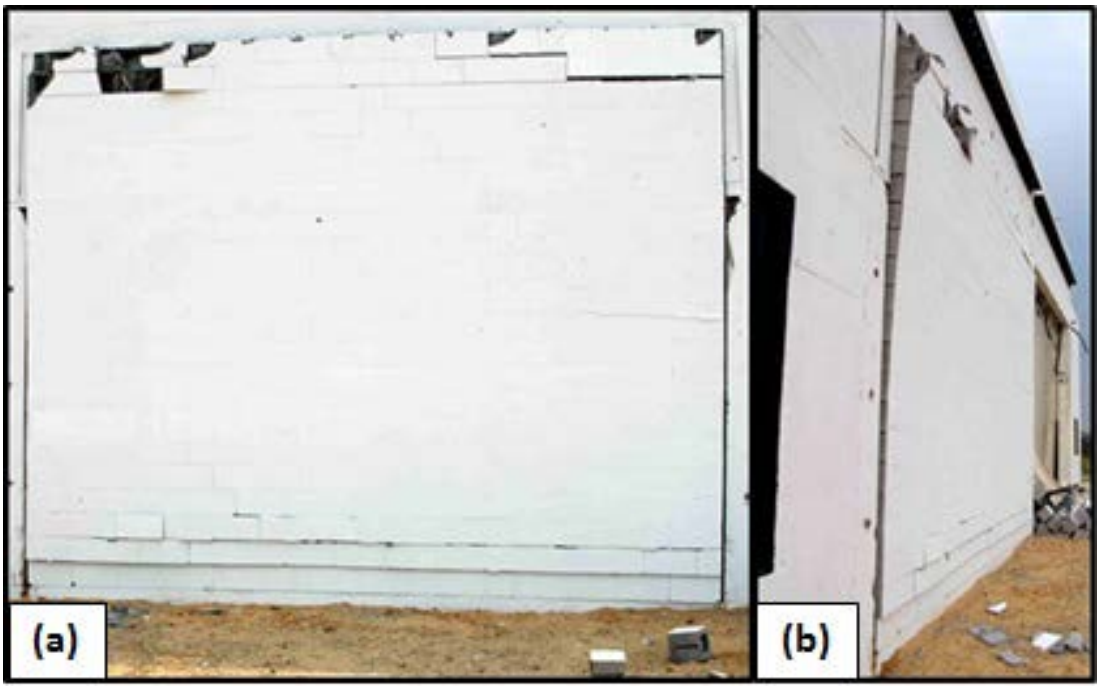

Figure 7.40. FS11. (a) Posttest view. (b) Posttest profile view.

7.5 Reinforced Film and Trowel-on Adhesive (FS12-FS13)

7.5.1 FS12

Wall FS12 was constructed in Bay 5 and retrofitted with the trowel-on epoxy used in FS11 and a reinforced elastomeric film (Figures 7.41a and b). At the time of the experiment, elastomeric films with a fiber reinforcement in a ±45-deg orientation could not be obtained. So the fiber reinforcement Fabric D was sent to a manufacturer to be encapsulated in the elastomeric resin to produce the reinforced film. However, the reinforcement could only be encapsulated in a 0/90-deg orientation in the film, and so the film had to be cut in a manner similar to the method used in FS2, FS3, and FS4 that allowed the film to be applied to the CMU wall with the fibers in a ±45-deg orientation

as illustrated in Figures 4.28 a and b in Section 4.5.2. The weight of the film and the lack of adhesion between the film and epoxy required temporary bracing during the application process (Figure 4.61). The overlap/seam dimensions along the length of the sheets were not uniform due to unexpected difficulties during the application process. To prevent a failure along the compromised seams, an additional 1-ft strip of reinforced film was added over these areas (Figure 4.62). Mechanical anchorage System 3 was used to secure the retrofit system to the reaction structure at the top and bottom supports. FS12 was evaluated at dynamic load level 1.

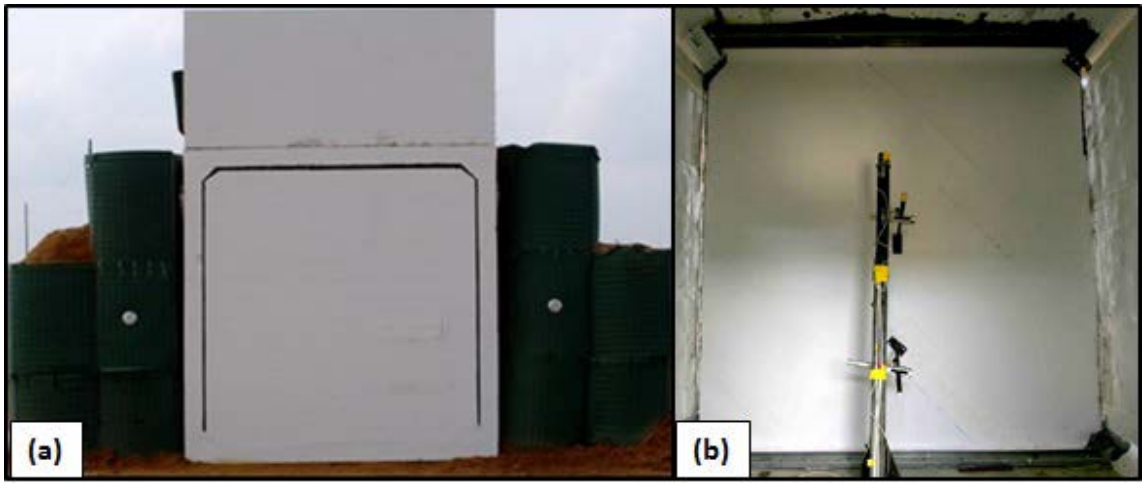

Figure 7.41. FS12. (a) Pretest exterior view. (b) Pretest interior view.

The retrofit prevented any debris from entering the reaction structure (Figure 7.42a). The displacement gauge at the center of the wall measured a maximum deflection of 0.251. Similar to FS11, the material started to disengage at the 1-in. gap between the CMU wall and the reaction structure at the center of the top support (Figure 7.43a

through d). The film continued to bubble until the entire sheet applied in the top right corner disengaged (Figure 7.42b). Approximately 12 face shells were damaged during the wall's response (Figure 7.44a). The top course of blocks was wedged between the reinforced concrete slab on the top of the reaction structure, the anchor plate, and the level of blocks just below the top course (Figure 7.44b). No damage was found on the elastomeric film during the posttest inspection.

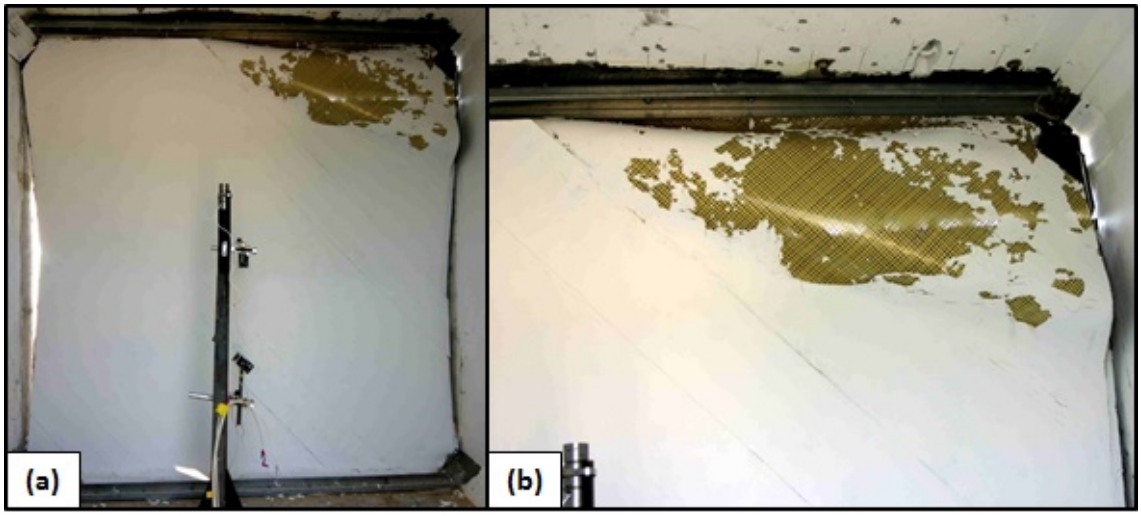

Figure 7.42. FS12. (a) Steel studs were not damaged during the blast response. (b) Film sheet disengaged but was held in place by anchor.

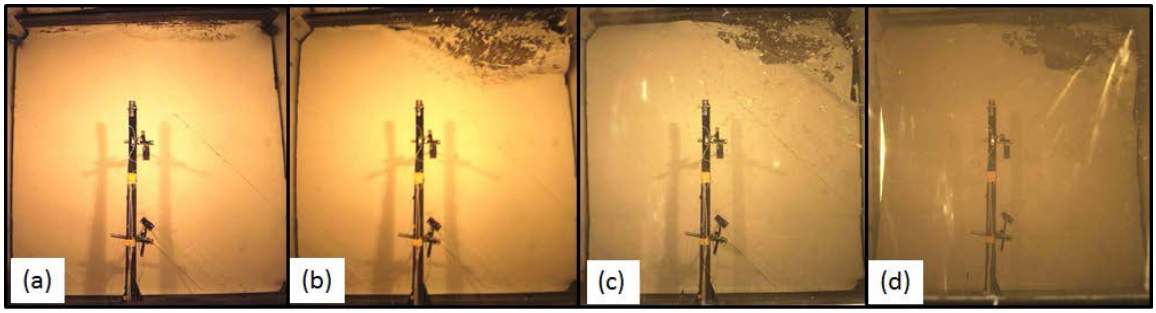

Figure 7.43. FS12: Frames from high-speed video. (a) Retrofit begins to bulge at top support. (b) Peel back contained to top right corner. (c) Corner sheet of film completely disengaged. (d) Sunlight through gap on side of wall during rebound phase.

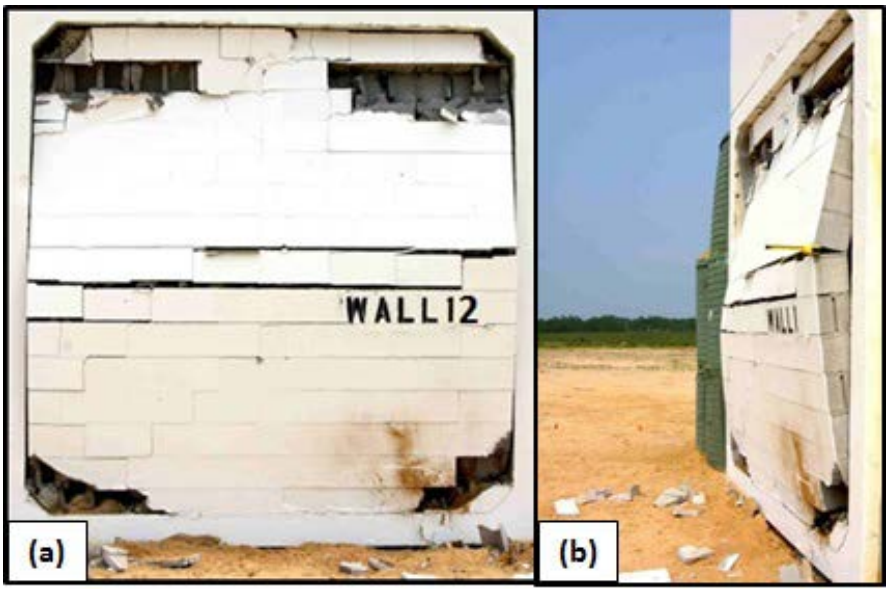

Figure 7.44. FS12. (a) Posttest exterior view. (b) Final location of CMU wall.

7.5.2 FS13

Wall FS13 was also constructed in Bay 5 and retrofitted with the trowel-on thermoset and an elastomeric film with Fabric F as the fiber reinforcement (Figures 7.45a and b). The elastomeric film was processed with the fiber reinforcement

at a ±45-deg reinforcement so that the film sheets could be applied vertically to the wall. Application time was reduced since the procedure did not require any special layout or application procedure. Mechanical anchor System 4 was used to secure the retrofit to the reaction structure. In an attempt to prevent the blast pressure from entering the reaction structure via the gaps, aluminum flashing was attached to the reaction structure to cover the gaps. FS13 was evaluated at dynamic load level 4.

The retrofit system used on the CMU wall failed straight across the mortar joint at the horizontal centerline of the wall creating two separate wall sections (Figure 7.46a).

Figure 7.45. FS13. (a) Pretest exterior view with aluminum flashing covering the gaps. (b) Pretest interior view.

After the retrofit failed along the centerline, the top half of the wall was too heavy for the anchor system and the wall section fell into the reaction structure (Figure 7.46b). The high-speed camera recorded the response but the footage could not be downloaded due

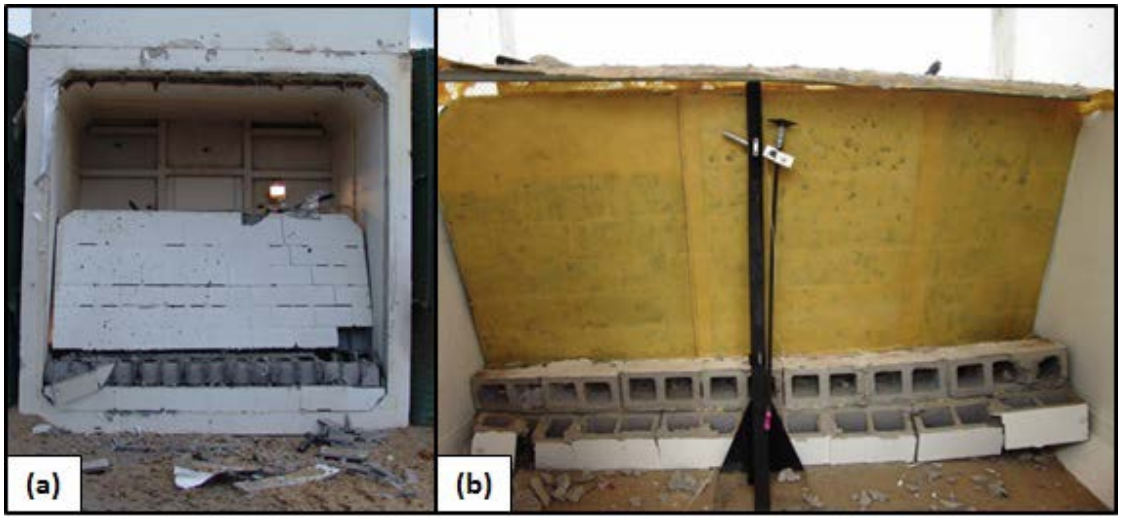

Figure 7.46. FS13. (a) Posttest exterior view. (b) Interior view.

to a computer malfunction. However, researchers were able to view the footage before it was lost. The footage showed that, at the area of maximum deflection (the centerline), a gap began to grow between the CMU blocks and the mortar. The film bridged the gap, and the fibers reoriented from 45 deg to 90 deg (perpendicular to the mortar line) until the fibers failed. The response mimicked the response observed in subscale experiments BLS9 and BLS10. After the fibers failed, the weight of the CMU blocks uniformly pulled the anchor plate out of the top support. The adhesion of the trowel-on thermoset to the elastomeric film and the CMU blocks was maintained throughout the experiment and during the posttest inspection (Figure 7.47a). The material did not disengage while the wall sections were removed for inspection. During the inspection process, it was noted that the fibers along the failure line pulled out of the elastomeric film (Figure 7.47b).

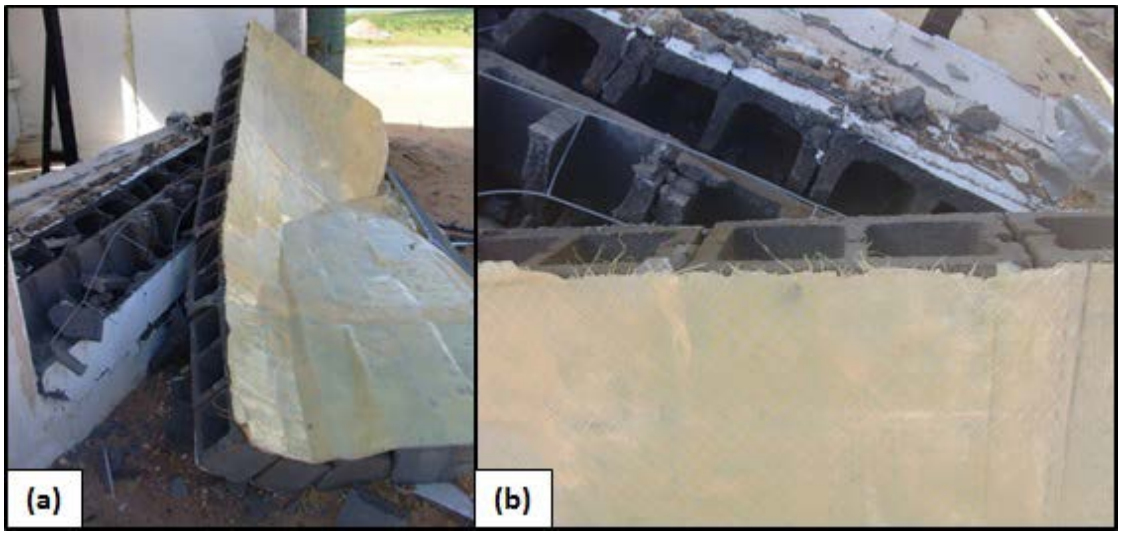

Figure 7.47. FS13. (a) Top half of the CMU wall removed from the reaction structure. (b) Fiber pull-out along the failure line.

7.6 Unreinforced Film with PSA (FS14-FS16)

7.6.1 FS14

Wall FS14 was constructed in Bay 2 with an extension to increase the height to 177 in. and was retrofitted with a PSA and elastomeric film (Figures 7.48a and b). The PSA, a COTS carpet tape, was applied to the elastomeric film first. Then the film was cut to length and applied to the CMU wall. The concrete supports were primed (Primer 4), and the trowel-on epoxy used in previous experiments was used to adhere the film to the supports. A temporary support system was used until the epoxy cured, then the mechanical anchor System 2 was installed. Wall FS14 was evaluated at dynamic load level 3.

**Figure 7.48. FS14. (a) Pretest exterior view.
(b) Pretest interior view.**

The retrofit system did not allow any of the debris to enter the reaction structure (Figure 7.49a). All of the blocks were thrown out of the reaction structure when the retrofit rebounded (Figure 7.49b). The carpet tape used as the PSA on the retrofit also

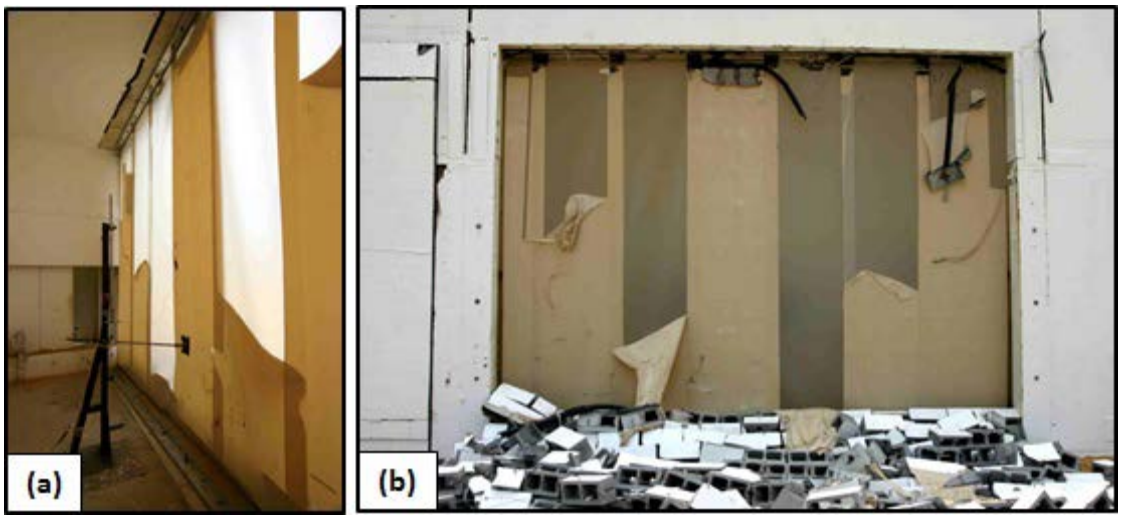

Figure 7.49. FS14. (a) Posttest interior view. (b) Exterior view.

peeled off the film as the CMU blocks disengaged (Figure 7.50a, b, and c). The film peeled off the top support until it engaged the anchor system, but the channel was not deformed by the force of the wall. The film did not appear to peel back from its original position on the bottom support, so the anchor system was not engaged.

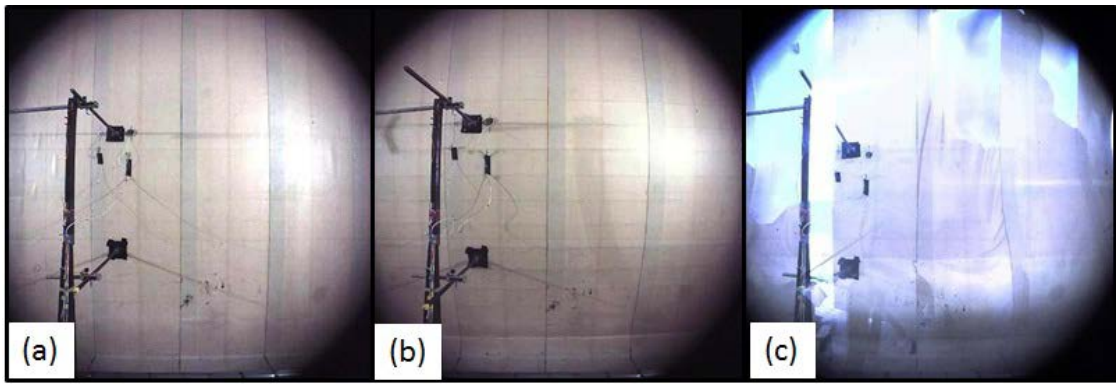

Figure 7.50. FS14: Frames from high-speed video. (a) Pretest view of wall. (b) Wall at maximum deflection. (c) CMU and tape peeling off the elastomeric film.

7.6.2 FS15

Wall FS15 was built in Bay 3 and retrofitted with a PSA and elastomeric film (Figures 7.51a and b). The PSA was purchased separately and applied to the elastomeric film in the field. The film was installed on the CMU wall, and the trowel-on thermoset from earlier experiments was used to create an adhesive bond on the top and bottom supports. Mechanical anchor System 4 was also installed on the top and bottom supports. FS15 was subjected to dynamic load level 2.

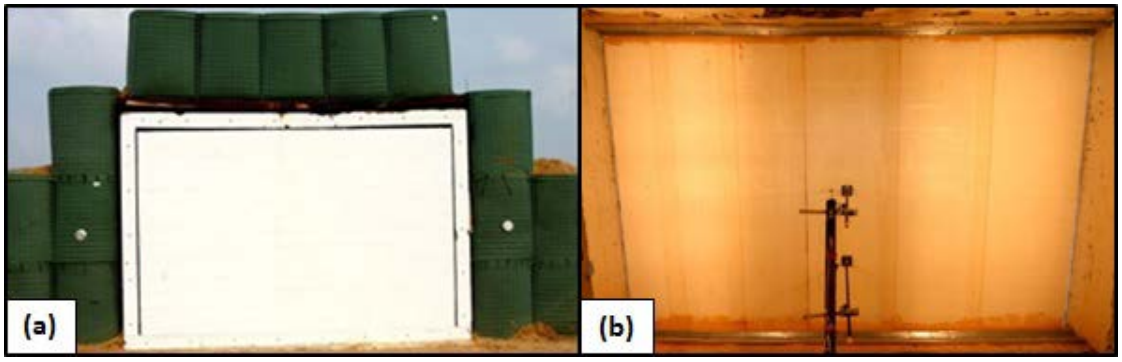

Figure 7.51. FS15. (a) Pretest exterior view. (b) Pretest interior view.

The retrofit prevented the CMU debris from entering the structure, and all of the blocks were propelled from the structure as the film rebounded (Figure 7.52a and b). The mechanical deflection rod and the accelerometer attached along the centerline of the wall indicated a maximum deflection into the reaction structure of 0.662 and 0.689, respectively. The film was transparent and allowed the high-speed video to capture the failure and deformation of the mortar joints (Figures 7.53a, b, and c). No damage was found on the elastomeric film during posttest inspection. The retrofit peeled back, and the anchor system on the top support was deformed (Figures 7.54a and b). The thin steel channel leg next to the CMU wall was folded completely over the full length of the wall.

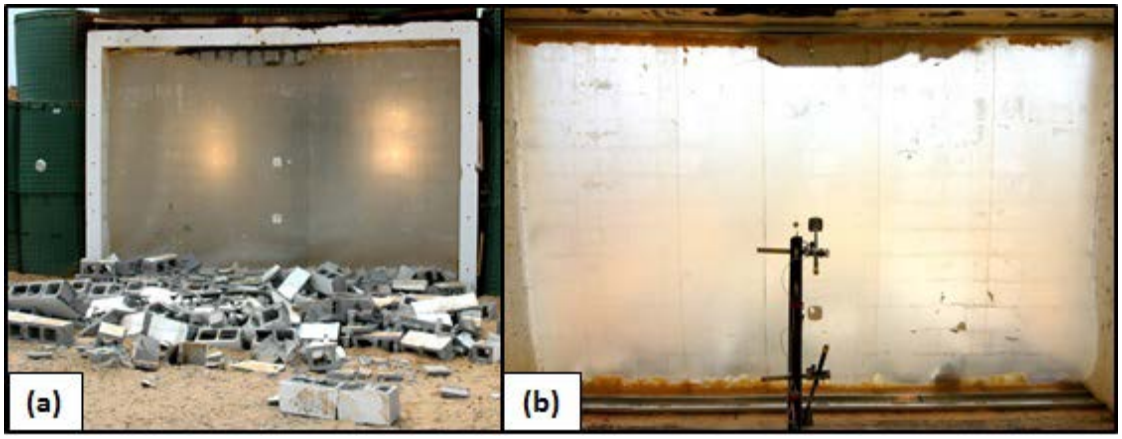

Figure 7.52. FS15. (a) Posttest exterior view. (b) Posttest interior view.

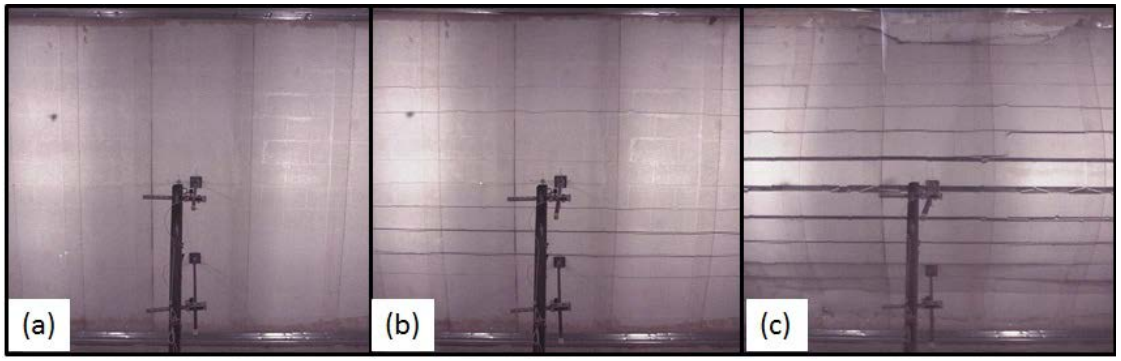

Figure 7.53. FS15: Frames from high-speed video. (a) Pretest camera view. (b) Cracks in mortar joints. (c) Maximum deformation.

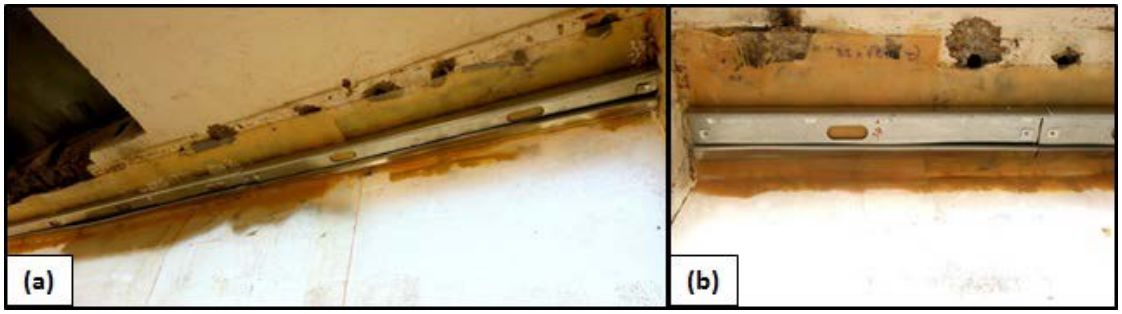

Figure 7.54. FS15. (a) Mechanical anchor at top support. (b) Close-up of deformed anchor.

7.6.3 FS16

Wall FS16 was built in Bay 1 with the extension added to the reaction structure and retrofitted with an unreinforced elastomeric film applied to the wall with a PSA (Figures 7.55a and b). The trowel-on epoxy was used to provide an adhesive bond between the film and the concrete substrate at the top and bottom supports. In addition to the adhesive bond, mechanical anchorage System 4 was used to secure the film to the reaction structure. The wall was evaluated at dynamic load level 4.

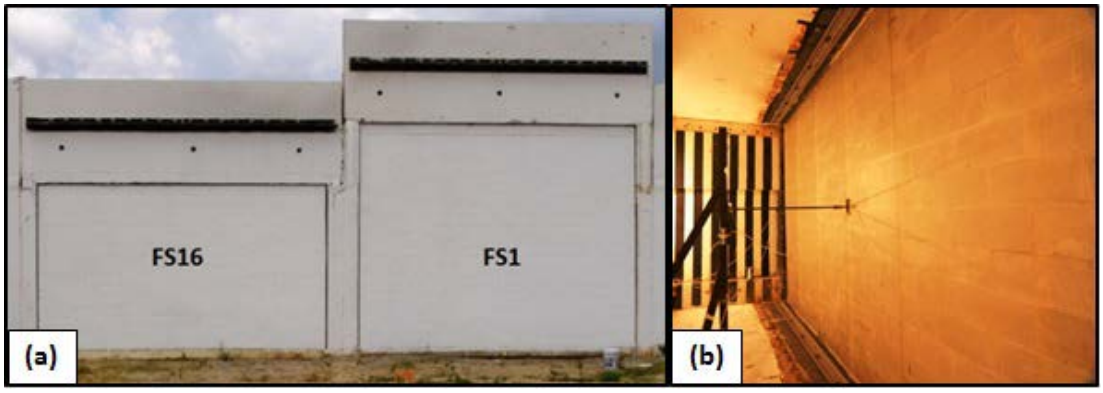

Figure 7.55. FS1 and FS16. (a) Pretest exterior view. (b) Pretest interior view of FS16.

The high-speed video showed the different phases of the retrofitted wall's response to the blast load as the wall deformed into the structure. First, cracks developed in the mortar joints, and then as the deformation continued, the film began to rip from left to right across the top support (Figures 7.56a, b, and c). The elastomeric film on the right half of the wall failed milliseconds later (Figures 7.57a, b, and c). The blocks and film

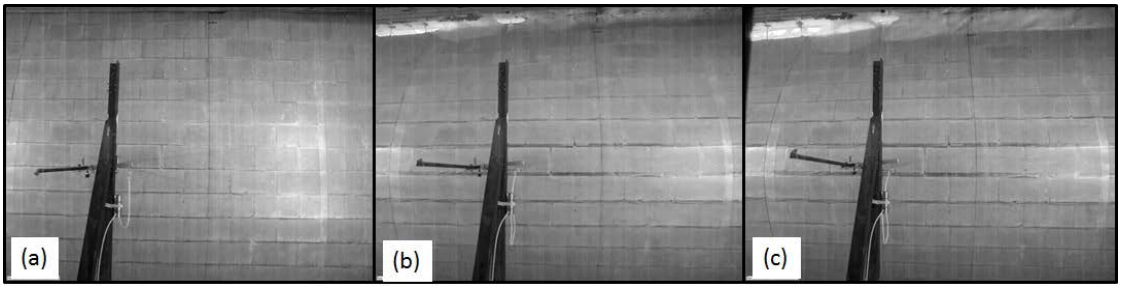

Figure 7.56. FS16: Frames from high-speed camera. (a) Cracks develop in mortar joints. (b) Tear in film propagates across the top of the support. (c) Point of maximum deflection into the reaction structure.

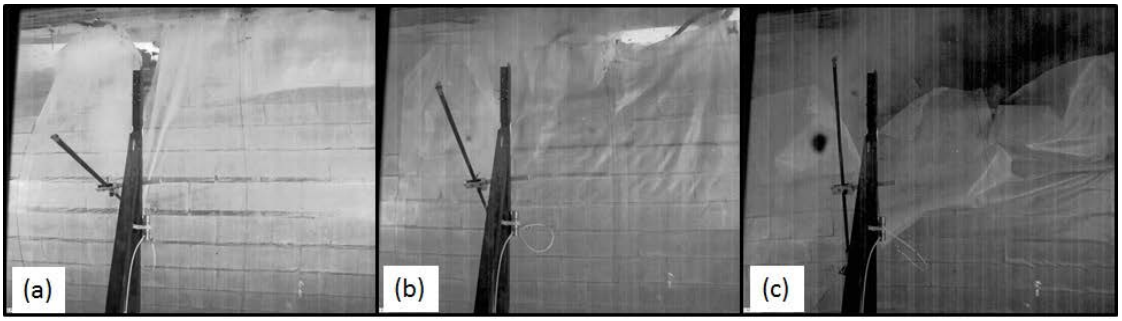

Figure 7.57. FS16: Frames from high-speed camera. (a) Blocks begin to disengage from the film. (b) Tear in film propagates the full length of the support. (c) Film and blocks fall into reaction structure.

on the left half of the wall, which failed early in the wall response, fell outside the reaction structure (Figure 7.58a). The blocks from the top right half of the wall and the film both fell into the reaction structure (Figure 7.58b). In Figure 7.59a, the torn edge of the film is shown. The film failed before the steel stud member was deformed as shown in Figure 7.59b.

Figure 7.58. FS16. (a) Half of the wall fell out of the reaction structure. (b) Half of the wall fell into the reaction structure.

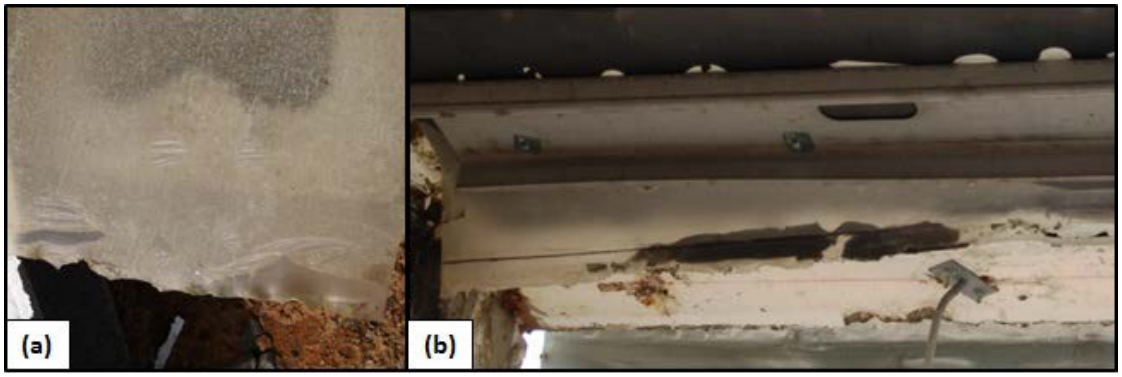

Figure 7.59. FS16. (a) Elastomeric film from top support. (b) Anchor undamaged and film remnants.

7.7 Reinforced Film and PSA (FS17-FS18)

7.7.1 FS17

Wall FS17 was constructed in Bay 3 and retrofitted with a reinforced elastomeric film with Fabric F encapsulated in the elastomeric resin. Trowel-on epoxy was used as an adhesive at the top and bottom supports. A temporary support was used until the

epoxy cured. Mechanical anchor System 4 was used to secure the retrofit system to the top and bottom supports. The wall was evaluated at dynamic load level 3.

The reinforced elastomeric film used on FS17 prevented the wall debris from entering the reaction structure (Figure 7.60a). All of the mortar joints in the CMU wall were compromised, and the blocks were propelled out of the reaction structure when the film rebounded (Figure 7.60b). Several of the seams were compromised in the experiment, but no debris entered the structure. The high-speed video documented the wall response under load (Figure 7.61a through d). The film lost adhesion along the top support and then propagated down to the centerline of the wall. The video also showed that the wall almost impacted the steel desk. As the wall deformed, the retrofit peeled back and engaged the anchor system. The bottom anchor was undamaged, but the top anchor was damaged the full length of the wall (Figures 7.62a and b).

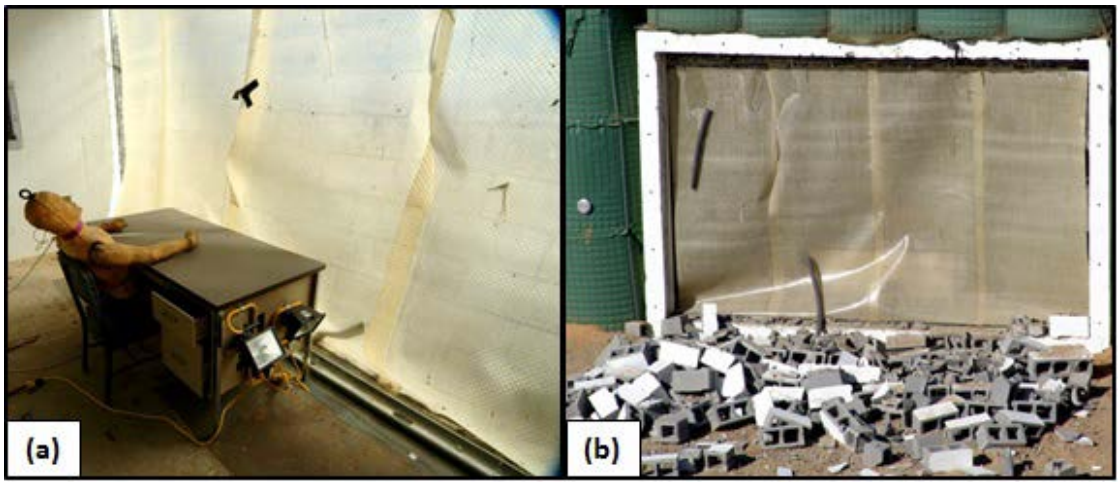

Figure 7.60. FS17. (a) Posttest interior view. (b) Posttest exterior view.

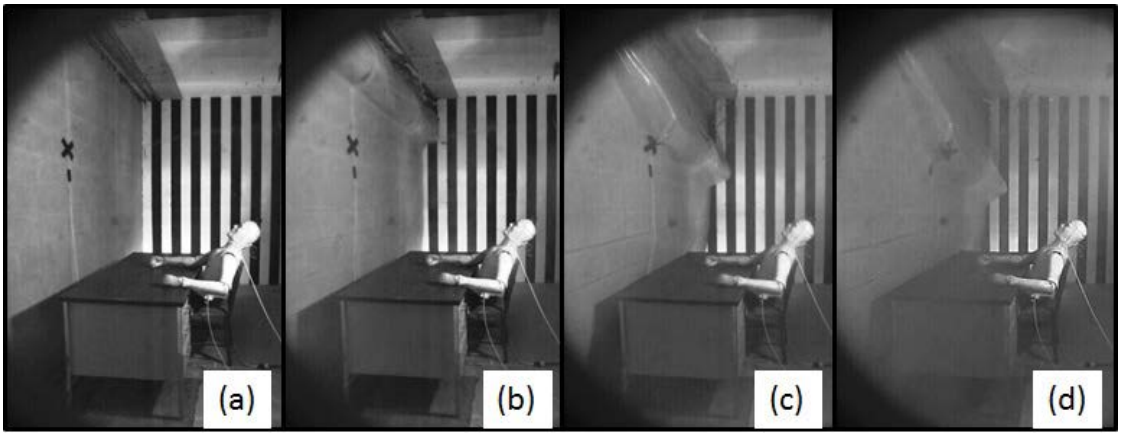

Figure 7.61. FS17: Frames from high-speed video. (a) Pretest camera view. (b) Film begins to disengage from the top of the wall. (c) Film continues to peel off the wall. (d) Point of maximum deformation in the retrofitted wall.

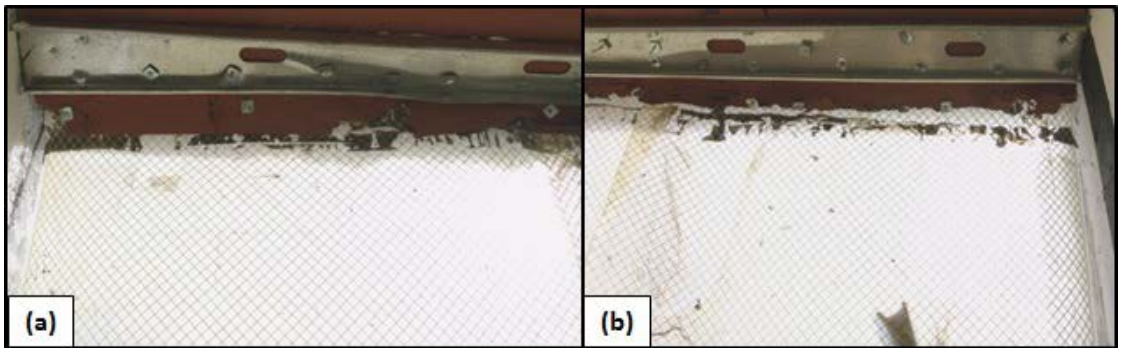

Figure 7.62. FS17. (a) Deformed anchor support on left side. (b) Right anchor support.

7.7.2 FS18

Wall FS18 was constructed in Bay 4, and the reinforced elastomeric film used in FS17 was used on FS18 (Figure 7.63a). The trowel-on epoxy used in FS17 was replaced with the trowel-on thermoset material that cured faster and did not require temporary

supports as the material cured. In addition to the trowel-on adhesive, mechanical anchor System 4 was added to secure the retrofit system to the top and bottom supports. The wall was evaluated at dynamic load level 4.

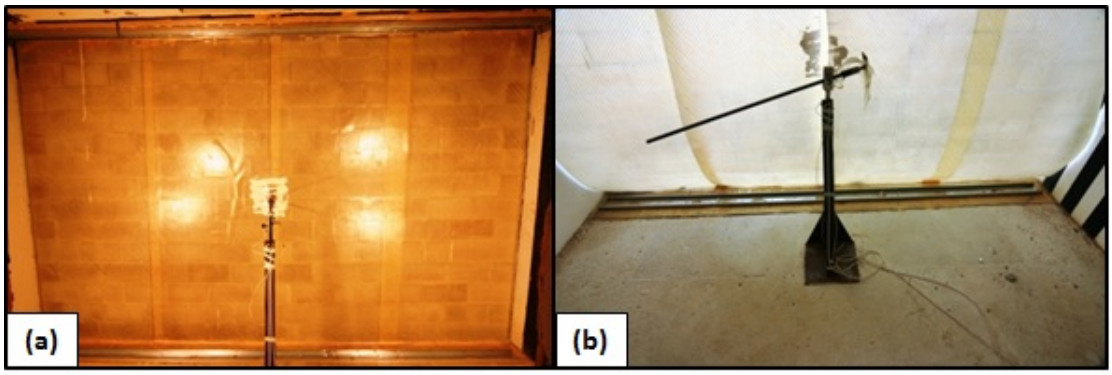

Figure 7.63. FS18. (a) Pretest interior view. (b) Posttest interior view.

The reinforced elastomeric film used on FS18 prevented the wall debris from entering the reaction structure (Figure 7.63b), but the film sustained damage during the experiment. The PSA was not strong enough to prevent the blocks from being propelled out of the structure during the film's rebound (Figure 7.64a). The film tore at three different locations along the anchor system on the top support, and the center seam was compromised (Figures 7.64b and 7.65a). The damage to the anchor system on the top support in FS18 mimicked the damage observed in FS17 (Figure 7.65b).

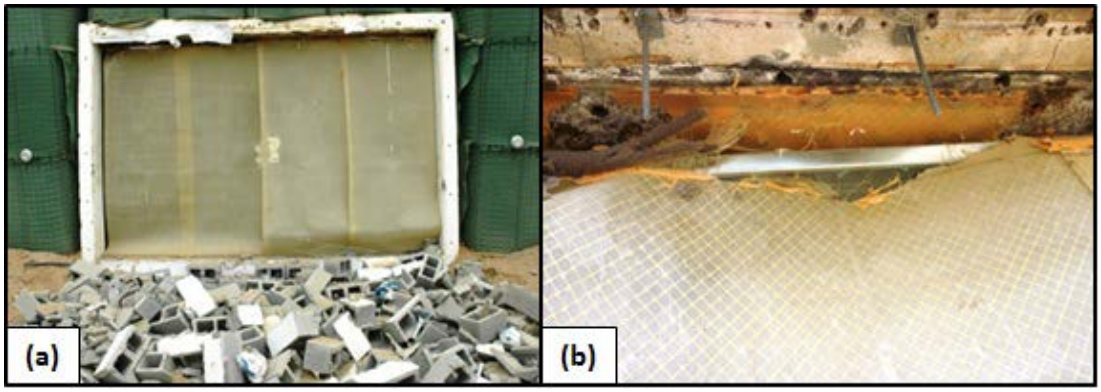

Figure 7.64. FS18. (a) Posttest exterior view. (b) Portions of the film tore and other sections peeled off the support.

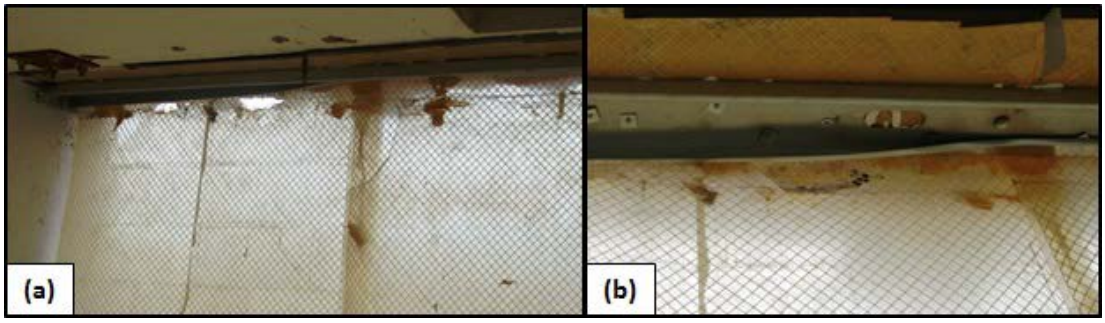

Figure 7.65. FS18. (a) The film tore in spots on the right and left sides. (b) Film peeled off the support in the center, and the steel anchor was deformed in these areas.

7.8 Summary of Full-Scale Dynamic Experiments

Six different retrofit systems were evaluated in eighteen full-scale CMU wall experiments. An unretrofitted CMU wall (FS1) was also added to the experimental plan to demonstrate the vulnerability and to document the debris hazard of a full-scale CMU wall subjected to an explosive event. The dynamic load levels for the unretrofitted and retrofitted walls evaluated are graphically depicted on Figure 7.66. Twelve of the eighteen experiments demonstrated that several different retrofit systems could be used

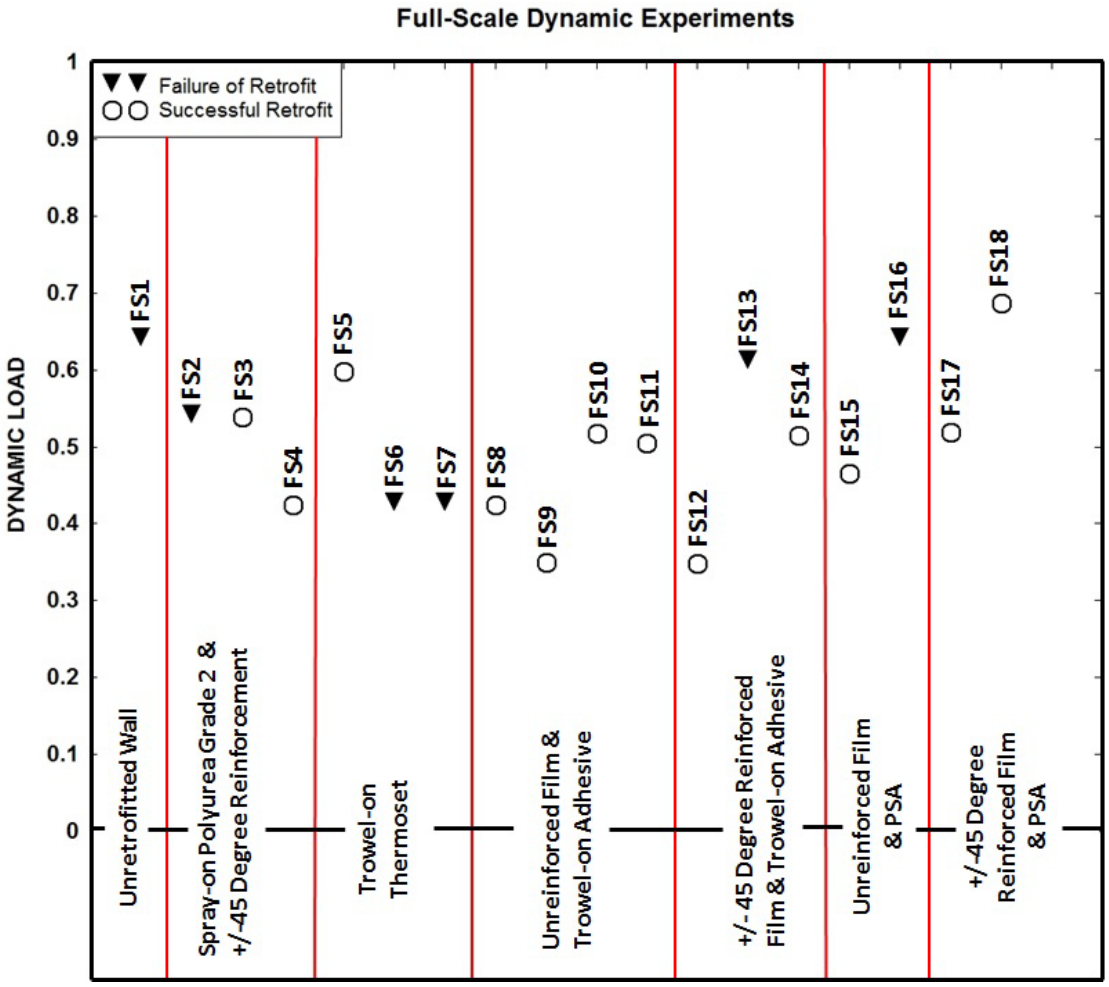

Figure 7.66. Summary of full-scale dynamic experiments.

to successfully retrofit a hollow unreinforced CMU wall. The ±45-deg fiber reinforced (Fabric F) elastomeric film applied to the CMU wall surface using a PSA and anchored to the reaction structure using a thin wall steel stud member survived the highest dynamic load (7) of all the retrofits evaluated in the full-scale experiments. The experiments were completed before the failure load was determined for the retrofit system. All of the data documented from the full-scale experiments is provided in Table 7.2.

Table 7.2. Summary of retrofit responses in full-scale dynamic experiments.

Exp. Label	Dynamic Load Level	Retrofit	Normalized Deflection	CMU Damage %	Failure Mode
FS2	3	Spray-on Polyurea Grade 2 Fabric D ±45 deg	Fail	Fail	5
FS3	3	Spray-on Polyurea Grade 2 Fabric E ±45 deg	0.396	99	Pass
FS4	2	Spray-on Polyurea Grade 2 Fabric E ±45 deg	0.52	92	Pass
FS5	3	Trowel-on Thermoset Grade 1	0.37	84	Pass
FS6	2	Trowel-on Thermoset Grade 2	Fail	Fail	5
FS7	2	Trowel-on Thermoset Grade 1	Fail	Fail	5
FS8	2	Trowel-on Thermoset Grade 1 & Thermoplastic Film	0.404	48	Pass
FS9	1	Trowel-on Thermoset Grade 1 & Thermoplastic Film	No Data	6	Pass
FS10	3	Trowel-on Thermoset Grade 1 & Thermoplastic Film	1	5	Pass
FS11	3	Trowel-on Epoxy & Polyurethane Film	0.712	1	Pass
FS12	1	Trowel-on Epoxy & Elastomeric Film Fabric D ±45 deg	0.251	12	Pass
FS13	4	Trowel-on Thermoset & Elastomeric Film Fabric F ±45 deg	Fail	Fail	1
FS14	3	PSA & Elastomeric Film	0.74	100	Pass
FS15	2	PSA & Thermoplastic Film	0.662	100	Pass
16	4	PSA & Elastomeric Film	Fail	Fail	2
17	3	PSA & Reinforced Film Fabric F ±45 deg	0.594	100	Pass
18	4	PSA & Reinforced Film Fabric F ±45 deg	0.594	100	Pass

Failure Mode: (1) Tear at mid-span; (2) Shear at top support; (3) Shear at bottom support; (4) Shear at both supports; (5) Peel-back failure at supports.

Two of the three walls (FS2, FS3, and FS4) retrofitted with the ±45-deg fiber reinforced Grade 2 spray-on polyurea effectively mitigated the debris hazard associated with dynamic load levels 2 and 3. All three walls used the Grade 2 spray-on polyurea to encapsulate the fiber reinforcement. FS2 used Fabric D oriented at ±45 deg to reinforce the polyurea layer, and FS3 and FS4 used Fabric E oriented at ±45 deg as reinforcement. FS2 and FS3 were evaluated on the same experiment, and both walls relied solely on the adhesive strength of the spray-on polyurea to anchor the material to the reinforced concrete roof and floor slabs of the reaction structure. The retrofit system on FS2 failed as the retrofitted wall rebounded from the pressure load. The retrofit on FS2 failed along the top support, but no fragments from the CMU wall were found inside the reaction structure, which implied that the retrofit system did mitigate the secondary debris hazard. FS3 remained attached to the reaction structure and also successfully mitigated the debris hazard. The dynamic load level was decreased to level 2 for FS4 since one of the two walls failed along the top support at level 3. To prevent a peel-back failure at the supports, a very robust anchor system was added to the top and bottom supports. The anchor plates worked well and the retrofit system once again successfully demonstrated the ability to mitigate the debris hazard. A robust system was needed for multiple reasons, i.e., the condition of the substrate at the supports was poor and the polyurea was relatively heavy, thick, and stiff.

The second retrofit system evaluated consisted of two grades of an unreinforced trowel-on thermoset material. The first wall (FS5) evaluated with the Grade 1 thermoset at dynamic load level 3 was the only wall to effectively mitigate the debris hazard.

However, the successful response obtained on FS5 could not be duplicated for FS6 or FS7, which were evaluated at a lower dynamic load level of 2. None of the walls used a mechanical anchor system. Wall FS6 was retrofitted with the Grade 2 thermoset, and FS7 used the Grade 1 material that was initially used on wall FS5.

The third group of walls (FS8, FS9, FS10, and FS11) were retrofitted with the unreinforced elastomeric (thermoplastic and polyurethane) films that were adhesively attached to the CMU wall surface using either the trowel-on thermoset from the previous retrofit system or a trowel-on epoxy. All four retrofitted walls successfully mitigated the debris hazard by preventing all of the fragments from entering the protected space at dynamic load levels 1, 2, and 3. The dynamic failure load for this retrofit system was not obtained during the current research program.

The ±45 deg fiber reinforced elastomeric film applied to the CMU wall surface using trowel-on adhesives was evaluated using two walls (FS12 and FS13). FS12 that was retrofitted with Fabric D at ±45 deg fiber orientation in the elastomeric film applied to the wall using the trowel-on epoxy effectively mitigated the debris hazard at dynamic load level 1. However, the retrofit system was difficult to apply to the wall surface due to the length of time it took for the epoxy to harden, the weight of the fiber reinforced film, and the special measurements and cuts required to apply the film to the wall to create the ±45 deg orientation. It is important to note that at the time FS12 was tested, fiber reinforced film was only available with a 0/90-deg fiber orientation, so the film had to be cut into specified shapes and lengths to create the desired 45-deg orientation. Most of the film sheets could only be anchored on one end due to the special orientation. FS13

was the first wall evaluated with an elastomeric film constructed with the fibers running in a ±45-deg orientation (Fabric F) in 4- to 5-ft rolls, which made the application procedure more efficient. The trowel-on thermoset was used as the adhesive for the elastomeric film on wall FS13. This system was evaluated at dynamic load level 4 which was larger than the load applied to the retrofitted wall in FS12. The retrofit on FS13 failed along the centerline and allowed debris to be propelled into the structure. The damage incurred during the blast response and the weight of the CMU adhered to the top half of the film caused the wall section to fall into the reaction structure. The maximum dynamic load the retrofit system could resist is between dynamic load levels 1 and 4.

The final two groups of retrofits used unreinforced and reinforced elastomeric films adhesively applied to the CMU wall surface using PSAs. Two of the three walls retrofitted with the unreinforced elastomeric films successfully mitigated the debris hazard for dynamic load levels 2 (FS15), and 3 (FS14), but the third wall (FS16) failed at dynamic load level 4. The unreinforced elastomeric film in FS16 failed when the film sheared along the top anchor plate. The left half of the wall fell into the reaction structure representing a high hazard, while the right side of the wall was propelled outside the reaction structure. It is unclear why the two halves of the wall responded differently. The maximum dynamic load the unreinforced films could resist is between dynamic load levels 2 and 4.

The two final walls (FS17 and FS18) evaluated in the full-scale program were retrofitted with the ±45-deg fiber reinforced films adhered to the CMU wall surface using a PSA. FS17 and FS18 successfully mitigated the debris hazard for dynamic load

levels 3 and 4, respectively. All of the CMU lost adhesion to the film and were propelled off the film and settled in front of the reaction structure.

8. DYNAMIC ANALYSIS: SDOF MODEL

One of the objectives in this research was to provide an analytical model or method to predict the structural response of hollow, unreinforced CMU infill walls retrofitted with unreinforced and reinforced elastomeric materials to blast loads. Each CMU wall was decoupled from the reinforced concrete or steel framed structure and transformed into an equivalent SDOF system. Then numerical integration techniques were used to solve the differential equation to determine the deflection at a critical point on the structural component under analysis. In this research, the point of interest was the mid-span deflection of the CMU walls.

The resistance functions generated from the subscale HTC experiments discussed in Chapter 5 were used as load-deflection data for the SDOF model developed using an Excel spreadsheet. In addition to the development of an analytical model, the ability to use subscale static experiments to predict the dynamic response of full-scale walls to blast loads was also evaluated. The resistance functions generated from the subscale static experiments were modified using common similarity/scaling methods discussed in Section 4.1 to predict the response of the full-scale retrofitted CMU walls using the two analysis techniques. The accuracy of the analysis techniques was defined by comparing the results of the full-scale HE experiments discussed in Chapter 7 to the predicted results using the scaled resistance functions for the full-scale prototypes.

The CMU wall used in the experimental and analytical methods was hollow, unreinforced, and simply supported at the floor and ceiling connections. The connection

at the ceiling consisted of a slip dowel grouted into the top course of blocks and a 1- to 1.5-in. gap left open or filled with a deformable material. A 1-in. gap was also left open on the right and left sides of each wall. The wall was analyzed as a single entity separate from the global structure. The SDOF model defined the dynamic response of the retrofitted CMU infill wall system to a blast load by limiting the motion of the wall to a single direction, i.e., the inward deflection of the wall. The position of the system at any instant in time, t, was defined in terms of a single coordinate, x.

The idealized model for the CMU wall was illustrated in Figures 2.2 and 8.1a, and to begin development, one must isolate the mass and define the effective forces acting on it (Figure 8.1b). The component under analysis in a blast event reaches its maximum response in a short time, so damping has little effect on the peak displacement and is specifically ignored during the analysis of infill CMU walls (Chopra 2001; Maji, Brown, and Urgessa 2008). In other dynamic applications damping can be very significant. Krauthammer (2008) in his book *Modern Protective Structures* states first that "the effect of damping is small, but the inertia effect may be significant and can dominate the response whenever loading durations are much shorter than structural response times. It should be noted that damping effects can be ignored during initial analysis considerations, as noted in the various design manuals." Damping was considered in Moradi's work involving CMU walls in 2003 and it was determined that damping proved to be insignificant to the walls' displacements and stresses. In a later publication (Resistance of Membrane Retrofit Masonry Walls to Lateral Pressure: A Design Tool for One-way Masonry Walls) by Moradi in 2009 the structural damping coefficient was

assumed to be zero, because the "structural damping during plastic response cannot be clearly defined or verified experimentally and has no physical significance during the plastic deformation of the structural element."

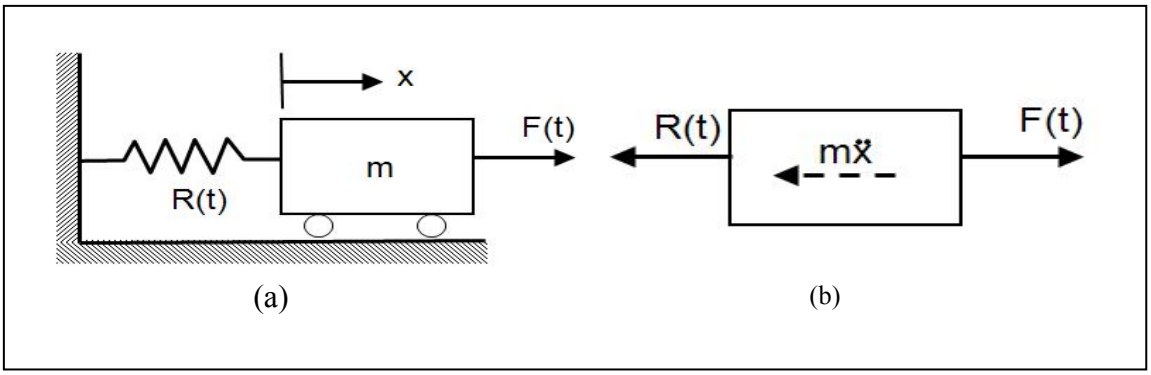

Figure 8.1. Idealized system for SDOF methodology. (a) SDOF model of CMU wall. (b) Free-body-diagram of SDOF model.

In an undamped system, three basic forces need to be defined, i.e., the external load, the resisting force, and the inertial force. The external load is the transient dynamic load created from the blast event, $F(t)$. The second force is the restoring force of the spring element and potential energy stored in the structural element, defined as the effective stiffness of the spring. For the non-linear, inelastic case associated with blast events, plastic behavior is anticipated, and the effective stiffness of the spring can be represented by, R, since the resistance changes based on the various ranges or stages of the resistance function of the structural component. The final force is the inertial force acting on the representative effective mass, $m\ddot{x}$, of the component under analysis, where

$\ddot{x}$ is the acceleration of the mass in the x direction. The equation of motion (Newton's second law),

$$F = m\ddot{x} \tag{8.1}$$

is the key equation in a SDOF model. The relationship between the blast load and the forces acting on the mass are shown in the free body diagram in Figure 8.1b. When all the forces acting on the system are summed, the equation of motion becomes

$$F(t) - R(t) = m\ddot{x}. \tag{8.2}$$

Now that the equation of motion has been defined, the deformed shape of the component must be assumed, and the equivalent system is selected so that the deflection of the concentrated mass is the same as a significant point on the structural component. The mid-point of the CMU wall was used to determine the transformation factors for the equivalent system based on an assumed shape of the actual structural component. When the load, mass, and resistance (stiffness) of the real structure are multiplied by the corresponding transformation factors, the equivalent single-degree factors are developed.

The methods and equations used to develop the transformation factors, K_M, K_L, and K_R, are well documented in *Introduction to Structural Dynamics* (Biggs, 1964). The equivalent mass, M_e, of the equivalent single-degree system for a structural element under uniform mass is given by

$$M_e = \int^{L} m\phi^2(x)dx \tag{8.3}$$

where ϕ is the assumed shape function on which the equivalent system is based, and m is the mass per unit length. The mass transformation factor, K_M, is defined as the ratio of the equivalent mass to the actual total mass of the structure.

$$K_M = \frac{M_e}{M_T} \tag{8.4}$$

where

M_T = mL

L = span.

$$K_M = \frac{1}{L}\int^{L} \phi^2(x)dx \tag{8.5}$$

The equivalent force on the idealized system for a distributed load is

$$F_e = \int^{L} w(x)\phi(x)dx \tag{8.6}$$

where $w(x)$ is the applied distributed load. The load transformation factor, K_L, is defined as the ratio of the equivalent force to the actual total force.

$$K_L = \frac{F_e}{F_T} \tag{8.7}$$

where $F_T = w(x)L$.

The strength and stiffness properties of a structural member are needed for modeling the response to dynamic loading. A resistance function defines the member's resistive force at any given deflection for the loading condition applied. The maximum resistance is the total load having the given distribution that the element can support statically. The stiffness is numerically equal to the total load of the same distribution that would cause a unit deflection at the point where the deflection is equal to the equivalent system. Therefore, the resistance factor, K_R, must always equal the load factor, K_L.

$$K_R = \frac{R_{me}}{R_m} = K_L \tag{8.8}$$

where

K_R = $\frac{k_e}{k}$

R_m = maximum value of wL, or the plastic-limit load the beam can support statically

R_{me} = R_m for the equivalent system

k_e = wL that would cause a unit elastic deflection at mid-span.

The resistance and deflection are related in the elastic range by Hooke's Law $R = kx$ and $R_e = k_e x$ for the equivalent system.

The load mass factor, K_{LM}, is the ratio of the mass and load factors. The equation of motion can now be written in the form of the real system with the equivalent transformation factors.

$$K_{LM} M_T \ddot{x}(t) + kx(t) = F(t) \tag{8.9}$$

Now, using the static resistance function, R, to replace $kx(t)$, the equation becomes

$$K_{LM} M_T \ddot{x}(t) + R(t) = F(t) \tag{8.10}$$

The SDOF model can effectively be used to describe the response of a CMU wall to blast effects. The incorporation of the characteristics of the retrofit techniques into the model results in an engineering level tool for wall retrofit design and analysis.

In blast design the element of interest is typically stressed beyond the elastic range, to the area of elasto-plastic behavior and then into the plastic zone where eventually hinges and final failure may occur. Analysis and design of these elements are usually too difficult to obtain from exact solutions in mathematical terms and simplifying assumptions and equivalent models to represent the elements must be developed to obtain solutions through numerical analysis and/or approximate design/analysis methods. Equation 8.11 was developed from Equation 8.10 to describe the response of a CMU wall to blast effects by calculating the variation of acceleration with time.

$$\ddot{x}(t) = \frac{1}{K_{LM} M_T}\big(F(t) - R(t)\big). \tag{8.11}$$

An approximate solution to the differential equation was obtained using a numerical technique that solved the equation iteratively starting at time zero when the displacement and velocity parameters were defined. The time scale was divided into discrete intervals,

and the solution was obtained by successively extrapolating the displacement from one time station (i) to the next using the recurrence formula (Biggs, 1964).

$$x^{(i+1)} = 2x^{(i)} - x^{(i-1)} + \ddot{x}^{(i)}(\Delta t)^2 \tag{8.12}$$

where

$x^{(i+1)}$ = the displacement in the next time station

$x^{(i-1)}$ = the displacement in the preceding time station

$\ddot{x}^{(i)}$ = the acceleration in the current time station

Δt = the time interval between stations.

Since an initial value for $x^{(i-1)}$ did not exist, the initial time step was calculated separately. The acceleration was assumed constant in the first time interval and equal to the initial value, so that the displacement at $x^{(1)}$ could be found using the following equation.

$$x^{(1)} = \frac{1}{2}\ddot{x}^{(0)}(\Delta t)^2. \tag{8.13}$$

The SDOF analysis described above to calculate the maximum mid-span deflection for each retrofitted wall subjected to the specified blast load was programmed into an Excel spreadsheet. The three components used to define the equation of motion for the equivalent system were calculated. The total mass required to determine the inertial force is completed in Table 8.1. The external load acting on the equivalent system is defined in Table 8.2 and the resisting force of the wall/retrofit system is entered into

Table 8.1. Wall and retrofit information.

Wall and Retrofit Data	**Input**
Wall Height	in.
Wall Width	in.
Wall Thickness	in.
CMU Wall Weight	lb
Weight/Unit Area of CMU Wall	$lb/in.^2$
Retrofit Thickness	in.
Weight/Unit Area of retrofit	$lb/in.^2$
Retrofit Weight	lb
Total Weight/Unit Area	$lb/in.^2$
M_t	$lb\text{-}sec^2/in.$

Table 8.2. Dynamic load.

Dynamic Load	**Input**	
Peak Reflected Positive Pressure		psi
Peak Reflected Impulse		psi-msec
F		lb/in.
t_{eo}		sec
Δt		sec

Table 8.3. A screenshot of the Excel spreadsheet used to predict the dynamic response is provided in Figure 8.2 and each table highlighted on the sheet is discussed in the following section.

Table 8.3. Resistance function.

Full-Scale Resistance Function				Subscale Resistance Function	
X Deflection, in.	**R Pressure, psi**	**Pressure/ Unit Width**	**Slope**	**R Pressure, psi**	**X Deflection, in.**
Column 1	Column 2	Column 3	Column 4	Column 5	Column 6

The physical dimensions of the CMU wall and retrofit used in each dynamic experiment were entered into Table 8.1, and the total mass, M_T, of the wall and retrofit was calculated using:

$$M_T = \left(\frac{\text{CMU and Retrofit Weight/Unit Area}}{g} \right) (\text{Height} \times \text{Unit Width}) \qquad (8.14)$$

where g is gravity (32.2 ft/sec^2 or 386 in./sec^2). The total mass of the system is used to determine the inertial component of the SDOF system. The mass of the wall remains unchanged due to the extremely short time duration of the event. One should also note that the mass of the retrofit system in the form of a membrane is minimal or negligible when compared to the mass of the CMU wall.

The external force acting on the system was determined based on the dynamic load for each full-scale retrofitted CMU wall experiment that was evaluated. The peak reflected pressure and impulse values used to represent the desired dynamic load were entered into Table 8.2. For simplification purposes, the assumption was made that the explosive event occurred at a sufficient range (standoff) to create a planar wave on the CMU wall, thereby applying a uniform load on the entire wall as it undergoes one-

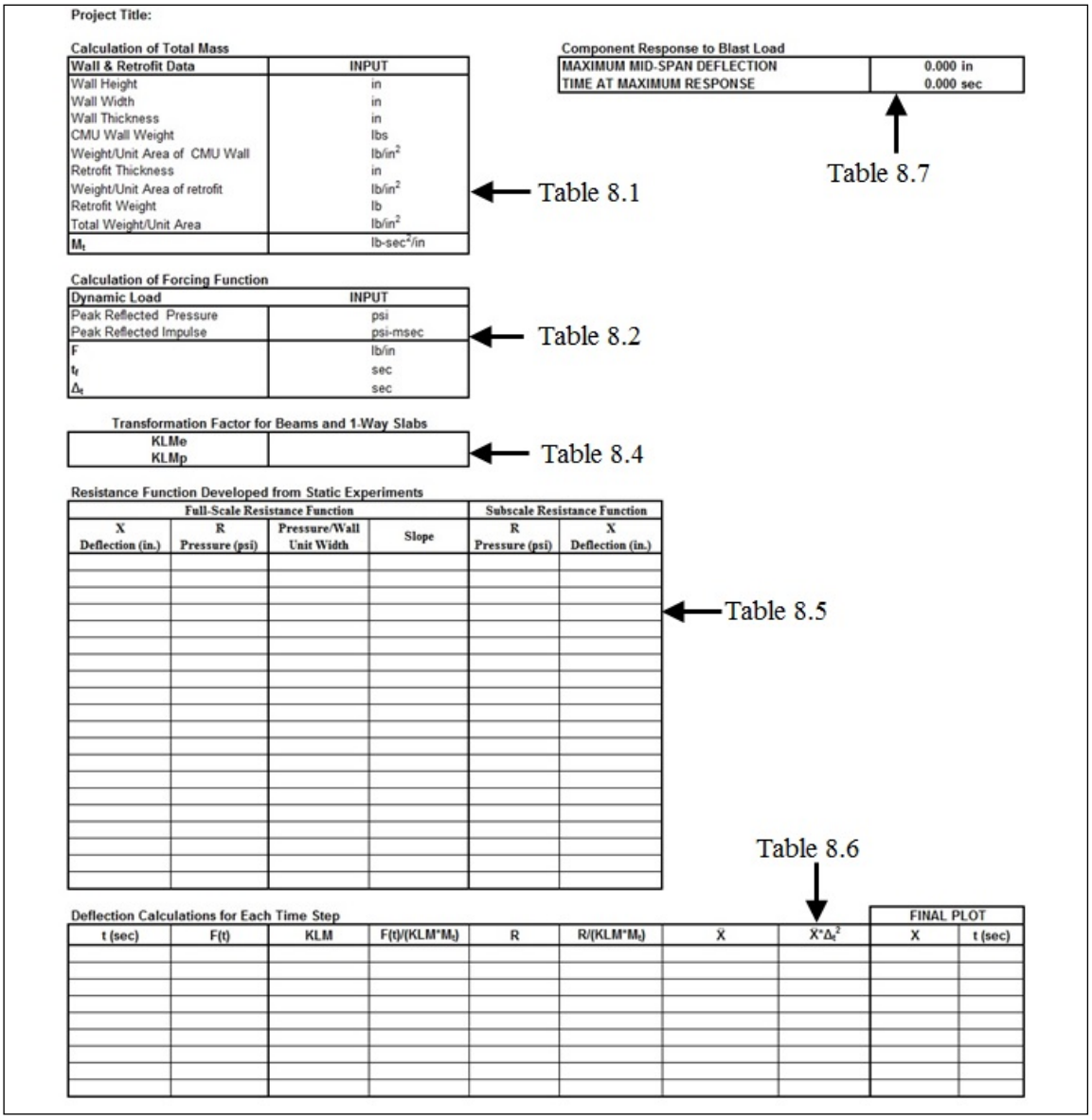

Figure 8.2. Screenshot of SDOF analysis using Excel.

dimensional curvature. A typical pressure versus time history plot for a HE blast wave is presented in Figure 8.3a. The wave initiates suddenly at a very high positive pressure. Then, the positive pressure wave decreases quickly to zero at time, t_o, which represents the duration of the positive phase. The initial positive phase is followed by a negative

pressure phase. The maximum negative pressure is usually much smaller than the positive pressure, but the duration of the negative pressure phase is normally much longer then the positive pressure phase. In most experimental situations, the negative impulse has been measured to be less than the positive impulse.

The peak reflected pressure (P_r) and impulse (I_r) values for each charge weight and standoff were used to create a simplified linearly decaying pressure-time history in the form of an equivalent positive triangular load followed by an equivalent negative rectangular load (Figure 8.3b). The peak pressure at time zero for the simplified load history was maintained as the maximum pressure for the dynamic load under consideration. The impulse calculated by determining the area under the true pressure-time history was also maintained for the simplified time history. This allows the duration of the positive phase, t_{eo}, for the simplified load history to be calculated using

$$t_{eo} = \frac{2I_r}{P_r} \tag{8.15}$$

The negative pressure for the equivalent rectangular load was calculated by finding the area (impulse) above the negative pressure curve. The magnitude of the negative impulse and the duration of the negative phase were maintained for the simplified time history. This allowed the magnitude of the negative pressure to be obtained

$$P_{en} = \frac{-I}{t_n}$$

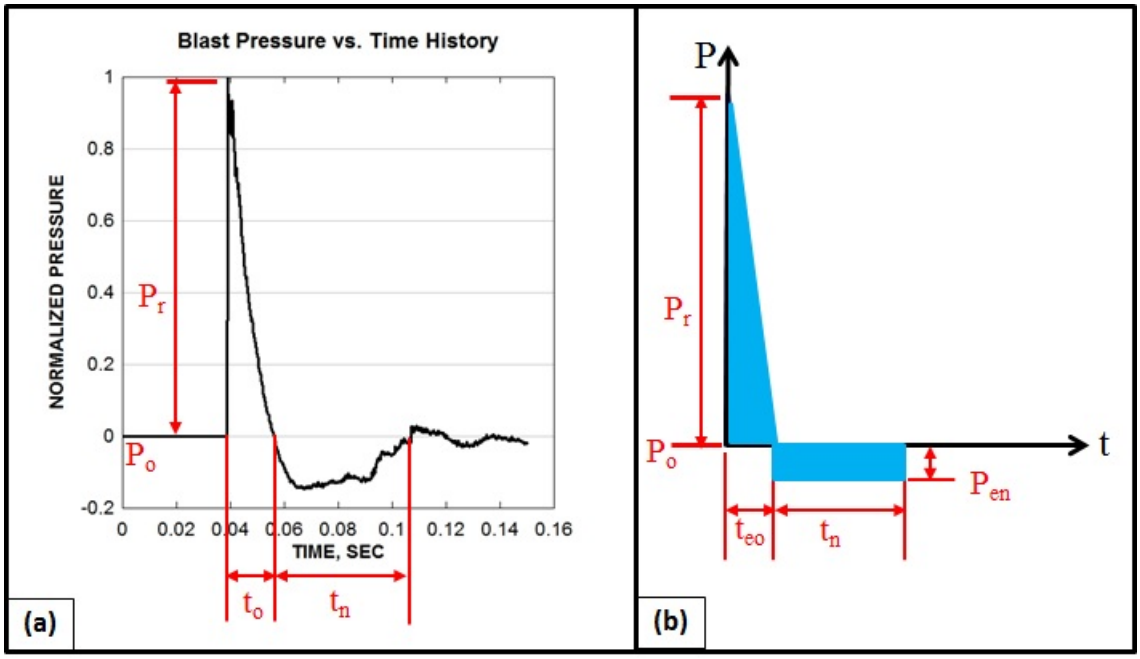

Figure 8.3. Waveform. (a) Typical blast pressure-time history. (b) Equivalent pressure-time history.

Most structural elements are designed to resist the positive pressure impulse. This design philosophy assures that the design of the structural element is conservative. In many cases, the stiffness of the element being designed is such that ignoring the negative phase results in a relatively small overall error in response. However, in the current situation, the stiffness of the reinforced CMU walls are such that neglecting the effects of the negative impulse results in a significant overestimation of the CMU wall's deflection. Therefore, in this effort both the positive and negative impulses were taken into account.

The accuracy of any numerical method in a step-by-step integration is dependent on the magnitude of the time increment, Δt. Several factors are considered when

determining the time increment: (1) the natural period of the structure, T; (2) the rate of variation of the loading function; and (3) the complexity of the stiffness and damping functions (Paz 1997). Biggs recommends an interval 1/10th of the natural period, while Paz suggests that sufficient results can be obtained with a time interval no longer than 1/6th the natural period of the structure. The natural period, T, and the natural frequency, f, of a one-degree-of-freedom system are:

$$T = 2\pi\sqrt{\frac{W}{kg}} \tag{8.16}$$

$$f = 1/T \tag{8.17}$$

Several time increments were evaluated beginning at $10^{-(n+1)}$ with n equal to 0 to 6 and as the time increment decreased the displacement values began to converge to the same value within 5 significant digits. No additional benefit was gained by continuing to decrease the time increment. Therefore, the time increment, Δt, selected for the analysis was entered into Table 8.2 as 0.0001.

The load-mass transformation factors, K_{LM}, for a simply-supported beam subjected to a uniform load across the entire span was published in Biggs (1964) and the values are provided in Table 8.4. The K_{LM} value for the strain response was entered into . 8.5 on the Excel spreadsheet as shown in Figure 8.2.

The experimentally determined resistance function for the respective retrofitted CMU walls was entered into Table 8.3. Columns 5 and 6 contain the experimentally derived pressure and deflection values respectively from the HTC. According to the laws

Table 8.4. Transformation factors for beams and one-way slabs. (Biggs 1964)

Strain Range	Load Factor, K_L	Mass Factor, K_M	Load-Mass Factor, K_{LM}	Maximum Resistance, R_m	Spring Constant	Dynamic Reaction, V
Elastic	0.64	0.5	0.78	$\frac{8M_p}{H}$	$\frac{384EI}{5L^3}$	0.39R+0.11P
Plastic	0.50	0.33	0.66		0	$0.38R_m$+0.12P

Table 8.5. Load/mass transformation factor.

Transformation Factor for Beams and 1-Way Slabs	
$K(LM)_e$	
$K(LM)_p$	

of geometrically similar scaling, the displacement values for the resistance function for the full-scale prototype in Column 1 were determined by multiplying the subscale displacement in Column 6 by the scaling factor discussed in Section 4.1. The pressure values from the subscale model (Column 5) were also used for the full-scale prototype (Column 2), because the magnitude of the pressure does not scale (β=1). Columns 1 and 2 represent the deflection and load, respectively, for the resistance function of the full-scale prototype. Columns 3 and 4 are additional terms used to calculate the appropriate values to use in the acceleration and displacement calculations to be conducted in Table 8.6. Column 3 is the resistance per unit width for the retrofitted wall, and Column 4 is the slope between two successive points on the resistance function.

Table 8.6. Calculation of displacement at mid-span.

t (sec)	F(t)	KLM	F(t)/ (K_{LM}*M_t)	R	R/ (K_{LM}*M_t)	$\ddot{X}$	$\ddot{X}$*Δt^2	X	t (sec)
Col. 1	Col. 2	Col. 3	Col. 4	Col. 5	Col. 6	Col. 7	Col. 8	Col. 9	Col. 10

The wall displacement at mid-span was calculated in Table 8.6 for each incremental time step. The time, *t*, for each calculation is provided in Column 1 and each successive time step was increased by the incremental time step, Δt, selected for the numerical integration process. Column 2 is the force applied at time, *t*, from the equivalent reflected pressure-time curve created in Table 8.2. Column 3 contains the appropriate load mass factors, K_{LM}, as determined by . 8.5 and the full-scale resistance function in Table 8.3. Columns 4, 5, and 6 contain the calculated force and resistance terms for the equation of motion. The acceleration values in Column 7 were obtained from subtracting the resistance term in Column 6 from the force term in Column 4. Column 9 contains the wall's mid-span displacement value for each time step as calculated using Equation 8.12. The magnitude of the maximum displacement and the associated time at the maximum response are provided in Table 8.7. The data used in the SDOF analysis are provided in Table 8.8.

The predicted mid-span deflections for the retrofitted CMU walls generated from the SDOF analysis are presented in Table 8.9. The normalized deflection versus time histories for the full-scale walls evaluated in the HE experiments and in the SDOF analysis are provided in Appendix F. The percent difference between the experimental

Table 8.7. Structural component response to blast load.

MAXIMUM MID-SPAN DEFLECTION	in.
TIME AT MAXIMUM RESPONSE	sec

Table 8.8. Wall and retrofit physical geometry and dynamic load level for full-scale SDOF model.

Wall					Retrofit		Dynamic Load Level
Label	**Height, in.**	**Width, in.**	**Thickness, in.**	**Weight, lb/in.^{3}**	**Thickness, in.**	**Weight, lb/in.^{3}**	
FS3	111	174	7.625	0.0455	0.2926	0.03996	3
FS4	130	224	7.625	0.0455	0.2926	0.03996	2
FS5	111	174	7.625	0.0455	0.2382	0.03031	3
FS8	130	224	7.625	0.0455	0.1195	0.04291	2
FS10	111	174	7.625	0.0455	0.1195	0.04291	3
FS11	177	224	7.625	0.0455	0.1195	0.04291	3
FS12	120	120	7.625	0.0455	0.091	0.0414	1
FS14	177	224	7.625	0.0455	0.0695	0.04081	3
FS15	111	174	7.625	0.0455	0.068	0.04289	2
FS17	111	174	7.625	0.0455	0.0715	0.03694	3
FS18	111	174	7.625	0.0455	0.076	0.04261	4

and predicted values were calculated using Equation 8.18 and are also provided in Table 8.9 for each full-scale retrofit that was evaluated.

$$\% \text{ Difference} = \frac{(x_{Experiment} - x_{Predicted})}{x_{Experiment}} \times 100 \tag{8.18}$$

Table 8.9. Normalized deflections from full-scale experiments and SDOF analysis.

Retrofit		Experimental Deflection Data	Displacement Calculated in SDOF	% Difference Exp. vs. Excel
Grade 2 ±45-deg Fiber Reinforced Spray-on Polyurea	FS3	0.396	0.397	0
	FS4	0.52	0.224	57
Trowel-on Thermoset	FS5	0.37	0.689	86
Trowel-on Thermoset and Unreinforced Film	FS8	0.404	0.379	6
	FS10	1	0.557	44
Trowel-on Epoxy and Unreinforced Film	FS11	0.712	0.475	33
Trowel-on Epoxy and ±45-deg Fiber Reinforced Film	FS12	0.251	0.218	13
Unreinforced Film and PSA	FS14	0.74	0.406	45
	FS15	0.662	0.361	45
±45-deg Fiber Reinforced Film and PSA	FS17	0.594	0.452	24
	FS18	0.594	0.621	5

The percent differences between the experimental and predicted values ranged from 0 to 86%. The average percent difference for all of the experiments was 33%. A significant amount of this average percent difference was caused by the results from full-scale wall FS5. This specimen was prepared using the trowel-on thermoset retrofit. The thickness of the retrofit used in the experiment was not well documented, and the structural response obtained in FS5 could not be repeated successfully in subscale or full-scale dynamic experiments. Therefore, it was determined that the FS5 result can be classified

as an outlier and removed from further review. Once the FS5 wall result was removed from the test matrix, the average percent difference between the measured and predicted mid-span deflections reduced to 27%. In all cases except for one, the predicted mid-span displacement underestimated the measured mid-span displacement.

The difference between the experimental and predicted values can be explained to some extent based on the observations recorded from the full-scale experiments. In Section 4.3.3, the different anchorage systems used in the experiments were discussed and the response of the retrofit systems at the supports were discussed for each retrofit evaluated in the respective section. The instrumentation that documented the mid-span deflection of the retrofitted wall during the response to the blast load measured the sum of the displacement of the CMU wall and the peel back of the retrofit materials at the supports. Unfortunately, it was not possible to separate the peel-back of the retrofit materials at the supports from the CMU displacement by either the instrumentation or high-speed video. However, examination of the high-speed video shows that significant peel-back of the retrofit materials at the supports did occur. In addition, damage to the mechanical anchorage was identified during the posttest inspections of the wall. The mechanical anchorage at the top and bottom supports was located 4-in. behind the surface of the CMU wall, so the maximum peel-back failure that could occur at the top and bottom supports was 4-in. If 4-in. is added to the SDOF predicted results presented in Table8.9, then the average percent difference decreases to 16%.

Based upon the results presented in this chapter, it is concluded that SDOF model can be combined with experimental scale-model results to do a reasonable job of predicting the full-scale response of the polymer reinforced CMU walls.

9. CONCLUSIONS AND RECOMMENDATIONS FOR FUTURE RESEARCH

The process of modifying an existing structure to withstand larger loads or to modify the structural response by adding additional materials or material systems is referred to as a retrofit. The research objective was to identify successful retrofit procedures for CMU walls and to provide a method to predict their response to blast loads. This objective was accomplished by developing several retrofit systems capable of mitigating the debris hazard associated with existing structures to airblast loads.

The research program contributed valuable information for engineers seeking retrofit solutions for steel- and concrete-framed structures with CMU infill walls. The application procedure, equipment requirements, and material characteristics for each retrofit system were outlined. Resistance functions and failure criterion for select retrofit systems were developed. Information obtained from the static and dynamic experiments used to characterize the responses of the retrofitted CMU walls to the blast loads will allow engineers, designers, and building owners to compare the various material systems and determine the retrofit that is applicable to specific explosive events and economic requirements.

Qualitative and quantitative information gathered from Chapters 4 to 8 was used to identify the most efficient and effective retrofit system evaluated in the research program. The characteristics, qualities, and physical properties that were deemed important during the development of the research program for the retrofit materials were ranked from 1 to 6 with 1 being the most desirable and 6 being the least desirable in

Table 9.1. By ranking the materials, it allowed the retrofit system with the lowest cumulative total to be identified as the most efficient retrofit system. Some of the items used to rank the retrofit systems included personnel safety equipment, training, equipment cost, time required to prep and install the retrofit systems, transportability of

Table 9.1. Ranking the retrofit systems evaluated in the research program.

	Spray-on Polyurea and Fiber Reinforcement	**Trowel-on Thermoset**	**Trowel-on Adhesive and Unreinforced Elastomeric Film**	**Trowel-on Adhesive and Reinforced Elastomeric Film**	**PSA and Unreinforced Elastomeric Film**	**PSA and Reinforced Elastomeric Film**
Equipment Cost	6	3	4	5	1	2
Transportability	4	3	2	2	1	1
Labor	6	5	3	4	1	2
Facility Down Time	4	3	2	2	1	1
Training/Difficulty	4	3	2	2	1	1
Quality Control	6	5	3	4	1	2
Dynamic Load	3	6	5	4	1	2
Availability	2	4	3	3	1	1
Safety Equipment	4	3	2	2	1	1
Analysis	5	6	3	2	4	1
Total Score	44	41	29	30	13	14

the retrofit materials, and equipment, quality control and assurance, the dynamic load mitigated, and the ability to analyze and predict the structural response of the retrofitted CMU wall.

All of the retrofit systems evaluated in the full-scale experiments were successful at some dynamic load level; as expected, some loads were higher than others. In Figure 9.1 all of the dynamic experiments were plotted, so that the level of the dynamic load for each retrofit system could be compared easily. To allow the subscale and full-scale experiments to be compared, a scale factor was applied to the impulse values obtained experimentally for each subscale dynamic experiment. Then, the impulse values for the subscale and full-scale walls were normalized, and the results are plotted on Figure 9.1.The open circles represent experiments where the retrofit performed successfully, and the solid data points represent the experiments where the retrofit failed to mitigate the secondary debris hazard. The subscale dynamic experiments were scaled to represent full-scale data and plotted with the full-scale experimental data.

The retrofit system evaluated successfully at the highest dynamic load was the unreinforced film applied to the wall using a PSA. The reinforced film applied to the wall using a PSA was a close second. The unreinforced film did have two occurrences at lower dynamic load levels where the retrofit failed, whereas the reinforced film only had one load in which it failed and it was quite a bit higher than the retrofit that was successful. This leads to more confidence in the retrofit systems containing the reinforced film over the unreinforced film. The unreinforced spray-on polyurea and trowel-on thermoset coatings were the least successful in the research program and

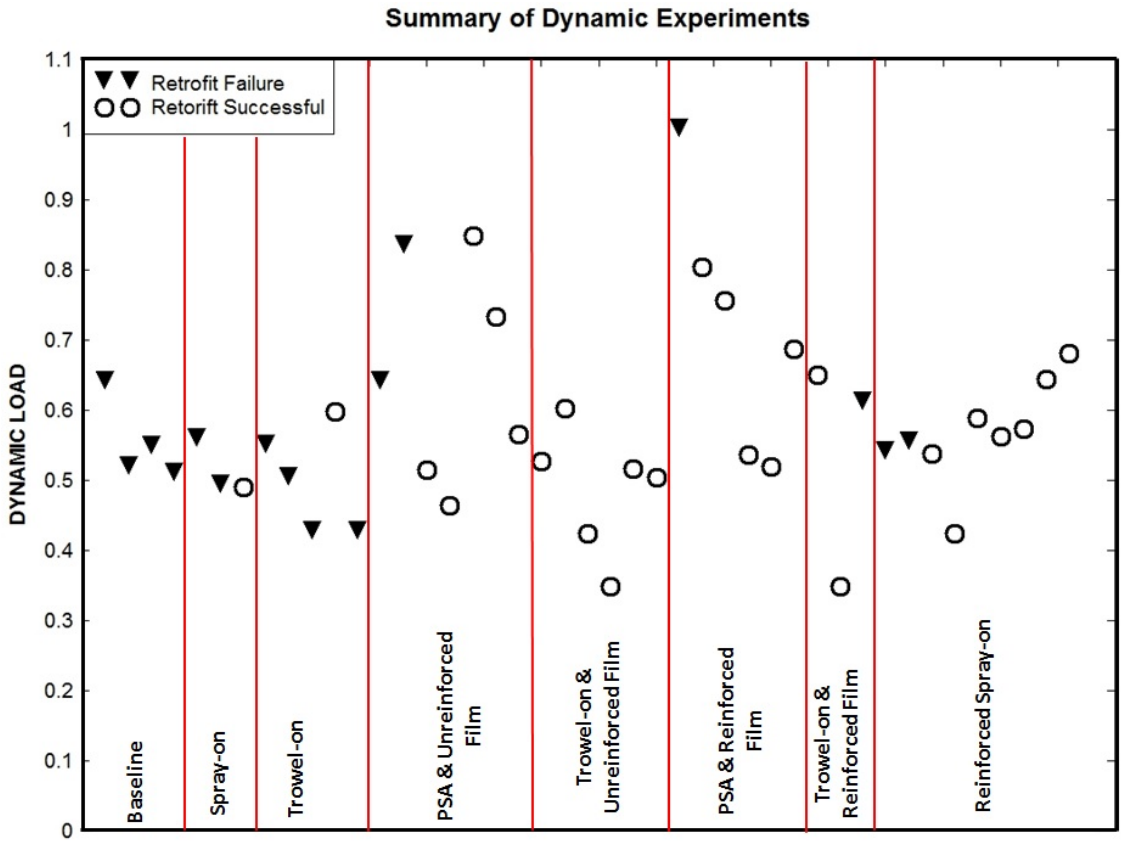

Figure 9.1. Dynamic load levels evaluated for each dynamic experiment.

are not recommended for use based on the structural responses observed in the dynamic experiments.

The reinforced spray-on retrofit systems successfully reduced the secondary debris hazard associated with CMU walls subjected to dynamic airblast loads. The effectiveness of the variations of the retrofit system was demonstrated in subscale static and dynamic experiments. The results from the subscale static and dynamic experiments identified the increase in ultimate flexural resistance through composite action, as well as the tensile membrane resistance achieved by both unreinforced and reinforced

elastomeric retrofit systems applied to hollow unreinforced CMU walls. From these experiments it was determined that the Grade 1 performed well, but the Grade 2 was more effective. Note that the two reinforced spray-on retrofitted walls (one subscale and one full-scale) that failed in the dynamic experiments did not use any mechanical anchorage system relying only on the adhesive strength between the polyurea and the steel or concrete supports. The subscale wall used fiber reinforcement in the 0/90-deg orientation and failed very early in the loading process, while the full-scale wall retrofitted with the ±45-deg fiber orientation failed after the initial deflection into the structure and during the rebound phase of the response, the material peeled off the top support. As expected, the stiffness of the polyurea material increased as the magnitude of the reinforcement increased. The stiffer reinforced material translated into smaller deflections; however, it was determined that the material can become too stiff, resulting in failure at the supports. The subscale static and dynamic experiments identified the importance of the fiber orientation and tensile strength. The 0/90-deg fiber orientation resulted in a retrofit system that was too stiff and resulted in failures at lower dynamic load levels than the corresponding walls retrofitted with the off-axis ±45-deg fibers. Therefore, fiber orientation significantly affected the ductility of the material.

The spray-on polyurea cures quickly after installation, and the spray rig ensures consistent mixing ratios, which are advantageous. However, the retrofit system has several characteristics that make it less than the ideal solution. The amount of equipment required for application is extensive, i.e., 220-volt electrical current, large air compressor, and spray-rig. The equipment and the two components housed in 50-gal

drums are not man–portable, and thus create additional logistical restraints. The spray-rig is expensive and maintenance intensive, which makes it difficult to use in austere environments. In addition to the high maintenance requirements, extensive training is also required to operate, clean, and maintain the equipment. Individuals who plan to operate the spray rig should be trained by professionals and maintain quality application techniques. The full-scale evaluation was performed in a sandy environment that made it extremely difficult to keep the spray tip clean. The crew suffered significant down time while the tip was cleaned or replaced frequently. The wall was retrofitted inside a reinforced-concrete reaction structure that was cleaned prior to the application process, but the spray tip still clogged. Those operating the system must wear extensive protective and safety gear. ERDC technicians wore a respirator and in some cases used a small air compressor to pump fresh air into the helmet. Areas not to be coated must also be protected because it is very easy to overspray the desired area.

The unreinforced and ±45-deg fiber reinforced elastomeric films applied to the CMU walls using a trowel-on adhesive successfully mitigated the debris hazard associated with airblast loads. It was noted in several posttest inspections of the dynamic experiments that the full CMU block or at least half of the blocks remained adhered to the elastomeric film after the blast event. This could be an important factor if the user would like to have additional protection from small arms fire after the initial blast event. The blocks that remained attached to the film after the blast event provided a visual barrier from potential follow-up or second wave attackers. However, it should be noted that the CMU wall was compromised and the weight of the blocks on the elastomeric

film may cause the film to tear away from the top support at some point after the initial blast attack. Unfortunately, long-term observations of the retrofit system were not conducted to determine the time it would take for the gravitational forces acting on the blocks to cause the film to fail due to posttest clean up requirements at the remote field site. The strong adhesion between the wall surface and film was created by the ability of the trowel-on materials to fill the air voids and discontinuities in the CMU surface. Therefore, if the user would like the CMU blocks or at least the face shells of the CMU blocks to remain attached to the retrofit system after the explosive event, then the trowel-on/film system should be selected for use. Out of the nine dynamic experiments conducted on the trowel-on/film system, only one failed. Additional experiments are recommended to establish the upper limit for this retrofit system.

The trowel-on/film retrofit systems had several advantageous characteristics and only a few drawbacks. Personnel safety equipment required for prep and installation were minimal, and no heavy equipment was required for installation. The ability to apply a manufactured film to the wall surface decreased the time required to apply the retrofit system and increased the quality control and assurance. However, the trowel-on adhesive had to be mixed to a particular ratio and was applied to the wall surface by technicians using notched trowels to control the material's thickness. Technicians had to work quickly so that the material would not begin the curing process before the film could be applied. A delay in film application compromised the adhesion between the film and adhesive. The training required to apply the trowel-on/film system was minimal and

could be accomplished on-site easily. The film can be shipped easily, but the trowel-on material was susceptible to high/low temperatures as discussed in Section 4.6.5.

The most effective and efficient retrofit system was the unreinforced and reinforced elastomeric films applied to the CMU walls using PSAs. The unreinforced film had a slight edge when comparing the highest dynamic load mitigated, but the reinforced film was evaluated at a very similar level. However, both systems could be evaluated at additional dynamic loads because the difference between the failure and success levels for the reinforced film was significant indicating that a dynamic load between those two values should be selected for additional evaluation. The PSA/film retrofit system was the easiest to apply and required little to no training. No heavy equipment was required, and safety equipment consisted of gloves and eye protection. In fact, the only equipment required for installation consisted of a paint roller and bucket to apply a primer and a knife and rubber roller to cut and apply the film. The material can be applied with minimal interruption to the facility. Other than moving the room's contents away from the wall surface, the operation and use of the facility was uninterrupted. The film was also applied to the wall quickly allowing the wall to be upgraded with little to no delay and no cure time is required because the PSA is applied to the film before the material arrives on site. Quality control and assurance are further increased or improved because the trowel-on material that requires mixing and application has been replaced by a PSA that was produced and applied to the film in a manufacturing facility. The only disadvantage, which was outside the scope of the research, was the inability of the current PSA to maintain adhesion of the blocks to the film after the initial blast event.

The bond between the film and CMU are much weaker using the PSA than when the trowel-on adhesive was used, so it will not provide a visual barrier against a follow-up attack. A visual barrier could be added to the system easily if a pigment was added to the resin or if the film was painted to create a visual barrier.

A full-scale fiber-reinforced polyurethane film has been produced by one of the manufacturers based on specifications developed during the progression of the research program and is available commercially. The retrofit system consists of a 48-in.-wide polyurethane film with open-weave ±45-deg Aramid fiber reinforcement with an aggressive hybrid acrylic PSA applied to one face of the film, and a primer for the wall/supports that emits no VOCs and requires no respirator materials for application. The film, including the removable liner protecting the PSA, was 71.5 mils thick. The adhesive and the removable liner are each 7 mils thick. The reinforcement is encapsulated in the film through an extrusion process.

The full-scale validation of the preferred retrofit systems demonstrated not only the effectiveness of the material against blast loads but also the ability to use subscale dynamic and static experiments to evaluate and develop retrofit systems. Some of the retrofit systems were removed from further evaluation due to poor performance in the subscale experiments. In Chapter 8, the ability to predict the responses of the retrofitted CMU walls to blast loads was assessed. The assessment was conducted by comparing the full-scale values from the HE experiments to the predicted values obtained using the SDOF model. It was determined that the best results were aachieved when both the positive and negative phases of the pressure wave were included in the SDOF analysis.

From the research program, one can apply the following procedure to determine the effectiveness of a retrofit material to blast loads.

- Step 1: Construct and execute a static experiment on a scale model.
- Step 2: Develop the static resistance function for the scale model.
- Step 3: Modify the static resistance function by applying the scale factor.
- Step 4: Execute the dynamic analysis using a SDOF model.
- Step 5: Based on the results from the SDOF model and observations in the static experiments, determine if the retrofit is worthy of final full-scale experimentation.
- Step 6: Conduct full-scale dynamic experiment.

While application of the above procedure allowed the pass/fail response to be accurately predicted for the full-scale wall retrofits examined, it is highly recommended that all potential retrofit materials used to protect high value assets be subjected to a full-scale dynamic experiment before deployment.

Future investigations should focus on materials and new systems that will continue to decrease the cost and improve the consistency of the material's response. It is highly recommended that the high strain rate effects on elastomeric and fiber-reinforced elastomeric materials be evaluated. Additional research could also be conducted on resin and fiber materials as well as fiber orientations. The contribution of the fibers and the optimal orientation of the fibers could also be investigated further. For example, a method similar to the one used in concrete design to determine a balance between the reinforcing steel and concrete could be developed to determine a balanced fiber strength and orientation in the resin to create an optimal response from the composite material.

The mechanical anchor systems could also be investigated further, and new techniques could be developed to anchor the retrofit systems.

If full-scale static and dynamic experiments could be conducted on the same size walls and retrofit materials, some of the questions regarding the scaling effects on the overall response of the wall as well as the strain rate effects on different material scales could be eliminated. This could be accomplished quite easily if a full-scale static test chamber and a dynamic test facility such as a BLS could be used to conduct the experiments efficiently and economically. To date, this has not been possible, but the construction of a new static test facility with an 8-ft by 8-ft loading area and a new target vessel for the BLS with an 8-ft by 8-ft target vessel to be completed at ERDC within the near future will allow future researchers to remove the scale factor from the unknowns.

The retrofits tested in the retrofit program proved that the secondary debris hazard from CMU walls subjected to HE events can be mitigated effectively. The retrofit systems could also be effective against other loading regimes. For example, a set of walls were unexpectedly subjected to hurricane force winds when the Category 3 Hurricane Dennis passed directly over the Florida test site in July of 2005. The walls were subjected to documented wind speeds of 131 to 155 mph. Four CMU walls were on the test site and all of them were retrofitted except for one. The CMU wall to the left in Figure 9.2a was retrofitted with an unreinforced elastomeric film adhered to the wall with a trowel-on epoxy. No visible signs of damage were found on the retrofitted wall during the post-storm inspection. The storm impacted the site before the wall to the right

in Figure 9.2a could be retrofitted. The unretrofitted wall failed, and the debris was propelled to the back of the reaction structure during the storm (Figure 9.2b).

Hollow, unreinforced, CMU walls were chosen as the structure to be retrofitted in the research program because it was one of the weakest structural components that could be evaluated. However, additional structures may also benefit from the retrofit systems. Tilt-up concrete panels or wood-stud walls could also benefit from the retrofit materials

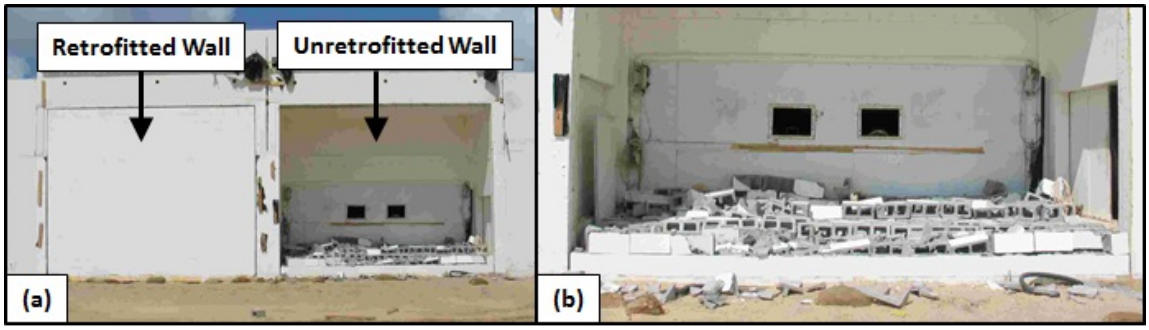

Figure 9.2. Wall response to huricane. (a) CMU walls after the hurricane. (b) Unretrofitted wall debris inside reaction structure.

discussed in the CMU research program. For example, an unretrofitted and a retrofitted wood-stud wall with brick veneers were added to test plans at Eglin AFB. The wood-stud walls were evaluated at dynamic load level 1. The target was built inside the reaction structure, Bay 5, and consisted of three walls and a ceiling. The three wood-stud walls were constructed with dimensional lumber and plywood sheathing (Figure 9.3a). The two side walls were anchored to the floor slab of the reaction structure with one concrete anchor bolt in the front corner (Figure 9.3b). No anchor bolts were used to secure the front wall panel to the reaction structure. The ceiling was constructed with

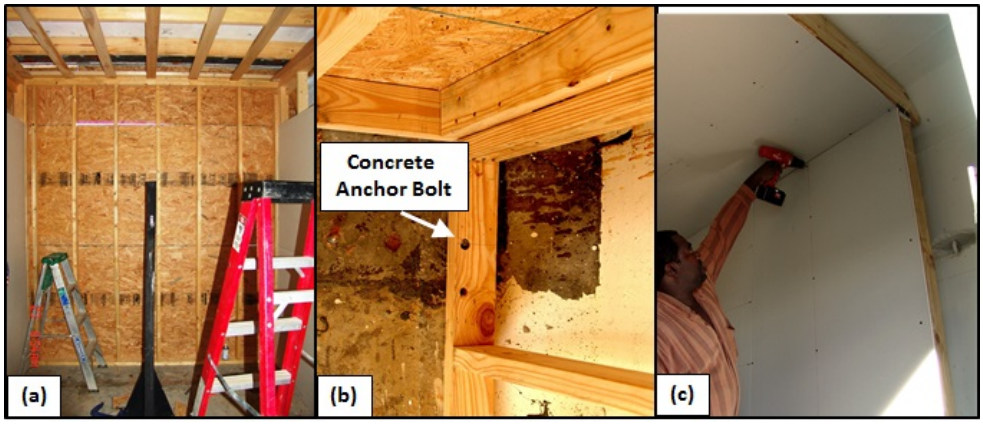

Figure 9.3. Conventional wood construction. (a) Dimensional lumber and plywood sheathing. (b) Concrete anchor bolts used to secure the lumber to the floor slab. (c) Sheetrock interior walls.

dimensional lumber, and standard sheetrock (gypsum board) was used on the interior walls and ceiling (Figures 9.3c and 9.4c). Veneers consisting of a single wythe of bricks were added to the front wall (Figures 9.4a and b) of each target. Unlike the CMU walls evaluated in the research program, a gap was not provided at the top or on the sides of the reaction structure to ensure a one-way response.

Figure 9.4. Brick façade. (a) Single wythe brick veneer. (b) Target exterior. (c) Target interior.

The unretrofitted target was heavily damaged during the HE event (Figure 9.5a). A majority of the brick veneer fell outside the reaction structure, but several large sections were propelled or fell into the reaction structure (Figure 9.5b, 9.6b, and 9.6c). The dimensional lumber and plywood used to frame the top half of the front wall were pulled away from the top support (Figure 9.6a). The bolts anchored the side walls and prevented the bottom plate from moving. This could be one reason that the primary

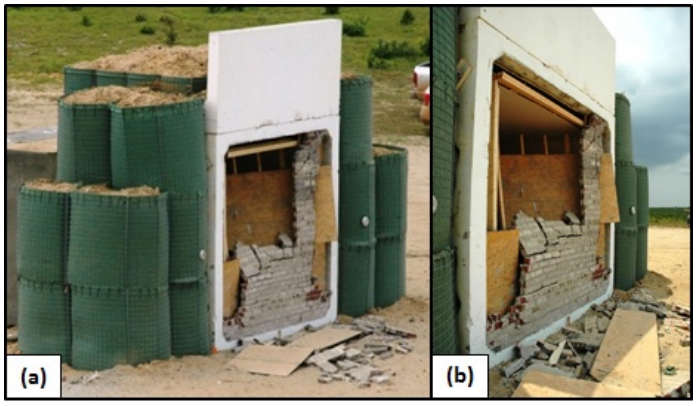

Figure 9.5. Unretrofitted wall response. (a) Posttest exterior view. (b) Debris outside of structure.

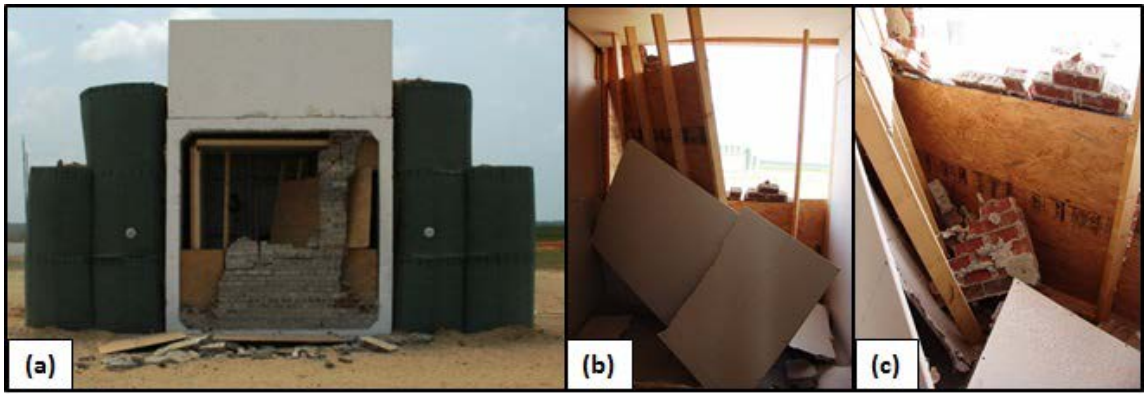

Figure 9.6. Wall response. (a) Heavy damage to top half of wall. (b) Sheetrock deflected into the structure. (c) Bricks from façade found inside structure.

damage occurred along the top of the wall that was not anchored. The ceiling panel remained in place. However, the ceiling may not have been able to deform because the framing for the ceiling panel was built tight against the concrete reaction frame. This may have prevented the ceiling from buckling under load. The retrofitted wall was built under the same conditions and subjected to the same dynamic load so that a one-to-one comparison was available.

The only difference between the two walls was the unreinforced polyurethane film that was installed to the interior of the retrofitted structure (Figure 9.7a). The film was applied to the sheetrock horizontally from one side wall to the opposite wall rather than vertically from the ceiling to the floor. The sheets of film were applied to at least a 2-ft section of the side walls adjacent to the front corners. The first sheet of film was applied to the top of the wall, and each successive sheet overlapped the previous sheet by 4 in. An additional 1-ft strip of material was applied over the first sheet of film to add additional support along the top edge of the wall. The film was anchored to the structure by attaching two 2-in. by 4-in. pieces of dimensional lumber on each side wall spaced 16 in. apart (Figure 9.7b and c). The film was sandwiched between the anchor boards, the sheetrock, and the 2-in. by 4-in. boards used to frame the side walls.

The retrofitted wall was damaged during the airblast, but no secondary debris was found inside the reaction structure. The brick veneer was cracked (Figure 9.8a), and the center of the wall deformed into the reaction structure (Figure 9.8d). The damage to the brick veneer implied that the wall developed a two-way response. As in the unretrofitted experiment, the largest amount of damage and deformation occurred in the top half of

the wall (Figure 9.8b). The accelerometer mounted on the center of the wall (Figure 9.8c) recorded a maximum deflection of 0.388.

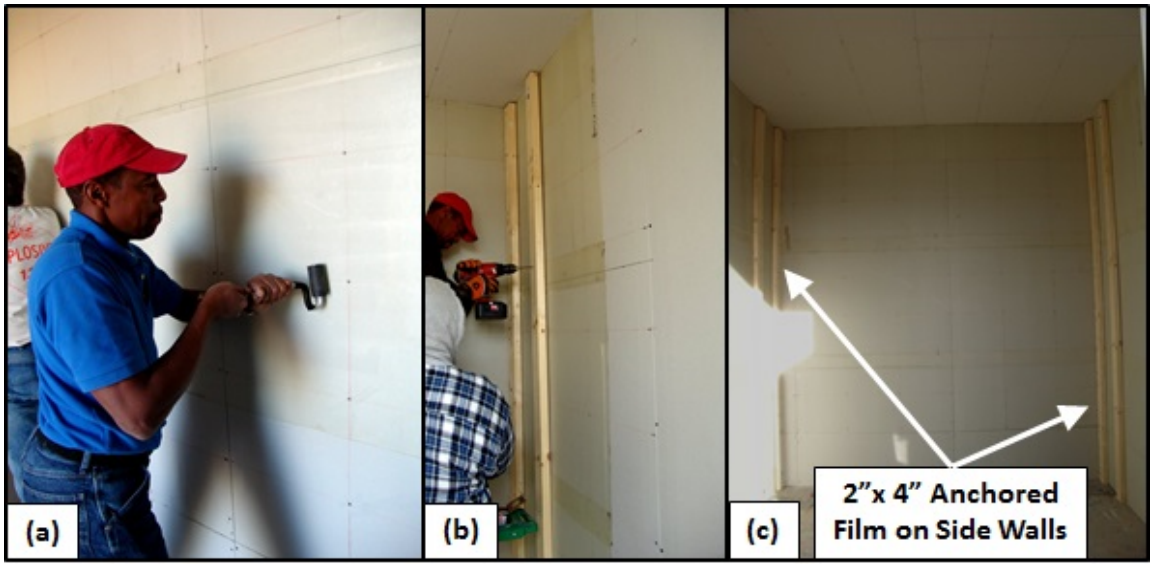

Figure 9.7. Retrofitted conventional wood construction. (a) Unreinforced elastomeric film applied horizontally across the front wall. (b) Dimensional lumber (2-in. by 4-in.) used to anchor retrofit to side walls. (c) Anchors were applied to both side walls.

Figure 9.8. Retrofitted wall response. (a) Posttest exterior of retrofitted wall. (b) Profile view of wall. (c) Posttest interior view of wall. (d) Retrofitted wall deflected into structure, but no debris fragments were found inside protected space.

Additional experiments should be conducted on a retrofitted wood-frame structure before the retrofits are deemed a successful mitigation technique because the side walls and ceiling were shielded in the above experiments and were not subjected to the airblast. To evaluate the capacity of a retrofitted conventional wood-frame structure to blast loads, the complete structure should be constructed on a typical foundation to define the additional damage that would be incurred due to the blast load on the side walls and roof of a complete structure. By constructing and retrofitting the entire structure, one can also determine if the current method to anchor the film on the side walls would be effective in a structure.

REFERENCES

3M. *Adhesives and Tapes: Design Guide for Bonding, Attaching, and Fastening.* St. Paul, MN: 3M, 2006.

Alkhrdaji, Tarek. "Blast Mitigation of Concrete Structures." *The Construction Specifier,* Vol. 59, no. 3, Alexandria, VA: Construction Specifications Institute, March 2006: 38-46.

Alkhrdaji, Tarek. "Blast Mitigation of Concrete Structures: An Overview of Assessment and Upgrade Processes." *Structural Engineer,* October 2006: 40-43.

Baker, Wilfred E., Peter S. Westine, and Franklin T. Dodge. *Similarity Methods in Engineering Dynamics: Theory and Practice of Scale Modeling*. Rochelle Park, NJ: Spartan Books, 1973.

Baylot, James T., Billy Bullock, Thomas R. Slawson, and Stanley C. Woodson. "Blast Response of Lightly Attached Concrete Masonry Unit Walls," *Journal of Structural Engineering*, Vol. 131, no. 8, American Society of Civil Engineers, August, 2005: 1186-1193. DOI: 10.1061(ASCE)0733-9445(2005)131:8(1186).

Biggs, John M., *Introduction to Structural Dynamics.* New York: McGraw-Hill, 1964.

Buchan, P.A. and J.F. Chen. "Blast Resistance of FRP Composites and Polymer Strengthened Concrete and Masonry Structures – A State-of-the-Art Review," *Composites: Part B*, Vol. 38, Issues 5-6, Elsevier Ltd., July-September 2007: 509-522. DOI: 10.1016/j.compositesb.2006.07.009.

Chopra, Anil K. *Dynamics of Structures: Theory and Applications to Earthquake Engineering.* 2nd ed. Upper Saddle River, NJ: Prentice-Hall, 2001.

Department of the Army, *Fundamentals of Protective Design for Conventional Weapons, Technical Manual TM 5-855-1*, Washington D.C., November 1986.

Dinan, Robert J., David R. Coltharp, and Phillip T. Townsend. *Fabric Retrofits of Concrete Masonry Exterior Walls – Blast Response Evaluation.* ERDC/GSL TR-02-18, US Army Corps of Engineers, Engineer Research and Development Center, Geotechnical and Structures Laboratory, Vicksburg, MS, 2002. (Limited Distribution).

Drysdale, Robert G., Ahmad A. Hamid, and Lawrie R. Baker. *Masonry Structures: Behavior and Design,* 2nd ed. Boulder, CO: The Masonry Society, 1999.

Graco Inc. *Reactor® E-30i and E-XP2i: Integrated Proportioning System.*Minneapolis, MN: Graco Inc., 2012. Accessed September 1, 2013. http://www.graco.com /content/dam/graco/aftd/literature/brochures/348500/348500EN-B.pdf.

Gurvin, Peter E. and Andrew C. Remson III. "U.S. Embassy Designs Against Terrorism: A Historical Perspective." *Structures 2001: A Structural Engineering Odyssey*. American Society of Civil Engineers, 2001: 1-10. DOI: 10.1061/40558(2001)73.

Huntsman Corporation. *Users Guide to Adhesives.*The Woodlands: Huntsman Corporation, 2007. http://www.freemansupply.com/datasheets/adhesiveguide.pdf.

Hyde, D. W. *User's Guide for Microcomputer Program CONWEP, Applications of TM 5-855-1, Fundamentals of Protective Design for Conventional Weapons SL-88-1*, U.S. Army Corp of Engineers Waterways Experiment Station Instruction, Vicksburg, MS, April 1988, revised February 1993.

Johnson, C.F., B.P. DiPaolo, and S.C. Woodson. "Evolution of Elastomeric Retrofits for Concrete Masonry Unit Walls for Enhanced Blast Resistance at the Engineer Research and Development Center." *Journal of Advanced and High Performance Materials,* Reno, NV: Matrix Group Publishing, Winter 2011: 27-30.

Johnson, Carol F., James L. Davis, David L. Coltharp, Bartley P. Durst, and Lonnie Smith. *X-Flex™ Retrofit: Results from Subscale Static and Dynamic Experiments.* ERDC/GSL TR-10-36, US Army Corps of Engineers, Engineer Research and Development Center, Geotechnical and Structures Laboratory, Vicksburg, MS, September 2010. (Limited Distribution).

Johnson, Carol F. and Lebron Simmons. *Blast Load Simulator/Shock Tube Testing Facilities in the United States,* U.S. Army Engineer Research and Development Center, Vicksburg, MS, 2008. (Unpublished).

Jones, Normon. *Structural Impact.* New York: Cambridge University Press. 1989.

Jones, P.A.S. *WAC: An Analysis Program for Dynamic Loadings on Masonry and Reinforced Concrete Walls.* Master's Thesis, Mississippi State University, 1989.

Kingery, Charles N. and Gerald Bulmash. *Airblast Parameters from TNT Spherical Air Burst and Hemispherical Surface Burst*, Report ARBL-TR-02555, U.S. Army Ballistic Research Laboratory, Aberdeen Proving Ground, MD, April 1984.

Knox, Kenneth J., Michael I. Hammons, Timothy T. Lewis, and Jonathan R. Porter. *Polymer Materials for Structural Retrofit.* Force Protection Branch, Air Expeditionary Force Technology Division, Air Force Research Laboratory, FL 2000. http://paxconamerica.com/documents/PAXCON%20Test%20Results1.pdf.

Krauthammer, Theodor. *Modern Protective Structures.* Boca Raton, FL: CRC Press, 2008.

Maji, Arup K., Jay P. Brown, and Girum S. Urgessa. "Full-Scale Testing and Analysis for Blast-Resistant Design." *Journal of Aerospace Engineering,* Reston: American Society of Civil Engineers, October 2008: 217-225. DOI: 10.1061/(ASCE)0893-1321(2008)21:4(217).

Mamlouk, Michael S. and John P. Zaniewski. *Materials for Civil and Construction Engineers.* Menlo Park, CA: Addison Wesley Longman, Inc., 1999.

Masonry Standards Joint Committee, American Concrete Institute, Structural Engineering Institute, and Masonry Society (U.S.). 2011. *Building Code Requirements and Specification for Masonry Structures: Containing Building Code Requirements for Masonry Structures (TMS 402-11/ACI 530-11/ASCE 5-11) [and] Specification for Masonry Structures (TMS 602-11/ACI 530.1-11/ASCE 6-11) and Companion Commentaries*. Boulder, CO: The Masonry Society.

Moradi, Lee. *Resistance of Membrane Retrofit Masonry Walls to Lateral Pressure: A Design Tool for One-way Masonry Walls.* Koln, Germany, LAP Lambert Academic Publishing, 2009.

Paz, Mario. *Structural Dynamics: Theory and Computation.* 4th ed. New York: Chapman & Hall, 1997.

Slawson, Thomas R., Carol F. Johnson, and Reed L. Mosher, "Development of a Blast Load Simulator," *Proceedings of the 72nd Shock and Vibration Symposium*, Falls Church, VA: Shock and Vibration Information Analysis Center, 2001. (Limited Distribution).

Troughton, Michael J., ed., *Handbook of Plastics Joining: A Practical Guide*. 2nd ed. Norwich, NY: William Andrew Inc., 2008.

Ugural, Ansel C. and Saul K. Fenster. *Advanced Strength and Applied Ealsticity.* 3rd ed. Englewood Cliffs, NJ: P T R Prentice Hall, 1995.

Wikipedia contributors, "History of terrorism," *Wikipedia, The Free Encyclopedia*, http://en.wikipedia.org/w/index.php?title=History_of_terrorism&oldid=582480488 (accessed February 8. 2010).

Woodson, Stanley C. "Blast-Resistant Structures." U.S. Army Engineer Research and Development Center Graduate Institute, Mississippi State University, Fall 1999. (Course Notes - Unpublished).

Woodson, S.C., Bullock, B.W., and Baylot, J.T., “CMU Wall Debris and Structural Response Experiments.” U.S. Army Engineer Research and Development Center, Vicksburg, MS, November 2001. (Unpublished).

APPENDIX A: ADDITIONAL RETROFIT AND BLAST ANALYSIS LITERATURE

Carney, Preston and John J. Myers. "Shear and Flexural Strengthening of Masonry Infill Walls with FRP for Extreme Out-Of-Plane Loading."*Architectural Engineering 2003 Building Integration Solutions.* American Society of Civil Engineers, September 2003: 246-250. DOI: 10.1061/40699(2003)45.

Connell, James D. "Evaluation of Elastomeric Polymers for Retrofit of Unreinforced Masonry Walls Subjected to Blast." PhD diss., University of Alabama at Birmingham, 2002.

Crawford, John E. "Modeling Blast-Resistant Protection Systems Composed of Polymers and Fabric." *Modeling the Performance of Engineering Structural Materials III*, The Minerals, Metals & Materials Society, 2002: 61-75.

Crawford, John E., Kenneth B. Morrill, Joseph M. Magallanes, and Youcai Wu. "Retrofit of Masonry Walls to Enhance Their Blast Resistance." *Structures Congress 2008: Crossing Borders,* 2008. DOI: 10.1061/41016(314)92.

Cummins, Magee, Kinnebrew, Durst, Davis and Johnson. Reinforced Elastomeric Configuration Tailored to Meet a User's Requirements for Protecting a Structure and a Structure Comprised Thereof, United States Patent Application Publication (US 2009/0004430 A1) 2009.

Davidson, James S., Jeff W. Fisher, Michael I. Hammons, Jonathan R. Porter, and Robert J. Dinan. "Failure Mechanisms of Polymer-Reinforced Concrete Masonry Walls Subjected to Blast." *Journal of Structural Engineering* 131, no. 8, American Society of Civil Engineers, August 2005: 1194-1205. DOI:10.1061/(ASCE)0733-9445(2005)131:8(1194).

Davidson, James S., Jonathan R. Porter, Robert J. Dinan, Michael I. Hammons, and James D. Connell. "Explosive Testing of Polymer Retrofit Masonry Walls." *Journal of Performance of Constructed Facilities* 18, no. 2, American Society of Civil Engineers, May 2004: 100-106. DOI: 10.1061/(ASCE)0887-3828(2004)18:2(100).

Dennis, Scott T. *Masonry Walls Subjected to Blast Loading*. Technical Report No. SL-00-2000, U.S. Army Corps. of Engineers, Waterways Experiment Station, Vicksburg, MS 2000.

Dennis, Scott T., James T. Baylot, and Stanley C. Woodson. "Response of ¼-Scale Concrete Masonry Unit (CMU) Walls to Blast." *Journal of Engineering Mechanics* 128, American Society of Civil Engineers. Febraury 2002: 134-142. DOI: 10.1061(ASCE)0733-9399(2002)128:2(134).

Department of Defense. *Unified Facilities Criteria: Structures to Resist the Effects of Accidental Explosions*, UFC 3-340-02, 2008.

Eamon, Christopher D., "Reliability of Concrete Masonry Unit Walls Subjected to Explosive Loads." *Journal of Structural Engineering,* Vol. 133, no. 7, American Society of Civil Engineers, July 2007: 935-944. DOI: 10.1061/(ASCE)0733-9445(2007)133:7(935).

Eamon, Christopher D., James T. Baylot, and James L. O'Daniel. "Modeling Concrete Masonry Walls Subjected to Explosive Loads." *Journal of Engineering Mechanics,* Vol. 130, no 9. American Society of Civil Engineers, September 2004: 1098-1106. DOI: 10.1061/(ASCE)0733-9399(2004)130:9(1098).

Fatt, M.S. Hoo, X. Ouyang, and R.J. Dinan. "Blast Response of Walls Retrofitted with Elastomer Coatings." *Structures Under Shock and Impact VIII.*WIT Press: 2004: 129-138. DOI: 10.2495/SU040131.

Ghobarah, A., and K. El Mandooh Galal. "Out-of-Plane Strengthening of Unreinforced Masonry Walls with Openings." *Journal of Composites for Construction* 8, American Society of Civil Engineers, July/August 2004: 298-305. DOI: 10.1061/(ASCE)1090-0268(2004)8:4(298).

Holland, T. J. *SOLVER User's Guide. Version 2.2 Dynamic Response Analysis of Single Degree of Freedom Systems.* No. NCEL-UG-0020. Naval Civil Engineering Laboratory, Port Hueneme, CA 1989.

Irshidat, Mohammad, Ahmed Al-Ostaz, Alexander Cheng, and Christopher Mullen. "Blast Resistance of Unreinforced Masonry (URM) Walls Retrofitted with Nano Reinforced Elastomeric Materials." *Structures 2009:Don't Mess with Structural Engineers.* American Society of Civil Engineers, 2009: 2133-2142. DOI: 10.1061/41031(341)234.

Loginow, Anatol. "Strength of Building Elements When Subjected to Airblast." *Practice Periodical on Structural Design and Construction* 13, American Society of Civil Engineers, August 2008: 106-108. DOI: 10.1061/(ASCE)1084-0680(2008)13:3(106).

Makovicka, D. and D. Makovicka Jr., "Dynamic Response of an Office Building Loaded by an Explosion-Generated Air Wave." *Structures Under Shock and Impact IX.* Vol. 87, 2006: 495-504. DOI: 10.2495/SU060471.

Muszynski, Larry C., and Michael R. Purcell. "Use of Composite Reinforcement to Strengthen Concrete and Air-Entrained Concrete Masonry Walls Against Air Blast." *Journal of Composites for Constructioin,* Vol. 7, no. 2, American Society of Civil Engineers, May 2003: 98-108. DOI: 10.106/(ASCE)1090-0268(2003)7:2(98).

Myers, John J., Abdeldjelil Belarbi, and Khaled A. El-Domiaty. "Blast Resistance of FRP Retrofitted Un-Reinforced Masonry (URM) Walls With and Without Arching Action." *The Masonry Society Journal*. September 2004: 9-26.

Ngo, T., P. Mendis, A. Gupta, and J. Ramsay. "Blast Loading and Blast Effects on Structures – An Overview." *EJSE Special Issue: Loading on Structures.* 2007: 76-91.

Slawson, Thomas R., David R. Coltharp, Scott T. Dennis, and Reed Mosher. "Evaluation of Anchored Fabric Retrofits for Reducing Hazards Involving Masonry Wall Debris." In *Proceedings, 9th International Symposium on the Interaction of Effects of Munitions with Structures.* 1999.

Slawson, Thomas R., *Wall Response to Airblast Loads: The Wall Analysis Code (WAC)*. U.S. Army Engineer Research and Development Center, Vicksburg, MS 1995.

Slawson, Thomas R., Carol F. Johnson, and James L. Davis. "Concrete Masonry Unit Wall and Retrofit Analysis Using Simplified Methods." *Structures 2004: Building on the Past, Securing the Future.*American Society of Civil Engineers, 2004:1-9. DOI: 10.1061/40700(2004)153.

U.S. Army Corps of Engineers Protective Design Center. *User's Guide for the Single-Degree-of-Freedom Blast Effects Design Spreadsheet (SBEDS).* PDC TR-06-02 Rev 1. September 2008.

Ward, Stephen P. "Retrofitting Existing Masonry Buildings to Resist Explosions." *Journal of Performance of Constructed Facilities*, Vol. 18, American Society of Civil Engineers, May 2004:95-99. DOI: 10.1061/(ASCE)0887-3828(2004)18:2(95).

APPENDIX B: AUTOCAD DRAWINGS

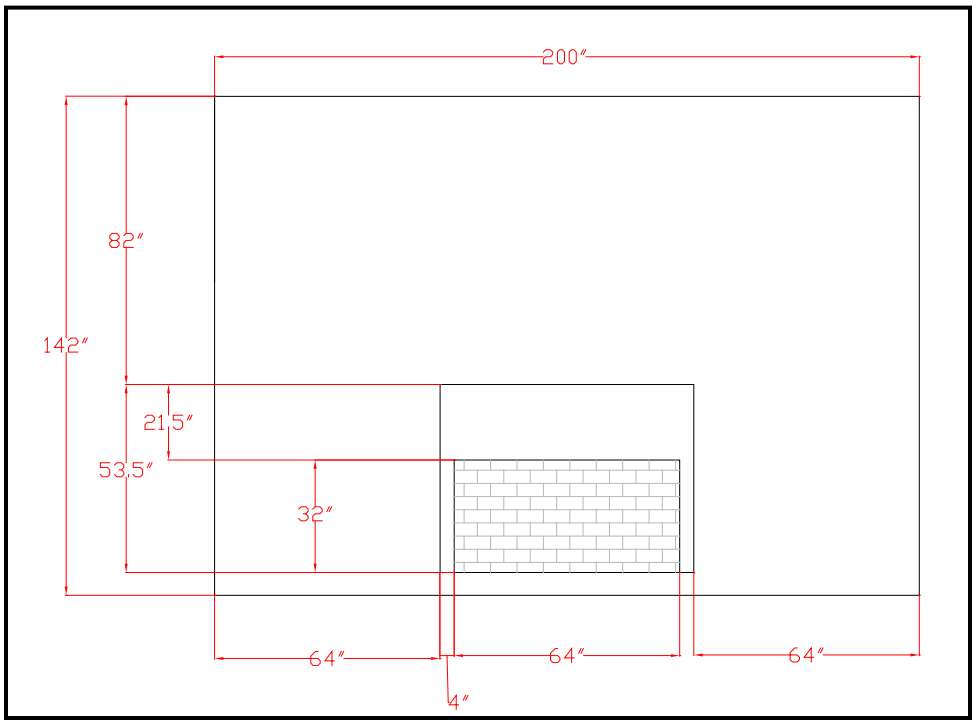

Figure B.1. Subscale dynamic reaction structure.

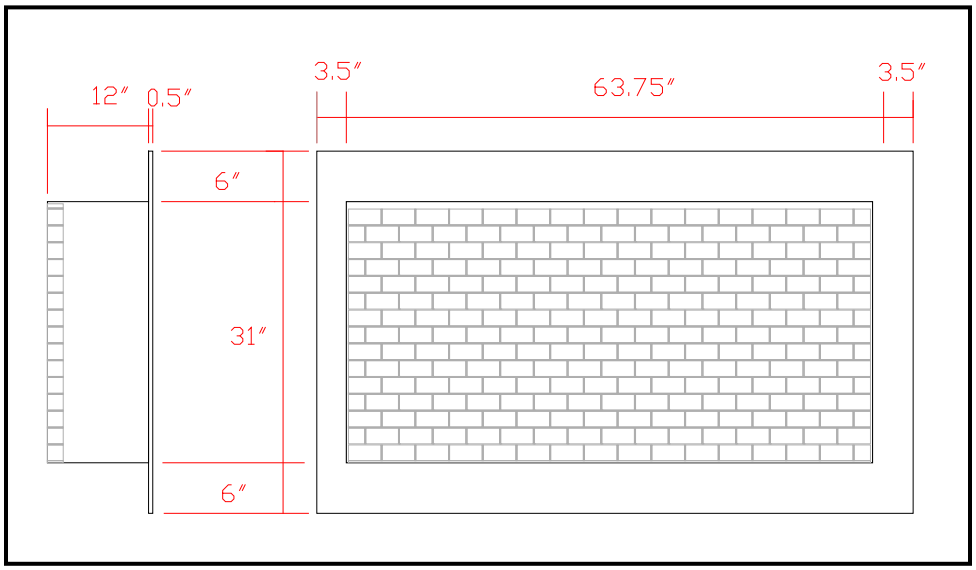

Figure B.2. Subscale CMU wall and steel frame.

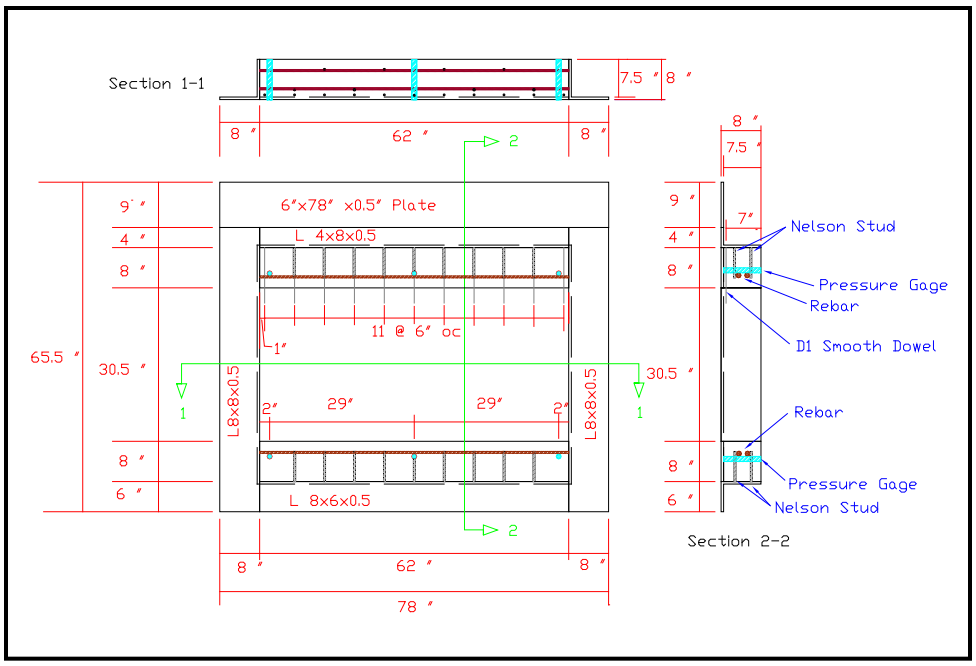

Figure B.3. Subscale concrete frame used in dynamic experiments.

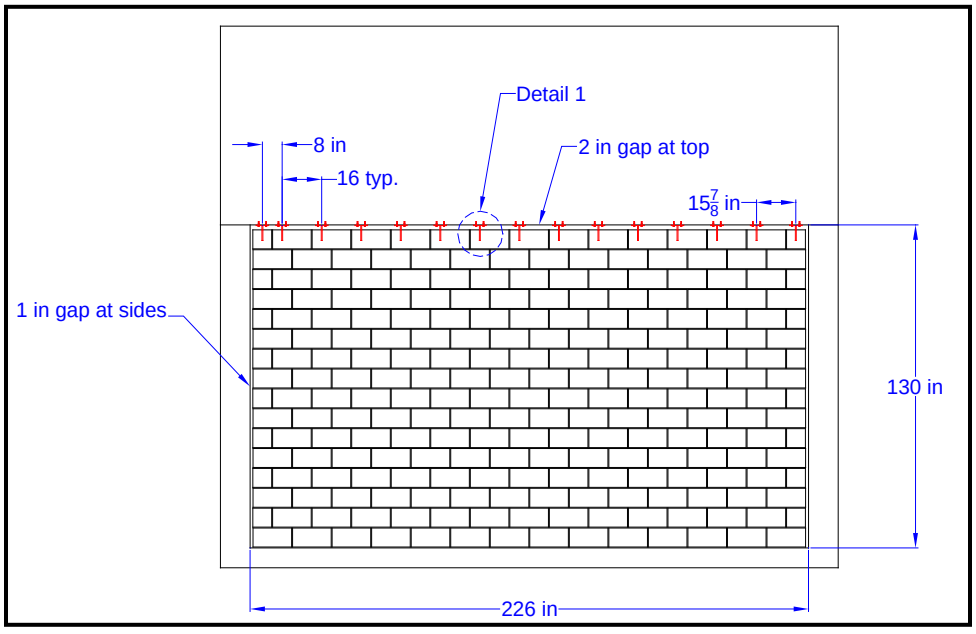

Figure B.4. Typical CMU wall construction details for Bays 1 and 2.

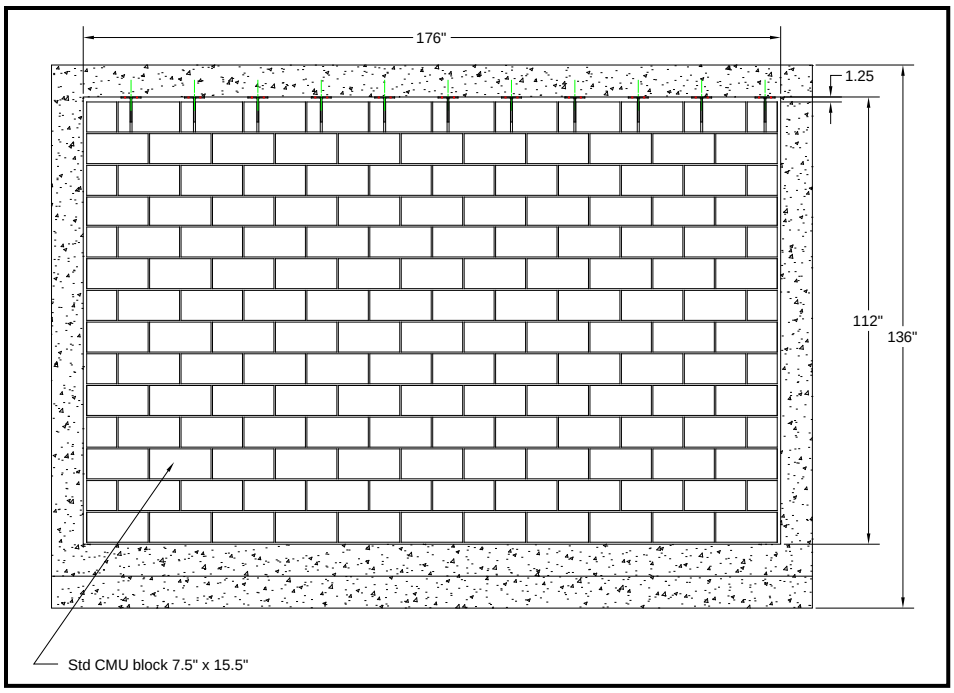

Figure B.5. Typical CMU wall construction details for Bays 3 and 4.

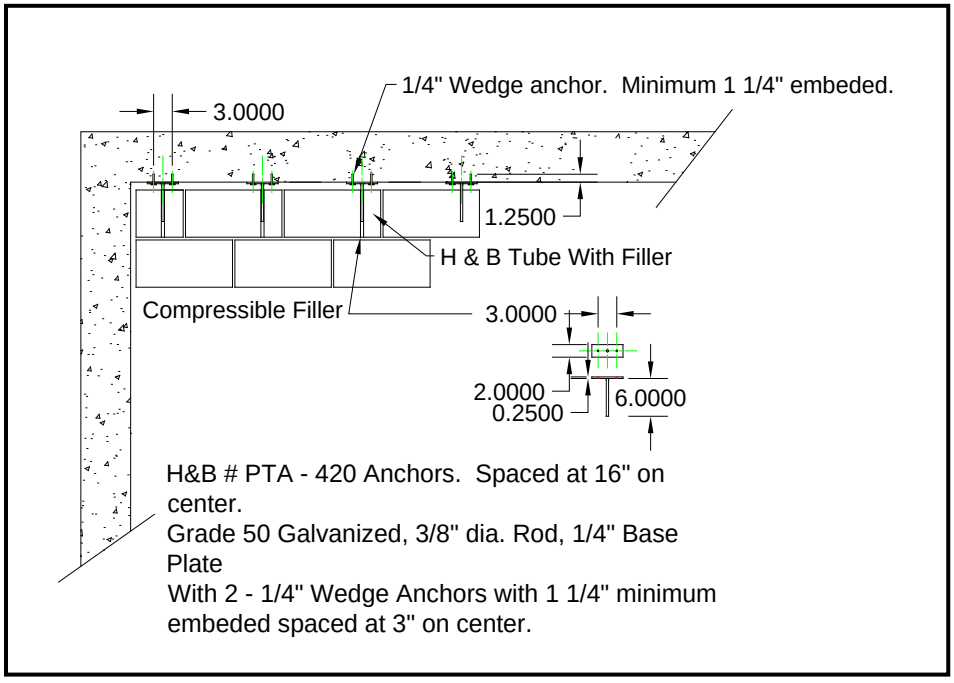

Figure B.6. Dowel details for CMU wall construction in all the full-scale reaction structures.

APPENDIX C: HTC STANDARD OPERATING PROCEDURE

The HTC (Figure C1) is a test apparatus used to develop static resistance functions for components or material systems. The test specimen constructed in a steel frame fits in a void centered between two water-filled chambers (Figure C2). One water chamber is a pressurized chamber, and the second chamber is open to the atmosphere.

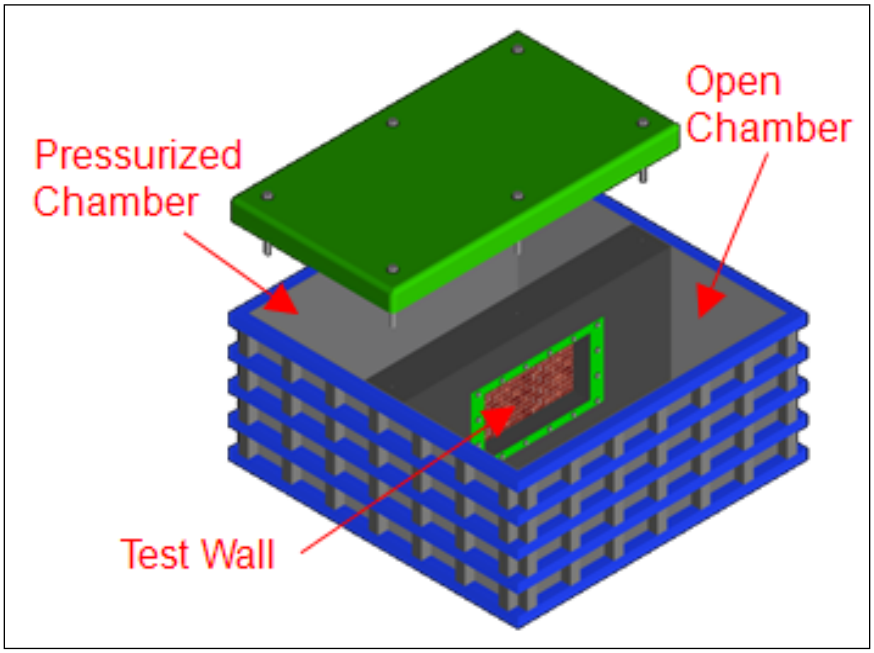

Figure C1. Hydrostatic Test Chamber (HTC).

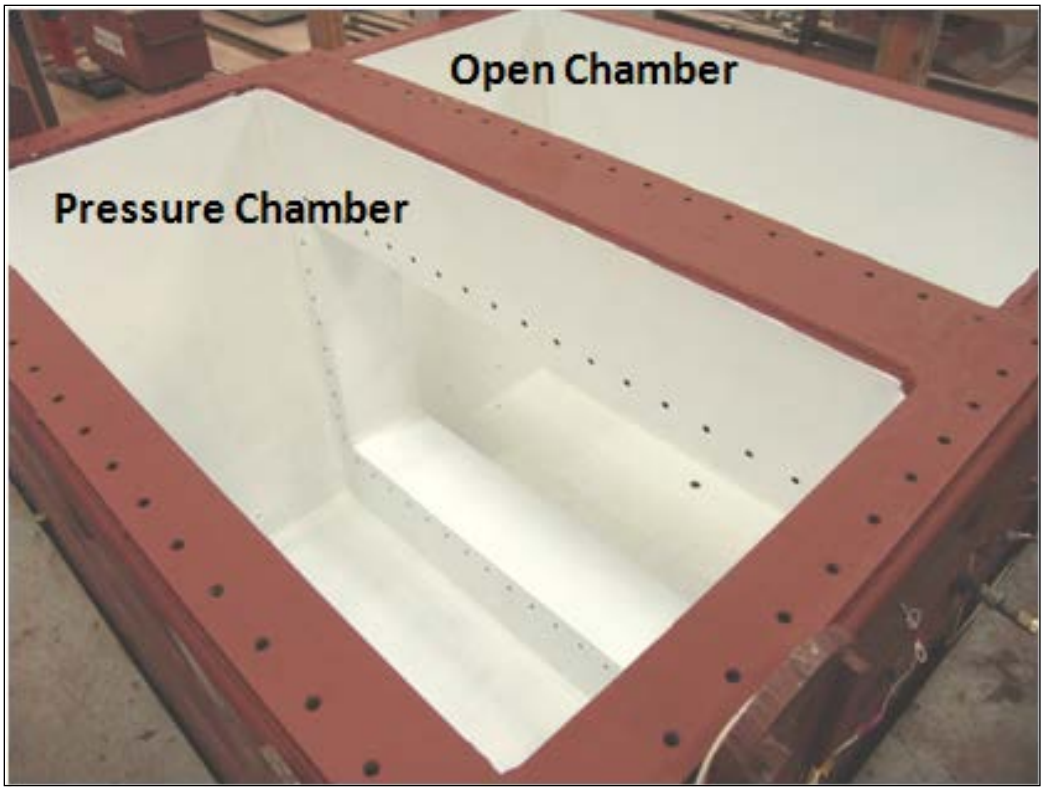

Figure C2. Test specimen is placed in void between the pressure and open chambers.

Step 1: Clean all neoprene seals for the lid, the neoprene membrane, steel membrane ring/frame, steel CMU wall frame, and steel pressure vessel flanges using a grinder with a wire cut-brush attachment. Only use the cut-brush along the perimeter of the neoprene membrane where the pass-through holes for the bolts are located as shown in Figure C3. Be careful not to let the cut-brush damage the interior of the neoprene membrane (the area inside the square in Figure C3). This is the area where the load will be applied to the test specimen, and a cut or weakened area will create a possible weak point in the membrane and failure of

the test. All of the old silicone used in previous experiments should be removed (Figure C4) before the setup process begins.

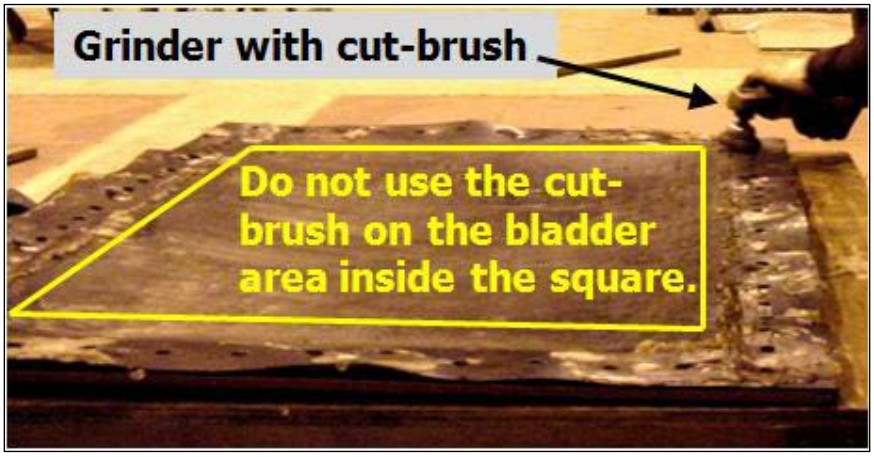

Figure C3. A grinder with a wire brush attachment is used to remove silicone on the neoprene membrane from the previous experiment.

Figure C4. Neoprene seal is cleaned prior to application of new silicone.

Step 2: A neoprene membrane is used to seal the pressurized chamber and to apply the hydrostatic load on the test specimen. Unreinforced and one- and two-fiber-reinforced neoprene materials have been used, but the single-fiber-reinforced material performs the best. The unreinforced material was too weak to sustain higher loads on the test specimen, and the two-fiber material was not ductile enough to sustain large deformations. The material can be cut to 42 in. by 74-3/8 in. using a simple work knife (Figures C5 and C6).

Figure C5. Steel ring and neoprene membrane.

Figure C6. Simple work knife used to cut neoprene material to correct size.

Step 3: Use the steel frame for the membrane to layout the proper bolt-hole placement in the neoprene. Use a punch and hammer to create pass through holes for the bolts that will be used to secure the membrane to the pressure vessel chamber (Figure C7).

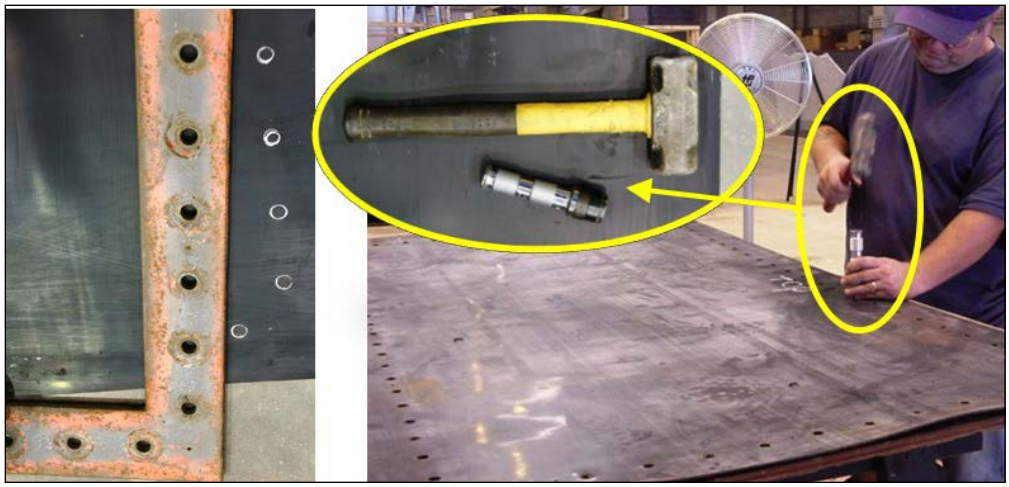

Figure C7. Use steel frame to layout bolt holes, then hammer and punch to create pass-through holes for bolts to secure the membrane to the HTC.

Step 4: Use small nuts, washers, and bolts to attach the neoprene to the steel frame forming the membrane (Figure C8). Silicone should be added around the small bolts to prevent any leakage (Figure C9).

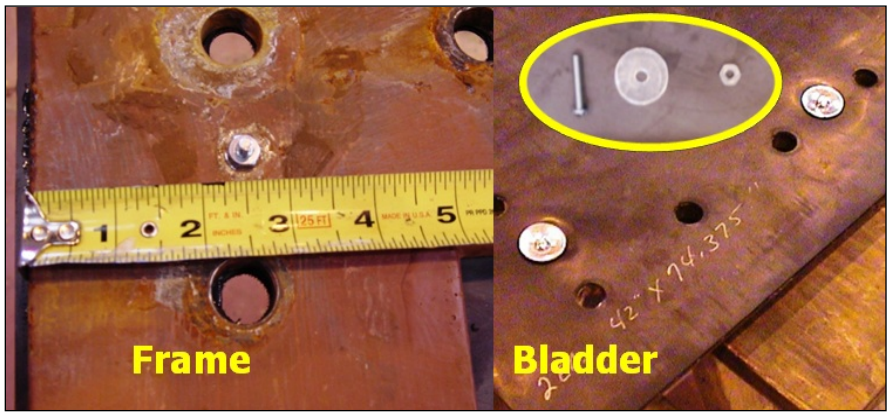

Figure C8. Use screw, washer, and nut to bolt membrane to steel frame. The nut should be on the steel side, and the washer and screw head should be on the membrane face.

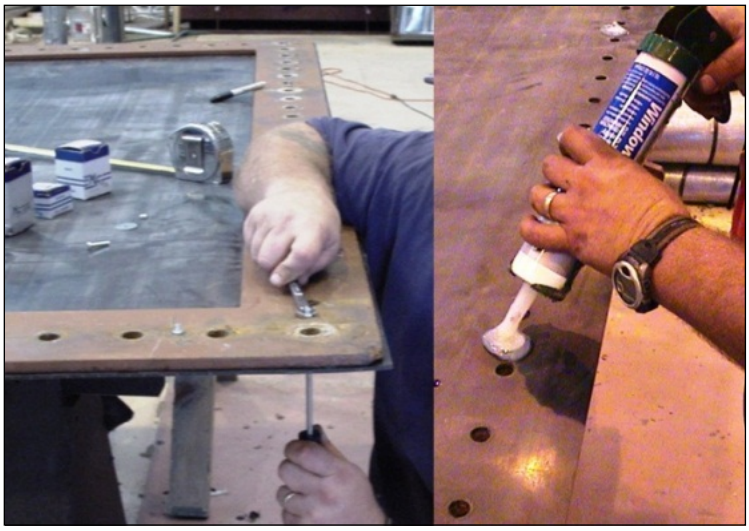

Figure C9. Bolt membrane to steel frame and apply silicone around bolts and washers.

Step 5: A solid bead of silicone should be placed along the perimeter of the membrane and on the interior line along the bolt holes. The full silicone bead should follow the dashed lines as shown in Figure C10. Use the crane to lift the membrane and lower it into the chamber on the pressure side (Figure C11).

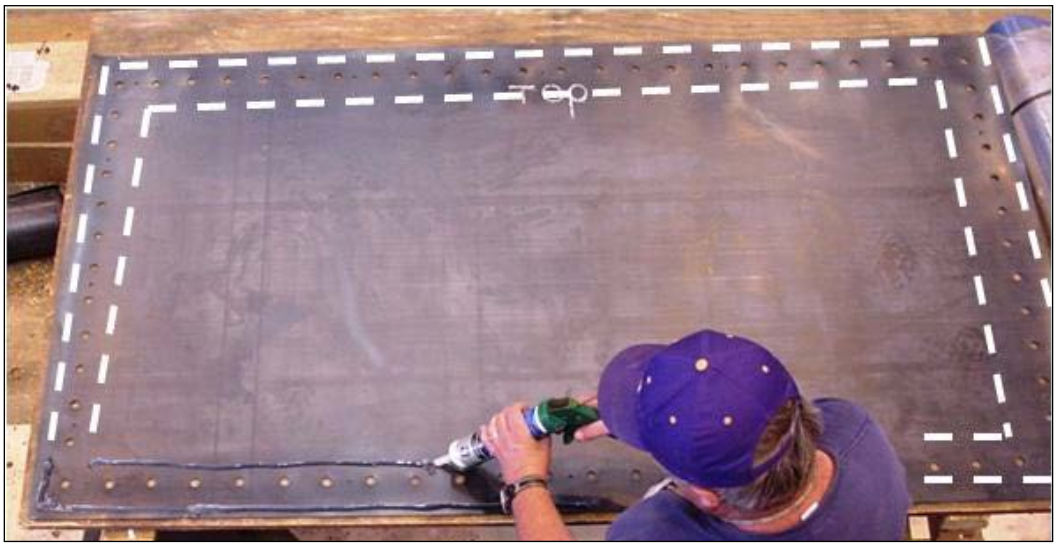

Figure C10. Apply two solid beads of silicone to membrane (one along perimeter and one just inside the bolt holes) before it is attached to pressure cavity.

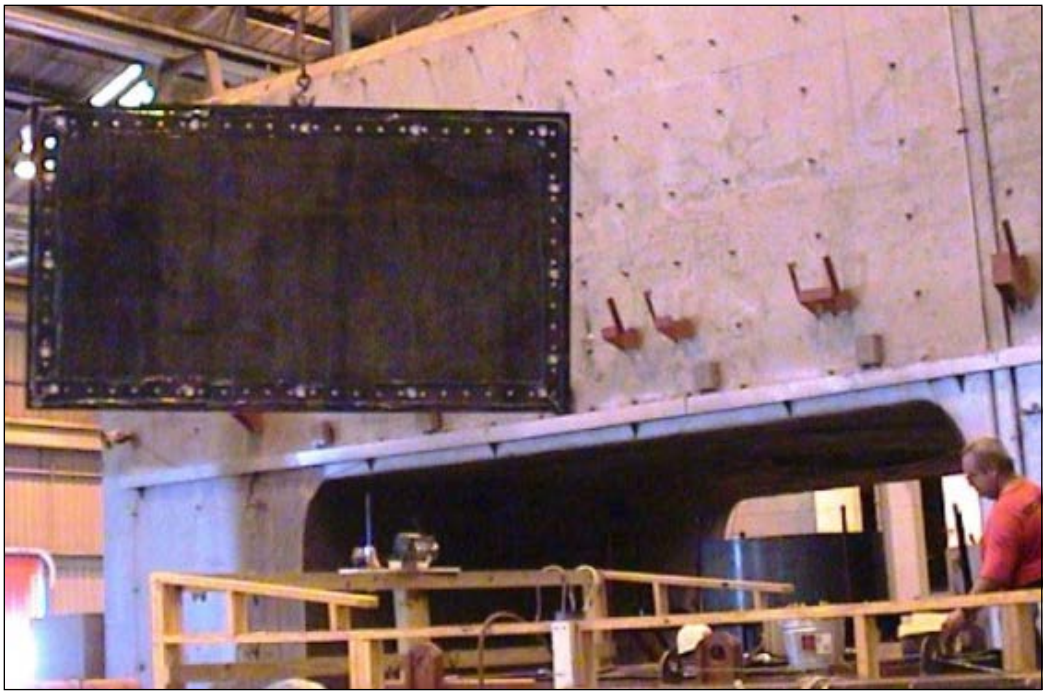

Figure C11. Use crane to load membrane and steel ring component.

Note: There will be multiple steps while setting up the HTC for an experiment that will require the user to bolt components to the walls of the HTC. When instructed to bolt a component to the HTC, DO NOT use an impact wrench (Figure C12). Use an air driven or socket (hand tool) wrench to tighten the bolts. The steel used to construct the HTC is thin, so an impact wrench will destroy the threads in the bolt holes.

Figure C12. Bolt membrane steel frame to pressure cavity. Do not use an impact wrench; use an air or torque wrench.

Step 6: Bolt the membrane into the pressure vessel. Check all the bolts used to secure the membrane before the top of the pressure chamber is attached. If a bolt is stripped and cannot be tightened, check to ensure the threads on the bolt are adequate. If the bolt threads look damaged, use another bolt. If the bolt is still loose and cannot be tightened, leave the bolt in place (as a plug) and silicone around the bolt to prevent any water leakage between the pressure and open chambers of the test apparatus (Figure C13).

Figure C13. Silicone around bolts that may be stripped.

Mark or note the bolt hole that is stripped so that a bolt insert or the hole can be re-tapped before the next experiment. A test can be conducted if one or two bolts are stripped. However, if more than six bolt holes are stripped or if two of the insecure bolts are consecutive, delay the experiment and re-tap the holes before proceeding. It takes 54 3/4-in.-diam bolts to attach the membrane to the HTC.

Step 7: The pressurized chamber has two bolts located under the membrane that are used as plugs (Figure C14). These holes are used to drain water that may be contained in the structural tube that separates the two chambers. Make sure the plugs are in place and apply silicone around each plug (Figure C15). If the plugs leak, the data obtained in the experiment will be compromised.

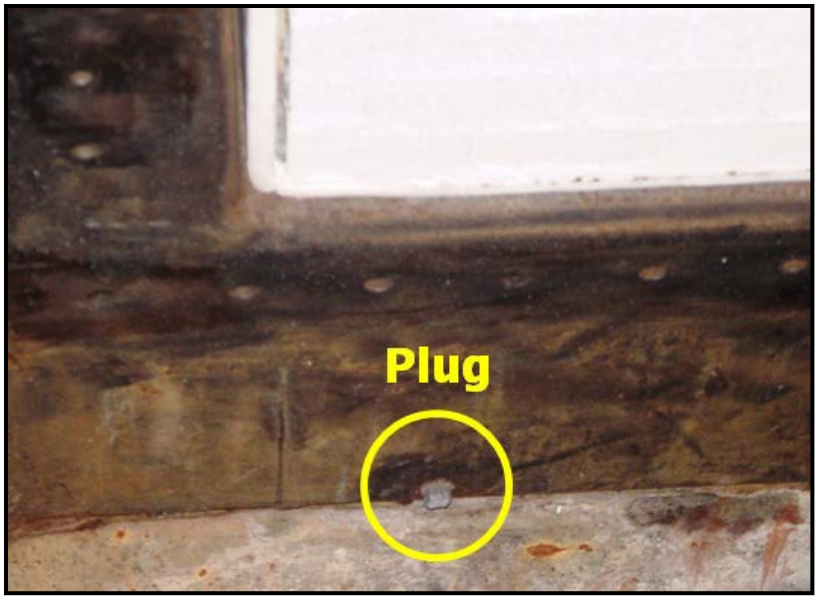

Figure C14. Make sure plugs under the membrane steel frame are in place.

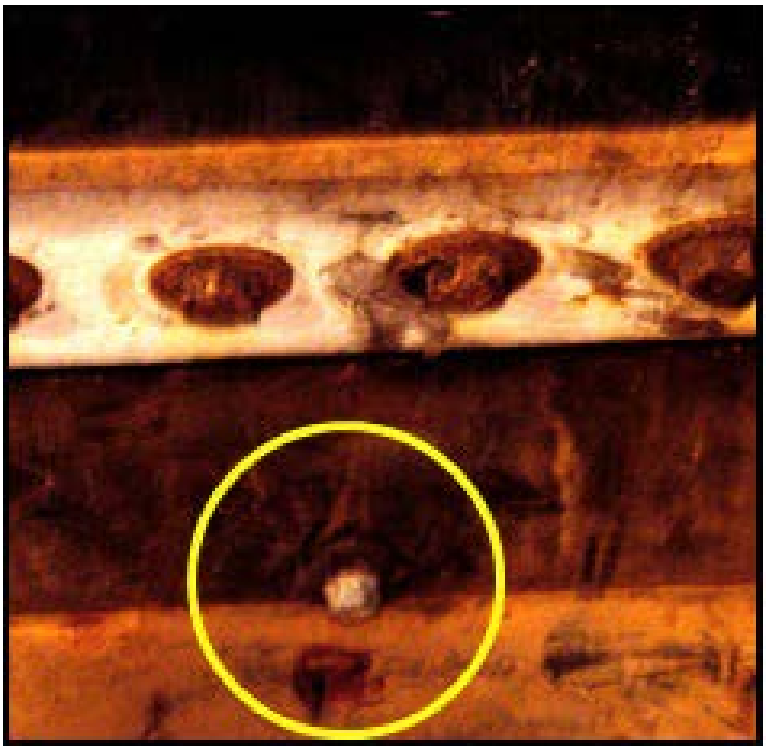

Figure C15. Silicone around both plugs.

Step 8: Remove all of the old silicone from the steel edges of the pressurized cavity using a wire brush or grinder with a cut-brush attachment (Figure C16). Inspect the previous neoprene layer; if the neoprene can be reused, simply clean the old silicone material off with a wire brush (Figure C17). If the neoprene cannot be reused, cut a new neoprene layer about 12 in. wide to fit along the edges of the chamber. Use the lid to layout the pass-through holes needed in the neoprene layer. Use the hammer and hole punch to create the pass-through holes. Note: To reduce the labor and time between experiments, it is recommended that an o-ring and a channel to house the o-ring be built into the top edges of the frame.

Figure C16. Cleaned side walls of pressure cavity.

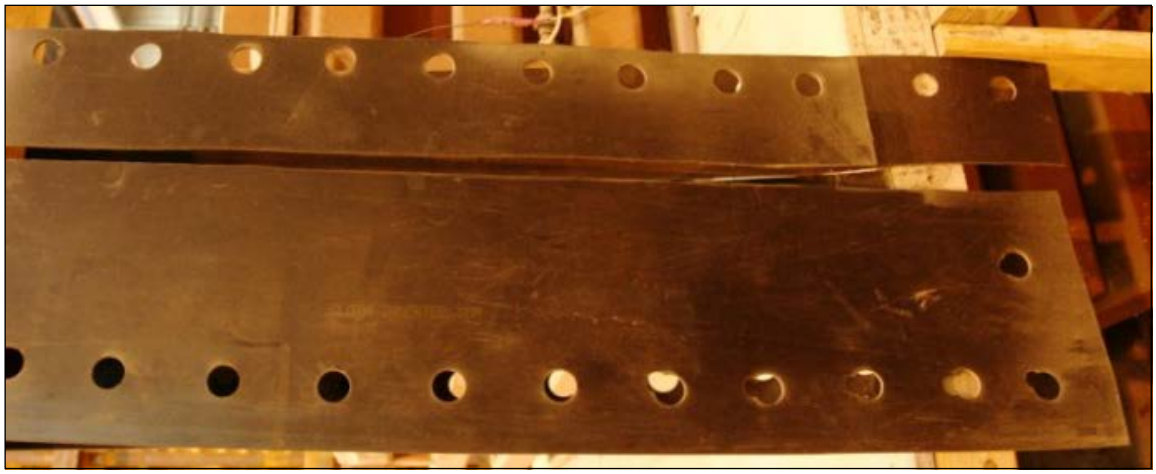

Figure C17. Neoprene seals used along side walls of pressure cavity.

Step 9: Use a shop vacuum to remove any debris in the pressurized and open chambers. Debris floating in the chamber will clog the relief pipes, equalizer, or drain pipes that will be discussed in future steps.

Step 10: Place a bead of silicone along the perimeter of the pressure cavity (Figure C18). Make sure that a bead is along the interior and exterior edges of the steel cavity frame. Then place the precut and punched neoprene layer along the pressure vessel. Apply another bead along the interior and exterior perimeters of the neoprene before the lid is applied (Figure C19).

Figure C18. Apply silicone to steel edges of pressure vessel then apply neoprene seals.

Figure C19. Apply another layer of silicone on neoprene seals before the lid is attached.

Step 11: Bolt the lid to the top of the pressure vessel (Figure C20). Use an air wrench or torque wrench to tighten the 64 3/4-in.-diam bolts (Figure C21). The lid and the pressure vessel will sandwich the neoprene layer (Figure C22). If a bolt hole is stripped or loose, leave the bolt in place and silicone around the bolt to prevent any water leakage. Mark or note the bolt hole that is loose or stripped so that it can be re-tapped before the next experiment. Because of the large number of bolts used to secure the top, a test can be conducted if one to six bolts are stripped as long as none of the stripped bolts are consecutive. The stripped bolts must have at least two good bolts between the stripped bolts. If more than six bolt holes are stripped, delay the experiment and re-tap the holes before proceeding.

Figure C20. Attach lid to pressure vessel.

Figure C21. Bolt lid into place using air or socket wrench.

Figure C22. Neoprene seal between lid and HTC.

Step 12: Open the four relief valves on the lid of the pressurized chamber (Figure C23).

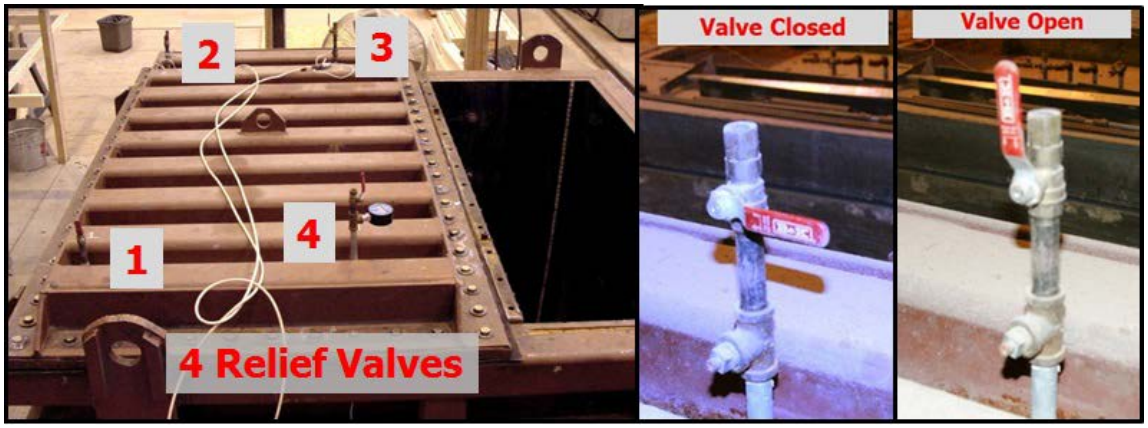

Figure C23. Open the four relief valves after the lid is bolted down.

Step 13: Prep the CMU wall frame before loading the test specimen into the HTC. If the support conditions are a concern, a mechanical connection can be added by bolting anchor plates to the top and bottom of the steel test frame (Figure C24). The anchor plates must be bolted into place before the wall is installed in the HTC. Deflection measurements should be painted on both side walls of the frame to allow test observers to monitor the wall's response as the test is in progress (Figure C25). Make sure the sides of the frame are clean and free of any material that could cause the wall to bind during the test, which would compromise the data collection.

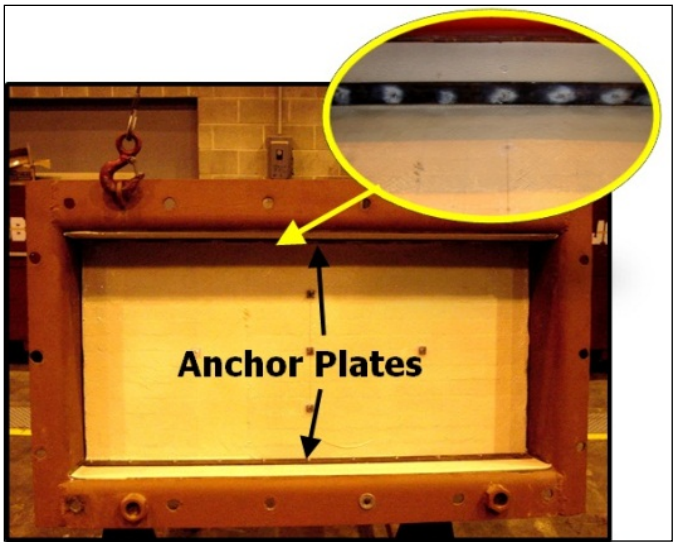

Figure C24. Apply anchor plates to top and bottom supports of test specimen.

Figure C25. Paint deflection measurements on the side walls of the test frame.

Step 14: Make deflection gauge mounts. If large displacements are expected, ensure that a material is used that will adjust to the test specimen's deformation. For example, neoprene squares were used to make the gauge mounts in this test series (Figure C26). Nails were deformed to make hooks for the gauge wire attachment. The nail head

prevented the nail from pulling through the neoprene. Adhere gauge mounts to the wall using epoxy, silicone, or SolidBond 24 hr before the day of the experiment. Five deflection gauges were used in this test series (Figure C27).

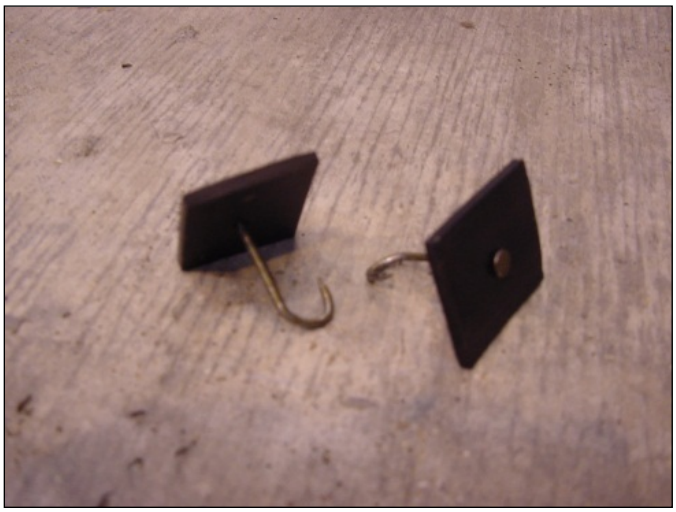

Figure C26. Deflection gauge mounts made from nails and neoprene squares.

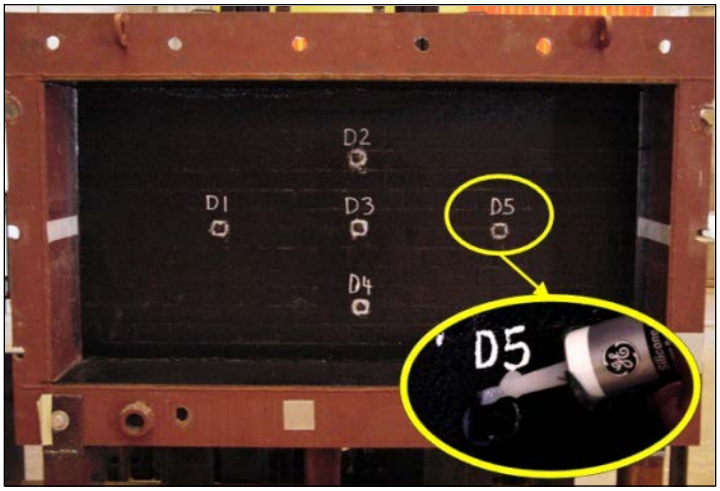

Figure C27. Five deflection gauge mounts were attached to wall specimen using silicon.

Note: Initially the wire potentiometers used to measure the deflection were attached to posts on the exterior wall of the open chamber (Figure C28). A small hole was drilled through the steel wall to allow the potentiometer wire to pass through the chamber wall and attach directly in line with the deflection points on the CMU wall. A small piece of rubber was used to cover the hole, and a needle was used to thread the wire through the neoprene. It was discovered during the test series that water leaked through the openings, and the wires tended to drag on the neoprene squares when the wall deformed significantly. A new deflection system that is discussed in later steps was used during the second half of the test series.

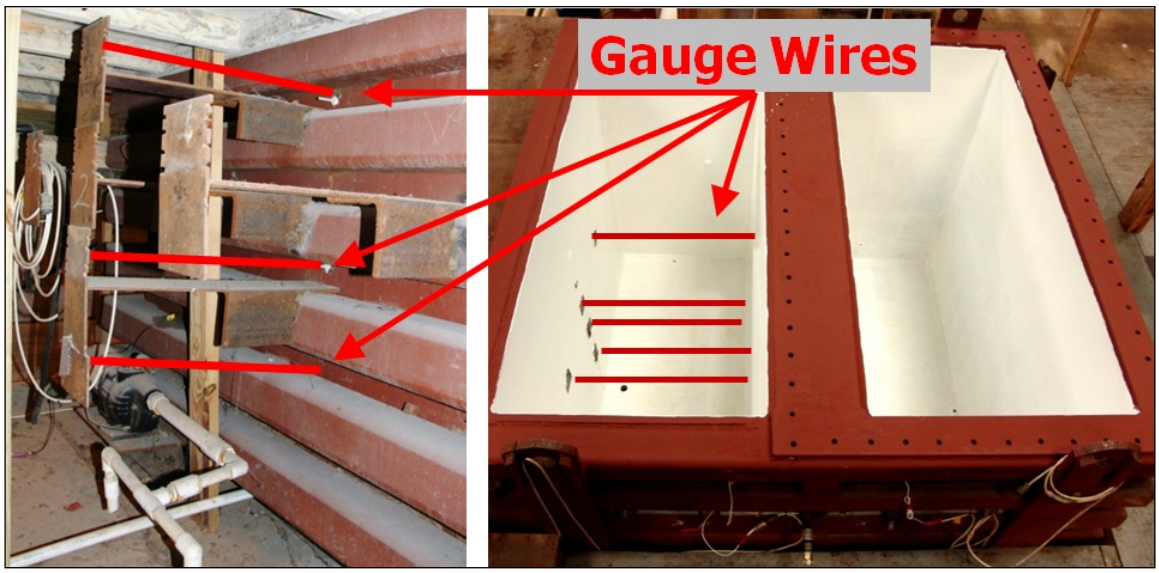

Figure C28. The old deflection setup (no longer used) had the potentiometers mounted outside the HTC, and the gauge wires passed through the open chamber wall to attach to the wall.

Step 15: Attach the crane to the wall frame and unbolt the frame from the stand (Figure C29). Ensure the crane is applying force to the frame before the frame is unbolted from the stand. Slowly move the wall into place and lower it into the open chamber (Figure C30). Load may need to be applied to the wall frame to position it in the vessel window (Figure C31).

Figure C29. Hook crane to wall frame and unbolt frame from stand.

Figure C30. Lower wall frame into position.

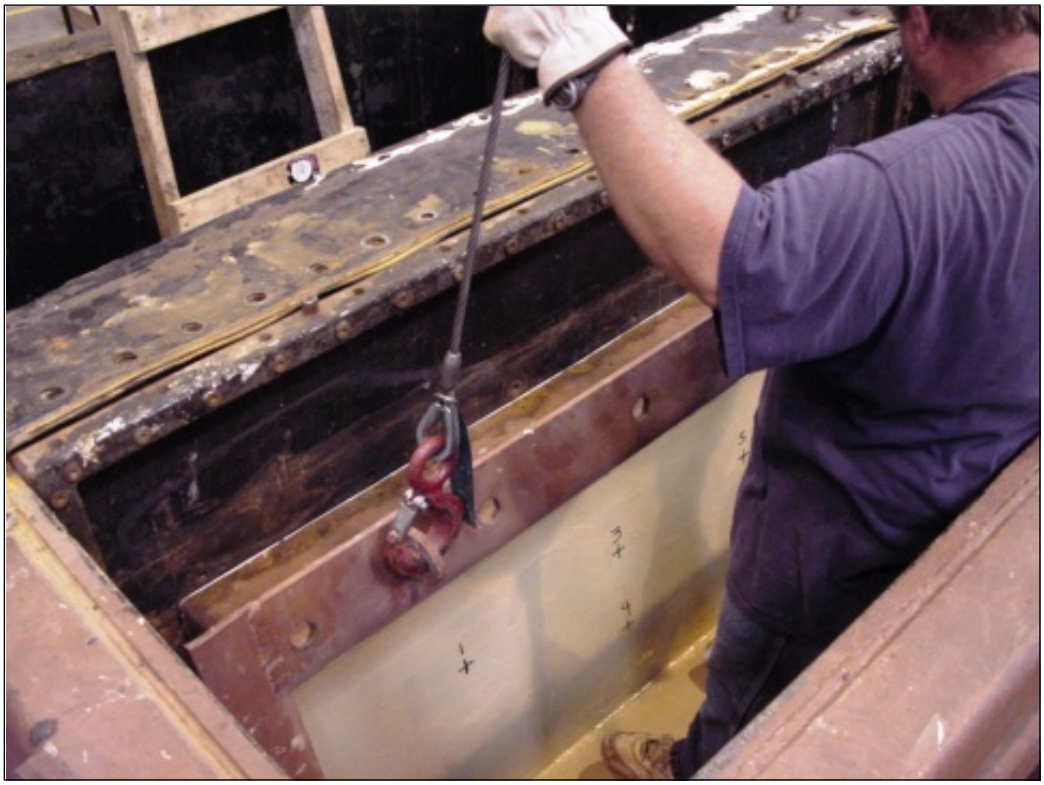

Figure C31. Technician counter balances frame to lower the wall into the chamber.

Step 16: Use an air wrench or torque wrench to tighten the 18 3/4-in.-diam bolts (Figure C32) used to attach the test specimen frame to the HTC. Check all bolts before the top of the pressure chamber is attached. If a bolt is stripped, silicone around the bolt to prevent any water leakage between the pressure and open chambers of the test apparatus (Figure C33). Mark or note the bolt hole that is stripped so that it can be re-tapped before the next experiment. A test can be conducted if one or two bolts are stripped, but if more than two bolt holes are stripped or if the two are consecutive, delay the experiment until repairs can be made.

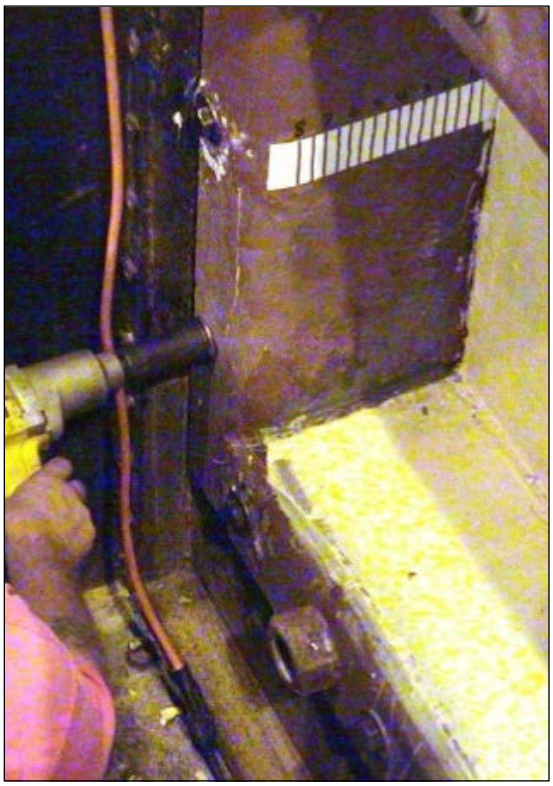

Figure C32. Bolt wall frame into the chamber.

Figure C33. If a bolt appears to be stripped, then silicone bolts.

Step 17: Close the two drain valves on the back wall of the open chamber (Figure C34). Open the equalizer valve on the pipe that connects the pressure and open chambers to aid in filling the two chambers equally (Figure C35).

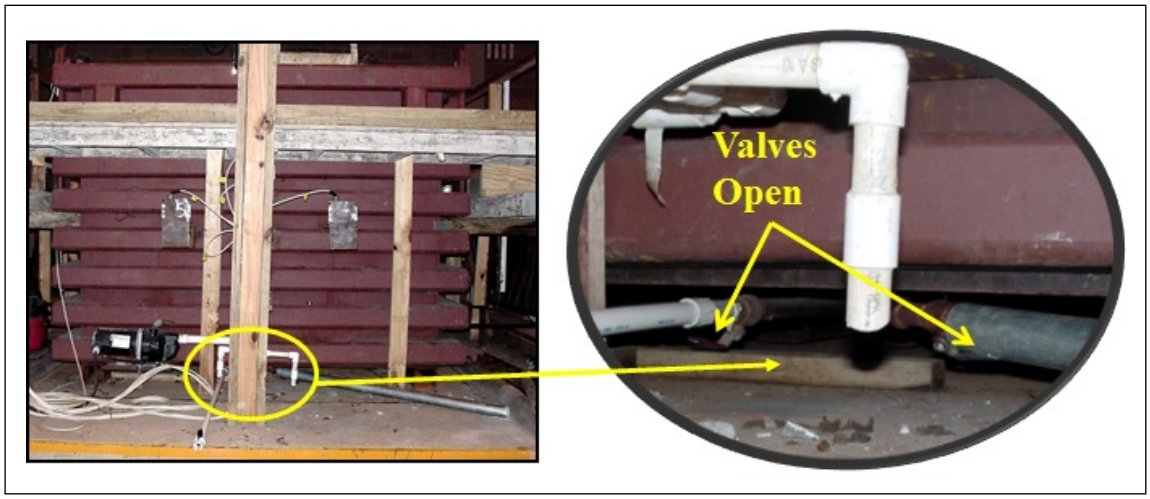

Figure C34. Close drain valves. Valves are closed when they are perpendicular to the pipe.

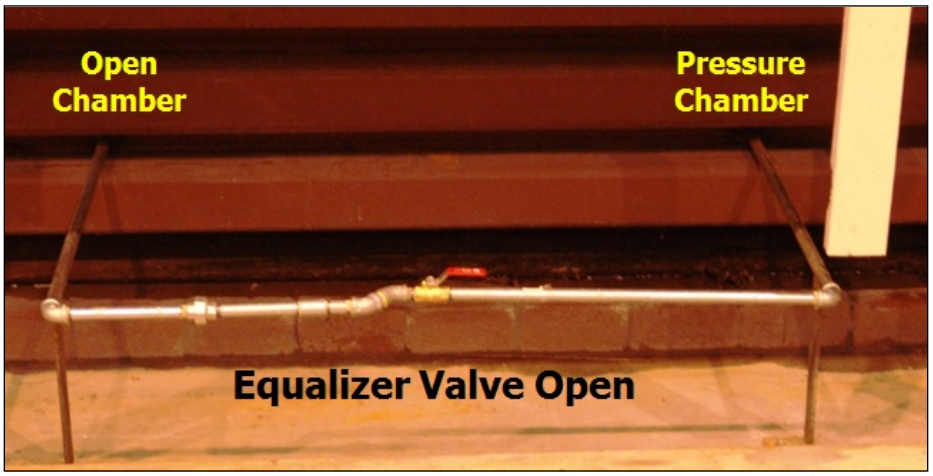

Figure C35. Open equalizer valve.

Step 18: Install pressure gauges in the mounts housed in the steel chambers and relief pipes (Figures C36 and C37). Six pressure gauge mounts are available for use on the HTC (Figure C38).

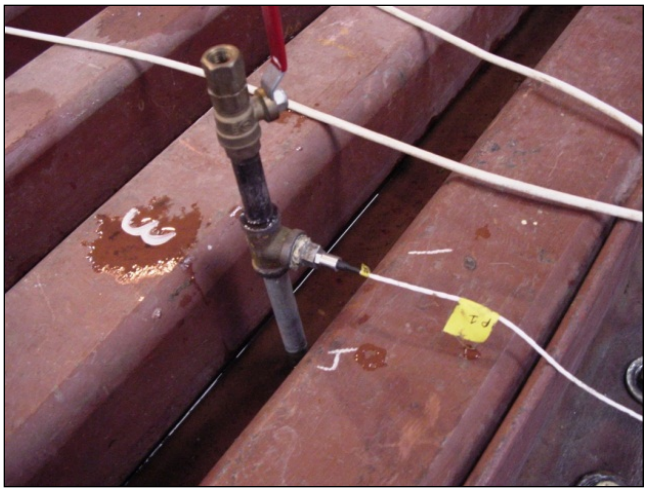

Figure C36. Pressure gauge installed on relief valve.

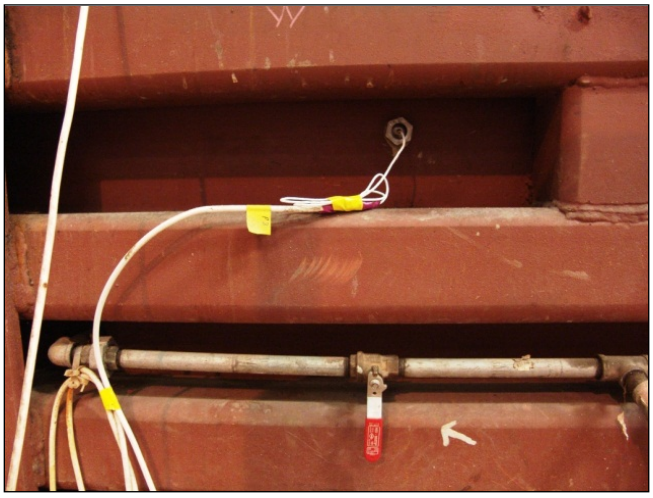

Figure C37. Pressure gauge installed in wall of the pressure vessel.

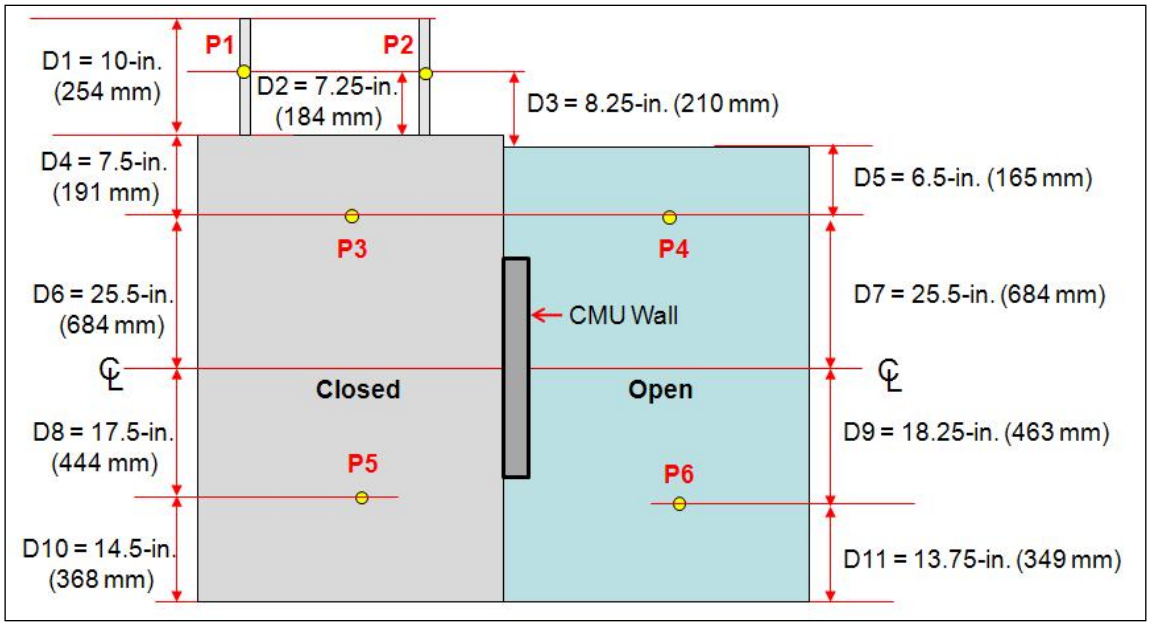

Figure C38. Locations of pressure gauge mounts on the HTC.

Step 19: Install deformation rack (Figure C39) and attach gauge wires to the wall hooks. Fishing line and quick-release hook extensions are used to extend the length of the wire potentiometers (Figure C40). The deformation rack was constructed to allow the gauge locations to be relocated from test to test. The old deflection method required additional holes to be drilled in the chamber wall to move the deflection measurement points. A steel frame is pinned across the exterior wall of the open chamber, and eye hooks are used to direct the gauge wires to the wall hooks (Figure C41). The wire potentiometers are attached to a steel u-channel that is clamped directly above the open chamber of the HTC (Figure C42). A spacer plate is used to maintain a designated distance from the wall to the deflection rack. The hook-and-eye turnbuckles are used to

prevent the deflection rods from rotating under load. The turnbuckles can be relocated and tightened to prevent distortion.

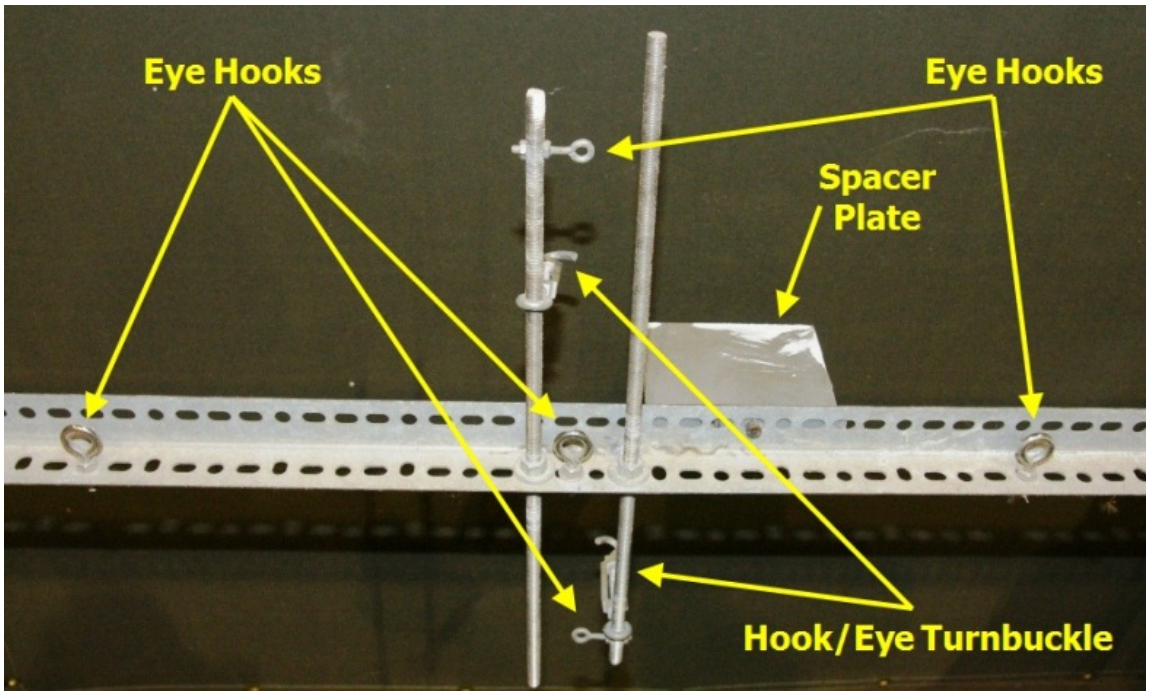

Figure C39. Deformation rack with eye hooks, turnbuckles, and spacer plate.

Figure C40. Fishing line used to create gauge wires and hook attachments.

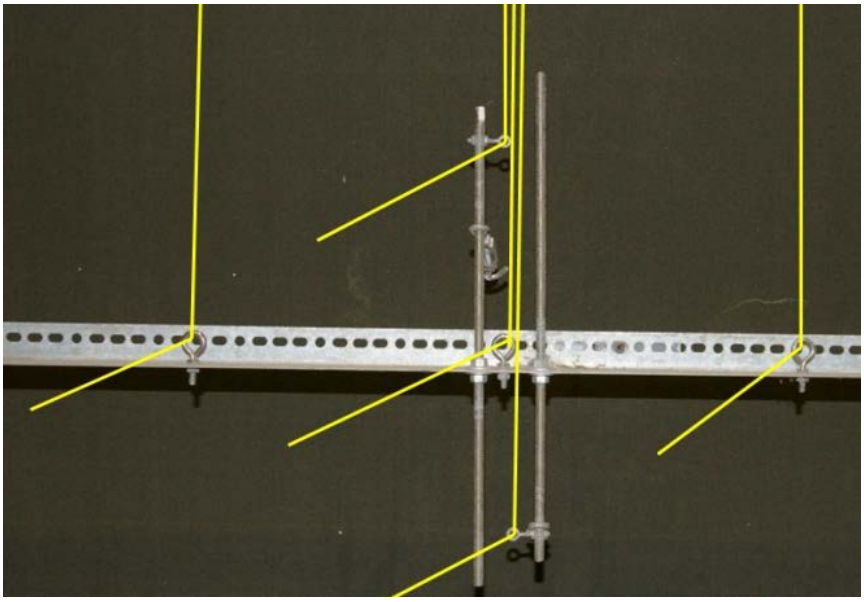

Figure C41. Deflection wires (yellow lines) originating from the potentiometer are passed through the eye hooks and attached to the deflection mounts on the wall.

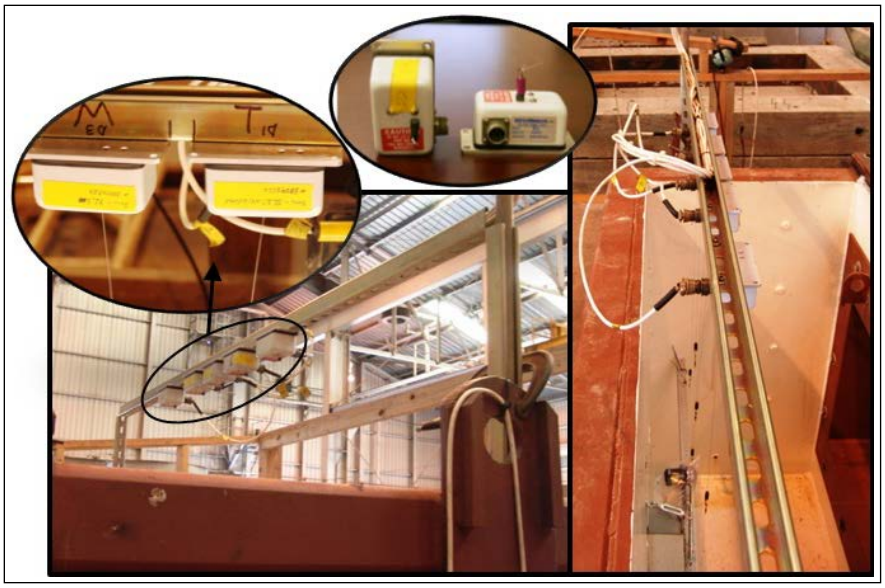

Figure C42. Linear potentiometers secured to u-channel to measure specimen deflection.

Step 20: Place underwater video camera in chamber on steel post in the corner (Figure C43). The camera can be moved during the experiment to video specific points on the test specimen (Figure C44). Attach lights to steel post secured over the open chamber. Ensure that lights and power cords are secured so that these items will not get wet in order to prevent injury from electric shock.

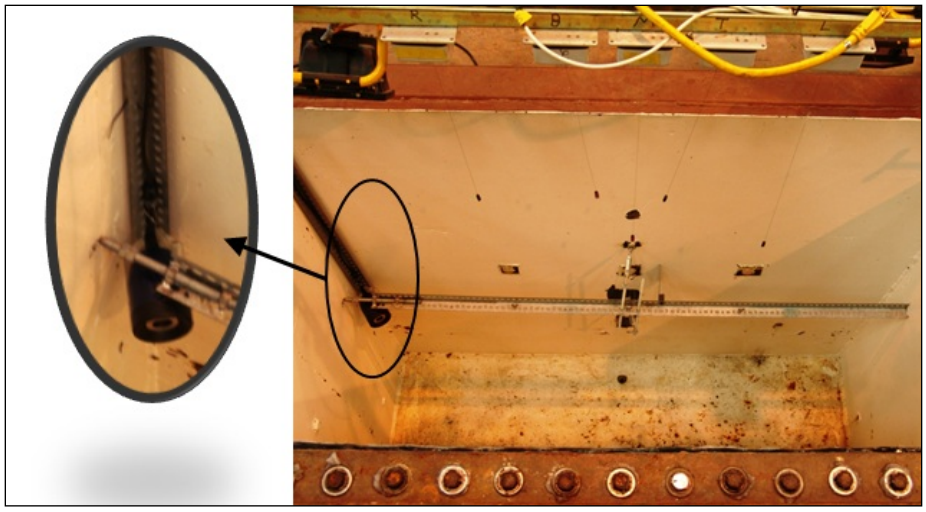

Figure C43. Underwater video camera placement in open chamber.

Figure C44. Underwater video camera.

Step 21: Open the valves at the bottom of the clear tubes that are used to monitor the water height in the open and pressure chambers (Figures C45 and C46). Check with instrumentation personnel to ensure that the data acquisition system is zeroed.

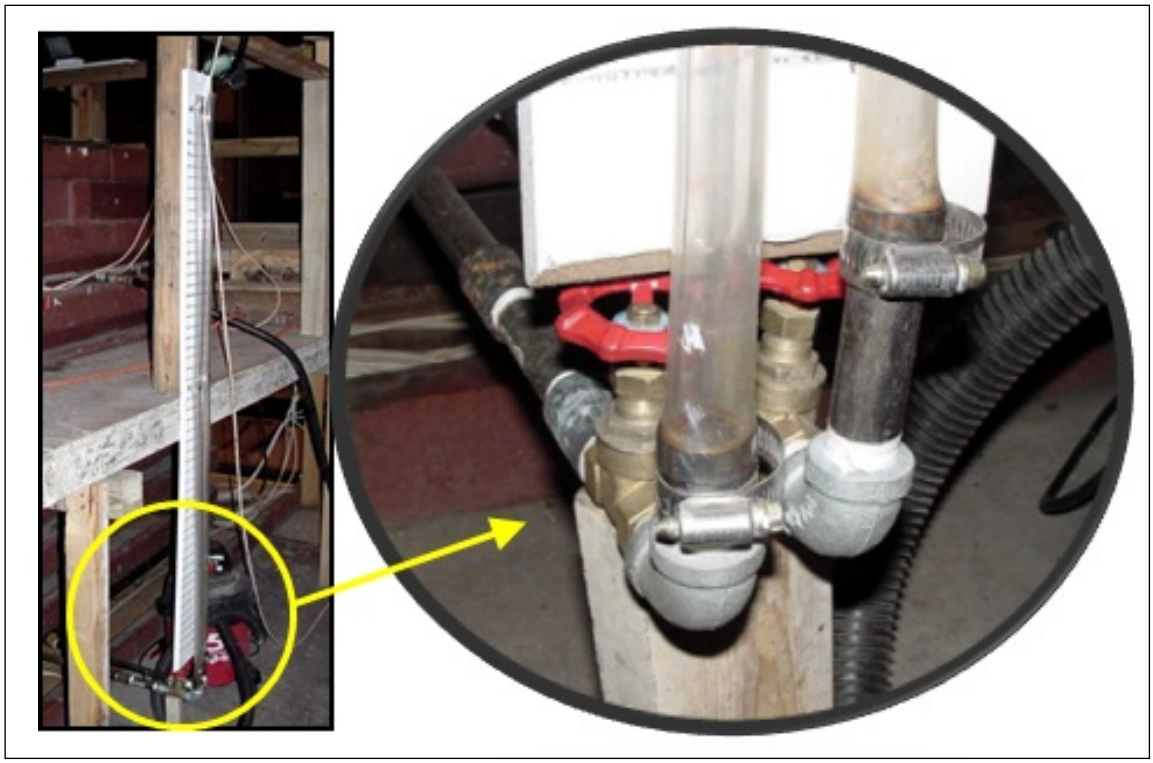

Figure C45. Open valves to monitor tubes.

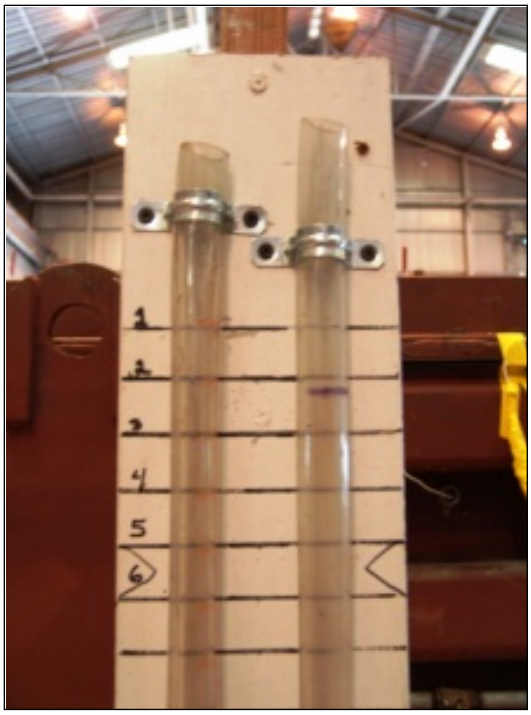

Figure C46. Monitor tubes.

Step 22: Open water inlet valves to HTC (Figure C47). To speed the process of filling both chambers, use a water hose to fill the open chamber (Figure C48). Be careful to monitor the water height in both chambers. If the chambers are not filled equally, a load will be applied to the wall during the filling process. Valves are open when they are parallel to the pipe. If a water hose is added to the open chamber, the water intake valve to the open chamber may be closed to allow a larger flow rate into the pressure chamber. The water flow into the chambers can be adjusted by opening or closing the valves on the water inlet pipe (Figure C49). As shown in Figure C49, the valve can be opened to any degree between 0 to 90.

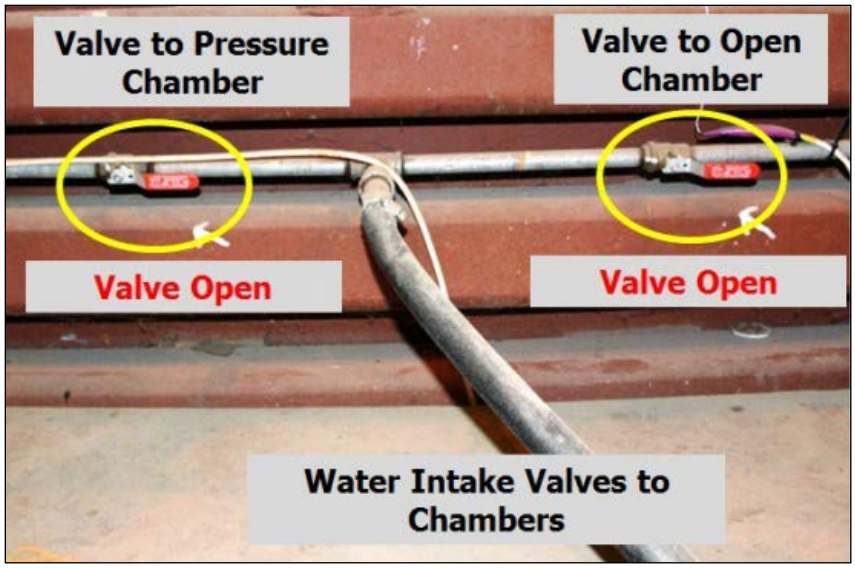

Figure C47. Valves to water inlet pipes.

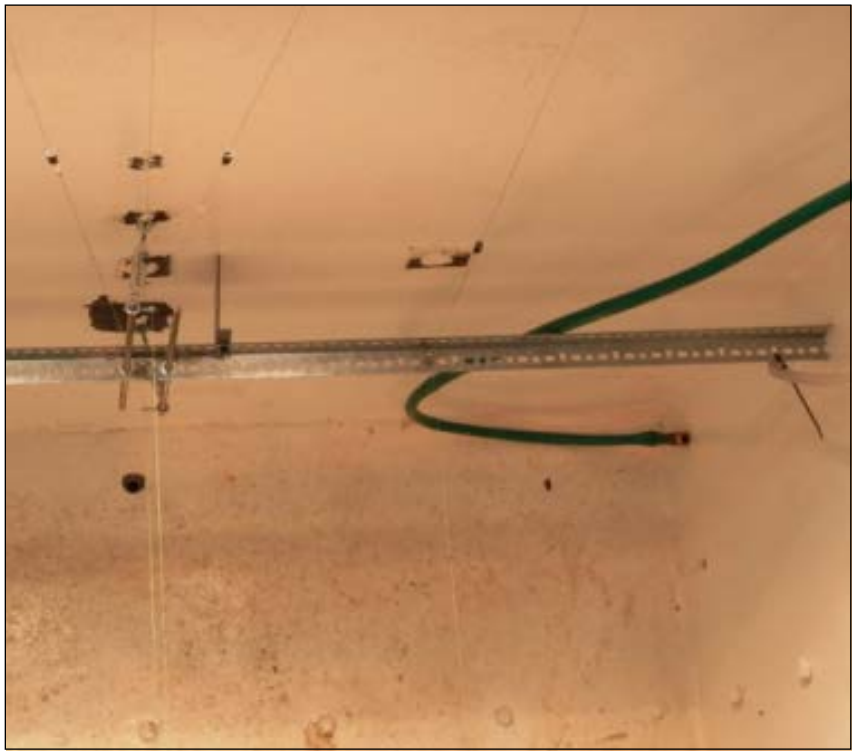

Figure C48. Water hose used in open chamber to speed the filling process.

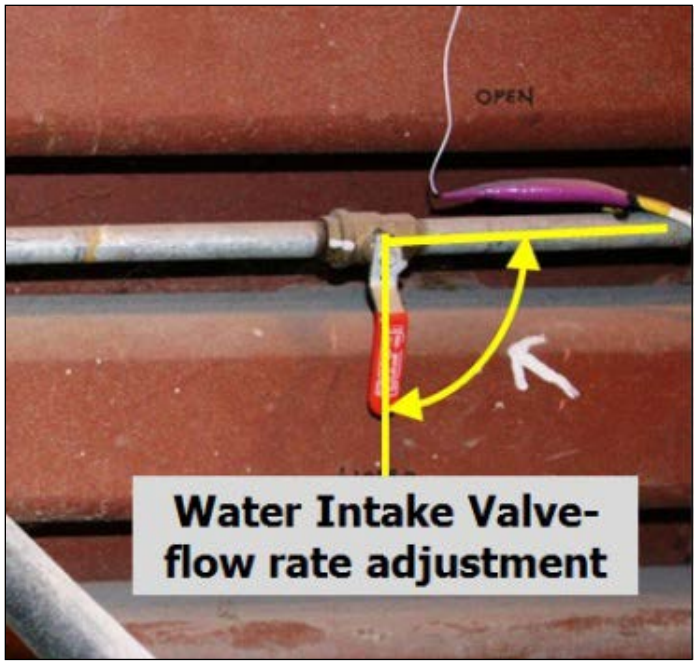

Figure C49. Water flow rate can be adjusted.

Step 23: Notify instrumentation personnel when the water starts to flow into the chambers. Start the data acquisition system when the water level reaches the lowest gauge in the structure. If a differential load is applied to the wall during the filling process, the magnitude of the pressure will be obtained as well as any deformation that may occur before the pressure chamber is actually closed and loading begins.

Step 24: Remove the water hose from the open chamber when the water is 3 in. from the top of the chambers. Close the equalizing pipe on the side of the test chamber that connects the two chambers (Figure C50). Continue to add water to the open chamber through the valve on the inlet pipe (Figure C51). Close the inlet valve to the open chamber when the water reaches the surface of the open chamber.

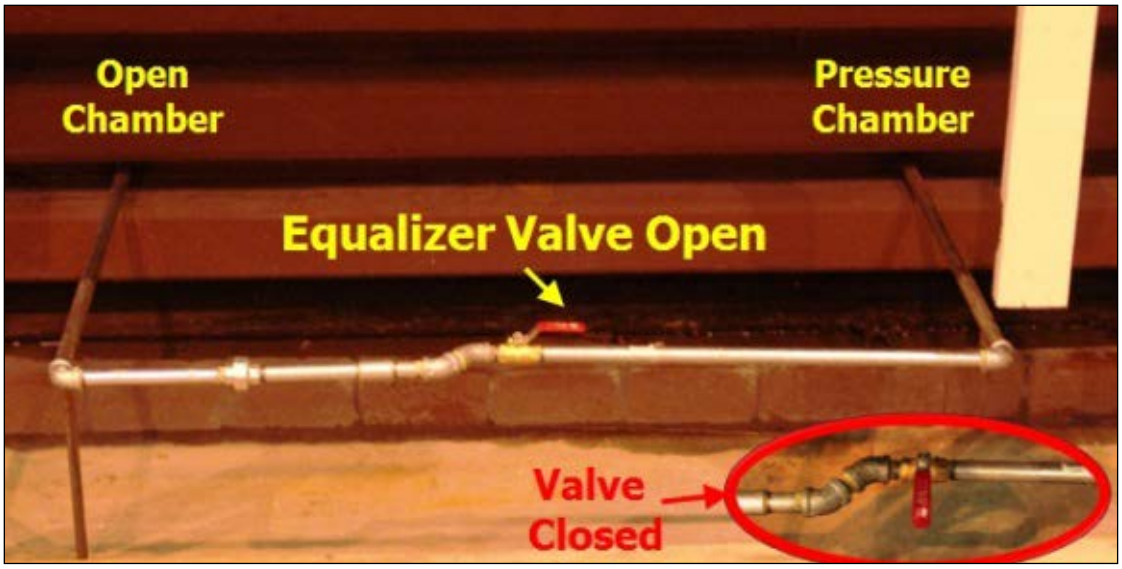

Figure C50. Close the equalizer valve.

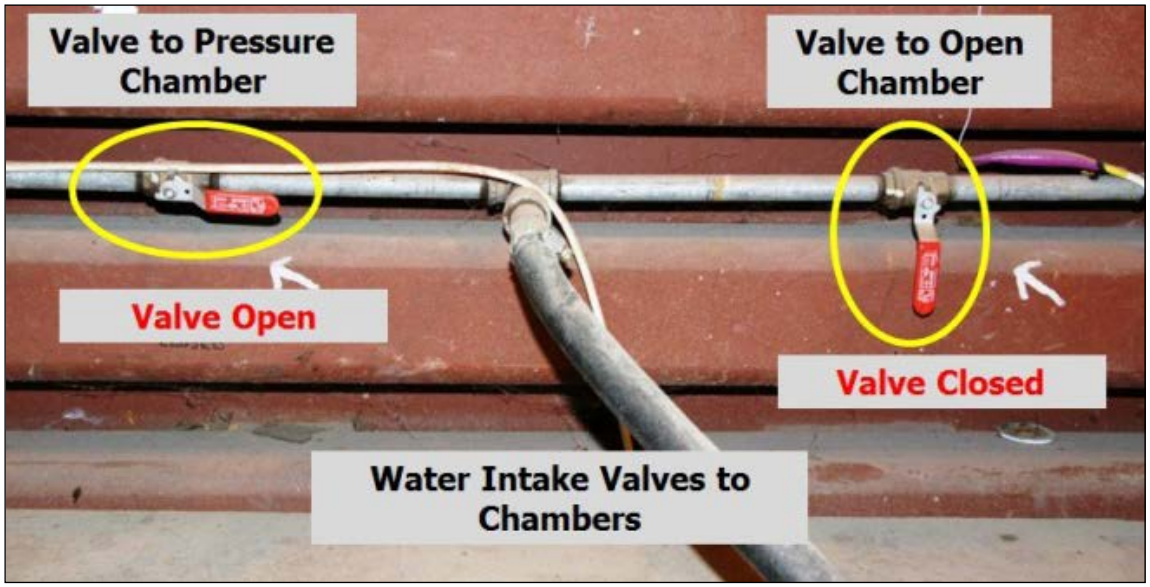

Figure C51. Close the valve to the open chamber when the water reaches the surface of the open chamber.

Step 25: When the water reaches the 1-in. mark on the monitoring tubes, close both of the valves at the bottom of the monitoring system (Figure C52). Also slow down the flow of the water into the pressure chamber as the chambers continue to fill. The inlet valve on both chambers can be partially opened to control the water flow (Figure C53).

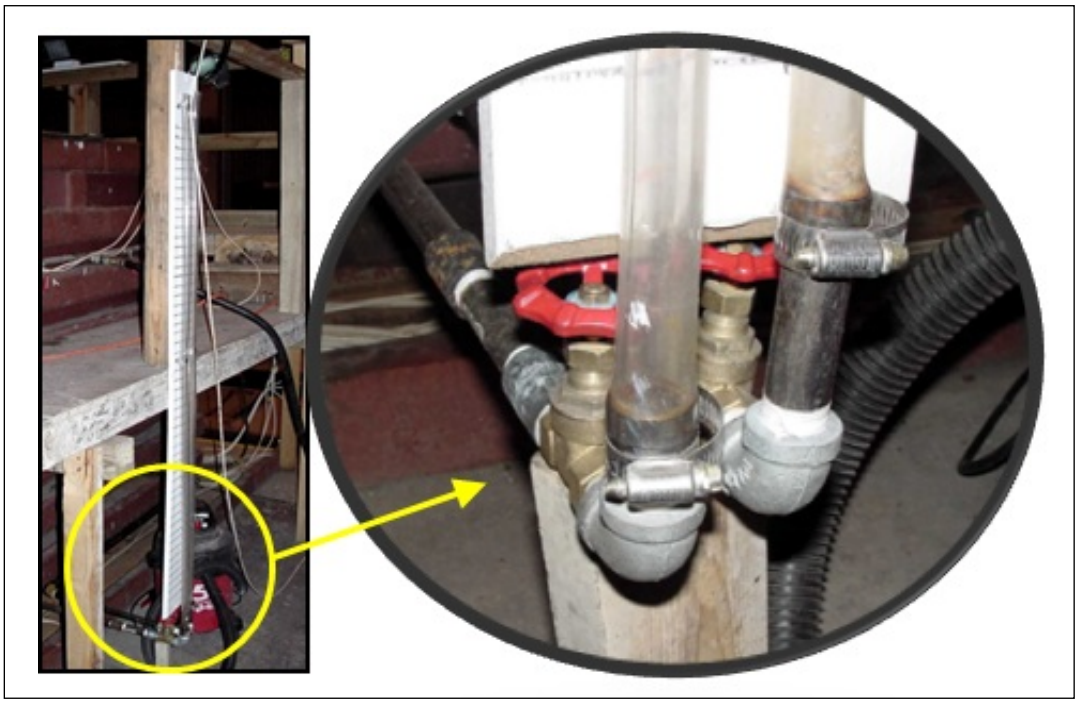

Figure C52. Close the monitoring tube valves.

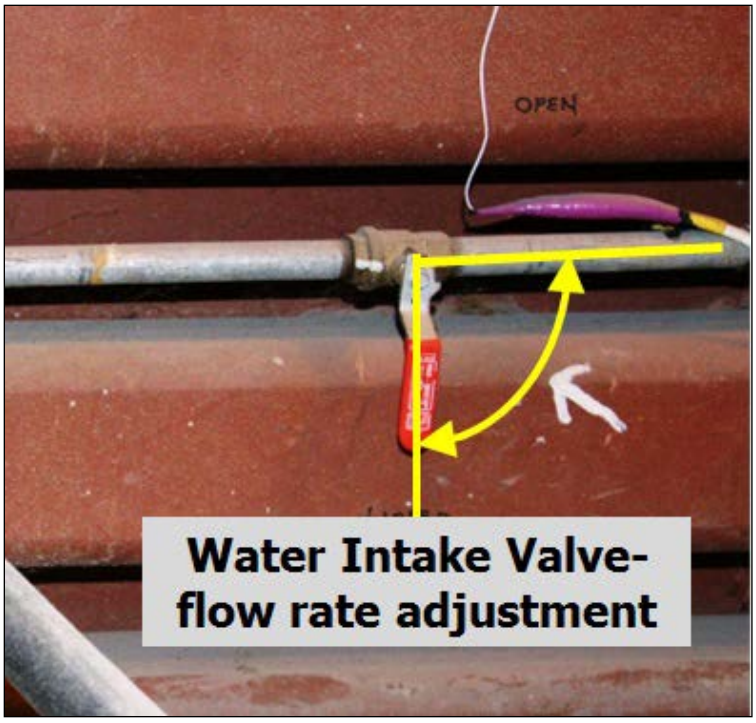

Figure C53. The water flow is controlled by the position of the inlet valve.

Step 26: Continue to add water to the pressure chamber while the air trapped in the chamber escapes through the relief valves on the top of the pressure chamber lid. When water begins to spray out of the relief valves (Figure C54), close the valves beginning at the shortest pipe (labeled 1) to the tallest (labeled 4) as shown in Figure C55. Before the relief valves are closed, slow the water flow in the intake valves. If the water flow is not decreased, the test specimen will be loaded very quickly when the final relief valve is closed.

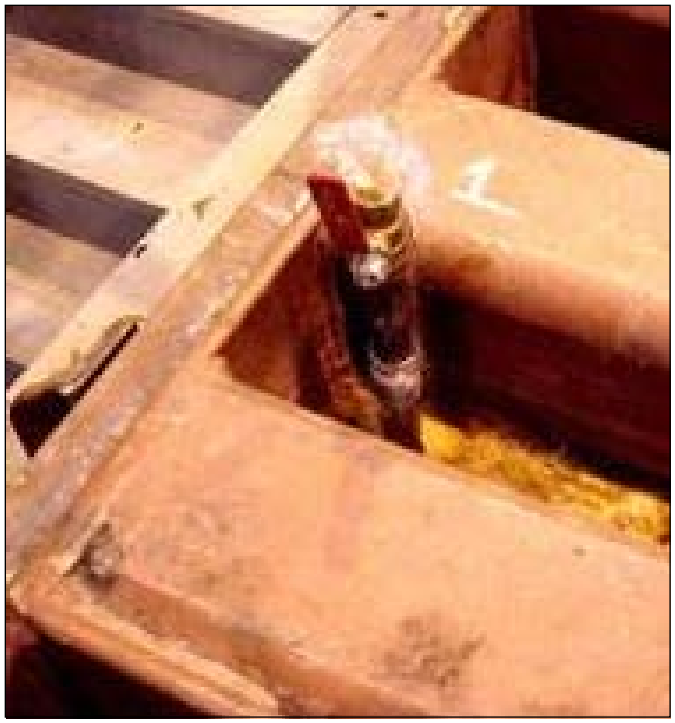

Figure C54. Close the relief valves when water begins to flow from relief valves.

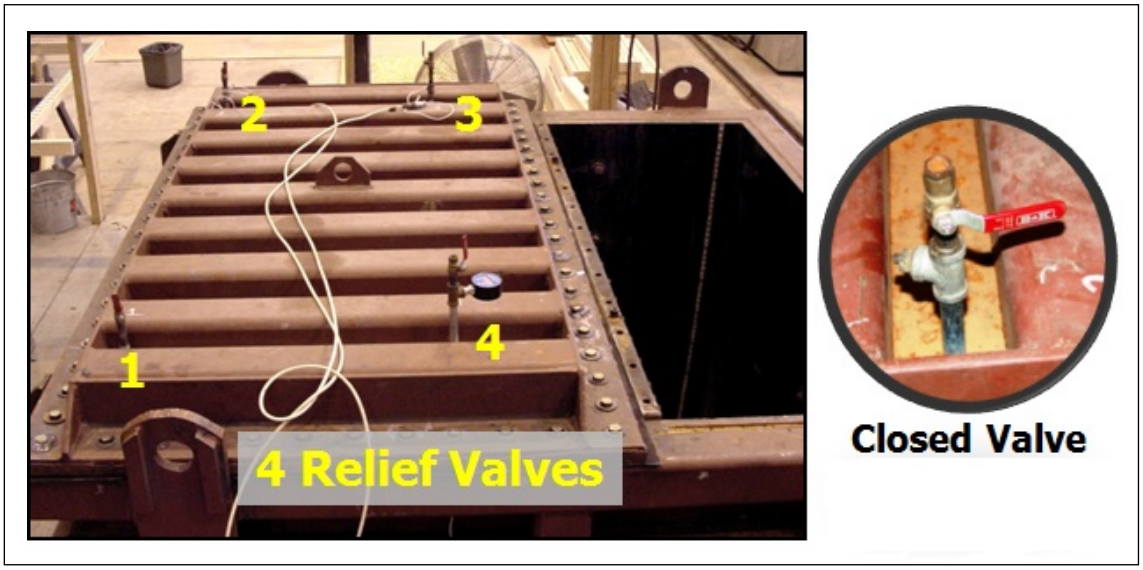

Figure C55. Before the four relief valves are closed, decrease the water flow in the inlet valves.

Step 27: Increase or decrease water flow depending on desired increase in pressure measurements. Be careful to monitor the time of the experiment to ensure that there is sufficient recording time left on the data acquisition system to complete the experiment. The time may dictate how quickly or slowly one can apply pressure to the wall. The flow of water can be controlled by the inlet pipe valve.

Step 28: When the desired wall response is obtained or the wall fails, stop adding water and notify instrumentation personnel. Open the drain valves (Figure C56), open the relief valves on the pressure lid, and drain both sides of the chamber (Figure C57).

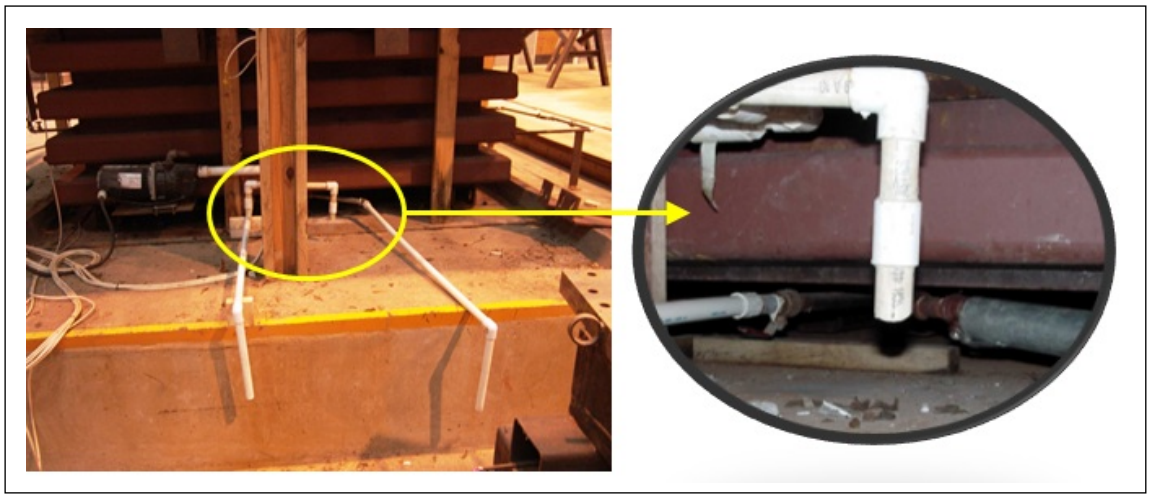

Figure C56. Open drain valves.

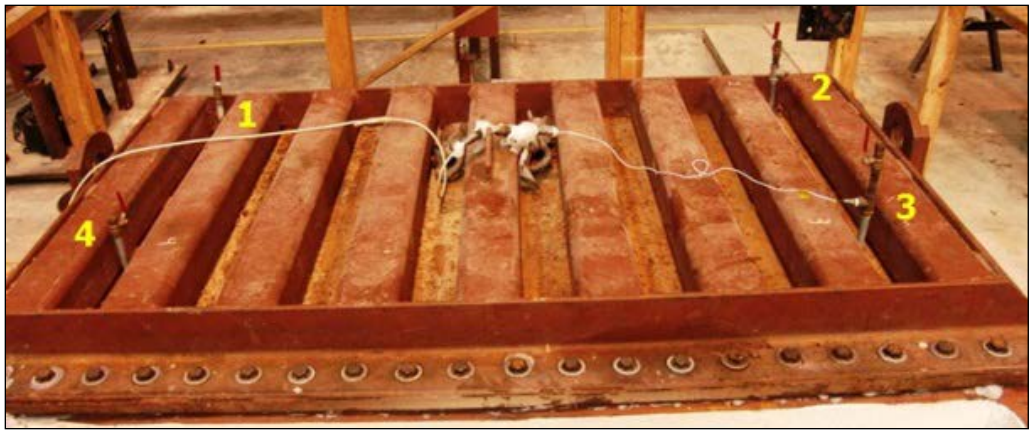

Figure C57. Open relief valves.

Step 29: Also drain the tubes that are used to monitor the height of the water during the filling process (Figure C58). Disconnect the deflection gauge wires as soon as possible to prevent damage to the potentiometers should the specimen fail (Figure C59). If the gauge wires are extended or pulled in too quickly, the gauge will be damaged and will not be available for the next experiment.

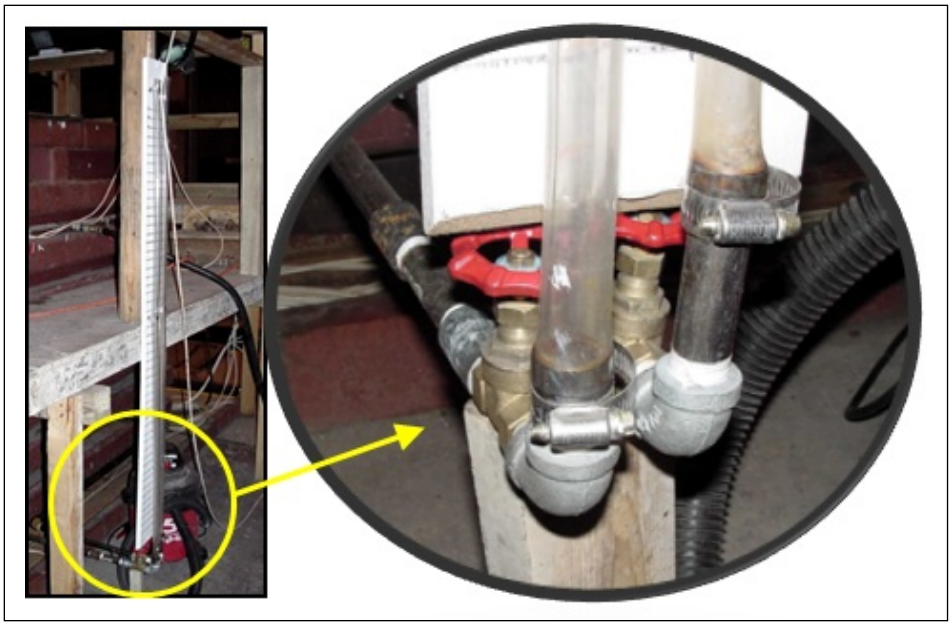

Figure C58. Open the monitor valves and drain water from tubes.

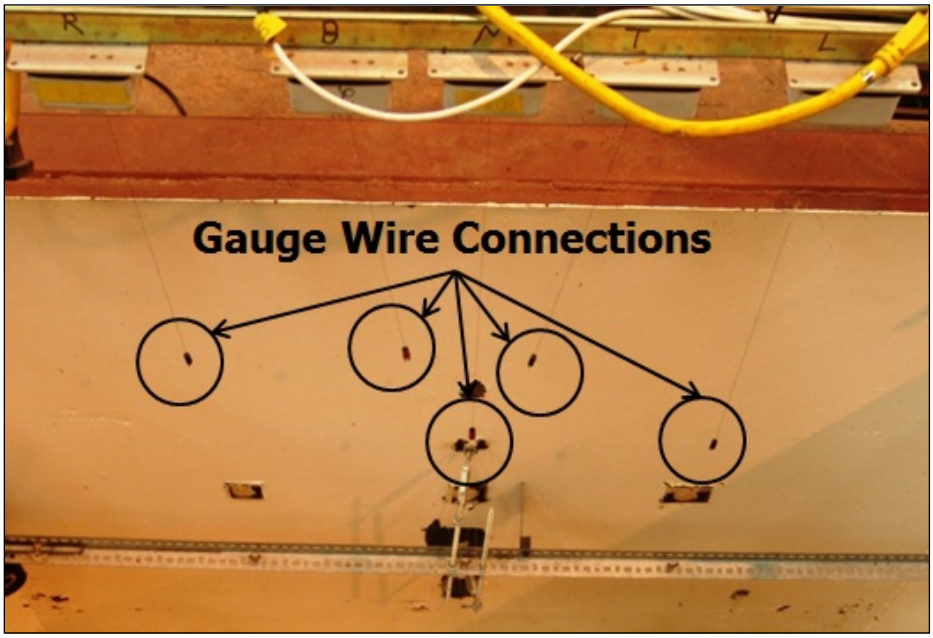

Figure C59. When the test is completed, undo the gauge connections to prevent damaging the linear potentiometers.

Step 30: Remove the test specimen. To determine if the membrane needs to be replaced, inspect the membrane from the open chamber. If the membrane has not been damaged, leave the membrane in place and use it on the next experiment. If the membrane does not need to be removed, the lid can stay in place reducing the amount of time and labor required before the next test can be conducted.

Step 31: If the next test will be delayed by more than 48 hr, remove the pressure chamber lid and allow the chamber to dry. This will minimize the development of rust in the HTC.

Step 32: Once the pressure chamber lid is removed, inspect all the seals. Remove all the silicone from the steel and neoprene components.

Step 33: Clean steel and neoprene components before next experiment. Be sure to follow Steps 10 and 11 before proceeding with the next experiment.

APPENDIX D: BLS OPERATIONAL LIMITS

The test matrix used to define the operational requirements for the BLS to be used in the CMU wall retrofit experiments is provided in Table D1.

Table D.1. BLS operational test matrix.

Test	DL in. (cm)	DP psi (MPa)	Air/HE %	Gap 1-C/R1 in. (mm)	Gap 2-R1/R2 in. (mm)	Gap 3-R2/CC in. (mm)	CC Length in. (mm)
29	12 (30)	40 (0.28)	20	6 (152)	6 (152)	0	0
23	12 (30)	600 (4.1)	100	0	12 (305)	6 (152)	18 (457)
25	12 (30)	1200 (8.3)	50	12 (305)	0	12 (305)	12 (305)
17	18 (46)	40 (0.28)	50	0	12 (305)	6 (152)	6 (152)
11	18 (46)	600 (4.1)	100	12 (305)	6 (152)	12 (305)	6 (152)
28	18 (46)	1200 (8.3)	20	6 (152)	0	12 (305)	0
24	24 (61)	40 (0.28)	100	0	0	6 (152)	0
12	24 (61)	600 (4.1)	50	6 (152)	6 (152)	6 (152)	18 (457)
18	24 (61)	1200 (8.3)	100	12 (305)	12 (305)	12 (305)	0
21	30 (76)	40 (0.28)	100	6 (152)	0	12 (305)	18 (457)
27	30 (76)	40 (0.28)	50	12 (305)	6 (152)	6 (152)	0
4	30 (76)	750 (5.2)	50	12 (305)	0	0	6 (152)
26	30 (76)	1200 (8.3)	20	0	6 (152)	0	12 (305)
14	36 (91)	40 (0.28)	20	12 (305)	6 (152)	12 (305)	6 (152)
5	36 (91)	750 (5.2)	100	6 (152)	12 (305)	0	0
3	36 (91)	1200 (8.3)	50	0	0	0	12 (305)
2	42 (107)	40 (0.28)	100	6 (152)	6 (152)	0	12 (305)
16	42 (107)	600 (4.1)	50	0	0	12 (305)	6 (152)
9	42 (107)	1200 (8.3)	20	12 (305)	12 (305)	6 (152)	6 (152)
20	48 (122)	40 (0.28)	50	12 (305)	12 (305)	0	12 (305)

Table D1. Continued.

Test	DL in. (cm)	DP psi (MPa)	Air/HE %	Gap 1- C/R1 in. (mm)	Gap 2- R1/R2 in. (mm)	Gap 3- R2/CC in. (mm)	CC Length in. (mm)
19	48 (122)	600 (4.1)	20	6 (152)	0	6 (152)	12 (305)
22	48 (122)	1200 (8.3)	50	0	6 (152)	12 (305)	0
1	54 (137)	40 (0.28)	20	0	0	0	18 (457)
8	54 (137)	1200 (8.3)	100	6 (152)	6 (152)	6 (152)	6 (152)
6	60 (152)	40 (0.28)	20	0	0	0	6 (152)
30	60 (152)	40 (0.28)	20	12 (305)	0	12 (305)	12 (305)
31	60 (152)	40 (0.28)	0	0	0	0	6 (152)
13	60 (152)	600 (4.1)	100	12 (305)	0	6 (152)	12 (305)
10	60 (152)	1200 (8.3)	50	6 (152)	12 (305)	12 (305)	6 (152)
15	66 (168)	600 (4.1)	20	0	12 (305)	12 (305)	12 (305)
7	66 (168)	1200 (8.3)	100	6 (152)	6 (152)	6 (152)	18 (457)

Note: DL - Driver Length and DP – Driver Pressure. The gaps are located between the listed components. These locations are abbreviated by: C- Transition Cone, R1 – Ring 1, and R2 – Ring 2, CC - Cascade.

APPENDIX E: DATA PROCESSING (DPLOT MACRO)

A DPLOT macro was written to automate many of the steps used in the software to process the raw data obtained in the dynamic experiments.

```
Filetype(9)
ForFilesIn("E:INPUT_PATH_TO_FILE*.wft")
        EditMultiplyY(-1)
        SelectCurve(-1)
        EditOperateX("X-5")
        EditTruncate(-5,60)
        TickInterval(1,5,5)
        ManualScale(-5,-10,60,90,-40,360)
        RunPlugin("Baseline Shift")
        Pause()
        DataProcess(1,"PRESSURE",2)
        DataProcess(0)
        Pause()
        SelectCurve(2)
        EditMultiplyY(1000)
        TextPointLabel(0,0,0,0,0,2,"X=$=(ROUND($X,2)) MSEC,
Y=$=(ROUND($Y,2)) PSI-MSEC")
        SelectCurve(1)
        TextPointLabel(0,0,0,0,0,2,"X=$=(ROUND($X,2)) MSEC,
Y=$=(ROUND($Y,2)) PSI")
        TextPointLabel(0,0,0,0,0,4,"X=$=(ROUND($X,2)) MSEC,
Y=$=(ROUND($Y,2)) PSI")
        LineWidth(-2,30)
        LineType(2,2)
        Title1("INPUT PLOT TITLE")
        Title2("INPUT PLOT DISCRIPTION")
        Title3("")
        Legend(1,"Pressure")
        Legend(2,"Impulse")
        LegendParams(.75,2,1,1,.5,.5)
        XAxisLabel("TIME, MSEC")
        YAxisLabel("PRESSURE, PSI")
        Y2AxisLabel("IMPULSE, PSI- MSEC")
        Size(0,5,5,0)
        RunPlugin("More Curve Fits...")
        Pause()
```

```
        Legend(3,"Pressure Equivalent")
        Legend(4,"Impulse Equivalent")
        GridLines(1)
        Color(1,0,0,0)
        Color(2,255,0,0)
        Pause()
        FileSaveAs(1,"E:INPUT_PATH_TO_SAVE_FILE\|TITLE2|.grf")
        FileSaveAs(4096,"E:INPUT_PATH_TO_SAVE_FILE \|TITLE2|.wmf")
        FileSaveAs("JPEG Picture","E INPUT_PATH_TO_SAVE_FILE
\|TITLE2|.jpg")
        Pause()
        FilePrint()
        FileClose()
        NextFile()
```

APPENDIX F: DISPLACEMENT-TIME PLOTS FOR FULL-SCALE WALL RETROFITS

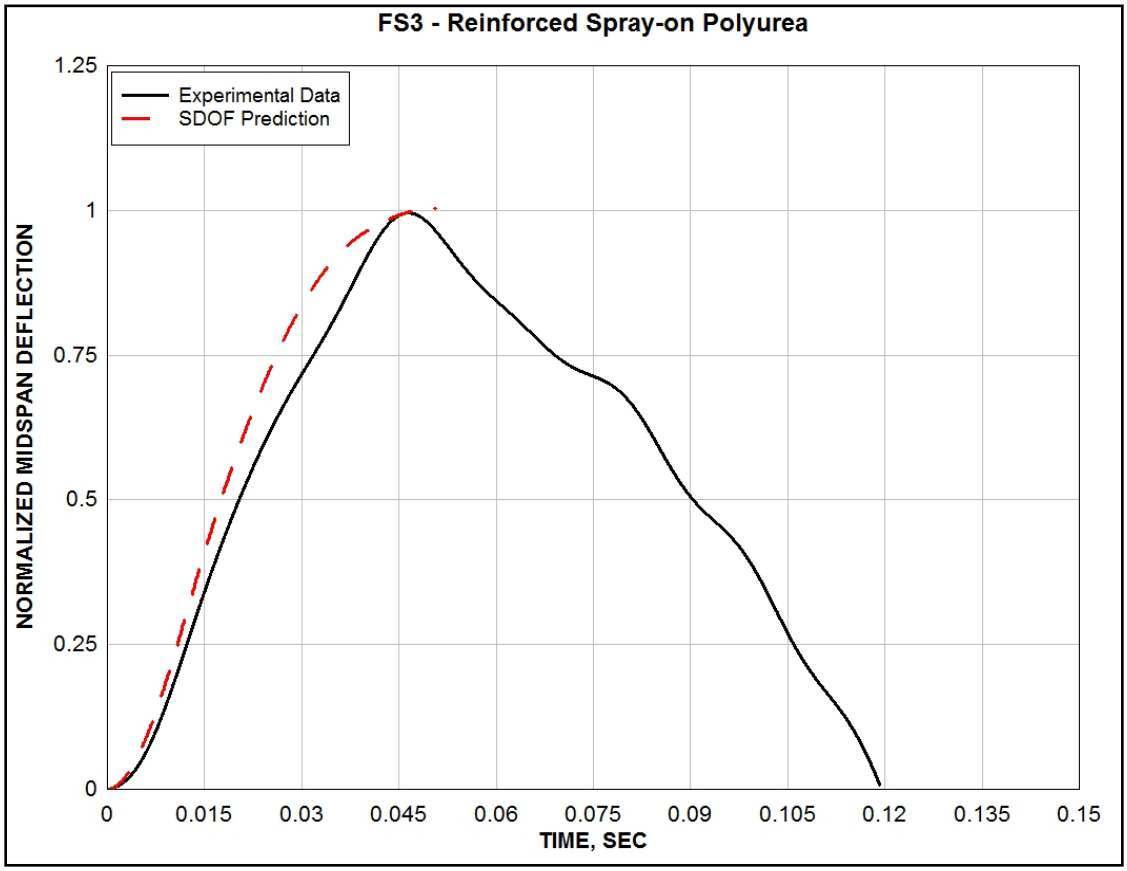

Figure F.1. Deflection for FS3-Reinforced Spray-on Polyurea.

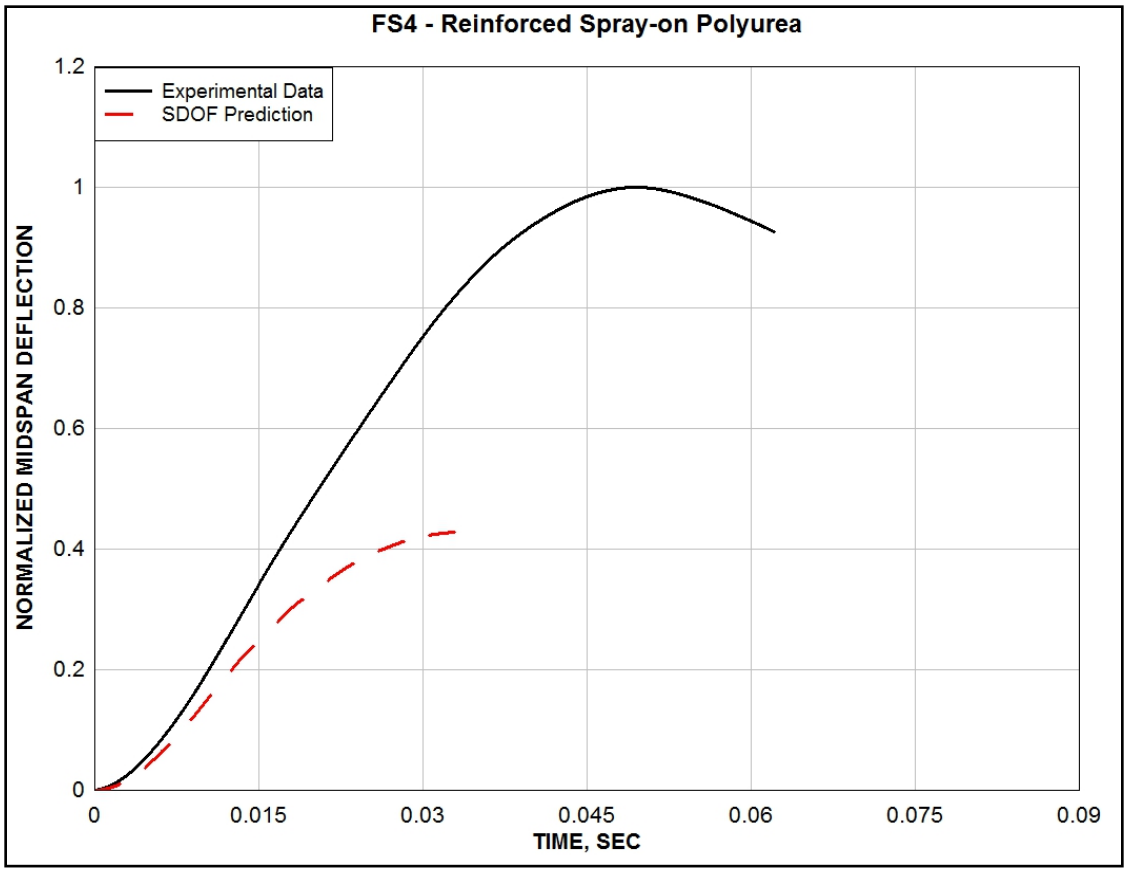

Figure F.2. Deflection for FS4 – Reinforced Spray-on Polyurea.

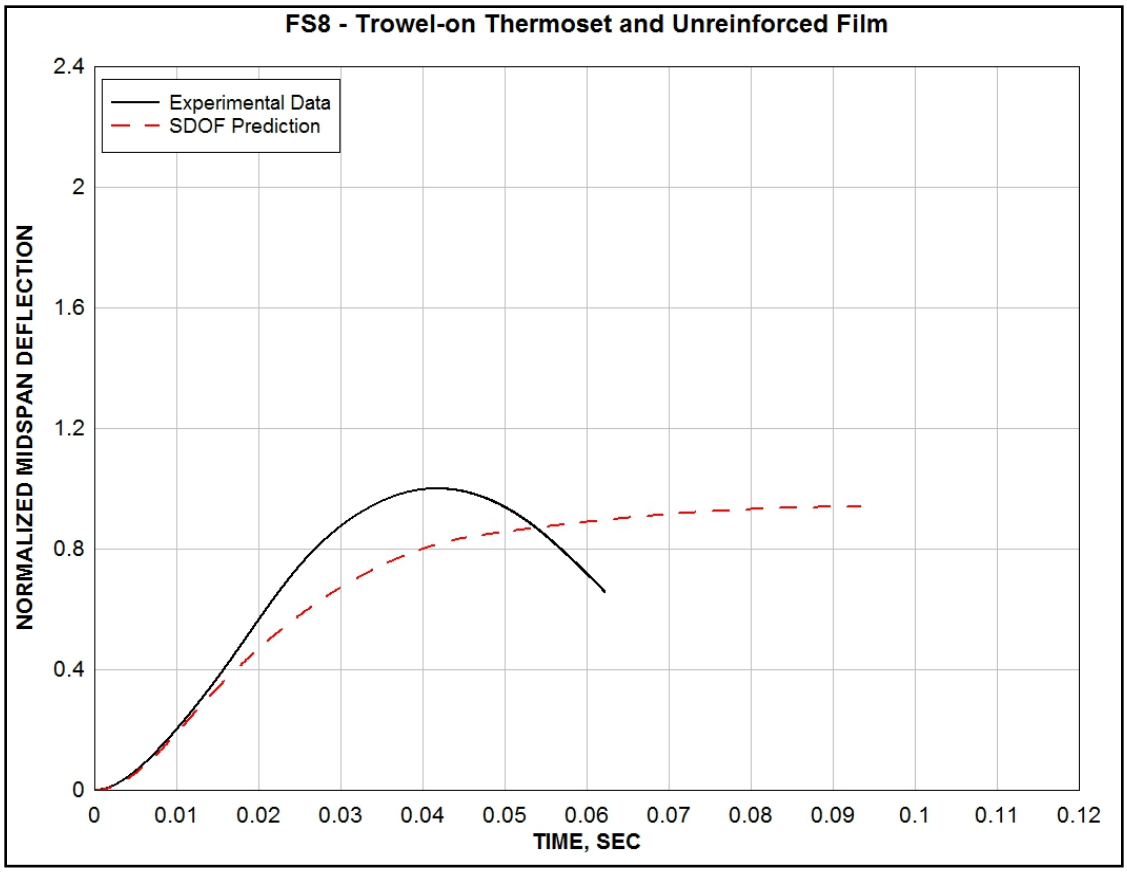

Figure F.3. Deflection for FS8 – Trowel-on Thermoset and Unreinforced Film.

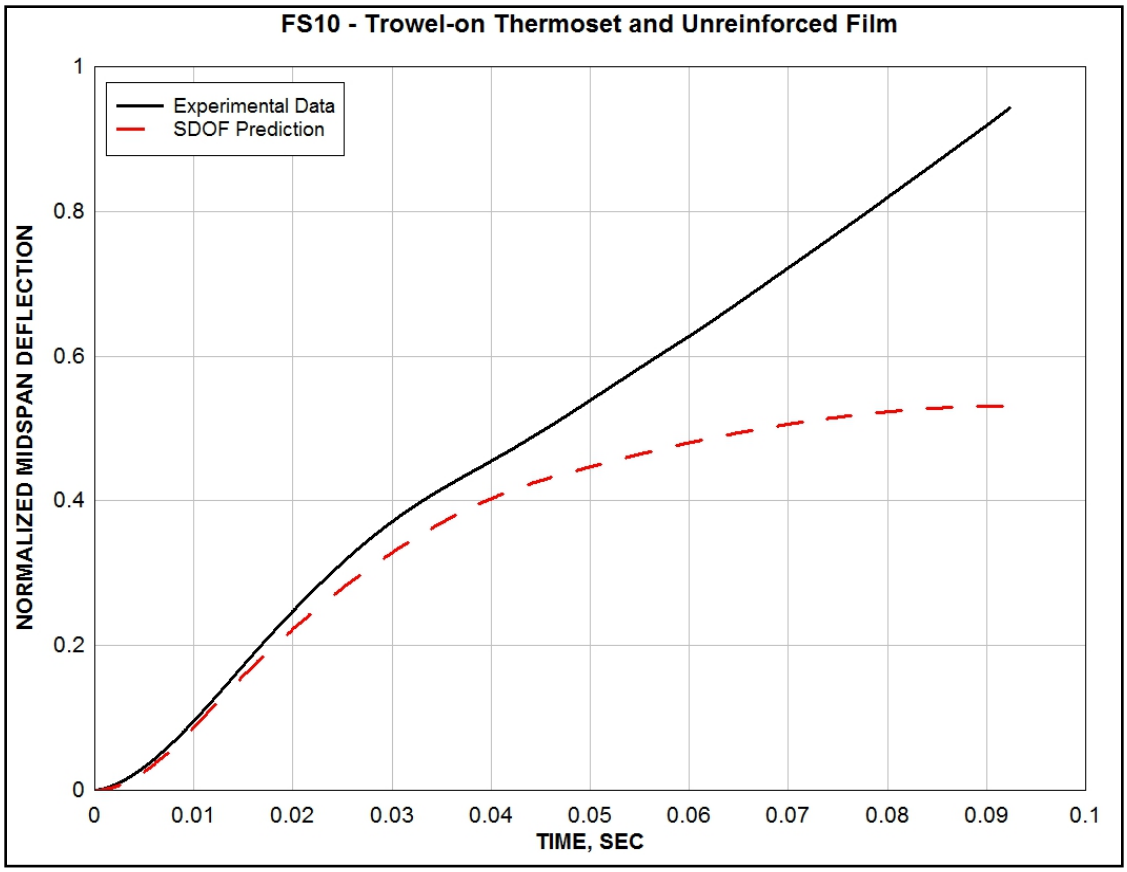

Figure F.4. Deflection for FS10 – Trowel-on Thermoset and Unreinforced Film.

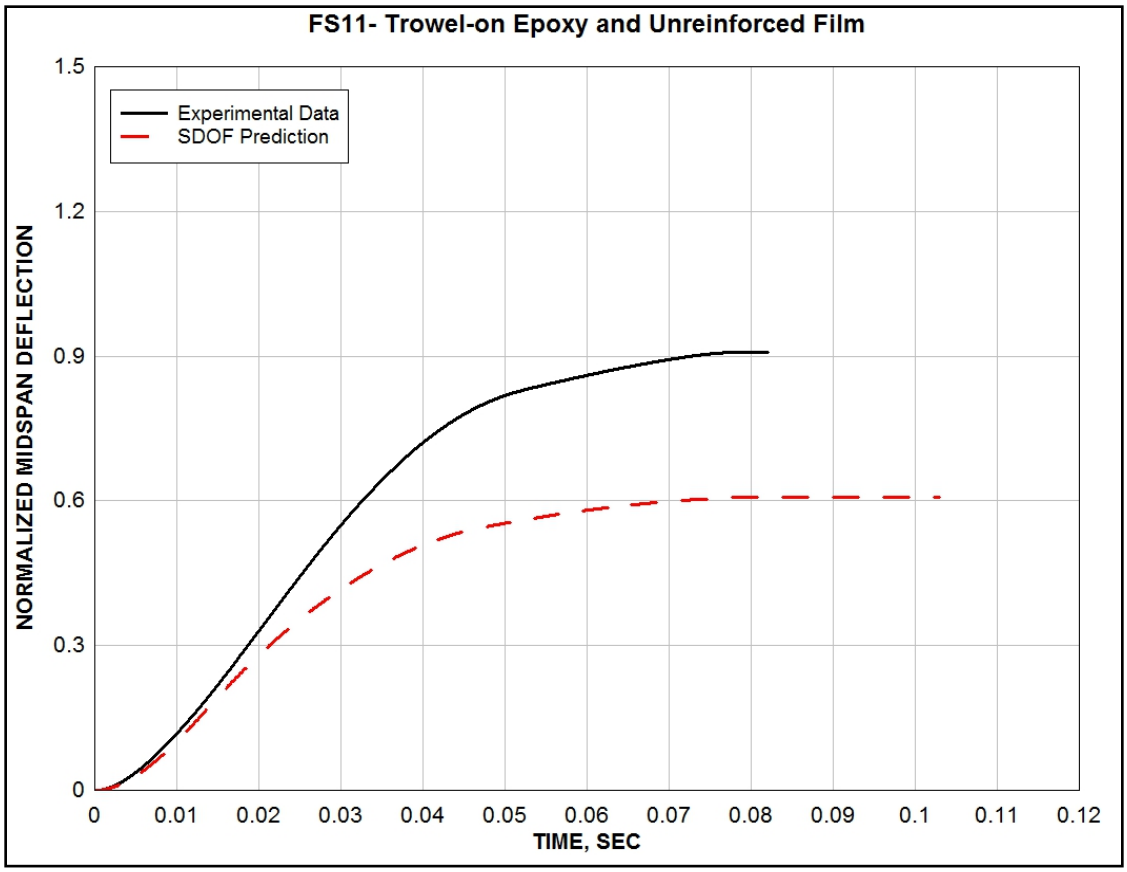

Figure F.5. Deflection for FS11 – Trowel-on Epoxy and Unreinforced Film.

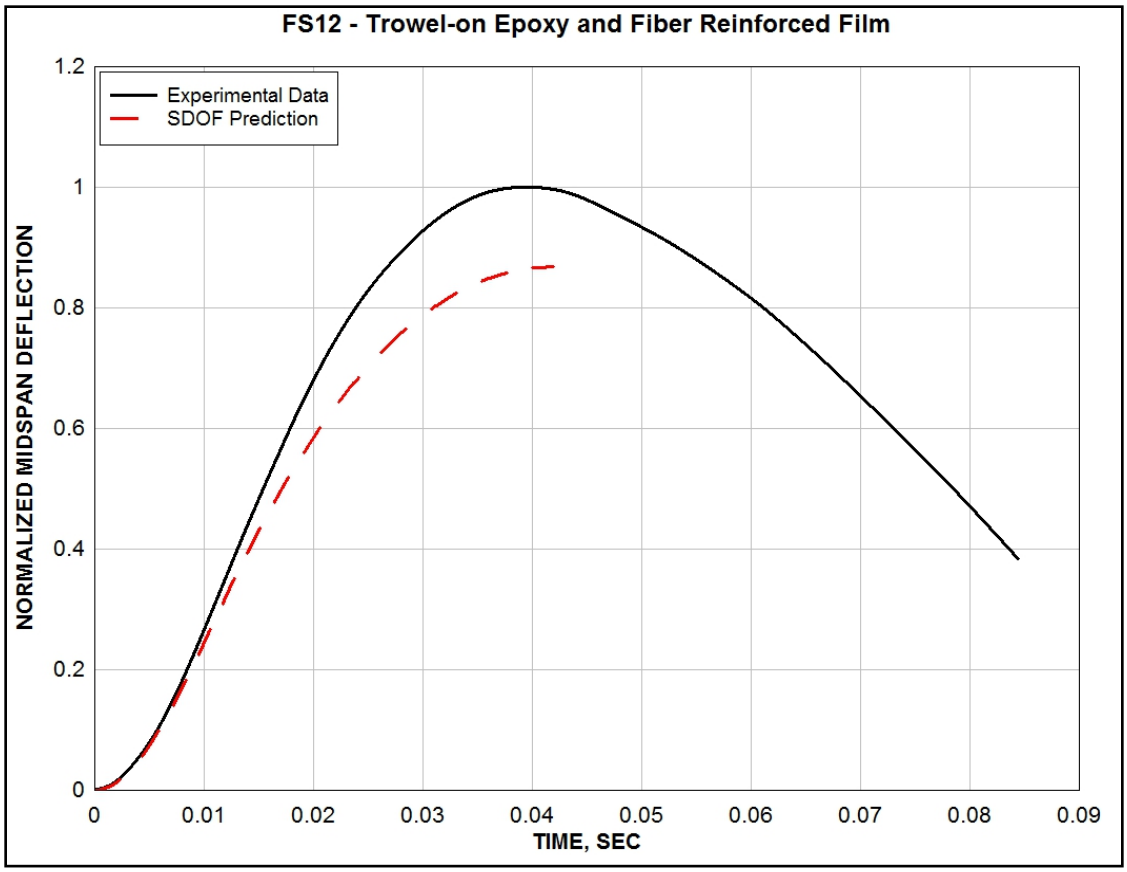

Figure F.6. Deflection for FS12 – Trowel-on Epoxy and Fiber Reinforced Film.

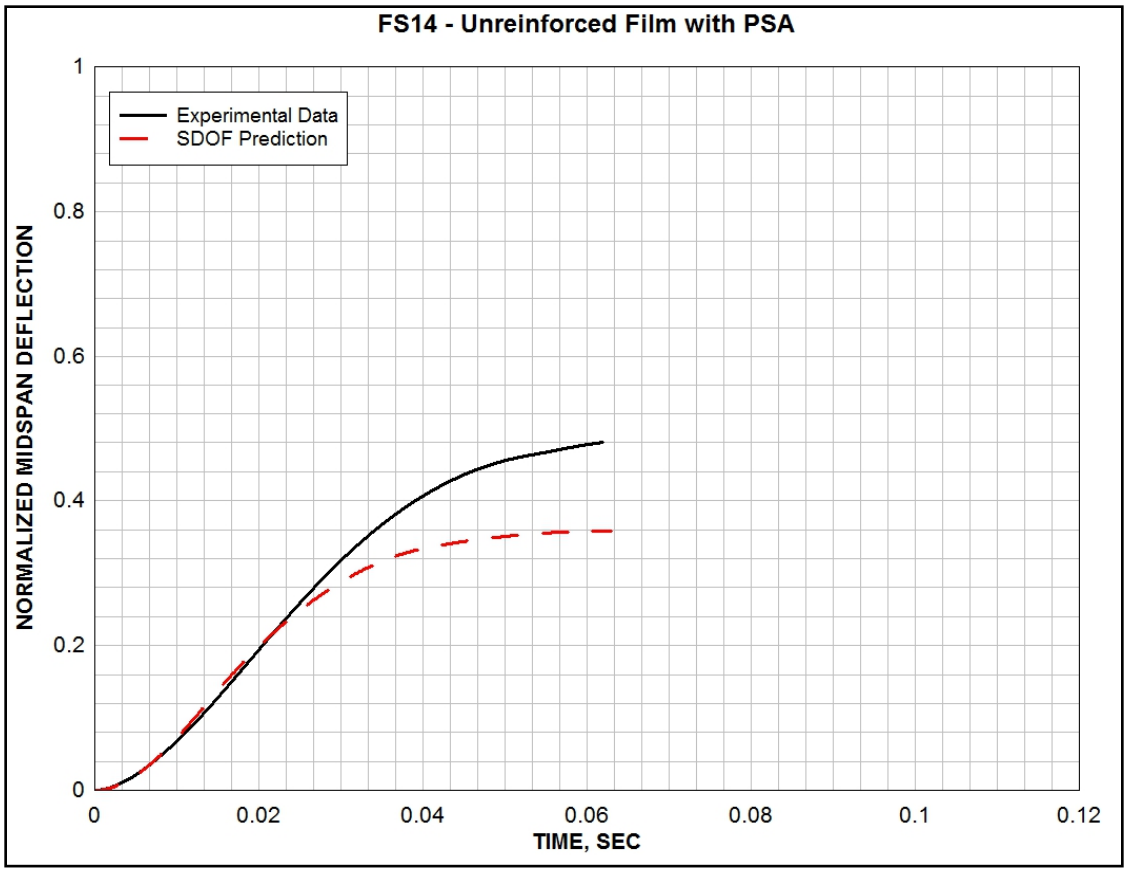

Figure F.7. Deflection for FS14 – Unreinforced Film with PSA.

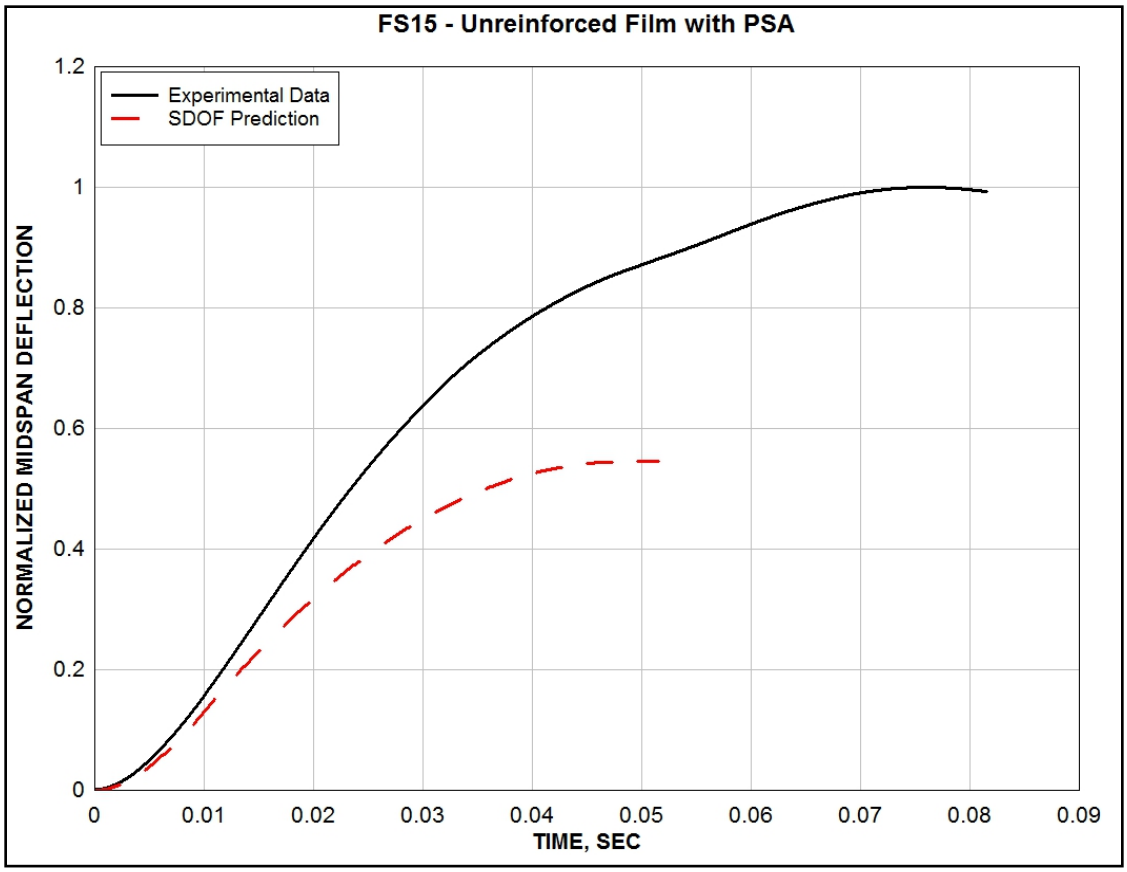

Figure F.8. Deflection for FS15 – Unreinforced Film with PSA.